

Some pages of this thesis may have been removed for copyright restrictions.

If you have discovered material in AURA which is unlawful e.g. breaches copyright, (either yours or that of a third party) or any other law, including but not limited to those relating to patent, trademark, confidentiality, data protection, obscenity, defamation, libel, then please read our [Takedown Policy](#) and [contact the service](#) immediately

THE BEHAVIOUR OF POLYMER QUENCHANTS

NICHOLAS ANTHONY HILDER

Doctor of Philosophy

THE UNIVERSITY OF ASTON IN BIRMINGHAM

January 1988

This copy of the thesis has been supplied on condition that anyone who consults it is understood to recognise that its copyright rests with its author and that no quotation from the thesis and no information derived from it may be published without the author's prior, written consent.

THE UNIVERSITY OF ASTON IN BIRMINGHAM

THE BEHAVIOUR OF POLYMER QUENCHANTS

NICHOLAS ANTHONY HILDER

DOCTOR OF PHILOSOPHY

1988

THESIS SUMMARY

The internationally accepted Wolfson Heat Treatment Centre Engineering Group test was used to evaluate the cooling characteristics of the most popular commercial polymer quenchants: polyalkylene glycols, polyvinylpyrrolidones and polyacrylates. Prototype solutions containing poly(ethyloxazoline) were also examined. Each class of polymer was capable of providing a wide range of cooling rates depending on the product formulation, concentration, temperature, agitation, ageing and contamination. Cooling rates for synthetic quenchants were generally intermediate between those of water and oil. Control techniques, drag-out losses and response to quenching in terms of hardness and residual stress for a plain carbon steel, were also considered. A laboratory scale method for providing a controllable level of forced convection was developed. Test reproducibility was improved by positioning the preheated Wolfson probe 25mm above the geometric centre of a 25mm diameter orifice through which the quenchant was pumped at a velocity of 0.5m/s. On examination, all polymer quenchants were found to operate by the same fundamental mechanism associated with their viscosity and ability to form an insulating polymer-rich-film. The nature of this film, which formed at the vapour / liquid interface during boiling, was dependent on the polymer's solubility characteristics. High molecular weight polymers and high concentration solutions produced thicker, more stable insulating films. Agitation produced thinner more uniform films. Higher molecular weight polymers were more susceptible to degradation, and increased cooling rates, with usage. Polyvinylpyrrolidones can be cross-linked resulting in erratic performance, whilst the anionic character of polyacrylates can lead to control problems. Volatile contaminants tend to decrease the rate of cooling and salts to increase it. Drag-out increases upon raising the molecular weight of the polymer and its solution viscosity. Kinematic viscosity measurements are more effective than refractometer readings for concentration control, although a quench test is the most satisfactory process control method.

KEYWORDS : Quenching.
 Polymer quenchants.
 Cooling characteristics.
 Hardenability.
 Residual stress.

DEDICATION.

To my parents: for their tolerance and support to which I owe more than I can possibly say.

ACKNOWLEDGEMENTS.

The author would like to take this opportunity to thank his supervisors, Dr. S. Murphy and Mr. H.C. Child, for their help and guidance. Particular thanks are due to all the staff of the Wolfson Heat Treatment Centre and to the members of its Engineering Group, without whom this project would not have been possible. He would also like to express his gratitude to the Department of Mechanical and Production Engineering. Finally, but not least, to Marie Paisley for her efforts in helping to produce this thesis.

"Strike while the iron is hot"

ενθνζ το πρηγμα κροτεισθω

(Addaeus, "Epigrams")

LIST OF CONTENTS

| | Page |
|--|------|
| 1.0 RATIONALE. | 25 |
| 2.0 LITERATURE SURVEY. | 28 |
| 2.1 Definition of Quenching. | 28 |
| 2.2 Requirements of a Quenching Medium. | 28 |
| 2.3 Methods of Quenching. | 29 |
| 2.3.1 Direct Quenching | 30 |
| 2.3.2 Time Quenching | 30 |
| 2.3.3 Interrupted Quenching | 30 |
| 2.3.4 Spray Quenching | 31 |
| 2.3.5 Fog Quenching | 32 |
| 2.4 Mechanism of Quenching. | 32 |
| 2.4.1 Stages of Quenching | 33 |
| 2.5 Quench Process Variables. | 35 |
| 2.5.1 Agitation | 35 |
| 2.5.2 Temperature of Quenchant | 35 |
| 2.5.3 Workpiece Temperature | 36 |
| 2.6 Test Methods for Evaluating Quenching Media. | 36 |
| 2.6.1 Thermocouple Techniques | 37 |
| 2.6.1.1 Silver test piece methods | 38 |
| 2.6.1.2 Wolfson Engineering Group quench test | 44 |
| 2.6.2 Magnetic Methods | 50 |
| 2.6.3 Hot Wire Tests | 52 |
| 2.6.4 Calorimetric Methods | 52 |
| 2.6.5 Hardening Response | 53 |
| 2.7 Quenching of Steel | 54 |
| 2.7.1 TTT and CCT Diagrams | 55 |
| 2.8 Theoretical Factors Influencing Heat Transfer During Quenching | 57 |
| 2.8.1 Quench Severity Factors | 62 |
| 2.8.2 Numerical Methods | 69 |
| 2.9 Hardenability Tests and Correlation Between Quench Cooling Data and Steel Hardening Response | 72 |
| 2.9.1 Hardenability Tests | 72 |
| 2.9.2 Correlation Between Quench Data and Hardening Response | 75 |
| 2.10 Traditional Quenching Media | 83 |
| 2.10.1 Water | 85 |
| 2.10.2 Quenching Oils | 86 |

| | | |
|----------|---|-----|
| 2.10.3 | Emulsions | 89 |
| 2.10.4 | Salt Bath | 89 |
| 2.10.5 | Air-Gas Hardening | 92 |
| 2.11. | Polymer Quenchants | 93 |
| 2.11.1 | Polyvinyl Alcohols (PVA) | 96 |
| 2.11.1.1 | Cooling characteristics of PVA solutions | 97 |
| 2.11.2 | Polyalkylene Glycols (PAG) | 98 |
| 2.11.2.1 | Cooling characteristics of PAG solutions | 100 |
| 2.11.2.2 | PAG quench tank control measures | 106 |
| 2.11.2.3 | Contamination of PAG quenchants | 108 |
| 2.11.2.4 | Ageing of PAG quenchants | 113 |
| 2.11.3 | Polyvinylpyrrolidone (PVP) | 114 |
| 2.11.3.1 | PVP quenchant variables | 115 |
| 2.11.4 | Polyacrylates | 118 |
| 2.11.4.1 | Polyacrylate quenchant variables | 118 |
| 2.11.5 | Polymer Quenchant Research in the Eastern Bloc | 122 |
| 2.11.6 | New Polymers For Use In Aqueous Quenching | 123 |
| 2.12 | Quenching Equipment and Conversion to Polymer Quenchants | 124 |
| 2.13 | Molecular Weight Distribution and Characterization of Polymers | 128 |
| 2.14 | The Development of Residual Stresses During Quenching | 132 |
| 2.14.1 | Residual Stresses and Quench Cracking | 135 |
| 3.0 | EXPERIMENTAL PROCEDURE | 137 |
| 3.1 | Polymer Quenchants Examined | 137 |
| 3.2 | Polymer Quenchant Characterization | 138 |
| 3.2.1 | Solid Content of Concentrates | 138 |
| 3.2.2 | Gel Permeation Chromatography | 138 |
| 3.2.3 | Limiting Viscosity Number Determination | 141 |
| 3.2.4 | Kinematic Viscosity Determination | 144 |
| 3.2.5 | Examination of the PAG Inverse Solubility Phenomenon | 175 |
| 3.2.5.1 | Nuclear magnetic resonance spectroscopy | 146 |
| 3.3 | Preparation of Polymer Quenchant Solutions | 147 |
| 3.4 | Polymer Quenchant Solution Concentration Control | 148 |
| 3.4.1 | Refractive Index | 148 |
| 3.4.2 | Kinematic Viscosity | 148 |
| 3.5 | Assessment of Polymer Quenchant Cooling Characteristics | 150 |
| 3.5.1 | Construction of a Revised Quench Test Rig | 150 |
| 3.5.2 | Measurement System | 155 |
| 3.5.3 | Surface Condition of Probe | 157 |

| | | |
|---------|--|-----|
| 3.5.4 | Quenchant Sample Volume and Temperature | 157 |
| 3.5.5 | Quenchant Sample Agitation | 158 |
| 3.5.5.1 | Impeller/Baffle systems | 158 |
| 3.5.5.2 | Pump agitation systems | 160 |
| 3.6 | Comparison of Polymer Quenchant Cooling Characteristics | 164 |
| 3.7 | Visual Examination of Polymer Quenchant Cooling Mechanism | 164 |
| 3.8 | Effect of Polymer Quenchant Concentration, Temperature and Agitation | 165 |
| 3.8.1 | Polymer Solution Concentration | 166 |
| 3.8.2 | Polymer Solution Temperature | 166 |
| 3.8.3 | Polymer Solution Agitation | 166 |
| 3.9 | Simulated Ageing of Polymer Quenchants | 166 |
| 3.10 | Shear Stability of Polymer Quenchants | 168 |
| 3.11 | Polymer Quenchant Solution Rheology | 170 |
| 3.12 | Contamination of Polymer Quenchants | 171 |
| 3.12.1 | Quench Oil Contamination | 171 |
| 3.12.2 | Ammonia Contamination | 172 |
| 3.12.3 | Salt Contamination | 173 |
| 3.13 | Drag-out | 174 |
| 3.14 | Quenched Hardness and Residual Stress | 176 |
| 3.14.1 | Residual Stress Measurements | 178 |
| 3.14.2 | Metallurgical Examination of Specimens | 181 |
| 3.15 | Cooling Characteristic Assessment for New Polymer Quenchant Systems | 181 |
| 4.0 | EXPERIMENTAL RESULTS | 183 |
| 4.1 | Physical Properties of Polymer Quenchants Examined | 183 |
| 4.2 | Polymer Quenchant Characterization | 183 |
| 4.2.1 | Gel Permeation Chromatography Data | 183 |
| 4.2.2 | Limiting Viscosity Number Data | 193 |
| 4.2.3 | Findings for the PAG Inverse Solubility Studies | 197 |
| 4.2.3.1 | Nuclear magnetic resonance spectroscopic analysis data | 202 |
| 4.3 | Concentration Control Data for Polymer Quenchant Solutions | 206 |
| 4.4 | Quenchant Sample Agitation Systems | 206 |
| 4.4.1 | Impeller/Baffle Systems | 206 |
| 4.4.2 | Pump Agitation Systems | 210 |
| 4.5 | Comparative Cooling Characteristic Data for Polymer Quenchant Products | 219 |
| 4.6 | Photographic Record of Cooling Mechanism for Representative Polymer Quenchants | 231 |

| | | |
|--------|--|------------|
| 4.7 | Effect of Polymer Quenchant Concentration, Temperature and Agitation on the Cooling Characteristics. | 240 |
| 4.7.1 | Polymer Solution Concentration | 240 |
| 4.7.2 | Polymer Solution Temperature | 240 |
| 4.7.3 | Polymer Solution Agitation | 240 |
| 4.8 | Ageing Data for Representative Polymer Quenchants | 259 |
| 4.8.1 | Polymer Quenchant Shear Stability Data | 265 |
| 4.9 | Polymer Quenchant Solution Rheology Data | 265 |
| 4.10 | Polymer Quenchant Contamination Data | 268 |
| 4.10.1 | Contamination with Oil | 268 |
| 4.10.2 | Contamination with Ammonia | 268 |
| 4.10.3 | Salt Contamination | 278 |
| 4.11 | Drag-out | 285 |
| 4.12 | Quenchant Hardness and Residual Stress Data | 285 |
| 4.13 | Cooling Data for New Polymer Quenchant Systems | 294 |
| 5.0 | DISCUSSION OF EXPERIMENTAL RESULTS | 299 |
| 5.1 | Development of an Agitated Quench Test System | 299 |
| 5.2 | Commercial Polymer Quenchants Examined | 307 |
| 5.3 | Cooling Mechanism for Polymer Quenchants | 312 |
| 5.3.1 | PAG Inverse Solubility Phenomenon | 313 |
| 5.4 | Effect of Polymer Concentration, Temperature and Agitation on Cooling Characteristics | 322 |
| 5.4.1 | Polymer Solution Concentration | 322 |
| 5.4.2 | Polymer Solution Temperature | 331 |
| 5.4.3 | Polymer Solution Agitation | 334 |
| 5.4.4 | Summary of the Effect of Polymer Quenchant Concentration, Temperature and Agitation on Cooling Characteristics | 338 |
| 5.5 | Simulated Ageing of Polymer Quenchants | 339 |
| 5.6 | Contamination of Polymer Quenchants | 350 |
| 5.6.1 | Contamination with Oil or Ammonia | 351 |
| 5.6.2 | Salt Contamination | 355 |
| 5.7 | Drag-out | 357 |
| 5.8 | Polymer Quenchant Control | 361 |
| 5.9 | Quenched Hardness and Residual Stress | 362 |
| 5.10 | New Polymer Quenchants | 370 |
| 6.0 | CONCLUSIONS | 371 |
| 7.0 | SUGGESTIONS FOR FURTHER WORK | 375 |
| | APPENDICES | 376 |
| | REFERENCES | 392 |

LIST OF TABLES

| | Page |
|---|------------|
| Table 1. Grossmann quench severity factors H. | 73 |
| Table 2. Quench data for polyvinylpyrrolidone and polyalkylene glycol. | 116 |
| Table 3. Polymer quenchant products examined. | 137 |
| Table 4. Perkin Elmer Series 10 high performance gel permeation chromatograph operating conditions. | 139 |
| Table 5. Viscosity - molecular weight relationships for PVP and sodium polyacrylate polymers. | 143 |
| Table 6. Polymer quenchant oil contamination programme. | 172 |
| Table 7. Polymer quenchant ammonia contamination programme. | 173 |
| Table 8. Polymer quenchant sodium nitrite / nitrate salt contamination programme. | 174 |
| Table 9. Analysis of steel specimens. | 176 |
| Table 10. Residual surface macrostress measurement conditions. | 179 |
| Table 11. Prototype polymer quenchant formulations incorporating PEO _x . | 182 |
| Table 12. Some physical properties of the polymer concentrates tested. | 184 |
| Table 13. GPC polystyrene-equivalent molecular weight distribution data for the PAG and PVP products. | 192 |
| Table 14. Viscosity number data for PVP samples. | 195 |
| Table 15. Viscosity number data for Aquaquench ACR. | 197 |
| Table 16. Viscosity number data for Quendila PA solutions. | 199 |
| Table 17. The effect of agitation created using impeller / baffle systems on the cooling characteristics of a 20% Quendila PA solution at 30°C. | 209 |
| Table 18. Cooling characteristics for a 20% Quendila PA solution at 30°C, tested using various annular flow conditions. | 213 |
| Table 19. Effect of probe position with respect to the pump outlet and inlet orifices, on the cooling characteristics for a 15% Quendila PA solution at 30°C and 0.5m/s. | 214 |
| Table 20. Comparative cooling characteristic data for 15% concentrate solutions tested at 30°C. | 229 |
| Table 21. Cooling characteristics for various concentration solutions of the representative polymer quenchants tested at 30°C and 0.5m/s agitation. | 241 |

| | |
|---|------------|
| Table 22. Cooling characteristics for 15% solutions of the representative polymer quenchants tested at various temperatures and 0.5m/s agitation. | 245 |
| Table 23. Cooling characteristics for 15% solutions for the representative polymer quenchants tested at 30°C and agitated at various fluid velocities. | 249 |
| Table 24. Cooling characteristics for the nominal 15% PAG (Quendila PA) solution at 30°C and 0.5m/s agitation following various throughput in the simulated ageing test. | 253 |
| Table 25. Cooling characteristics for the nominal 15% PVP (Parquench 90) solution at 30°C and 0.5m/s agitation following various throughput in the simulated ageing test. | 254 |
| Table 26. Cooling characteristics for the nominal 15% polyacrylate (Aquaquench ACR) solution at 30°C and 0.5m/s following various throughput in the simulated ageing test. | 255 |
| Table 27. Fresh polymer concentrate and distilled water additions required to maintain a 2 litre sample of constant refractive index (equivalent to an initial 15% solution) for a cumulative quench load of 100kg/litre in the simulated ageing test. | 259 |
| Table 28. Cooling characteristics for nominally 18% polyacrylate (Aquaquench ACR) solutions supplied by T.I. Desford Tubes Ltd., following various periods of use. Test conditions 30°C and 0.5m/s agitation. | 264 |
| Table 29. Apparent viscosity values for 15% solutions of each representative polymer quenchant type measured at 15°C. | 265 |
| Table 30. Cooling characteristics for 15% representative polymer quenchant solutions contaminated with quench oil and tested at 30°C and 0.5m/s agitation. | 273 |
| Table 31. Cooling characteristics for 15% representative polymer quenchant solutions contaminated with ammonia and tested at 30°C and 0.5m/s agitation. | 279 |
| Table 32. Cooling characteristics for distilled water at 30°C contaminated with various sodium nitrite/nitrate salt additions (AVS 250). Test conditions 30°C and 0.5m/s agitation, probe preheat temperature 500°C. | 278 |

| | |
|---|------------|
| Table 33. Cooling characteristics for 15 and 30% (Quendila PA) solutions contaminated with various sodium nitrite/nitrate salt additions (AVS 250). Test conditions 30°C and 0.5m/s agitation, probe preheat temperature 500°C. | 279 |
| Table 34. Cooling characteristics for 15% PVP (Parquench 90) solutions contaminated with various sodium nitrite/nitrate salt additions 0.5m/s agitation, probe preheat temperature 500°C. | 284 |
| Table 35. Cooling characteristics for 15% polyacrylate (Aquaquench ACR) solutions contaminated with various sodium nitrite/nitrate salt additions (AVS 250). Test conditions 30°C and 0.5m/s agitation, probe preheat temperature 500°C. | 285 |
| Table 36. Drag-out for various quenchants. | 286 |
| Table 37. Surface residual hoop stress and hardness data for 12.5mm diameter 080H41 cylinders quenched under various conditions, including selected Wolfson quench test data. | 289 |
| Table 38. Cooling characteristics for the prototype quenchant solutions containing poly(ethyloxazoline) ($\bar{M}_w = 500,000$) tested at 30°C. | 298 |
| Table 39. Viscosity-average molecular weight data for the PVP's examined during extra work. | 310 |

LIST OF FIGURES.

| | Page |
|--|-------------|
| Figure 1. Temperature gradients and other major factors affecting the quenching of a gear. | 32 |
| Figure 2. The three stages of cooling during quenching shown on (a) the conventional time-temperature cooling curve, and (b) the corresponding cooling rate-temperature plot. | 34 |
| Figure 3. Diagram of the silver ball apparatus. | 38 |
| Figure 4. (a) Cooling curves for various quenching media measured at 40°C using the silver ball test; (b) corresponding cooling rate-temperature plots, and (c) hardness profiles across test bars, 50mm in diameter of steel 50MN7 (0.5%C, 1.8%Mn, <0.4%Si), after hardening in various media. | 40 |

| | | |
|-------------------|--|-----------|
| Figure 5. | Silver specimen for measuring the cooling curves in the Japanese Standards Association (JIS,K2242.1980) test. | 41 |
| Figure 6. | Cooling curves for the centre of bars 16mm diameter and 48mm long on being cooled in mineral oils A and B: (a) silver,(b) steel XC 48 (0.48%C, 0.65%Mn, 0.25%Si) and (c) hardness profiles across the steel bars after being quenched in each oil. | 43 |
| Figure 7. | Wolfson Engineering Group thermal probe: (a) probe details and (b) general assembly. | 45 |
| Figure 8. | Schematic of the original Wolfson Heat Treatment Centre test rig. | 46 |
| Figure 9. | Liscic's equipment for evaluating quenching media with centrifugal pump agitation. | 48 |
| Figure 10. | Diagram of the nickel ball test apparatus. | 51 |
| Figure 11. | Time-temperature plots obtained for quench oil samples in both the new and used conditions, measured at 40°C using the Wolfson Engineering Group test method. | 51 |
| Figure 12. | Hardness distribution across quenched bars of various diameters: (a) 0.45%C steel and (b) 0.4%C,1%Cr-V steel. | 54 |
| Figure 13. | (a) Time Temperature Transformation and (b) Continuous Cooling Transformation curves for a 0.44% plain carbon steel (German CK45) austenitized at 880°C. | 56 |
| Figure 14. | Curves for estimating the cooling power (Grossmann quench severity factor, H) of quenching baths. | 63 |
| Figure 15. | Curves for Russell's quench severity factor h against time to cool through the 0.05 intervals for 12.5mm (1/2 in.) diameter bars. | 66 |
| Figure 16. | Effect of increasing concentration of a commercially available water soluble quenchant on Russell's quench severity factor h,measured using a 12.5mm diameter by 50mm long 25/15 Cr-Ni steel test piece with a centrally located thermocouple. | 66 |
| Figure 17. | Change of Grossmann quench severity factor H with distance from quenched surface of a 3 in. (76mm) round of 18%Cr-8%Ni steel quenched in water at 60°F (16°C). | 67 |
| Figure 18. | Variation of Grossmann quench severity factor H with temperature and size for SAE/AISI 9460 (0.6%C, 1.0%Mn, 0.5%Ni, 0.4%Cr) steel oil quenched from 1550°F (845° C). | 67 |

| | | |
|--------------------|--|----|
| Figure 19. | Thermal diffusivity of various structures. | 68 |
| Figure 20. | Variation of Grossmann quench severity factor H with temperature and size for 17%Cr steel water quenched from 1550°F (845°C)(52). | 68 |
| Figure 21. | Effect of surface temperature on heat transfer coefficient for (a) water (5 consecutive tests),and (b) average result for six quenches into a 25% PAG solution. | 70 |
| Figure 22. | Relationships among ideal critical diameter, D_i , actual diameter, D , and Grossmann severity of quench, H . | 73 |
| Figure 23a. | Jominy end-quench test of hardenability. | 74 |
| Figure 23b. | Jominy end-quench curves for:(a) plain carbon steel (0.4%C, 0.7%Mn); (b) low alloy steel (1%Ni, 0.35%C); and (c) alloy steel (3%Ni,1%Cr, 0.3%C). | 74 |
| Figure 24. | Grossmann chart relating bar diameter, hardenability of steel and severity of quench. | 76 |
| Figure 25. | Location on end-quenched Jominy hardenability specimen corresponding to: (a) the centre of round bars, (b) the half - radius position in round bars. | 77 |
| Figure 26. | Cross-section hardness in rounds related to end-quench bar locations and Grossmann severity of quench H . | 78 |
| Figure 27. | Tamura quench severity V values for various cooling patterns for materials quenched in oils. | 82 |
| Figure 28. | Typical cooling rate-temperature curves for some common quenchants at 30°C as measured under non-agitated conditions by the Wolfson Engineering Group test. | 84 |
| Figure 29. | The cooling characteristics of water and inorganic salt solutions measured under non-agitated conditions by the Wolfson Engineering Group test. | 85 |
| Figure 30. | Cooling characteristics for different categories of quench oil measured at 40°C using the Wolfson Engineering Group test. | 87 |
| Figure 31. | The effect of agitation on the cooling characteristics of a medium-speed oil tested using the Wolfson Engineering Group method at 40°C. Agitation created by a two-blade impeller used at the speeds indicated, in conjunction with an H-baffle. | 88 |
| Figure 32. | (a) The Edwin Cooper accelerated ageing test rig for oils, (b) typical results for a straight mineral oil before and after ageing determined using the Wolfson Engineering Group test. | 90 |

| | | |
|-------------------|--|------------|
| Figure 33. | Cooling curves for the centre of an 18/8 stainless steel specimen (13mm diameter by 64mm long) on being quenched into non-agitated water, conventional oil, and soluble oil emulsions. | 91 |
| Figure 34. | Cooling curves for the centre of an 18/8 stainless steel specimen (12.7mm diameter by 37.5mm long) on being quenched into a salt bath and non-agitated conventional quenching media. | 91 |
| Figure 35. | The synthesis of polyvinyl alcohol (PVA). | 96 |
| Figure 36. | Cooling curves for aqueous PVA solutions as a function of concentration and temperature. Measured by a thermocouple at the geometric centre of type 304 stainless steel specimens (13mm diameter by 100mm long) quenched under non-agitated conditions. | 97 |
| Figure 37. | The molecular structure of polyalkylene glycol (PAG) derived from the random polymerization of ethylene and propylene oxides. | 98 |
| Figure 38. | Schematic representation of the effect of (a) concentration (b) temperature and (c) agitation on the cooling characteristics of a typical PAG solution. | 101 |
| Figure 39. | Effect of concentration of PAG solutions on maximum cooling rate as measured using the Wolfson Engineering Group test but with an austenitic stainless steel probe. | 101 |
| Figure 40. | The effect of agitation on the cooling characteristics of a 25% solution of a typical PAG tested using the Wolfson Engineering Group method at 40°C. Agitation created by a two-bladed impeller used at the speeds indicated, in conjunction with an H-baffle. | 104 |
| Figure 41. | West Bromwich College of Commerce and Technology test system, agitation created by 4 pumps in 2 parallel circuits. | 105 |
| Figure 42. | Effect of quenchant flow rate (employing the system illustrated in figure 41) on the cooling characteristics of a 20% PAG quenchant at 40°C using the Wolfson Engineering Group test. | 105 |
| Figure 43. | Results of Wolfson Engineering Group tests on polymer solutions with the same refractive index, comparing fresh quenchant with polluted quenchants. | 107 |

| | | |
|-------------------|--|-----|
| Figure 44. | Cooling curves for a 10% PAG solution, at 20°C with moderate agitation, contaminated with (a) a rust preventive oil and (b) ammonia. Curves produced using the drasticimeter technique with a silver test probe 8mm diameter by 24mm long. | 108 |
| Figure 45. | Schematic representation of the influence of contaminants on useful life of polymer quenchants: (a) life span of a polymer quenchant with low maintenance; (b) "delta" accumulation as a function of water quality. | 109 |
| Figure 46. | (a) Schematic illustration of the membrane separation process for polymer quenchants; (b) cutaway view of spiral-wound element for polymer separation. | 113 |
| Figure 47. | Comparison of the cooling characteristics of new and used 23.5 wt % PAG solution. | 114 |
| Figure 48. | Six-step polyvinylpyrrolidone (PVP) synthesis. | 115 |
| Figure 49. | Sodium polyacrylate produced by the polymerization of sodium acrylate (or hydrolysis of polyacrylate ester). | 118 |
| Figure 50. | Cooling curves of polyacrylate quenchant as a function of concentration and temperature. | 120 |
| Figure 51. | Cooling rate-temperature curves for a polyacrylate quenchant, showing the effect of concentration at a bath temperature of 52°C(non-agitated). Measured in accordance with the Wolfson Engineering Group test, but with an austenitic stainless steel probe. | 120 |
| Figure 52. | (a) Drag-out of polymer quenchants at 30°C and of a quench oil at 70°C; (b) Specially-designed test probe. | 121 |
| Figure 53. | General formula of a substituted oxazoline polymer. | 124 |
| Figure 54. | Batch quench tank with (a) pump system agitation, and (b) propeller agitation. | 125 |
| Figure 55. | Integral quench furnace with draft tube and directional flow manifold. | 127 |
| Figure 56. | A typical normalized weight distribution curve for the molecular weights of a polymer sample. | 130 |
| Figure 57. | A plot of viscosity number versus concentration. | 130 |
| Figure 58. | Development of thermal stresses on cooling . | 137 |
| Figure 59. | The effect of bar diameter on the residual stress pattern from both thermal and transformation stresses. | 134 |
| Figure 60. | GPC calibration plot for polystyrene samples dissolved in THF. | 140 |

| | | |
|-------------------|---|------------|
| Figure 61. | Typical glass capillary viscometers: (a) U-tube type BS/U, and (b) suspended level type BS/IP/SL. | 142 |
| Figure 62. | View through eyepiece of refractometer. | 149 |
| Figure 63. | Replacement quench test rig. | 151 |
| Figure 64. | Circuit diagram for pneumatic probe transfer system using CETOP standard symbols and indicating the sequence. | 152 |
| Figure 65. | Computerized quench data acquisition system. | 154 |
| Figure 66. | Linearizer and amplifier circuit. | 154 |
| Figure 67. | Schematic diagram of the impeller/ H-baffle agitation system. | 159 |
| Figure 68. | Schematic diagram of the prototype quench tank used in conjunction with the variable speed pump, showing the inlets for either vertical or horizontal flow. | 159 |
| Figure 69. | West Bromwich College of Commerce and Technology quench unit modified to incorporate a 25mm internal diameter pump outlet tube. | 162 |
| Figure 70. | Preferred centrifugal pump agitation system. | 163 |
| Figure 71. | Apparatus for shear stability testing. | 169 |
| Figure 72. | Schematic diagram of the Epprecht Rheomat 15 cone and plate viscometer. | 170 |
| Figure 73. | Drag-out specimen. | 175 |
| Figure 74. | Residual stress specimen. | 175 |
| Figure 75. | X-ray diffraction focussing geometry. | 177 |
| Figure 76. | Gel permeation chromatograms for Quendila PA samples dissolved in THF in both the as-received condition, and following a quench load of 100kg/litre in the accelerated ageing test. | 185 |
| Figure 77. | Gel permeation chromatogram for Quendila PHT dissolved in THF. | 186 |
| Figure 78. | Gel permeation chromatogram for Breox NF-18 dissolved in THF. | 187 |
| Figure 79. | Gel permeation chromatogram for Aquaquench 1250 dissolved in THF. | 188 |
| Figure 80. | Gel permeation chromatogram for Ucon E dissolved in THF. | 189 |
| Figure 81. | Gel permeation chromatogram for Parquench 60 dissolved in chloroform. | 190 |

| | | |
|-------------------|--|------------|
| Figure 82. | Gel permeation chromatograms for Parquench 90 samples, dissolved in chloroform in both the as-received condition, and following a quench load of 100kg/litre in the accelerated ageing test. | 191 |
| Figure 83. | Concentration-viscosity number plots for the aqueous PVP samples at 30°C. | 194 |
| Figure 84. | Concentration-viscosity number plots for polyacrylate (Aquaquench ACR) samples dissolved in 1.25M aqueous NaSCN at 30°C. | 196 |
| Figure 85. | Concentration-viscosity number plots for aqueous PAG (Quendila PA) solutions at 25, 40 and 60°C. | 198 |
| Figure 86. | Effect of temperature on the kinematic viscosity of a 1 weight per cent Quendila PA solution. | 200 |
| Figure 87. | Effect of temperature on the kinematic viscosity of a 10 weight per cent Quendila PA solution. | 201 |
| Figure 88. | 300MHz proton magnetic resonance spectrum for Quendila PA dissolved in deuteriochloroform. | 203 |
| Figure 89. | 300MHz proton magnetic resonance spectrum for Quendila PHT dissolved in deuterchloroform. | 204 |
| Figure 90. | Relationship between the percentage of oxypropylene units in the PAG products Quendila PA and PHT and an integral ratio R. | 205 |
| Figure 91. | Concentration control for representative polymer quenchant products using a refractometer. | 207 |
| Figure 92. | Concentration control for representative polymer quenchant products using a suspended level viscometer. | 208 |
| Figure 93. | Effect of fluid velocity on the maximum cooling rate for Quendila PA (PAG) solutions of various concentrations at 30°C, using both vertical and horizontal flow. | 211 |
| Figure 94. | Effect of Quendila PA (PAG) concentration on the critical fluid velocity to instantaneously strip the stable polymer film and eliminate stage A cooling, for vertical and horizontal flow at 30°C. | 212 |
| Figure 95. | Effect of probe height H with respect to the pump outlet orifice on the cooling characteristics for a 15% Quendila PA solution at 30°C. Fluid velocity through outlet 0.5m/s. | 215 |

| | |
|--|-----|
| Figure 96. Effect of horizontal probe displacement X with respect to the pump outlet orifice on the cooling characteristics for a 15% Quendila PA solution at 30°C, fluid velocity through outlet 0.5m/s. | 216 |
| Figure 97. Effect of pump inlet position D on the cooling characteristics for a 15% Quendila PA solution at 30°C, fluid velocity through outlet 0.5m/s. | 217 |
| Figure 98. Cooling data for a 15 volume per cent solution of Quendila PA tested at 30°C in both the static condition and 0.5m/s agitation. | 220 |
| Figure 99. Cooling data for a 15 volume per cent solution of Quendila PHT tested at 30°C in both the static condition and 0.5m/s agitation. | 221 |
| Figure 100. Cooling data for a 15 volume per cent solution of Breox NF-18 tested at 30°C in both the static condition and 0.5m/s agitation. | 222 |
| Figure 101. Cooling data for a 15 volume per cent solution of Aquaquench 1250 tested at 30°C in both the static condition and 0.5m/s agitation. | 223 |
| Figure 102. Cooling data for a 15 volume per cent solution of Ucon E tested at 30°C in both the static condition and 0.5m/s agitation. | 224 |
| Figure 103. Cooling data for a 15 volume per cent solution of Parquench 60 tested at 30°C in both the static condition and 0.5m/s agitation. | 225 |
| Figure 104. Cooling data for a 15 volume per cent solution of Parquench 90 tested at 30°C in both the static condition and 0.5m/s agitation. | 226 |
| Figure 105. Cooling data for a 15 volume per cent solution of Aquaquench 110 tested at 30°C in both the static condition and 0.5m/s agitation. | 227 |
| Figure 106. Cooling data for a 15 volume per cent solution of Aquaquench ACR tested at 30°C in both the static condition and 0.5m/s agitation. | 228 |
| Figure 107. Stages during quenching for a non-agitated 15 volume per cent PAG (Quendila PA) solution at 30°C. | 236 |
| Figure 108. Stages during quenching for a 15 volume per cent PAG (Quendila PA) solution at 30°C and 0.5m/s agitation. | 234 |

| | |
|--|-----|
| Figure 109. Stages during quenching for a 15 volume per cent PVP (Parquench 90) solution non-agitated at 30°C. | 235 |
| Figure 110. Stages during quenching for a 15 volume per cent PVP (Parquench 90) solution at 30°C and agitated at 0.5m/s. | 236 |
| Figure 111. Stages during quenching for a 15 volume per cent Polyacrylate (Aquaquench ACR) solution non-agitated at 30°C. | 238 |
| Figure 112. Stages during quenching for a 15 volume per cent Polyacrylate (Aquaquench ACR) solution at 30°C and 0.5m/s agitation. | 239 |
| Figure 113. Typical cooling data for various concentration PAG (Quendila PA) solutions tested at 30°C and 0.5m/s agitation. | 242 |
| Figure 114. Typical cooling data for various concentration PVP (Parquench 90) solutions tested at 30°C and 0.5m/s agitation. | 243 |
| Figure 115. Typical cooling data for various concentration polyacrylate (Aquaquench ACR) solutions tested at 30°C and 0.5m/s agitation. | 244 |
| Figure 116. Typical cooling data for a 15 volume per cent PAG(Quendila PA) solution tested at various temperatures and 0.5m/s agitation. | 246 |
| Figure 117. Typical cooling data for a 15 volume per cent PVP (Parquench 90) solution tested at various temperatures and 0.5m/s agitation. | 247 |
| Figure 118. Typical cooling data for a 15 volume per cent polyacrylate (Aquaquench ACR) solution tested at various temperatures and 0.5m/s agitation. | 247 |
| Figure 119. Typical cooling data for a 15 volume per cent PAG (Quendila PA) solution at 30°C and agitated at various fluid velocities. | 250 |
| Figure 120. Typical cooling data for a 15 volume per cent PVP (Parquench 90) solution at 30°C and agitated at various fluid velocities. | 251 |
| Figure 121. Typical cooling data for a 15 volume per cent polyacrylate (Aquaquench ACR) solution at 30°C and agitated at various fluid velocities. | 252 |

| | |
|---|-----|
| Figure 122. Typical cooling data for a 15 volume per cent PAG (Quendila PA) solution at 30°C and agitated at 0.5m/s following various cumulative quench loads in the simulated ageing test. | 256 |
| Figure 123. Typical cooling data for a 15 volume per cent PVP (Parquench 90) solution at 30°C and agitated at 0.5m/s following various cumulative quench loads in the simulated ageing test. | 257 |
| Figure 124. Typical cooling data for a 15 volume per cent polyacrylate (Aquaquench ACR) solution at 30°C and agitated at 0.5m/s following various cumulative quench loads in the simulated ageing test. | 258 |
| Figure 125. Typical cooling data for nominally 18 volume per cent polyacrylate (Aquaquench ACR) solutions supplied by T.I. Desford Tubes Ltd. following various periods of use. Test conditions 30°C and 0.5m/s agitation. | 263 |
| Figure 126. Kurt Orbahn shear stability results for 15 volume per cent solutions of the representative polymer quenchants. | 266 |
| Figure 127. Epprecht Rheomat cone-and-plate viscometer results for 15 volume per cent solutions of the representative polymer quenchants at 15°C. | 267 |
| Figure 128. Typical cooling data for a 15 volume per cent PAG (Quendila PA) solution at 30°C and agitated at 0.5m/s with various weight per cent levels of quench oil contamination (Houghtoquench 3s). | 269 |
| Figure 129. Typical cooling data for a 15 volume per cent PAG (Quendila PA) solution at 30°C and agitated at 0.5m/s with varying weight per cent levels of soluble quench oil contamination (Klenquench 3). | 270 |
| Figure 130. Typical cooling data for a 15 volume per cent PVP(Parquench 90) solution at 30°C and agitated at 0.5m/s with varying weight per cent levels of quench oil contamination (Houghtoquench 3s). | 271 |
| Figure 131. Typical cooling data for a 15 volume per cent polyacrylate (Aquaquench ACR) solution at 30°C and agitated at 0.5m/s with varying weight per cent levels of quench oil contamination (Houghtoquench 3s). | 272 |

| | |
|--|-----|
| Figure 132. Typical cooling data for a 15 volume per cent PAG (Quendila PA) solution contaminated with various weight per cent additions of ammonia. | 274 |
| Figure 133. Typical cooling data for a 15 volume per cent PVP (Parquench 90) solution contaminated with various weight per cent additions of ammonia. | 275 |
| Figure 134. Typical cooling data for a 15 volume per cent polyacrylate (Aquaquench ACR) solution contaminated with various weight per cent additions of ammonia. | 276 |
| Figure 135. Typical cooling curves for a 15 volume per cent PAG (Quendila PA) solution, and for water contaminated with AVS 250 sodium nitrite/nitrate salt. Test conditions 30°C, 0.5m/s agitation, probe preheat temperature 500°C. | 280 |
| Figure 136. The effect of sodium nitrite/nitrate salt additions on the refractometer readings for the representative polymer quenchant solutions. | 281 |
| Figure 137. The effect of sodium nitrite/nitrate salt additions on the kinematic viscosities of the representative polymer solutions. | 282 |
| Figure 138. The effect of sodium nitrite/nitrate salt additions on the inversion temperature for 15 and 30 volume per cent PAG (Quendila PA) solutions. | 283 |
| Figure 139. Results of drag-out experiment for representative polymer solutions of various concentrations at 30°C in both the static and the agitated conditions. | 284 |
| Figure 140. Chromium K_{α} diffraction profiles for the fully annealed 12.5mm diameter 080H41 specimen. | 290 |
| Figure 141. Chromium K_{α} diffraction profiles for the 12.5mm diameter 080H41 specimen quenched into a 15 volume per cent PAG (Quendila PA) solution at 30°C and 0.5m/s agitation | 291 |
| Figure 142. Chromium K_{α} diffraction profiles for the 12.5mm diameter 080H41 specimen quenched into a 15 volume per cent PVP (Parquench 90) solution at 30°C and 0.5m/s agitation. | 292 |
| Figure 143. Chromium K_{α} diffraction profiles for the 12.5mm diameter 080H41 specimen quenched into a 15 volume per cent polyacrylate (Aquaquench ACR) solution at 30°C and 0.5m/s. | 293 |

| | |
|---|-----|
| Figure 144. Cooling data for a 2.25 weight per cent solution of poly(ethyloxazoline) tested at 30°C in both the static condition and 0.5m/s agitation. | 295 |
| Figure 145. Cooling data for a solution containing 1.5 weight per cent Parquench 90: poly(ethyloxazoline) mixed in the ratio 3:1, and tested at 30°C in both the static condition and 0.5m/s agitation. | 296 |
| Figure 146. Cooling data for a solution containing 10 weight per cent of Quendila PA: poly(ethyloxazoline) mixed in the ratio of 9:1, and tested at 30°C in both the static condition and 0.5m/s agitation. | 297 |
| Figure 147. Maximum cooling rates for a 20 volume per cent PAG (Quendila PA) solution as a function of calculated Reynolds numbers for annular flow produced using the West Bromwich College of Commerce and Technology agitation system. | 302 |
| Figure 148. Schematic representation of the submerged jet illustrated in Plate 5 for a 15 volume per cent PAG (Quendila PA) at 30°C and 0.5m/s fluid velocity. | 304 |
| Figure 149. Schematic representation of the cooling mechanism for polymer quenchants. | 319 |
| Figure 150. The effect of solution concentration on the maximum cooling rate for each of the representative polymers tested at 30°C, 0.5m/s fluid velocity. | 323 |
| Figure 151. The effect of solution concentration on the cooling rate at 300°C for each of the representative polymers tested at 30°C, 0.5m/s fluid velocity. | 324 |
| Figure 152. Effect of solution kinematic viscosity measured at 40°C on the stage A/B transition temperature for the various concentration PAG (Quendila PA) and polyacrylate (Aquaquench ACR) solutions tested at 30°C, and 0.5m/s agitation. | 325 |
| Figure 153. Effect of solution kinematic viscosity measured at 40°C on the stage A/B transition cooling rates for the various concentration PAG (Quendila PA) and polyacrylate (Aquaquench ACR) solutions, tested at 30°C, and 0.5m/s agitation. | 326 |

| | |
|---|-----|
| Figure 154. The maximum cooling rate for the various concentration representative polymer solutions measured at 30°C and 0.5m/s agitation, as a function of kinematic viscosity. | 329 |
| Figure 155. The cooling rate at 300°C for the various concentration representative polymer solutions measured at 30°C and 0.5m/s agitation, as a function of kinematic viscosity. | 330 |
| Figure 156. The effect of solution temperature on the maximum cooling rate for each of the representative polymers tested at 15 volume per cent concentration and 0.5m/s agitation. | 332 |
| Figure 157. The effect of solution temperature on the cooling rate at 300°C for each of the representative polymers tested at 15 volume per cent concentration and 0.5m/s agitation. | 333 |
| Figure 158. The effect of agitation on the maximum cooling rate for 15 volume per cent solutions of the representative polymers at 30°C. | 336 |
| Figure 159. The effect of agitation on the cooling rate at 300°C for 15 volume per cent solutions of the representative polymers at 30°C. | 337 |
| Figure 160. The effect of usage on the maximum cooling rate for a nominal 15 volume per cent solution of each representative polymer quenchant, tested at 30°C and 0.5m/s agitation. | 340 |
| Figure 161. The effect of usage on the cooling rate at 300°C for a nominal 15 volume per cent solution of each representative polymer quenchant, tested at 30°C and 0.5m/s agitation. | 341 |
| Figure 162. The effect of usage on the kinematic viscosity of nominal 15 volume per cent solutions of each representative polymer quenchant at 40°C. | 342 |
| Figure 163. The effect of oil contamination (Houghtoquench 3S) on the maximum cooling rate of 15 volume per cent solutions of each representative polymer quenchant tested at 30°C, 0.5m/s fluid velocity. | 351 |

- Figure 164.** The effect of ammonia contamination on the maximum cooling rate of 15 volume per cent solutions of each representative polymer quenchant. Tested at 30°C, 0.5m/s fluid velocity. 352
- Figure 165.** The effect of additions of AVS 250 nitrite/nitrate salt on the maximum cooling rate of water and both 15 and 30 volume per cent PAG (Quendila PA) solutions. Tested at 30°C, 0.5m/s with probe preheated to 500°C. 353
- Figure 166.** The effect of additions of AVS 250 nitrite/nitrate salt on the maximum cooling rate of water and 15 volume per cent solutions of a typical PVP (Parquench 90) and a polyacrylate (Aquaquench ACR) quenchant. tested at 30°C, 0.5m/s with probe preheated to 500°C. 354
- Figure 167.** The effect of the representative polymer solution viscosity on the level of drag-out in the static tests. 358
- Figure 168.** The relationship between the residual hoop stress in quenched 12.5mm diameter 0.45%C steel bars and the maximum cooling rates for the various quenchants measured using the Wolfson Engineering Group test. 364
- Figure 169.** The relationship between the residual hoop stress in quenched 12.5mm diameter 0.45%C steel bars and the cooling times to 360°C for the various quenchants measured using the Wolfson Engineering Group test. 365
- Figure 170.** The relationship between the core hardness in quenched 12.5mm diameter 0.45%C steel bars and the maximum cooling rates for the various quenchants measured using the Wolfson Engineering Group test. 366
- Figure 171.** The relationship between the core hardness in quenched 12.5mm diameter 0.45%C steel bars and the cooling times to 360°C for the various quenchants measured using the Wolfson Engineering Group test. 367

LIST OF PLATES

| | Page |
|--|------|
| Plate 1. Illustration of the flame and smoke hazard when quenching into oil, even when using a damper shield. | 95 |
| Plate 2. Quenching into a 20 per cent PAG solution following conversion to a polymer quenchant. | 95 |
| Plate 3. Atago N1 hand refractometer for monitoring the concentration of polymer quenchant solutions. | 149 |
| Plate 4. Revised Wolfson Engineering Group quench test rig for evaluating the cooling characteristics of polymer quenchants. | 155 |
| Plate 5. Flow visualization for a 15 per cent Quendila PA (PAG) solution at the standardized test conditions. | 218 |
| Plate 6. Change in appearance of a nominally 15 volume per cent solution of the representative PAG (Quendila PA) with increased throughput in the accelerated ageing test. (a) Fresh, (b) 10kg/litre, (c) 50kg/litre and (d) 100kg/litre. | 261 |
| Plate 7. Change in appearance of a nominally 15 volume per cent solution of the representative PVP (Parquench 90 with increased throughput in the accelerated ageing test. (a) Fresh, (b) 10kg/litre, (c) 50kg/litre and (d) 100kg/litre. | 261 |
| Plate 8. Change in appearance of a nominally 15 volume per cent solution of the representative Polyacrylate (Aquaquench ACR) with increased throughput in the accelerated ageing test. (a) Fresh, (b) 10kg/litre, (c) 50kg/litre and (d) 100kg/litre. | 262 |
| Plate 9. Change in appearance of 15 volume per cent solutions of each representative polymer quenchant 14 days after the addition of 1 weight per cent of oxidized mild steel filings. (a) PAG (Quendila PA), (b) PVP (Parquench 90) and (c) Polyacrylate (Aquaquench ACR). | 262 |

CHAPTER 1

1.0 RATIONALE

The quenching of heat treatable metal is the rapid cooling of that metal from some suitable elevated temperature in order to achieve desired metallurgical properties. Traditionally the principal quenchants were water, possibly modified by the addition of inorganic salts; and oils, either naturally occurring or refined. However, during the past thirty years a number of water soluble organic polymers have become commercially available for the quenching of both ferrous and non-ferrous metals. In order of historical use, these are polyvinyl alcohol, polyalkylene glycols, polyvinylpyrrolidone and sodium polyacrylate. The manufacturers of these polymer quenchants are understandably very secretive about the formulation of their products, in fact it is only in recent years that they have been prepared to disclose even the generic nature of the polymer employed.

Polymer quenchants offer the heat treater a number of environmental, economic and technical advantages, the principal advantage undoubtedly being the elimination of the quench-oil fire hazard. Despite this, heat treaters are still reluctant to change over from the traditional quenching media. This reluctance is mainly associated with early operational difficulties encountered with polymer quenchants caused by insufficient understanding regarding their behaviour. Nevertheless, improved products and greater experience have led to a slow yet progressive increase in the demand for polymer quenchants in the last decade, with a corresponding increase in the number of suppliers. Polymer quenchants are today frequently used for the tank quenching of ferrous components, induction and flame hardening operations and the solution treatment of precipitation-hardenable aluminium alloys.

The cooling mechanism for polymer quenchants has received very little attention and is unclear. Polyalkylene glycols are by far the most popular form of polymer quenchant in use today. This class of polymer exhibits inverse solubility, which means that it becomes insoluble at a critical temperature below the boiling point of the

solution. This reversible phenomenon is not well understood, and because of the prevalence of polyalkylene glycols, it is often mistakenly used to describe the cooling behaviour of all classes of polymer quenchant.

Most of the papers published on the cooling characteristics of polymer quenchants have been written by authors with a vested interest in one particular type of polymer, with cooling data provided using a range of different thermocouple techniques, test conditions and methods of indicating polymer concentration. Consequently, direct comparison of the results is practically impossible. However, what is clear from this earlier work is that close control of polymer quenchant solutions is essential for their successful application. No attempt has ever been made to explain the characteristics of polymer quenchants in terms of their molecular structure. Therefore, the aim of this research was to establish a better understanding of the behaviour and quench effectiveness of existing commercial polymer quenchants, from consideration of their properties on a molecular level.

In order to allow tentative comparisons to be made, this research has involved testing three of the most popular polymer quenchant types in industrial use today under identical conditions. The cooling characteristics of the polymer solutions were measured using the Wolfson Heat Treatment Centre Engineering Group method which has recently been accepted as an international standard for static quench oils. Since agitation of polymer quenchants is believed to be essential for their successful application, a controllable means for providing agitation was required when evaluating their cooling characteristics. Consequently, the first objective of this work was to devise a suitable method for agitating the polymer quenchant test samples.

To obtain a greater understanding of the behaviour of polymer quenchants a number of parameters, known to influence their behaviour, were studied. These parameters included the polymer solution concentration, temperature and agitation as well as the influence of long term usage, contamination and drag-out. Hardening response and residual stress data have also been determined for 12.5mm diameter 0.45 per cent carbon steel bars quenched into each polymer solution type.

The overall objective of this research was to establish a better understanding of the behaviour and quench effectiveness of existing commercial polymer quenchants. A better understanding of their behaviour and the heat transfer mechanisms involved will increase the scope for their application. As polymer quenchants have both technical and economic advantages over the conventional products and are inherently fire resistant, their wider use is of considerable industrial and social benefit.

CHAPTER 2

2.0 LITERATURE SURVEY

2.1 Definition of Quenching

In metallurgy the term "quenching" simply refers to the rapid cooling of a material from some elevated temperature⁽¹⁾. The basic principle behind all quenching operations is that by rapidly cooling certain materials, a metastable form of their high temperature state is preserved at room temperature. The quench may involve a polymorphic change, but this depends on the material being quenched. Steels, for example, are hardened by quenching from their austenitic condition to produce martensite, whilst certain aluminium alloys are quenched to form a supersaturated solution before being age-hardened. Both processes dramatically improve the properties of the alloys compared with their equilibrium condition.

The quench hardening of steel is probably the oldest and most widely used heat treatment process. Consequently, most of the available literature on quenching is associated with steel, and this is the area which will be covered in most detail during this review.

2.2 Requirements of a Quenching Medium

The main requirement of a quenching medium is that it should cool the component at the correct rate, throughout its section, to provide the optimum structure and properties consistent with its anticipated service performance; or provide the correct starting conditions for subsequent treatments. For example, a steel may be air cooled to provide the correct starting conditions for machining, whilst oil or water quenching, followed by tempering, may be required for other applications. The cooling rate achieved in the body of the component is dependent on the rate of heat extraction through its surface, the section size, and the temperature gradient set up within the part. The rate of heat extraction is principally associated with the type of quenchant chosen. Cook has listed some of the requirements for an "ideal quenchant".⁽²⁾ The ideal quenchant should:-

- (a) Cool the component sufficiently rapidly, to the transformation temperature required, to prevent the formation of higher temperature transformation products.
- (b) Maintain the temperature of the component in the transformation range to provide sufficient time for the reaction to be completed, with the smallest possible temperature gradient.
- (c) Cool slowly during transformation and when transformation is complete.
- (d) Minimize oxidation on the surface of "bright" components.
- (e) Maintain a consistent quenching efficiency with time.
- (f) Have low adherence to reduce drag-out.

Unfortunately, it is not possible to have an ideal quenchant, nor is it possible to quench a component in an ideal manner, that is with the entire section cooling at the same rate. The cooling rate at the centre of a component is dependent on the physical properties of the material as well as the heat extraction rate of the quenchant. Even if the surface of the component was instantaneously cooled to the temperature of the quenchant, subsurface positions would cool at a slower rate. Therefore, the cooling rate at the critical position within the component is the important factor, and a quenchant should be chosen to provide the correct temperature gradient to ensure that the required structure is produced at this critical depth. In some cases it may be necessary to have a steep temperature gradient in order to obtain the required structure at the centre. However, increasing the cooling rate of a quench, in addition to raising the temperature gradient, produces secondary effects which may be very important. Residual stress can be higher, and the tendency for both distortion and cracking increases. These factors must obviously be taken into account when choosing a quenchant. Ideally, a quenchant should be chosen which will produce the required structure at the slowest possible cooling rate.

2.3 Methods of Quenching

A quenchant's rate of heat extraction is greatly modified by the manner, or condition, in which it is used. These modifications have resulted in the assignment of specific names to various quenching methods, which will now be discussed⁽³⁾ :-

2.3.1 Direct-Quenching is the most widely used method and, as its name implies, the components are plunged directly into the appropriate quenchant. For example, when carburized work is quenched from the carburizing temperature, or from a slightly lower temperature, the term "direct-quenching" is used to distinguish this method from the more indirect practice of carburizing, slow cooling, reheating and quenching. Direct-quenching is simple and economical, and distortion of carburized parts is less likely than with reheating and quenching.

2.3.2 Time Quenching is applied when the cooling rate of the component being quenched has to be changed abruptly at some time during the cooling cycle. The change in cooling rate may be either an increase or a decrease. The usual practice is to quench in one medium (for instance, water) for a short time to avoid the formation of higher temperature transformation products, and then to quench the component in a second medium (for instance, oil), so that it cools more slowly through the martensitic transformation range. Still air is often used as the second medium in many applications. Great care is required when using this method, since precise control of the time of immersion in the first quenching medium is necessary. Time-quenching is mainly used for minimizing distortion, cracking and dimensional changes.

2.3.3 Interrupted-Quenching is essentially a form of time-quenching in which the first quenching medium is a molten bath, usually fused salt, maintained at a constant temperature. This method is used in the austempering and martempering processes for ferrous alloys. When austempered the component is quenched from the austenitizing temperature at a rate fast enough to avoid the formation of ferrite or pearlite and then held at a temperature just above its martensite start temperature (M_s), until transformation to bainite is complete.

In martempering the austenitized component is quenched in an appropriate medium whose temperature is maintained substantially at the M_s of the part. It is then held in the medium until its temperature is uniform throughout, but not long enough to permit bainite to form, and then cooled in air. The treatment is frequently followed by

tempering. When the process is applied to carburized material, the controlling M_s temperature is that of the case. This variation of the process is frequently called marquenching.⁽¹⁾

2.3.4 Spray-Quenching In this technique, streams of quenching liquid are directed at specific areas of the component at high pressure, up to 825kPa (120 psi). The cooling rate is fast and uniform over the entire quench temperature range because of the large volume of coolant used, and because all the coolant makes direct contact with the component. The velocity of the stream displaces any vapour bubbles and provides spray droplets, which are available for heat transfer. With certain polymer quenchants low pressure spraying is preferred, which produces a flood-type flow⁽⁴⁾.

2.3.5 Fog-Quenching. This method employs a fine fog or mist of liquid droplets and a carrier gas as cooling agents. Although similar to spray-quenching it is less effective, because the hot mist or fog in contact with the component being quenched is not easily replaced by cooler mist or fog.

2.4 Mechanism of Quenching

The mechanism of quenching is dependent upon a number of factors: (a) internal characteristics of the component that affect the supply of heat to the surface; (b) surface and other external characteristics that influence the removal of heat; (c) the heat-extracting potential of the static quenchant at normal fluid temperatures and pressures; and (d) variations in the heat-extracting potential of the quenchant as a result of agitation or changes in temperature or pressure. The combined effect of these factors makes the quenching mechanism highly complex for real components. This is demonstrated in *Figure 1* for a furnace heated gear that is quenched edgewise into a static liquid.⁽³⁾

The irregular configuration of the gear affects the flow of heat from within the gear to the quenching area as shown in part A of *Figure 1*. High temperatures persist near the surface at the roots of the teeth where large vapour bubbles are trapped. If the gear were induction or flame heated, a uniform thin heated layer conforming to the

complex contour of the gear would be produced. In this case the heat supply to the quenching area would be more consistent, and quenching would progress more rapidly because heat would simultaneously flow to the underlying cold metal.

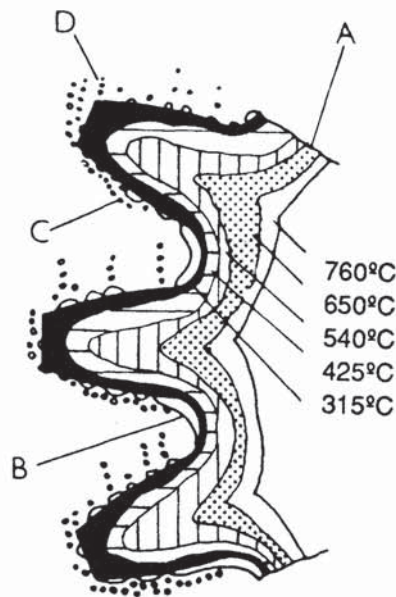


Figure 1. Temperature gradients and other major factors affecting the quenching of a gear^(3,4). See text.

The liquid experiences unavoidable movement as a result of the act of immersion, the turbulence of boiling, and convection currents. This minimum agitation will eventually dissipate the accumulated heat to the surrounding large body of fluid. However, local volumes of liquid may be heated sufficiently for vaporization to occur. Volatile quenching liquids produce vapour at all operating temperatures. Above the boiling point, so much vapour is produced that an envelope of gas is formed around the surface of the component. This envelope, or "vapour blanket", is maintained principally by radiated heat for as long as the heat is available (part B in *Figure 1*). The temperature above which a total vapour blanket is maintained is called the "characteristic temperature" of the liquid.

At lower temperatures, the vapour continues to exist in the form of bubbles, which vary in size depending on the relative interfacial tensions for the liquid, gas and solid, at the temperatures concerned. For example, in one liquid a few large adherent bubbles may be formed (part C in *Figure 1*), whilst numerous small easily detached

bubbles may be formed in another (part D in *Figure 1*): this is referred to as the "bubble size characteristic" of the liquid. The mechanical trapping of vapour bubbles (such as part C) will severely retard the transfer of heat at the affected location.

Other factors which may affect the heat-extracting potential of a quenchant are: (a) solids that are deposited on the surface of components when they are quenched in some oils, brines or water-glass solutions; (b) gels that may form at the liquid-gas interface of the vapour blanket in polymer or other gelling solutions; (c) deposits that form or changes that occur in the liquid which affect its viscosity; and (d) permanent loss of volatile constituents with low boiling points.

2.4.1 Stages of Quenching. The most useful way of accurately describing the complex mechanism of quenching is to produce a time-temperature plot or "cooling curve" for the quenching liquid under controlled conditions. This involves quenching either the real component, or a test piece, containing an embedded thermocouple. The cooling curve produced relates to the size, shape and material of the quenched piece, its preheat temperature, thermocouple location, and the conditions of the quench fluid during the test. Nevertheless, the cooling curve is sensitive to the factors that may affect the cooling ability of the quenchant, because the test simulates conditions of actual practice. Practical methods and equipment for obtaining cooling curves will be discussed in detail later.

Figure 2a shows a typical cooling curve for a liquid quenching medium showing schematically what happens at the surface of the quenched part.⁽⁵⁾ It is clear that quenching occurs in three distinct stages, each of which has very different characteristics. This now classic theory was originally postulated by Pilling and Lynch,⁽⁶⁾ and later confirmed by Scott.⁽⁷⁾

The three cooling stages can also be represented as a differential graph of cooling rate against temperature (*Figure 2b*). The rate of cooling on a time-temperature curve is given by its slope. Some authors prefer to present the cooling rate as the ordinate, but

this is strictly speaking incorrect, since the cooling rate causes a change in temperature.

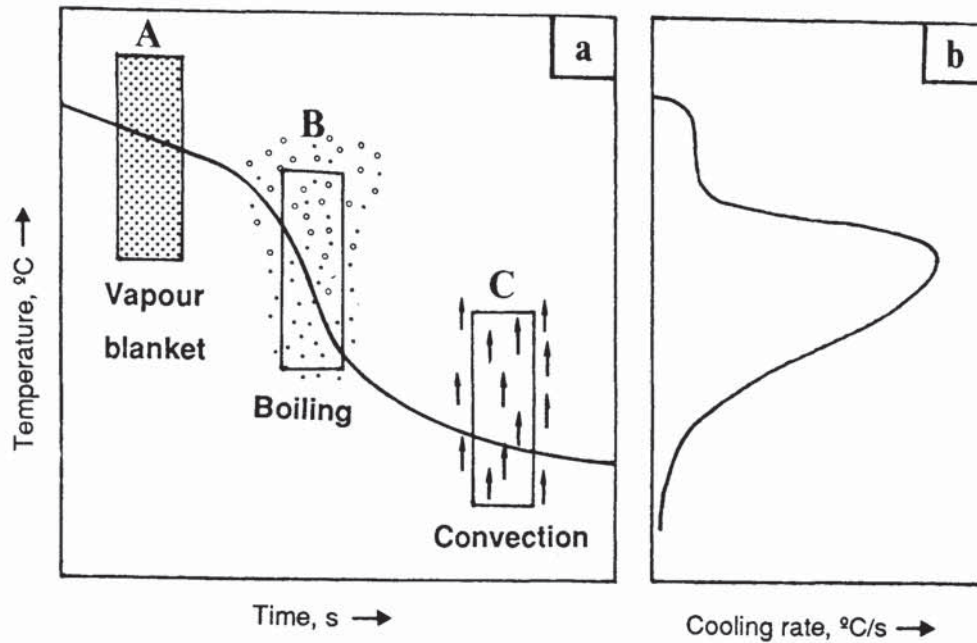


Figure 2. The three stages of cooling during quenching shown on (a) the conventional time-temperature cooling curve, and (b) the corresponding cooling rate-temperature plot⁽⁵⁾.

The three stages of heat extraction will now be described in detail:-

Stage A: Vapour blanket or film boiling stage.

In this first stage, the temperature of the metal is so high that after the initial liquid contact time (approximately 0.1s), the quenching medium is vaporized at the metal's surface and a thin stable film of vapour is produced around the hot metal. This occurs when the supply of heat from the surface of the hot metal exceeds the amount of heat needed to form the maximum vapour per unit area of the metal, and is known as the "Leidenfrost phenomenon".⁽³⁾ Cooling is by radiation and conduction through the gaseous film, and since vapour films are poor heat conductors, the cooling rate is relatively slow during this stage.

Stage B: Vapour transport or nucleate boiling stage.

This, the fastest stage, starts when the metal has cooled to the characteristic temperature at which the vapour film is no longer stable. As the vapour blanket collapses, cool quenchant wets the metal surface, and violent boiling occurs. Heat is removed from the metal very rapidly, predominantly as the latent heat of vaporization. The size and shape of the vapour bubbles are important in controlling the duration of this stage, as well as the cooling rate developed within it.

Stage C: Liquid cooling or convection stage.

This stage starts when the surface temperature of the metal reaches the boiling point (or boiling range) of the quenching liquid. Below this point, boiling stops and slow cooling takes place by conduction and convection through the liquid. The difference in temperature between the boiling point of the liquid and the bath temperature is a major factor influencing the rate of heat transfer. The viscosity of the quenchant also affects the cooling rate in stage C.

2.5 Quench Process Variables

2.5.1 Agitation. Enhanced movement of the quenching medium has a significant effect on its heat transfer characteristics. Agitation causes an earlier mechanical disruption of the vapour blanket (stage A), and smaller more frequently detached vapour bubbles during nucleate boiling (stage B). It also mechanically disrupts or dislodges gels and solids, either on the surface of the component, or suspended at the edge of the vapour blanket, thus producing faster liquid cooling (stage C). In addition, agitation replaces the hot fluid adjacent to the quenched metal with cool, therefore providing the first step in the disposal of the accumulated heat.

2.5.2 Temperature of Quenchant. The temperature of the fluid may markedly affect its ability to extract heat. Higher fluid temperatures tend to lower the characteristic temperature and thus lengthen the duration of stage A. The viscosity of the quenchant is likely to be lowered, which may influence its cooling characteristics. Other factors being equal, high fluid temperatures generally decrease the rate of heat transfer during stage C.

2.5.3 Workpiece Temperature. Raising the temperature of the workpiece has relatively little effect on its ability to transfer heat to the quenchant. The rate of heat extraction may be increased, simply because of the larger temperature differential. However, the more rapid oxidation of the workpiece at higher temperatures can have a significant effect on its ability to transfer heat. Beck et al⁽⁸⁾ and Segerberg⁽⁹⁾ both concluded that the stage A, vapour blanket phase, would disappear partly or completely when quenching oxidized surfaces. The oxide layer was also found to be thermally insulating and likely to reduce the cooling rate. Price and Fletcher,⁽¹⁰⁾ on the other hand, demonstrated that an oxidized surface increased the stability of stage A cooling. This discrepancy is most probably attributable to differences in the thickness of the oxide layers involved; the layers developed during the work of Price and Fletcher were considerably thinner than those for the other workers.

2.6 Test Methods for Evaluating Quenching Media

The testing of industrial quenching media encompasses a wide range of techniques, because of the need to supplement conventional quality control procedures for physical and chemical parameters, with those of cooling characteristic assessment. Most quality control techniques, such as for the measurement of pH, colour and viscosity, have well established internationally standardized test procedures.⁽¹¹⁾ However, it was not until June 1985, that a test method was adopted as an international standard for assessing the cooling characteristics of certain quenchants.⁽¹²⁾ The "Scientific and Technological Aspects of Quenching" Technical Committee of the International Federation for the Heat Treatment of Materials (IFHT), agreed to base its recommended standard for testing quenching oils, on the now widely used method, developed by the "Testing of Quenching Media" working party of the Wolfson Heat Treatment Centre Engineering Group. In addition, the American Society for Metals (ASM) "Quenching and Cooling Committee" is evaluating the Wolfson Engineering Group quench test method as part of its "round-robin" exercise to establish a standard.

Nevertheless, today a wide range of different quenchant cooling power tests are still

being used throughout the world, often on a geographical basis. For example, the nickel-ball test is still popular in the USA, and the silver ball/cylinder in France and Germany.⁽¹¹⁾ Direct comparison of the results obtained using these different tests is impossible. Rather than describing a large number of individual tests, it is more convenient to classify them according to their various operating principles:^(13,14)

- (a) thermocouple techniques
- (b) magnetic methods
- (c) hot -wire tests
- (d) calorimetric methods
- (e) hardening response.

2.6.1 Thermocouple Techniques. These are probably the most useful way of accurately determining the cooling characteristics of a quenchant. A high-speed recorder or computer is used for recording temperature changes for one or more thermocouples embedded in a quenched test piece. The resulting cooling curve depicts the stages of heat transfer that occur, and cooling rates may be established throughout the complete quenching process. However, the cooling curve produced reflects not only the cooling characteristics of the quenchant, but also the characteristics of the test piece employed. For example, the test piece material, geometry, surface finish and thermocouple position all influence the results. The preheat temperature and volume ratio of metal to quenchant are also critical. Therefore, each of these factors must be precisely defined in order to produce a reproducible test method.

The transfer of heat from the metal to the quenchant takes place at the surface of the solid body. Consequently, surface cooling data would be required for absolute characterization of the quenchant. Unfortunately, the direct measurement of surface cooling curves poses acute experimental difficulties, as was described by French,⁽¹⁵⁾ and only approximate determinations can be made. Centrally-located thermocouple measurements average out surface effects, and increase the time factor, so that characteristic points on the cooling curve appear at higher temperatures than if they were recorded at the surface of the test piece.⁽³⁾

Test pieces are being fabricated from silver, stainless steel, nickel, or from selected carbon and alloy steels related to specific studies.⁽¹⁶⁾ When hardenable steel test pieces are used, the cooling curves show not only the stages of cooling for the quenchant, but also the heats of transformation for the steel. Non-ferrous test pieces could also be used to simulate particular quenching applications. The two most popular forms of thermocouple techniques in use today are those employing silver test pieces, and those using stainless steels or nickel alloys, such as the IFHT preferred Wolfson Engineering group test. These tests will now be examined in detail:

2.6.1.1 Silver test piece methods. The advantages claimed for using silver test pieces are that they are easy to machine, free from transformation effects and resistant to corrosion.⁽³⁾ In addition, the thermal conductivity of silver (419W/mK at 293K) is nearly seven times greater than that for steel (typical mild steel, 63W/mK).⁽¹⁷⁾ Consequently, the temperature gradient induced in a quenched silver test piece would be less steep than for an equivalent steel specimen; and a centrally-measured cooling curve would more accurately reflect surface temperature changes.

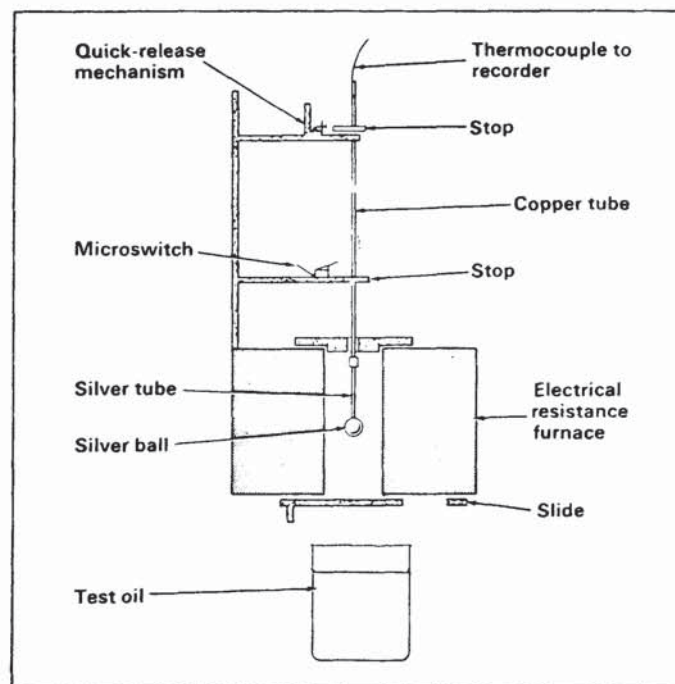


Figure 3. Diagram of silver ball test apparatus⁽¹⁴⁾.

The first popular silver test piece method incorporated a ball 20mm in diameter with a thermocouple located at its centre. The silver ball was heated and equalized at 800°C prior to quenching into a fixed volume (usually 600ml) of quenchant (*Figure 3*). The thermocouple was connected to a high-speed recorder, the latter being automatically started by the microswitch illustrated. The test is a very sensitive method of detecting differences between quenchants, as the cooling curves obtained by Rogen and Sidan⁽¹⁸⁾ illustrated (*Figure 4a*). The corresponding cooling rate- temperature curves can be seen in *Figure 4b*. However, this test has a number of practical limitations which were outlined in a critique of quench test methods by Lakin:⁽¹⁴⁾

- (a) Since the thermocouple hot junction has to be located exactly at the geometric centre of the ball, it is difficult to manufacture the test assemblies without introducing some probe to probe response differences.
- (b) The high thermal conductivity of silver compared with steel means that the results obtained do not correspond to practical quenching conditions.
- (c) It is important to maintain a consistent surface finish, by polishing with emery paper between runs. Due to silver's extreme softness, this rapidly affects the geometry of the probe.

Several other problems could be added to this list, namely:

- (d) The expense of silver, combined with the relatively short life of the probe, makes the test costly to perform.
- (e) Silver is susceptible to contamination by certain constituents of quench oils, such as sulphur.
- (f) The screw thread joining the probe to the thermocouple support tube is prone to quenchant ingress.

The silver ball has today been largely superseded by cylindrical probes. Provided the cylinder's length is at least three times its diameter, it can be considered to be infinitely long, and heat loss from its ends can be ignored.⁽¹⁹⁾

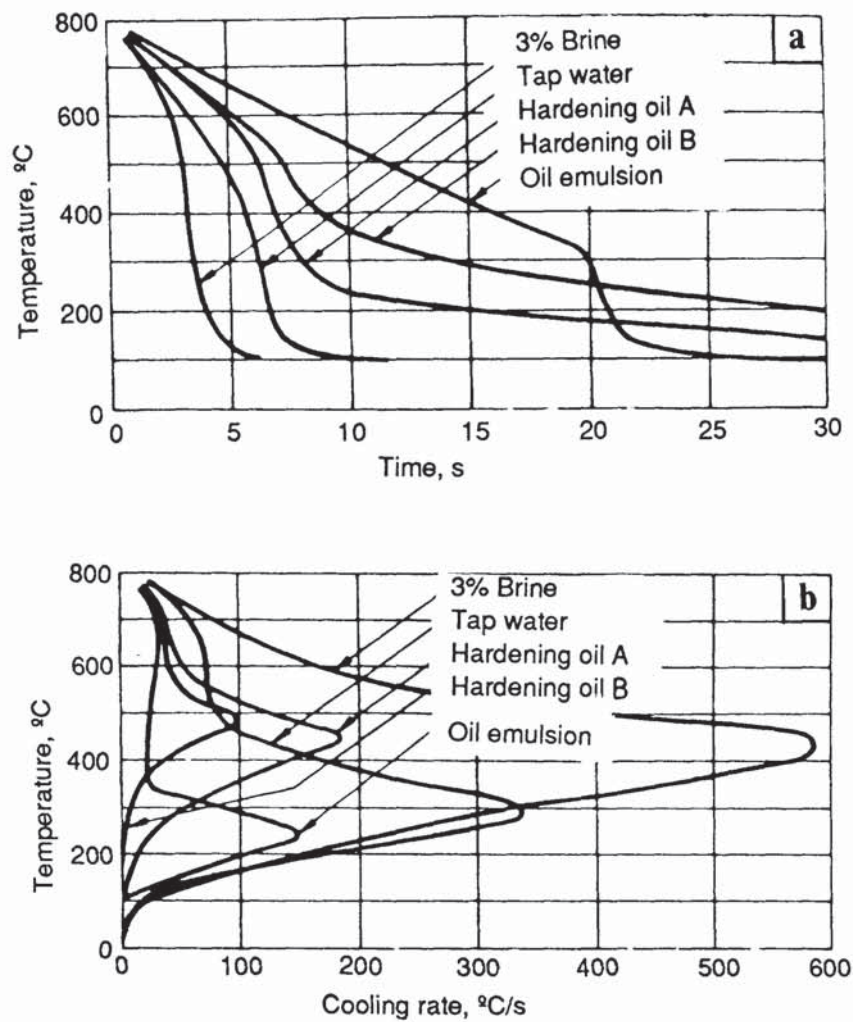
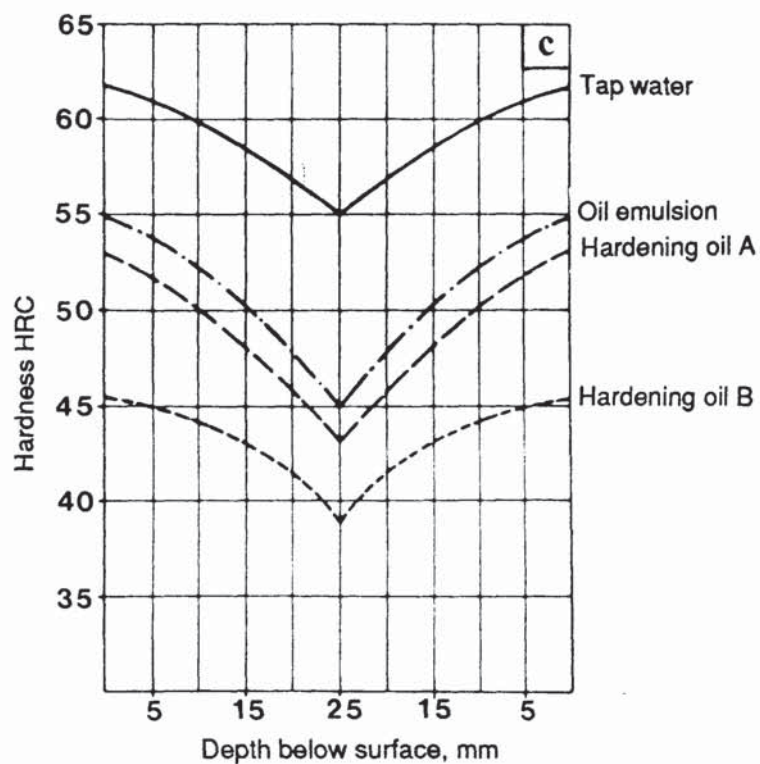


Figure 4.(a) Cooling curves for various quenching media measured at 40 °C using the silver ball test; (b) corresponding cooling rate-temperature plots, and (c) hardness profiles across test bars, 50mm in diameter of steel 50MN7 (0.5%C, 1.8%Mn, <0.4%Si), after hardening in various media⁽¹⁸⁾.



In France, CETIM (Centre Technique des Industries Mecaniques) have developed the "drasticimeter" or "diacpot" test using a silver cylinder, 16mm diameter and 48mm long, with a thermocouple at its centre. Both time-temperature curves and cooling rate-temperature curves are recorded. This method is IFHT's second choice for a standard oil test. Initially, a cylinder 8mm diameter and 24mm long was used, but this was found to produce inconsistent results for aqueous quenchants.⁽²⁰⁾ The diacpot method suffers from the same problems listed previously for the silver ball test, except for problem (a) which is not applicable for cylinders.

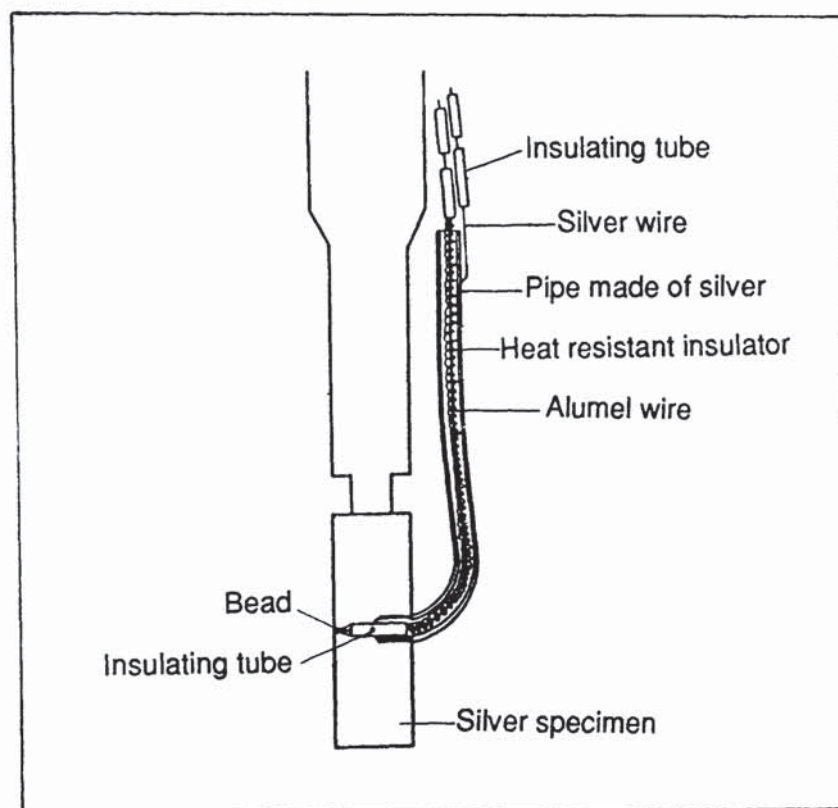


Figure 5. Silver specimen for measuring cooling curves in the Japanese Standards Association (JIS.K2242.1980) test⁽²¹⁾.

The Japanese Standards Association (JIS) have also developed a quench test, using a 10mm diameter by 30mm long silver cylinder, with a near surface mounted thermocouple⁽²¹⁾ (Figure 5). The probe itself actually constitutes one element of the silver-alumel thermocouple used. A 0.6mm alumel wire is attached at the hot junction which is touched with a silver

nitrate crystal. The volume of quench sample used during this test is only 250ml. Time-temperature, and occasionally time-cooling rate curves, are recorded. This novel approach also suffers from the problems (b), (c), (d) and (e) already listed for the silver ball test. In addition, the attachment of the alumel wire at the hot junction is critical,⁽²²⁾ and, because of the complexity of fabrication, inter-probe consistency could prove a problem. The method is also open to the objection that the spot over which the temperature is measured is not backed up by metal, as is the surface of a specimen without a hole. Furthermore, a very high-speed recorder is required, capable of registering rates of temperature change of at least 540°C in 0.1s.⁽³⁾

Thelning⁽²²⁾ has reviewed the problem of trying to correlate cooling data from silver test pieces with practical steel quenching situations. The problem is exacerbated by silver's much higher thermal conductivity than steel, and its lack of phase transformations which influence the rate of cooling. Rogan and Sidan⁽¹⁸⁾ highlighted the problem using the silver ball test. It is clear from examination of *Figures 4a* and *4b* that the brine (3 per cent sodium chloride solution) produced the highest cooling rate, and hardening oil B the slowest. However, when a series of 50mm diameter bars manufactured from a steel equivalent to 50MN7 (nominal composition 0.5% C, 1.8% Mn, <0.4% Si) were hardened in each quenchant excluding the brine, the hardness profiles shown in *Figure 4c* were produced. The results are as would be predicted from *Figures 4a* and *4b*, except for the emulsified oil. The emulsion had the slowest cooling curve down to 300°C and yet produced a higher hardening response than the oils.

Beck et al⁽⁸⁾ have also demonstrated these problems by comparing the cooling curves for two mineral oils using 16mm diameter by 48mm long cylinders manufactured from both silver and steel:

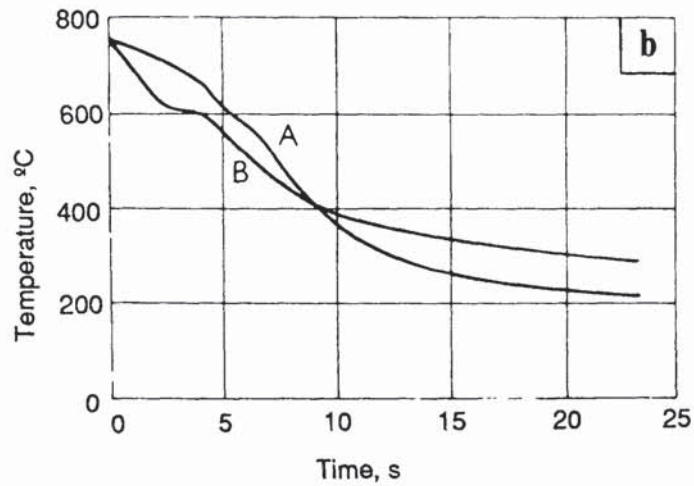
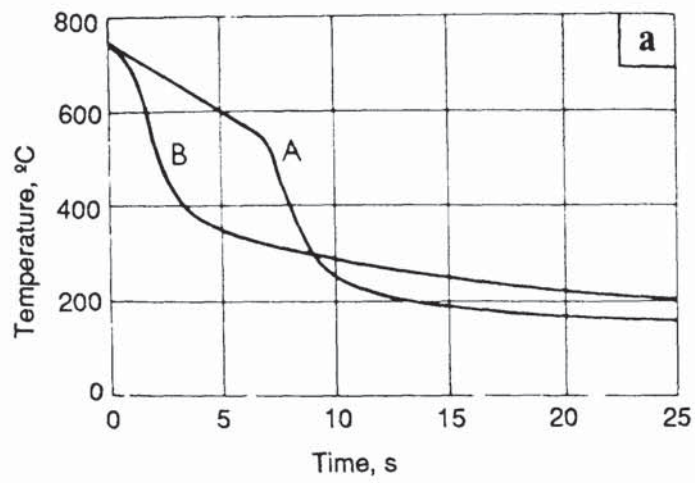
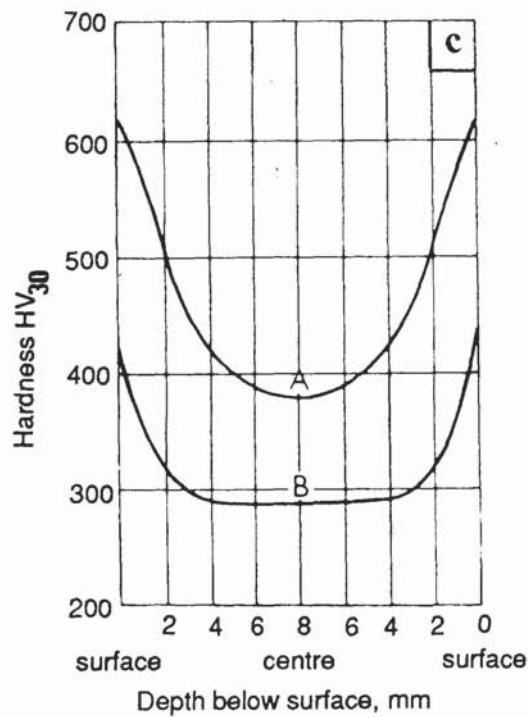


Figure 6. Cooling curves for the centre of bars 16mm diameter and 48mm long on being cooled in mineral oils A and B: (a) silver, (b) steel XC 48 (0.48%C, 0.65%Mn, 0.25%Si) and (c) hardness profiles across the steel bars after being quenched in each oil⁽⁸⁾.



The silver test piece was equivalent to the one used in the diapot test. The steel used was grade XC48 (nominal composition 0.48% C, 0.65% Mn, 0.25% Si). The cooling curves from this test are shown in *Figures 6a* and *6b*. The silver cylinder curves show that the nucleate boiling stage occurred considerably later in hardening oil A than oil B. As regards the steel cylinders, the progress of the cooling was basically the same as that for the silver cylinders, except at 600°C, where there was a break in the cooling of about 2s in oil B. The practical result of these oil quenches on the hardness profiles for the steel cylinders is shown in *Figure 6c*. It can be seen that oil A yielded a higher hardness than oil B; however, the authors had expected the reverse from consideration of the cooling curve data.

2.6.1.2 Wolfson Engineering Group quench test. In 1982, following extensive trials to ensure accuracy and reproducibility, the Wolfson Heat Treatment Centre Engineering Group issued the specification "Laboratory Test for Assessing the Cooling Characteristics of Industrial Quenching Media".^(24,25) As described previously, IFHT have adopted this specification for testing non-agitated quench oil samples in its entirety, adding a clause permitting the optional use of a computer-based system for measurement and recording of results.⁽¹²⁾ During round-robin trials IFHT found the Wolfson Engineering Group method more reproducible than the diapot test, which they selected as their second choice. IFHT have now submitted the specification to the International Organization for Standardization (ISO) in Geneva. In addition, the specification has been proposed as a British Standard by the Wolfson Engineering Group.

The test uses a cylindrical probe, 12.5mm in diameter and 60mm long, manufactured from Inconel¹ 600, a heat resisting nickel-chromium-iron alloy. The probe has a chromel-alumel thermocouple at its geometric centre, and is TIG-welded onto a support tube (*Figure 7*).

¹Trademark of the Inco group of companies



Figure 7. Wolfson Engineering Group thermal probe: (a) probe details and (b) general assembly⁽²⁴⁾.

The support tube which is the same diameter as the probe, and of specified minimum length, prevents quenchant ingress problems. The probe is heated to the specified temperature 850°C and then transferred into a fixed volume (2 litres) of the quenchant under test⁽²⁶⁾ (*Figure 8*). A tenacious surface oxide is maintained on the probe to ensure reproducible characteristics and thus avoiding the problem, associated with the silver test pieces, of having to recondition the surface with emery paper after each test. The specification also describes a paraffinic mineral oil-based reference quenching fluid, with defined physical characteristics and known cooling response, which is used for regular cross-checking of probes. The thermal conductivity of Inconel 600 is much closer to that of steel than silver, thus making the results more applicable to practical quenching situations. However, the lower thermal conductivity makes interpretation of the points of inflexion on the cooling curves more difficult and, like silver, no account is made of the possible phase transformations which occur in steel. Correlation between Wolfson Engineering Group test data and practical quenching situations will be described in more detail later.

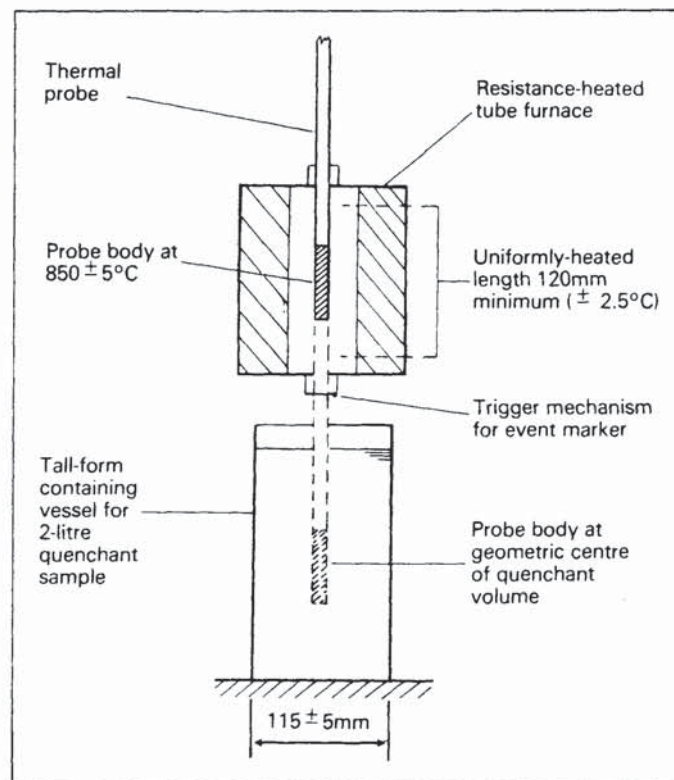


Figure 8. Schematic of the Wolfson Engineering Group quench test rig⁽²⁶⁾.

The specification, as published, relates principally to oil samples, but with modification is applicable to other quenching media. Lakin,⁽¹¹⁾ for example, has outlined three areas in which the basic test may need to be modified for the evaluation of polymer quenchants:

(1) Quenchant sample agitation. The specification advises a static quench sample for oil tests. Nevertheless, it is generally believed that agitation is essential for the effective use of polymer quenchants in order to prevent thermal stratification and inconsistent quench performance. Lakin therefore suggested the use of a propeller/baffle type agitation system to direct the flow of the quenchant towards the probe. He recommended a two-bladed, 40mm diameter high pitch model boat propeller, rotating at 1900rpm, in a 3 litre squat form beaker. The probe was required to be accurately positioned in the middle of a chord equidistant between the beaker edge and the central H-shaped baffle, and at the centre of the 2.6 litre test volume in the vertical plane.

Propeller agitation systems have been used by many workers in recent years.^(11,26,27,28,29,30,31) Unfortunately, most of these workers gave no precise details regarding the propeller agitation system used, preferring to describe the level of agitation in only general terms such as "moderate" or "vigorous". Correlation between these different systems is therefore virtually impossible, due to the variations in propeller size and tank/baffle geometry.

Pump agitation systems offer the advantage that the quenchant fluid velocity past the test piece can be relatively easily assessed. One such system designed by Liscic,⁽³²⁾ for testing bars of various diameter, is shown in *Figure 9*. The major drawback with this system is that it requires a very large sample volume (over 100 litres), therefore making it totally impracticable as a routine laboratory scale test. Several workers^(16,33,34) have developed similar systems, but each suffered from the same basic problem of excessive quenchant sample volume. A small sample volume is

essential for process control, or for field trials where the sample is frequently required to be transported by post.



Figure 9. Liscic's equipment for evaluating quenching media with centrifugal pump agitation⁽³²⁾.

The Wolfson Engineering Group working party "Testing of Quenching Media", realizing the need for agitation in a realistic test for aqueous quenchants, set up a specific committee to examine different agitation systems in 1983. A wide range of techniques, including propeller/baffle, pump, turntable and magnetic stirrer tests, have been examined.⁽³⁵⁾ Generally, it has been found that impeller/baffle systems have little effect on the cooling characteristics, and that vortex problems can arise using magnetic stirrers. Turntable tests have been found to accelerate the cooling

characteristics drastically. The quenchant velocity past the probe may be changed by adjusting either the speed of the turntable or the probe's position with respect to the axis of rotation. By adjusting both these parameters, it was possible to conduct tests with equal fluid velocities but with different probe positions. The results from these tests showed inconsistent cooling characteristics, suggesting that not only the fluid velocity is critical but also the nature of the flow pattern. A pump system appears to offer the most effective means of providing agitation. The level of agitation is readily quantified in terms of fluid velocity, which may be related to practical situations, and the flow pattern is fairly easy to control.

The "Agitation of Quenching Media" committee has therefore begun a series of round-robin trials to assess the accuracy and reproducibility of pump systems. The present author has proposed a variable speed centrifugal pump system, with a capacity of 2 litres, which forms the basis of the systems presently being investigated.⁽³⁵⁾ Preliminary trials have highlighted that, not only the fluid velocity, but also the flow pattern is critical. Consequently, the geometry of the quench tank and its associated pipework must be specified precisely.⁽³⁶⁾ This centrifugal pump system was submitted to IFHT's Technical Committee on "Scientific and Technological Aspects of Quenching", at its June 1985 meeting in Berlin.⁽¹²⁾ This international committee is also trying to establish a standard agitated test method for evaluating polymer quenchants.

(2) Quenchant temperature. The second modification to the basic Wolfson Engineering Group test which Lakin⁽¹¹⁾ thought necessary, for evaluating polymer quenchants, was sample temperature control. He believes that the sample test temperature is more critical with polymer quenchants than with oils, and that control to within $\pm 1^\circ\text{C}$ is necessary.

(3) Recording instrumentation. The Wolfson Engineering group test, like the diaplot method records both time-temperature and cooling rate-

temperature curves. The original specification described a way of producing simultaneous real time records of both curves using a battery powered electronic differentiator, combined with Y-t and X-Y recorders of specified characteristics. Some polymer quenchant solutions have cooling characteristics faster than cold water and thus require recorders of high writing speed; because of this, and in order to facilitate data handling, many test centres have converted to computer based systems. In fact, the IFHT form of the specification which has been submitted to ISO for evaluating quench oils, has an additional section permitting the optional use of a suitable computer technique.

2.6.2 Magnetic Methods. These tests make use of the phenomenon known as the Curie point (i.e. the temperature at which the magnetic properties of certain materials change). Although no longer popular, the most extensively used magnetic method was the General Motors or GKN nickel ball test illustrated in *Figure 10*.⁽¹³⁾ This technique measures the time taken by a standard amount of quenchant (normally, 200ml) to cool a nickel ball (usually 22 or 25mm diameter) from between 800 and 850°C to its Curie point. The Curie point temperature for nickel is 354°C, below the nose of the isothermal transformation diagrams for most steels. The nickel balls are heated in a controlled atmosphere before being released individually. A timer is activated as the ball falls past a microswitch. The ball settles in a tray and continues to cool. When the Curie point temperature (354°C) is reached, the timer is stopped automatically by a second microswitch activated by the attraction between the nickel and the electromagnet.

An obvious problem with this test is that only comparative data is produced, lacking the detail provided by the thermocouple techniques. This is exemplified in *Figure 11*, which shows the cooling curves for a new and used sample of the same oil tested under identical conditions.⁽¹⁴⁾

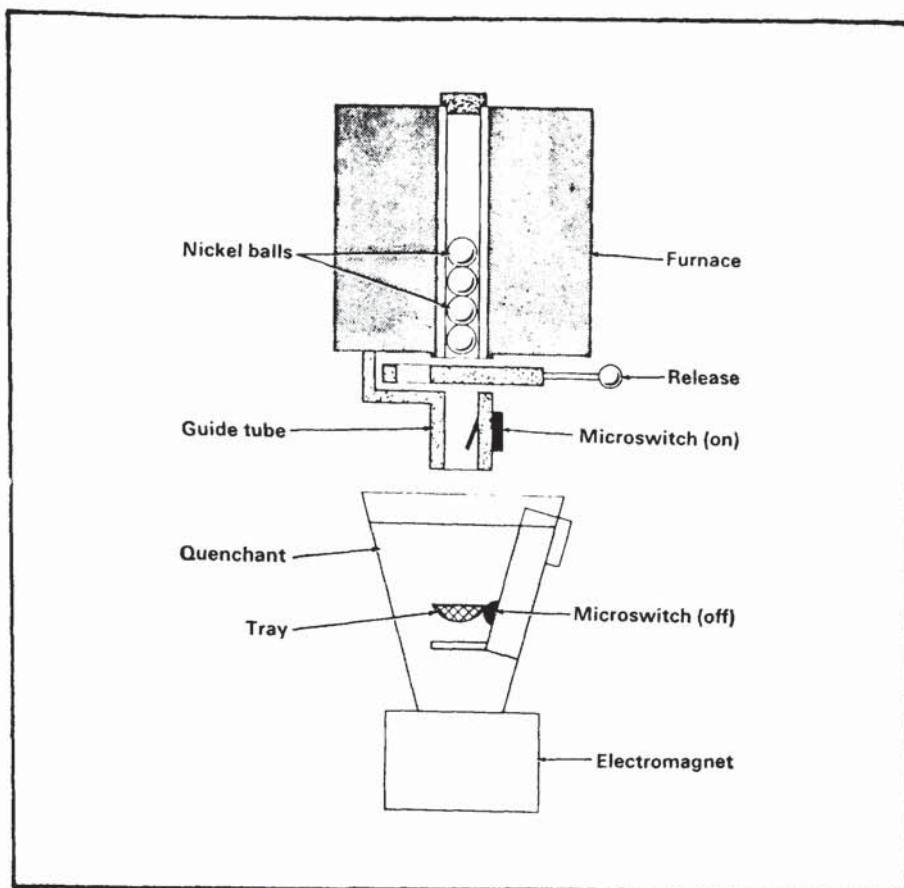


Figure 10. Diagram of the nickel ball test apparatus⁽¹⁴⁾.

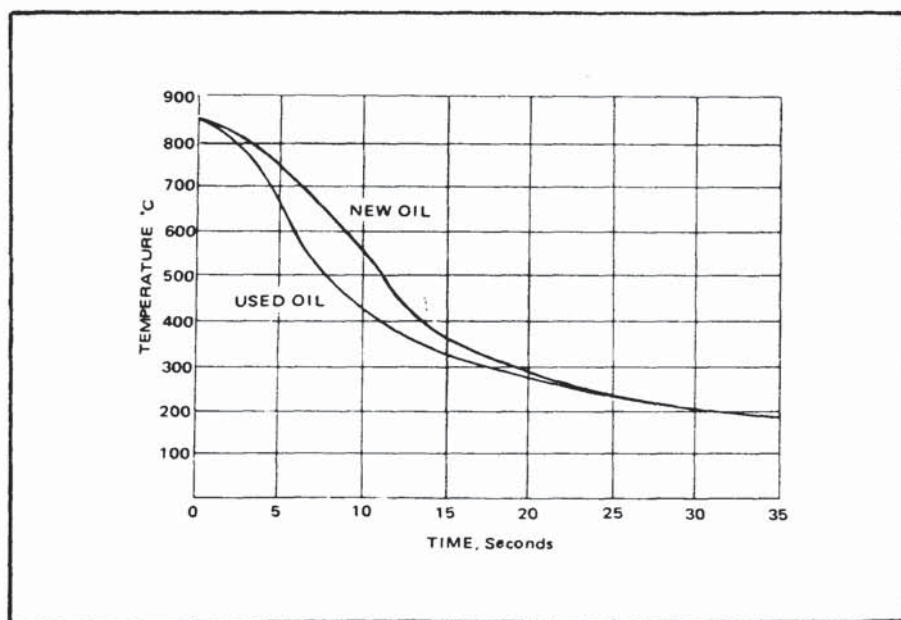


Figure 11. Time-temperature plots obtained for quench oil samples in both the new and used conditions, measured at 40 °C using the Wolfson Engineering Group test method⁽¹⁴⁾.

It can be seen that the used oil is faster than the new, as would be expected, and that the nickel ball test would give an increased time result for the new oil as compared with the used. However, had the curves converged at 350°C instead of 250°C the magnetic method would have considered both samples to be equal, due to the lack of information at intermediate temperatures. Problems also arise in maintaining a consistent surface finish and ball diameter.

2.6.3 Hot Wire Tests. This method consists of heating a nichrome or cupron wire (of standard gauge and electrical resistance) by means of an electrical current, in a small volume (100 to 200ml) of quenchant. The quenchant is normally tested at room temperature, and the wire is supported by two copper or brass electrodes. Heating of the wire is accomplished by steadily increasing the current by means of a rheostat. The cooling power of the quenchant is indicated by the maximum current reading, as measured by an ammeter.⁽¹⁴⁾ Quenchants capable of fast heat extraction permit the passage of higher currents through the wire before "burn-out" (i.e. melting of the wire).

These tests are again limited in that the data cannot be directly related to practical quenching problems since the cooling is accomplished well above normal heating ranges for steels, and would not show much difference between fast quenchants. Furthermore, the current value determined is dependent upon factors additional to the cooling power of the quenchant, e.g. variable contact resistance and variations in wire diameter and melting point.

2.6.4 Calorimetric Methods. These measure the rise in temperature of a known volume of quenchant after a fixed time following the quenching of a standard specimen from a specified temperature. The maximum ultimate rise in temperature is also recorded and the ratio of these two temperatures used to rate the quenchant. The more efficient quenchants have the highest ratio.

A typical example of this type of test is the "interval" or "five-second" test.⁽³⁾ A 250g bar of stainless steel is heated to 815°C and quenched for 5s. The two litre sample of

quenchant is then stirred to ensure temperature equalization, and the rise in temperature noted to the nearest tenth of a degree Celsius. This process is repeated for a series of test bars. Finally, an identical bar is fully quenched in a second two litre sample and the rise in temperature recorded. The quenching power of the medium is computed according to the following equation:

$$\text{Quench Speed (\%)} = A/B \quad (1)$$

Where A represents the average rise in quenchant temperature for the 5s quench bars, and B represents the maximum temperature rise of the sample for the fully quenched specimen.

The five-second test was once popular for determining gross changes in the characteristics of quench oils, because it was expedient and required no special equipment. But, although simple in concept, the test is difficult to perform in practice because of the very precise control required of the short time interval involved, and the need for a consistent specimen surface finish. In addition, the data obtained is not directly applicable to practical quenching situations, since the short time interval (5s) constitutes only a comparison in the higher temperature region of the quench, and the results may be misleading.

2.6.5 Hardening Response. Traditionally, metallurgists have compared the quenching efficiency of different media by examination of the effect that such quenching has on the structure and hardness distribution within steel bars of various diameters.⁽³⁷⁾ However, the hardening response of steel is dependent not only on the cooling power of the quenchant, but also the size, microstructure and composition of the steel being quenched (*Figure 12*).⁽³⁸⁾ Therefore, no one steel is suitable for all quenchants. Hardening response tests are also time consuming, costly and relatively difficult to perform. Since the quench hardening of steel is so industrially important, many workers have attempted to correlate quenchant characteristics with hardening power. These areas will be examined in detail in the next few sections.

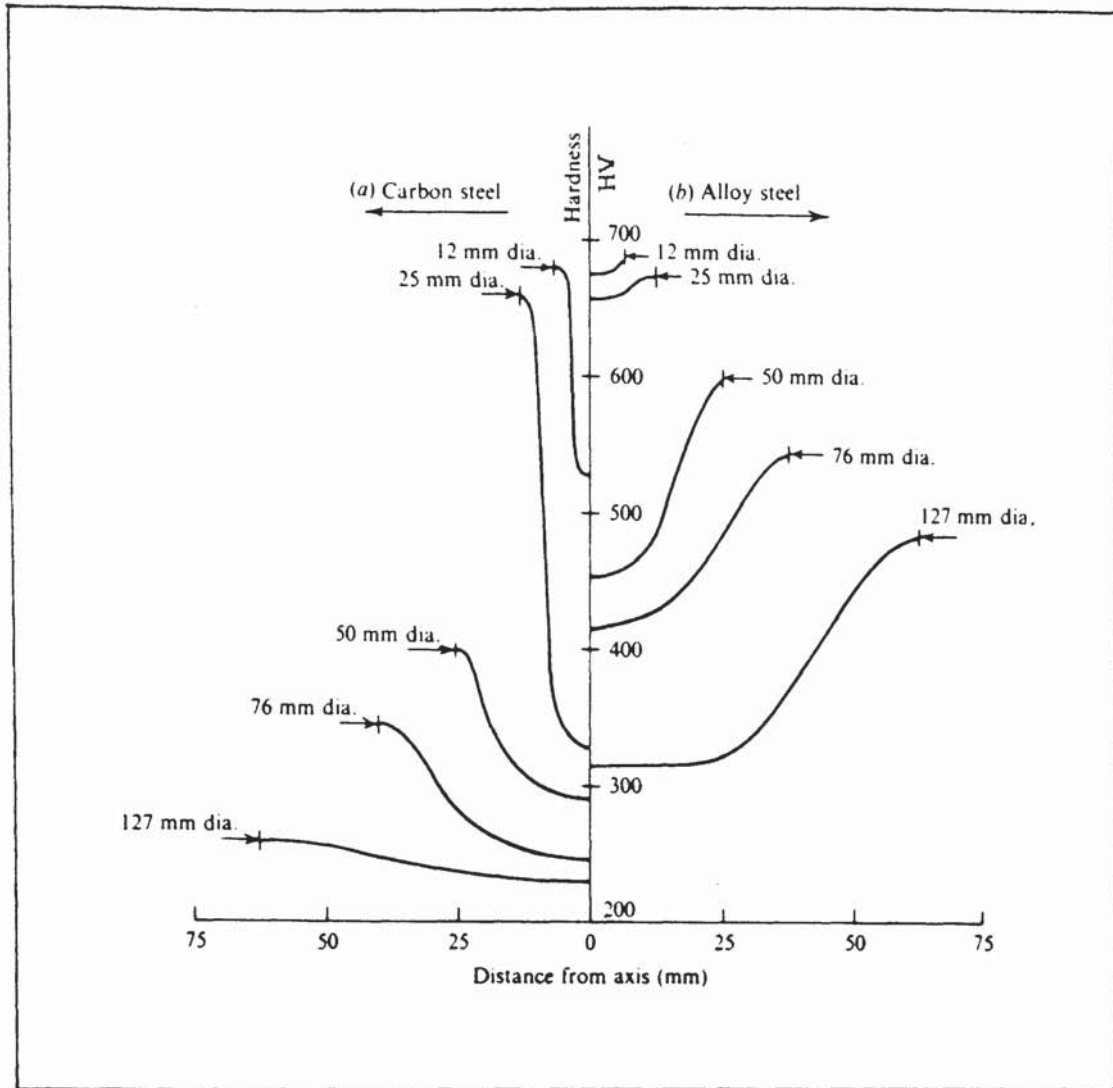


Figure 12. Hardness distribution across quenched bars of various diameters: (a) 0.45%C steel and (b) 0.4%C, 1%Cr-V steel⁽³⁸⁾.

2.7 Quenching of Steel

Steel is quenched to control the transformation of austenite to desired microconstituents. The cooling from austenite may produce structures which are fully martensitic, bainitic or ferritic depending on the steel composition, its hardenability and rate of cooling. The term "hardenability" simply refers to the ability of a steel to be transformed to martensite at a given depth when cooled under prescribed conditions.⁽³⁹⁾ Components that are quenched range from small bolts and pins to items weighing many tonnes, such as rotor forgings.⁽⁴⁰⁾ In each case, the objective is to produce the optimum microstructure and hence properties throughout the section to meet the necessary service requirements. Often the as-quenched structure required is

martensite and the component is subsequently tempered.

2.7.1 TTT and CCT Diagrams. The cooling rates required to achieve particular microstructures for steels are often represented by time-temperature-transformation (TTT) diagrams and continuous-cooling-transformation (CCT) diagrams. Two such diagrams are shown in *Figures 13a* and *13b* respectively, for a 0.44 per cent plain carbon steel austenitized at 880°C.⁽⁴¹⁾

TTT diagrams (sometimes called I-t diagrams for isothermal transformation) do not provide quantitative hardenability data since they are constructed from an examination of the microconstituents that are produced at intermediate temperatures during the quench. However, they do throw some light onto the time-temperature interrelationship in the transformation of austenite and, therefore, a qualitative insight into the hardenability of the steel. It can be seen from *Figure 13a* that the transformation of austenite into ferrite and then pearlite is slow in starting and progressing at temperatures just below AC_1 . The process then accelerates as the temperature is lowered, reaching a maximum at approximately 540°C; it then decelerates and the transformation product changes progressively to bainite, until the M_s temperature is reached where martensite is formed athermally.

CCT diagrams are more relevant to the continuous cooling conditions that occur during quenching. The conversion of TTT diagrams to CCT diagrams seemed possible at one time, but these attempts were found to be unreliable.⁽³⁹⁾ The most complete information on the continuous cooling transformation in steel is obtained using small specimens which can be heated and cooled at controlled rates in a dilatometer. This method takes advantage of the principle that austenite (face-centred-cubic lattice) has a distinctly different thermal expansion coefficient from ferrite, or any other body-centred-cubic transformation product of austenite. However, the method of controlling the cooling rate varies between test-centres. It may be completely natural or Newtonian cooling, controlled linear cooling, or for practical convenience a mixture of the two.

(a)

TTT

Austenitized at 880°C
Heat-up time: 1 min.
Held for 5 mins.

Temperature, °C

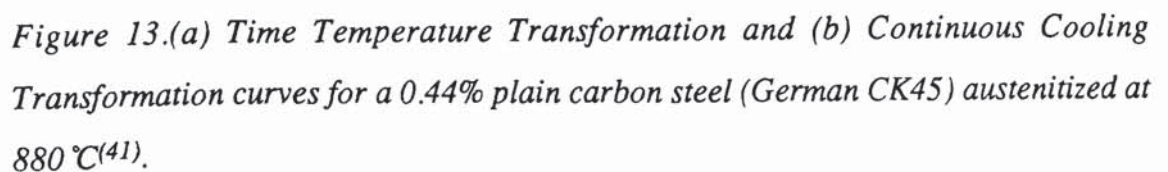
Time, s

Ac₃
Ac₁

A: Austenite
F: Ferrite
P: Pearlite
B: Bainite
M: Martensite

○ : Hardness, HV
25;75: % Transformation

Ms
M₅₀
M₉₀



Sachs⁽⁴²⁾ reviewed the presentation of transformation data in 1974, and included in his summary the major contributors of CCT diagrams at that time. It was clear from this review that the data was being collected and presented in many different forms. Sachs believes that the most convenient form of CCT diagram is the graph of transformation temperature against time (rather than having cooling rate or bar diameter as the abscissa), since it permits any cooling cycle to be superimposed. *Figure 13b* shows such a diagram based on a "grid" of experimental cooling curves. The percentage of each microconstituent is marked on the curves, as well as the resulting hardness. This particular diagram was constructed from dilatometric and metallographic data from 4.5mm diameter by 15mm long test pieces. Essentially Newtonian cooling was used, but zero time was taken when the specimen had reached AC₃. If the steel was cooled fast enough from the austenitizing temperature (880°C) to reach 100°C in about 12s, it would form 2 per cent bainite and 98 per cent martensite, with a resulting hardness of 548HV. Slower cooling taking about 40s to 100°C would lead to the formation of 10 per cent ferrite, 80 per cent pearlite, 5 per cent bainite and 5 per cent martensite with a hardness of 274HV.

Many CCT diagrams are illustrated in the literature without stating how they were constructed. Great care must be taken when trying to correlate cooling curves with such published data. It could be misleading, for example, to superimpose arbitrary cooling curves on diagrams constructed from linear cooling data.⁽²³⁾

2.8 Theoretical Factors Influencing Heat Transfer During Quenching

The rate at which heat is removed from a quenched component is dependent on several material and quenchant characteristics. For instance, the hardening of steel by austenitizing and quenching involves a highly complex process of unsteady-state heat transfer. Even in a hypothetical "infinite" quench (i.e. instantaneous cooling of the surface of the component to the temperature of the quenchant), the heat-flow process depends on the specific heat, thermal conductivity, and diffusivity of the steel, each of which varies for a given phase and temperature range. The situation is further complicated because heat is evolved as austenite transforms. In practice, the cooling rate is also controlled by the vapour blanket formation, boiling characteristics and the

velocity, temperature, specific heat, heat of vaporization, conductivity, density, viscosity and wetting characteristics of the quench fluid.⁽³³⁾

During the last century, numerous workers have tackled the quench heat transfer problem. However, because of the extreme mathematical difficulties, one or more questionable assumptions have always been required in order to simplify the calculations. Mathematically, Newton's empirical law of cooling can be used to describe the heat transfer from a quenched metal component:

$$q = cA (T_1 - T_2) \quad (2)$$

where q = rate of heat transfer (W)
 c = heat transfer coefficient at the metal-quenchant interface (W/m²K)
 A = surface area of metal in contact with fluid (m²)
 T_1 = surface temperature of metal (K)
 T_2 = fluid temperature away from surface (K)

Equation (2) defines the heat transfer coefficient, c , at the interface between the metal surface and the quench fluid. From a purely theoretical standpoint, the only satisfactory method of absolutely defining the cooling characteristics of the quenchant is in terms of this interfacial heat transfer coefficient. However, the value of c is sensitive to the geometry of the situation, such as the size, shape and surface condition of the part, plus the properties of the fluid and its velocity. In some situations, such as quenching, c also varies with the temperature difference ΔT , which equals $T_1 - T_2$. During nucleate boiling, c has been found to typically vary as a function of ΔT^2 , whereas for natural convection, weaker powers of ΔT such as $\Delta T^{0.25}$ or $\Delta T^{0.33}$ are more likely.⁽¹⁹⁾ The value of the heat transfer coefficient can be determined using one of two approaches:

(1) An analytical approach, based solely on the physical properties of the fluid and its dynamics.

(2) An empirical approach, based on the determination of surface cooling characteristics from the conduction within a quenched test piece of known physical properties.

An example of the first type of approach has been outlined by Terrier,⁽⁴³⁾ and later by Monroe and Bates.⁽³³⁾ When austenitized steel components are quenched in practice, the flow of the quenchant at the surface of the component will normally be turbulent. The above authors attempted to model this situation using three dimensionless parameters known as transport coefficients. The parameters used were:

- (a) Reynold's number, Re , which is the ratio of inertia to viscous forces, and relates to the stability of the fluid flow. Re is a function of V , ρ , X and η .
- (b) Prandtl's number, Pr , which defines the thermal properties of the fluid and is a function of η , S_p and K .
- (c) Nusselt's number, Nu , which is a measure of the efficiency of heat flow and is a function of c , K and X .

where V = fluid velocity (m/s)
 ρ = fluid density (kg/m³)
 η = fluid viscosity (Ns/m² or Pas)
 S_p = specific heat of fluid (J/kgK)
 K = thermal conductivity of fluid (W/mK)
 X = characteristic dimension (m)
 c = interfacial heat transfer coefficient (W/m²K)

As can be seen, the transport coefficients are only defined in general terms; the specific relationships have to be established for particular applications. Terrier, and Monroe and Bates, draw an analogy between the conditions within a quench tank and turbulent flow through a pipe, which is one of the most frequently studied situations. Unfortunately, the latter authors incorrectly defined the Nusselt number in their derivation of c , which was consequently also incorrect. Their derivation of Nu had the characteristic length and the thermal conductivity the wrong way around. In addition, they quoted a relationship between the three transport coefficients without stating for which boundary conditions it was valid. Turbulent Nusselt numbers are

highly dependent on the range of Reynold's and Prandtl numbers concerned.⁽¹⁹⁾ The physical properties of the quench fluid change considerably during the quench, due to the large temperature differences involved. Terrier's derivation was more accurate, since the Nusselt number was correctly defined and a broader relationship between the three transport coefficients was used. Although simplistic, this analytical approach does provide a useful insight into the effect of certain variables. A revised form of this approach is given below for a fluid flowing through a pipe of diameter D.

$$Re = \frac{DVP}{\eta} \quad (3)$$

The value of Re indicates the level of flow stability: empirical studies have shown that, for $Re < 2200$, the flow of fluid through the tube is laminar, while for greater values it becomes turbulent. However, the flow is not considered to be fully turbulent until $Re > 10,000$.⁽⁴⁴⁾ For pipe flow the Prandtl and Nusselt parameters may be defined as:

$$Pr = \frac{\eta S_p}{K} \quad (4)$$

$$Nu = \frac{cD}{K} \quad (5)$$

and for turbulent flow:

$$Nu = A Re^a Pr^b \quad (6)$$

where A, a and b depend on the chosen boundary conditions and the value of Re and Pr. (Typically, $0.5 \leq a \leq 0.88$ and $0.33 \leq b \leq 0.5$).⁽¹⁹⁾

$$\text{therefore: } c = \frac{A K Re^a Pr^b}{D} \quad (7)$$

Even though equation (7) cannot be explicitly solved, it implies that the interfacial heat transfer coefficient c increases with the value of the Reynold's number and hence the level of turbulence. However, this analytical solution for c relates only to heat

transfer between the inner wall of a pipe and a fluid which is flowing through it. Flow past irregular shaped objects such as cast, forged or machined components has not been examined in sufficient detail to define relationships which would enable c to be solved for practical quenching situations. The properties of the quenchant mentioned in this approach are important in controlling the heat transfer, but, in the absence of functional equations, empirical approaches for determining the rate of heat removal are usually adopted.

The actual heat flow from the interior of a quenched part to its surface can be described using Fourier's law which defines the thermal conductivity of the material.

$$q = -k A \frac{\delta T}{\delta x} \quad (8)$$

where q = heat transfer rate (W)

k = thermal conductivity of part (W/mK)

A = area of part (m^2)

$\delta T/\delta x$ = thermal gradient in part (K/m)

From equation (8), Fourier deduced the following fundamental partial differential equation for the flow of heat in three directions at right angles to one another:

$$\frac{\delta^2 T}{\delta x^2} + \frac{\delta^2 T}{\delta y^2} + \frac{\delta^2 T}{\delta z^2} = \frac{1}{\alpha} \frac{\delta T}{\delta t} \quad (9)$$

where α = thermal diffusivity of the part = $k/C_p \lambda$ (m^2/s)

λ = density of the part (kg/m^3)

C_p = specific heat of the part (J/kgK)

Equation (9) forms the basis of empirical methods for determining the surface temperature history of quenched test pieces from which c can be deduced. The equation may need to be modified, depending on the geometry of the test piece being used. For example, transferring equation (9) from cartesian to cylindrical co-ordinates for a quenched bar gives:

$$\frac{\delta^2 T}{\delta r^2} + \frac{1}{r} \frac{\delta T}{\delta r} + \frac{1}{r^2} \frac{\delta T}{\delta \theta^2} + \frac{\delta^2 T}{\delta z^2} = \frac{1}{\alpha} \frac{\delta T}{\delta t} \quad (10)$$

However, if the bar is considered sufficiently long ("infinite"), so that axial heat flow can be neglected, and symmetrical radial flow assumed, the equation becomes:

$$\frac{\delta^2 T}{\delta r^2} + \frac{1}{r} \frac{\delta T}{\delta r} = \frac{1}{\alpha} \frac{\delta T}{\delta t} \quad (11)$$

2.8.1 Quench Severity Factors. The first major breakthrough in attempting to find a solution to equation (9) for practical quenching situations came from Russell⁽⁴⁵⁾ in 1936. Russell examined the mathematical problem in detail and defined "h", as a measure of the severity of the quench and equal to c/k (units length^{-1}). This "quench severity factor" facilitated the calculations, as did his assumption that the physical characteristics of the steel and the quenching power of the bath remained constant. Russell was therefore able to present condensed tables for applying the calculations to quenched plates and cylinders.

Three years later, Grossmann et al,⁽⁴⁶⁾ using the same basic assumptions as Russell, introduced a similar quench severity factor "H", equal to half of that proposed by Russell (i.e. $H = 1/2h$). The difference arose from the use of diameters instead of radii in the calculations by the American workers. The Grossmann approach, although not popular in the UK, has been overwhelmingly accepted in the USA as a means of ranking quenchants for hardenability studies. The value of H for a quench bath can be derived from a hardening response test. Grossmann et al⁽⁴⁶⁾ introduced the criterion of "half-temperature time" as a means of relating cooling rate to the hardness obtained. The half temperature was defined as being the midpoint between the maximum temperature and that of the quench bath. (The fact that it encompassed the time/temperature zone of incubation of pearlite in many steels was put forward as justification for its choice, and also that it gave relatively good agreement with experimental results). They also defined a term D_u , the "diameter of the unhardened core", as the diameter where the microstructure was 50 per cent martensite.

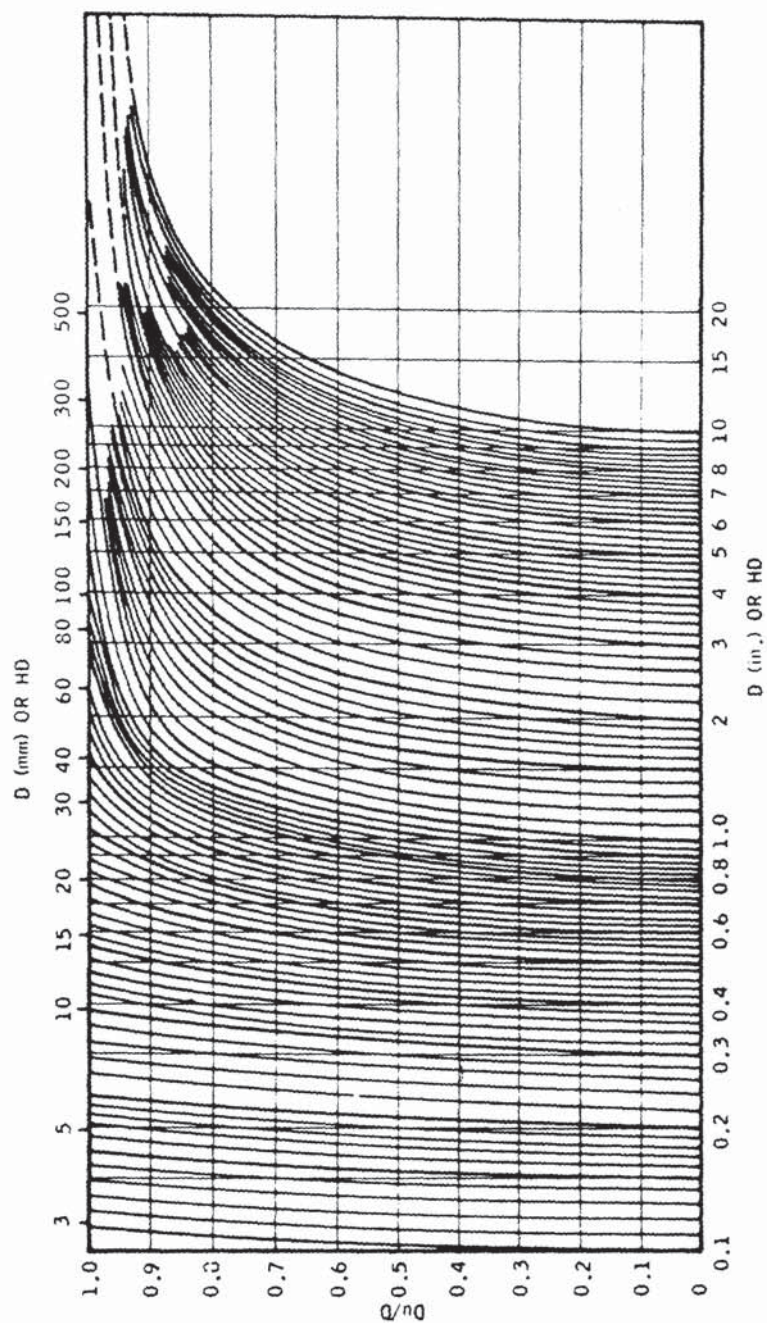


Figure 14. Curves for estimating the cooling power (Grossmann quench severity factor, H) of quenching baths⁽⁴⁷⁾.

Various times to half-temperature were calculated for various positions in different sized rounds, with baths of varying H values, and the chart shown in *Figure 14* was constructed.⁽⁴⁷⁾ The chart is used for determining the H value for any quenching bath by quenching various sized rounds of the same steel and determining Du for each bar diameter, D . By placing a sheet of tracing paper on *Figure 14* and plotting each of the various values of Du/D versus D , a curve can be drawn through the points. The curve can then be moved horizontally until the drawn curve matches one of the calculated curves, which then corresponds to the HD values. Dividing each value of HD by the D of the corresponding bar results in a value for H . The chart has only limited practical utility since it is impossible to match the experimental points determined by quenching different sized rounds, to any curve, when there is a very large difference in bar diameter and depth of hardening.⁽³⁹⁾

Both Russell's and Grossmann's quench severity factor approaches suffer from the same basic shortcomings associated with the assumption implicit in their original derivation. Papers by Carney and Janulionis,⁽⁴⁸⁾ and then later by Hopkins and Riley,⁽⁴⁹⁾ both critically examined the relevance of such quench severity factors. The latter authors listed four invalid assumptions:

(1) That Newton's law of cooling, equation (2), is obeyed and hence the interfacial heat transfer coefficient c , remains constant. Heindlhofer,⁽⁵⁰⁾ as far back as 1922, showed that this was not true for large temperature differences such as occur during quenching. If a single mode of heat transfer occurred at the surface, this assumption would be realistic, but as has been shown earlier there are three distinct stages of heat transfer during quenching.⁽⁶⁾

Realizing this, the USC (United Steel Companies) produced a report,⁽⁵¹⁾ based on Russell's original analysis and describing how the variation of h with temperature could be derived from time-temperature data recorded at the centre of quenched bars. The time taken to cool through intervals of 0.05 of the difference between the maximum temperature and that of the surroundings is required. The method uses a dimensionless temperature parameter U , known as the "fractional temperature" in

order to simplify the heat flow calculations.

$$U = \frac{T_1 - T_2}{T_0 - T_1} \quad (12)$$

where T_0 = initial temperature of body (K)

T_1 = instantaneous temperature at the centre of the body (K)

T_2 = initial temperature of the quenchant (K)

In addition, a graphical solution was given for 12.5mm diameter bars, in the form of a set of curves of h against the time to cool through the 0.05 time intervals (*Figure 15*). Cook⁽²⁾ used this method to demonstrate the change in h with temperature for a number of different quenchants, as the results for various concentration solutions of an unspecified water soluble quenchant illustrate (*Figure 16*).

Not only do the quench severity factors vary with temperature, but they also change with the bar diameter, and position within the bar at which the time-temperature measurements are made.⁽⁵¹⁾ Carney et al^(48,52) demonstrated these effects as can be seen in *Figures 17* and *18*. (To avoid confusion it must be noted that the quench severity factors quoted in these graphs were calculated using Russell's analysis and then halved to produce Grossmann equivalent H factors). Since the value of the quench severity factor is a surface phenomenon, it is not surprising that it increases with smaller bars, since they have a larger surface area to volume ratio.

(2) That the physical properties of the steel (in particular the thermal diffusivity) remain constant. *Figure 19* demonstrates the change in thermal diffusivity with temperature and hence structure.⁽⁵³⁾ Variations in composition also affect the physical properties, and hence the quench severity factor, as can be seen from comparing *Figures 18* and *20* taken from Carney.⁽⁵²⁾

(3) The heats of transformation do not affect the cooling process. Experimental work, such as that conducted by Carney, disprove this.

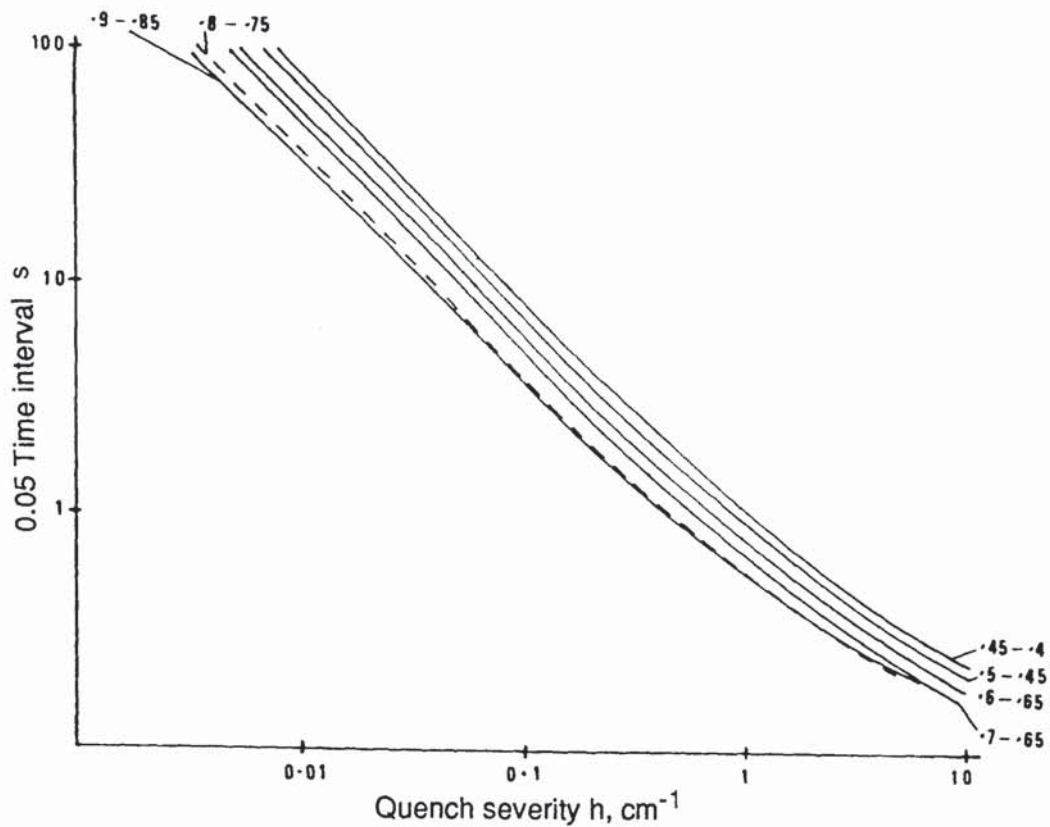


Figure 15. Curves for Russell's quench severity factor h against time to cool through the 0.05 intervals for 12.5mm (1/2 in.) diameter bars⁽⁵¹⁾.

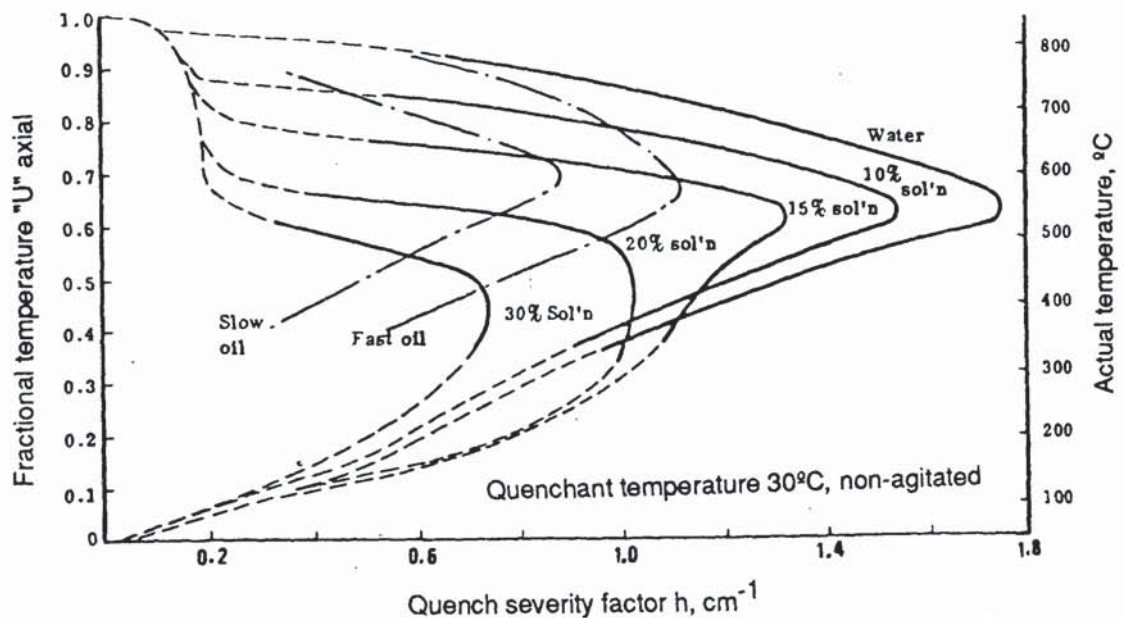


Figure 16. Effect of increasing concentration of a commercially available water soluble quenchant on Russell's quench severity factor h , measured using a 12.5mm diameter by 50mm long 25/15 Cr-Ni steel test piece with a centrally located thermocouple⁽²⁾.

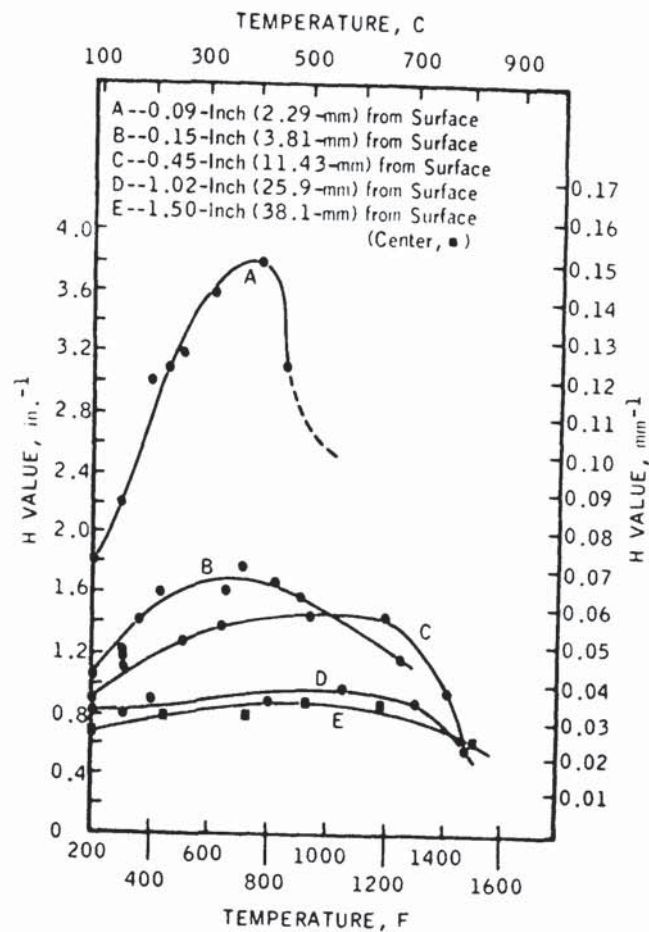


Figure 17. Change of Grossmann quench severity factor H with distance from quenched surface of a 3 in. (76mm) round of 18%Cr-8%Ni steel quenched in water at 60 °F (16 °C)⁽⁴⁸⁾.

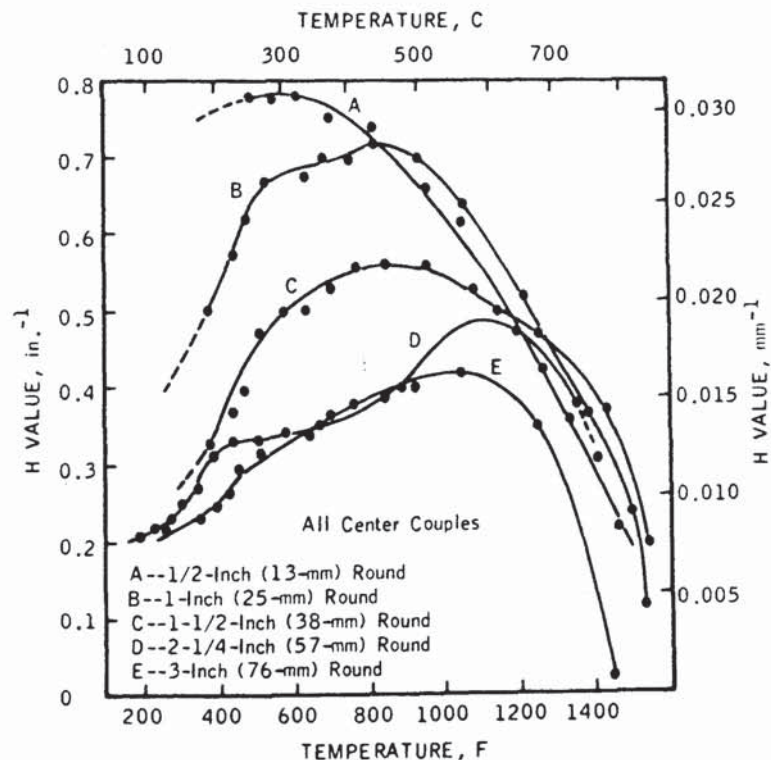


Figure 18. Variation of Grossmann quench severity factor H with temperature and size for SAE/AISI 9460 (0.6%C, 1.0%Mn, 0.5%Ni, 0.4%Cr) steel oil quenched from 1550 °F (845 °C)⁽⁵²⁾.



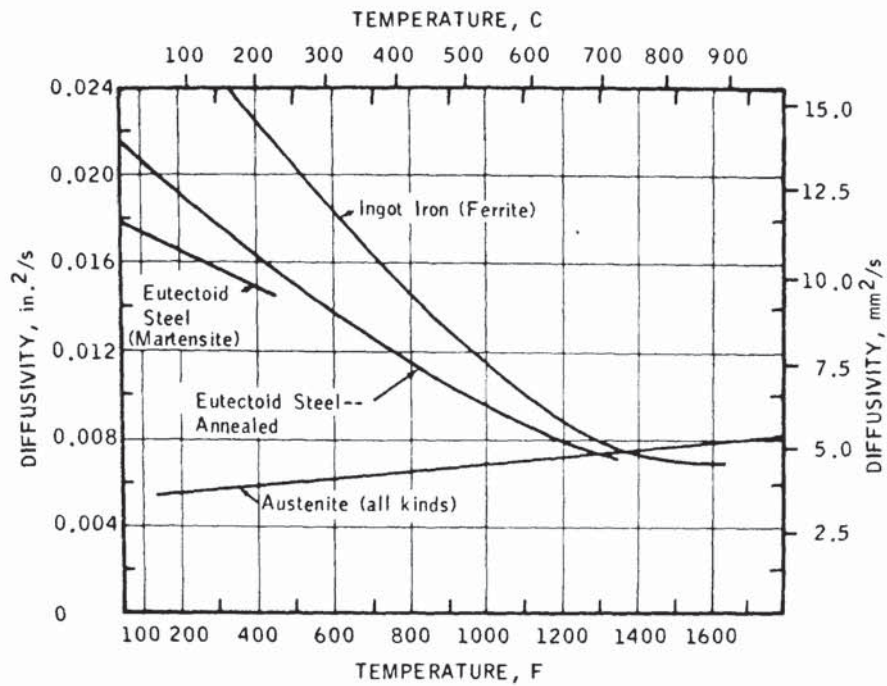


Figure 19. Thermal diffusivity of various structures⁽⁵³⁾.

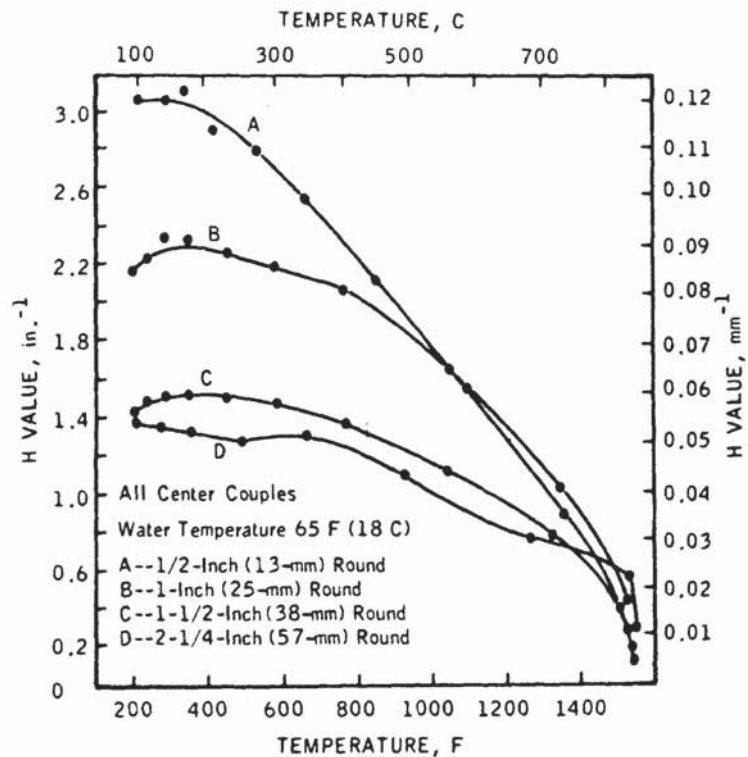


Figure 20. Variation of Grossmann quench severity factor H with temperature and size for 17%Cr steel water quenched from 1550 F (845 °C)⁽⁵²⁾.

(4) That the composition and structure remain constant and homogeneous throughout. Metallographic evidence clearly shows that this is not true of hardenable steels.

In addition to these problems, Hopkins and Riley⁽⁴⁹⁾ showed that the cooling curves, and derived quench severity factors, also changed considerably with the shape of the test piece being quenched. The surface condition of the test piece would also influence the result.

2.8.2 Numerical Methods. In recent years, with the advent of much greater computing power, more accurate determinations of the interfacial heat transfer coefficient for quenched test pieces have been possible using approximate, numerical procedures. These methods involve hypothetically splitting the quench specimen up into a number of discrete spatial and temporal locations called "nodes". The nodes are arranged along patterned grid lines in "finite difference techniques", or in almost arbitrary arrangements for "finite element analysis".⁽¹⁹⁾ Several workers^(10,54,55,56) have chosen finite difference methods to model the heat conduction in quenched test pieces since they are expedient for simple geometrical shapes. The governing partial differential equation for the geometry of specimen involved, is replaced by a number of algebraic equations which must be solved simultaneously at discrete time intervals. The paper by Chevrier and Beck⁽⁵⁴⁾ is recommended for the derivation of such equations for cylindrical test pieces. The method relies on the step-by-step calculation of a large number of approximate solutions. This process continues until the iterates converge toward the true solution. The error depends on the number of iterations and the stability of the calculations; consequently, test pieces with multiple thermocouples embedded at different depths below the surface are required in order to check the calculated time-temperature profiles.

Price and Fletcher⁽¹⁰⁾ used such a technique to determine the effect of surface temperature on the magnitude of the surface heat transfer coefficient in water, polymer and oil quenchants. The test piece used for most of the results comprised a

120mm square by 15mm thick AISI 304 stainless steel (19% Cr, 10% Ni, 0.08% C) plate, containing three thermocouples. The test piece was preheated to 850°C and then quenched into at least 100 litres of the quenchant sample at 20°C.

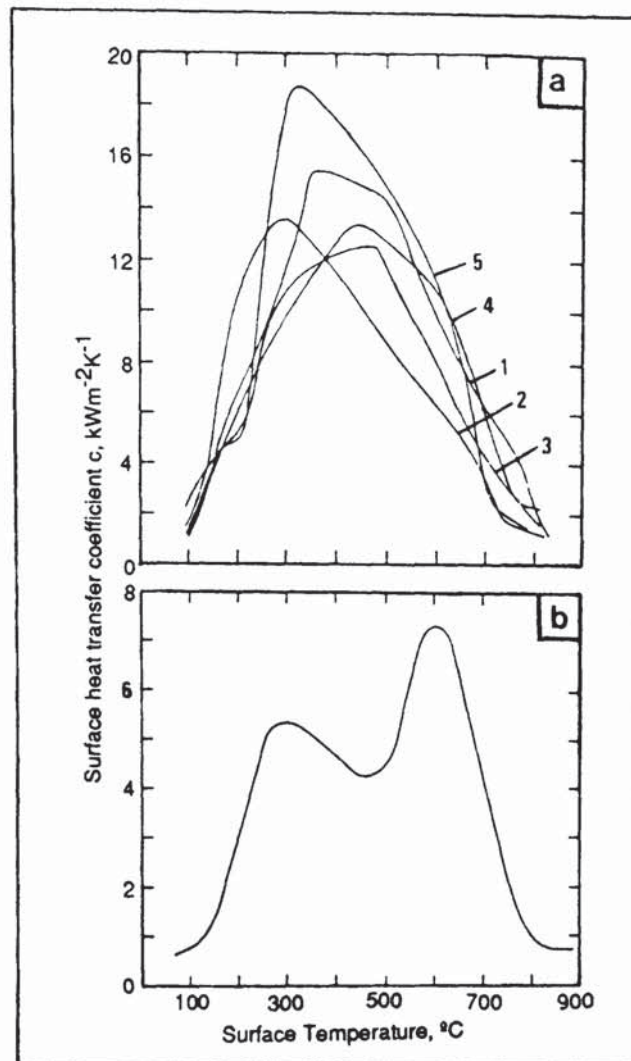


Figure 21. Effect of surface temperature on the heat transfer coefficient for (a) static water (5 consecutive tests), and (b) average result for six quenches into an agitated 25% Aquaquench 1250² solution.

Figure 21a shows the results for five tests using static water. There was considerable scatter, even though the plate was repolished after every test. Figure 21b gives the average result for six quenches into a 25 per cent polyalkylene glycol (Aquaquench 1250²) solution. Agitation of the polymer solution was created by two 290mm

²Aquaquench 1250 is the tradename of a polymer quenchant marketed by Edgar Vaughan and Co. Ltd., Birmingham.

diameter propellers, rotating at 50rpm. It can clearly be seen that the polymer quenchant exhibited a much lower maximum surface heat transfer coefficient compared with those for the unagitated water sample. Unfortunately, no indication of the amount of scatter was given for the polymer quenchant results. As would be expected, these graphs reflect the stages of cooling that occur, and are very similar in shape to the more directly produced cooling rate-temperature plots.

Since numerical methods such as the one described above are very costly and time consuming, they are not really suitable for the routine evaluation of quenchants. The manufacture of consistent test pieces poses a considerable problem because of the need for precise positioning of the thermocouples. Obviously the problem is exacerbated as the number of thermocouples increases, although the corresponding level of confidence in the results is also raised.

Several workers ^(54,57,58,59) have examined the possibility of using a single, centrally-located thermocouple to calculate surface cooling characteristics using an explicit solution to the inverse problem of transient heat conduction. Considerable computing power is needed for these highly complex mathematical solutions based on Duhamel's theorem. A detailed description of this technique has recently been given for cylindrical silver test pieces by Qun and Xijing.⁽⁵⁹⁾ A collaborative project between these workers and the Wolfson Heat Treatment Centre has recently been organized in order to modify the technique for Wolfson Engineering Group quench test probes.⁽⁶⁰⁾ However, the stability of such calculations needs to be carefully scrutinized, since without supplementary temperature measurements, the accuracy of the results cannot easily be checked.

Numerical methods offer the advantage that the temperature profile for the test piece can be evaluated at any one moment during the quench. This is essential for the accurate prediction of the hardness and residual stress distribution within the quenched piece.^(10,61) Nevertheless, it must be remembered that numerical methods provide only approximate solutions, and experience the same restrictions associated

with all empirical techniques (i.e. the results are highly sensitive to the experimental conditions, especially the size, shape and properties of the test piece). Vast amounts of data are needed, including accurate details concerning the physical properties of the test piece material over the entire quench temperature range. Furthermore, as was shown by Chevrier and Beck,⁽⁵⁴⁾ generalization of such results is impossible due to the anisothermal nature of the test piece surface. A novel method of demonstrating this effect was recently described by Tensi et al⁽⁵⁶⁾ These German workers studied the progression of the nucleate boiling stage along the length of a quenched cylinder using conductivity measurements between the test piece and a tubular electrode surrounding it. They called the speed at which the nucleate boiling front proceeded along the cylinder the "rewetting rate".

2.9 Hardenability Tests and Correlation Between Quench Cooling Data and Steel Hardening Response.

2.9.1 **Hardenability Tests.** Various methods can be used to assess the hardenability of steel. In the Grossmann method,⁽⁶²⁾ the microstructure is observed in several quenched bars of various diameters. The position of the 50 per cent martensite zone, which is more clearly seen than the 100 per cent region, is determined in each bar and hence the critical diameter for the steel, D_c (i.e. the diameter which would harden to 50 per cent martensite at the centre). The ideal diameter for a given steel, D_i , is then the critical diameter for an ideal quench when $H = \infty$. This is obtained by means of *Figure 22* and *Table 1*, which gives the values of H for various quenching procedures.

The commonest measure of hardenability is the Jominy end-quench test. This requires much less time and material than the Grossmann method, but the results are not so directly related to practice. A 25mm (1 inch) diameter bar, 100mm (4 inches) long is austenitized just above the critical temperature range and then quenched by a jet of water impinging on one end, see *Figure 23a*. After cooling, a flat, 0.4mm (0.015 inch) deep, is ground along the side and hardness measurements made every 1.5mm (1/16 inch).

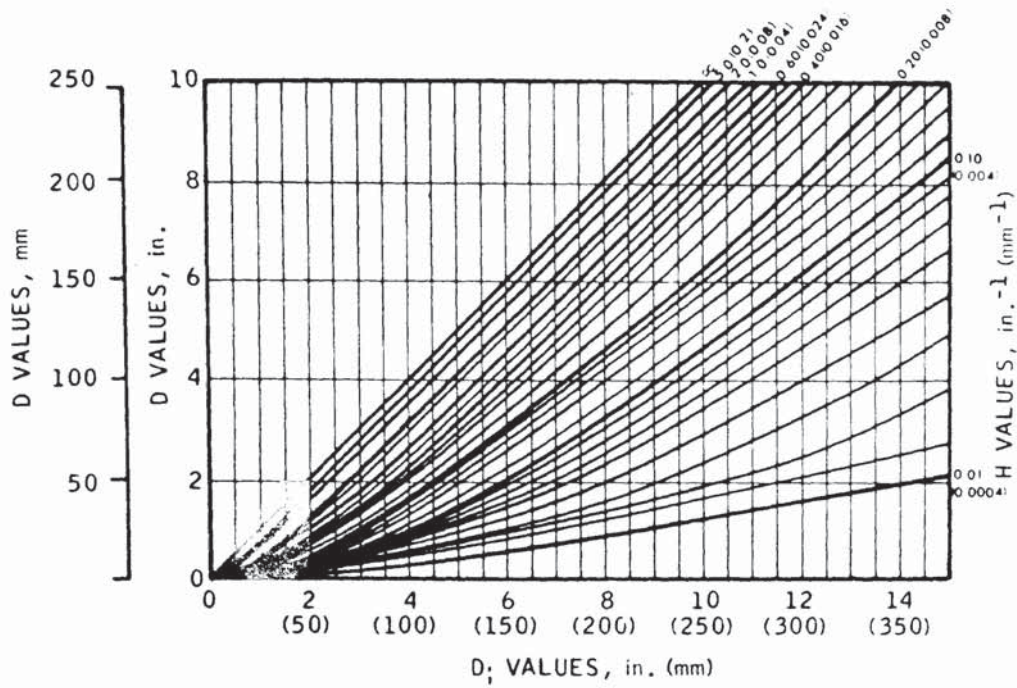


Figure 22. Relationships among ideal critical diameter, D_i , actual diameter, D , and Grossmann severity of quench, $H^{(46)}$.

| H Value | | Quenchant | Agitation |
|--------------------|---------------------|--------------|-----------|
| inch ⁻¹ | (mm ⁻¹) | | |
| 0.20 | (0.0079) | Oil | No |
| 0.35 | (0.0138) | Oil | Moderate |
| 0.50 | (0.0197) | Oil | Good |
| 0.70 | (0.0276) | Oil | Strong |
| 1.0 | (0.0394) | Water | No |
| 1.5 | (0.0591) | Water | Strong |
| 2.0 | (0.0787) | Brine | No |
| 5.0 | (0.1969) | Brine | Strong |
| Infinity | | Ideal quench | |

Table 1. Grossmann quench severity factors $H^{(46)}$.

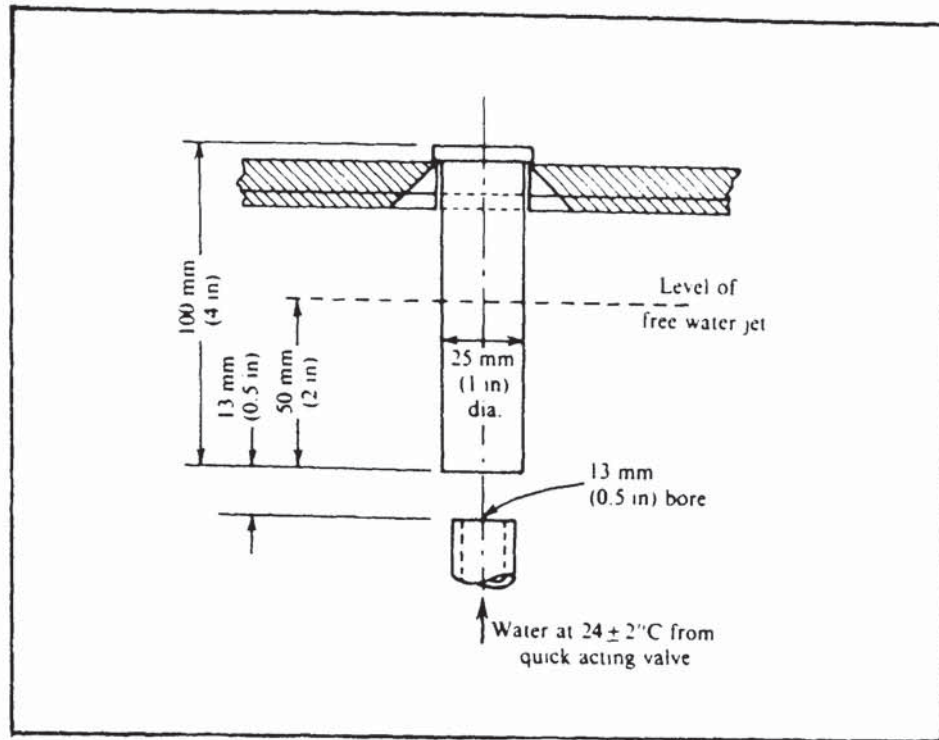


Figure 23a. Jominy end-quench test of hardenability⁽³⁸⁾.

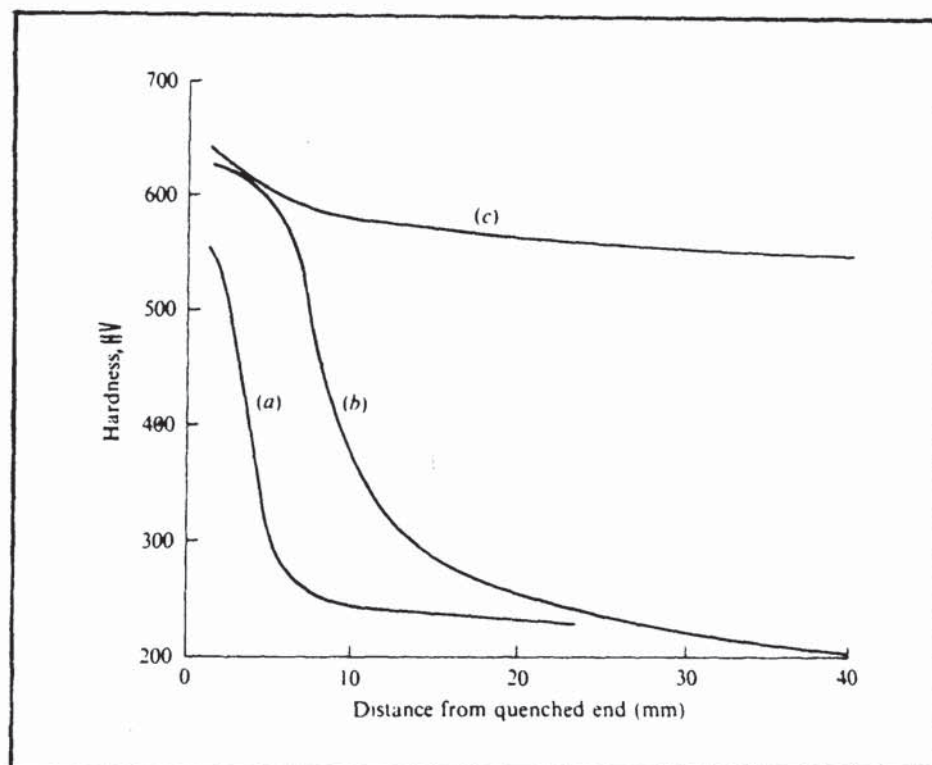


Figure 23b. Jominy end-quench curves for: (a) plain carbon steel (0.4%C, 0.7%Mn); (b) low alloy steel (1%Ni, 0.35%C); and (c) alloy steel (3%Ni, 1%Cr, 0.3%C)⁽³⁸⁾.

Typical Jominy test results are given in *Figure 23b*.⁽³⁸⁾ The 0.4 per cent plain carbon steel has relatively low hardenability with the hardness dropping off rapidly at about 4mm from the quenched end. The low alloy steel (1 per cent nickel, 0.35 per cent carbon) has slightly better hardenability with the median hardness occurring at about 10mm. The third curve shown is for a high hardenability steel containing 3 per cent nickel, 1.0 per cent chromium and 0.3 per cent carbon.

2.9.2. Correlation Between Quench Data and Hardening Response.

Many workers have attempted to predict the hardening response of steel components from some measure of the quenchants' cooling power. The prediction is complicated by the fact that the hardness developed depends not only on the cooling rate of the quenchant over some particular temperature range, but also on the composition of the steel. In addition, the rate of cooling varies across the section of the quenched component. It is not surprising, therefore, that such attempts have generally been disappointing.

Some of the first attempts were made in the 1940's by German workers such as Rose,⁽⁶³⁾ and Krainer and Swoboda.⁽⁶⁴⁾ These authors used mathematical relationships based on the cooling curves obtained using the silver ball test. These results were disappointing, as were the later attempts using a silver ball by Rogen and Sidan,⁽¹⁸⁾ (*Figure 4*) described previously.

The most commonly used techniques have been based on some hardenability equivalence criterion, using end-quench data for the steel in question. Asimow et al⁽⁴⁷⁾ related the hardness at a given distance on the Jominy bar, with that in steel bars using a mathematical relationship between D_i and D_c . This work was later extended to produce *Figure 24*, commonly used in the USA and referred to as the "Grossmann chart".⁽⁴⁾ The application of the chart is limited because the quench conditions are described only in general terms (for example, "very good oil quench - good agitation"). An added complication is the fact that what appears to be good agitation in a quenching system that has no parts in it, may be poor agitation, when a

load of components is immersed in the tank.

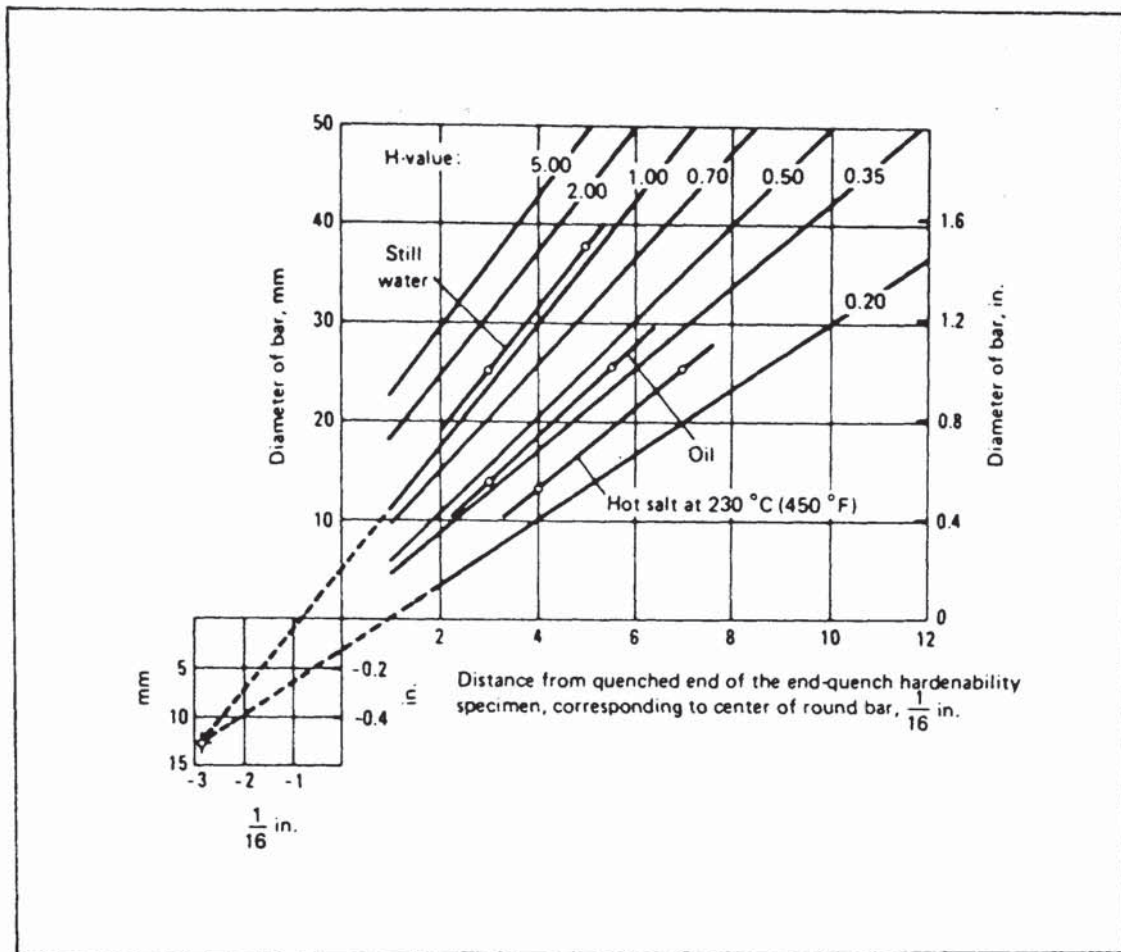


Figure 24. Grossmann chart relating bar diameter, hardenability of steel and severity of quench⁽⁴⁾.

Lamont⁽⁶⁵⁾ used Russell's tables for the cooling of round steel bars, to enable the hardness at graduated positions, from bar surface to centre, to be estimated for various values of the Grossmann quench severity factor H. Examples of the curves he presented are given in *Figures 25a* and *25b*. Three years later, in 1946, Russell⁽⁶⁶⁾ showed how his calculations could be applied to Jominy test bars. In 1971, Jatzak⁽⁶⁷⁾ manipulated Lamont's curves to give *Figure 26*, relating calculated half-temperature times in round bars to those of various distances along the Jominy test bar, for various values of H. This is probably one of the most widely used approximations used in industry.

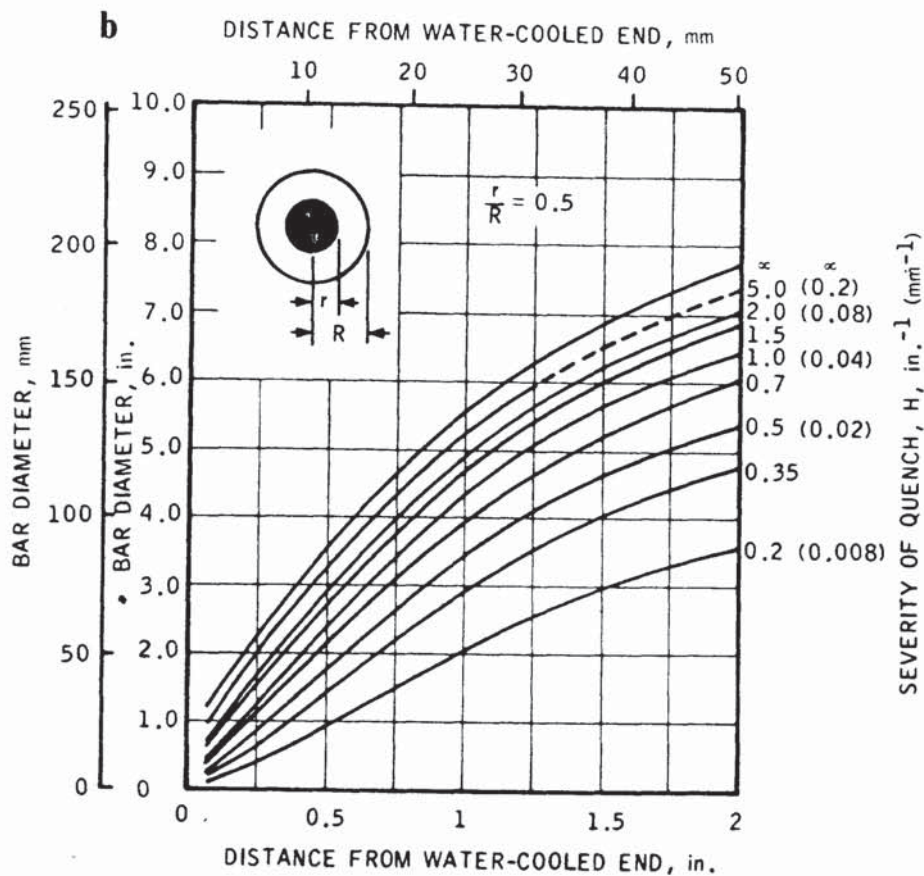
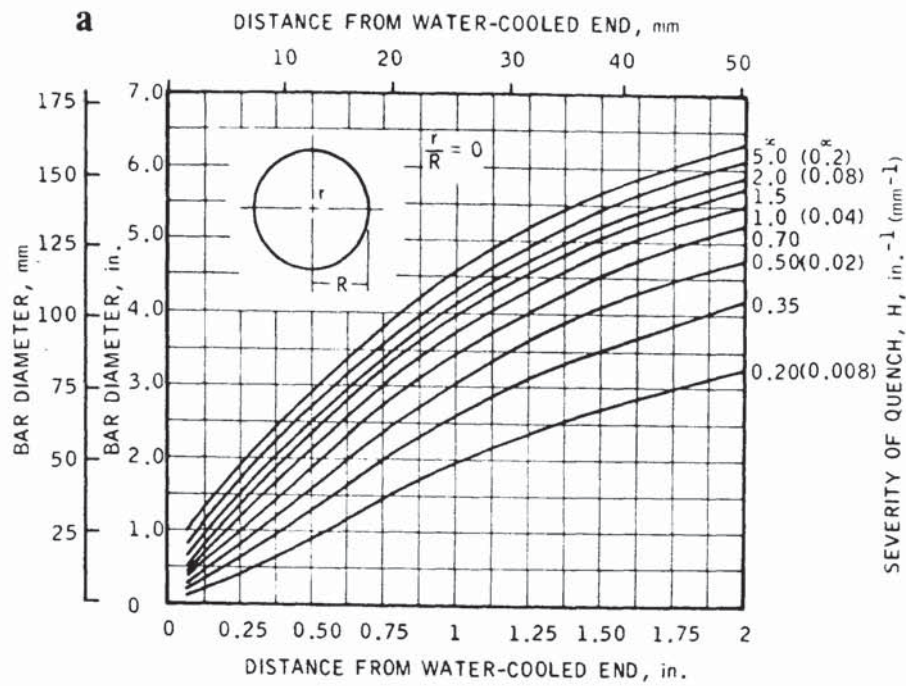


Figure 25. Location on end-quenched Jominy hardenability specimen corresponding to: (a) the centre of round bars, (b) the half-radius position in round bars⁽⁶⁵⁾.

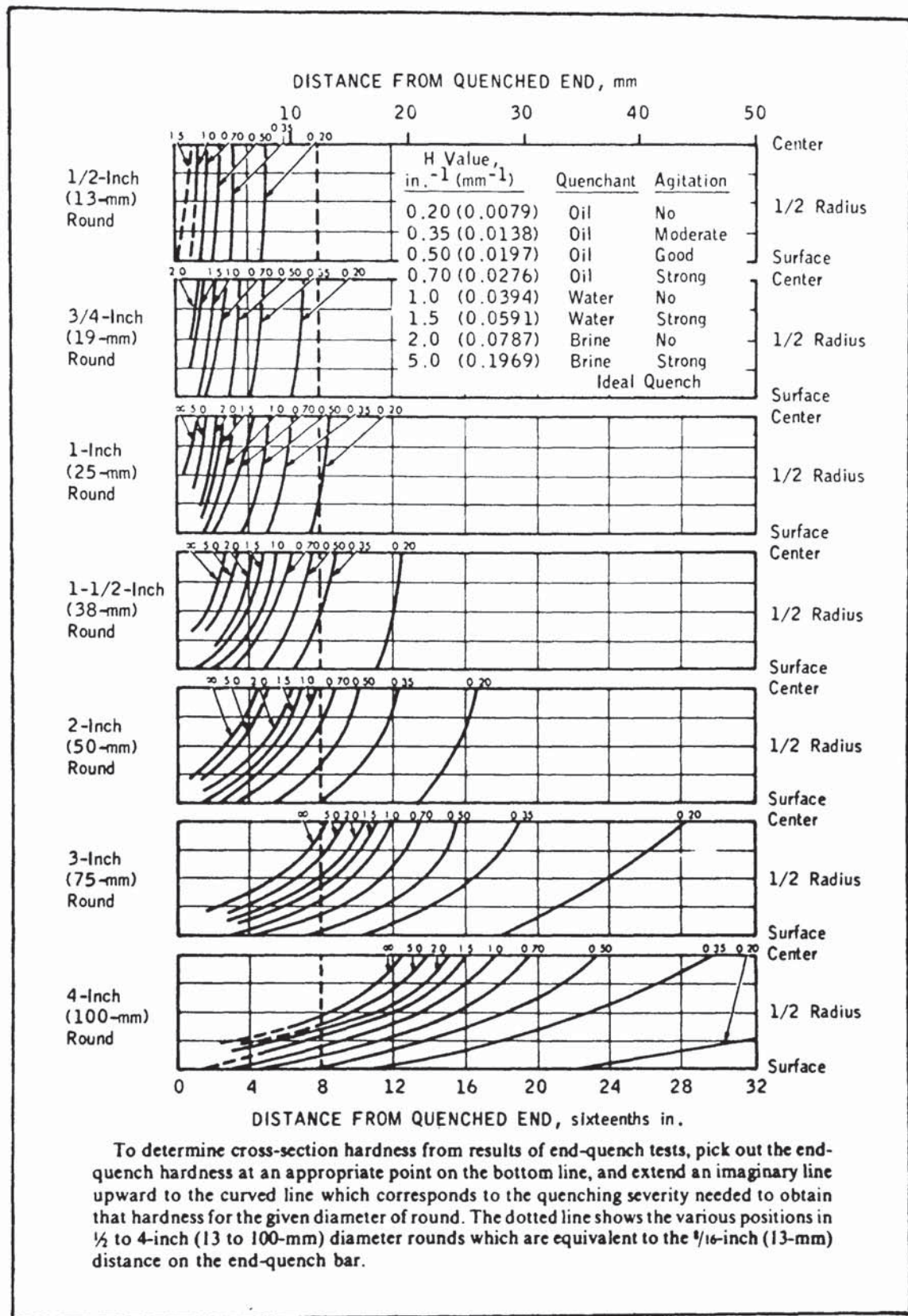


Figure 26. Cross-section hardness in rounds related to end-quench bar locations and Grossmann severity of quench $H^{(67)}$.

The Wolfson Heat Treatment Centre Engineering Group "Testing of Quenching Media" working party has also attempted to correlate the information obtained from probe quench data, with that obtained from the quenching of actual components in industrial heat transfer plant. The first trial carried out by the working party was to quench bars of different size, made from a cast of known hardenability 080H41 (En8, 0.4% C, 0.8% Mn), from production furnaces into various quenchants, at different temperatures and levels of agitation. After quenching, the test bars were sectioned and the hardness measured at their central point. From a knowledge of the centre hardness, bar diameter and Jominy hardenability characteristics, the quench severity factors H for the various units were determined. From this exercise it was found that:

- (a) sealed quench furnaces with high levels of agitation gave high values of H;
- (b) accelerated oils gave higher values of H than hot oils;
- (c) scale on the surface of the bars resulted in lower values of H.

The next test work was performed by Bateman,⁽⁶⁸⁾ who carried out quenches into an oil tank placed on a rotating turntable. The shortcomings of this agitation method were described earlier. The Wolfson probe was positioned in the tank so that it experienced laminar flow (100mm from centre at 33rpm). Once the quench probe results had been obtained for a range of quench fluids, 12.5mm diameter bars of 080M30 (En5, 0.3% C, 0.8% Mn) of known hardenability were quenched into the same moving oils. The H values obtained during this work were consistently lower than those measured in the previous trials on production furnaces, and a water quench only achieved an H value of 0.55 against the widely quoted value of 1.0. Hampshire⁽⁶⁹⁾ compared these H values with the data obtained from the probe quench tests, and established the following equation using regression analysis:

$$\begin{aligned} H = & 0.395 \times 10^{-1} (\text{time to } 600^{\circ}\text{C}) - 0.139 \times 10^{-1} (\text{time to } 400^{\circ}\text{C}) \\ & + 0.123 \times 10^{-2} (\text{maximum cooling rate}) + 0.224 \times 10^{-2} (\text{rate at } 300^{\circ}\text{C}) \\ & + 0.224 \times 10^{-4} (\text{temperature of maximum rate}) \end{aligned} \quad (13)$$

where: cooling times (s), temperatures ($^{\circ}\text{C}$) and cooling rates ($^{\circ}\text{C/s}$)

Nicklin⁽⁷⁰⁾ carried this work further, by attempting to correlate quench severity factors estimated from time-temperature data using the Wolfson Engineering Group quench test, with those obtained using both Russell's⁽⁶⁶⁾ and Jataczak's⁽⁶⁷⁾ methods for industrial furnace/oil quench combinations. Cylindrical specimens manufactured from three steels of various diameter were quenched in each industrial unit to test a range of hardenabilities, and quench severity factors h , determined from the resulting core hardness values. Oil samples from each unit were then tested using standard Wolfson conditions, and values of h determined using *Figure 15*. The resulting level of correlation between the h values determined was generally poor. The accuracy of the correlations was found to be better for certain steels such as 080H41 (En8), where the half -temperature time criterion was considered more suitable, since the 50 per cent martensite hardness coincided with the middle of the steepest slope of the Jominy curve. Agitation was found to have a significant effect, and some means of quantifying it was believed necessary. Direct correlation between hardness and certain cooling variables seemed to be more effective, especially for certain materials. For example, the regression equation below yielded a correlation coefficient of 0.98 for a 12.5mm diameter bar of 080H41 (En8):

$$H_v = 1108 + 1.05A - 50.7t_{600} \quad (14)$$

where: H_v = core hardness (HV_{30})

A = correction factor

t_{600} = cooling time to 600°C (s)

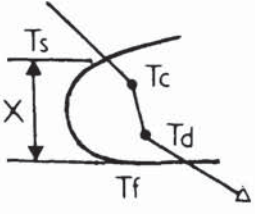
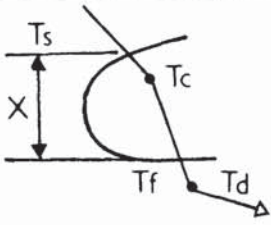
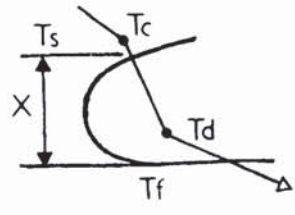
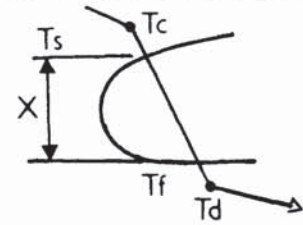
The correction factor A , takes into account variables such as quench bath agitation and temperature. The value of A could thus provide a useful means of ranking industrial quench tank installations. Nicklin therefore concluded that direct correlation between hardness and cooling variables is more significant than calculating quench severity factors, which have been derived using a number of invalid assumptions (described previously).

Most correlation work has relied on some form of hardenability equivalence criterion. The above work used the half-temperature time criterion; however, if the time to cool to a temperature halfway between the hardening temperature and the bulk quenchant temperature is not the major cooling parameter affecting the hardness, poor correlation will occur. The results of Jones and Pumphrey⁽⁷¹⁾ and more recently Nicklin,⁽⁷⁰⁾ cast serious doubt on its general applicability. Other criteria have been suggested such as the cooling rate at 700°C, with which Jominy⁽⁷²⁾ obtained fairly good correlation; rate at 538°C, which Grossmann⁽⁴⁶⁾ rejected in favour of the half-temperature time method; and times to cool through various temperature ranges chosen for their effect on transformation. Monroe and Bates⁽³³⁾ have chosen to characterize quenchant using an H factor related to the cooling rate at 700°C. They utilized a polynomial least squares fit to relate H values calculated using the Grossmann method, with rate data obtained from cooling curves.

It is believed unlikely that any one hardenability equivalence criterion will give valid results for all steels, because of their varying response to hardening. This is clearly seen by examining published CCT diagrams for steels of varying composition. Some steels have hardenability controlled by pearlite, whilst others which contain alloying elements, such as chromium, molybdenum and vanadium, form complex carbides which delay the pearlite reaction, producing bainite.

Tamura et al⁽²²⁾ have proposed a radical new quench severity factor, V, derived from the cooling curve for the quenchant and the relevant CCT diagram for the steel of interest. The characteristic temperature (T_c) and the temperature corresponding to the beginning of the convection stage (T_d) are determined from the cooling curve for the quenchant. A factor X is also used which equals the temperature range requiring rapid cooling to produce the desired microstructure, obtained from the CCT diagram (*Figure 27*). A range of V values are quoted for a number of oil/steel combinations. For example, the value of V for a 0.45 per cent plain carbon steel quenched into a hot oil was 0.31, compared with a value of 0.66 for the same steel quenched into an accelerated oil. However, the authors believe that the criterion, as described, is not suitable for aqueous polymer quenchant solutions. This is because, compared with

oils, the characteristic temperature (T_c) was higher and less consistent, and the value of T_d (the convection stage transition temperature) much lower. These Japanese workers used the previously described JIS test employing a silver test piece with a near surface mounted thermocouple (*Figure 5*).

| | | | |
|----------------|----------------|---|-------------------------------|
| $T_s \geq T_c$ | $T_d \geq T_f$ |  | $V = \frac{(T_c - T_d)}{(X)}$ |
| $T_s \geq T_c$ | $T_d \leq T_f$ |  | $V = \frac{(T_c - T_f)}{(X)}$ |
| $T_s \leq T_c$ | $T_d \geq T_f$ |  | $V = \frac{(T_s - T_d)}{(X)}$ |
| $T_s \leq T_c$ | $T_d \leq T_f$ |  | $V = \frac{(T_s - T_f)}{(X)}$ |

KEY

T_s : Transformation Start Temperature
 T_f : Transformation Finish Temperature
 T_c : Characteristic Temperature
 T_d : Convection Stage Start Temperature

Figure 27. Tamura quench severity V values for various cooling patterns for materials quenched in oils⁽²²⁾.

Recently, Thelning⁽⁷³⁾ co-ordinated a round-robin exercise amongst members of the IFHT's "Technical Aspects of Quenching" Technical Committee. The aim was to correlate cooling data for quench oils from industrial units using Wolfson equivalent

probes, with the practical hardening result for a number of steels of varying hardenability. Unfortunately, the level of correlation was generally disappointing, since no account was made of the varying oil temperatures and level of agitation in the industrial quench units. Both these factors have a significant effect, as was demonstrated by Nicklin.⁽⁷⁰⁾ In addition, there were inconsistencies between the different test centres regarding the oil sample volume and temperature for the cooling characteristic tests. Nevertheless, it was possible to list the oils in order of hardening power, by measuring the area contained by their cooling rate-temperature curves and two limiting temperature horizontals enclosing the diffusion dependent transformation range. These temperature ranges were chosen from the relevant CCT diagram and were typically 600-300°C for unalloyed steels and 500-200°C for alloy steels.

It is often stated that in order to obtain good hardening response a quenchant should provide a high initial rate of cooling so as to avoid the noses of the non-martensitic transformation products seen on the CCT diagram. However, Thelning^(23,73) has postulated that there is an optimum duration of slow vapour blanket (stage A) cooling for a particular steel to achieve the best hardening result. This is because, if the cooling through the upper metastable austenite range is slow, nucleation proceeds slowly, which enhances hardening. Should the slow cooling continue till just before the nucleation range and then change over to rapid cooling, the steel passes into a temperature range where any nuclei previously formed will grow slowly. The nucleate boiling stage for the quenchant should thus coincide with the critical temperature range for the steel. This hypothesis is considered to be more relevant to materials such as low alloy steels, in which the noses for the high temperature transformation products have been shifted to the right of the CCT diagram. With plain carbon steels a high initial rate of cooling is necessary, simply in order to miss the non-martensitic noses.

2.10 Traditional Quenching Media

The choice of quenching fluid and technique depends on the type of material to be quenched and the shape and thickness of the part being quenched. When hardening

tool steel, the heat treater generally aims at obtaining a martensitic structure, at least in the surface layers of the steel. Therefore, the cooling rate must be controlled to avoid the formation of pearlite or bainite. Since the dimensions of the tool are usually decided in advance, the correct quench conditions must be chosen to produce the required depth of hardening within the predetermined dimensional tolerance. Plain carbon steels and precipitation-hardening alloys are commonly quenched in water. Alloy steels require less severe cooling rates and hence less distortion problems arise. A wide range of cooling rates are capable of being achieved, depending on the quench fluid chosen as illustrated in *Figure 28*.

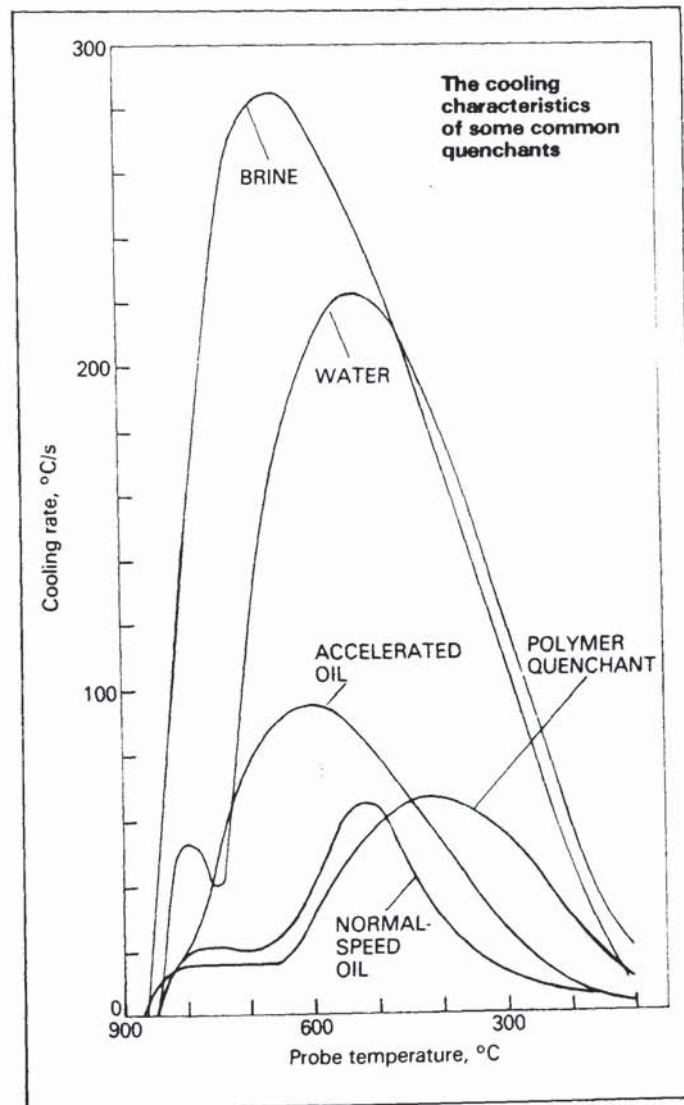


Figure 28. Typical cooling rate-temperature curves for some common quenchants at 30 °C as measured under non-agitated conditions by the Wolfson Engineering Group test⁽²⁶⁾.

A brief survey of the most commonly used traditional quenching media will now be given.

2.10.1 Water. Water is probably the oldest cooling medium used for hardening and today still finds widespread use. It has several advantages, it is readily available, cheap, non-hazardous and can be used to provide high rates of cooling. However, it has the disadvantage that its cooling rate is still relatively high around 300°C, the temperature range at which martensite formation starts in many steels. This subjects the steel to the simultaneous influence of thermal and transformation stresses, the combined effect of which will increase the risk of crack formation. Water quenching is particularly prone to cracking parts with significant differences in cross-sectional area and parts containing holes and grooves. One method of reducing the danger of cracking is to remove the steel from the water bath when it has cooled some 200-400°C, and then rapidly transferring it to an oil bath. This has been found to be a very effective means of increasing the depth of hardening of oil-hardening, low alloy steels.⁽⁷⁴⁾

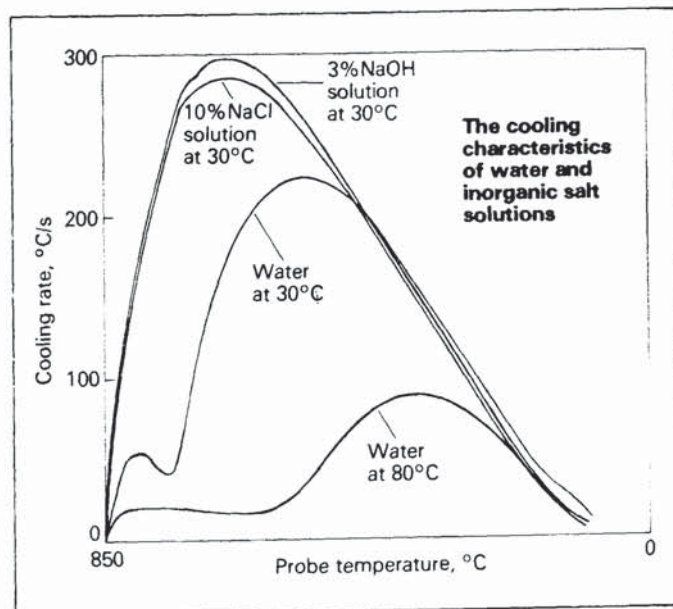


Figure 29. The cooling characteristics of water and inorganic salt solutions measured under non-agitated conditions by the Wolfson Engineering Group test⁽²⁶⁾.

The optimum temperature for water quenching has been found to be between 20 and 40°C, since the cooling capacity falls rapidly when the temperature of the water exceeds 60°C (*Figure 29*).⁽²⁶⁾ At the higher temperatures the vapour blanket phase (stage A) is prolonged, encouraging vapour entrapment and subsequent problems such as uneven hardness, distortion and cracking. By adding 5-10 weight per cent of common salt or soda to water, its cooling capacity is greatly increased due to destabilization of the vapour blanket, and its maximum rate of cooling is shifted to a higher temperature around 650°C (*Figure 29*). The main disadvantage with brine is its corrosive nature and the high alkalinity of caustic solutions can cause dermatitis. Contamination of water with salt tends to increase the cooling rate whilst soaps, algae, slimes or emulsion formers generally reduce the cooling rate.⁽⁴⁾

2.10.2 Quenching Oils. Oils can be formulated to provide a range of cooling rates, but oil quenching is generally much slower than water quenching as was seen in *Figure 28*. Although considerably more expensive than water, oils are often described by the heat treater as "more forgiving", i.e. they are less prone to cause cracking or soft spots when excursions in quenchant temperature or local variations in fluid velocity occur.⁽³³⁾

All modern quenching oils are closely fractionated, solvent-refined, paraffin-based mineral oils. These have much better ageing stability than naturally occurring fatty oils. The simplest and cheapest oil used for hardening is a straight mineral oil with a kinematic viscosity μ (i.e. dynamic viscosity/density) of around 20mm²/s at 40°C.⁽⁷⁵⁾ This type of oil is usually referred to as a spindle or normal speed cold quenching oil. By the introduction of certain additives which suppress the formation of a vapour blanket in the early stages, the cooling capacity can be considerably increased (accelerated oil). The additives used range from accelerating wetting agents such as metal sulphonates to antioxidants and detergents.⁽⁷⁶⁾ Furthermore, there are oils that are formulated to give good thermal and oxidation stability, for use at elevated temperatures up to around 200°C (hot quenching or martempering oils). A typical hot quenching oil would be a "dumb-bell" blend of two base oils with a kinematic viscosity of around 115mm²/s at 40°C. *Figure 30* gives typical cooling

characteristics for each class of oil tested using the Wolfson Engineering Group test at the standard conditions (i.e. unagitated at 40°C).⁽⁷⁷⁾ Proprietary oils are usually specified with reference to their physical properties such as viscosity, density and flash point.

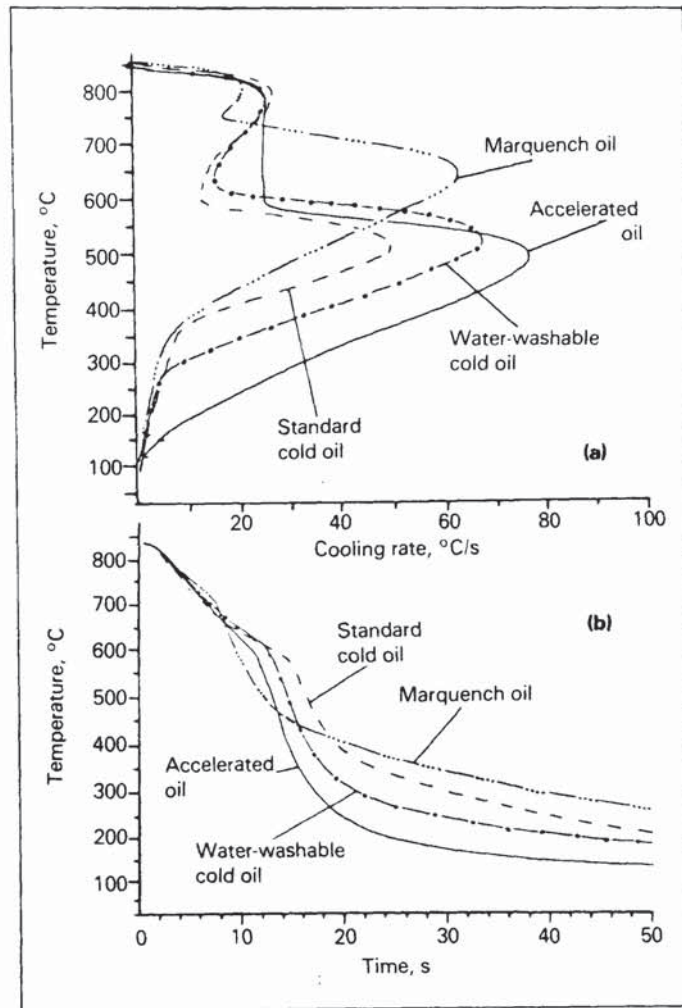


Figure 30. Cooling characteristics for different categories of quench oil measured at 40 °C using the Wolfson Engineering Group test⁽⁷⁷⁾.

The maximum cooling rate for oils generally occurs between 500-600°C, the cooling rate being relatively slow in the range of martensite formation. Since oil has a rather low capacity for heat extraction relative to water, its use as a quenchant for medium to low-alloy steels is restricted to light sections. A well established way of increasing the

cooling capacity of the oil is by vigorously agitating either the bath or the charge. This is demonstrated in *Figure 31* for a medium speed oil using the Wolfson Engineering Group test.⁽²⁶⁾ The agitation was created by a 75mm diameter two blade impeller used in conjunction with an H-shape baffle. Tests in which air bubbles are formed during the agitation of the quenchant have been found to be unsatisfactory, since the bubbles form a heat-insulating film and result in uneven hardening and even cracking.⁽⁷⁴⁾ Another way of increasing the cooling capacity is to raise the temperature of the oil to between 50-80°C. This increase in temperature reduces the viscosity of the fluid and thus results in enhanced heat transfer.

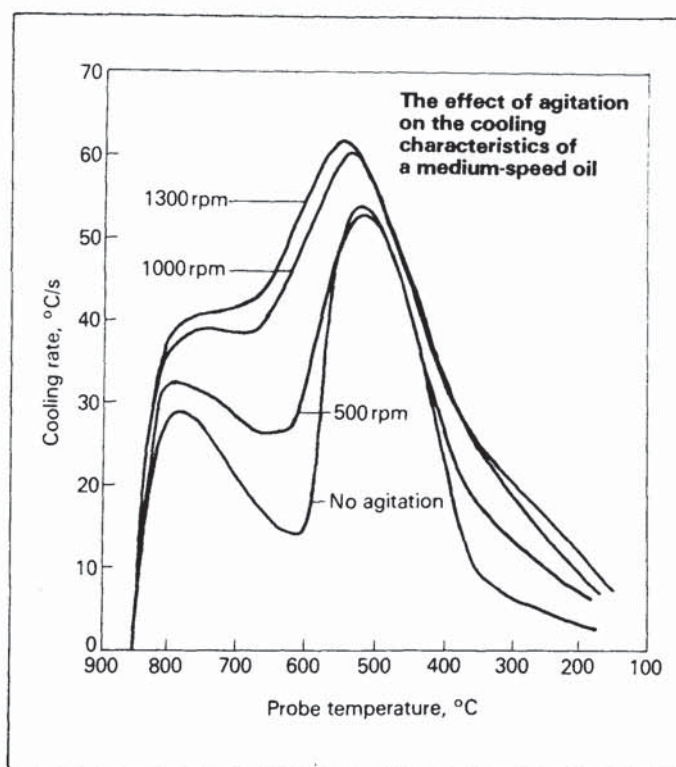


Figure 31. The effect of agitation on the cooling characteristics of a medium-speed quench oil tested at 40 °C. Agitation created by a two-bladed impeller used at the speeds indicated, in conjunction with an H-baffle⁽²⁶⁾.

There are a number of problems associated with using oils. The cooling characteristics of oils are known to change with age. Bashford and Mills⁽⁷⁶⁾ have highlighted this using a service simulation test in which oil samples were subjected to a repeated thermal shock cycle under oxidizing conditions. A schematic diagram of

the test rig used and typical results for a straight mineral oil are shown in *Figures 32a* and *32b* respectively. Other objections to the use of oil as a quenchant are the cost, its inability to rapidly quench parts, the surface residue left on parts, environmental problems and the fire hazard.

2.10.3 Emulsions. By mixing water and water soluble oil in various proportions, it is possible to obtain cooling media of various cooling capacities. As indicated by the comparison of cooling curves presented in *Figure 33*,⁽⁴⁾ water/oil emulsions combine the worst features of water and oil quenchants. An emulsion containing 10 per cent soluble oil and 90 per cent water is clearly seen to form massive vapour envelopes at the beginning of the quench cycle. Therefore, at the higher bath temperature 50°C, the initial severity of the quench is reduced to below that of conventional oil. Cooling in the latter stage corresponding with the critical martensite transformation range is essentially the same as water. For emulsions containing 90 per cent soluble oil and 10 per cent water, cooling rates are lower over the entire cooling range compared with conventional oil. If the water and oil are not properly emulsified, the water will collect at the bottom of the tank, and if rapid heating ensues, the generation of steam may give rise to an explosion. For these reasons oil and water emulsions are generally inferior to other quenchants.

2.10.4 Salt Baths. Salt baths made up of approximately equal parts of sodium nitrite and potassium nitrate are the most popular for cooling purposes. Salts are available to enable temperature ranges of 160-500°C and 500-600°C to be used.⁽⁷⁴⁾ *Figure 34* illustrates that molten salt cools faster than oil down to about 500°C.⁽⁷⁸⁾ This is due to the fact that there is no vapour phase in the cooling mechanism of molten salt. Salt bath quenching is particularly useful for steels having reasonably good hardenability (such as tool steels), and parts with not too heavy a section. The lower the bath temperature and the greater the agitation, the better is its cooling capacity. Contamination greatly reduces the salt bath's cooling efficiency and stirring keeps the foreign particles suspended in the molten salt. Consequently, it is better to move the quenched part in the supernatant molten salt and let the impurities sink to the bottom.

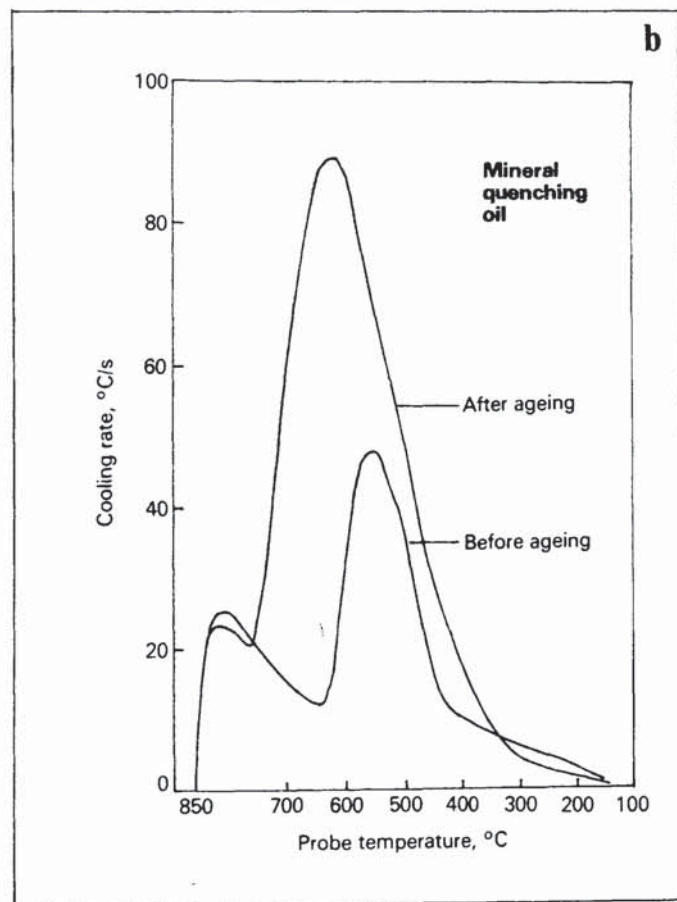
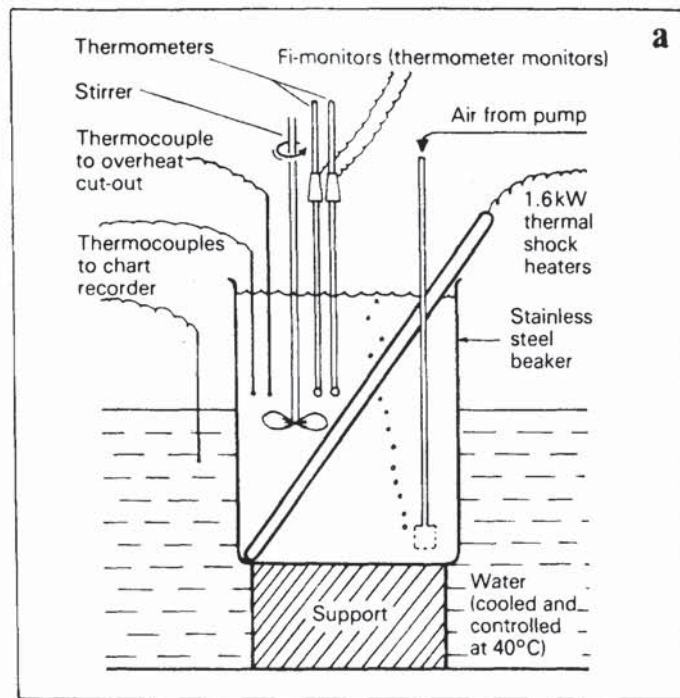


Figure 32. (a) The Edwin Cooper accelerated ageing test rig for oils, (b) typical results for a straight mineral oil before and after ageing determined using the Wolfson engineering Group test⁽⁷⁶⁾.

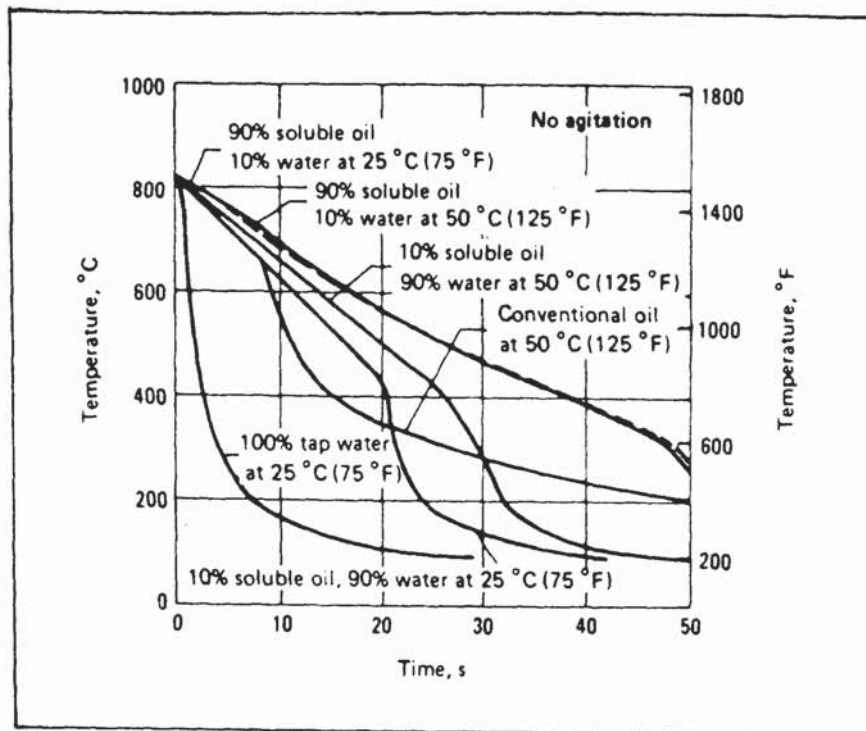


Figure 33. Cooling curves for the centre of an 18/8 stainless steel specimen (13mm diameter by 64mm long) on being quenched into non-agitated water, conventional oil, and soluble oil emulsions⁽⁴⁾.

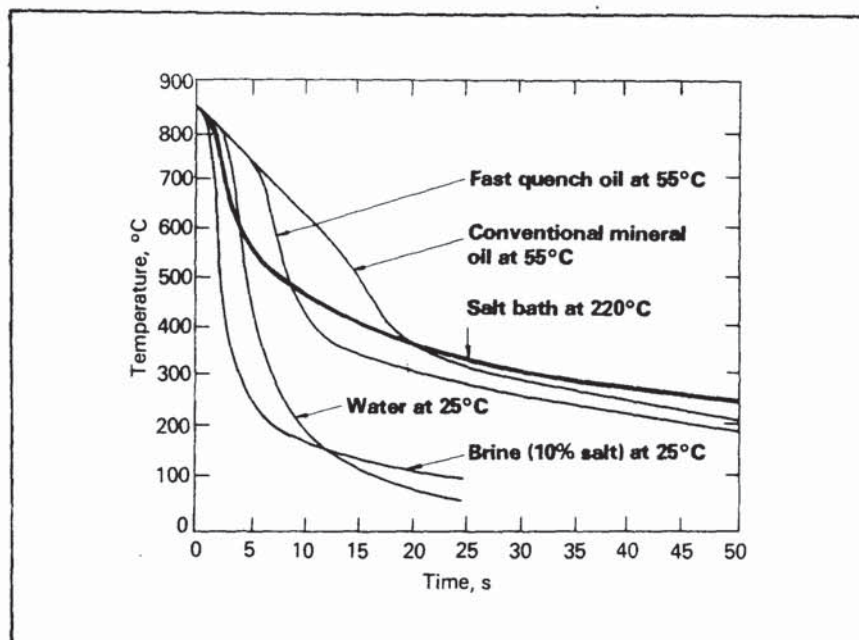


Figure 34 Cooling curves for the centre of an 18/8 stainless steel specimen (12.7mm diameter by 37.5mm long) on being quenched into a salt bath and non-agitated conventional quenching media⁽⁷⁸⁾.

The cooling capacity may be increased by adding water to the salt. The amount of water must be kept within close limits; 0.3-0.5 per cent approximately doubles the cooling capacity.⁽⁷⁴⁾ Care must be taken when adding the water to avoid the risk of explosion. For the same reason parts that have been treated in a traditional cyanide bath containing in excess of 10 per cent cyanide must not be quenched in a nitrite-nitrate bath.

2.10.5 Air-Gas Quenching. The typical composition of a conventional air-hardening structural steel is 0.3% C, 1.2% Cr, 4% Ni and 0.3% Mo. Such a steel would be wholly martensitic after air hardening in sections up to 100mm diameter. Nowadays, structural parts are rarely made in air-hardening steel on account of the high cost of the necessary alloying elements, and also because such steels must inevitably be annealed after forging or rolling and before subsequent machining.⁽⁷⁴⁾ In some applications, quenching in still air is too slow, and oil quenching undesirable because of distortion, cost factors, handling problems, or the final hardness obtained. In these applications gas quenching constitutes a useful compromise. Protective gases are now commonly used to avoid the oxidation problem associated with air. Low alloy steels in light sections and high alloy steels may be successfully hardened by means of compressed gas. The advantages of using gas are that distortion is negligible and that the steel can be easily straightened during the cooling process. Gas quenching is an essential feature of vacuum hardening, where pressures up to 500kPa (5 bar) are currently being applied. To ensure uniform cooling, the part is either rotated in a steady current of compressed gas which may be recirculated via a heat exchanger, or the gas flow direction periodically reversed. The cooling rate is related to the surface area and mass of the part and to the type, velocity and pressure of the cooling gas. The cooling rate can be adjusted and controlled by altering the last two of these variables.^(4,79)

Compressed gas also comprises a vital component in the relatively new technique of quenching into fluidized beds.⁽⁸⁰⁾ Fine aluminium oxide (alumina) particles are fluidized in the gas stream. Fluidized beds at ambient temperature exhibit cooling rates between those of oil and air, whilst heated beds offer a medium for

marquenching and austempering operations.

2.11 Polymer Quenchants

The term "polymer quenchants" is relatively new. It is only in the last thirty years that certain water-soluble organic polymers have been found to be useful in modifying the cooling characteristics of water, and less than twenty years since the most widely-used type of polymer quenchant was first marketed in the UK.

Initially, insufficient basic understanding and experience with polymer quenchants resulted in operational problems and cracked components; consequently, heat treaters were reluctant to change over from the tried and tested traditional quenching media. However, improved polymer products and greater understanding have led to a progressive increase in their usage over the last decade, for the quenching of both ferrous and non-ferrous materials. Today, polymer quenchants account for approximately 15 per cent of the quenchant market,⁽⁸¹⁾ and it has been predicted that they will surpass oil in use before the turn of the century.⁽⁸²⁾

The advantages of polymer quenchants have been outlined by numerous authors and include:-

- (1) **Reduced fire hazard:** the principal advantage of polymer quenchants is the elimination of the oil fire hazard. A disturbing number of heat treatment shops have been badly damaged or totally destroyed as a result of oil fires. Ignition of the quench oil generally occurs when the hot components are not fully immersed (usually due to mechanical failure of the lowering gear or low oil levels in the tank), or when quenching into very high viscosity oils which do not rapidly distribute the heat.⁽⁴⁾
- (2) **Flexibility in operation:** by controlling the concentration, temperature and agitation of the polymer solution, it is possible to achieve a range of cooling rates, thus enabling a wide variety of materials and components to be quenched.
- (3) **Lower quenchant costs:** polymer quenchants are generally supplied as concentrated solutions. The purchase cost of these solutions is higher than oil per unit volume, but the polymer concentrates are subsequently further diluted, resulting in an

overall cost saving. The concentrates contain an unstated volume of water which is required to aid handling and further dilution. Compared with increasingly expensive refined quenching oil, polymer quenchants are produced from cheaper petrochemical feedstocks, natural gas and, in some instances, coal.⁽⁸³⁾

(4) Cleaner environment: heat treatment shops are notoriously dirty places, with oil spillages, sludge and scale particular problems. Certain oil products are also known to be carcinogenic and can cause dermatitis. Polymers result in a much cleaner and safer working environment, with the noxious smoke and fumes produced during oil quenching being replaced by steam. This is clearly illustrated in *Plates 1* and *2* which compare typical oil and polymer quench installations.⁽⁸⁴⁾ In the USA, a number of companies have been banned from using oils by the Environmental Protection Agency, and in this country more stringent rules may be introduced by the Health and Safety Executive.⁽²⁹⁾

(5) Reduced process costs: other factors to be considered in the overall economics of use include the cost of post-quench treatments, quenchant quality control, maintenance procedures, disposal, life of equipment, part inspection and insurance costs. On balance, these usually favour polymer quenchants.⁽⁸²⁾ In particular, products quenched in polymer solution do not require degreasing prior to further treatment and insurance premiums may be considerably lower because of the reduced fire risk.⁽²⁹⁾ Polymer quenchant solutions have almost double the specific heat of mineral quench oils. Higher productivity is thus possible, since the temperature of the quenchant will rise only half of that of the same volume of oil, for a given charge weight.

Even though polymer quenchants offer all these advantages, they are by no means the answer to all the heat treater's problems. Since polymer quenchants are aqueous solutions, they generally exhibit faster cooling rates, compared with oils, through the critical martensite transformation temperature range. Therefore, polymer solutions are used predominantly for applications requiring rates of cooling intermediate between those of water and normal-speed oils.⁽⁴⁾ This obviously precludes the treatment of certain materials, particularly high carbon or high alloy steels, and also components with surface defects or stress raisers.⁽²⁹⁾



Plate 1. Illustration of the flame and smoke hazard when quenching into oil, even when using a damper shield.⁽⁸⁴⁾



Plate 2. Quenching into a 20 per cent PAG solution following conversion to a polymer quenchant.⁽⁸⁴⁾

(Above photographs reproduced by courtesy of both Edgar Vaughan and Co. Ltd., and Flather Bright Steels Ltd., Telford.)

Closer control of the quench tank conditions and more frequent monitoring is also required for the successful application of polymer products.

Although all polymer quenchants have some similarities, they also exhibit significant differences depending on their composition. Relatively few papers have been published concerning the cooling characteristics of polymer quenchants, those available tending to be by authors working for polymer quenchant suppliers, with a natural bias towards their own products. Accordingly, direct comparison of the results is difficult since, as this review unavoidably illustrates, the authors use a range of thermocouple techniques, test conditions, and methods of indicating polymer concentration (complicated by the use of as-supplied concentrates of normally unspecified make-up). Whereas the patent literature has described numerous potential polymer candidates, in reality only four classes of product have achieved commercial prominence as quenchants in the Western world.⁽⁴⁾ These main classes of polymer will now be discussed in order of historical precedence.

2.11.1 Polyvinyl Alcohols (PVA). Aqueous solutions of polyvinyl alcohol were first described as quenching media in US patent 2,600,290, issued in 1952,⁽⁸⁶⁾ PVA having been first synthesized in Germany in 1925.⁽⁸⁷⁾ In producing PVA resin, a multi-step process is used since the vinyl alcohol monomer, $\text{CH}_2=\text{CHOH}$, rapidly rearranges to form acetaldehyde, CH_3CHO . Thus, it is first necessary to produce polyvinyl acetate resin from vinyl acetate monomer, and follow with alcoholysis of the polyvinyl acetate to PVA. These reactions are illustrated in *Figure 35*.⁽⁸⁷⁾

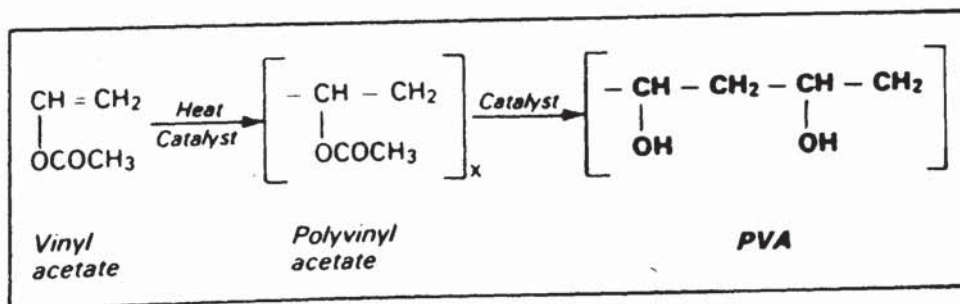


Figure 35. The synthesis of polyvinyl alcohol (PVA)⁽⁸⁷⁾.

Chemically, PVA can be classified broadly as a polyhydric alcohol with secondary hydroxyl groups on alternate carbon atoms. As is true with most polymeric materials, variations in structure or composition can have a profound effect on characteristics and hence end-use. PVA is a solid, its solubility in water depending upon molecular weight and the extent of residual polyvinyl acetate. The degree of hydrolysis can govern commercial applications and may vary from partial (87-89%) through fully hydrolysed (95%) to "super" hydrolysed (99.7%). The principle uses of PVA include paper and textile sizes, solvent-resistant films, adhesives, emulsifiers, and as an intermediate for the manufacture of polyvinyl butyral, a safety glass laminate.

2.11.1.1 Cooling characteristics of PVA solutions.

PVA was introduced in the mid 1950's as an additive to water to modify its rate of cooling.⁽⁸⁸⁾ The concentrations used in practice range from 0.05-0.30 weight per cent; for convenience in handling, an aqueous concentrate is used. As the curves in *Figure 36* illustrate, only slight variations in solution concentration are needed to produce significant changes in the cooling characteristics of PVA solutions and, accordingly, close control is necessary for successful quenching. At concentrations of less than 0.01 weight per cent, the cooling characteristics at room temperature are only moderately different from those of water alone.

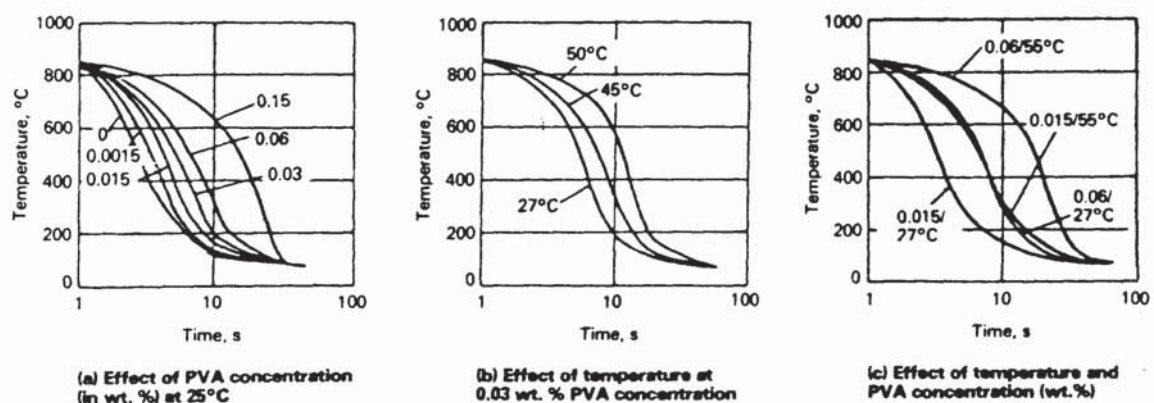


Figure 36. Cooling curves for aqueous PVA solutions as a function of concentration and temperature⁽⁴⁾. Measured by a thermocouple at the geometric centre of type 304 stainless steel (19% Cr, 10% Ni, 0.08% C) specimens (13mm diameter by 100mm long) quenched under non-agitated conditions. Water hardness 130ppm.

Only a limited number of industrial PVA quench installations remain today, because of major concentration control problems which arise from the formation of crusty residues on components.

2.11.2 Polyalkylene Glycols (PAG). Polyalkylene glycols, or polyalkylene glycol ethers, were first sold commercially by Union Carbide, under the trademarks Ucon and Prestone, as synthetic lubricants for industrial and automotive use in the early 1940's.⁽⁸⁹⁾ These neutral or nonionic materials are formulated by the random polymerization of ethylene and propylene oxides as shown in *Figure 37*. (Higher alkylene oxides and/or aryl oxides may also be used). The original Ucon LB and D series products were insoluble in water, whilst the 50HB and 75-H products were water soluble and led to the development of aqueous quenchants. Roberts and Fife⁽⁹⁰⁾ stated that a water soluble polyethylene-polypropylene derivative could be prepared by adding aldehyde-free ethylene oxide and propylene oxide to aliphatic monohydric alcohols (such as methanol and butanol), in substantially anhydrous conditions at 80-160°C and a pressure of 35 to 350kPa (5-50psi). Block polymerizations of these same oxides are possible but these derivatives are more costly to manufacture and less attractive as quenchants. By varying the molecular weights and the ratio of oxides, polymers having broad applicability may be produced. PAG's find use in a wide range of applications including cosmetics, hydraulic fluids, lubricants and heat transfer agents.

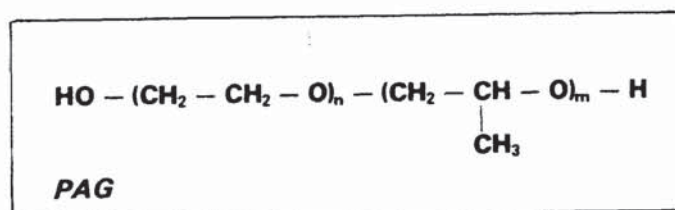


Figure 37. The molecular structure of polyalkylene glycol (PAG) derived from the random polymerization of ethylene and propylene oxides⁽⁸³⁾.

Some of the higher-molecular weight derivatives (12,000-14,000) were shown by Blackwood and Cheesman⁽⁹¹⁾ to have utility as metal quenchants when used in

aqueous solutions. Commercial introduction of PAG quenchants occurred during the mid 1960's⁽⁹²⁾ and today they hold 90 per cent⁽⁸¹⁾ of the market for polymer quenchants as a whole. These products exhibit inverse solubility in water, i.e. they are completely soluble in water at room temperature, but insoluble at elevated temperatures. This phenomenon provides the mechanism of cooling hot metal by surrounding it with a polymer-rich coating that governs the rate of heat extraction, but, once the metal has been cooled, the polymer goes back into solution. PAG quenchants are available with inversion temperatures ranging from 71 to 88°C.⁽⁹³⁾ The inverse solubility phenomenon is not well understood; the only published attempts to describe the mechanism for PAG quenchants have been by the present author, and will be described in detail later.^(36,85)

Commercial PAG quenchants contain a number of additives such as inhibitors, defoamers and bactericides, all of which affect the cooling characteristics.⁽²⁸⁾ Rusting can be a serious problem where recirculation of treated water is not employed. PAG solutions are inhibited to provide corrosion protection of the quench system components. Commercial products typically contain approximately 2.5 per cent sodium nitrite as a rust preventative,⁽⁹⁴⁾ although a number of manufacturers are now producing more complex nitrite-free inhibitors because of the likelihood of future legislation banning the use of nitrites on the grounds of health and safety.^(95,96) However, care must be taken to avoid mixing polymer products which contain nitrites and those which are nitrite-free, since a reaction between the inhibitors could produce potentially carcinogenic nitrosamines. These inhibitors are subject to depletion in service, so there is no guarantee that corrosion protection will last indefinitely. Sample analyses can provide the guidance needed for supplemental inhibitor make-up, the quenchant supplier usually providing this service.⁽⁹⁷⁾ Corrosion inhibition imparted to quenched parts will be of short duration, so that specific protection should be provided following the tempering operation.⁽⁴⁾

The wetting characteristics of PAG quenchants can be enhanced by the addition of water soluble alcohols, glycols or glycol ethers with 2-7 carbon atoms,⁽⁹⁸⁾ but control

of these multicomponent systems becomes more complex since these low boiling point additives are quickly depleted.

2.11.2.1 Cooling characteristics of PAG solutions.

In the application of PAG quenchants for heat treating, three principal parameters are recognized to control the rate of cooling:

- (1) quenchant concentration
- (2) quenchant temperature
- (3) quenchant agitation

The influence of each of these parameters on cooling rate has been shown schematically, in the form of cooling curves, by Blackwood and Mueller⁽⁹³⁾ (*Figure 38*). The slower rates of cooling achieved at the higher concentrations reflect the thickness of the precipitated polymer-rich layer that surrounds the heated part during quenching. Mason and Lake⁽⁹⁹⁾ showed a linear decrease in maximum cooling rate with increased concentration as illustrated in *Figure 39*.

The cooling rate of PAG solutions can thus be varied to suit particular requirements by simply changing the concentration. One source⁽⁸⁴⁾ gives the following general guidance:

- (a) Low concentrations of up to 5 per cent improve wettability on the component surface, thereby imparting a more uniform quench and preventing problems of soft-spotting frequently associated with water quenching.
- (b) Solutions of 10-20 per cent achieve quenching rates comparable to those of fast quenching oils, and are therefore suitable for low-hardenability applications where maximum mechanical properties are required.
- (c) Solutions of 20-30 per cent offer cooling rates to suit a wide range of through-hardening and case-hardening steels.

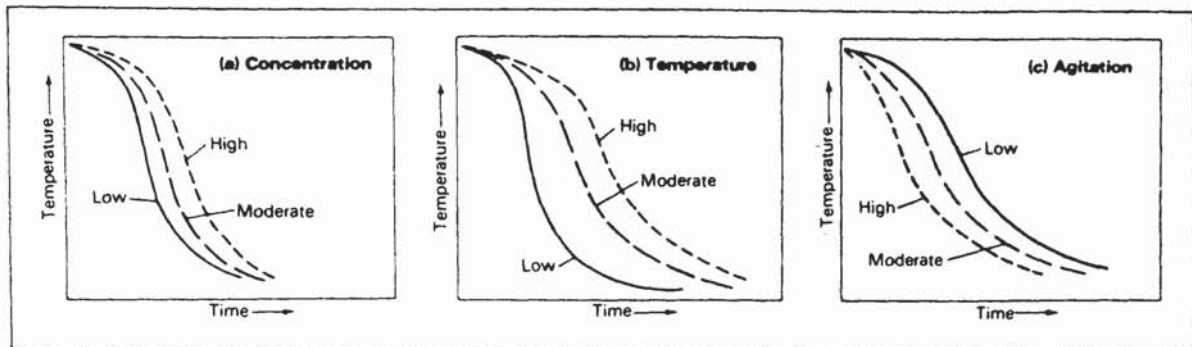


Figure 38. Schematic representation of the effect of (a) concentration, (b) temperature and (c) agitation on the cooling characteristics of a typical PAG solution^(4,93).

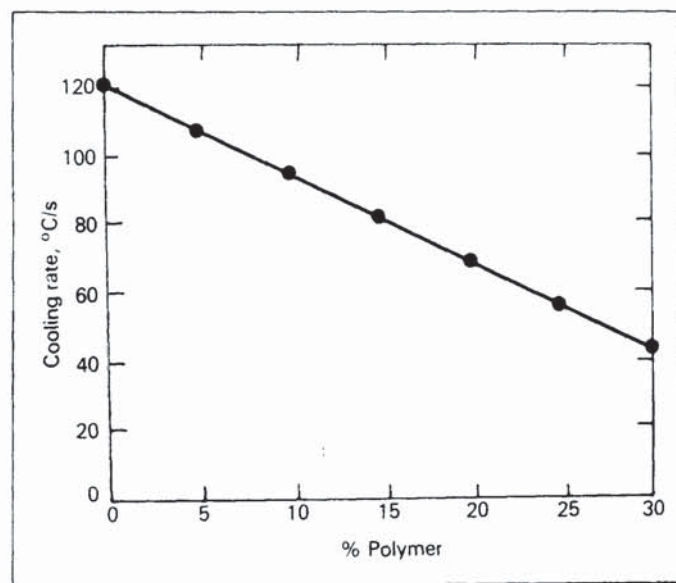


Figure 39. Effect of concentration of PAG solutions on maximum cooling rate as measured using the Wolfson Engineering Group test, but with an austenitic stainless steel probe⁽⁹⁹⁾.

PAG quenchants are claimed by Metals Handbook⁽⁴⁾ to be less sensitive to minor fluctuations in polymer concentration than polyvinyl alcohol solutions.

Just as water exhibits a marked decrease in cooling capability as its temperature is elevated, this same loss is translated to aqueous PAG solutions (*Figure 38b*). One of the disadvantages when using plain water above about 50°C as a quenchant is the prolonged vapour blanket phase, stage A. This prolongation could produce vapour entrapment which may result in uneven hardness and unfavourable distribution of stress, which in turn may cause cracking and/or distortion. By using PAG quenchants, uniform wetting of the metal surface results, thus avoiding the problems.⁽⁴⁾

In the heat treatment of precipitation-hardenable aluminium alloys, quenching from the solution treatment temperature (typically 470-565°C) is aimed at avoiding pre-precipitation effects and retaining hardening elements in solid solution so that controlled hardening/strengthening is promoted on ageing. Several authors⁽¹⁰⁰⁻¹¹⁰⁾ have described how distortion problems associated with quenching aluminium alloys have been minimized by replacing water baths with those containing PAG solutions. The American Aerospace Metals Engineering Committee (AMEC), reflecting the consensus of major airframe manufacturers and the US Government, provides specification guidelines for the use of both single polymer (Type I) and multiple polymer (Type II) PAG quenchants.⁽¹¹¹⁾ The most critical temperature range in the quenching of these alloys is from 400-250°C. It is between these temperatures that undesirable precipitation of the solute phase is most likely to occur if cooling is too slow, resulting in lower corrosion resistance and reduced mechanical properties on subsequent ageing. Suttie⁽¹⁰⁷⁾ showed that an 11 per cent PAG solution gave a similar cooling rate to 25°C water over

the critical temperature range, but was slower below 250°C, thereby reducing thermal stress and hence distortion. Other advantages of PAG solutions for the heat treatment of aluminium alloys include greater freedom of design because configurations of thick and thin sections can be considered, and the elimination of costly heated tanks and post quench straightening or machining operations. The last point has the added bonus that the compressive layer formed during quenching can be maintained in the fully-machined condition.

Mechanical refrigeration to maintain PAG solution temperatures below 25°C may provide performance benefits for aluminium alloys. At the other extreme, massive sections of high-hardenability alloy steels may require both high quenchant concentrations and high bath temperatures to avoid undue stress in the component. For certain crack sensitive parts of AISI 5160 (0.6% C, 0.88% Mn, 0.22% Si, 0.8% Cr), quenching at a bath temperature of 70°C was found to be the best answer.⁽⁹³⁾ However, care must be taken to prevent the temperature of the bath exceeding the inversion point for the polymer.

Agitation is considered to be critical for the successful use of PAG quenchants, as stated by many authors.^(4.11.26.34.35.112-119) Different rates of agitation, via variable-speed pumps or propeller agitators, provide flexibility where parts of different sizes, mass, geometry, etc., are processed. It is now fairly well established that as the level of agitation is increased, the cooling curves are shifted to more rapid rates as seen in *Figure 38c*. A paper by the present author has highlighted that the effectiveness of the agitation depends not only on the fluid velocity but also on the nature of the flow pattern with respect to the quenched piece.⁽³⁵⁾ Early Wolfson Engineering Group quench tests by Close,⁽²⁶⁾ for a PAG solution agitated using an impeller/baffle system were found to be inconsistent (*Figure 40*).

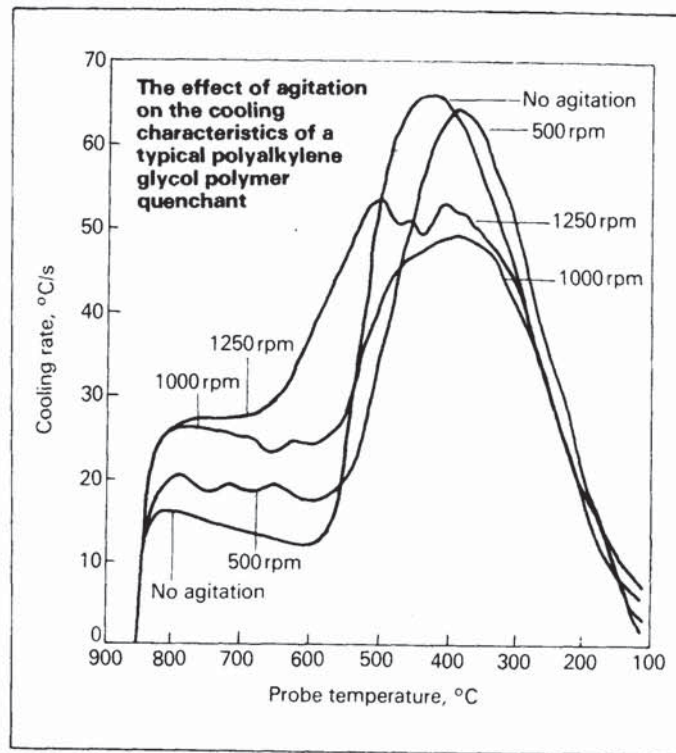


Figure 40. The effect of agitation on the cooling characteristics of a 25% solution of a typical PAG tested using the Wolfson Engineering Group method at 40 °C. Agitation created by a two-blade impeller used at the speeds indicated, in conjunction with an H-baffle⁽²⁶⁾.

Mason and Capewell⁽³⁴⁾ later used a pump agitation system based on a design by Heins and Mueller,⁽¹⁶⁾ shown in Figure 41. Their results for a 20 per cent PAG solution at 40 °C (Figure 42) exhibited the same basic trends as those reported by the present author, who used a considerably smaller system. Unfortunately direct comparison of the results was not possible since different test conditions were used. The maximum cooling rate is increased with increased fluid velocity, whilst the duration of stage A is decreased until instantaneous nucleate boiling occurs. In general, low to moderate agitation is believed essential in order to (a) ensure that adequate replenishment of polymer occurs at the hot metal surface and (b) provide uniform heat transfer from the hot part to the surrounding reservoir of cooler quenchant. Vigorous agitation may be essential for achieving a rapid cooling rate, such as may be required with a low-hardenability steel to avoid undesirable transformation products.⁽⁴⁾

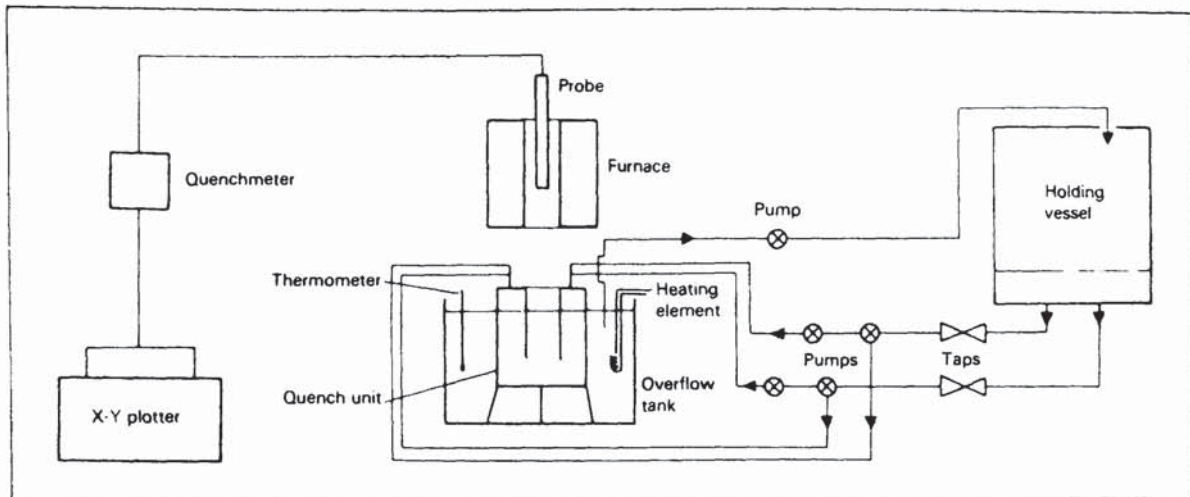


Figure 41. West Bromwich College of Commerce and Technology test system, agitation created by 4 pumps in 2 parallel circuits.(Minimum sample volume:25 litres)⁽³⁴⁾.

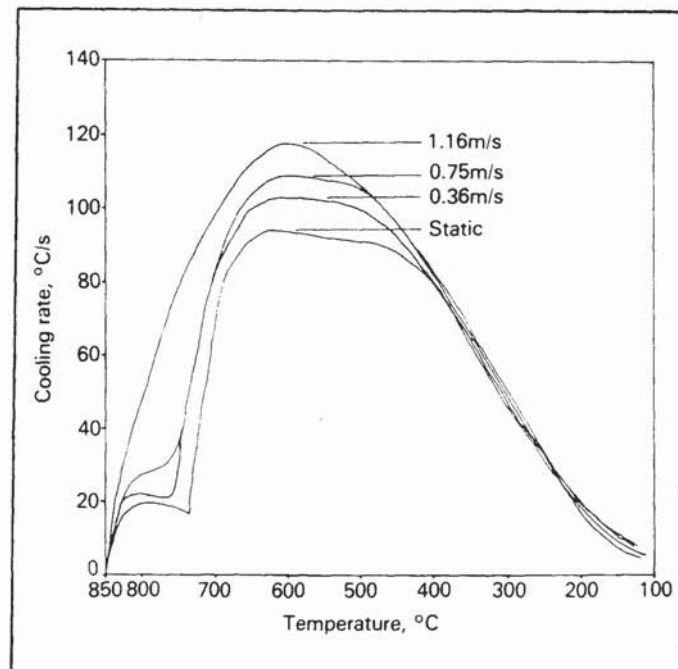


Figure 42. Effect of quenchant flow rate (employing the system illustrated above) on the cooling characteristics of a 20% PAG quenchant at 40 °C using the Wolfson Engineering Group test⁽³⁴⁾.

Monroe and Bates⁽³³⁾ found that PAG solutions were more sensitive to changes in temperature and agitation than oil or water, and that the optimum conditions for a 16 per cent solution were bath temperatures between 25 and 30°C, with agitation to produce fluid velocities of 0.5 to 1.0m/s, resulting in quench severity factors H ranging from 1.1 to 1.3. These values were higher than those produced by oil, but lower than those achieved with water at the same temperature and velocities. Higher bath temperatures or inadequate agitation resulted in lower values of H, in the range 0.15 to 0.5.

2.11.2.2 PAG quench tank control measures.

Certain routine maintenance practices are required with all polymer quenchant solutions to ensure that the proper concentration is maintained at all times.⁽⁸³⁾ The refractive index of PAG solutions (in the range employed for quenching), is essentially linear with concentration. Relatively small hand-held optical refractometers that employ an arbitrary scale and which are capable of being calibrated, are used.⁽⁴⁾ Whereas such instruments prove invaluable for day-to-day monitoring of the concentration, water-soluble contaminants alter the refractometer readings.⁽¹¹³⁾

Seegerberg⁽¹²⁰⁾ has recently questioned the validity of refractometer readings, by comparing the cooling data for a polluted polymer quenchant with that for a freshly made-up solution with the same refractive index (*Figure 43*). The polluted solution produced highly inconsistent cooling characteristics. No indication was given of the nature of the pollution, or even the test conditions for the solutions. Foreman⁽⁸²⁾ has reported that the refractometer reading increases with thermal degradation. Thus, it is clear that back-up procedures are necessary to verify (or correct) the refractometer reading.

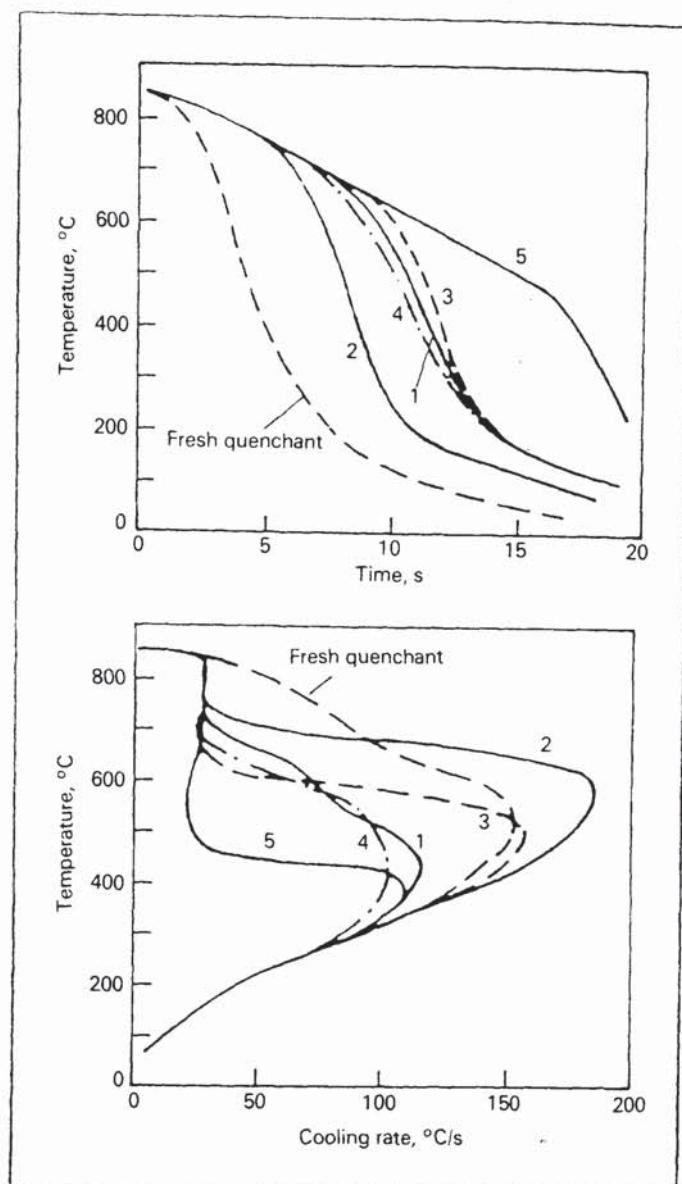


Figure 43. Results of Wolfson Engineering Group test on polymer solutions with the same refractive index, comparing fresh quenchant with polluted quenchants (curves 1-5)⁽¹²⁰⁾.

With PAG quenchants, kinematic viscosity measurements (which are correlated with concentration) have proven to be the most useful,^(4,83) although specific gravity measurements may also be utilized.⁽⁹⁵⁾ Other analytical tests, such as the measurement of pH (for alkalinity), inhibitor level (for corrosion protection), and specific conductance (for inorganic salt concentration), are useful adjuncts to monitoring polymer quenchant facilities. These latter tests are generally required at reduced time frequency intervals.⁽⁸³⁾

2.11.2.3 Contamination of PAG quenchants.

Both Burgdorf⁽²⁸⁾ and Mueller⁽¹²¹⁾ have investigated the effect of contamination on PAG quenchants. Burgdorf considered the influence of several types of contaminant on cooling curve performance. It was found that the quenching characteristics of a 10 per cent PAG solution were strongly influenced by certain contaminants such as oils, caustic soda and ammonia (a constituent of carbonitriding atmospheres), whilst others, such as soot, scale or nitrate-containing cleaner had little or no effect. Oil contaminants resulted in a longer stage A phase or, in other words, the start of the nucleate boiling phase (stage B) was delayed, as illustrated, for contamination by a rust-preventive oil in *Figure 44a*.

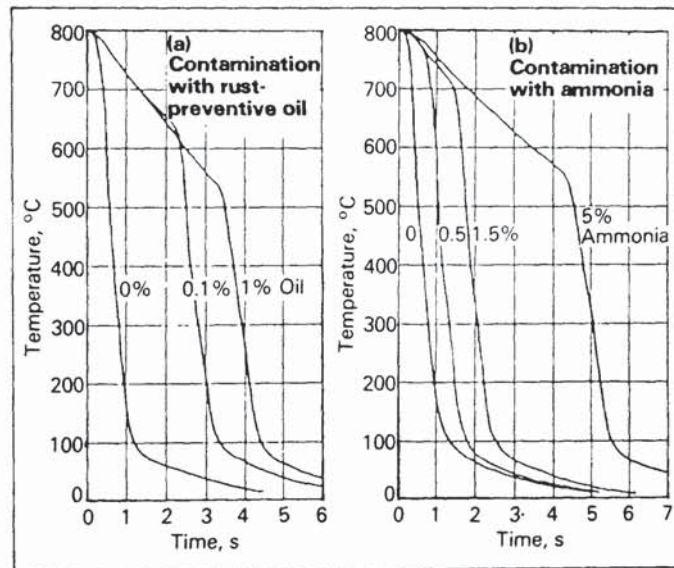


Figure 44. Cooling curves for a 10% PAG solution, at 20°C with moderate agitation, contaminated with (a) a rust-preventive oil and (b) ammonia. Curves produced using the drasticimeter technique with a silver test probe 8mm diameter by 24mm long⁽²⁸⁾.

Ammonia has a high solubility in water and was found to have a significant effect, considerably decreasing the cooling rate at the upper temperature range of the quenching process (*Figure 44b*). This was thought to be due to the formation of stable vapour films on the surface of the hot metal, similar to the case of oil-contaminated solutions. Carbon

dioxide and carbon monoxide, which are also constituents of controlled furnace atmospheres, were also found to exhibit similar effects, but on a much smaller scale, since under normal pressures these gases have a much lower solubility. These results were obtained using the 8mm diameter by 24mm long silver drasticimeter test piece which was subsequently found unreliable for aqueous quenchants and superceded by the diacpot test with a larger specimen.

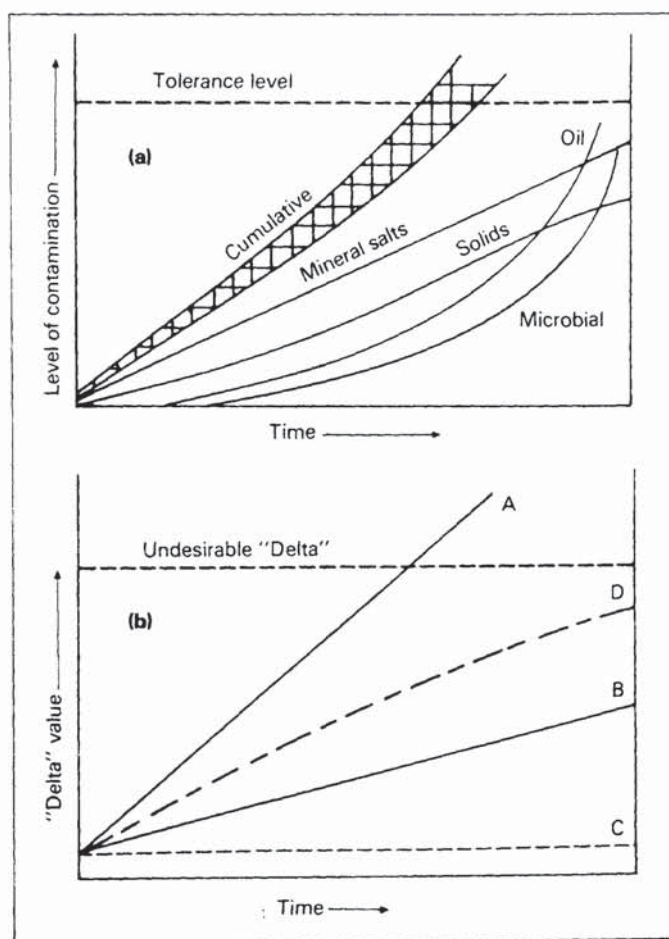


Figure 45. Schematic representation of the influence of contaminants on useful life of polymer quenchants: (a) life span of a polymer quenchant with low maintenance; (b) "delta" accumulation as a function of water quality⁽¹²¹⁾.

Mueller⁽¹²¹⁾ outlined the five principal reasons that could lead to the disposal of PAG quenchant solutions (although it is likely that most of these factors would also apply to all types of polymer quenchant):

- (1) Solids contamination (e.g. scale, soot)
- (2) Tramp fluids build-up (e.g. oils, hydraulic fluids)
- (3) Biological contamination (e.g. bacteria, fungi, moulds)
- (4) Dissolved materials (e.g. inorganic salt from water make-up or from salt bath carry-over; water-soluble organic materials; dissolved gases)
- (5) Breakdown of the polymer.

In a situation where contaminant levels increase with time, there must be a specific tolerance level as illustrated in *Figure 45a*. The extent of tolerable contamination in any one system is governed by a multitude of factors including the crack sensitivity of the quenched material, the geometry of the part, the influence of quenchant flow, the functioning of mechanical conveyors, elevators, etc. As was described by Burgdorf, scale and soot have little effect on the cooling characteristics, but can result in abrasive wear of pumps and heat exchangers, etc. Tramp fluids, such as residual oils, can have a significant effect on the cooling characteristics as was shown in *Figure 44a*.

Any aqueous polymer solution is susceptible in use to bacterial and/or fungal infection via air-borne or other inoculation. The growth of micro-organisms can cause fluid deterioration, corrosion and physical plugging of circulation lines. In addition, the appearance of slime and/or the generation of foul odours can seriously influence working conditions. Single-polymer PAG quenchants are simple mixtures of polymer, water and corrosion inhibitor. PAG's are bioresistant so that they do not represent a nutrient for biological growth under normal quenching practices. By avoiding complex multi-component systems, the possibility of susceptibility to biodegradation is inherently reduced. Recently, Blackwood et al⁽¹²²⁾ carried out a survey to determine the frequency of microbiological activity in single polymer PAG quenchants. Commercially available agar-coated bio-dip-sticks were employed, and 80 per cent of the

systems tested showed some biological activity. However, for only a small percentage of these was a biocide addition thought necessary. Thus it was concluded that, although microbiological contamination is prevalent in many quench systems, PAG's will not support bacterial growth, and biocides are rarely required.

Mueller⁽¹²¹⁾ believes that the most prevalent source of contamination in a polymer quenchant system, and yet the least likely to be recognized, is the accumulation of inorganic salts from the water used for the initial solution and make-up. The hardness of the water used is not critical, since PAG's are nonionic and hence not influenced by the presence of calcium or magnesium salts. Rather, the concern lies with the accumulation of all inorganic salts that concentrate in the quenchant as water evaporates during normal quenching practice. Softening the water is thus not the answer; ideally, deionization or reverse osmosis should be employed to reduce the total dissolved solids.

Mueller⁽¹²¹⁾ has introduced the concept of a "delta " value which quantifies the extent of contamination and is defined as the difference in concentration measured by refractometer and the effective concentration measured by viscosity. *Figure 45b* illustrates the method of determining contamination tolerances. Curve A represents either a high rate of water make-up (high evaporation), or a high level of salt in the make-up, or both. Obviously, the delta accumulation is most rapid. Curve B relates to some lower level of salt content and/or a lower make-up level. Curve C reflects the use of deionized water where the rate of make-up is not a factor. Curve D represents a water of some known hardness level where, upon evaporation, the solubility limits of the calcium and/or magnesium salts are reached. When this occurs, the salts precipitate out from solution and either accumulate as sludge or are removed by filtration. Thus, the salt accumulation is not a straight line function, but some curved measure of delta development that could eventually end in an equilibrium plateau.

The inverse solubility of PAG's can provide a unique advantage when it becomes necessary to isolate the quenchant from certain contaminants. In the aerospace industry, for example, where quenching from nitrite-nitrate salt baths is practised, the carried-over salts can be removed by thermal separation where necessary, although in practice the presence of a certain amount of salt in the PAG solution has been found tolerable. There is a discrepancy in the literature regarding this critical salt tolerance level. Von Bergen⁽⁹⁵⁾ and Simmonds⁽¹²³⁾ claim salt levels up to between 12 and 14 weight per cent are acceptable, whereas Anderson et al⁽¹²⁴⁾ claim the level to be between 3 and 5 per cent. It must be noted that the first two workers represent PAG quenchant manufacturers, whilst the latter market a system for salt separation. Thermal separation simply involves heating the polymer solution to a temperature above its inversion point at which stratification occurs. The separation is not one hundred per cent efficient due to the chemical properties of the PAG, and approximately 2-5 per cent polymer remains with the separated salt-rich aqueous layer, which can be removed and discarded.⁽¹²⁵⁾

Croucher et al^(124,125) have examined the use of ultrafiltration as a means of separating the PAG concentrates at room temperature. Goettsh et al⁽¹²⁶⁾ have recently given more precise details about this technique. At the heart of the system described in *Figure 46* are eight spiral-wound membrane elements containing a composite membrane through which water and most salt, but not polymer, will pass. The output is dependent on the surface area of the membrane, PAG concentration, temperature, operating pressure and the ratio of permeate to feed flows. It is important to remove suspended solids prior to entry into the membrane system to prevent fouling, and inhibitor is lost during the process. Nevertheless, ultrafiltration systems are claimed to be more economical than heat separation systems, and more efficient by providing a more complete

polymer separation. A pay-back time of less than one year is claimed, due mainly to PAG and energy savings.

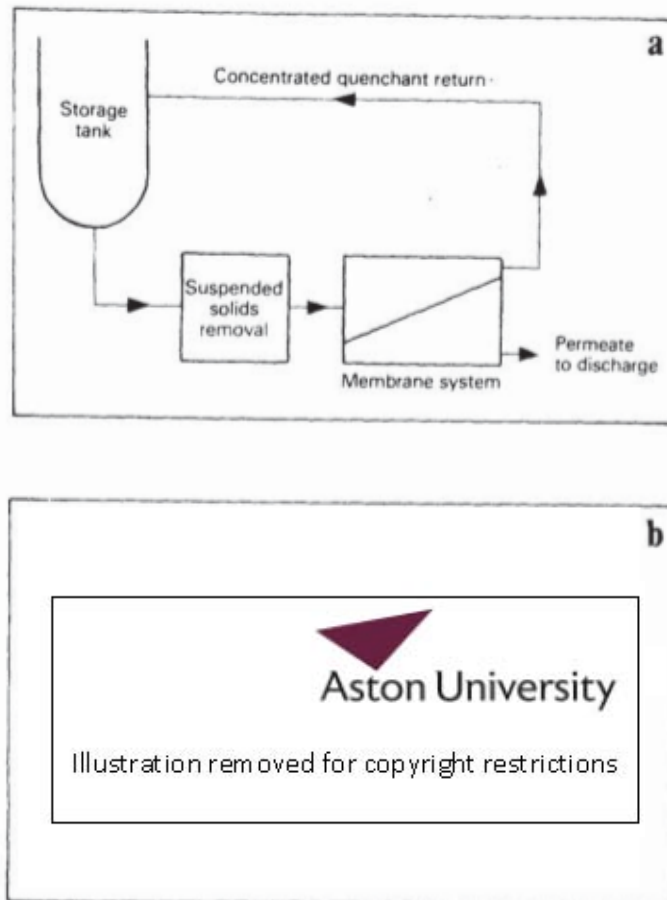


Figure 46. (a) Schematic illustration of the membrane separation process for polymer quenchants; (b) cutaway view of spiral-wound element⁽¹²⁶⁾.

2.11.2.4 Ageing of PAG quenchants.

Burgdorf⁽²⁸⁾ and, more recently, Kopietz⁽⁹⁴⁾ have considered the effect of ageing on the cooling properties of PAG solutions. Both authors reported the same basic trends. After prolonged use, the film boiling phase (stage A) was extended and the cooling rate during the convection phase (stage C) was considerably increased, resulting in a greater risk of quench cracking. Kopietz compared five commercial PAG quenchants from industrial units after prolonged use (one over 14 years!) with freshly-prepared solutions of the same concentration. *Figure 47* compares time-temperature and cooling rate-temperature curves for a 23.5 weight per cent

PAG solution tested as new and after short-term use. The used solution exhibits a faster cooling rate in the convection stage, following a general tendency observed in other tests. Kopietz concluded that the reason for this increased quenching effect in used PAG solutions could be depolymerization, oxidation and certainly contamination. He did not attempt to analyse the degradation products. On the basis of personal experience, he did not believe that mechanical shearing of the polymer molecule played a major role.

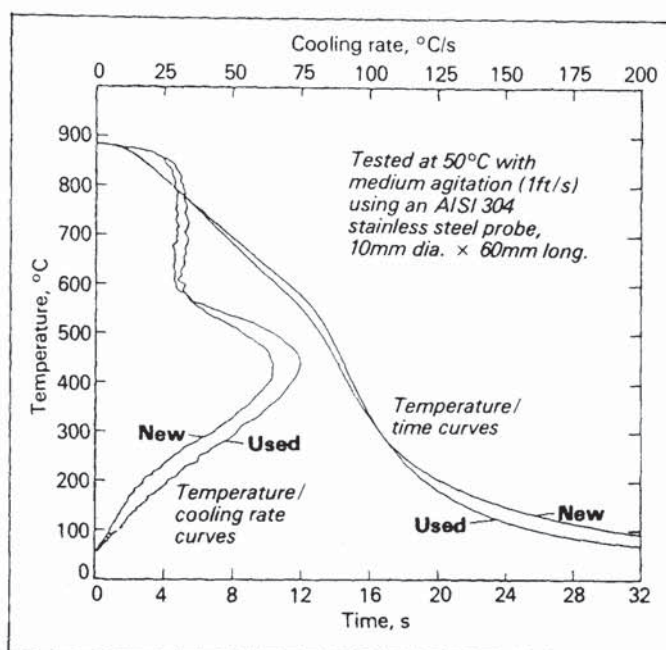


Figure 47. Comparison of the cooling characteristics for a new and used 23.5 weight per cent PAG solution⁽⁹⁴⁾.

2.11.3 Polyvinylpyrrolidone (PVP). Polyvinylpyrrolidone was developed in Germany during the late 1930's. It is derived from the polymerization of N-vinyl-2-pyrrolidone. The six-step synthesis shown in Figure 48 is used by General Aniline to produce PVP from the basic raw materials, acetylene, formaldehyde, ammonia, and hydrogen.⁽⁸⁷⁾

PVP is a water-soluble polymer characterized by its unusual complexing and colloidal properties and by its physiological inertness. Four viscosity grades are currently offered for industrial use in the USA, supplied as white free-flowing powders. The

commercial uses of PVP include cosmetics and toiletries (because of emulsifying, thickening and emollient properties), the clarification of beverages, in pharmaceuticals and as a blood-plasma extender.^(83,87)

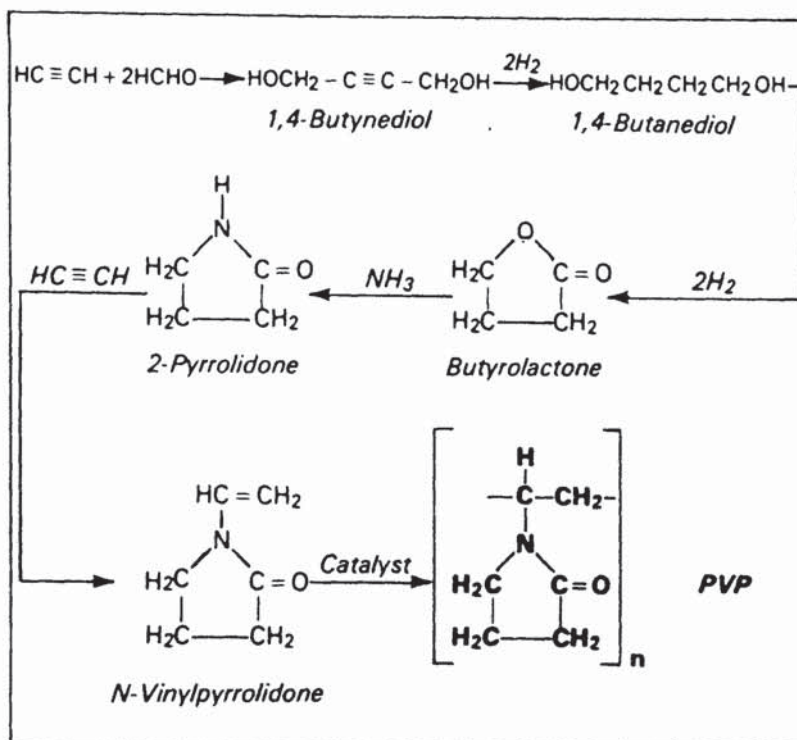


Figure 48. Six-step polyvinylpyrrolidone (PVP) synthesis⁽⁸⁷⁾.

Solutions of PVP in water were first produced as quenchants by Meszaros in US patent 3,902,929, issued in 1975.⁽¹²⁷⁾ The patent defined the preferred average molecular weight (160,000 PVP-K60 grade), the quantity of polymer recommended for a solution concentrate (generally about 10 per cent polymer solids), and the preferred use of borax and sodium nitrite rust inhibitors and paraformaldehyde as a bactericidal preservative. PVP products have found use as quenchants in the USA, Japan and Germany, although they are not at present distributed within the UK.

2.11.3.1 PVP quenchant variables. As with other polymer quenchants, concentration, bath temperature and agitation all affect the cooling characteristics. PVP products are claimed to have certain operating

advantages compared with the more widely-used PAG's, namely faster stage A and B heat transfer, yet slower stage C convective heat transfer.^(82,128)

Table 2. Quench data for polyvinylpyrrolidone and polyalkylene glycol (25.4mm diameter probes manufactured from either AISI 304 (19%Cr, 10%Ni, 0.08%C) or 4140 (0.4%C,1%Cr, 0.65%Mn, 0.2%Mo) steel with centre thermocouple and austenitized between 870-900°C⁽⁸²⁾.

| Type and conc ⁿ . of polymer | Bath temp. (°C) | Fluid velocity (m/s) | Cooling rate at 704°C (°C/s) | Cooling rate at 204°C |
|---|-----------------|----------------------|------------------------------|-----------------------|
| 16% PVP | 52 | 0 | 33 | 5 |
| " | 52 | 0.75 | 57 | 13 |
| 25% PVP | 54 | 0.75 | 48 | 7 |
| 16% PAG | 52 | 0 | 16 | 11 |
| " | 52 | 1.0 | 35 | 15 |

Table 2 gives data published by Foreman and Meszaros⁽⁸²⁾ which corroborate these points. However, no information was given concerning the volume of quenchant tested or the means by which the various flow velocities were produced. In addition, 25mm diameter probes manufactured from two different materials were utilized, and no mention is made of which results refer to which material. The authors also briefly describe a method for selecting quench conditions from CCT and quench test data, in order to provide desired microstructures and hardnesses. The following equation was offered for calculations relating to PVP solutions:

$$\begin{aligned} \text{Predicted cooling rate} = & B_0 + (B_1 \times \text{concentration}) + (B_2 \times \text{velocity}) \\ & + (B_3 \times \text{quenchant temperature}) \end{aligned} \quad (15)$$

where predicted cooling rate is in °F/s, concentration in per cent, velocity in ft/min. and quenchant temperature in °F, the American workers preferring non SI units (Système Internationale d'Unités). The coefficients B_0 , B_1 , B_2 and B_3 are derived from the quench test data for a given quenchant type, section size and temperature point on the cooling curve. B_0 is representative of a fixed rate of cooling for water, which is modified by the remaining terms in the equation. In relation to B_0 , as the concentration increases, the cooling rate decreases and B_1 is a negative value; as the velocity increases (or section size decreases) the cooling rate increases and B_2 is a positive value; as the temperature increases, cooling rate decreases and B is a negative value.

Since PVP does not exhibit inverse solubility in water, only very small amounts of polymer film are retained on quenched parts at quenchant temperatures ranging from 30°C to near boiling point. Therefore, a wider range of working temperatures for quenching can be employed.⁽⁴⁾ Bates et al⁽¹¹⁰⁾ have included 25 per cent solutions of PVP at temperatures between 25 and 40°C as suitable quenchants for use during aluminium heat treatment.

Concentration control can be maintained by monitoring regularly with a calibrated refractometer and with back-up viscosity measurements, as is the case for PAG solutions. An ultrafiltration method (similar to that described previously for PAG's) for removing insoluble contaminants and lower-molecular-weight constituents, without interrupting the quenching process, has been patented.⁽¹²⁹⁾

2.11.4 Polyacrylates. One of the more recent types of polymer to be marketed as a commercial aqueous quenchant, these products, based on sodium polyacrylate, were first introduced at an ASM Heat Treating Conference/Workshop in May 1977⁽¹³⁰⁾ and patented by Kopietz and Munjat⁽¹³¹⁾ in 1978. The polymer has the structure illustrated in *Figure 49* and may be produced via direct polymerization of sodium acrylate, or the alkaline hydrolysis of sodium polyacrylate ester. By using an alkali metal salt, in this case sodium, the polymer is soluble in water. Polyacrylic acid salts find a broad range of end uses such as thickening agents, flocculants and for soil conditioning.⁽⁸⁷⁾

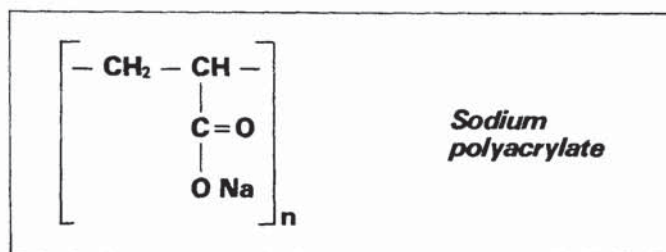


Figure 49. Sodium polyacrylate produced by the polymerization of sodium acrylate (or hydrolysis of polyacrylate ester)⁽⁸³⁾.

Polyacrylate products represent a class of quenchants whose structure and hence properties are significantly different from those of PVA, PAG or PVP types. The latter polymers are nonionic, that is, they are neutral or not ionizable. Polyacrylate polymers are negatively charged or anionic. This characteristic imparts strong polarity, which not only provides water solubility, but is also suspected of causing the quenchant to operate by a different mechanism of heat extraction.⁽⁴⁾

2.11.4.1 Polyacrylate quenchant variables.

Again, the cooling effect of the polyacrylate quenchants is a function of the three basic parameters of polymer concentration, bath temperature and bath agitation. By varying the molecular weight of the polymer and these three parameters, a wide range of cooling rates is claimed possible, from

the fast quenching of water to the slow cooling of oils.⁽⁴⁾ The cooling curves of the polyacrylate solutions can be almost straight as illustrated in *Figure 50*.^(4,132) Straight cooling curves are claimed by Kopietz⁽¹³²⁾ to be a result of stable vapour blankets, and hence uniform heat extraction, which makes polyacrylate solutions useful for non-martensitic quenching, and also for hardening crack-prone parts made of high-hardenability steels. Applications of this kind are usually not possible with other polymer quenchants.

Mason and Griffin⁽¹³³⁾ have described how polyacrylate solutions can be employed for patenting medium-to-high-carbon steel rod or wire, instead of the commonly used lead or salt bath process at 510 to 565°C. Patenting is a process which produces fine lamellar pearlite, with higher hardness than obtained with air cooling and very good drawability of the rod or wire. A 30 to 40 per cent polyacrylate solution at 70°C was found to produce properties only slightly inferior to those of lead-patented steel, but with reductions in cost, drag-out losses and toxicity problems. The authors made an interesting observation: premature breakdown of the stage A film was indicated by cooling rate-temperature curves determined by static Wolfson Engineering Group tests, as shown in *Figure 51*.

Early polyacrylate products were known to suffer from a certain degree of instability.^(68,95) However, more recent formulations are now being applied successfully in critical heat treatment operations^(81,84,134) such as the hardening of seamless low-alloy steel tubes for the oil industry, forged axle shafts and thin section alloy-steel crankshafts. 15 to 20 per cent solutions are preferred for high-alloy steel grades, while 5 to 10 per cent solutions are required for low hardenability carbon steels. Emphasis is placed on the ability of the polyacrylate solutions to produce cooling rates through the martensite transformation temperature range, which are significantly closer to those of normal-speed quenching oils than those achieved by other classes of polymer quenchant.

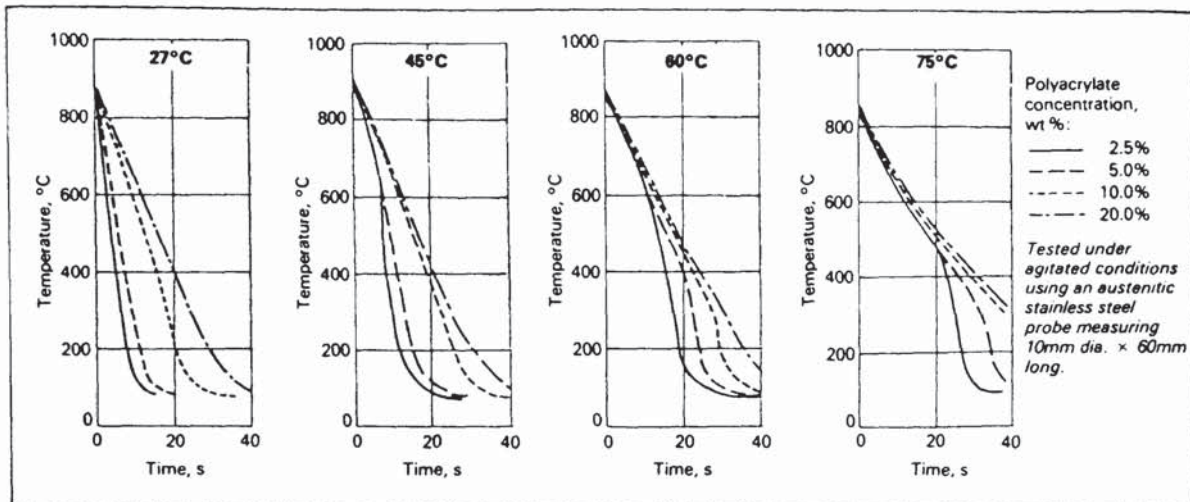


Figure 50. Cooling curves of polyacrylate quenchant as a function of concentration and temperature^(4,132)

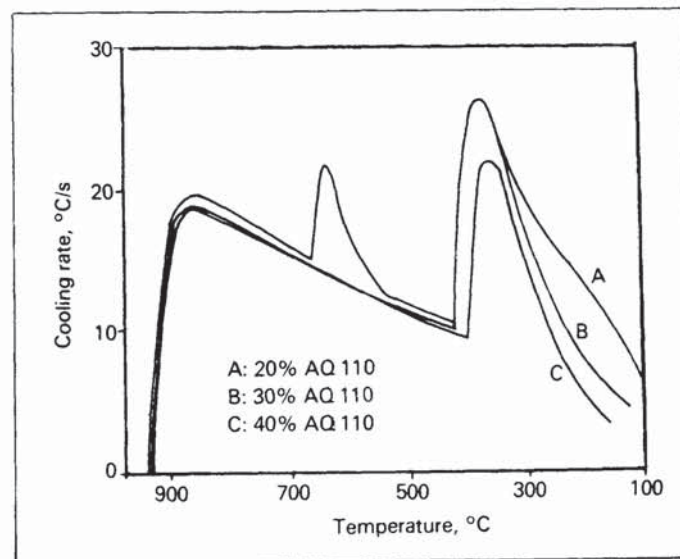


Figure 51. Cooling rate-temperature curves for a polyacrylate quenchant (Aquaquench 110*), showing the effect of concentration at a bath temperature of 52 °C (non-agitated). Measured in accordance with the Wolfson Engineering Group test, but with an austenitic stainless steel probe⁽¹³³⁾. * Aquaquench 110 is the tradename of a polymer quenchant marketed by Edgar Vaughan and Co. Ltd., Birmingham.

As with other polymer quenchants, it is believed that agitation is essential for the optimum performance of polyacrylate solutions.⁽¹³⁵⁾ Metals Handbook⁽⁴⁾ recommends a high degree of agitation for hardening operations, and minimal agitation for non-martensitic quenching.

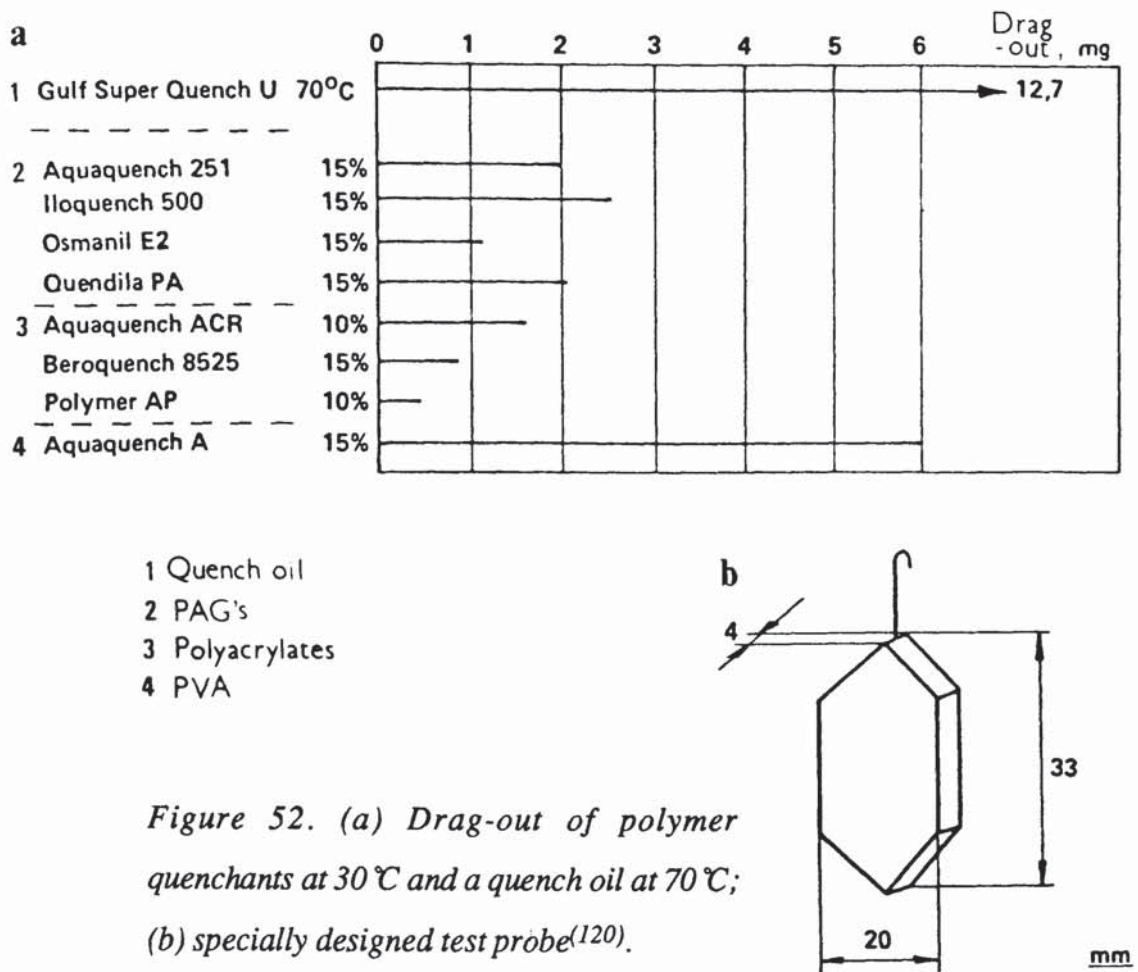


Figure 52. (a) Drag-out of polymer quenchants at 30 °C and a quench oil at 70 °C; (b) specially designed test probe⁽¹²⁰⁾.

Seegerberg⁽¹²⁰⁾ claims that polyacrylates exhibit slightly lower drag-out losses compared with PAG's, as shown in Figure 52a. Unfortunately, precise details regarding the test method were not given, although a specially designed test probe seen in Figure 52b was used and the quenchants were tested in the static condition. The relatively high level of drag-out for the PVA solutions was ascribed to the formation of a solid polymer film on the test probe surface. Generally, polymer quenchants

have lower drag-out than quench oils. The amount of drag-out per unit area is dependent on the type of polymer, its concentration and temperature, the surface temperature of the component when taken out of the bath, and the shape and surface condition of the component.

Concentration control is possible using both refractometry and viscosity measurement. Mueller⁽⁸³⁾ described how the sodium may ionize in aqueous solution due to the anionic nature of the polymer, resulting in sensitivity to hard waters containing alkaline metals such as calcium, magnesium or iron producing changes in viscosity and concentration measurements, etc. Consequently, he believed control measures may prove to be a problem.

The present author has recently published a paper in which the effect of concentration, temperature and agitation on the cooling rate for typical PAG, PVP and polyacrylate quenchants were compared; contamination, ageing and drag-out were also examined.⁽³⁶⁾

2.11.5 Polymer Quenchant Research in the Eastern Bloc.

Polymer quenchants are generating considerable interest in the Eastern bloc. Research is actively being pursued, although it appears less advanced than in the West, with fewer polymer quenchants used industrially. In addition to the polymer quenchants which are analogous to those already employed in the West, other polymer types are also being examined.

Khina,⁽¹³⁶⁾ Tolstousov⁽¹³⁷⁾ and, more recently, Zakamaldin et al⁽¹³⁸⁾ have reviewed the most popular quenchants in the USSR, including PVA, PAG, sulphite alkali and polyacrylamide solutions. Sulphite alkali solutions form a colloidal film around the hot part, retarding heat transfer. Operational problems, such as fermentation, mould formation, and unpleasant odours, have limited their acceptance as industrial products. Polyacrylamide solutions appear to be more attractive

quenchants, although they are still in the development stage. These are film-forming polymers of high molecular weight, and with mineral salts added to improve the cooling properties. Concentrations as low as 0.2 to 0.5 weight per cent are claimed by Zakamaldin et al⁽¹³⁸⁾ to lower cooling rates considerably compared with water.

Bedarev et al⁽¹³⁹⁾ have shown that polyethylene oxide solutions are suitable quenchants for aluminium alloys. Concentrations between 0.12 to 0.25 weight per cent result in four to five times less distortion compared with water, whilst conferring equivalent mechanical properties and corrosion resistance. An interesting paper by Bozhko et al⁽¹⁴⁰⁾ shows the importance of polymer solution viscosity on the cooling characteristics. It is proposed that there is a critical viscosity for polymer solutions, above which there is little effect on the cooling rate. This work was based on solutions containing various molecular weight derivatives of a nonionic polymer, described only as "PPS". The critical kinematic viscosity was found to be approximately 4.5mm²/s. Above this level there was little reduction in the average cooling rate, calculated from steel test pieces containing a central thermocouple and quenched into static solutions of the polymer. No details were given regarding the test conditions.

2.11.6 New Polymers For Use in Aqueous Quenching.

Warchol⁽¹⁴¹⁾ has described the latest developments in polymer quenchant research. The aim is to produce stable polymer formulations which, in comparison with oils, exhibit faster cooling in the early stages of quenching, but slower rates in the convection stage. One of the most exciting developments is the introduction of a new class of polymer. Substituted oxazoline polymers, such as poly(ethyloxazoline) (PEOx), offer certain quench advantages. This polymer was patented in December 1984⁽¹⁴²⁾ and has the structure illustrated in *Figure 53*. The polymers are nonionic in character and provide the same quenching effect as PAG's. However, only one half to one third of the amount of polymer is required, resulting in lower bath viscosities and hence reduced drag-out.

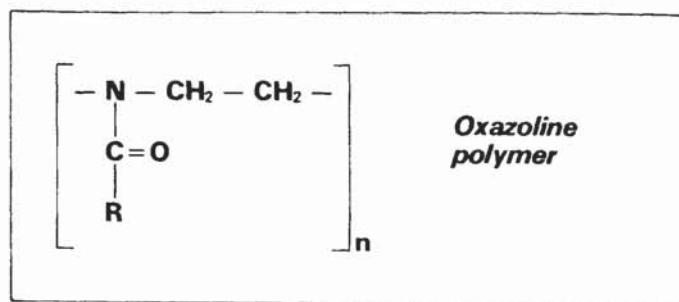


Figure 53. General formula of a substituted oxazoline polymer, where *R* is an organic radical consisting of a phenyl or an aryl group containing 1 to 7 carbon atoms which may be halogen substituted. Homopolymers or copolymers may be produced depending upon whether the substituents *R* are the same for all units or different. Polymerization of the respective monomers or comonomers occurs in the presence of a cation catalyst. Poly(ethyloxazoline) (PEOx) homopolymers where $R = C_2H_5$ and with molecular weights ranging from 200,000 to 500,000 are particularly preferred⁽¹⁴²⁾.

Other areas of ongoing research include the examination of various high-molecular-weight copolymers. Mixtures based on PVP's and PEOx's are also being studied.⁽¹⁴³⁾ Field trials are being conducted using these new polymer formulations, and new polymer quenchant ranges are expected to be announced soon as a result of this, and other, work.

2.12 Quenching Equipment and Conversion to Polymer Quenchants.

Equipment requirements for quenching may vary widely, depending on the number and size of parts to be quenched each day. For a complete quenching system, the following functional equipment is usually required and installed⁽³⁾:

(a) work tank or machines, (b) facilities for handling the parts quenched, (c) quenching medium, (d) agitation equipment, (e) coolers, (f) heaters, (g) pumps and filters, (h) quenchant supply tank, (i) equipment for ventilation and for protection against hazards, and (j) equipment for automatic removal of scale from tanks.

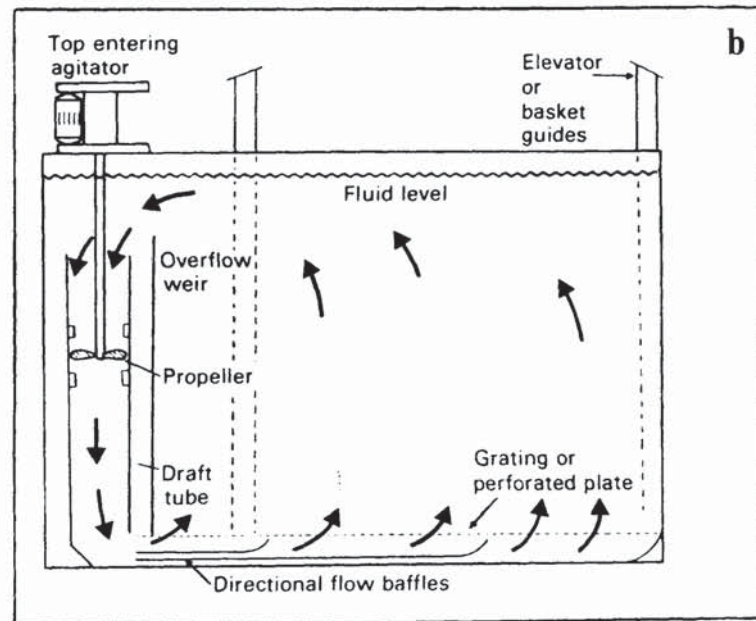
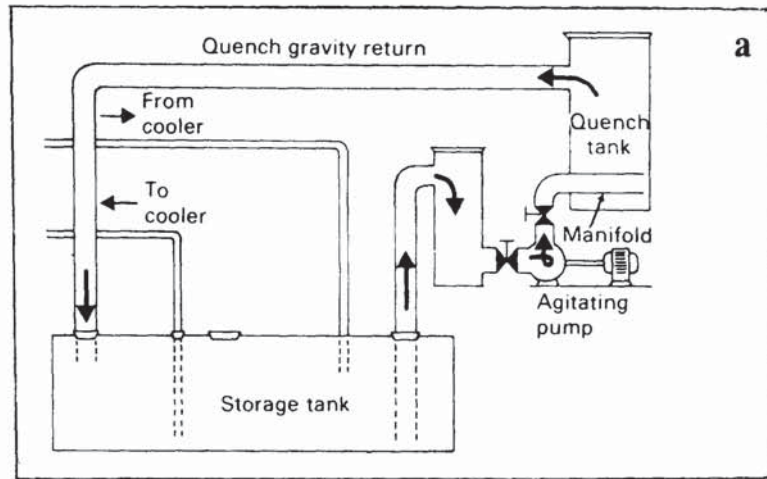


Figure 54. Batch quench tank with (a) pump system agitation, and (b) propeller agitation⁽¹¹⁸⁾.

Several authors^(93,114,118) have described quench tank modifications required when converting from conventional quench media to polymer quenchants. Thorough cleaning of the quench system is usually necessary to avoid contamination problems. Even though polymer solutions generally contain inhibitors, additional corrosion controls may be required, such as the painting of the quench tank with a suitable paint which will resist dissolution by the quenchants.⁽⁹⁷⁾ A two-pack epoxy or polyurethane based paint system is normally recommended. In conventional oil quenching operations, the quenchant volume is often calculated on the basis of 10 litres of fluid per kilogramme of total charge weight. For polymer quenchant operations (especially when PAG solutions are used with inversion temperatures around 75°C), this ratio should be regarded as the minimum to avoid soft spotting or cracking. Ideally a ratio of 15 litres of polymer solution per kilogramme of quench load should be utilized.^(114,118) The conversion may also require the installation of more efficient tank agitation to ensure uniform polymer coatings on the quenched parts. Valuable guidelines for design factors in quench systems using polymer quenchants have been outlined by both Beck⁽¹¹⁴⁾ and Lakin.⁽¹¹⁸⁾

Figures 54a and 54b illustrate two typical bath quench tanks agitated using either pump or propeller systems respectively. The agitation system should provide directional flow through the charge region with the fluid being replaced approximately once per minute.

Conversion to polymer quenchants is relatively straightforward when the furnace and quench tank are separate entities. However, in the case of sealed-quench furnaces, such as that shown in *Figure 55*, attention to the sealing of the inner vestibule door and gas flow levels is necessary to counter possible water vapour contamination of the furnace atmosphere. Ammonia-containing atmospheres such as used in nitrocarburizing could also affect the cooling characteristics of the polymer quenchant as was demonstrated by Burgdorf (*Figure 44b*).⁽²⁸⁾ Effective agitation, to produce surface movement of the quenchant, is also essential in order to avoid localized heating and excessive water vapour build-up. Nevertheless, PAG quenchants have

been employed successfully in a number of sealed-quench furnaces^(114,118,144) and some major furnace manufacturers are now offering units suitable for use with polymers. A specially formulated PAG quenchant, with a higher inversion temperature (88°C), is marketed to reduce the risk of bulk inversion in sealed-quench tanks.⁽¹¹⁸⁾

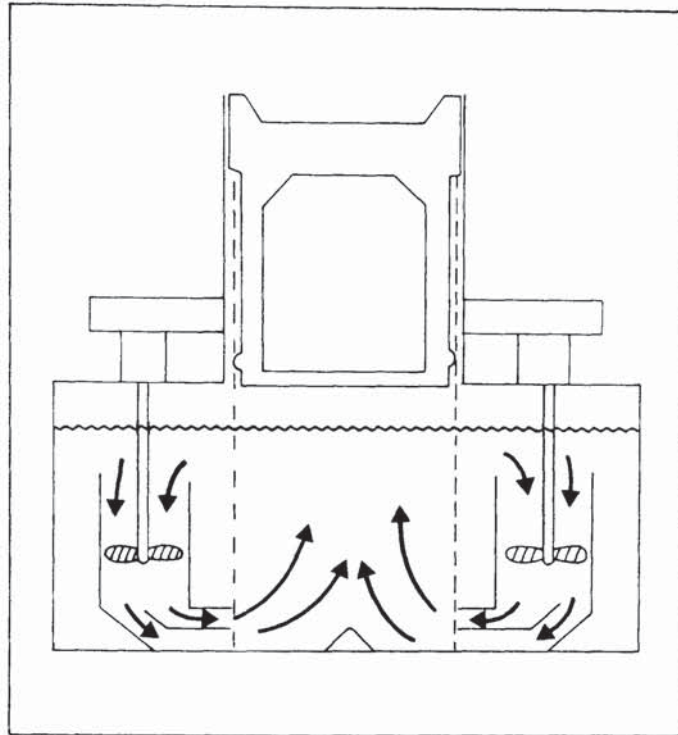


Figure 55. Integral quench furnace with draft tube and directional flow manifold⁽¹¹⁸⁾.

Polymer quenchants are also being successfully employed in special quenching systems such as used for induction and flame hardening operations and with press quenching machines. Long shafts are frequently induction hardened in scanning operations with a spray of quenchant applied through a separate ring or from hollow inductors. PVA solutions, made-up with 5 to 30 parts by weight of polymer with 10,000 parts water, were initially used as replacements for pure water in order to provide more uniform heat transfer characteristics.⁽³⁾ However, a "varnish-like" coating on the spray orifices interfered with the proper quenching action. Consequently, 1 to 20 per cent PAG solutions are more commonly used today.⁽¹⁴⁵⁾ The quench flow must be sufficient to wet the surface of the part to the point where

the quench medium does not boil off after the part progresses away from the point of initial quench impingement. Polymer quenchants are also occasionally used with commercial quenching presses which are designed for controlled quenching of ring gears and other round, flat or cylindrical parts, to permit heat treatment with minimum distortion.

2.13 Molecular Weight Distribution and Characterization of Polymers.

All polymer molecules consist by definition of large numbers of simple repeat units, derived from small molecules (monomers) and joined together by covalent bonds to form high molecular weight polymer molecules. The length of the polymer chain is specified by the number of repeat units in the chain and is called the "degree of polymerization" (DP).⁽¹⁴⁶⁾ The molecular weight of the polymer is the product of the molecular weight of the repeat unit and the DP. It is rare for the repeat units to be distributed evenly between all the polymer molecules. Random processes occurring during polymerization produce chains containing varying numbers of repeat units, so that the polymer contains a distribution of molecular chain lengths and is said to be "polydisperse".

The chemical reactions which produce synthetic polymers are of two types⁽³⁸⁾: addition (or chain) polymerization and condensation (or step) polymerization. The former occurs between monomers with an unsaturated, or double, bond. One half of the bond opens to provide two half bonds able to unite with similar bonds in two adjacent monomers. The double bond is opened by a reactive substance with one unpaired electron (free radical) derived from the decomposition of a suitable initiator. Chain growth is terminated when two free radicals annihilate each other. Condensation polymerization does not require an unsaturated bond in the monomer. In polymer formation the condensation takes place between two polyfunctional molecules to produce one large polyfunctional molecule, with the possible elimination of a small molecule such as water. Functionality refers to the number of reactive groups within the monomer. The condensation reaction continues until almost all of one of the reagents is used up.

The polymer chain produced may be linear or branched depending on the functionality of the monomer. Difunctional monomers form linear chains, whilst monomers with more than two active bonds enable reactions in several directions producing two or three dimensional molecules. Linear polymers form the basis of thermoplastics which soften and become liquid as the temperature is raised; cross-linked or network structures swell rather than dissolve, do not soften appreciably on heating and decompose before melting.

When more than one monomer is polymerized at the same time, a copolymer is produced. In block copolymers long runs or blocks of each monomeric repeat unit are formed along the chain. Random copolymers are more common and involve long runs of one monomer or the other in an irregular sequence. A third variety is the graft copolymer. In this case branches of one monomer are grown on a previously formed polymer molecule.

Due to the polydisperse nature of polymers it is not generally possible to characterize a polymer by a single molecular weight, and the mass of the polymer molecules can only be completely described by a molecular weight distribution. *Figure 56* illustrates a typical normalized distribution in which the weight fraction ω of molecules of molecular weight M is plotted against M .⁽¹⁴⁷⁾ For a polydisperse polymer sample there are a number of ways in which the molecular weight may be averaged, of which the most useful are the number-average, \bar{M}_n , and the weight-average, \bar{M}_w . Consider a dispersion of molecular weights, say N_1 molecules with molecular weight M_1 , N_2 with molecular weight M_2 and N_i with molecular weight M_i , then:

$$\bar{M}_n = \frac{\sum N_i M_i}{\sum N_i} \quad (16)$$

since the mass of the i th fraction $\omega_i = N_i M_i$

$$\bar{M}_w = \frac{\sum N_i M_i^2}{\sum N_i M_i} \quad (17)$$

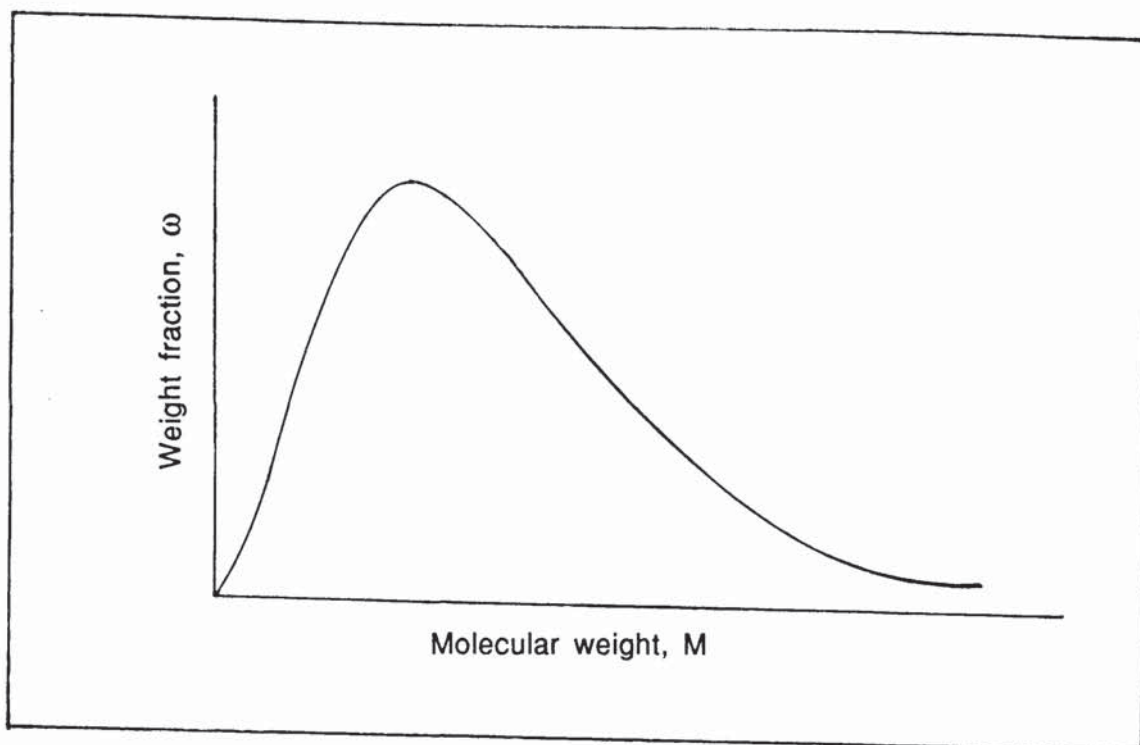


Figure 56. A typical normalized weight distribution curve for the molecular weights of a polymer sample⁽¹⁴⁷⁾.

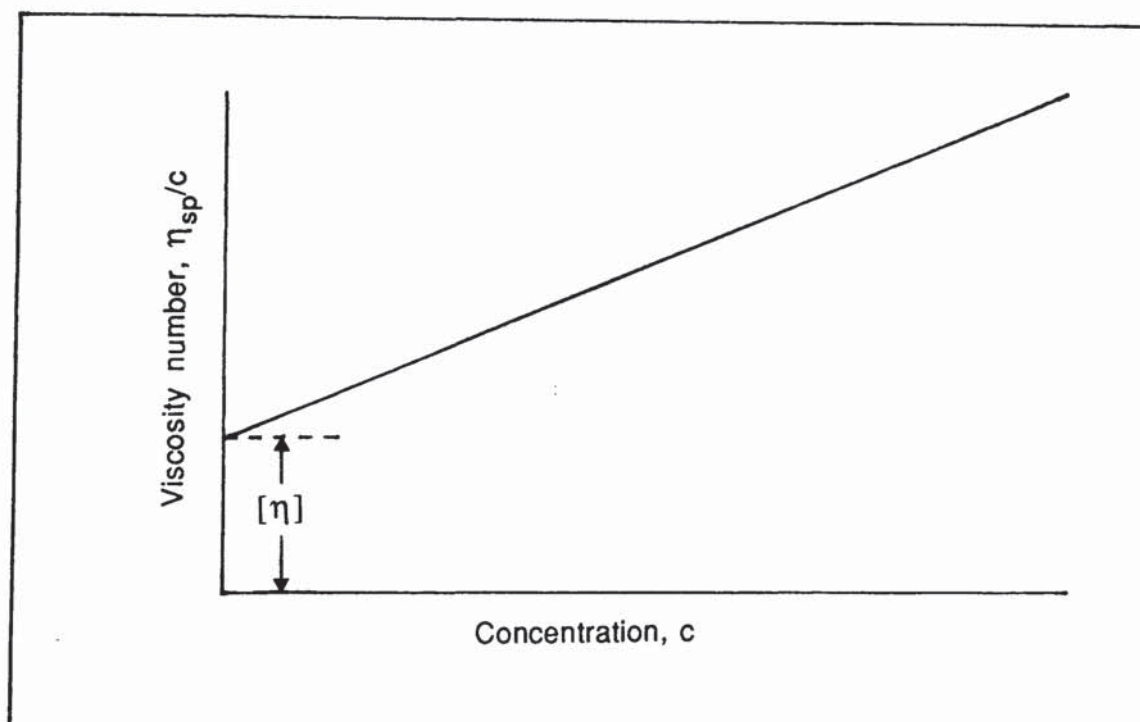


Figure 57. A plot of viscosity number versus concentration is generally linear for small concentrations. The value of the viscosity number extrapolated to zero concentration is the limiting viscosity number (intrinsic viscosity), $[\eta]$ ⁽¹⁴⁶⁾

The ratio \bar{M}_w/\bar{M}_n provides a simple measure of the breadth of the molecular weight distribution; this polydispersity ratio is 1.0 for a monodisperse sample, whilst most commercial synthetic polymers have a polydispersity ratio in the range 2 to 20, with a value as high as 250 possible.⁽¹⁴⁷⁾

In solution, a polymer molecule may be considered as a randomly coiling chain, whose conformation or shape is constantly changing.⁽¹⁴⁶⁾ In very dilute solution the individual molecules may be considered as acting independently. In more concentrated solutions chain entanglement interactions occur. The viscosity of a polymer solution is basically a measure of the size or extension in space of the polymer molecule. If η is the effective viscosity of the solution and η_0 that of the pure solvent, the viscosity ratio of the solution is defined by η/η_0 , and the specific viscosity η_{sp} , by $(\eta - \eta_0)/\eta_0$. The viscosity number (reduced specific viscosity) is defined by η_{sp}/c , where c is the mass concentration of the polymer (g/dl). The most useful term is the limiting viscosity number (intrinsic viscosity) $[\eta]$, which may be used to characterize the shape and molecular weight of a linear polymer. The value of $[\eta]$ is determined by measuring the viscosity of a series of solutions of different concentration, then plotting the viscosity number against the concentration and extrapolating to zero concentration. (*Figure 57*). The limiting viscosity number has the dimensions of reciprocal concentration.

The effect of molecular weight on the solution viscosity is given by the Mark-Houwink-Sakurada relationship:

$$[\eta] = \kappa M^a \quad (18)$$

where M is the molecular weight and κ and a are constants whose values depend on the nature of the polymer, solvent and temperature. The value of κ normally varies from 0.5 to 5×10^{-4} and a from 0.5 to 1.0.⁽³⁸⁾ Equation (18) provides a convenient method for estimating the molecular weight of a polydisperse sample of a linear polymer. Viscosity measurement leads to a viscosity average molecular weight,

defined as:

$$\bar{M}_v = \left[\frac{\sum N_i M_i^{1+a}}{\sum N_i M_i} \right]^{1/a} \quad (19)$$

The constants in equations (18) and (19) can be determined from viscosity measurements using monodisperse or fractionated polymers. If $a = 1$, then $\bar{M}_v = \bar{M}_w$, but for any polydisperse polymer $\bar{M}_n < \bar{M}_v < \bar{M}_w$.

The limiting viscosity number has also been related to the molecular dimensions of the polymer molecule.⁽¹⁴⁸⁾ For a broad spectrum of polymer-solvent systems:

$$[\eta] = \phi \frac{(\bar{r}^2)^{3/2}}{M} \quad (20)$$

where ϕ is nearly a universal constant, equal to 2.50×10^{21} , provided the mean square end-to-end distance for a freely jointed chain (\bar{r}^2) is given in cm^2 , $[\eta]$ in dl/g and $M > 10^6$.

The molecular weight of polymers can be determined in a number of ways. Measurement of colligative properties yields \bar{M}_n values, whilst light scattering measurements provide values of \bar{M}_w . Other techniques include end group analysis using chemical or physical methods, ultracentrifugation and dilute solution viscosity measurements. All these methods except the last are, in principle, absolute. However, most commercial test apparatus provide only relative values.⁽¹⁴⁶⁾ The technique which is most widely used today for measuring molecular weight distributions is gel permeation chromatography (GPC), which is more correctly termed size exclusion chromatography.⁽¹⁴⁷⁾

2.14 The Development of Residual Stresses During Quenching.

Residual stresses arising from quenching may be classified as those arising from a thermal gradient alone, as in the rapid cooling of a hot solid with no phase transformation taking place, and those from a thermal gradient in combination with a phase transformation, as in heat treating steel.

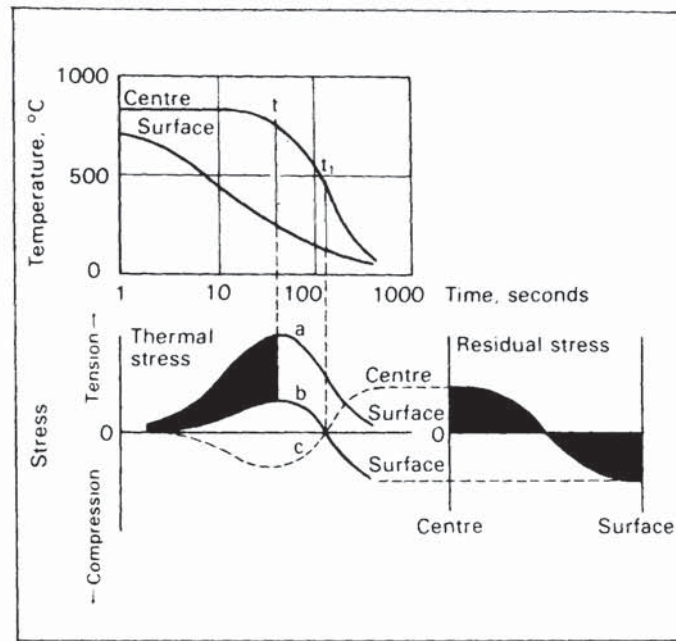


Figure 58. Development of thermal stresses on cooling (transformation stresses not taken into account)^(149,150).

When considering thermal stresses only, a typical tangential or hoop stress distribution is shown in *Figure 58*, which applied to a bar 100mm in diameter and quenched in water from 850°C.^(149,150) The temperature difference between the surface and the core is greatest (about 500°C) at time t . This corresponds to a linear differential expansion of approximately 0.6 per cent and results in a stress in excess of 1000N/mm². If the body of the material were elastic enough to accommodate this stress, the stress diagram for the surface layer would take the shape of curve "a". Once the temperature at the centre of the bar equals that of the surface, the stress should fall to zero. However, because the yield point of steel is considerably lower at elevated temperatures the material will flow plastically, following curve "b". The stresses at the centre will be opposite in sign as indicated by curve "c". After time t , contraction in the core will exceed that at the surface, resulting in complete stress neutralization at time t_1 . Consequently, after cooling to room temperature, there will be tangential compressive residual stresses at the surface and tensile at the core. The room temperature residual stress distribution is given in the right-hand diagram of *Figure 58*. The greater the quench severity and the larger the bar size, the higher will be the residual stresses.^(74,150)

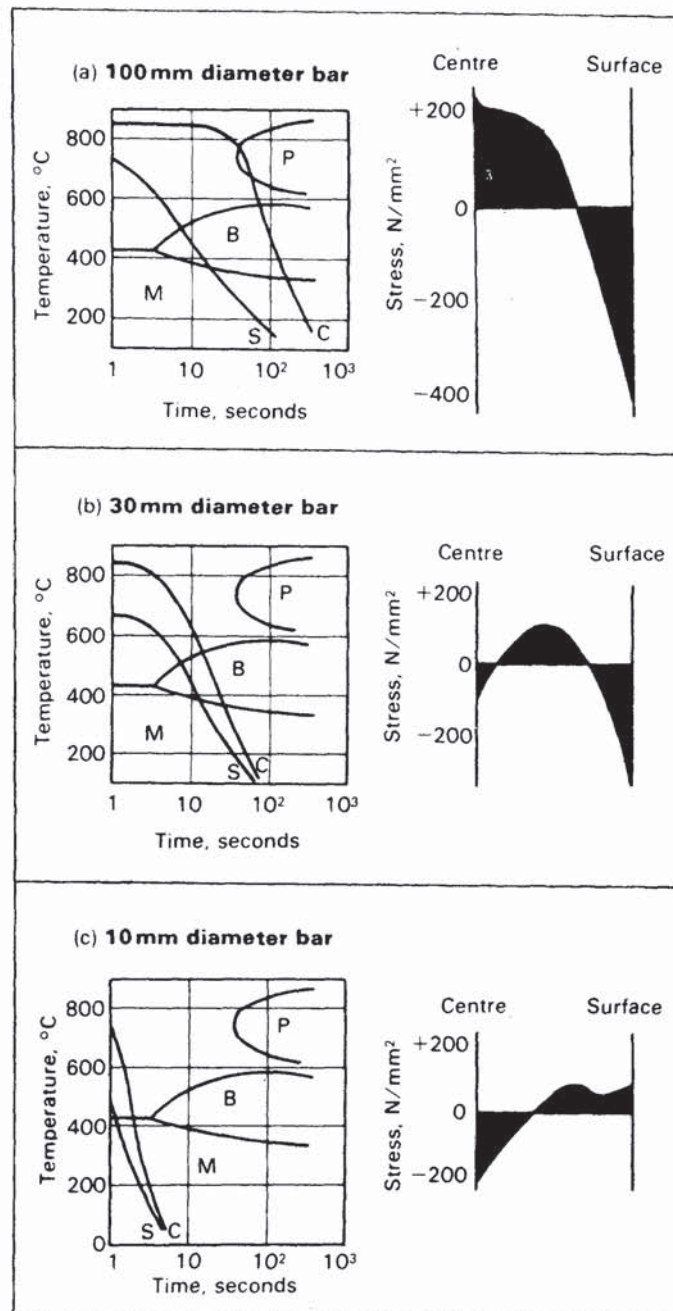


Figure 59. The effect of bar diameter on the residual stress pattern from both thermal and transformation stresses, in a water quenched steel DIN 22CrMo44 (0.22%C, 0.65%Mn, 1.05Cr, 0.44%Mo). The diagrams on the left show the cooling curves at the surface (S) and centre (C) superimposed on the CCT diagram. Those on the right show the distribution of residual stresses, with tensile positive and compressive stresses negative^(149,150).

With the quench hardening of steel, additional stresses are involved due to the increase in volume that takes place as austenite transforms to other structures. For example, the formation of martensite results in an approximate 4 per cent volume expansion (1.3 per cent linear growth), whilst higher temperature transformation products result in somewhat less growth.⁽¹⁵⁰⁾ If the main part of the transformation takes place in the centre before the surface starts to transform, which is the course of events in shallow-hardening steels, the same stress pattern as has been described in *Figure 58* is set up. However, when the main part of the transformation starts in the surface, tensile stresses are produced there and compressive stresses at the centre.

Rose⁽¹⁴⁹⁾ performed a series of tests in which (0.22% C, 0.65% Mn, 1.0% Cr, 0.44% Mo) steel bars of various diameter were quenched in water. The results shown in *Figure 59* illustrate how a variety of residual stress patterns may be produced depending on the transformation characteristics and cooling rate/section size. The stress distribution in the 100mm bar (*Figure 59a*) corresponds roughly to that due solely to thermal stresses; if the nose of the pearlite curve had been located further to the left, an additional increment of stress would have resulted. With reference to the 30mm diameter bar (*Figure 59b*), the start of the bainite formation at the centre approximately coincides with that of martensite in the surface; compressive stresses were measured both in the surface and at the centre with tensile stresses in the intervening region. The 10mm bar (*Figure 59c*) is through hardened with a smaller temperature difference between the surface and centre compared with the larger diameter bars; most of the martensite formation in the core occurs when the martensite reaction in the surface zone is nearly complete. Both of these factors contribute to the creation of tensile surface stresses and core compressive stresses.

2.14.1 Residual Stresses and Quench Cracking. Thelning⁽⁷⁴⁾ has outlined two critical size groups in which quench cracking is likely to occur, when hardening steel, due to the residual stress pattern induced. The most common cause of quench cracking is when the section size of the steel is at its maximum for through-hardening. In this case, tensile stresses greater than the tensile strength of the steel may build up in the outer layers, resulting in a longitudinal crack emanating from

the surface, a high cooling rate increases the likelihood of this form of cracking.

The second size group is the one where transverse cracks start at the core. This type of cracking occurs when sufficiently high compressive stresses have been built up in the outer layers and correspondingly high tensile stresses at the core. Flaws in the central region of the steel and a high cooling rate favour this form of quench cracking.

CHAPTER 3

3.0 EXPERIMENTAL PROCEDURE

3.1 Polymer Quenchants Examined

A number of commercially available polymer quenchant products were acquired for evaluation. *Table 3* lists the supplier, the tradename and the class of each polymer quenchant examined. PVA quenchants were excluded from this study since they are no longer available in the UK, and now find only very limited use.

Table 3. Polymer quenchant products examined.

| Polymer type | Trade name | Supplier |
|--------------|-----------------|---|
| PAG | Quendila PA | BP Chemicals Ltd, |
| " | Quendila PHT | The British Petroleum Co.plc. |
| " | Breox NF-18 | " |
| PAG | Aquaquench 1250 | Edgar Vaughan and Co.Ltd. (A member of the Houghton group of companies). |
| PAG | Ucon* E | Tenaxol Incorporated. (*Ucon is a registered trade mark of Union Carbide Corporation). |
| PVP | Parquench 60 | Park Chemical Company |
| " | Parquench 90 | (A subsidiary of Whittaker Corporation). |
| Polyacrylate | Aquaquench 110 | Edgar Vaughan & Co Ltd. |
| " | Aquaquench ACR | " |

3.2 Polymer Quenchant Characterization

3.2.1 Solids Content of Concentrates. Each product was supplied as a viscous "concentrate", containing an unstated amount of water to aid subsequent handling and further dilution. In order to estimate the solids-content of these products, approximately 25ml of each concentrate was accurately weighed, and then "dried" by heating to 50°C in a vacuum oven at a pressure of 10kPa for 5 hours. The reduced pressure above the concentrate enabled the water to be boiled away at a lower temperature, thus reducing the risk of oxidation and decomposition of the polymer. A cryogenic trap was utilized to prevent the extracted water from contaminating the oil in the rotary pump. The dehydrated samples were then re-weighed and their change in mass recorded. This process was repeated twice, and mean values for the solids-contents of each concentrate calculated in weight per cent.

3.2.2 Gel Permeation Chromatography. Gel permeation chromatography (GPC), more correctly termed size-exclusion chromatography, is a well established means of determining the molecular weight distribution of polymers.⁽¹⁴⁷⁾ The GPC process can be described very simply. A sample of the polymer is diluted with a suitable solvent and then injected into a stream of the pure solvent which is flowing through a set of columns. The columns are packed with solvent-swollen gel with a range of pore sizes. The separation into molecular size is obtained because the larger molecules cannot diffuse into the pores, and are rapidly eluted, while the smaller ones penetrate further with decreasing size and are retarded correspondingly.

A Perkin-Elmer Series 10 Liquid Chromatograph was used for this work. The columns employed were packed with highly cross-linked poly(styrene-co-divinyl benzene), a material which has proved successful with a wide range of polymer types. The system utilized 5 columns linked in series. These comprised a precolumn to filter unwanted particulate matter in the eluent plus analytical columns with pore sizes of 10^2 , 10^3 , 10^4 and 10^5 Å respectively. The equipment was limited to two solvents, "spectrasol grade" tetrahydrofuran (THF) was preferred, although chloroform could also be used. The "dried" PAG samples were soluble in THF but

the other polymer types were not. The samples had to be dehydrated since water reduced the retention efficiency of the columns. A 2 weight per cent sample of each PAG product was tested using the operating conditions shown in *Table 4*.

Table 4. Perkin-Elmer Series 10 High Performance Gel Permeation Chromatograph operating conditions.

| | |
|----------------------------|---|
| Differential refractometer | Attenuation: 32X Polarity: -ve |
| Pump | Pressure limits: upper 13MPa lower 2MPa Flowrate: 1ml/minute |
| Sample | Loop size: 100 µlitre Concentration: 2 wt% Solvents: THF and chloroform |
| Y-t recorder | chart speed: 10mm/minute |

Only relative molecular weight values could be calculated since the columns had been calibrated with almost monodisperse polystyrene samples. The calibration plot is given in *Figure 60*. The concentration of the eluent was monitored using a differential refractometer detector, from which a gel chromatogram was plotted on the Y-t recorder. From this trace, the peak intensity at each 0.1ml elution volume was measured and the polymers polystyrene-equivalent number and weight-average molecular weights were calculated using the computer program listed in Appendix A. The calculation is based on the fact that the detector response (i.e. perpendicular height h_i) for each elution volume is proportional to the solution concentration and hence the weight fraction of the polymer ω_i . Thus from equations (16) and (17) it can be seen that: $\bar{M}_n = \sum h_i / \sum (h_i / M_i)$ and $\bar{M}_w = \sum h_i M_i / \sum h_i$.

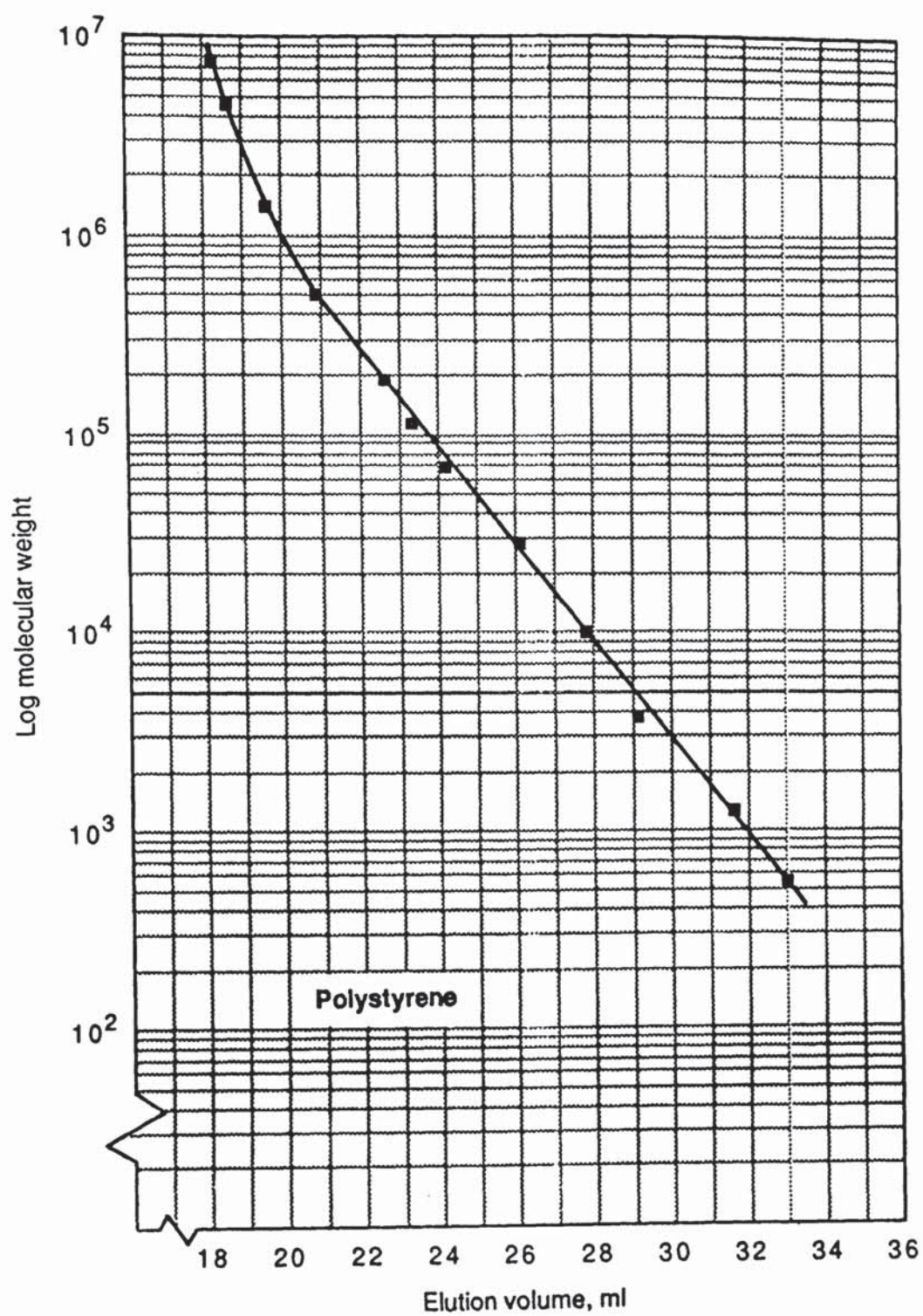


Figure 60. GPC calibration plot for polystyrene samples dissolved in THF.

Since the dehydrated PVP samples were soluble in chloroform, the chromatograph was converted for use with this solvent. Unfortunately the polyacrylates were insoluble in both solvents.

3.2.3 Limiting Viscosity Number Determination. The limiting viscosity number for a polymer can be determined by measuring the viscosity of a series of solutions of different concentration and then plotting the viscosity number against the concentration as was described in Section 2.13 (*Figure 57*). The viscosity-average molecular weight of the polymer \bar{M}_v , can thus be obtained using equation (18), provided values for the Mark-Houwink-Sakurada constants are available. Such data is available only for the most popular polymer/solvent systems. The value of a and κ in equation (18) for a particular PAG would depend upon that copolymer's precise molecular architecture. Consequently, as far as it is known, no such data has ever been published for PAG molecules. However, values for these constants have been published from tests using fractionated samples of both PVP and sodium polyacrylate whose weight-average molecular weights have been measured using an absolute method (*Table 5*).

Dehydrated samples of Parquench 60, Parquench 90 and Aquaquench ACR were diluted with the appropriate solvent to obtain solutions with concentrations ranging from 1.0 to 0.06g/dl. The viscosity numbers for these solutions were determined using a U-tube (Ostwald) glass capillary viscometer as shown in *Figure 61a*. The viscosity number is equal to $t - t_0 / t_0 c$, where t is the efflux time (which is the time required for the polymer solution to flow between two rings etched on the capillary tube), t_0 is the efflux time for the pure solvent and c is the concentration. The procedure for using this type of viscometer was as follows: a clean dry viscometer was charged with a slight excess of the sample through tube L, using a long pipette to minimize any wetting of the tube above mark G (*Figure 61a*). The viscometer was then mounted vertically in a Gallenkamp thermostatic bath, preset at the required temperature and to within $\pm 0.01^\circ\text{C}$. Once temperature equilibrium with the bath had been achieved (minimum 30 minute immersion), the volume of the sample was adjusted so that the bottom of the meniscus settled at mark G.

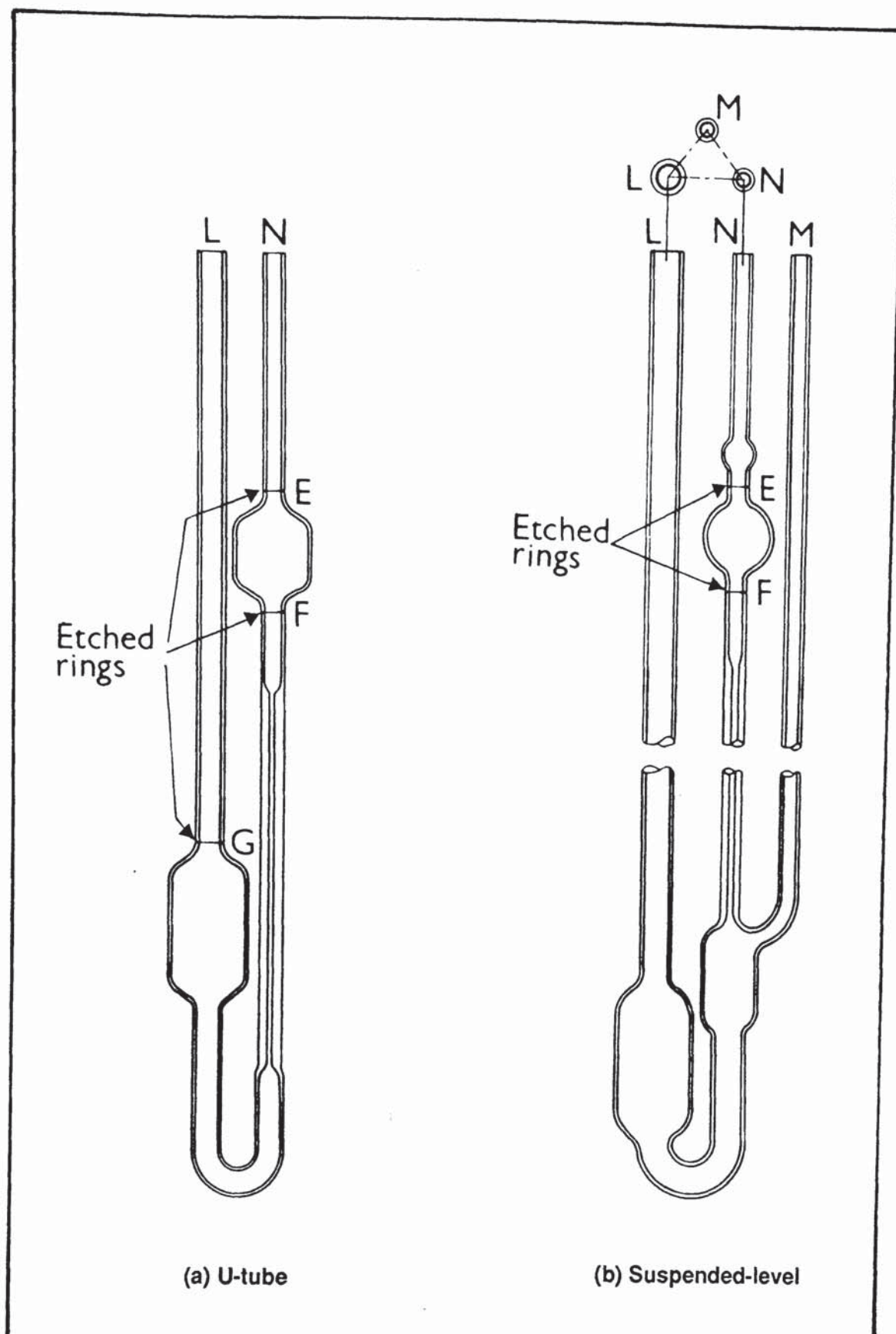


Figure 61. Typical glass capillary viscometers: (a) U-tube type BS/U, and (b) suspended level type BS/IP/SL⁽¹⁵²⁾.

Suction was then applied at N using a rubber bulb to bring the liquid level to a point approximately 5mm above timing mark E. The suction was then released and the flow time taken for the bottom of the meniscus to pass from the top edge of mark E to the top edge of mark F. The efflux time was measured using an electronic stopwatch to an accuracy of at least 0.2s. This process was repeated until two successive flow times agreed to within 0.2 per cent. The temperature of the bath was checked with a thermometer before and after each test. Prior to each series of tests the viscometer was cleaned by immersion overnight in chromic acid. It was then rinsed at least five times with distilled water, filled with acetone, drained and then dried in an air-circulating oven. Between successive determinations, the viscometer was drained, thoroughly rinsed with warm water and then acetone, and again dried in the electric oven.

Table 5. Viscosity-molecular weight relationships for PVP and sodium polyacrylate polymers ⁽¹⁵¹⁾

| Polymer | PVP | Sodium polyacrylate |
|---|-----------------------------|-----------------------|
| Solvent | Water | Aqueous NaSCN (1.25M) |
| Temperature (°C) | 30 | 30 |
| Mark-Houwink-Sakurada constants:- $\kappa \times 10^5$ (dl/g) a | 14 0.7 | 121 0.5 |
| Molecular weight range $M \times 10^{-4}$ | 1-340 | 12-83 |
| Absolute method | Sedimentation and diffusion | Light scattering |

3.2.4 Kinematic Viscosity Determination. The kinematic viscosity of a liquid, μ , equals its dynamic viscosity divided by its density (i.e. $\mu = \eta / \rho$). During this work, kinematic viscosities were measured in accordance with BS188:1977,⁽¹⁵²⁾ using the two designs of glass capillary viscometer illustrated in *Figure 61*. U-tube viscometers (*Figure 61a*) were used for very dilute solutions with values of μ below $3.5\text{mm}^2/\text{s}$. Suspended-level (Ubbelohde) viscometers, *Figure 61b*, were more suitable for normal concentration polymer quenchant solutions, since they offer the advantage of measurements independent of sample volume.

For both viscometer designs, the kinematic viscosity is related to the efflux time, t . As long as liquid flow is not infinitely slow, potential energy is partially lost in overcoming friction. Some of the potential energy is also lost through conversion to kinetic energy, which in turn is dissipated through the formation of vortices on exit from the capillary. The relationship between μ and t is derived from Poiseuille's law:

$$\mu = Ct - B / t \quad (21)$$

where $C = \frac{\pi d^4 h g}{128LV}$

and $B = \frac{aV}{8\pi L}$

μ = kinematic viscosity

t = efflux time

d = diameter of capillary tube

h = mean head of liquid

g = acceleration due to gravity

L = length of capillary tube plus 3 times its diameter

V = volume of liquid which flows in time t

a = constant

However, if the flow rates are sufficiently slow, i.e. if t is sufficiently large ($>200s$), the effect of the kinetic energy correcting term B/t becomes negligible and equation (21) is simplified to:

$$\mu = Ct \quad (22)$$

Equation (22) was used throughout this work, with the viscometer factor C given on a calibration certificate supplied by the manufacturer. The operating procedure for the suspended-level viscometers was slightly different to that previously described for the U-tube. The viscometer was charged with the polymer quenchant solution through tube L, ensuring that the ventilation tube M was not blocked (*Figure 61b*). The viscometer was immersed in the thermostatic bath and, after temperature equalization, tube M was closed and suction applied to capillary tube N until the liquid reached a level about 5mm above E. The liquid was held at this level by closing tube N. Tube M was then opened so that the solution dropped from the lower end of the capillary tube. When the sample was clear of both the capillary end and the lower end of tube M, tube N was again opened. The efflux time was the time taken for the bottom of the meniscus to pass from the top edge of mark E to the top edge of mark F. The opening and closing of the tubes was simply performed by applying finger pressure. As for the U-tube viscometer, two successive measurements to within 0.2 per cent were used to calculate μ from equation (22).

3.2.5 Examination of the PAG Inverse Solubility Phenomenon.

The inversion temperature for a 15 volume per cent solution of each as-supplied PAG concentrate listed in Table 3 was assessed visually, using a technique based on the standard test method for evaluating the cloud point of nonionic surfactants.⁽¹⁵³⁾ A 50ml sample of each solution was poured into a 25mm by 200mm test tube and then heated in a water bath to a temperature above its cloud point. The test solution was agitated during the heating phase with a partial immersion thermometer and again when air cooled. The inversion temperature was equal to that at which the sample lost its trace of turbidity. The process was repeated until consecutive results agreed to within 1°C.

In order to study the effect of temperature on the conformation of a typical PAG molecule in solution (equation 20), limiting viscosity numbers were measured for aqueous Quendila PA solutions at 25°C, 40°C and 60°C as described in Section 3.2.3. Furthermore, kinematic viscosity measurements were made for both 1.0 and 10.0 weight per cent solutions of the dehydrated Quendila PA concentrate at temperatures between 25 and 80°C.

The higher inversion temperature of Quendila PHT, compared with Quendila PA, was thought to be due to an increased proportion of oxyethylene units in the polymer chain (*Figure 37*). Therefore, in order to examine this hypothesis, proton nuclear magnetic resonance (NMR) spectroscopy was employed. This technique enabled the ratio of ethylene oxide to propylene oxide derived units to be established for each of these PAG quenchant products.

3.2.5.1 Nuclear magnetic resonance spectroscopy

NMR spectroscopy makes use of the property of spin possessed by nuclei whose atomic number and mass number are not both even. Such nuclei have an associated magnetic moment and, when placed in a strong magnetic field, align themselves with spin parallel and antiparallel with respect to the field: these different orientations have different energies. Thus, by applying an oscillating field in the radio frequency range, the nuclei become excited and their change in energy level may be observed as a resonance peak.

The value of the magnetic field, at a given nucleus, depends on the electronic structure surrounding it; therefore nuclei absorb energy at different frequencies when in different electron environments. In proton NMR spectroscopy, which was used during this work, the spectrum obtained for a compound is made up of peaks which represent hydrogen atoms surrounded by different atomic groups. The difference measured in parts per million (ppm) on a scale labelled δ , between the frequency of an isolated hydrogen atom taken as a reference point, and a particular hydrogen

atom in a given compound, is defined as its chemical shift. The chemical shift and spin coupling (i.e. the splitting of a signal from a single nucleus or group of closely related nuclei into $n+1$ protons, where n is the number of equivalent neighbouring protons) give qualitative structural information. Since the intensity of the NMR signal is directly proportional to the number of nuclei producing it, quantitative measurements can be made without requiring pure standards and calibration curves.⁽¹⁵⁴⁾

A Bruker AC300 high resolution NMR spectrometer with associated integration system was used during this work. This unit operated at 300MHz for proton resonances. Dehydrated samples of both Quendila PA and PHT were run as 50 weight per cent solutions in deuteriochloroform which is virtually "transparent" in the proton spectrum. The hydrogen atoms of tetramethylsilane were assigned as the reference point with a corresponding δ value of zero.

3.3 Preparation of Polymer Quenchant Solutions.

In industry, the most popular way of quoting polymer quenchant concentrations is as a volume percentage of the as-supplied concentrate. This figure gives no real indication of the true polymer concentration in solution. Nevertheless, since this is the most common method, and because the concentrate formulations are unspecified by the suppliers, it was also generally used throughout this work.

Fresh polymer quenchant solutions were prepared by diluting the as-supplied concentrates with distilled water prior to each series of tests. The method for dissolving the concentrates was the same irrespective of polymer type. For example, 2 litres of a 15 per cent by volume solution was made up by accurately pouring 300 ± 5 ml of polymer concentrate into a 500ml measuring cylinder, and then topping up with distilled water at 50°C to the required volume. Warm water was used in order to facilitate solvation. The cylinder was then vigorously shaken and the contents

carefully poured into a 2 litre beaker. Due to the high inherent viscosity of the concentrates, it was necessary to use the remaining 1500ml of warm distilled water to wash away residual polymer from the inner walls of the measuring cylinder. Finally, the fluid within the beaker was stirred to ensure homogeneity before being transferred to the quench tank.

3.4 Polymer Quenchant Solution Concentration Control.

3.4.1 Refractive Index. The most popular method of monitoring the concentration of polymer quenchants is by using a hand-held refractometer. An Atago N1 refractometer, illustrated in *Plate 3*, was used during this work. A small drop of the polymer solution was placed onto the glass slide of the refractometer, which was then held up to the light and a number read directly from the scale seen through the eyepiece (*Figure 62*). It was important when making the measurements to compensate for temperature variations, by adjusting the refractometer to read zero for distilled water at the same temperature as the polymer solution.

The refractive index was given in terms of an arbitrary "Brix number", relating to the concentration of sugar solutions. The refractometer was calibrated for the Quendila PA, Parquench 90 and Aquaquench ACR products, using a number of freshly prepared solutions of absolute concentration between 5 and 30 per cent. A calibration plot was then produced showing the relation of solution concentration (in volume per cent of the as-supplied concentrate) to the corresponding Brix number. The slide of the refractometer was thoroughly cleaned using warm water after each measurement in order to prevent possible contamination, and hence spurious results.

3.4.2 Kinematic Viscosity. Kinematic viscosity measurements may also be used to monitor the concentration of polymer quenchant solutions. The kinematic viscosities for the various concentration Quendila PA, Parquench 90 and Aquaquench ACR solutions were measured at 40°C as described in Section 3.2.4.



Plate 3. Atago NI hand refractometer for monitoring the concentration of polymer quenchant solutions.

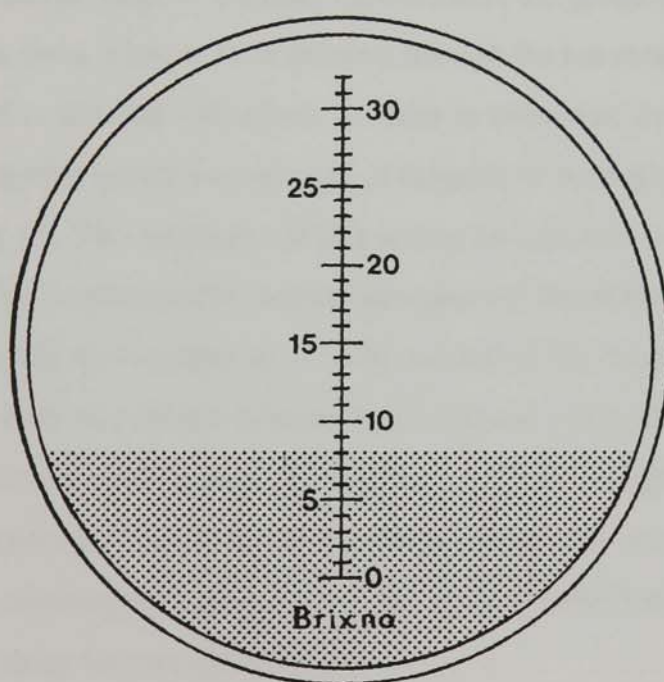


Figure 62. View through eyepiece of refractometer.

3.5 Assessment of the Polymer Quenchant Cooling Characteristics.

The test used to assess the cooling characteristics of the polymer quenchants was based on that outlined in the Wolfson Engineering Group quench test specification.^(24,25) The standard form of the test, which has been submitted as both a British and ISO standard for evaluating static quench oils, was adapted to include agitation of the polymer quenchant samples. A schematic diagram of the original gravity-drop quench test rig, operated by the Wolfson Heat Treatment Centre at Aston University prior to August 1985, was given in *Figure 8*. Preliminary trials were performed using this rig in order to optimize the test conditions for polymer quenchants. From the experience gained, a new test rig was assembled.

3.5.1 Construction of Revised Quench Test Rig. The original gravity-drop probe transfer system had a number of shortcomings, the principal one being that the probe tended to bounce upon contact with its end-stop resulting in vibration and premature breakdown of stage A cooling. Furthermore, the probe was difficult to clean between tests, since it had to be withdrawn through the hot zone of the furnace whilst still covered in residual quenchant. In order to overcome these problems a pneumatic probe transfer system was adopted. A diagram of this replacement test rig is shown in *Figure 63*. Two miniature double-acting air cylinders with a stroke of 160mm controlled the vertical and horizontal movement of the probe, whilst a series of ancillary valves and moving-part logic units controlled the sequence of events. *Figure 64* shows both the circuit diagram and sequence using standard CETOP (European Oil Hydraulic and Pneumatic Committee) symbols. A regulator was used to maintain the operating pressure at 550kPa (80psi) Originally a compressor was used, but this was replaced by a compressed gas cylinder which was quieter, and eliminated the time delay for pressure build-up.

The quench probe was connected to the piston of the vertically acting cylinder (A) by a support plate. Cylinder A was in turn mounted on an 8-wheeled aluminium shuttle trolley. This trolley was propelled in the horizontal plane by cylinder B, running on four bright nickel plated steel rails which prevented lateral movement of the probe.

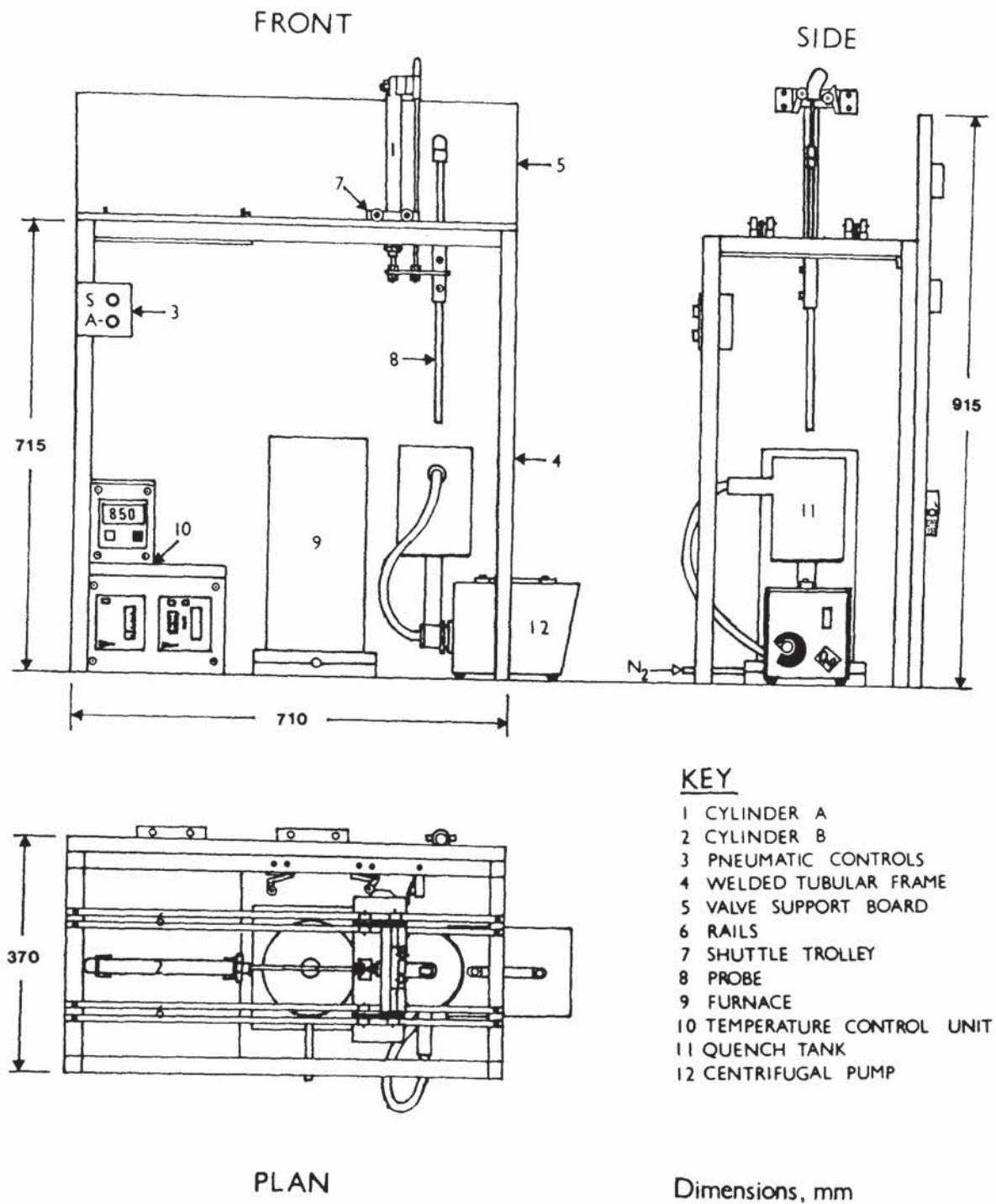


Figure 63. Replacement quench test rig.

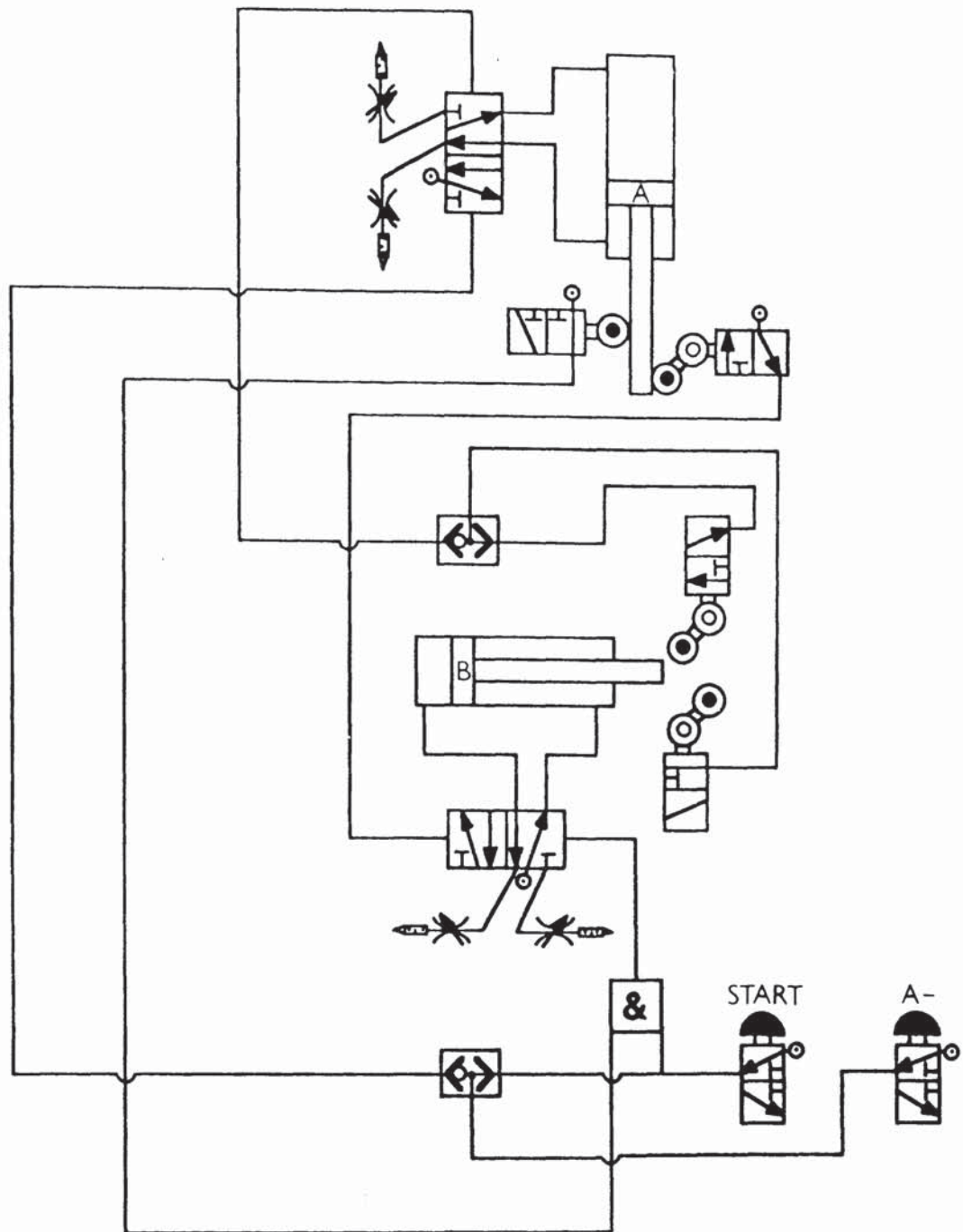


Figure 64. Circuit diagram for pneumatic probe transfer system using CETOP standard symbols.

SEQUENCE: A-, B+, A+, STOP. (QUENCH)

A-, STOP.(CLEAN)

B-, A+, STOP.(FURNACE)

Radial probe movement was prohibited by a stainless steel shaft which was connected to the support plate and ran through a bush in the base of the trolley. This shaft also supported a specially sculptured aluminium block which activated the roller-trip-pilot valves attached to the top of cylinder A. The transfer system was bolted onto a welded 25mm square tubular steel frame, which was in turn bolted to a bench to prevent movement. A wooden back-board supported the lubricator, eight outlet manifold and pneumatic control valves. The trolley had a profiled edge which activated both the roller-trip-pilot valves connected to the tubular frame, and a microswitch which commenced data collection as the probe was lowered into the quenchant. The probe transfer time between the furnace and the quench tank was controlled by throttle valves, which were adjusted so as to complete the operation in 1.0 ± 0.2 s (within the maximum specified time of 2s)⁽²⁴⁾.

As can be seen from *Figure 64*, the probe followed an up-across-down quench sequence. Once cooled, it could be raised from the quenchant by retracting cylinder A's piston, to facilitate cleaning prior to being replaced in the furnace. Warm water was used to clean the probe when using aqueous quenchants, methylated spirit when testing oils. Single handed operation of the system was possible, since just two push buttons controlled the transfer sequence and data collection was started automatically. Furthermore, probes with about a fifty per cent shorter support tube were used (see *Figure 7*), compared with those required for the original gravity-drop system.

A resistance-heated tube furnace insulated with ceramic fibres for rapid heating (approximately 20 minutes) was custom made for the new test rig. The 25mm internal diameter refractory tube was wound such that a uniform heating zone 150mm long was developed. A Eurotherm thyristor controller maintained the probe preheat temperature at $850 \pm 5^\circ\text{C}$. The controller type K (chromel/alumel) thermocouple was positioned midway along the length of the hot zone. In addition, supplementary thermocouples were used in conjunction with a Eurotherm multichannel digital readout to monitor the temperature of both the furnace and the quenchant sample. In an attempt to prolong the life of the probe, the furnace was designed so that it could be purged with nitrogen. During probe preheat a nitrogen flowrate of around 2 litres/minute was maintained.

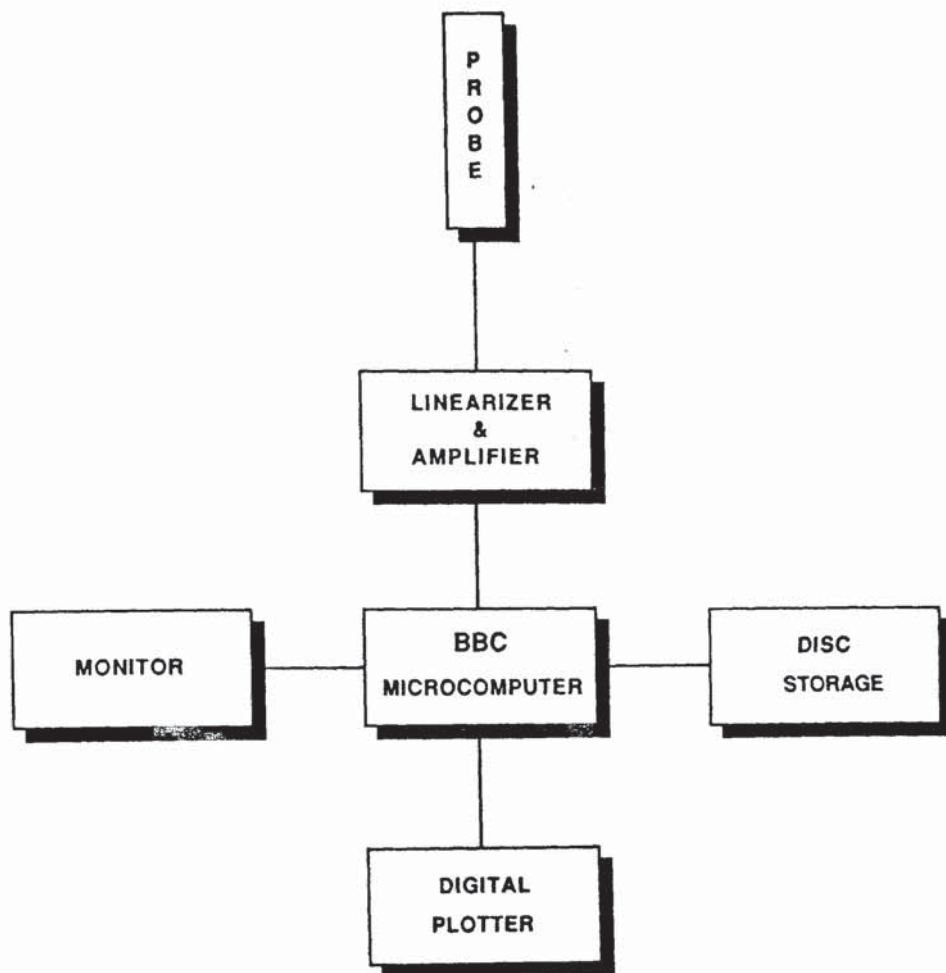


Figure 65. Computerized quench data acquisition system.

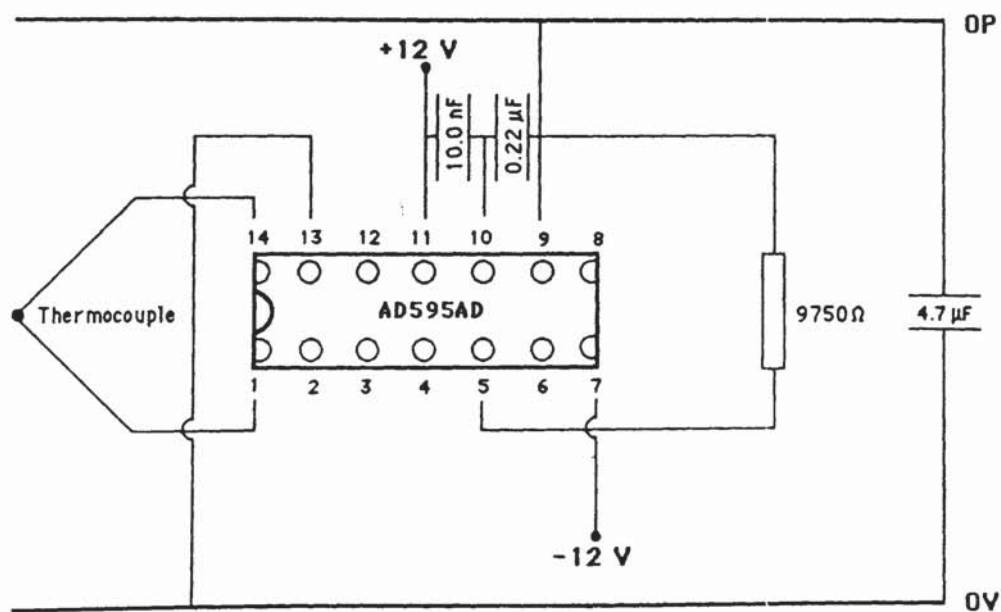


Figure 66. Linearizer and amplifier circuit.

3.5.2 Measurement System. The original test rig used an electronic differentiator to produce a rate signal proportional to the variation in probe thermocouple output with time; this cooling rate signal was recorded relative to probe temperature using an X-Y recorder. Simultaneously, a time-temperature plot was produced using a Y-t recorder. However, in order to facilitate data handling this system was replaced by a computer technique. A BBC model B microcomputer formed the nucleus of the new system, as can be seen in *Figure 65*. *Plate 4* illustrates the revised quench test rig and associated measurement system hardware.

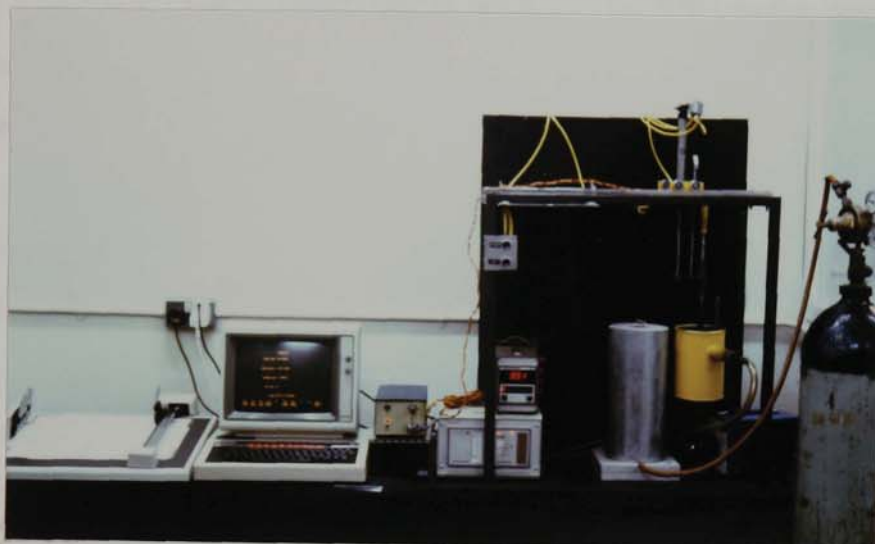


Plate 4. Revised Wolfson Engineering Group quench test rig for evaluating the cooling characteristics of polymer quenchants.

The software was based on a package developed by GKN Technology Ltd.,⁽¹⁵⁵⁾ and incorporated three programs written in BASIC for equipment calibration, data recording, and the analysis and plotting of both time-temperature and cooling rate-temperature curves. A listing of these programs is given in Appendix B. Twin 80-track single density 5.25 inch (133mm) disc drives were used in conjunction with a Kenda Professional DMFS (Disc Management Filing System). Drive A was used to

run the quench test software, whilst drive B provided an archive for the data. Up to 400 kbytes of data, equivalent to about 125 one minute tests, could be stored on each disc.

A linearizer and amplifier (*Figure 66*) were required to transform the probe thermocouple output into a form compatible with the BBC microcomputers in-built analogue to digital converters (input voltage 0 - 1.8V). A sampling frequency of 30 points/s was employed, and throughout this work the data was averaged on a sliding basis over five points in order to smooth the curves; as a result six readings were actually recorded every second. Consequently, since quench data was always recorded for 60s, 360 data points were recorded during each test. The computer programs were very "user friendly", being driven by the BBC microcomputers red user defined function keys. The first program was devoted to probe calibration using up to five soak temperatures. Each probe was calibrated individually and the soak temperatures normally used were room temperature, 232°C, 438°C, 644°C and 850°C, thus maintaining approximately equal temperature increments. The computer calculated a least squares fit, recording both the zero error and the number of bits/°C for the probe. Before each series of tests, the calibration was checked before data collection could commence. If the discrepancy between the measured and calculated temperatures exceeded either 2 per cent or 5°C, recalibration was necessary.

The second program was devoted to the collection of the quench data. After input of the test conditions, the temperature of the probe was displayed on the monitor. Once the probe had been soaked for 5 minutes at $850 \pm 5^\circ\text{C}$ it was transferred to the quench tank. The data collection was triggered automatically by the event marker microswitch previously described. Following the predetermined sample time of 60s, an audible signal was given to indicate that the data could be ascribed a filename and saved on disc.

Due to the limited memory capacity of the BBC microcomputer, the data had to be recalled from the disc in order to run the final analysis program. The shape of both

the time-temperature and cooling rate-temperature curves could be displayed on the screen of the monitor, plus a numerical listing of the data. This last feature was extremely useful since the cooling parameters used to characterize the quenchant could be read directly. These parameters, outlined in the specification,⁽²⁴⁾ were the cooling times to 600°C, 400°C and 200°C, the maximum cooling rate and temperature at which this occurred, and the rate at 300°C. In addition, when evaluating polymer quenchants both the characteristic temperature and cooling rate for the stage A/B transition were recorded. At least duplicate tests were performed on each quench sample and the mean values for these parameters calculated. The time-temperature and cooling rate-temperature curves were then plotted on A3 size paper using a serial interface five pen flat-bed digital plotter (Watanabe MP1000).

3.5.3 Surface Condition of Probe. A vital element affecting the achievement of reproducible quench test results was the formation of a tenacious surface oxide on the probes. New probes required conditioning prior to initial use as described in the Wolfson specification,⁽²⁴⁾ by carrying out a minimum of six dummy quenches from 850°C into a hydrocarbon oil. Before each series of tests, the condition of the test probe was checked by quenching into a static 2 litre sample of the reference quenching fluid at 40°C. The reference fluid was supplied by the National Physical Laboratory and is an unblended paraffinic mineral oil with specified physical and cooling characteristics. If the measured cooling characteristics from duplicate tests were within their specified range of values, testing could commence. However, if these cooling criteria could not be fulfilled, reconditioning of the probe was necessary. This was performed by mounting the probe in a lathe at 500rpm. and repolishing its surface with 600-grit emery paper (taking care not to round the edges). The dummy quench routine was then repeated until the measured cooling characteristics for the reference fluid were once again within their specified range.

3.5.4 Quenchant Sample Volume and Temperature. A quench sample volume of 2 litres was normally used. Larger samples were only used during trial runs with prototype quench tanks. The samples were heated to the test temperature using an internal electric resistance heater, thermal gradients being minimized by

agitation. A cooling coil could also be immersed in the sample to control its temperature to within $\pm 1^{\circ}\text{C}$. Neither the resistance heater or the cooling coil remained in the tank during the test. The test temperatures which were generally used were 40°C for quench oils and 30°C for polymer quenchants. The latter temperature was chosen on the advice of the Wolfson Engineering Group which comprised both polymer quenchant suppliers and users.

3.5.5 Quenchant Sample Agitation. The standard Wolfson Engineering Group test for evaluating quench oils specifies the use of a non-agitated sample. However, agitation is believed essential for the successful application of polymer quenchants (as was described in Section 2.11). Some form of agitation was therefore required for a realistic test when evaluating the cooling characteristics of such solutions. Consequently, a number of different agitation systems were examined. This work was carried out in conjunction with the Wolfson Engineering Group's committee "Agitation of Quenching Media".

3.5.5.1 Impeller / baffle systems.

The first system to be evaluated consisted of a variable speed 75mm twin-flat-bladed impeller, used in conjunction with an H-shaped baffle (*Figure 67*). The circular vessel used contained 2.5 litres of quenchant. A 20 per cent PAG (Quendila PA) solution at 30°C was chosen for these initial trials, being within the range most frequently employed in industry. An electric drill was used to drive the impeller via a flexible coupling. The speed of rotation was measured using a hand-held tachometer, and could be adjusted by means of a rheostat. The probe was positioned at the midpoint of a chord, equidistant between the container edge and the central baffle, and at the centre of the fluid volume in the vertical plane. The impeller was similarly positioned, parallel to the centre of the probe in the opposite half of the container, inclined at an angle of about 10° to the vertical. Impeller speeds up to 1300rpm. were used; higher speeds resulted in air-entrapment and foaming. The 75mm flat-bladed impeller was then replaced by a 40mm diameter high pitch model boat propeller (preferred by Lakin⁽¹¹⁾) and the tests repeated.

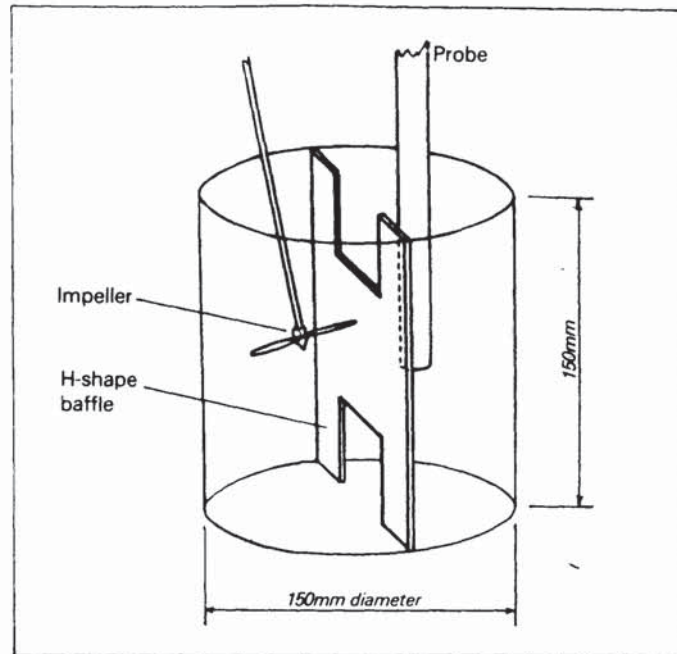


Figure 67. Schematic diagram of the impeller/ H-baffle agitation system.

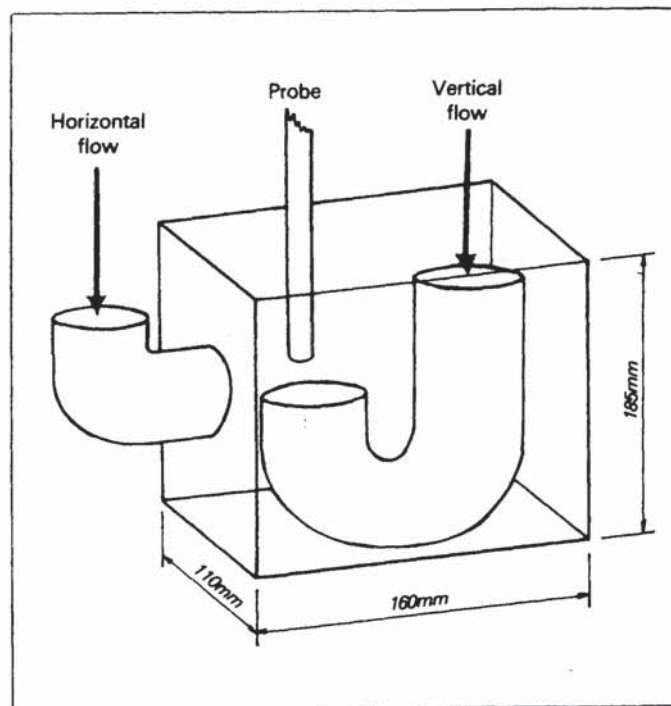


Figure 68. Schematic diagram of the prototype quench tank used in conjunction with the variable speed pump, showing the inlets for either vertical or horizontal flow.

3.5.5.2 Pump agitation systems.

A number of pump agitation systems of various design were evaluated. Most of this work was performed using a Charles Austen (Type C16C) centrifugal pump which had a 25W motor and rheostat speed control, producing a maximum flowrate in excess of 23 litres per minute at zero head. It was portable and had a nylon-filled bakelite housing and impeller, neoprene lip seals and a stainless steel shaft. Thus, cleaning between polymer quenchant tests was simply a matter of thoroughly flushing with warm water.

The first pump system to be examined incorporated an oblong shaped perspex tank which enabled the probe to be photographed as it cooled. The pump outlet could be connected to one of two positions enabling either vertical or horizontal quenchant flow with respect to the axis of the probe, as illustrated in *Figure 68*. Two 12.5mm internal diameter by 500mm long flexible PVC tubes were used to make the necessary connections. The pump inlet tube (not shown in the diagram) was positioned against the side of the tank opposite the horizontal orifice. This system also had a total capacity of 2.5 litres.

The level of agitation could be quantified in terms of the fluid velocity emerging from the pump outlet orifice. The fluid velocity was equal to the flowrate divided by the cross sectional area of the outlet. The fluid velocity could thus be varied by adjusting either the speed of the pump (and hence the flowrate), or the size of the outlet orifice. Since the flowrate at a particular pump setting was dependent on the viscosity of the fluid, calibration was required for each polymer solution concentration and temperature tested. The calibration was performed by measuring the time taken to pump a known volume of quenchant. Using the same pipework, the pump inlet was connected to a graduated cylinder which was positioned so as to maintain the same average head of liquid above the pump as when it was connected to the quench tank. At least 500ml of solution was pumped prior to commencing the timing in order to ensure that the pump was fully primed and that its impeller

had gained momentum. An electronic stopwatch was used to measure the time taken for the fluid level to drop between two gradations. This process was repeated until two consecutive readings agreed to within 0.2s. The flowrate and hence fluid velocity could then be calculated. If on the other hand, a predetermined fluid velocity was required, the speed of the pump had to be adjusted until the required flowrate was achieved. For example, in order to obtain a fluid velocity of $0.50 \pm 0.02\text{m/s}$ through a 25mm diameter outlet, a flowrate of 14.73 litres per minute was required. Therefore, 2 litres of the quenchant needed to be pumped in $8.1 \pm 0.2\text{s}$.

Tests were performed using 10, 20 and 30 per cent PAG (Quendila PA) solutions at 30°C , with both vertical and horizontal flow conditions. By controlling the pump speed, and the outlet orifice size using pierced rubber stoppers, fluid velocities up to 1m/s were possible. The pump was always run intermittently for at least five minutes prior to quenching in order to dissipate any entrapped air bubbles, thus avoiding dual phase flow conditions. The quenched probe was positioned 25mm above the geometric centre of the vertical outlet. When using horizontal flow conditions the probe was positioned such that its surface was 25mm from the outlet, and with its thermocouple hot junction at the centre of the submerged jet.

A series of tests were also performed at West Bromwich College of Commerce and Technology, using the quench test system which was shown in *Figure 41*. Once again a 20 per cent PAG (Quendila PA) solution was tested at 30°C . The solution was pumped from a large holding vessel to the quenching unit shown in *Figure 69*, using four 120W (Type 175 DP/C) Totton centrifugal pumps. The original quench unit was modified by the incorporation of an aluminium sleeve in order to reduce the diameter of the outlet from 42 to 25mm. The flowrate was measured by recording the time taken to pump 10 litres of the quenchant through the annulus formed when the probe was positioned such that its thermocouple hot junction was 105mm from the top of the unit. By adjusting the speed of the pumps using a rheostat,

and from knowledge of the area of the annulus formed between the probe and the outlet tube, tests were performed using fluid velocities of 0.5, 1.0 and 2.0m/s. Fluid velocities in excess of 2.0m/s were not practicable since the jet of fluid produced impinged on the base of the furnace which was vertically above the quench unit. This system had a minimum quenchant sample capacity of 25 litres.

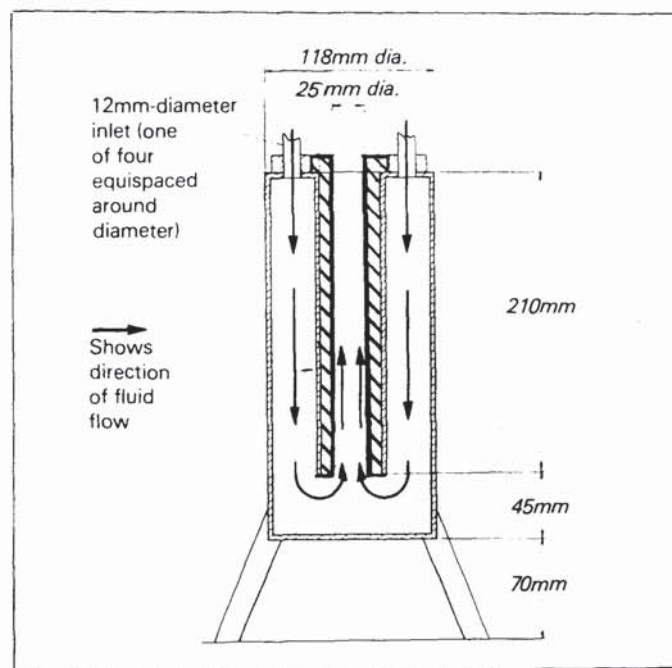


Figure 69. West Bromwich College of Commerce and Technology quench unit modified to incorporate a 25mm internal diameter pump outlet tube.

From the experience gained using these various systems, that shown in *Figure 70* was finally chosen. The diameter of the tank was within the range specified by the Wolfson Engineering Group, as was the required sample volume (2 litres).⁽²⁴⁾ Furthermore, when the probe was positioned 25mm above the geometric centre of the 25mm diameter pump outlet orifice, its thermocouple hot junction coincided with the centre of the quenchant sample volume.

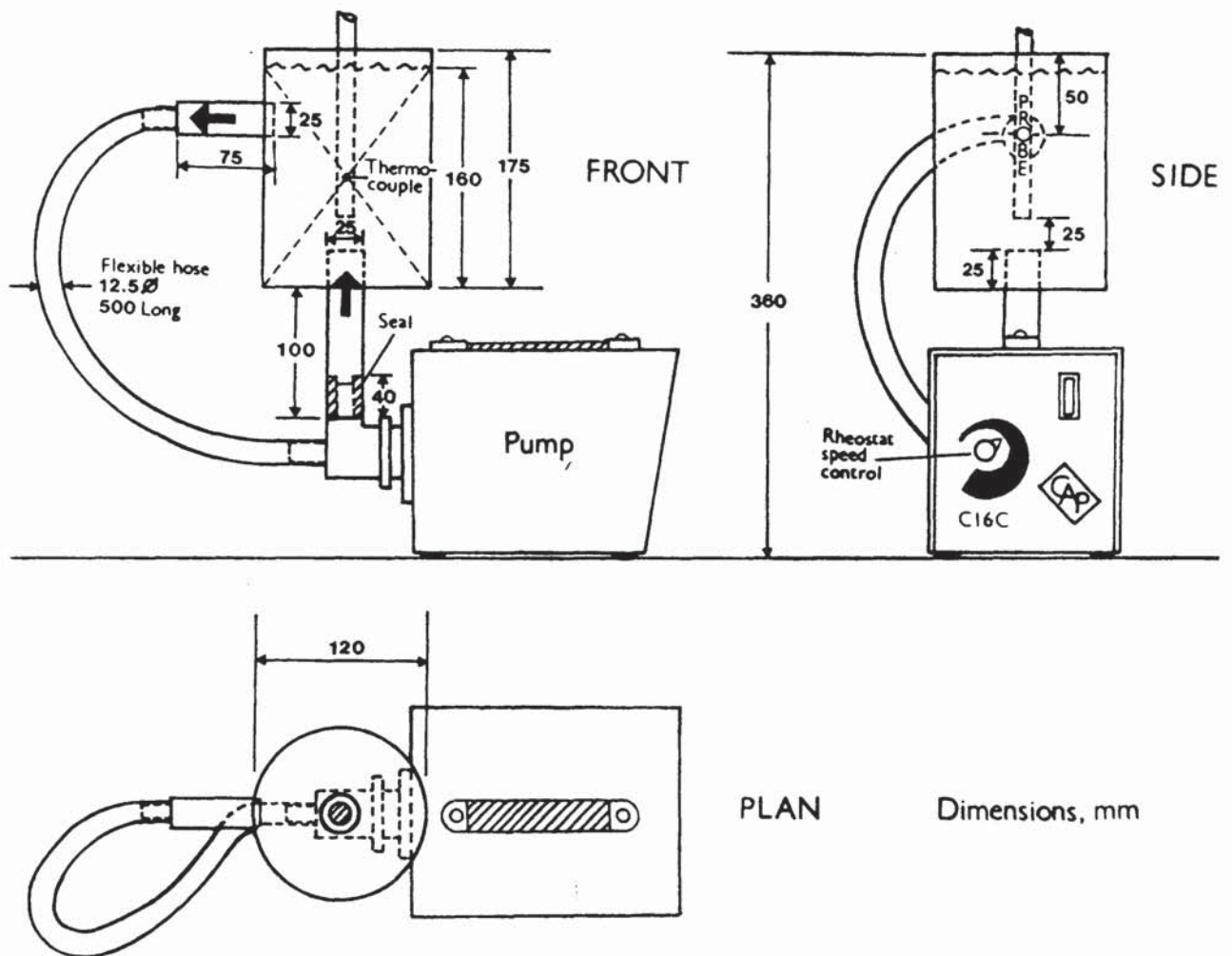


Figure 70. Preferred centrifugal pump agitation system.

In order to assess the influence of probe position with respect to the pump outlet orifice, trials were performed at different heights and horizontal displacements from its geometric centre. This was facilitated by the pneumatic probe transfer system which ensured precise positioning of the probe. These trials were conducted using a 15 per cent PAG (Quendila PA) solution at 30°C and a fluid velocity of 0.5m/s. In addition, the effect of pump inlet position was examined using a specially manufactured tank. This tank was of the same dimensions as that shown in *Figure 70* having two inlets with centres 100mm and 150mm from the top of the unit. A rubber stopper was used to seal the redundant inlet.

3.6 Comparison of Polymer Quenchant Cooling Characteristics.

The cooling characteristics for each of the polymer quenchant products listed in *Table 3* were evaluated using identical test conditions. A 15 per cent by volume solution of each concentrate was tested at 30°C in both the static condition and agitated at 0.5m/s. These conditions were chosen since they lay within the range of industrial application for each polymer type. The probe was always positioned 25mm above the geometric centre of the 25mm pump outlet orifice. A typical and popular example of each class of polymer was then chosen for a more comprehensive analysis. The "representative" products chosen were as follows:

PAG (Quendila PA)

PVP (Parquench 90)

Polyacrylate (Aquaquench ACR)

3.7 Visual Examination of Polymer Quenchant Cooling Mechanism.

Initially, videorecordings of the probe as it cooled in each of the representative polymer solutions were made. The tank shown in *Figure 68* was used for this preliminary work. A Sony U-matic professional videorecorder and camera were employed. The best results were obtained with a dark background produced by placing a black card behind the tank. Incident illumination was provided by two 500W photoflood lamps which were positioned approximately 500mm in front of the probe, and at an angle of about 45° either side of it. Both static and agitated results for

the 15 per cent solutions at 30°C were recorded. However, the resolution of the videorecordings was fairly poor, especially with the polyacrylate which, unlike the other two polymer types, formed a virtually opaque solution.

In order to improve the resolution, 35mm photography was adopted. The illumination conditions remained the same as for the videorecording work. A Canon T70 camera with a built in motor winder and command back was used so that the time interval between successive shots could be controlled. The camera was mounted on a tripod, and the pneumatic transfer system enabled it to be prefocussed on the probe in the quenched position. A Tokina zoom lens, set at a focal length of 80mm and combined with a 31mm extension tube, was employed for this close-up work.

A circular perspex tank identical to that shown in *Figure 70* was used to photograph a series of flow visualization experiments. A 15 per cent PAG solution at 30°C and 0.5m/s was chosen since it had a viscosity intermediate between the equivalent concentration PVP and polyacrylate solutions. The flow pattern around a cool probe positioned 25mm above the pump outlet orifice was recorded by injecting ink into the flexible tubing connecting the pump inlet to the tank.

Perspex tanks were found to be incompatible with PAG quenchants, since acute crazing developed following prolonged use. Unacceptable distortion was also experienced when photographing through circular tanks. Consequently, a flat sided glass tank 140mm x 140mm x 180mm high was constructed. This tank had a 25mm pump outlet positioned 50mm from its front face. A quench test for each of the representative polymer solutions was photographed in both the static and 0.5m/s agitated condition.

3.8 Effect of Polymer Quenchant Concentration, Temperature and Agitation.

The three most important parameters which are known to influence the cooling capacity of a polymer quenchant are the solution concentration, temperature and level of agitation. In order to study the relative influence of each of these variables, for each representative polymer, it was necessary to standardize a set of test conditions, and

then to change the level of one parameter at a time. The "standard" conditions used were a 15 volume per cent solution tested at 30°C and agitated at 0.5m/s. These particular conditions were chosen since they lie within the range of industrial application for each polymer type.

3.8.1 Polymer Solution Concentration. Polymer solution concentrations between 1.0 ± 0.1 and 30.0 ± 0.3 volume per cent were examined. A fresh solution was prepared for each test and its concentration checked using both refractive index and kinematic viscosity measurements. Upon completion of the duplicate quench tests the concentration was again checked using the hand-held refractometer.

3.8.2 Polymer Solution Temperature. Polymer solution temperatures between 10 and 70°C were employed. Prior to quenching, the temperature was controlled to within $\pm 1^\circ\text{C}$. The temperature of each polymer solution after quenching was also recorded.

3.8.3 Polymer Solution Agitation. Each polymer solution was evaluated in the static condition and at a range of fluid velocities. The maximum fluid velocity obtainable for each polymer solution was dictated by its viscosity.

3.9 Simulated Ageing of Polymer Quenchants.

An accelerated ageing programme was undertaken to study the progressive effect of long-term usage on the characteristics of the representative polymer quenchant solutions. Three 63.5mm diameter by 40mm long austenitic stainless steel bars (En58b, nominal composition 0.07% C, 0.5% Si, 0.9% Mn, 0.9% Ni, 17.0% Cr, 0.4% Ti), weighing 1kg each, were repeatedly heated in a muffle furnace to 850°C and quenched into 2 litre samples of the polymer quenchants. Each bar was thoroughly cleaned before being reheated in order to prevent decomposition of residual polymer on its surface and contamination of the quenchant. The bars were suspended on nichrome wire to facilitate transfer and manual agitation when immersed in the quenchant. The tall-form corrosion resistant vessels, used to contain the quenchant samples, were partially immersed in a cold water bath to prevent the

temperature of the quenchants exceeding 70°C. Each vessel had a lid to reduce evaporative losses and any sedimentary scale was regularly removed. A constant refractive index (equivalent to an initial 15 per cent solution) was maintained throughout the testing. This required the addition of fresh water and polymer to compensate for evaporation and drag-out. The levels of each of these additions were monitored.

The test was accelerated since a ratio of 1kg of quench load per 2 litres of quenchant was maintained. In industrial practice a ratio of 1kg per 15 litres is advised;^(114,118) therefore, the test was approximately 7.5 times more arduous than normal operating conditions. Consequently, the final test quench load of 100kg/litre corresponded to 3/4 tonne of steel per litre industrially, which was equivalent to between two and three years continuous use for some quench tanks.⁽⁷⁶⁾

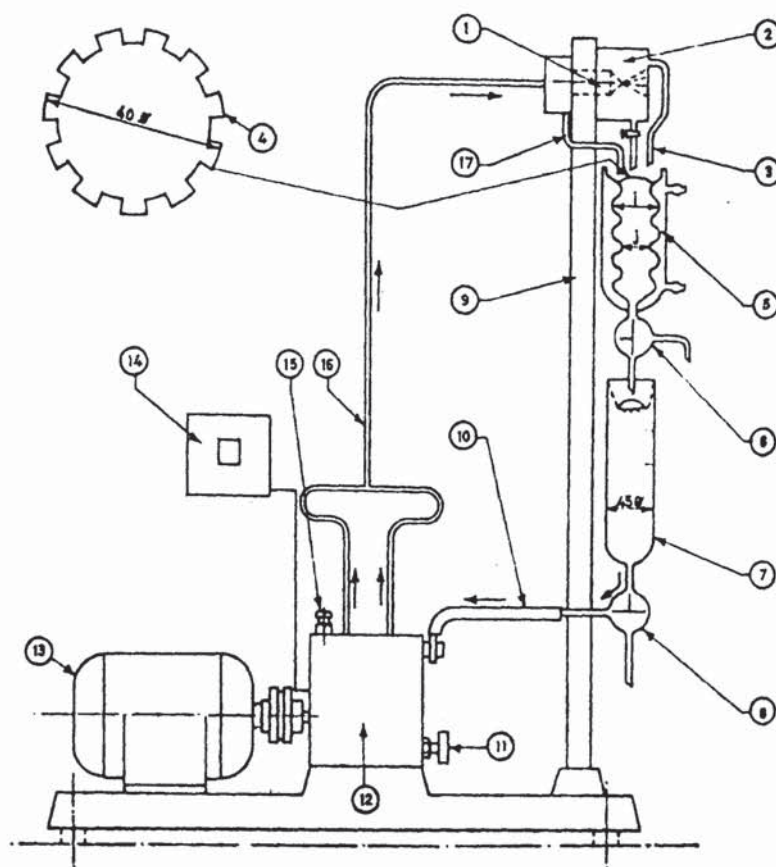
The cooling characteristics of each solution at the standard conditions were evaluated every 2.5kg/litre up to 10kg/litre, and then every 10kg/litre up to the final quench load (100kg/litre). Prior to each quench test the kinematic viscosities of the solutions were measured at 40°C, and pH values recorded every 50kg/litre. The latter measurements were made at room temperature using a glass electrode in conjunction with a Russel 640 digital pH meter, which had been calibrated using both pH7 and pH9 buffer solutions. A 10ml sample of each solution was retained after 10, 50 and 100kg/litre in order to compare their change in appearance. Upon completion of the ageing programme, GPC analysis was performed on the used PAG and PVP samples as described in Section 3.2.2, and limiting viscosity numbers determined for the PVP and polyacrylate (Section 3.2.3).

This ageing work was supplemented by the periodic analysis of polyacrylate samples extracted from an actual industrial installation. T.I. Desford Tubes Limited supplied samples of a nominally 18 per cent Aquaquench ACR solution from their 12,000 gallon (~55,000 litre) tank used for quenching AISI 4140 (nominal composition: 0.4% C, 0.9% Mn, 1.0% Cr, 0.4% S, 0.2% Mo) tubes up to 10m in length. Their

custom built tank, designed for this purpose, provided pumped circulation of quenchant to both external and internal surfaces. A flocculent phase was observed in both the samples supplied by T.I. and from the accelerated ageing programme. This floc appeared to contain traces of scale. Consequently, the interaction between scale and polymer quenchants was examined by adding 1 weight per cent of mild steel filings, which had been oxidized in a muffle furnace, to 15 per cent solutions of each representative polymer product. The appearance and refractive index of these samples were monitored after 14 days.

3.10 Shear Stability of Polymer Quenchants.

The shear stability of a 15 per cent solution of each representative polymer was evaluated using the Kurt-Orbahn standard test method.⁽¹⁵⁶⁾ The apparatus belonging to Hythe Chemicals Limited consisted of a fluid reservoir, a double-plunger pump with an electric motor drive, an atomization chamber with a diesel injector spray nozzle and a fluid cooling vessel (*Figure 71*). The equipment was calibrated with a reference fluid of known shear stability and cleaned by flushing three times with the test solution. The test required 220ml of solution to be added to the fluid reservoir with the cock below the atomization chamber in the closed position. The pump was then started and 50ml of solution removed using the three-way-cock below the cooling vessel. The stroke counter was adjusted for automatic shut-off at the required number of cycles. The flow rate was set at 170ml/minute so that each cycle was completed in one minute. The pressure between the pump and nozzle was 19.0 ± 0.35 MPa. By adjusting the cooling water flow, the fluid temperature measured at the point of discharge of the fluid reservoir was maintained between 30 and 35°C. At the end of the test the cock below the atomization chamber was opened and the sheared fluid collected in a beaker through the three-way cock below the fluid reservoir. The kinematic viscosities of the unsheared and the sheared polymer solutions were then measured at 40°C and the percentage change in their viscosity calculated. Each polymer quenchant was tested at 15, 30, 60 and 90 cycles. A fresh solution was used for each test.



- | | |
|--|--|
| 1. Spray nozzle. | 9. Support column. |
| 2. Atomization chamber. | 10. Connection with pump-suction opening. |
| 3. Outlet for the atomized liquid. | 11. Pump setting screw. |
| 4. Distributor plate for 5. | 12. Double-plunger injection pump, Bosch Type PE 2 A/90. |
| 5. Glass container with cooling jacket (250ml). i = approx. 50mm. j = approx. 25mm. Length = approx. 180mm. | 13. Electric motor, 1.1kW, 900rpm. |
| 6. Three-Way cock. | 14. Automatic stroke-count measuring and cut-off device. |
| 7. Graduated glass reservoir 45mm diameter (250ml). | 15. Ventilating screw/pump. |
| 8. Three-Way cock. | 16. Pressure tubing from pump to injector. |
| | 17. Return line for overflowing liquid. |

Figure 71. Apparatus for shear stability testing⁽¹⁵⁶⁾.

3.11 Polymer Quenchant Solution Rheology.

An Epprecht Rheomat 15 cone and plate viscometer was used to examine the dynamic viscosity of the representative 15 volume per cent polymer solutions over a range of shear rates. A schematic diagram of the test apparatus is given in *Figure 72*. The tests were performed at room temperature (15°C).

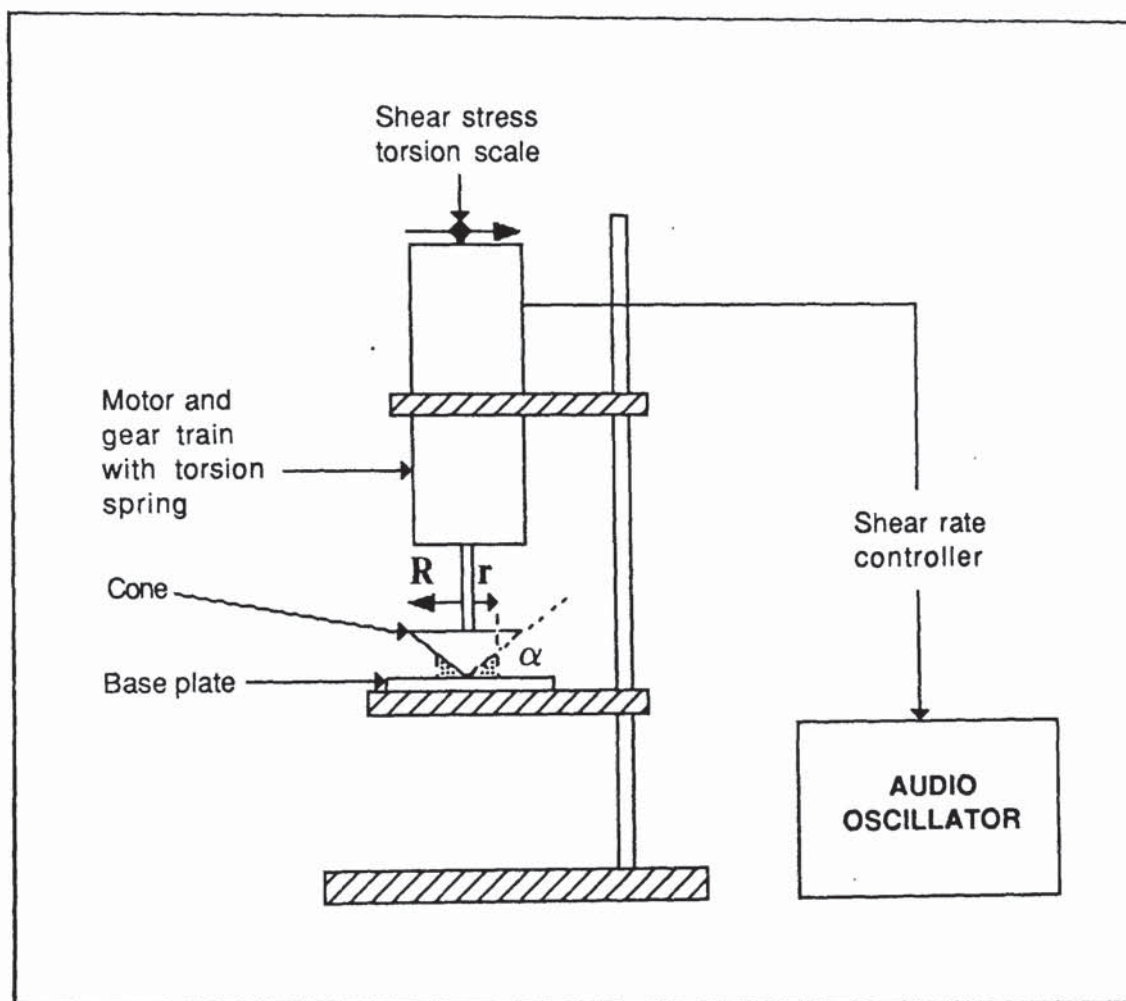


Figure 72. Schematic diagram of the Epprecht Rheomat 15 cone and plate viscometer.

Approximately 10ml of each test solution was spread uniformly onto the fixed base plate of the viscometer. The cone was then lowered onto the base plate, where it rotated upon a ball bearing joint. The cone was rotated by the motor suspended above it. It was driven through a chain of gears by an audio oscillator, which provided a number of fixed frequencies. This generating unit had 15 speed settings. At each

setting the angular velocity, Ω , attained a constant value. Consequently, as can be seen from equation (23), the shear rate $\dot{\gamma}$ over the entire radius of the cone was also constant.

$$\text{shear rate at radius } r \quad \dot{\gamma} = \frac{r \Omega}{r \alpha} = \frac{\Omega}{\alpha} \quad (23)$$

where α is the angle subtended between the cone and the base plate. The shear stress τ was proportional to the torque M , as shown in equation (24). A spiral torsion spring enabled the shear stress to be read directly from a pointer moving over a fixed scale.

$$\tau = \frac{3 M}{2 \pi R^3} \quad (24)$$

Where R equals the radius of the cone. Thus, by adjusting the speed of the cone, and hence the shear rate, the resultant shear stress could be read directly from the scale. The experimental conditions used during the tests allowed values of shear rate up to 3970 s^{-1} . A plot of shear stress against shear rate could thus be produced. Since the dynamic viscosity is given by:

$$\eta = \tau / \dot{\gamma} \quad (25)$$

apparent viscosity values could be calculated for non-Newtonian fluids at different values of shear rate.

3.12 Contamination of Polymer Quenchants.

Experiments were conducted to examine the influence of oil, ammonia and salt contaminants on the cooling characteristics of each class of polymer quenchant. Once again, the standard quench test conditions were maintained for the representative polymer quenchants.

3.12.1 Quench Oil Contamination. The first contaminant to be investigated was a normal speed quench oil (Houghtoquench 3S³). Contamination levels

between 0.10 ± 0.02 and 2.50 ± 0.03 weight per cent oil were examined. The level of contamination was progressively increased by adding a predetermined mass of oil to 1998g of the test solution as shown in Table 6. The Brix number for each contaminated solution was measured using the hand-held refractometer. This process was then repeated for the PAG using a water soluble form of the quench oil (Klenquench 3³).

Table 6. Polymer quenchant oil contamination programme.

| Oil contamination level (wt %) | Oil weight addition (g) | Oil cumulative addition (g) | Total weight of solution (g) |
|--------------------------------------|-------------------------------|-----------------------------------|------------------------------------|
| 0 | 0 | 0 | 1998 |
| 0.1 | 2 | 2 | 2000 |
| 1.0 | 18 | 20 | 2018 |
| 2.5 | 32 | 52 | 2050 |

3.12.2 Ammonia Contamination. The effect of ammonia contamination was also examined. Ammonia is a constituent of carbonitriding atmospheres and has a very high solubility in water. The ammonia was supplied in the form of a 35 weight per cent solution. 1003g of stock fluid was prepared for each quenchant by adding 103g of the representative polymer concentrate to 900g of the as-supplied ammonia solution. This stock fluid then contained 31.4 weight per cent ammonia, combined with 68.6 weight per cent of a 15 weight per cent solution of the polymer. The discrepancy encountered in using a weight per cent form of the polymer solution in the stock fluid was considered negligible. Various levels of ammonia contamination were then produced, by adding the stock fluid in a predetermined ratio to the standard 15 volume per cent polymer solutions as shown in Table 7.

³ Houghtoquench 3S and Klenquench 3 are the trade names of quench oils marketed by Edgar Vaughan and Co. Ltd., Birmingham.

Table 7. Polymer quenchant ammonia contamination programme.

| Ammonia contamination level (wt %) | 31.4 wt% NH ₃ stock fluid addition (g) | Weight of standard solution | Total weight of solution (g) |
|--|---|-----------------------------------|------------------------------------|
| 0 | 0 | 2000 | 2000 |
| 0.5 | 32 | 1968 | " |
| 2.5 | 159 | 1841 | " |
| 5 | 318 | 1682 | " |

A fresh solution was prepared for each quench test since ammonia is volatile and therefore rapidly lost during boiling. Once again the refractometer reading for each solution was recorded.

3.12.3 Salt Contamination. A specific industrially-important example where salt contamination of PAG quenchants occurs is the heat treatment of aluminium alloys. Precipitation-hardenable aluminium components are quenched from nitrite/nitrate salt baths at around 500°C; contamination of the quenchant is inevitable due to inadvertent drag-out of the salt on the parts. To assess the effect of such contamination on the cooling characteristics, distilled water and each of the representative polymer solutions were contaminated with various levels of a typical sodium nitrite/nitrate salt (AVS 250⁴) as shown in *Table 8*. A 30 per cent PAG solution was also tested since this is currently the only class of polymer used for this application.⁽¹¹¹⁾

In order to simulate the aluminium heat treatment conditions the Wolfson probe was heated to 500°C before being quenched. As usual the standard test conditions were employed, i.e. 30°C and 0.5m/s agitation. The kinematic viscosity of each test sample

⁴Degussa Ltd. designation (formerly Cassel TS330)

was measured at 40°C and a refractometer reading taken. Furthermore, inversion temperature measurements were made for the PAG samples as was described in Section 3.2.5.

Table 8. Polymer quenchant sodium nitrite/nitrate salt contamination programme.

| AVS 250 contamination level (wt %) | AVS 250 weight addition (g) | AVS 250 cumulative addition (g) | Total weight of solution (g) |
|--|-----------------------------------|---------------------------------------|------------------------------------|
| 0 | 0 | 0 | 1990 |
| 0.5 | 10 | 10 | 2000 |
| 1.0 | 10.1 | 20.1 | 2010.1 |
| 2.5 | 31.0 | 51.1 | 2041.1 |
| 5 | 53.7 | 104.8 | 2094.8 |
| 10 | 116.2 | 221 | 2211 |
| 12.5 | 63 | 284 | 2274 |
| 15 | 67 | 351 | 2341 |
| 20 | 147 | 498 | 2488 |
| 25 | 165 | 663 | 2653 |

3.13 Drag-Out.

Residual polymer removed from the quench tank on the surface of cooled components reduces the effective concentration of the solution. A simple experiment was performed in order to compare the amount of drag-out for each polymer type. A purely arbitrary test piece was manufactured from 2mm thick austenitic stainless steel (AISI 304, nominal composition 19% Cr, 10% Ni, 2% Mn, 0.08% C). The test piece had a complex shape, as shown in *Figure 73*, featuring a hole and both squared and rounded edges to simulate the sort of profiles which may be encountered with real components. The same test piece was used throughout this work.

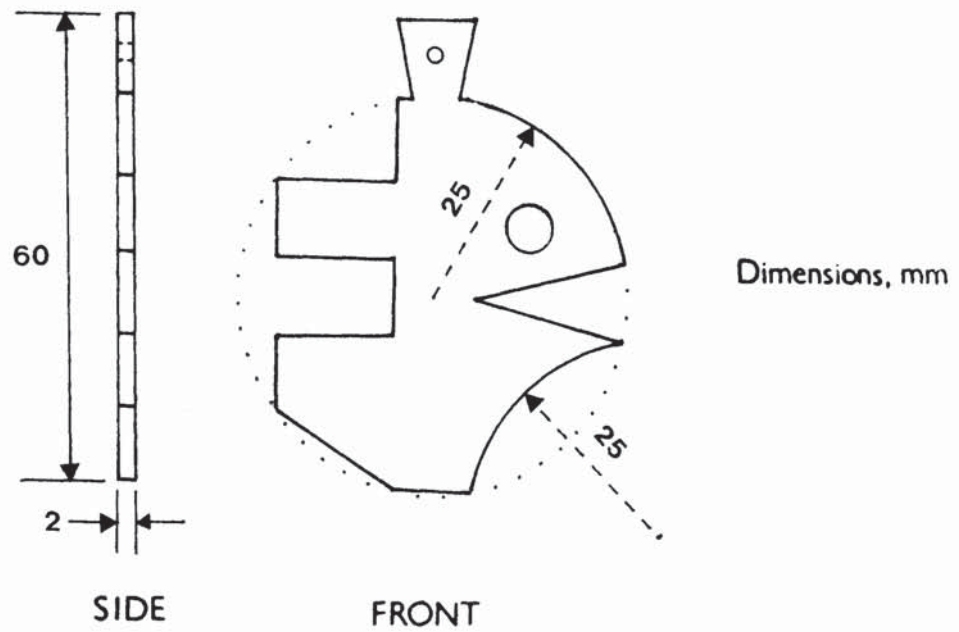


Figure 73. Drag-out specimen manufactured from AISI 304 austenitic stainless steel.

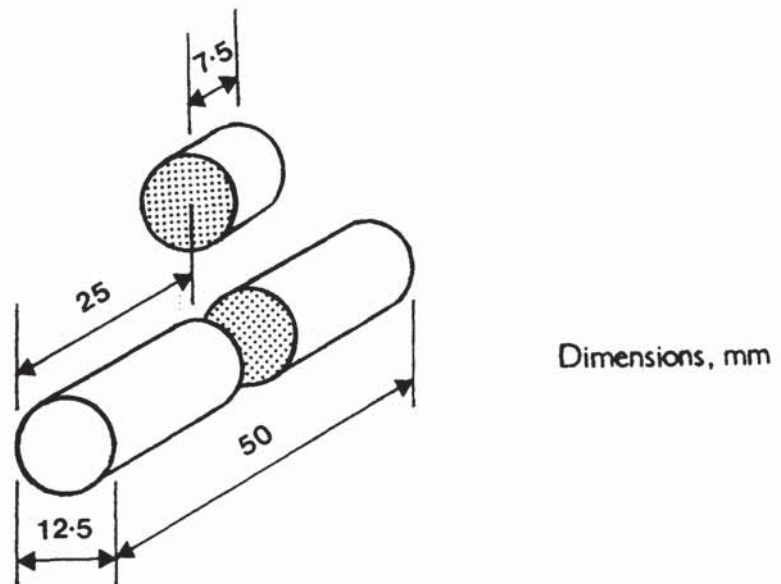


Figure 74. Residual stress specimen manufactured from 080H41 showing section removed for hardness tests.

The test piece was accurately weighed and then heated to 850°C in a Metals Research vertical-tube vacuum furnace at 6.7Pa (5×10^{-2} Torr) to minimize oxidation. It was soaked for 5 minutes at temperature before being rapidly transferred into the quenchant. Nitrogen was purged through the furnace during transfer. The quench tank which was used for evaluating the cooling characteristics (*Figure 70*) was also utilized during this experiment in order to enable both static and agitated quench conditions. In the agitated test, the test piece was suspended approximately 25mm above the pump outlet orifice through which the quench sample was flowing at 0.5m/s. The representative polymers were evaluated at 5, 15 and 25 per cent concentrations and at 30°C. The test piece was immersed in the quenchant for precisely 60s after which it was removed and allowed to drain for a further 60s and then re-weighed. Its gain in mass was used as a means of quantifying the level of quenchant drag-out. Each test was repeated five times. Errors due to oxidation of the test piece were considered minimal for these comparative tests. Both static water at 30°C and a normal speed quench oil (Fenso 40⁵) at 40°C were included in the test programme.

3.14 Quenched Hardness and Residual Stress.

Cylindrical test specimens were manufactured from 080H41 (En8c) steel of composition given in *Table 9*

Table 9. Analysis of steel specimens.

| Composition wt % | C | Mn | Si | S | P |
|---------------------|------|------|------|-------|-------|
| | 0.45 | 0.89 | 0.19 | 0.022 | 0.010 |

The specimens were 12.5mm diameter and 50mm long (*Figure 74*), the length being four times the diameter to simulate an "infinite bar" (i.e. equivalent geometry to Wolfson test probe). This particular material and specimen size were chosen since

⁵Fenso 40 is the trade name of a quench oil marketed by Esso Petroleum Co. Ltd.

they correspond with the conditions with which Nicklin⁽⁷⁰⁾ obtained the greatest success when attempting to correlate the centre hardnesses and cooling parameters determined from static Wolfson Engineering Group tests (Equation (14)). Plain carbon steels such as this have a steeper Jominy curve than alloy steels (*Figure 23*), which means that their as-quenched hardness is likely to be more sensitive to cooling rate. Furthermore, a diameter of 12.5mm corresponds approximately with the maximum for through hardening in a static water quench for this particular steel.

The specimens were austenitized for 30 minutes at 850°C in the Metals Research vertical-tube vacuum furnace, a nitrogen purge being used during transfer to the quench tank in order to minimize oxidation, and thus produce an acceptable surface finish for the stress measurements. The specimens were quenched longitudinally into the same quench tank that was used for measuring the cooling characteristics of the quenchants. Each of the representative polymer quenchants were employed both at the standard agitated conditions and static. Specimens were also quenched into a static normal-speed oil (Fenso 40) at 40°C and into static distilled water at both 30 and 40°C. An additional specimen was fully annealed by furnace cooling from 850°C.

3.14.1 Residual Stress Measurements. The surface residual tangential (hoop) macrostress was measured midway along the length of each quenched cylinder. A well established X-ray diffraction method known as the "two-exposure" technique was used. This technique is preferred by most UK and American workers.⁽¹⁵⁷⁾ The experimental conditions which were used are given in *Table 10*; and correspond with those preferred by Kirk,⁽¹⁵⁸⁾ and which are recommended in the SAE residual stress measurement handbook.⁽¹⁵⁹⁾ Cr K α radiation and the (211) martensite/ferrite crystallographic plane with 2θ diffraction angles around 156° were used. X-ray stress analysis is based upon the accurate measurement of the change in θ . The two-exposure method required the shift in diffraction line position to be recorded as the specimen orientation ψ was changed from 0 to 45° (*Figure 75*).

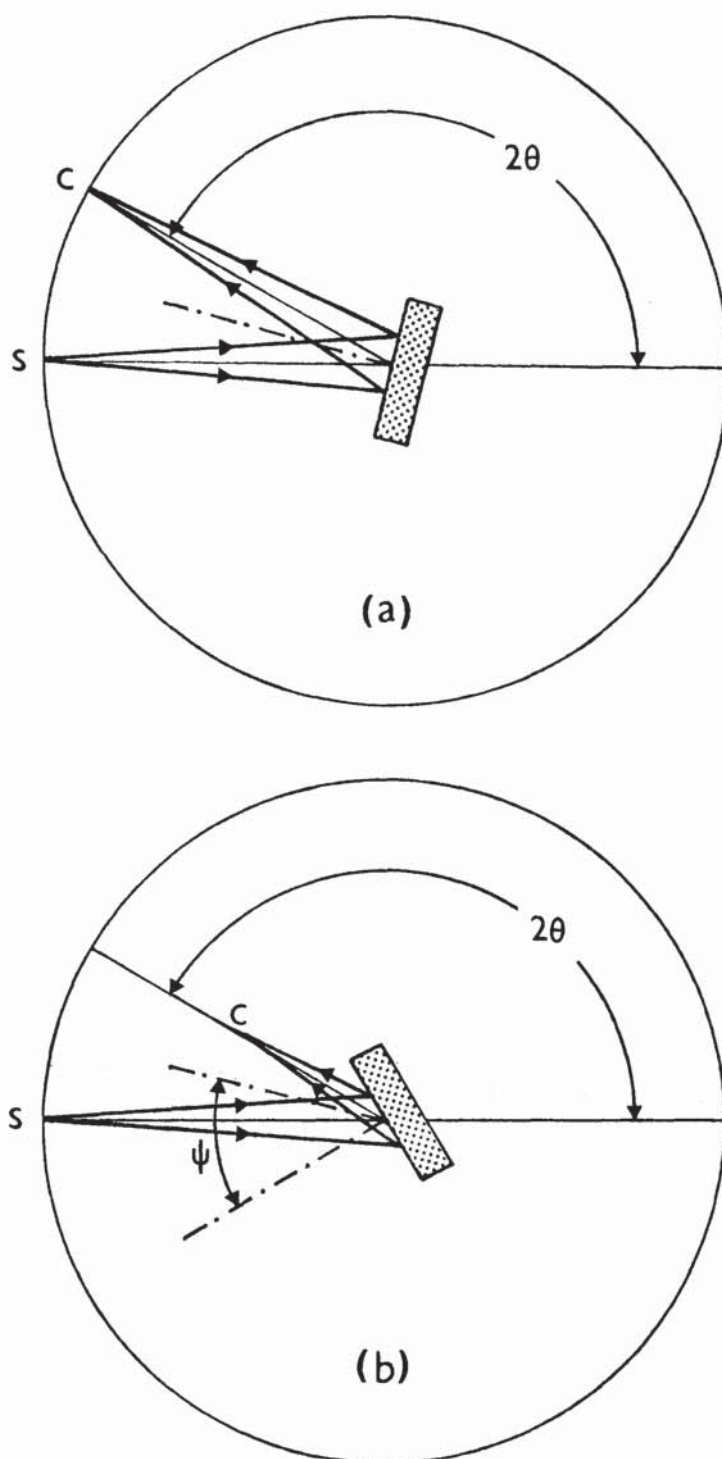


Figure 75. Focussing geometry for samples (a) when $\psi=0^\circ$, and (b) when $\psi=45^\circ$. The X-ray source is at S, the counter should be at C for optimum intensity measurements⁽¹⁶¹⁾.

The residual macrostress was then calculated using equation (26), which was derived by Cullity.⁽¹⁶⁰⁾

$$\sigma = \frac{E}{(1 + \gamma) \sin^2 \psi} \left[\frac{\sin \theta_{\psi=0}}{\sin \theta_{\psi=45}} - 1 \right] \quad (26)$$

where E is the elastic modulus for the material and γ is the Poisson's ratio.

Table 10. Residual surface macrostress measurement conditions

| |
|---|
| Philips PW1120 X-ray generator and PW1050 vertical goniometer diffractometer. |
| Cr K α radiation, wavelength 2.28970 Å |
| V - filter |
| Xe filled proportional counter detector. |
| Voltage 36kV |
| Amperage 42mA |
| Divergent slit 4° |
| Receiving slit 0.2mm |
| Fixed count, 3 x 10 ⁴ counts |
| Two-exposure parafocus method |
| $\psi = 0^\circ$ Focusing distance 172mm |
| $\psi = 45^\circ$ " " 111.75mm |
| Elastic modulus for steel E = 206,850MPa |
| Poisson's ratio for steel $\gamma = 0.29$ |

The specimens were supported on the X-ray stress stage so that their circumference was parallel to the plane of the goniometer table rotation and perpendicular to the goniometer axis of rotation. The specimens were secured to the stage using a custom made "V" block shaped clamp. A metallurgical kit was employed with a dial gauge which permitted accurate placement of the specimen surface on the goniometer axis, and a robust slide track which facilitated precise parafocusing. This involved moving the receiving slit and detector along a radius toward the specimen, in order to fulfill the beam focusing conditions as ψ changed from 0 to 45° (*Figure 75*). The parafocus

technique was used to obtain high diffracted intensities, thereby reducing the time required for the stress determination. The slits were chosen to obtain as many suitably-orientated crystals as possible in the irradiated area, and to produce the maximum diffracted intensity and peak to background ratio with resolution of peak doublets (if such existed). A vanadium filter was placed over the receiving slit in order to minimize undesirable iron fluorescent radiation.

It has been estimated that for these test conditions, 90 per cent of the information is derived from a surface layer approximately 14 μ m thick when $\psi=0$ and 9 μ m thick when $\psi=45^\circ$,⁽¹⁵⁷⁾ the length of the irradiated region on the sample being around 6 and 7mm respectively. Fixed count (inverse intensity) scaling allowed the use of a constant probable error, since the standard deviation in the measurements is proportion to \sqrt{N} , where N is the number of counts. Therefore for this work, where N was equal to 3×10^4 counts, the standard deviation was approximately 0.6 per cent of N.

Before each series of tests the goniometer calibration was checked using a gold standard with a 2θ diffraction angle of 151.96° . A graphical plot of the diffraction line profile was first made so as to include at least the top ten per cent of the peak during the fixed count step scan. A step size of 0.05° was used during the scan. Due to the relatively broad nature of the peaks for hardened steel, the measured inverse intensities were multiplied by the Lorentz-polarization and absorption factors (equation (27)) to make the peaks more symmetrical.

$$\text{LPA factors} = \left[\frac{1 + \cos^2 2\theta}{\sin^2 \theta} \right] (1 - \tan \psi \cot \theta) \quad (27)$$

The peak centres were determined using a maximum of least-squares quadratic method proposed by Kirk.⁽¹⁶¹⁾ The intensity was measured at $2n+1$ points distributed approximately equally on either side of the peak, the centre being taken as

the working origin. If the measured intensity y_i occurred at position x_i , then:

$$2\theta_p = 2\theta_{x_0} - \frac{\delta(2n+3)(2n-1)}{30} \cdot \frac{\sum_{i=n}^n (x_i y_i)}{\sum_{i=n}^n [(x_i^2 - x^{-2}) y_i]} \quad (28)$$

where $2\theta_p$ is the angular position of the peak, $2\theta_{x_0}$ the angular position of the working origin x_0 , and δ the angular step size. An algorithm supplied by Kirk was used for this peak fitting operation and for analysis of the variance. A listing of the stress calculation program used is given in Appendix C. Duplicate tests were performed on each quenched steel cylinder.

3.14.2 Metallurgical Examination of Specimens. Upon completion of the stress measurements, each specimen was sectioned as was shown in *Figure 74* using a Eurospark 650 spark machining unit to avoid tempering. The centre section of each specimen was mounted in bakelite and the midlength face polished in accordance with the standard techniques; roughing with grinding wheels was followed by a series of increasingly fine diamond grit abrasives on soft cloths. Each time the abrasive particle size was reduced the specimen was turned through 90° to produce scratch marks at right angles to the previous set. Following the $1\mu\text{m}$ diamond grit polish, the microstructure of each specimen was examined using a Polyvar metallurgical microscope. Hardness tests were then performed using a Vickers Pyramid machine and a 30kg load. The accuracy of the machine was checked with three blocks of known hardness. Five impressions were made near the core and adjacent to the surface of the specimens, and mean values calculated.

3.15 Cooling Characteristic Assessment for New Polymer Quenchant Systems.

A sample of poly(ethyloxazoline) PEOx (*Figure 53*) with a weight-average molecular weight of 500,000 was acquired from the Dow Chemical Company. Prototype quenchant solutions were then prepared with reference to the filed patent information regarding this class of polymer. The first solution to be evaluated was a straight 2.25 weight per cent solution (*Table 11a*), tested both in the static condition

and agitated at 0.5m/s at 30°C. This particular concentration was chosen since it was the mean value described in US patent 4,486,246.⁽¹⁴²⁾

A more recent patent⁽¹⁴³⁾ describes the use of an aqueous PVP/PEO_x mixture as a quenchant. Consequently, a 1.5 weight per cent solution of PVP and PEO_x in the ratio 3:1 was produced as shown in *Table 11b*. Parquench 90 was the PVP product used. Once again these conditions were chosen since they corresponded with the mean values outlined in Warchol's patent. This solution was also tested at 30°C in both the static and agitated condition.

Finally, a solution was prepared according to *Table 11c*, containing 10 weight per cent of PAG and PEO_x mixed in a ratio of 9:1. Quendila PA was the PAG utilized, the test conditions being the same as for the previous prototype solutions.

Table 11. Prototype polymer quenchant formulations incorporating PEO_x.

| Test | Condition | Weight of water (g) | Weight of PEO _x (g) | Weight of concentrate (g) | Total weight (g) |
|------|--|---------------------|--------------------------------|---------------------------|------------------|
| a | 2.25 wt% PEO _x | 1955 | 45 | - | 2000 |
| b | 1.5 wt% PVP:PEO _x (3:1) | 1767.5 | 7.5 | 225* | 2000 |
| c | 10 wt% PAG:PEO _x (9:1) | 1680 | 20 | 300** | 2000 |

NOTE: * The Parquench 90 concentrate contains approximately 90 per cent water.

** The Quendila PA concentrate contains approximately 40 per cent water.

CHAPTER 4

4.0. EXPERIMENTAL RESULTS

4.1 Physical Properties of Polymer Quenchants Examined.

Table 12 outlines some of the physical properties of the commercial polymer quenchant concentrates examined. The concentrates were all pale, straw-coloured fluids with varying levels of viscosity and pituitousness. The results for the Quendila PA, PHT and Aquaquench 1250 and ACR concentrates were obtained using samples from two different batches; the remainder were single source samples. As can be seen, there were slight variations in the kinematic viscosities of polymer products of the same type from different batches.

The concentrates spanned a fairly wide kinematic viscosity range. The least viscous product at 40°C was Parquench 60 with a value of 17mm²/s, whilst Aquaquench ACR had the highest kinematic viscosity (602 ± 22mm²/s). The solids-contents ranged from 9 ± 1 weight per cent for the Parquench 60 sample to 60 ± 1 weight per cent for Quendila PA.

4.2 Polymer Quenchant Characterization

4.2.1 Gel Permeation Chromatography Data. Polystyrene-equivalent molecular weight distribution data for each of the PAG and PVP products examined is given in *Table 13*. The chromatograms from which this data was derived are given in *Figures 76 to 82*. The results given in *Table 13* are clearly not absolute values since the elution volume is related to the hydrodynamic volume of the polymers, and the calibration plot for polystyrene in THF (*Figure 60*) was used in all the calculations. Furthermore, the samples examined during this characterization work were not pure polymer since, being commercial products, they contained other additives. The deviation from the true molecular weights is likely to be greater for the PVP samples since they were eluted using chloroform.

Table 12. Some physical properties of the polymer concentrates tested

| Product name | Polymer type | Solubility in water (Inversion temp. $\pm 1^\circ\text{C}$) | Electrolytic character | Kinematic viscosity at 40°C (mm^2/s) | pH (± 0.1) | Solids content (wt %) | Dry residue |
|------------------|--------------|--|-------------------------|--|------------------|-----------------------|----------------|
| * Quendila PA | PAG | Inverse (74) | Nonionic | 430 \pm 11 | 8.5 | 60 \pm 1 | Viscous liquid |
| Quendila PHT | " | " (88) | " | 558 \pm 18 | 8.5 | 58 \pm 2 | " |
| Breox NF-18 | " | " (78) | " | 531 | 8 | 50 \pm 1 | " |
| Aquaquench 1250 | " | " (77) | " | 229 \pm 4 | 9.5 | 50 \pm 1 | " |
| Ucon E | " | " (74) | " | 245 | 8 | 40 \pm 1 | " |
| Parquench 60 | PVP | Normal | " | 17 | 9.2 | 9 \pm 1 | Brittle Solid |
| * Parquench 90 | " | " | " | 75 | 9.2 | 10 \pm 1 | " |
| Aquaquench 110 | Polyacrylate | " | Anionic polyelectrolyte | 526 | 9 | 12 \pm 1 | " |
| * Aquaquench ACR | " | " | " | 602 \pm 22 | 8.6 | 23 \pm 2 | " |

* Representative polymer products.

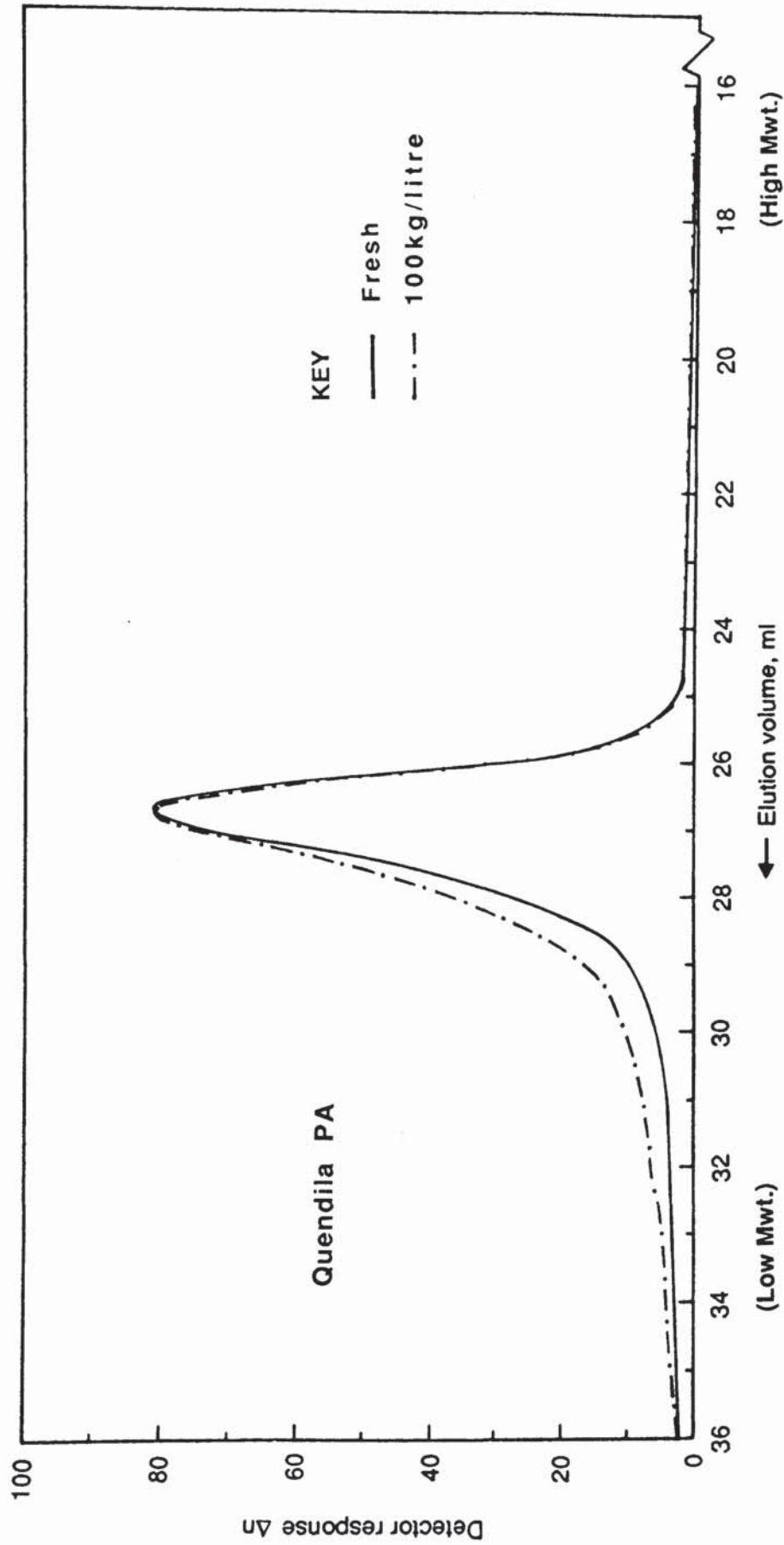


Figure 76. Gel permeation chromatograms for Quendila PA samples dissolved in THF in both the as-received condition, and following a quench load of 100kg/litre in the accelerated ageing test.

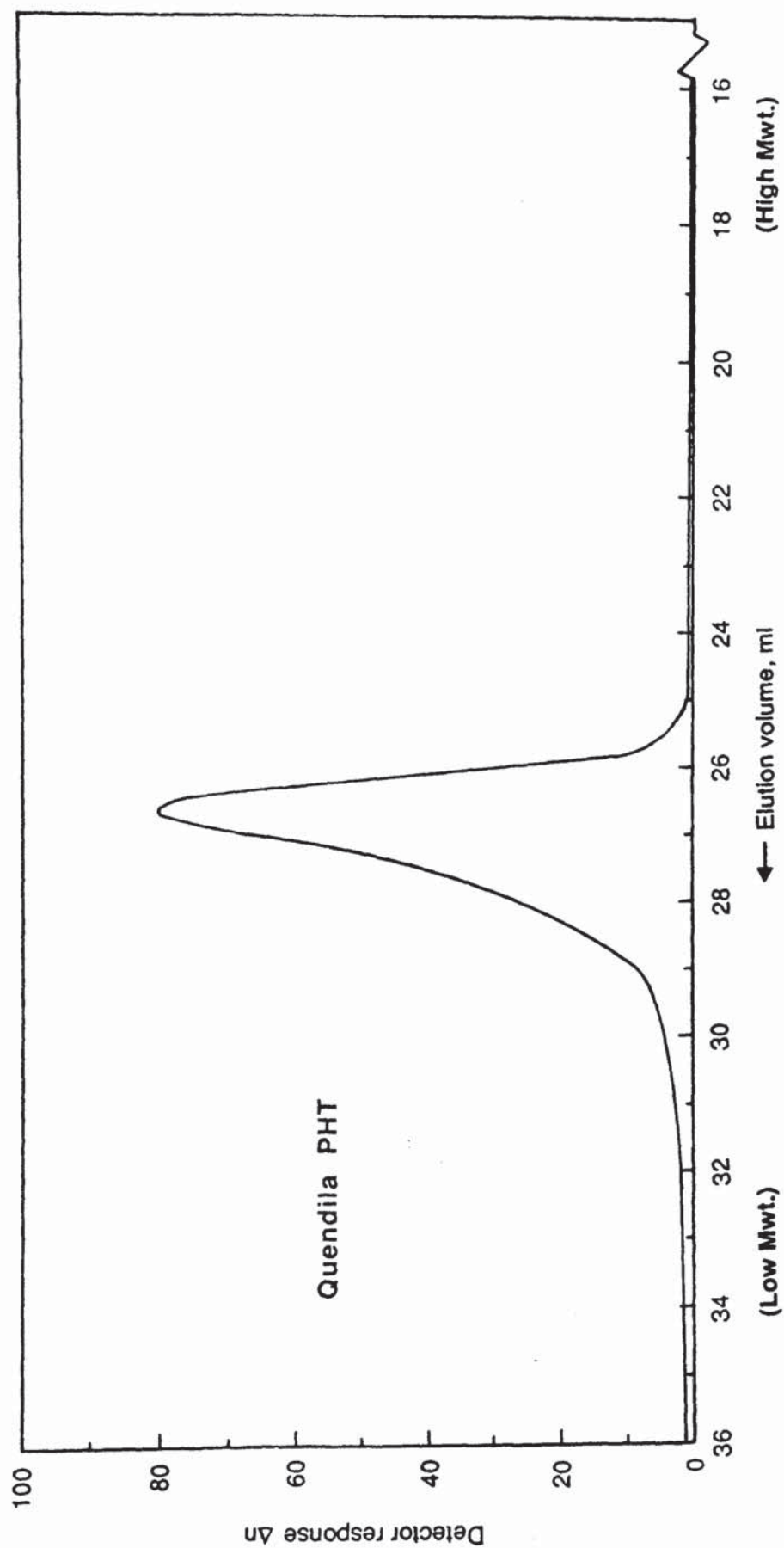


Figure 77. Gel permeation chromatogram for Quendila PHT dissolved in THF.

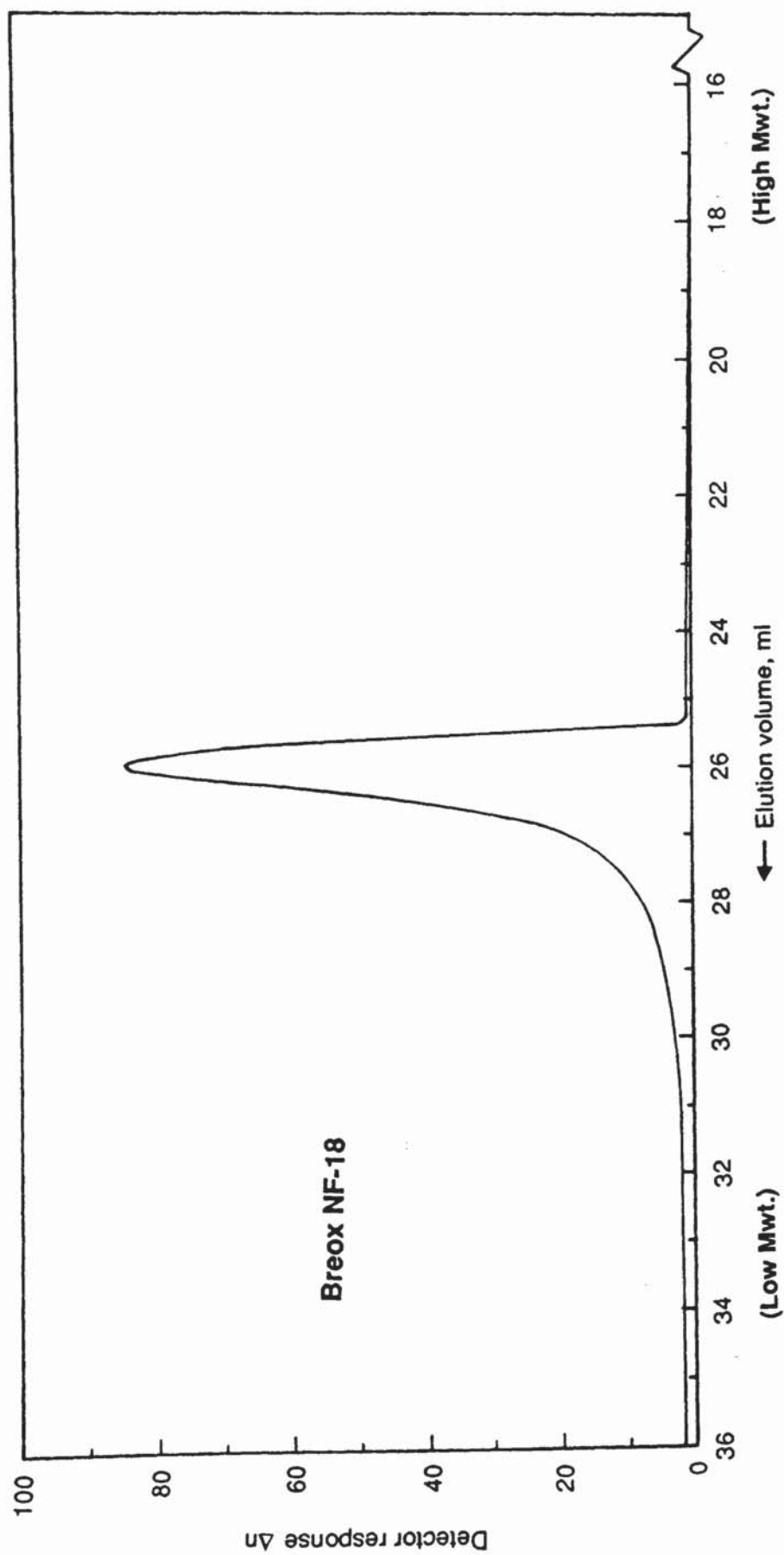


Figure 78. Gel permeation chromatogram for Breox NF-18 dissolved in THF.

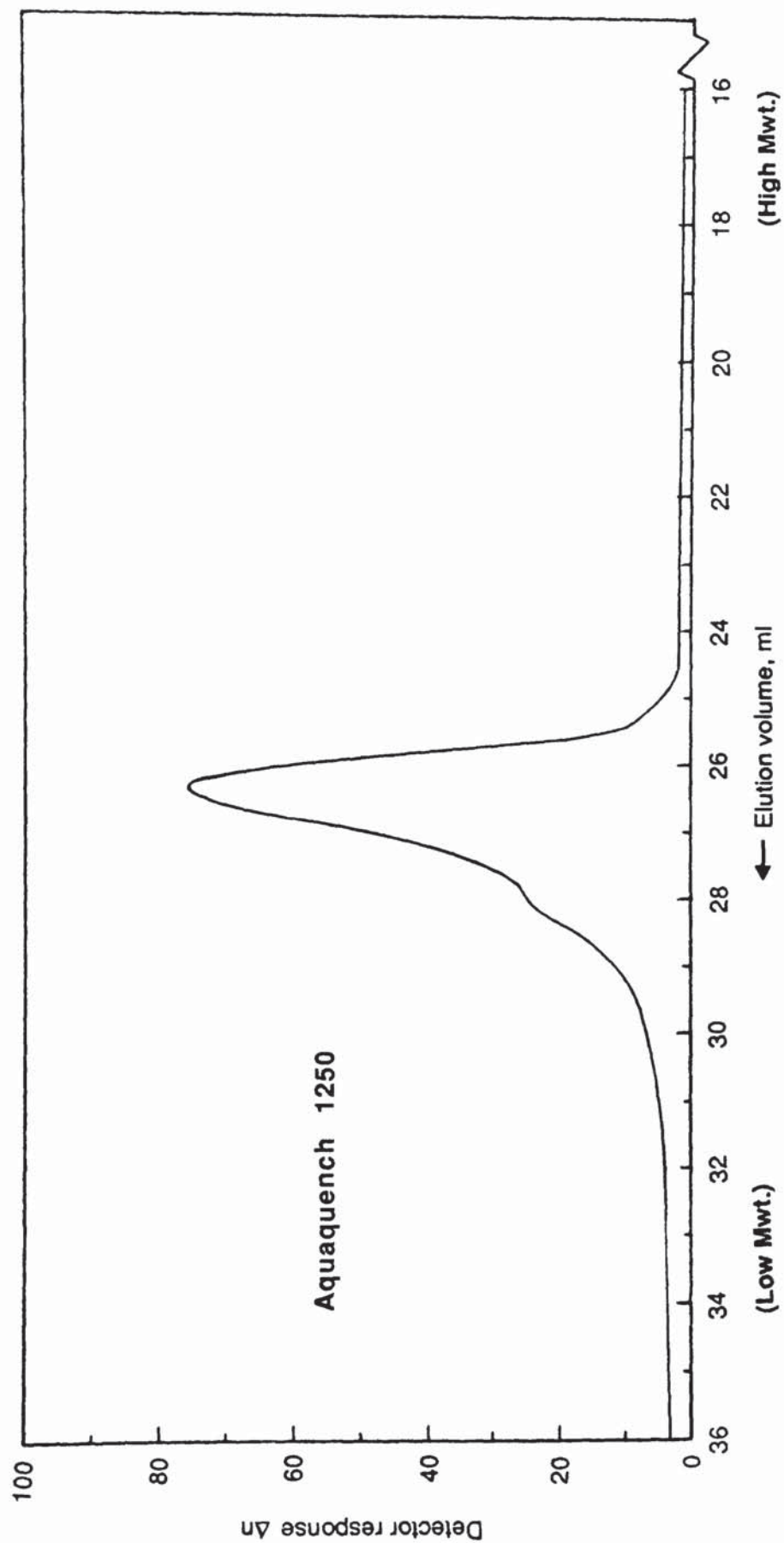


Figure 79. Gel permeation chromatogram for Aquaquench 1250 dissolved in THF.

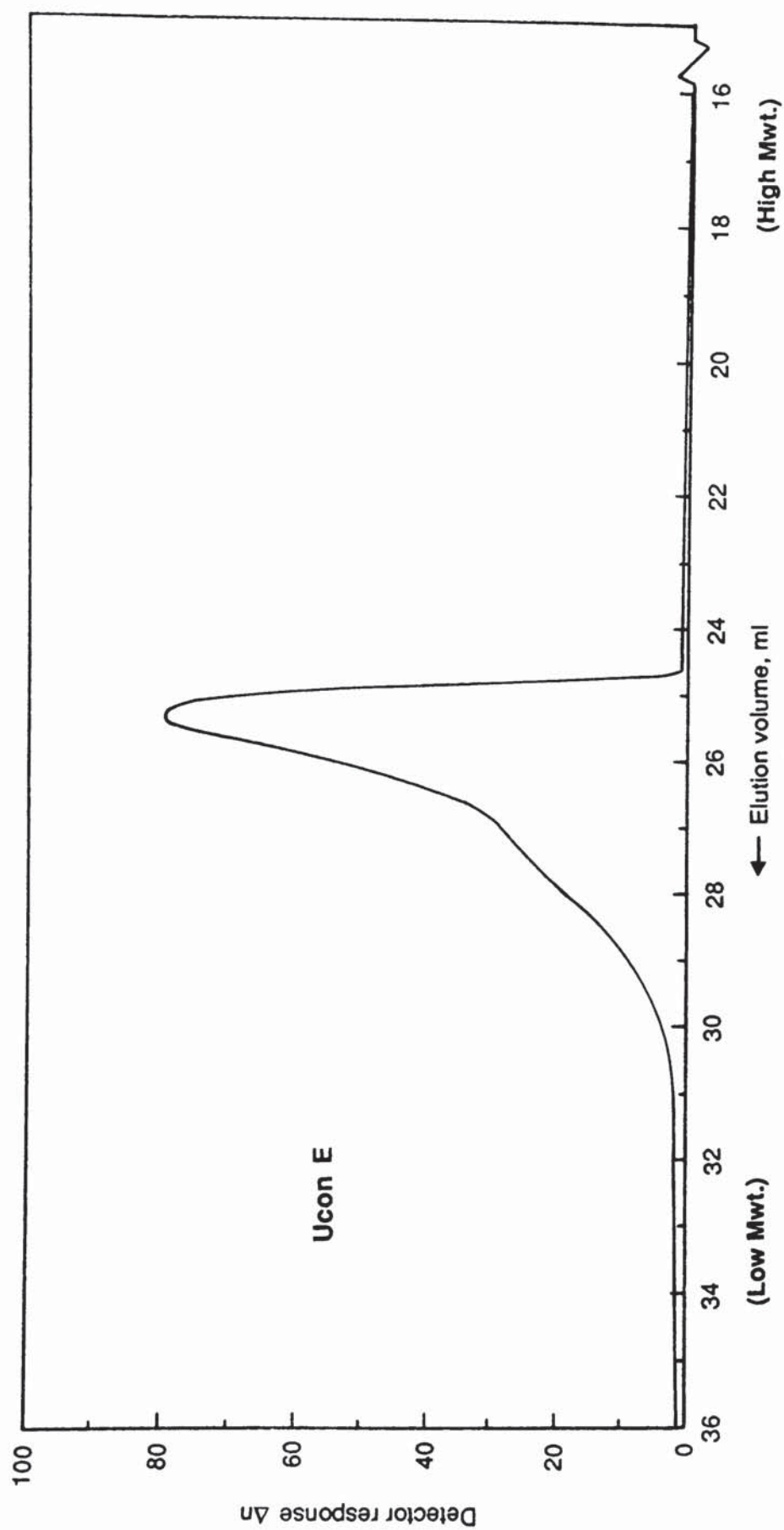


Figure 80. Gel permeation chromatogram for Ucon E dissolved in THF.

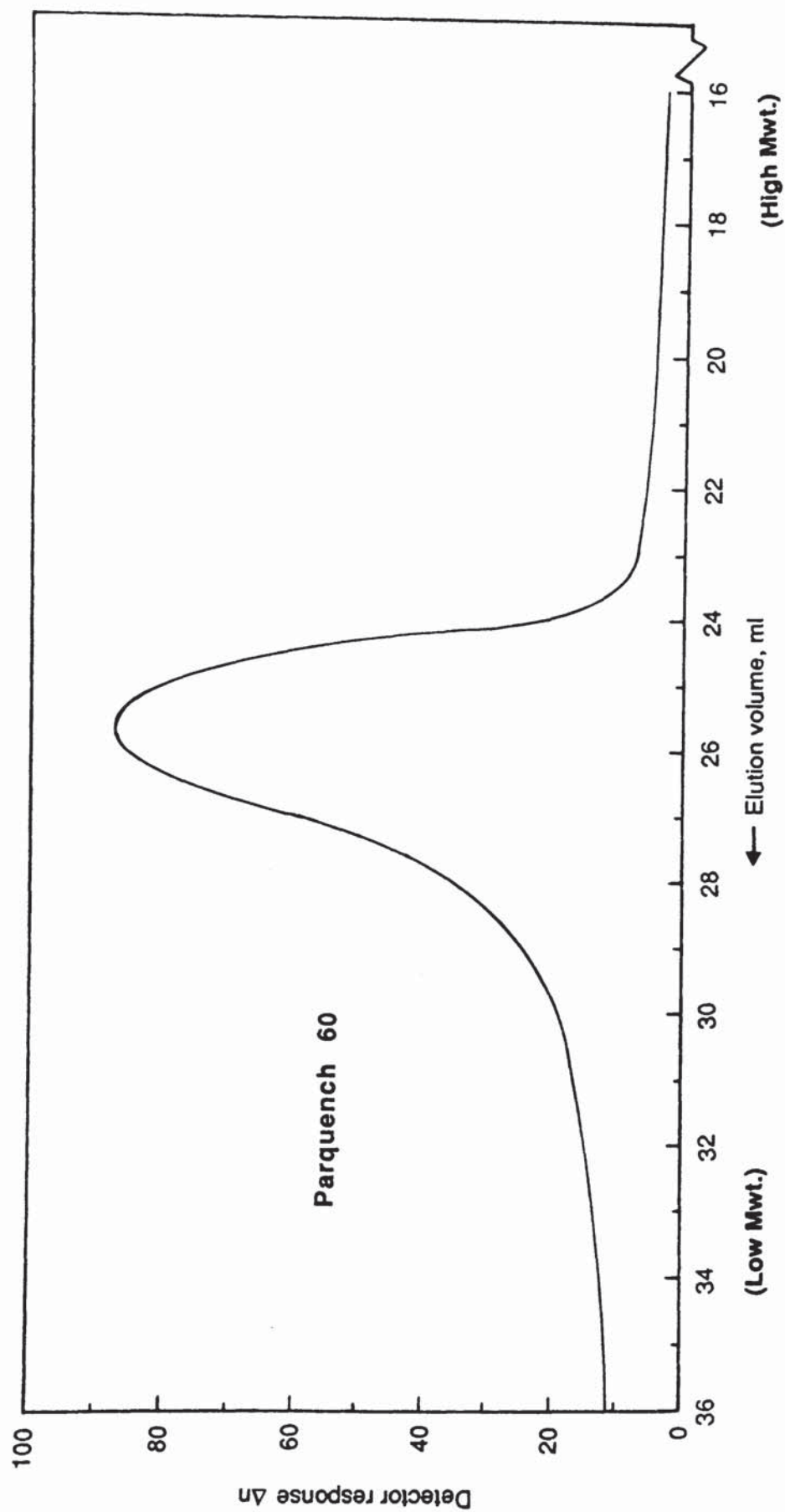


Figure 81. Gel permeation chromatogram for Parquench 60 dissolved in chloroform.

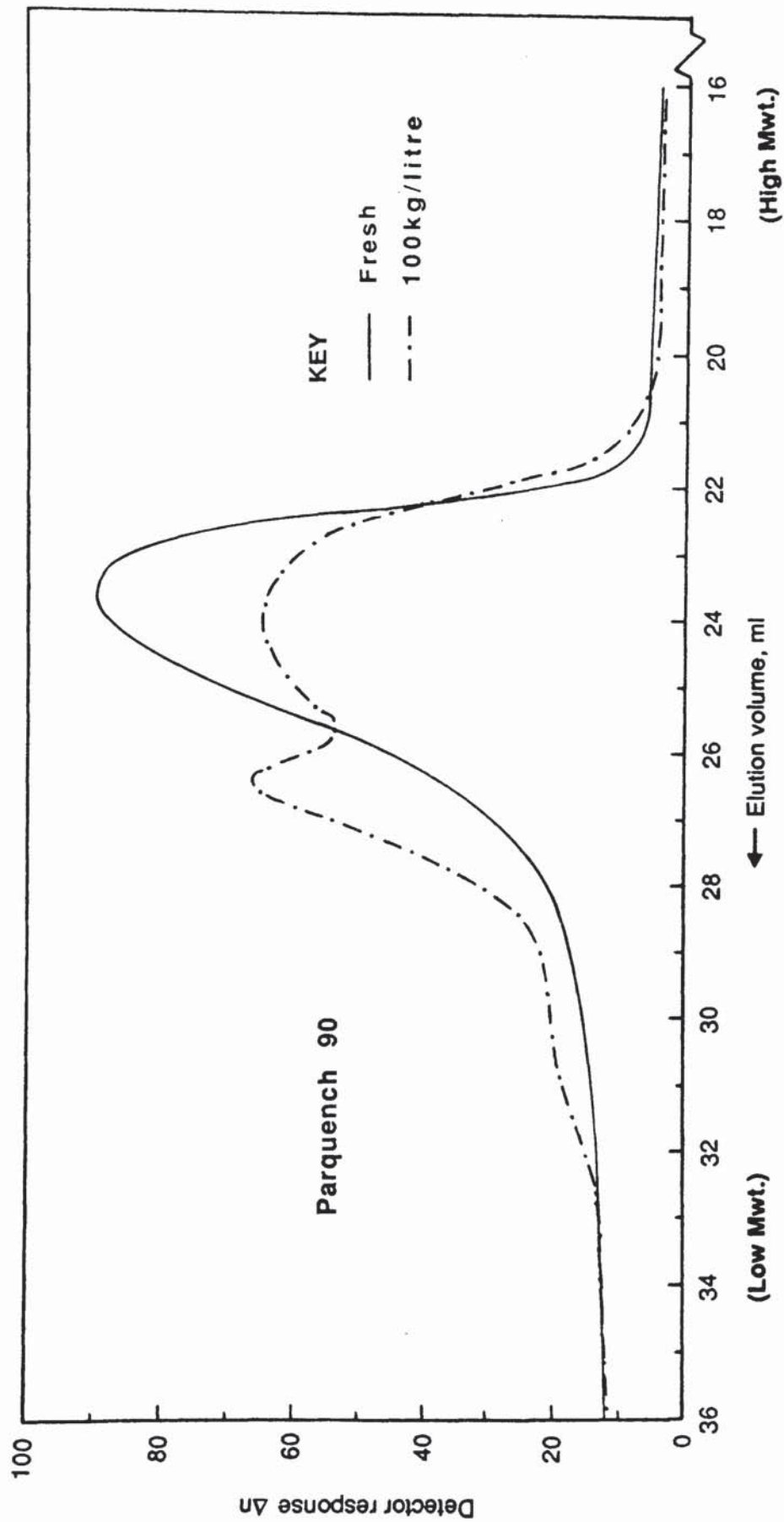


Figure 82. Gel permeation chromatograms for Parquench 90 samples dissolved in chloroform in both the as-received condition, and following a quench load of 100kg/litre in the accelerated ageing test.

The PAG products had polystyrene-equivalent weight-average molecular weights ranging from about 12,000 to 20,000; the newer generation products such as Breox NF-18 and Ucon E had the highest values. The polystyrene-equivalent average molecular weights for the PVP products were higher than those for the PAG's, with Parquench 90 having a weight-average value 2.7 times higher than that of Parquench 60.

Table 13. GPC polystyrene-equivalent molecular weight distribution data for the PAG and PVP products.

| Sample | Weight-average molecular weight \bar{M}_w | Number-average molecular weight \bar{M}_n | Polydispersity ratio |
|-----------------|---|---|-------------------------|
| PAG's | | | |
| Quendila PA: | | | |
| Fresh | 12,480 | 4,200 | 2.96 |
| 100kg/litre | 11,280 | 3,420 | 3.29 |
| Quendila PHT | 12,470 | 6,220 | 2.00 |
| Breox NF-18 | 17,900 | 9,150 | 1.95 |
| Aquaquench 1250 | 13,960 | 3,790 | 3.67 |
| Ucon E | 20,110 | 9,580 | 2.09 |
| PVP's | | | |
| Parquench 60 | 27,330 | 10,120 | 2.70 |
| Parquench 90: | | | |
| Fresh | 74,560 | 25,040 | 2.97 |
| 100kg/litre | 65,670 | 7,530 | 8.72 |

Figures 76 and 82 compare the chromatograms of both the fresh Quendila PA and Parquench 90 samples, and those obtained after a quench load of 100kg/litre in the accelerated ageing test. For both classes of polymer, there was a general shift in the

distribution for the aged samples towards lower molecular weights with correspondingly increased polydispersity ratios. The distribution for the aged Parquench 90 sample exhibited a pronounced lower molecular weight peak and tail, plus a contribution of higher molecular weight, compared with that for the fresh sample.

4.2.2 Limiting Viscosity Number Data. The concentration-viscosity number plots for each of the PVP products are given in *Figure 83*. The corresponding efflux time data is given in *Table 14*. Linear regression equations and correlation coefficients R are presented adjacent to each plot. From these it can be seen that the limiting viscosity number $[\eta]$ for the Parquench 60 sample was 0.74dl/g and the value for Parquench 90 1.59dl/g when fresh, dropping to 0.68dl/g following a quench load of 100kg/litre in the accelerated ageing test.

A frequently used and commonly recognized method of distinguishing between different molecular weight grades of PVP is the K-value. These K-values are normally derived from the viscosity ratio, η_r , for a 1g/dl concentration aqueous solution using Fikentsher's equation:⁽⁸⁷⁾

$$\frac{\log \eta_r}{c} = \frac{75 k_0^2}{1 + 1.5 k_0 c} + k_0 \quad (29)$$

where c equals the concentration in g/dl, η_r is the viscosity of the solution compared to that of the solvent (η / η_0), and $K = 1000k_0$. Solving equation (29) directly for K :

$$K = \frac{[\sqrt{300c \log \eta_r + (c + 1.5c \log \eta_r)^2} + 1.5c \log \eta_r - c]}{(0.15c + 0.003c^2)} \quad (30)$$

Thus, since η_r is equal to 2.05 for a 1g/dl solution of Parquench 60 and 4.07 for an equivalent Parquench 90 solution, the corresponding values of K are 60.4 and 88.7 respectively. The aged Parquench 90 sample had a η_r value of 2.38 producing a K-value of 67.

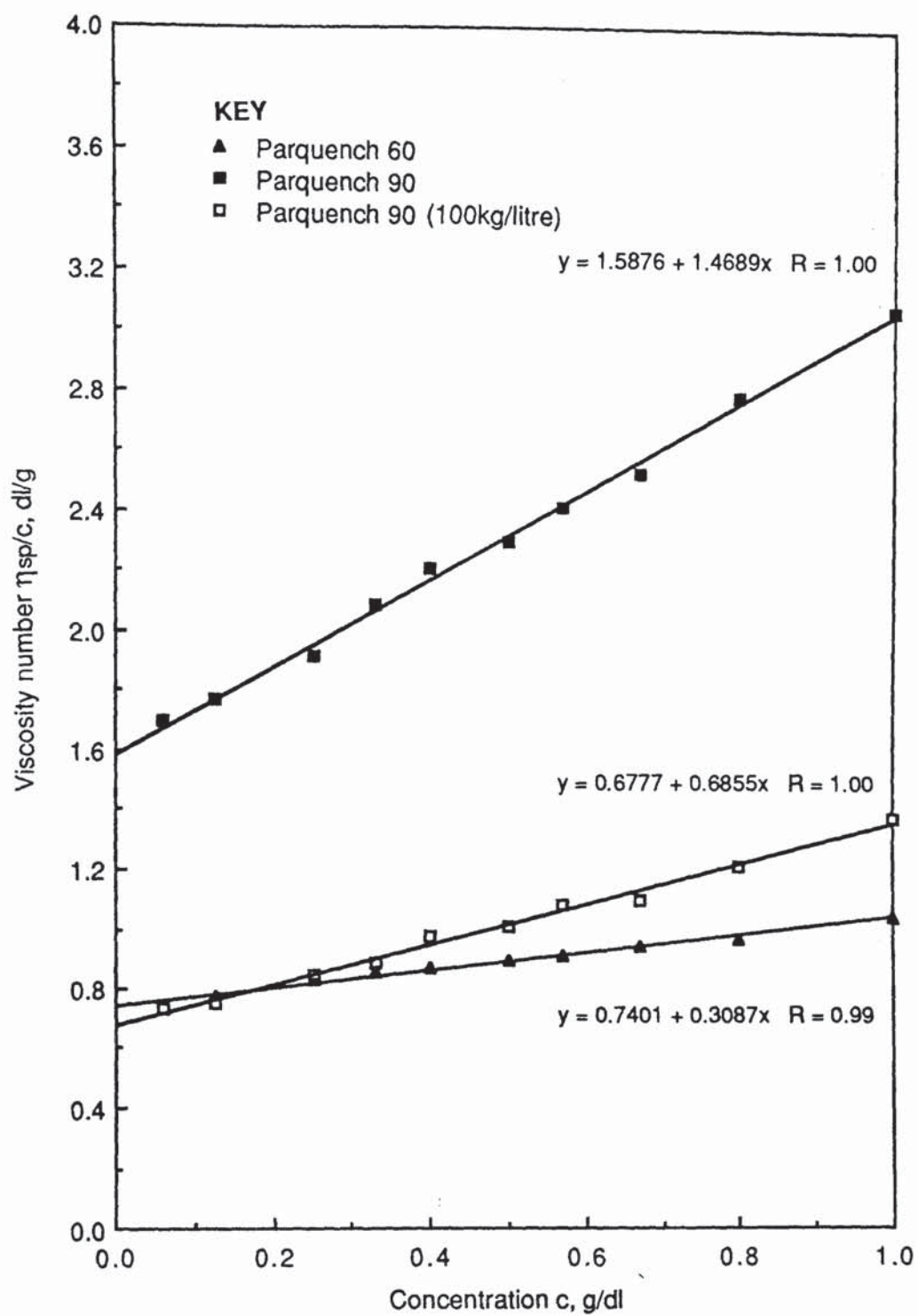


Figure 83. Concentration-viscosity number plots for the aqueous PVP samples at 30 °C.

Table 14. Viscosity number data for the PVP samples.

| Concentration (g/dl) | Parquench 60 | | Parquench 90 (fresh) | | (100kg/litre) | |
|-------------------------|-------------------|---------------------------|----------------------|---------------------------|-------------------|---------------------------|
| | Efflux time(s) | Viscosity number(dl/g) | Efflux time(s) | Viscosity number(dl/g) | Efflux time(s) | Viscosity number(dl/g) |
| 1.0 | 2235 | 1.047 | 4448 | 3.073 | 2599 | 1.380 |
| 0.8 | 1939 | 0.970 | 3521 | 2.780 | 2158 | 1.220 |
| 0.67 | 1788 | 0.951 | 2943 | 2.530 | 1897 | 1.100 |
| 0.57 | 1663 | 0.917 | 2596 | 2.416 | 1770 | 1.089 |
| 0.50 | 1584 | 0.901 | 2350 | 2.304 | 1643 | 1.009 |
| 0.40 | 1472 | 0.870 | 2057 | 2.209 | 1520 | 0.980 |
| 0.33 | 1401 | 0.857 | 1846 | 2.092 | 1413 | 0.891 |
| 0.25 | 1319 | 0.831 | 1615 | 1.916 | 1325 | 0.853 |
| 0.125 | 1198 | 0.777 | 1334 | 1.773 | 1194 | 0.747 |
| 0.06 | 1140 | 0.733 | 1203 | 1.694 | 1140 | 0.733 |
| 0.0 | 1092 | - | 1092 | - | 1092 | - |

The currently preferred values of the Mark-Houwink-Sakurada parameters κ and a for aqueous PVP solutions at 30°C were given in *Table 5*. Since equation (18) can be written in the form:

$$\bar{M}_v = \left[\frac{[\eta]}{\kappa} \right]^{1/a} \quad (31)$$

the viscosity-average molecular weight, M_v , for Parquench 60 was thus calculated to be 208,314 and the value for Parquench 90 found to equal 621,214. The value of M_v dropped nearly 70 per cent to 184,611 for the aged Parquench 90 sample.

Figure 84 gives the concentration-viscosity number plots for samples of Aquaquench ACR in both the fresh condition, and following a quench load of 100kg/litre:

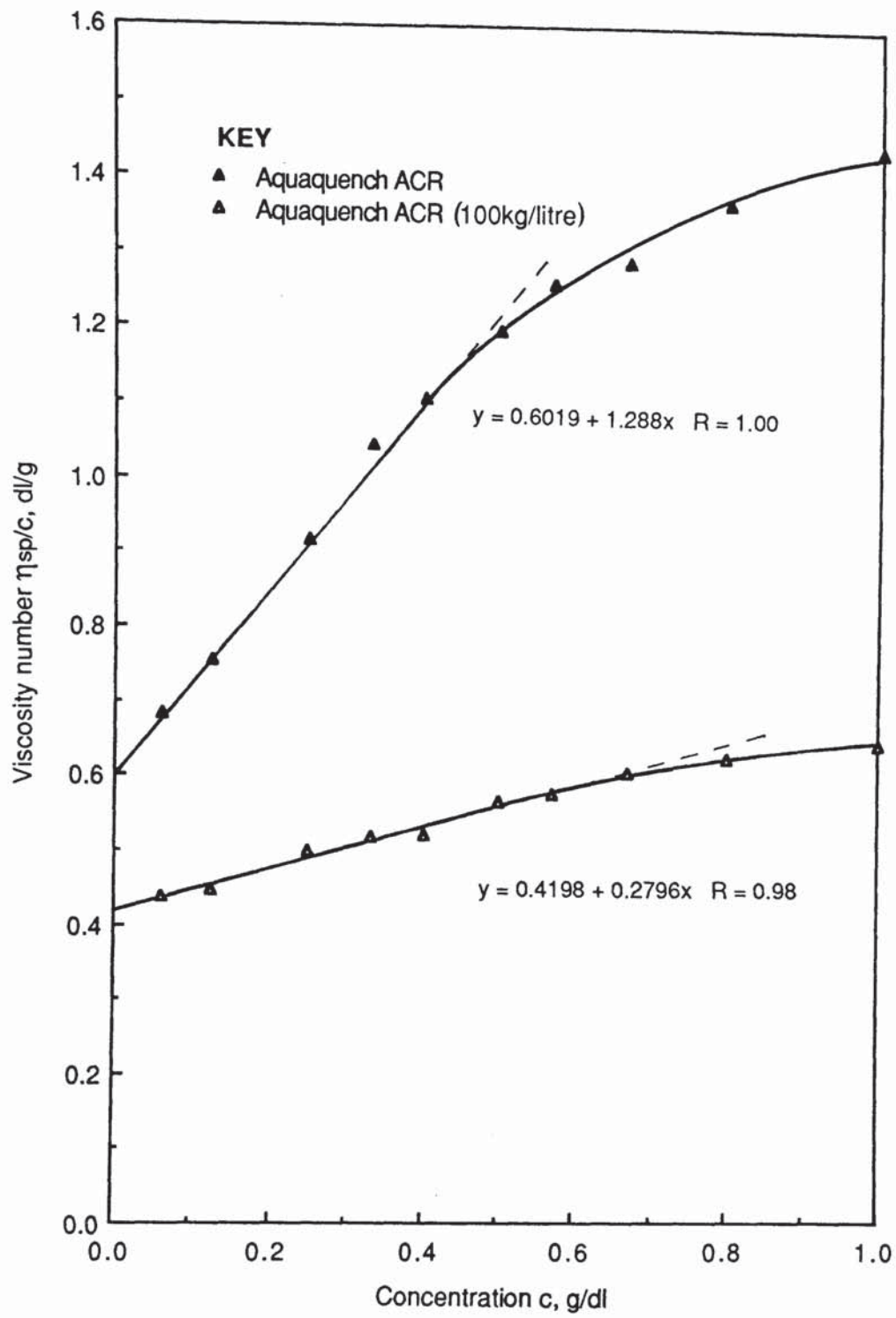


Figure 84. Concentration-viscosity number plots for polyacrylate (Aquaquench ACR) samples dissolved in 1.25M aqueous NaSCN at 30 °C.

Both plots exhibit curvature for concentration levels above 0.5g/dl. However, limiting viscosity numbers were derived by extrapolating the lower concentration linear portions of the plots back to c equals zero. The regression equations for these lines are given in *Figure 84*. The value of $[\eta]$ for the fresh Aquaquench ACR sample was 0.60dl/g, dropping to 0.42dl/g after ageing. The Mark-Houwink-Sakurada constants for sodium polyacrylates tested under these conditions were given in *Table 5*. Thus from equation (31), \bar{M}_v for Aquaquench ACR was found to be 245,884 when fresh, dropping 51 per cent to 120,483 after 100kg/litre.

Table 15. Viscosity number data for Aquaquench ACR.

| Concentration (g/dl) | Fresh | | Aged (100kg/litre) | |
|-------------------------|--------------------|---------------------------|--------------------|---------------------------|
| | Efflux time (s) | Viscosity number(dl/g) | Efflux time (s) | Viscosity number(dl/g) |
| 1.00 | 2795 | 1.441 | 1887 | 0.648 |
| 0.80 | 2397 | 1.367 | 1719 | 0.627 |
| 0.67 | 2135 | 1.290 | 1611 | 0.607 |
| 0.57 | 1967 | 1.259 | 1523 | 0.579 |
| 0.50 | 1830 | 1.197 | 1471 | 0.569 |
| 0.40 | 1652 | 1.107 | 1384 | 0.522 |
| 0.33 | 1540 | 1.045 | 1341 | 0.519 |
| 0.25 | 1408 | 0.919 | 1288 | 0.500 |
| 0.125 | 1253 | 0.755 | 1209 | 0.447 |
| 0.06 | 1192 | 0.684 | 1175 | 0.437 |
| 0.0 | 1145 | - | 1145 | - |

4.2.3 Findings for the PAG Inverse Solubility Studies. Concentration-viscosity number plots for the Quendila PA solutions at 25, 40 and 60°C are given in *Figure 85*.

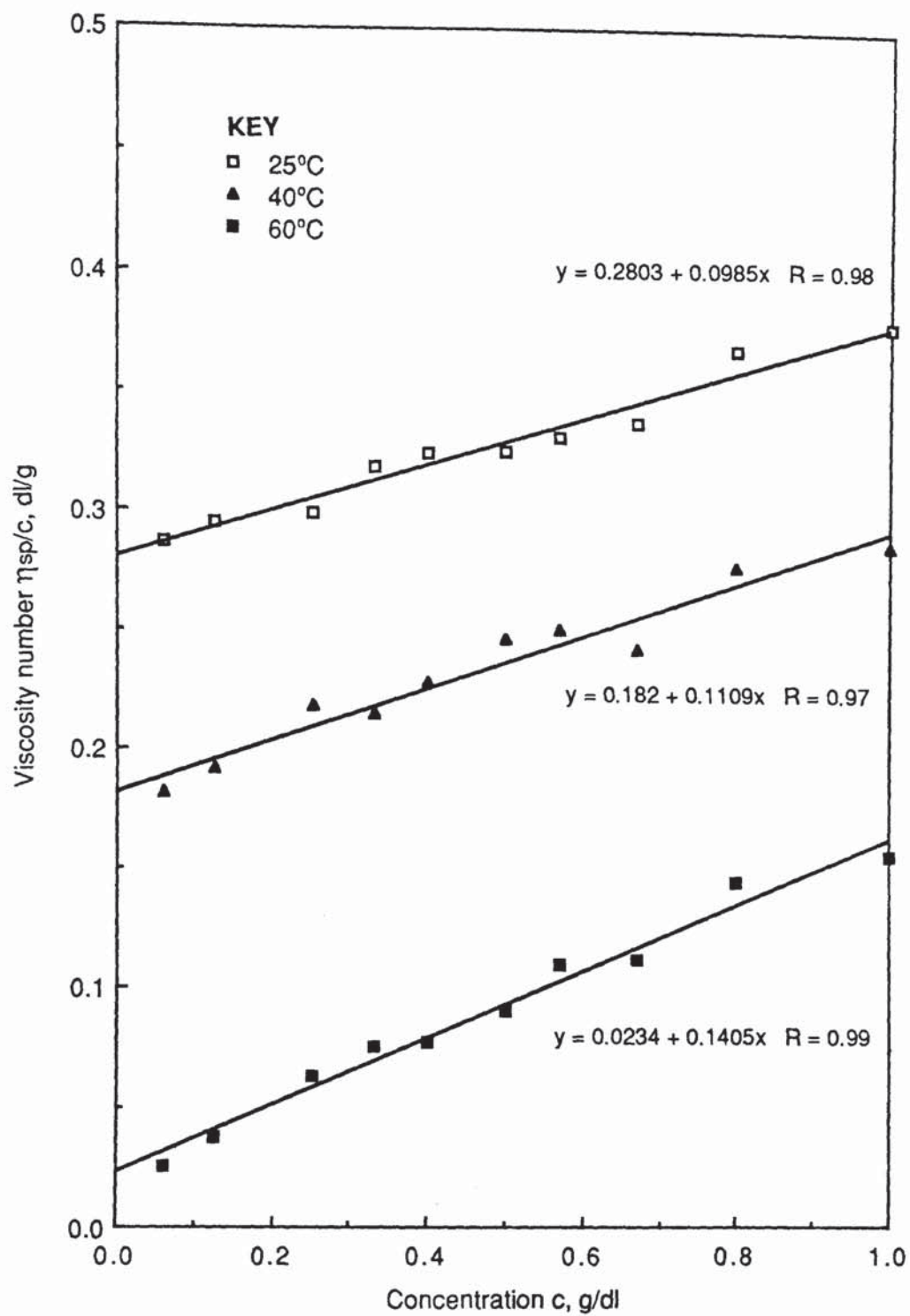


Figure 85. Concentration-viscosity number plots for aqueous PAG (Quendila PA) solutions at 25, 40 and 60 °C.

From the linear regression equations shown in this figure, it can be seen that the limiting viscosity numbers dropped from 0.28dl/g at 25°C through 0.18dl/g at 40°C to 0.02dl/g at 60°C. The corresponding efflux time data is given in *Table 16*.

Table 16. Viscosity number data for the Quendila PA solutions.

| Concentration (g/dl) | 25°C | | 40°C | | 60°C | |
|-------------------------|-------------------|---------------------------|-------------------|---------------------------|-------------------|---------------------------|
| | Efflux time(s) | Viscosity number(dl/g) | Efflux time(s) | Viscosity number(dl/g) | Efflux time(s) | Viscosity number(dl/g) |
| 1.0 | 1681 | 0.379 | 1179 | 0.287 | 740 | 0.156 |
| 0.8 | 1578 | 0.368 | 1120 | 0.278 | 714 | 0.145 |
| 0.67 | 1495 | 0.338 | 1065 | 0.243 | 688 | 0.112 |
| 0.57 | 1450 | 0.332 | 1047 | 0.251 | 680 | 0.110 |
| 0.50 | 1418 | 0.326 | 1029 | 0.247 | 669 | 0.091 |
| 0.40 | 1377 | 0.324 | 1000 | 0.229 | 660 | 0.078 |
| 0.33 | 1347 | 0.318 | 981 | 0.215 | 656 | 0.076 |
| 0.25 | 1310 | 0.299 | 966 | 0.218 | 650 | 0.063 |
| 0.125 | 1264 | 0.295 | 938 | 0.192 | 643 | 0.038 |
| 0.06 | 1240 | 0.287 | 926 | 0.182 | 641 | 0.026 |
| 0.0 | 1219 | - | 916 | - | 640 | - |

Figures 86 and 87 demonstrate the effect of temperature on the kinematic viscosities of 1.0 and 10.0 weight per cent solutions of the dehydrated Quendila PA concentrate. The viscosity of both solutions decreased upon raising the temperature. The discontinuities in the curves correspond with the inversion points for these particular PAG solutions. The inversion temperature for the 1.0 weight per cent solution was $78.0 \pm 0.5^\circ\text{C}$, whilst that for the 10.0 weight per cent solution was $74.0 \pm 0.5^\circ\text{C}$.

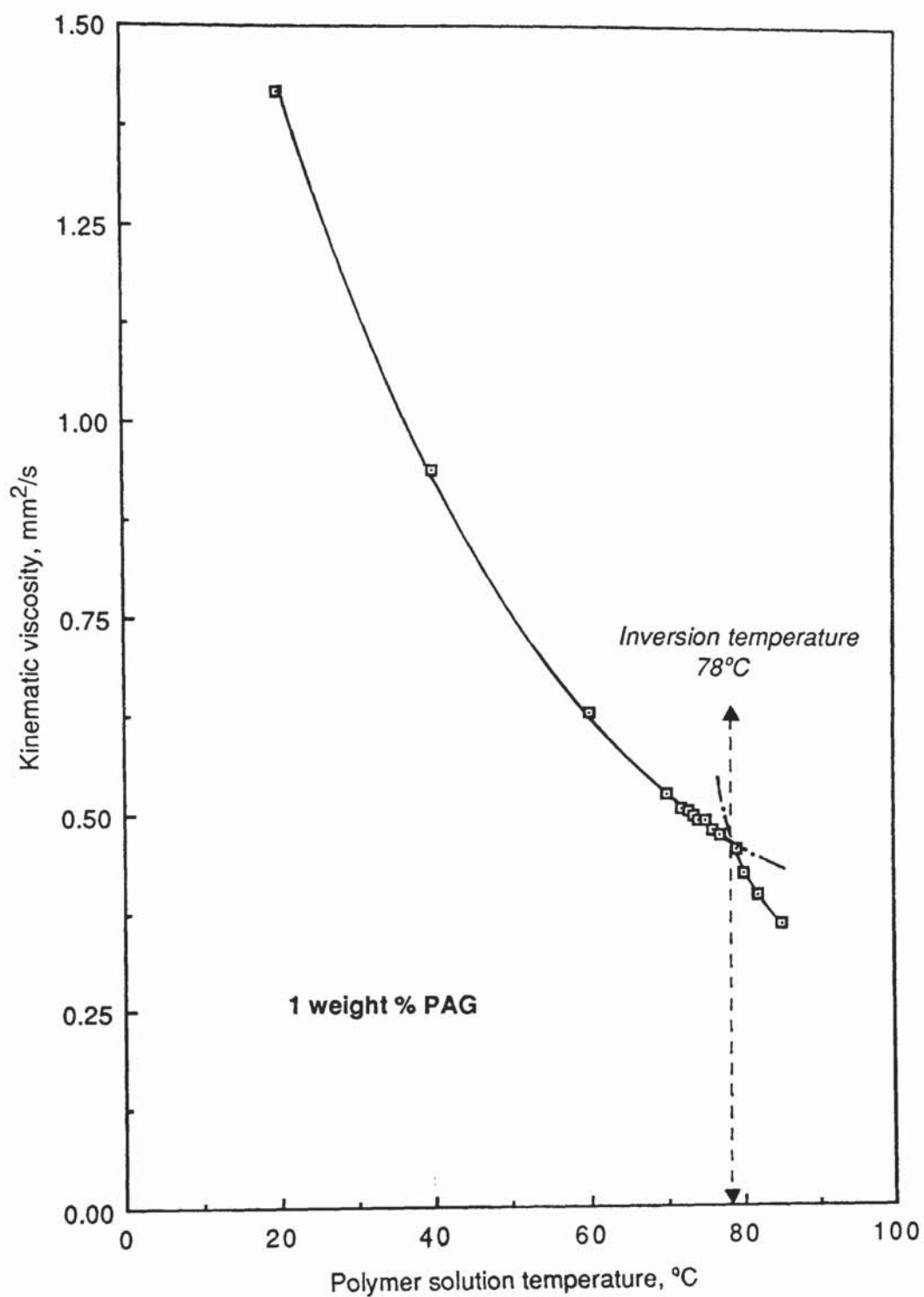


Figure 86. Effect of temperature on the kinematic viscosity of a 1 weight per cent Quendila PA solution.

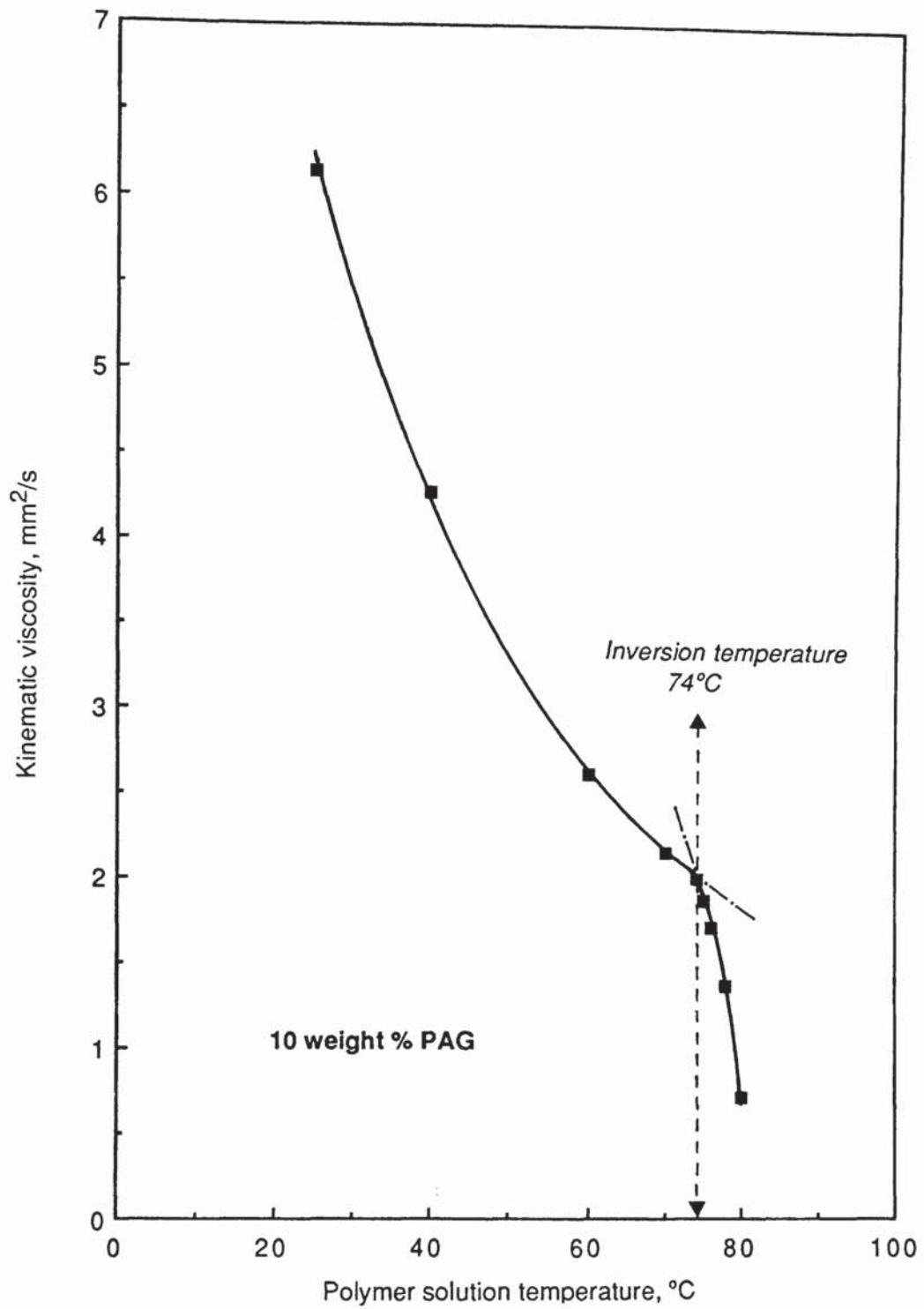


Figure 87. Effect of temperature on the kinematic viscosity of a 10 weight per cent Quendila PA solution.

4.2.3.1. Nuclear magnetic resonance spectroscopic analysis data.

The proton NMR spectra for Quendila PA and Quendila PHT are given in *Figures 88 and 89*. The signal corresponding to the chemical shift (δ) of around 1.1ppm is from the methyl group protons of the propylene oxide derived units, whilst the group seen at about 3.5ppm is due to the protons on carbon atoms attached to oxygen. The multiplet structure of these signals is associated with proton spin-spin coupling. From these two signals, an estimation for the ratio of ethylene oxide to propylene oxide derived units can be obtained.⁽¹⁵⁴⁾

The midfield signal (2.6ppm) is believed to be due to the CH₂ and CH groups attached to terminal hydroxyl protons. A trace amount of water can also be seen in the Quendila PHT spectrum at about 4.3ppm. The integrated intensity values for these signals are given on each spectrum.

From examination of the molecular structure of a PAG (*Figure 37*), a relationship was deduced between the percentage of oxypropylene units in the polymer and a specific ratio (R): where R equals the number of protons connected to oxygen atoms divided by the number of methyl group protons of propylene oxide (*Figure 90*). The proportion of oxyethylene units to oxypropylene units could thus be estimated for each polymer from the integral ratio R, obtained by dividing the integral of the signal at around 3.5ppm by that at about 1.1ppm. Therefore, R was equal to 6.9 for Quendila PA (173.82 / 25.08), and 10.5 for Quendila PHT (76.38 / 7.25). From *Figure 90*, it was thus estimated that the Quendila PA polymer contained about 12.5 per cent oxypropylene units and that the Quendila PHT contained 18 per cent oxypropylene units. However, these ratios are more usually quoted in terms of weight per cent. Propylene oxide has a molecular mass of 58 and ethylene oxide a value of 44. Consequently, the respective oxyethylene : oxypropylene ratios for Quendila PA and PHT were found to be 76 : 24 and 84 : 16 when considered in terms of weight per cent.

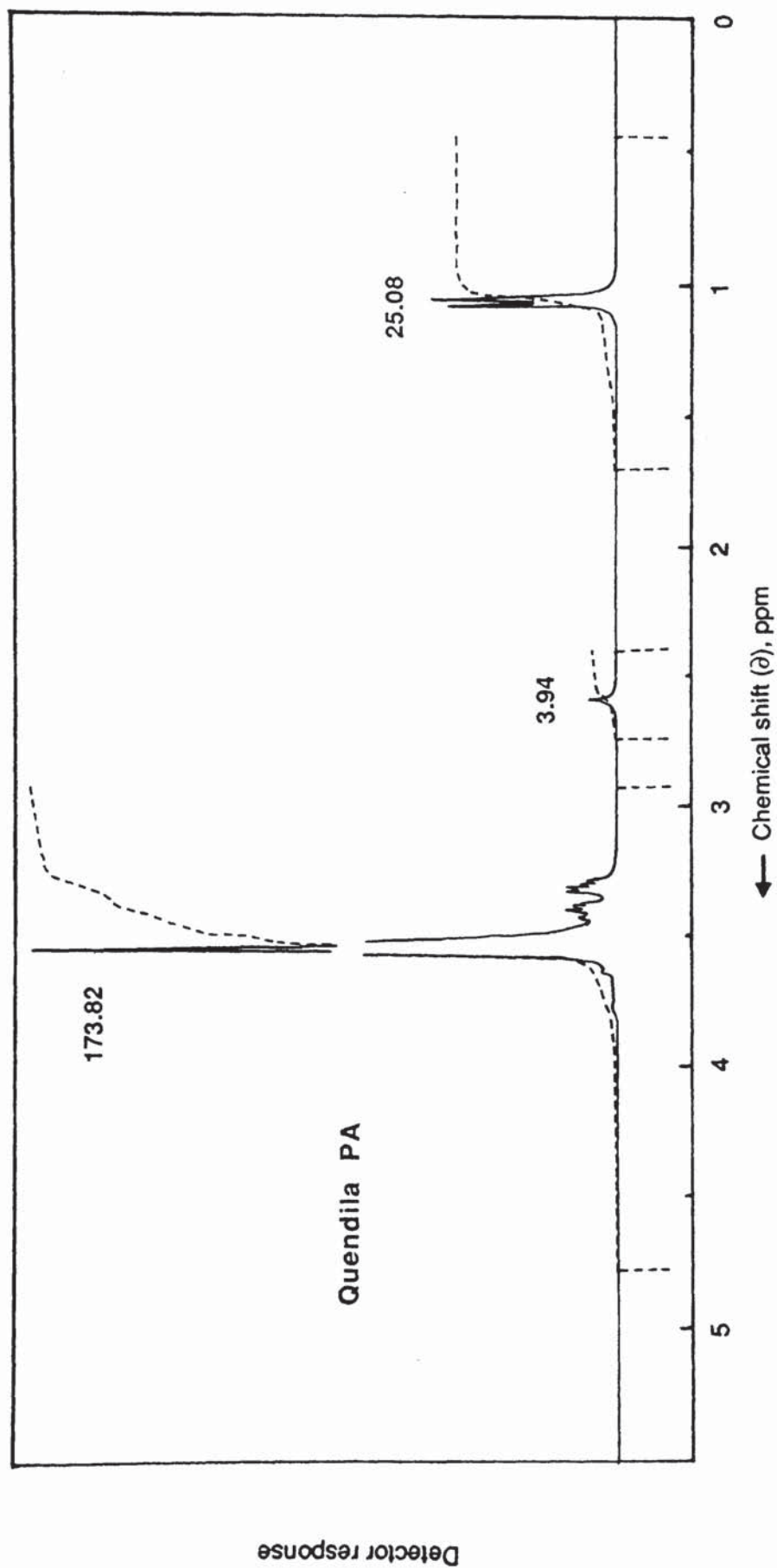


Figure 88. 300MHz proton magnetic resonance spectrum for Quendila PA dissolved in deuteriochloroform.

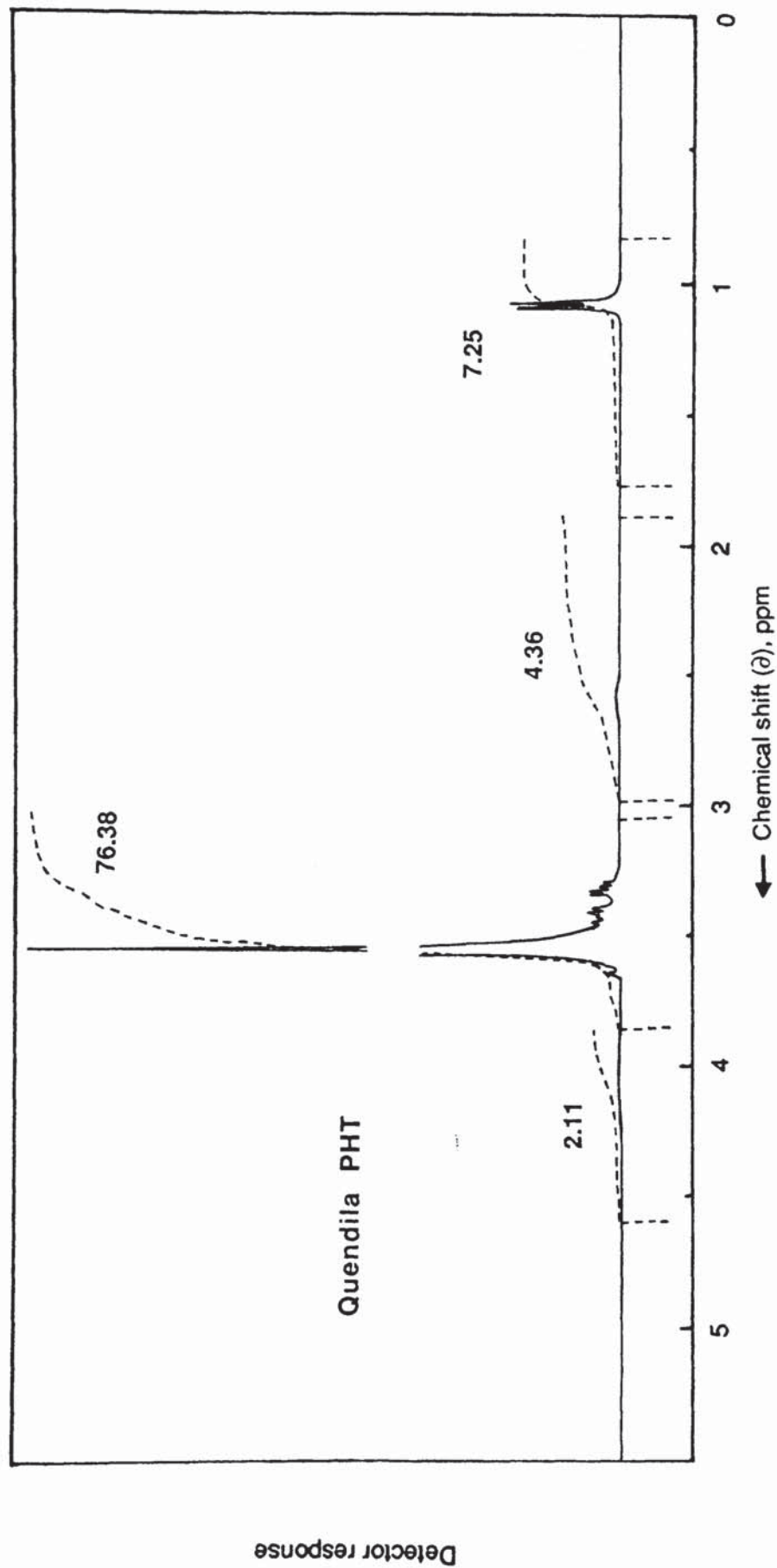


Figure 89. 300MHz proton magnetic resonance spectrum for Quendila PHT dissolved in deuterchloroform.

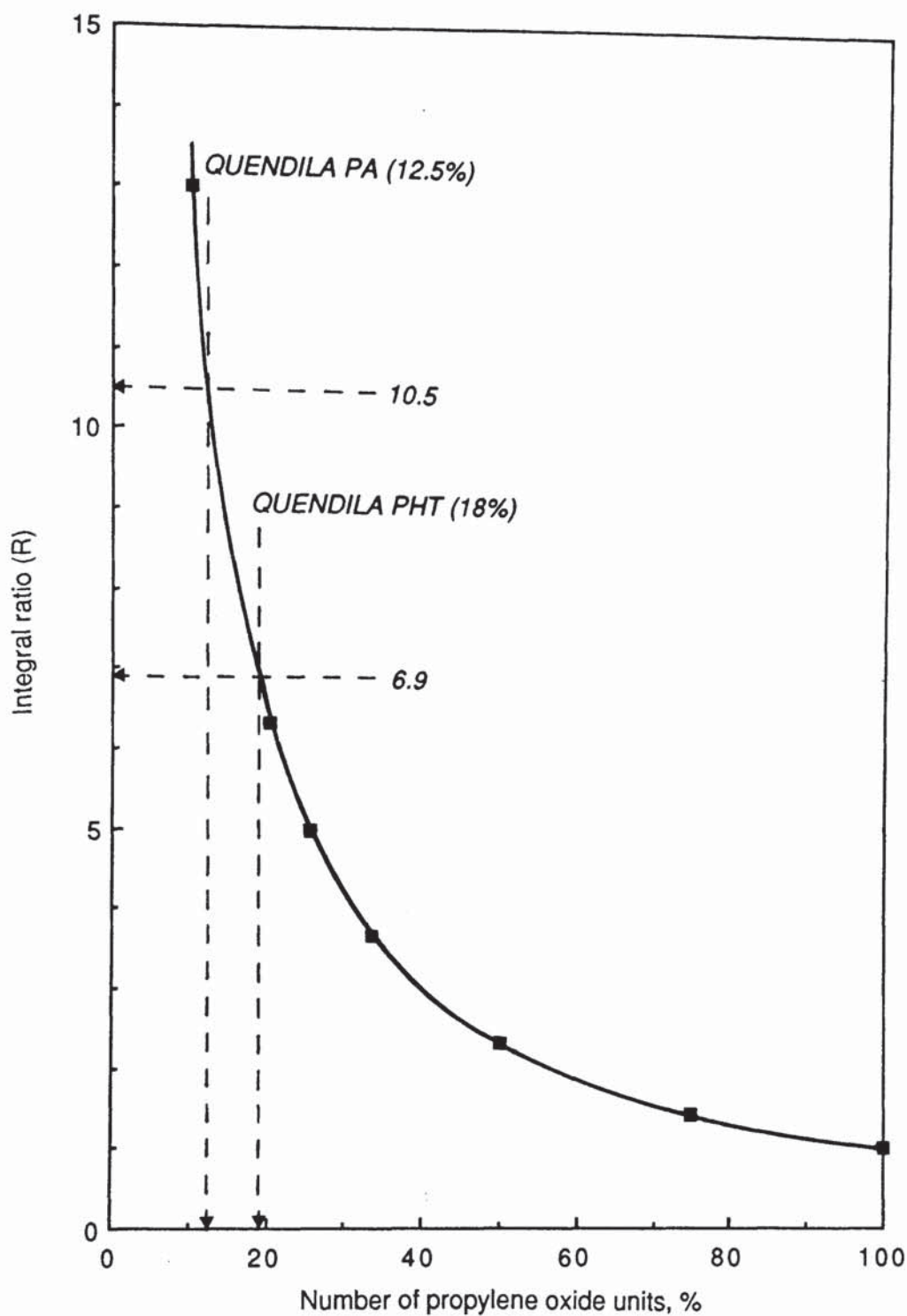


Figure 90. Relationship between the percentage of oxypropylene units in the PAG products Quendila PA and PHT and the integral ratio R. (Where R equals the number of protons connected to oxygen atoms divided by the number of methyl group protons of propylene oxide).

4.3 Concentration Control Data for Polymer Quenchant Solutions.

Typical concentration versus refractometer reading plots for the three representative polymer quenchants examined (*Table 12*) are given in *Figure 91*. The calibration plots are linear for each polymer type over their normal working concentration range. The steeper the lines, the greater the true solution concentration.

Figure 92 shows the kinematic viscosities of the various concentration representative polymer solutions at 40°C. These plots reflect the variations in viscosity between the original polymer concentrates. For a given concentration the polyacrylate tended to have a much higher kinematic viscosity when compared with the PAG, which in turn had a higher viscosity than the PVP. However, these concentration figures take no account of the real level of polymer in the solutions. Using the solids-content values for each product as a guide, and disregarding the other additives present, a 1.5 weight per cent solution of the Aquaquench ACR yielded a kinematic viscosity of 6.65mm²/s at 40°C; and the Quendila PA, 0.94mm²/s. Thus, when comparing more truly equivalent solution concentrations, the polyacrylate still had the highest kinematic viscosity but the PVP now had a value nearly three times higher than the PAG.

4.4 Quenchant Sample Agitation Systems.

4.4.1 Impeller / Baffle Systems. A schematic diagram of the first agitation system to be evaluated was given in *Figure 67*. Both a 75mm twin-flat-bladed impeller and a 40mm diameter high pitch model boat propeller were studied. The effect of the speed of rotation of both stirrers on the cooling characteristics of a 20 per cent Quendila PA solution at 30°C is given in *Table 17*.

The results given are the mean values \pm the standard deviations from at least duplicate tests. Both systems had little effect on the overall cooling characteristics of the PAG solution. Foaming problems were encountered with each system at speeds greater than 1000rpm. Static quench sample results are given for both series of tests. The variation in the cooling rate at 300°C may be attributable to the fact that the later high-pitch propeller tests were performed using a different probe and batch of Quendila PA.

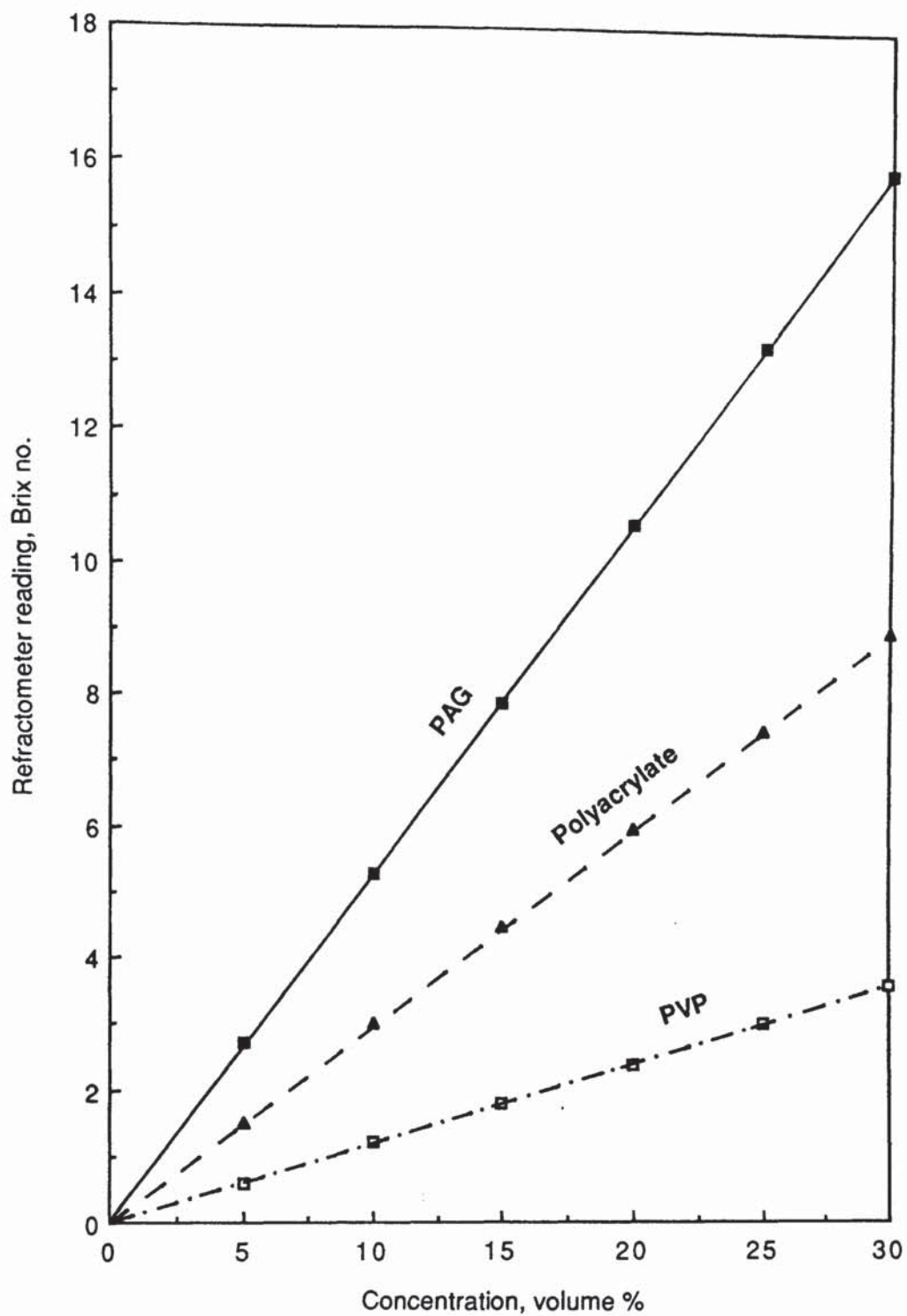


Figure 91. Concentration control for representative polymer quenchant products using a refractometer.

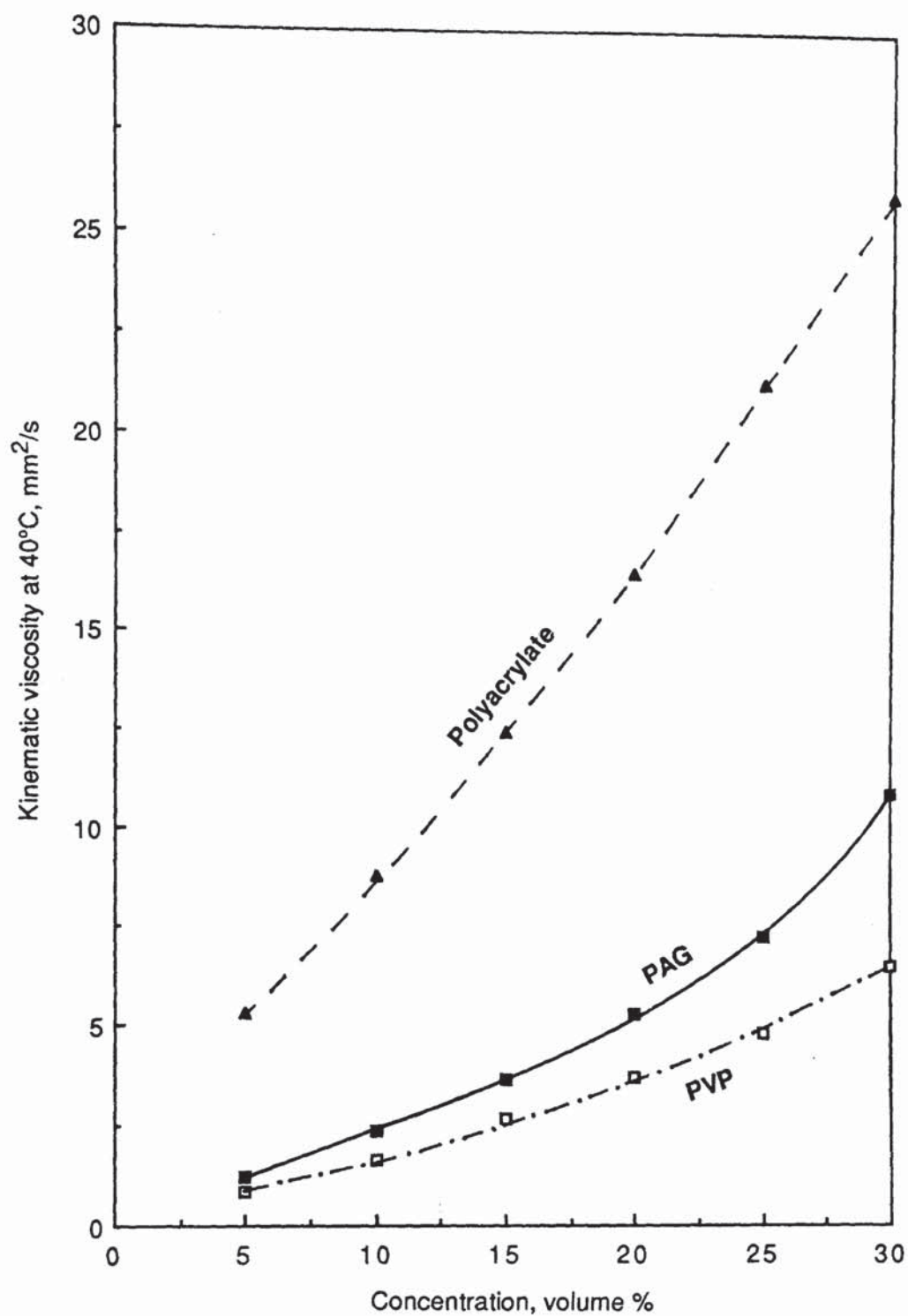


Figure 92. Concentration control for representative polymer quenchant products using a suspended level viscometer. ($1\text{mm}^2/\text{s} = 1\text{cSt}$).

Table 17. The effect of agitation created using impeller/baffle systems on the cooling characteristics of a 20% Quendila PA solution at 30°C.

| Test Impeller speed (rpm) | Time (s) to | | | Maximum cooling rate (°C/s) | Temp. of max ^m rate (°C) | Cooling rate at 300°C (°C/s) | Stage A/B | |
|---------------------------------|-------------|--------|--------|--------------------------------------|--|---------------------------------------|---------------|----------------|
| | 600°C | 400°C | 200°C | | | | Temp. (°C) | Rate (°C/s) |
| 75mm Flat-bladed | | | | | | | | |
| static | 11 ± 2 | 12 ± 2 | 18 ± 2 | 101 ± 7 | 556 ± 41 | 57 ± 2 | 723 ± 13 | 17 ± 1 |
| 500 | 9 ± 2 | 11 ± 2 | 16 ± 2 | 104 ± 9 | 599 ± 25 | 56 ± 2 | 746 ± 1 | 21 ± 2 |
| 1000 | 8 ± 2 | 10 ± 2 | 15 ± 2 | 102 ± 6 | 577 ± 23 | 55 ± 2 | 724 ± 14 | 28 ± 5 |
| 1300 | 8 ± 1 | 10 ± 1 | 15 ± 1 | 94 ± 7 | 549 ± 43 | 56 ± 2 | 702 ± 38 | 31 ± 1 |
| 40mm ϕ High-pitch | | | | | | | | |
| static | 10 ± 1 | 12 ± 1 | 17 ± 1 | 105 ± 1 | 547 ± 14 | 52 ± 1 | 742 ± 5 | 16 ± 1 |
| 500 | 10 ± 1 | 12 ± 1 | 16 ± 1 | 105 ± 2 | 556 ± 13 | 47 ± 1 | 747 ± 5 | 16 ± 2 |
| 1000 | 9 ± 1 | 11 ± 1 | 17 ± 1 | 110 ± 4 | 587 ± 24 | 46 ± 2 | 763 ± 6 | 16 ± 3 |

4.4.2 Pump Agitation Systems. *Figure 93* shows the effect of fluid velocity on the maximum cooling rate for Quendila PA solutions of various concentration at 30°C, using both vertical and horizontal flow directions with respect to the probe. This data was obtained using the quench tank, shown in *Figure 68*, which was used in conjunction with the Charles Austin centrifugal pump. Further information regarding both this and the impeller/baffle tests can be found in a published paper,⁽³⁵⁾ which is enclosed unbound.

The severity of the quench was raised by either reducing the polymer concentration or by increasing the fluid velocity. For example, in the static tests, the maximum cooling rate decreased from 130°C/s for the 10 per cent solution; through 102°C/s for the 20 per cent solution; to 63°C/s for the 30 per cent solution. This was an approximately linear decrease. The standard deviations tended to be greater for the static tests, whereas greater consistency was achieved when fluid velocities around 0.5m/s were used. By increasing the fluid velocity past the probe, a number of distinct trends were observed:

- (i) a progressive decrease in the cooling times to 600, 400 and 200°C;
- (ii) a progressive increase in maximum cooling rate associated with smaller more frequently detached vapour bubbles;
- (iii) a progressive increase in the temperature of maximum rate;
- (iv) the characteristic stage A/B transition temperature and rate increased until a critical fluid velocity was reached at which no stable film heat transfer was observed and nucleate boiling commenced the instant the probe was immersed (*Figure 94*).

The direction of the quenchant flow with respect to the probe was also very important. For example, in the case of the 20 per cent solution, the stage A film was stripped instantaneously upon quenching with a horizontal fluid velocity of 0.37m/s compared with 0.97m/s for vertical flow. The maximum rate was approximately 5 per cent higher for a given fluid velocity when using horizontal flow for the 10 and 20 per cent concentration solutions, and about 20 per cent higher for the 30 per cent Quendila PA solution.

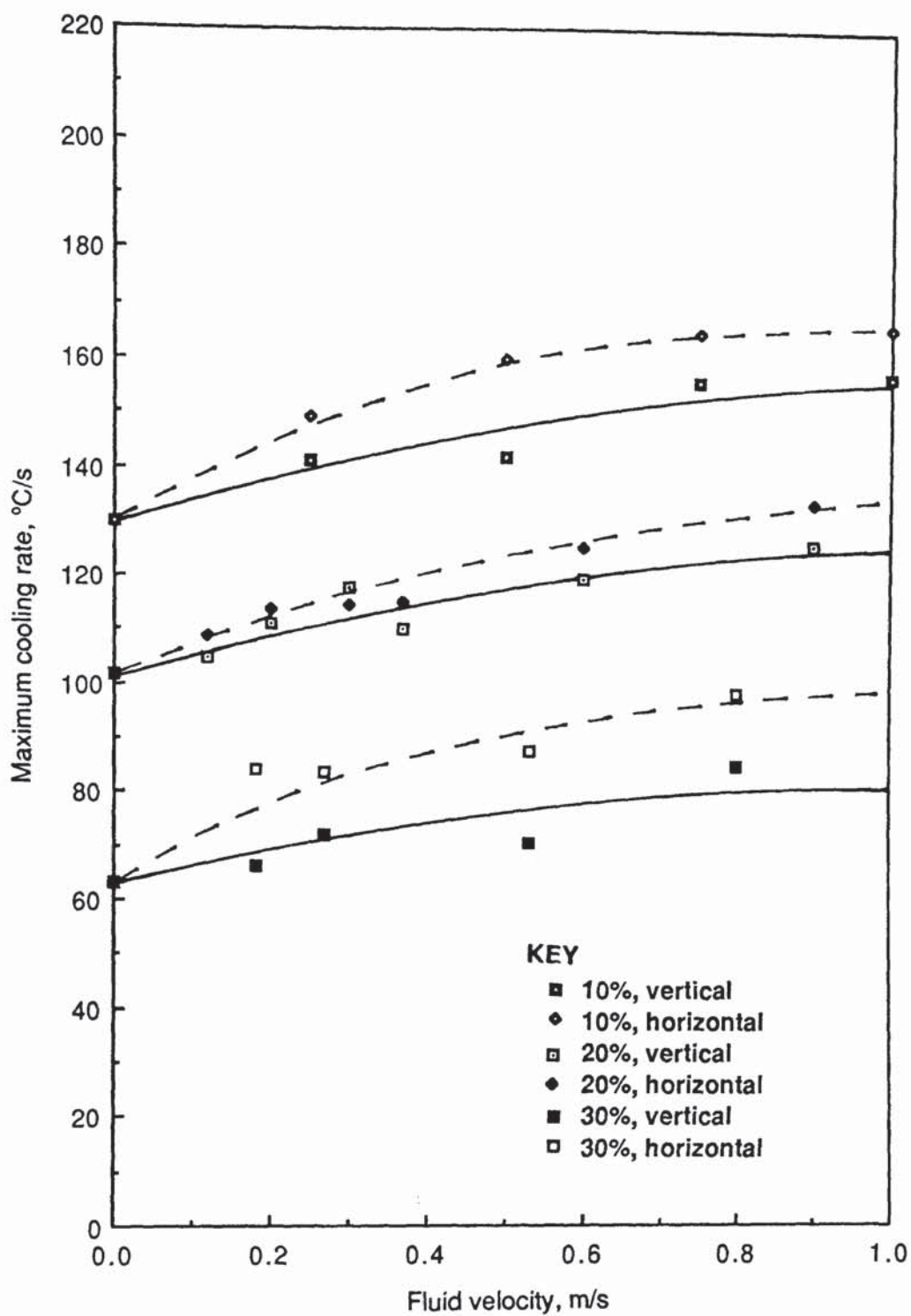


Figure 93. Effect of fluid velocity on the maximum cooling rate for Quendila PA (PAG) solutions of various concentrations at 30 °C, using both vertical and horizontal flow.

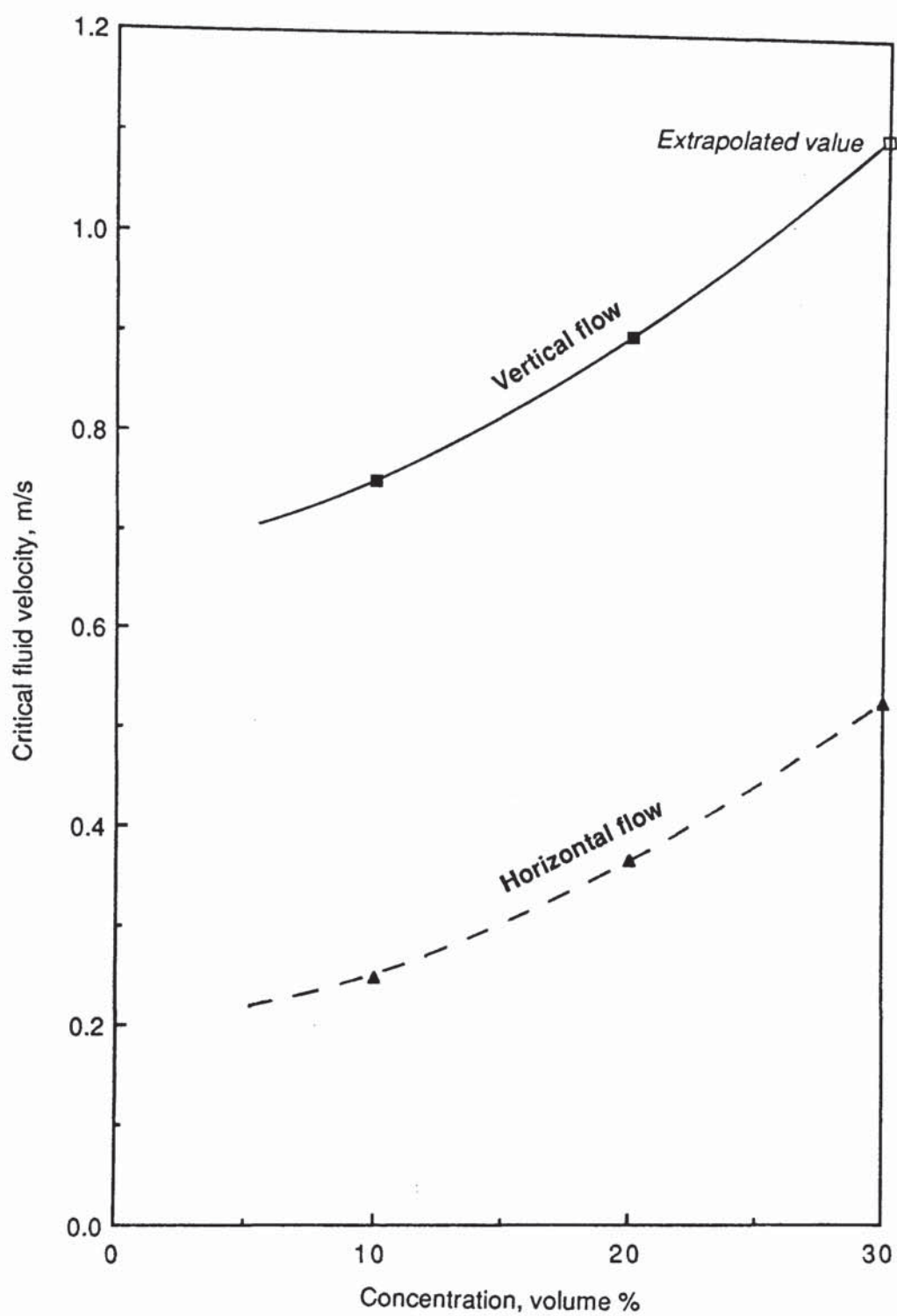


Figure 94. Effect of Quendila PA (PAG) concentration on the critical fluid velocity to instantaneously strip the stable polymer film and eliminate stage A cooling, for vertical and horizontal flow at 30 °C.

Regression and correlation analysis revealed positive curvilinear relationships between the fluid velocity and the cooling times to 600, 400 and 200°C, and for the maximum cooling rates. Correlation coefficients ranging from 0.99 to 0.92 were achieved for a second order fit for the maximum cooling rate data shown plotted in *Figure 93*. The correlation was much poorer for the temperature of maximum rate and rate at 300°C. Generally, the horizontal flow conditions resulted in greater correlation than the vertical, and the correlation improved with increased concentration for the stage A/B transition data.

Table 18. Cooling characteristics for a 20% Quendila PA solution at 30°C, tested using various annular flow conditions.

| Flow condition | Maximum cooling rate (°C/s) | Temp.of max ^m rate (°C) | Cooling rate at 300°C(°C/s) | Stage A/B transition | |
|------------------------------|-----------------------------|------------------------------------|-----------------------------|----------------------|-------------|
| | | | | Temp (°C) | Rate (°C/s) |
| static | 103 ± 3 | 593 ± 29 | 50 ± 1 | 766 ± 18 | 16 ± 1 |
| 0.5m/s 25mm ϕ outlet | 116 ± 2 | 595 ± 3 | 53 ± 1 | 785 ± 20 | 23 ± 2 |
| 0.5m/s 42mm ϕ outlet | 125 ± 2 | 596 ± 12 | 53 ± 1 | 800 ± 7 | 23 ± 2 |
| 1.0m/s 25mm ϕ outlet | 128 ± 1 | 632 ± 31 | 53 ± 1 | - | - |
| 2.0m/s 25mm ϕ outlet | 136 ± 2 | 652 ± 14 | 53 ± 1 | - | - |

Table 18 gives the cooling rate data for the tests performed at West Bromwich College of Commerce and Technology using the system which was shown in *Figure 41*. Time-temperature data was not obtained from these tests. The same trends as for the previous system were observed upon increasing the fluid velocity. With this system the probe formed an annulus with the quench unit tube which had an internal

diameter of either 25 or 42mm. Therefore, by adjusting the speed of the pumps, two tests could be performed at a fluid velocity of 0.5m/s past the probe, but with different sized annuli. The maximum cooling rate was about 7 per cent higher when using the larger diameter outlet tube.

Table 19. Effect of probe position with respect to the pump outlet and inlet orifices, on the cooling characteristics for a 15% Quendila PA solution at 30°C. Fluid velocity through outlet 0.5m/s.

| Test | Time (s) to | | | Maximum cooling rate (°C/s) | Temp of max ^m rate (°C) | Cooling rate at 300°C (°C/s) |
|----------------|-------------|---------|----------|-----------------------------------|--|------------------------------------|
| | 600°C | 400°C | 200°C | | | |
| Height | | | | | | |
| H (mm) | | | | | | |
| 5 | 2.9±0.1 | 4.6±0.1 | 8.7±0.1 | 158 ± 1 | 672 ± 6 | 56 ± 1 |
| 15 | 3.0±0.1 | 4.7±0.1 | 8.9±0.1 | 155 ± 2 | 668 ± 9 | 53 ± 1 |
| 25 | 3.1±0.1 | 4.9±0.1 | 9.1±0.1 | 152 ± 1 | 666 ± 8 | 51 ± 1 |
| 35 | 3.6±0.7 | 5.5±0.8 | 9.7±0.9 | 149 ± 1 | 656 ± 21 | 51 ± 1 |
| 45 | 3.7±0.1 | 5.5±0.1 | 9.9±0.1 | 147 ± 1 | 690 ± 1 | 50 ± 1 |
| Horizontal | | | | | | |
| Displacement | | | | | | |
| X (mm) | | | | | | |
| 0 | 3.2±0.1 | 4.9±0.1 | 9.2±0.1 | 153 ± 1 | 675 ± 29 | 53 ± 2 |
| 5 | 3.2±0.1 | 5.0±0.2 | 9.3±0.2 | 152 ± 1 | 675 ± 14 | 54 ± 1 |
| 10 | 3.1±0.1 | 4.9±0.1 | 9.2±0.1 | 151 ± 1 | 669 ± 7 | 52 ± 1 |
| 15 | 3.2±0.2 | 5.0±0.2 | 9.2±0.2 | 148 ± 1 | 701 ± 13 | 52 ± 1 |
| 20 | 3.6±0.3 | 5.4±0.3 | 9.6±0.3 | 139 ± 2 | 707 ± 15 | 52 ± 1 |
| 25 | 4.9±1.1 | 6.8±1.1 | 11.1±1.3 | 129 ± 2 | 647 ± 23 | 50 ± 1 |
| Inlet Position | | | | | | |
| D (mm) | | | | | | |
| 50 | 3.1±0.1 | 4.9±0.1 | 9.2±0.1 | 152 ± 2 | 669 ± 5 | 52 ± 1 |
| 100 | 3.2±0.1 | 5.0±0.2 | 9.3±0.1 | 150 ± 1 | 664 ± 18 | 52 ± 1 |
| 150 | 3.2±0.1 | 5.0±0.1 | 9.3±0.1 | 153 ± 1 | 674 ± 9 | 52 ± 1 |

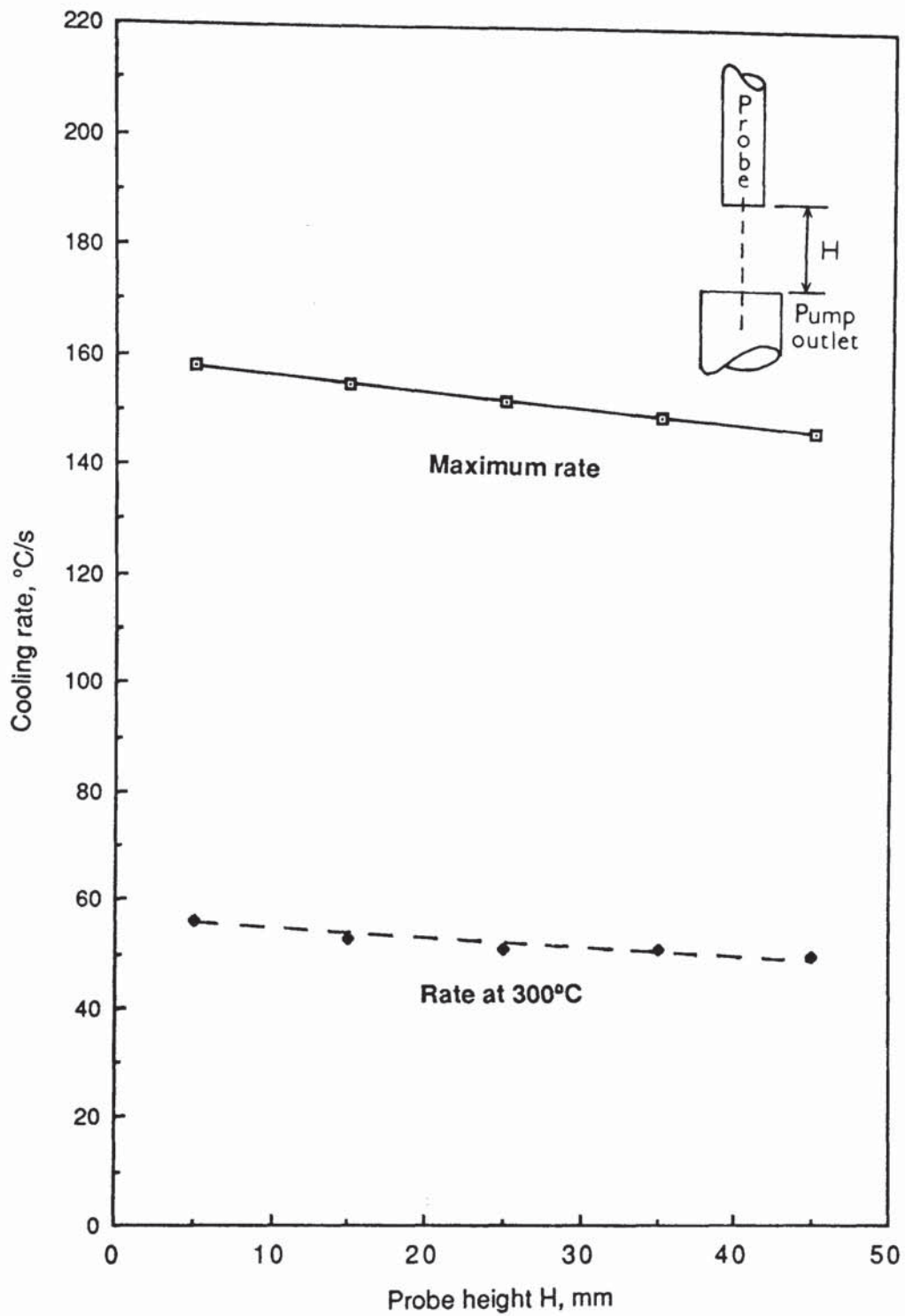


Figure 95. Effect of probe height H with respect to the pump outlet orifice on the cooling characteristics for a 15% Quendila PA solution at 30 °C. Fluid velocity through outlet 0.5m/s.

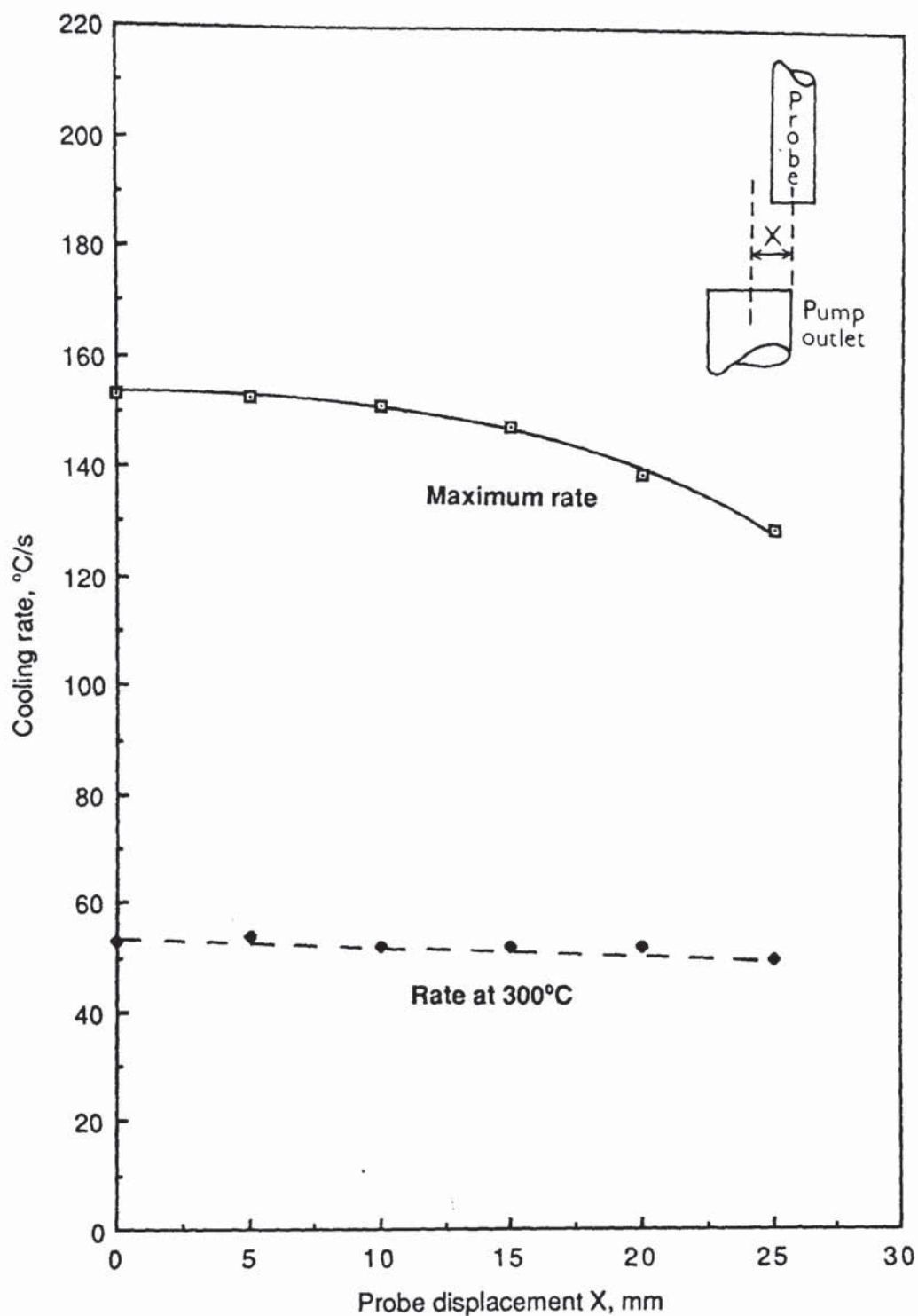


Figure 96. Effect of horizontal probe displacement X with respect to the pump outlet orifice on the cooling characteristics for a 15% Quendila PA solution at 30 °C, fluid velocity through outlet 0.5m/s.

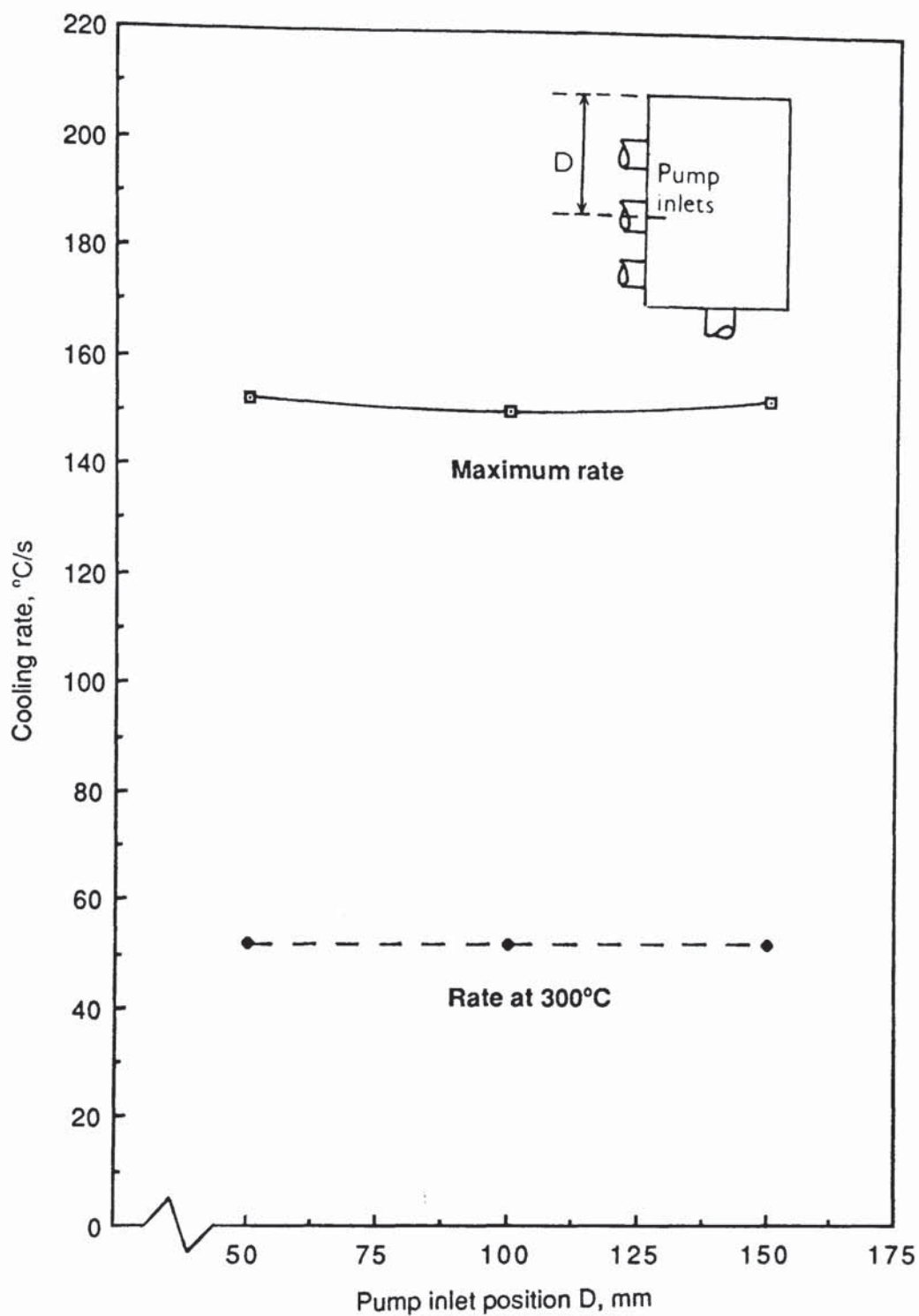


Figure 97. Effect of pump inlet position D on the cooling characteristics for a 15% Quendila PA solution at 30 °C, fluid velocity through outlet 0.5m/s.

The final pump agitation system to be examined was that shown in *Figure 70*. This system was used for all subsequent quenchant cooling assessment work. *Table 19* shows the effect of probe position on the cooling characteristics of a 15 per cent Quendila PA solution at 30°C. A fluid velocity of 0.5m/s emerging from the 25mm diameter outlet orifice was maintained throughout the tests. Results are also given which illustrate the effect of pump inlet position on the characteristics.

Figures 95 to 97 demonstrate more clearly these effects. There was a linear decrease in both the maximum cooling rate and the rate at 300°C upon increasing the probe height *H*. Horizontal probe displacements *X* of up to about 10mm had little effect, whereas greater displacements resulted in a more pronounced decrease in the cooling rates. However, varying the inlet position *D* did not appear to significantly influence the results.



Plate 5. Flow visualization for a 15 per cent Quendila PA (PAG) solution at the standardized test conditions (probe 25mm above 25mm diameter outlet through which the 30 °C solution is being pumped at a fluid velocity of 0.5m/s).

The fluid flow pattern around the probe (highlighted with red ink) for the 15 per cent Quendila PA (PAG) solution at the standardized conditions is shown in *Plate 5*. The fluid jet can be seen emerging from the 25mm diameter orifice in an essentially laminar pattern, and then diverging at a height of approximately 5mm above the orifice at an angle of about 15° to the normal in a turbulent fashion.

4.5 Comparative Cooling Characteristic Data for Polymer Quenchant Products.

Figures 98 to 106 show both the time-temperature and cooling rate-temperature curves for each of the polymer quenchant products which were listed in *Table 12*. The 15 volume per cent solutions of each concentrate were tested at 30°C in both the static condition and when agitated at 0.5m/s. The results shown represent average curves derived from at least duplicate tests. The cooling parameter data from these tests is given in *Table 20*.

The slowest PAG was Ucon E with a maximum rate of $143 \pm 1^\circ\text{C/s}$ and a rate at 300°C of $40 \pm 1^\circ\text{C/s}$ in the agitated test. Breox NF-18 was the PAG with the highest maximum rate ($172 \pm 2^\circ\text{C/s}$) whereas Quendila PHT was the fastest at 300°C with a rate of $58 \pm 1^\circ\text{C/s}$. The static PAG's all experienced stage A cooling, agitation at a fluid velocity of 0.5m/s either eliminated or greatly reduced stage A cooling for each product. Even in the static tests neither of the PVP products produced stage A cooling. The cooling rate at 300°C was significantly increased (>100%) in the agitated PVP tests. The Parquench 90 sample had slightly slower cooling characteristics when compared with Parquench 60. The polyacrylates exhibited prolonged stage A cooling in the static tests. The instability in this film boiling stage resulted in inconsistent results and the highest standard deviations. Multiple nucleate boiling peaks were commonly observed for the static Aquaquench 110 samples as seen in *Figure 105*. Agitation greatly reduced the duration of stage A cooling for the polyacrylates, which in turn produced a significant improvement in the level of test reproducibility. When compared with the other polymer types at these test conditions, the polyacrylates tended to have the lowest cooling rates.

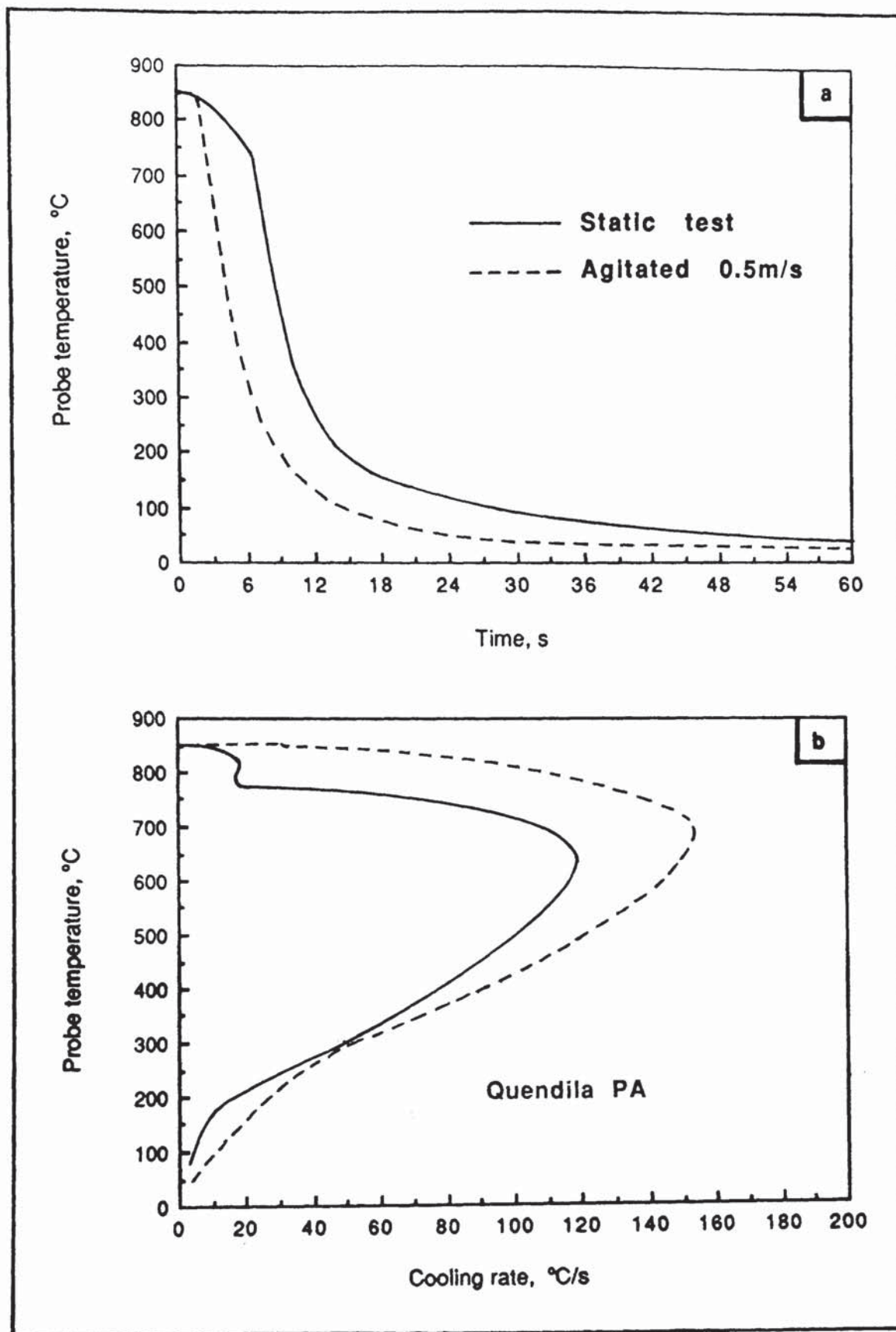


Figure 98. Cooling data for a 15 volume per cent solution of Quendila PA tested at 30 °C in both the static condition and 0.5m/s agitation.

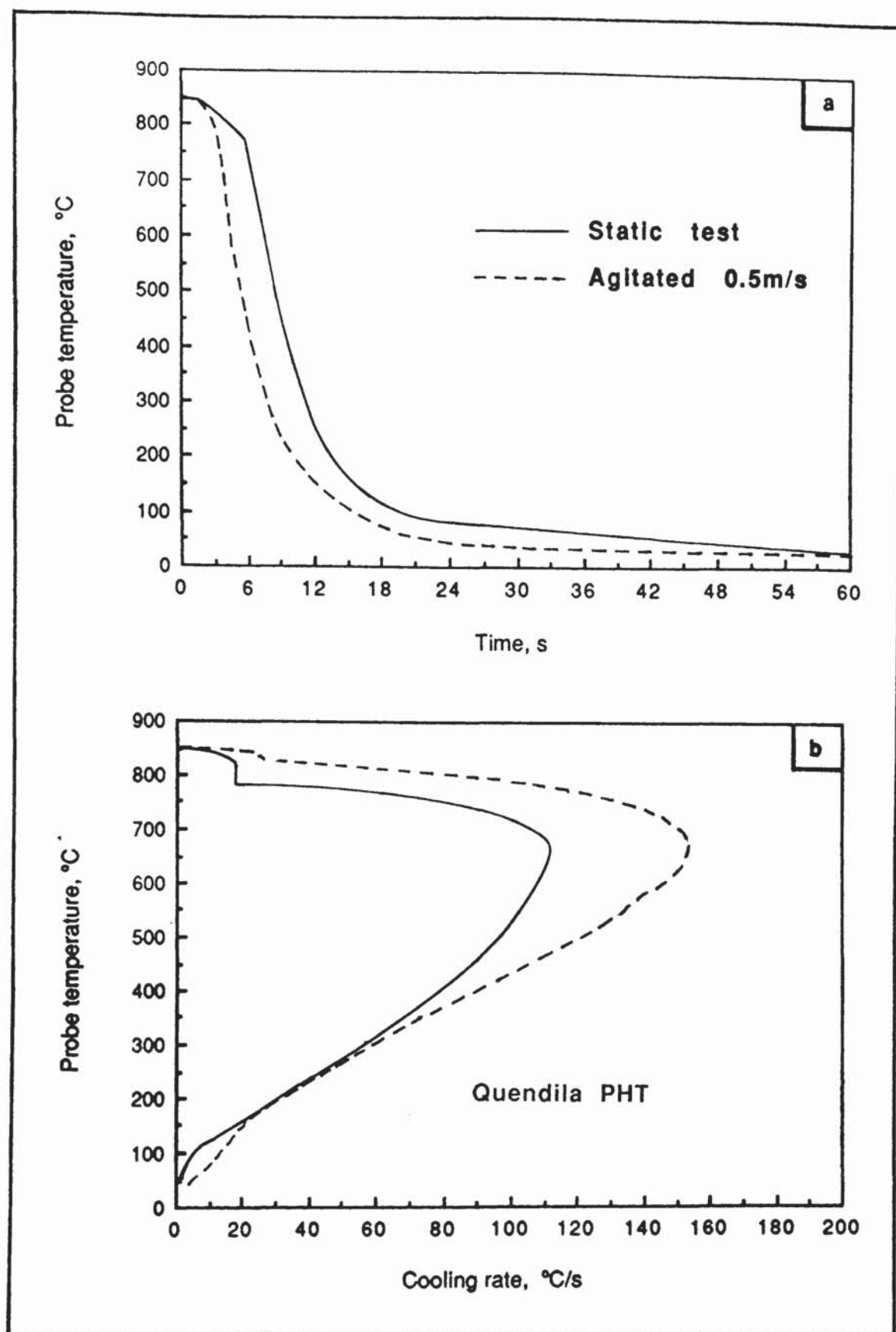


Figure 99. Cooling data for a 15 volume per cent solution of Quendila PHT tested at 30 °C in both the static condition and 0.5m/s agitation.

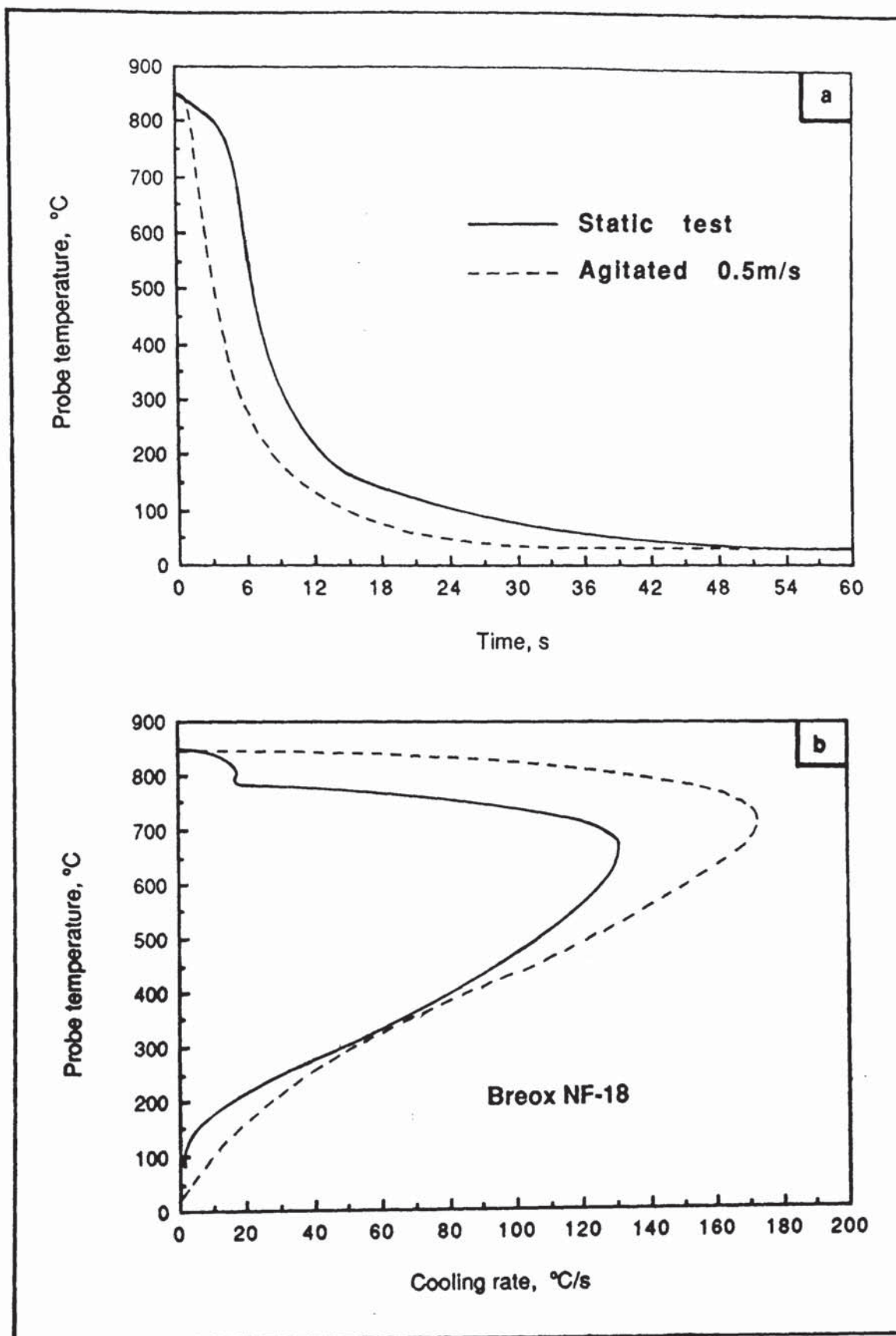


Figure 100. Cooling data for a 15 volume per cent solution of Breox NF-18 tested at 30 °C in both the static condition and 0.5m/s agitation.

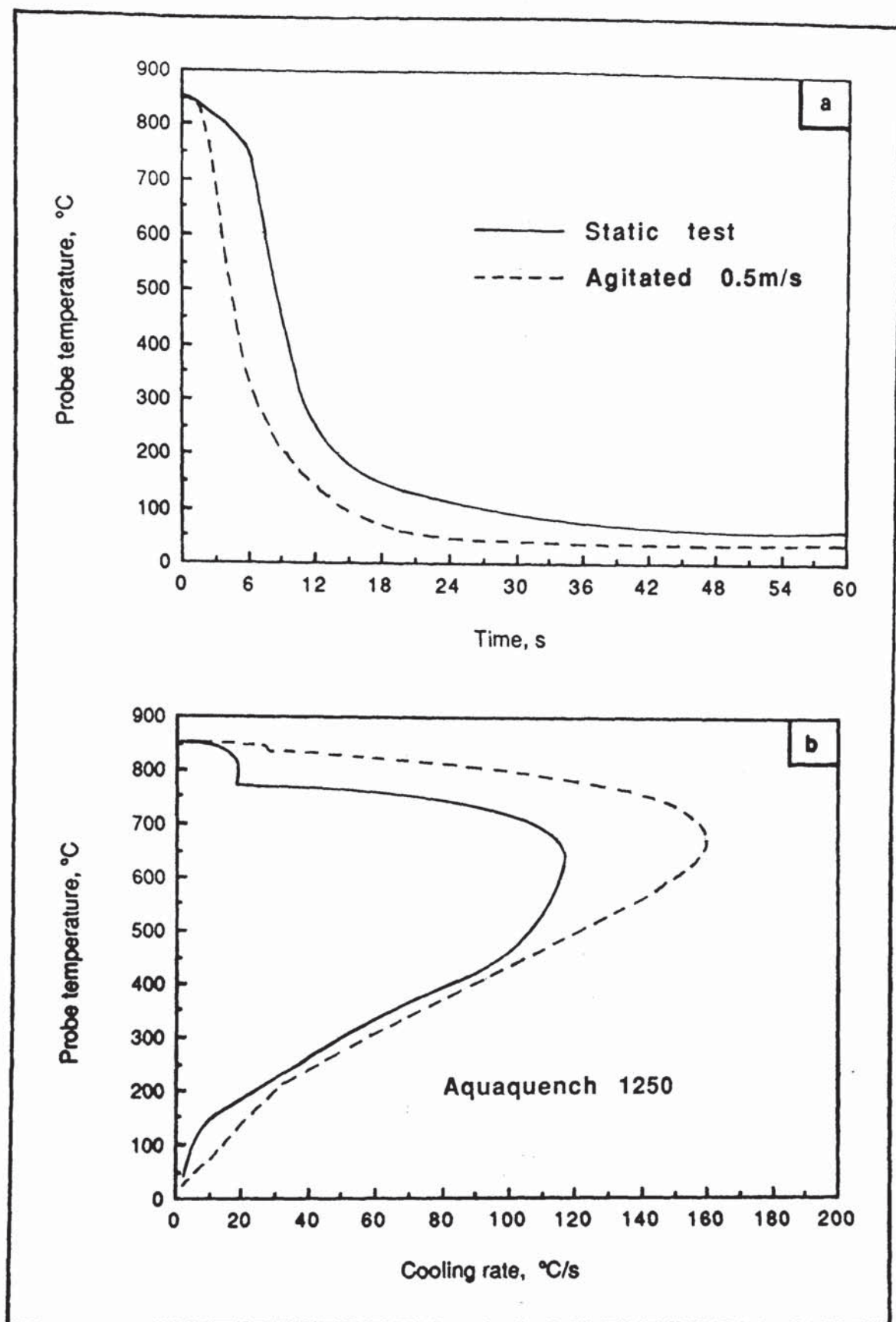


Figure 101. Cooling data for a 15 volume per cent solution of Aquaquench 1250 tested at 30 °C in both the static condition and 0.5m/s agitation.

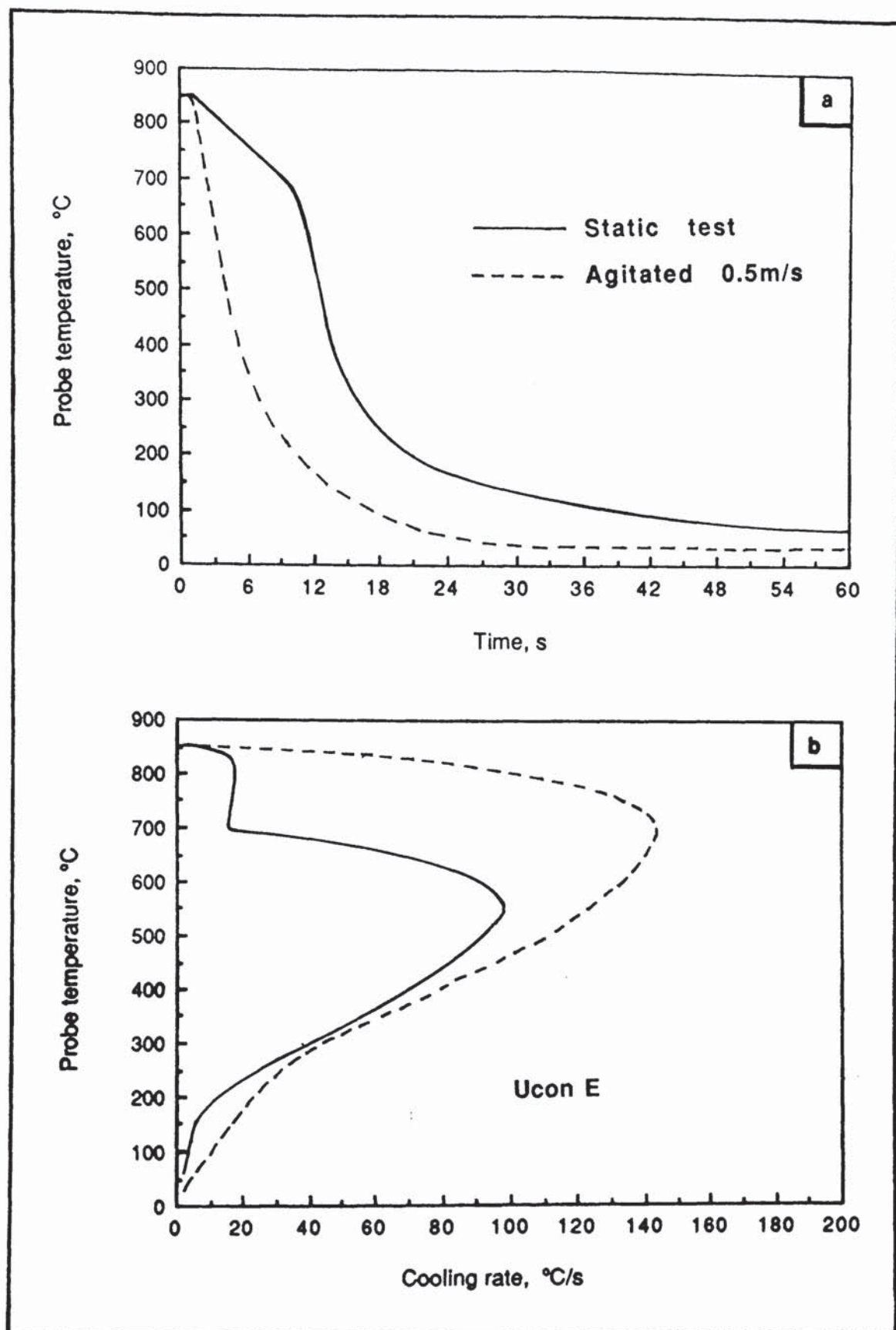


Figure 102. Cooling data for a 15 volume per cent solution of Ucon E tested at 30°C in both the static condition and 0.5m/s agitation.

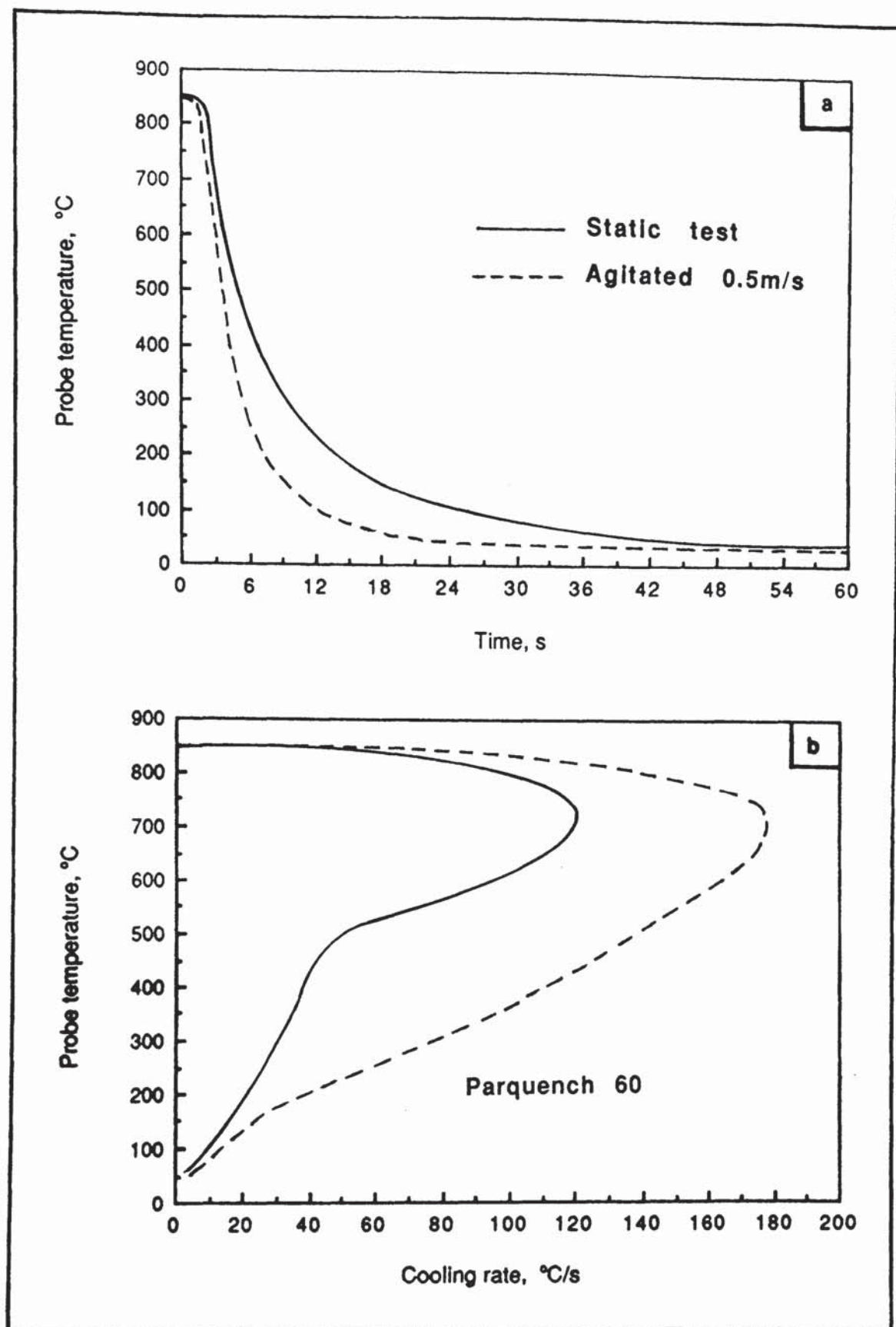


Figure 103. Cooling data for a 15 volume per cent solution of Parquench 60 tested at 30 °C in both the static condition and 0.5m/s agitation.

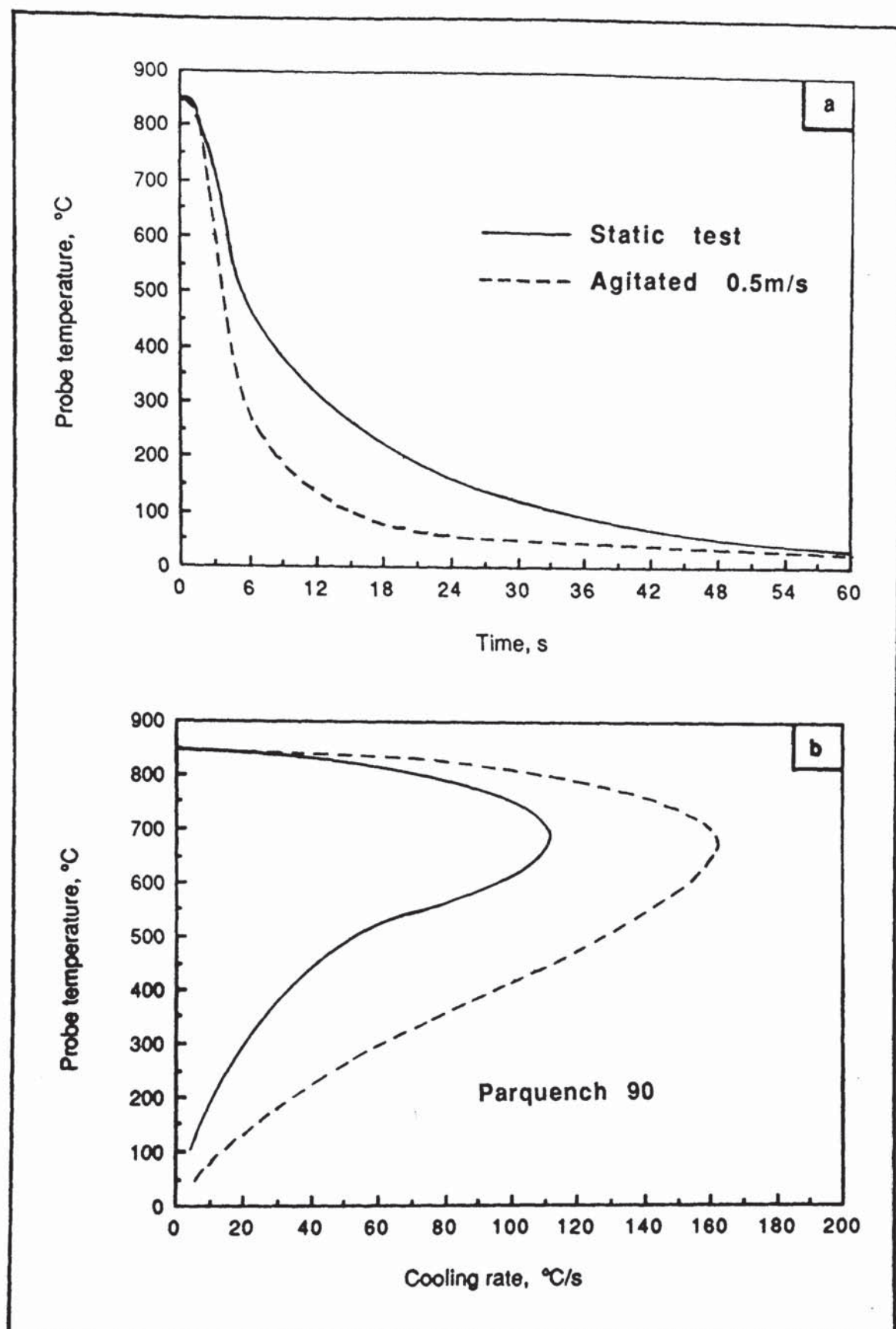


Figure 104. Cooling data for a 15 volume per cent solution of Parquench 90 tested at 30 °C in both the static condition and 0.5m/s agitation.

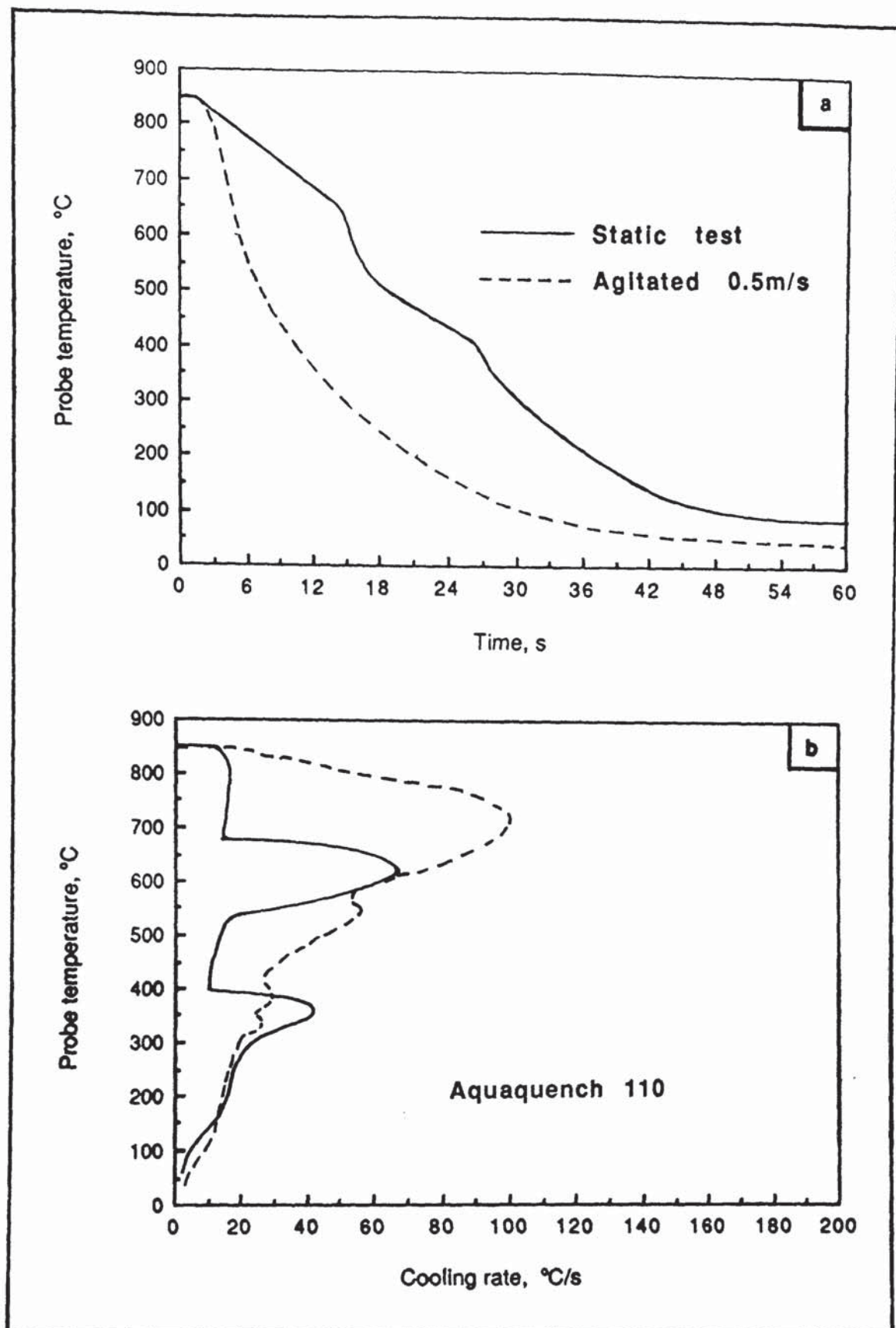


Figure 105. Cooling data for a 15 volume per cent solution of Aquaquench 110 tested at 30 °C in both the static condition and 0.5m/s agitation.

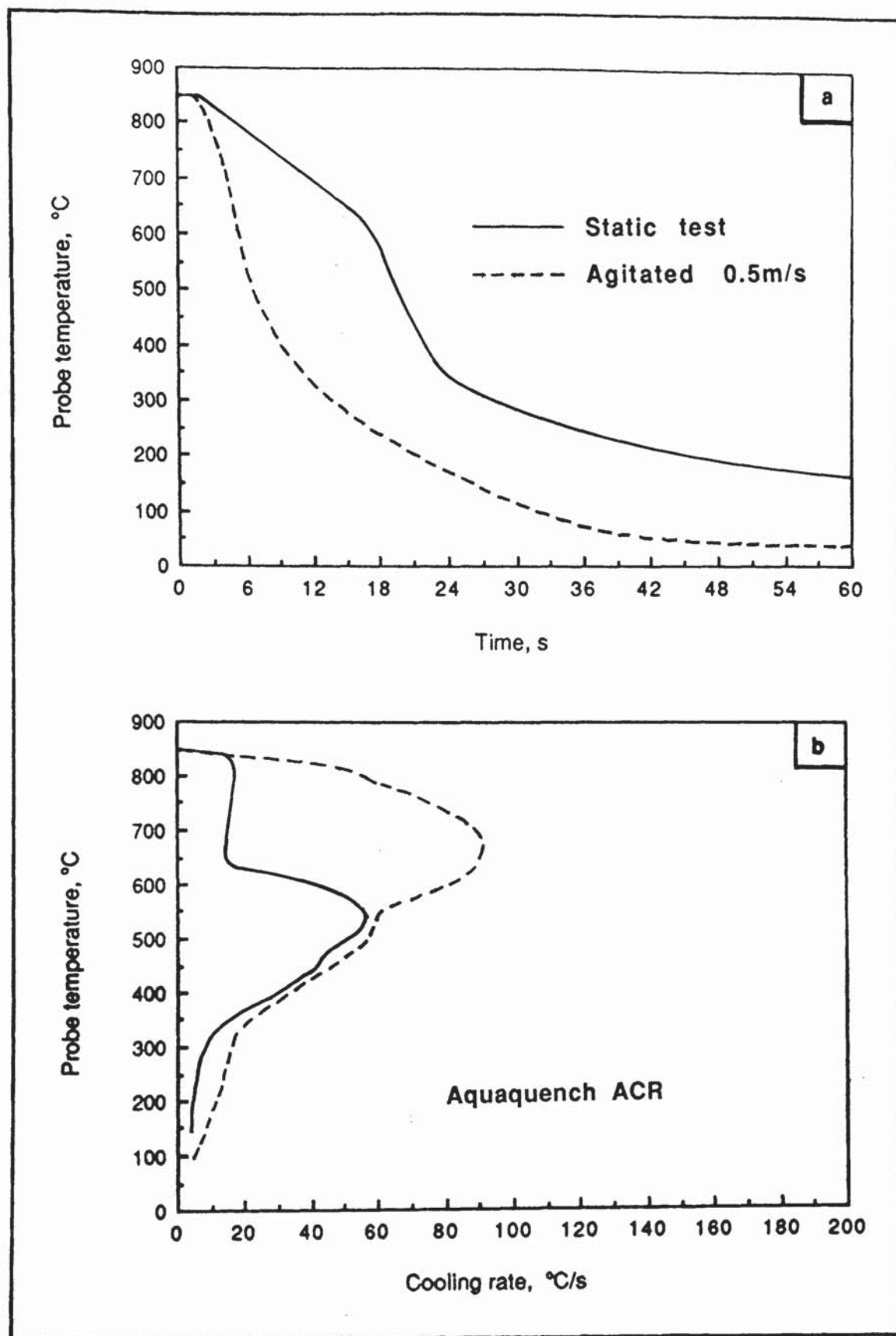


Figure 106. Cooling data for a 15 volume per cent solution of Aquaquench ACR tested at 30 °C in both the static condition and 0.5m/s agitation.

Table 20. Comparative cooling characteristic data for 15 volume per cent concentrate solutions tested at 30°C

| Test | Time (s) to | | Maximum cooling rate | Temp. of max ^m rate | Cooling rate at 300°C | Stage A/B transition | |
|---------------------|-------------|----------|----------------------|--------------------------------|-----------------------|----------------------|-------------|
| PAG's | 600°C | 400°C | 200°C | (°C/s) | (°C) | Temp. (°C) | Rate (°C/s) |
| Quendila PA | | | | | | | |
| static | 7.6±0.4 | 9.5±0.3 | 14.0±0.7 | 119 ± 3 | 634 ± 27 | 48 ± 3 | 776 ± 8 |
| 0.5m/s | 3.4±0.2 | 5.0±0.1 | 9.4±0.2 | 154 ± 1 | 676 ± 16 | 50 ± 1 | 831 ± 5 |
| | | | | | | | 18 ± 2 |
| | | | | | | | 32 ± 1 |
| Quendila PHT | | | | | | | |
| static | 7.2±0.8 | 9.4±0.9 | 13.3±0.9 | 111 ± 3 | 657 ± 16 | 55 ± 1 | 778 ± 18 |
| 0.5m/s | 4.2±0.1 | 5.8±0.1 | 9.7±0.1 | 153 ± 3 | 656 ± 33 | 58 ± 1 | 826 ± 1 |
| | | | | | | | 17 ± 1 |
| | | | | | | | 27 ± 1 |
| Breox NF-18 | | | | | | | |
| static | 5.6±1.3 | 7.6±1.3 | 12.8±0.9 | 131 ± 3 | 673 ± 20 | 47 ± 3 | 786 ± 12 |
| 0.5m/s | 2.2±0.1 | 4.0±0.1 | 8.6±0.1 | 172 ± 2 | 707 ± 18 | 51 ± 3 | 17 ± 1 |
| | | | | | | | - |
| Aquaquench | | | | | | | |
| 1250 static | 7.4±0.1 | 9.3±0.1 | 14.0±0.1 | 117 ± 2 | 627 ± 13 | 50 ± 1 | 773 ± 3 |
| 0.5m/s | 3.5±0.1 | 5.2±0.1 | 9.3±0.2 | 159 ± 2 | 659 ± 17 | 57 ± 1 | 834 ± 1 |
| | | | | | | | 18 ± 1 |
| | | | | | | | 27 ± 2 |
| Ucon E | | | | | | | |
| static | 11.1±1.4 | 13.5±1.5 | 20.7±1.6 | 98 ± 4 | 544 ± 4 | 37 ± 1 | 689 ± 1 |
| 0.5m/s | 3.1±0.1 | 5.1±0.1 | 10.4±0.1 | 143 ± 1 | 671 ± 21 | 40 ± 1 | 16 ± 1 |
| | | | | | | | - |

Table 20 continued.

| Test | Time (s) to | | Maximum cooling rate (°C/s) | Temp.of max ^m rate (°C) | Cooling rate at 300°C (°C/s) | Stage A/B transition | |
|---------------|-------------|----------|--------------------------------|---------------------------------------|---------------------------------|----------------------|------------|
| | 600°C | 400°C | | | | 200°C | Temp. (°C) |
| PVP's | | | | | | | |
| Parquench 60 | | | | | | | |
| static | 3.5±0.3 | 6.7±0.7 | 13.0±2.4 | 119 ± 4 | 728 ± 40 | 36 ±9 | - |
| 0.5m/s | 2.8±0.1 | 4.2±0.1 | 7.0±0.1 | 178 ± 1 | 704 ± 8 | 76 ± 1 | - |
| Parquench 90 | | | | | | | |
| static | 3.9±0.4 | 8.2±0.3 | 19.7±1.9 | 112 ± 3 | 690 ± 3 | 21 ± 4 | - |
| 0.5m/s | 2.8±0.1 | 4.4±0.1 | 8.1±0.2 | 162 ± 3 | 676 ± 23 | 60 ± 1 | - |
| Polyacrylates | | | | | | | |
| Aquaquench | | | | | | | |
| 110 static | 15.3±3.4 | 26.5±1.1 | 38.0±3.2 | 67 ± 6 | 603 ± 49 | 22 ± 6 | 645 ± 59 |
| 0.5m/s | 5.0±0.1 | 10.6±0.5 | 21.3±0.8 | 102 ± 4 | 711 ± 2 | 19 ± 1 | 833 ± 5 |
| Aquaquench | | | | | | | |
| ACR static | 17.2±1.1 | 22.2±2.0 | 48.2±3.2 | 56 ± 2 | 528 ± 56 | 8 ± 1 | 640 ± 25 |
| 0.5m/s | 5.0±0.6 | 9.0±0.2 | 21.2±0.3 | 90 ± 2 | 670 ± 2 | 17 ± 1 | 770 ± 37 |
| | | | | | | | 14 ± 1 |
| | | | | | | | 60 ± 1 |

4.6 Photographic Record of the Cooling Mechanism for the Representative Polymer Quenchants

Figures 107 to 112 illustrate the cooling stages for each of the representative polymer quenchant solutions, tested in both the static condition and when agitated at 0.5m/s. From knowledge of the camera winder speed, it was possible to compare selected photographs synchronously with the measured cooling rate-temperature curves. However, it must be remembered that the cooling curves are being measured at the centre of the probe and show a subsequent time lag compared with the surface cooling phenomena.

Figure 107 represents a static 15 per cent PAG quench at 30°C where : (a) inversion of the polymer occurs, with the residual water vaporizing to produce a steam blanket adjacent to the hot metal, encapsulated by the polymer film. This composite film-boiling region is approximately 0.2 - 0.4mm thick. (b) Nucleate boiling is initiated at the fastest cooling base of the probe where the polymer film is thinnest. The pressure of the steam blanket becomes sufficient to break through this polymer film and an explosive boiling reaction occurs as the cool liquid wets the edge of the probe. (c) Nucleate boiling has spread along the entire length of the probe; once initiated, steam bubbles grow (with occasional coalescence) before escaping from the surface encapsulated in polymer. The diameter of the escaping bubbles is typically several millimetres. (d) Nucleate boiling has begun to decline with a concurrent reduction in bubble size. When the surface temperature of the probe reaches the inversion point, the polymer redissolves, giving rise to liquid cooling by convection.

The results for the same PAG solution in the agitated condition are shown in *Figure 108* where: (a) stable film-boiling has already broken down with nucleate boiling fronts simultaneously moving inwards from both ends of the probe. (b) The entire surface of the probe is now "active" i.e. nucleate boiling is occurring, with small bubbles continuously escaping through a tenuous polymer film. These bubbles can

only just be resolved because of their small characteristic size (a few tenths of a millimetre) combined with their rapid departure rate, compared with the camera shutter speed of 1/125s. This last parameter was limited by the amount of light that could be directed towards the probe without producing excessive reflections from the front of the glass tank. (c) The polymer film is beginning to redissolve in the fastest cooling portions of the probe such as near its base. (d) Only patches of polymer remain on the probe surface. It is interesting to compare this with the equivalent point (d) in *Figure 107*, after a quench time of 15s. Less polymer remains on the surface of the probe in the agitated solution and its core temperature is nearly 100°C lower. Thus, the effect of agitation was to speed up the quench producing smaller more frequently detached bubbles and thinner more uniform polymer films.

Figure 109 examines the characteristics of a 15 per cent PVP solution at 30°C in the non-agitated conditions where: (a) a cloud of polymer has been ejected and nucleate boiling has commenced near the probe's base with partial-film-boiling over the rest of its surface. (b) Nucleate boiling is now in operation over the entire probe length. A film of polymer attempts to constrain the release of the bubbles. Vapour coalescence towards the top of the probe has resulted in large bubbles (3 - 4mm) being formed, whilst smaller bubbles (0.5 - 1.0mm) depart the cooler base. (c) As the probe continues to cool, a more stable yet still active film is produced. This film is approximately 1.4mm thick, containing a fairly even distribution of bubbles between 0.5 and 2.0mm in size. (d) The polymer redissolves near the base of the probe as its temperature falls below the boiling point of the solution.

The results for the agitated PVP solution are shown in *Figure 110* where: (a) polymer is being jettisoned from the surface of the probe. A tenuous active polymer film covers most of the probe, although bare metal is already exposed at its base. (b) More of the base of the probe is revealed, with sub-millimetre size bubbles being formed further up. (c) The bubble size and film thickness have continued to decrease. (d) No visible polymer film remains on the surface of the probe.

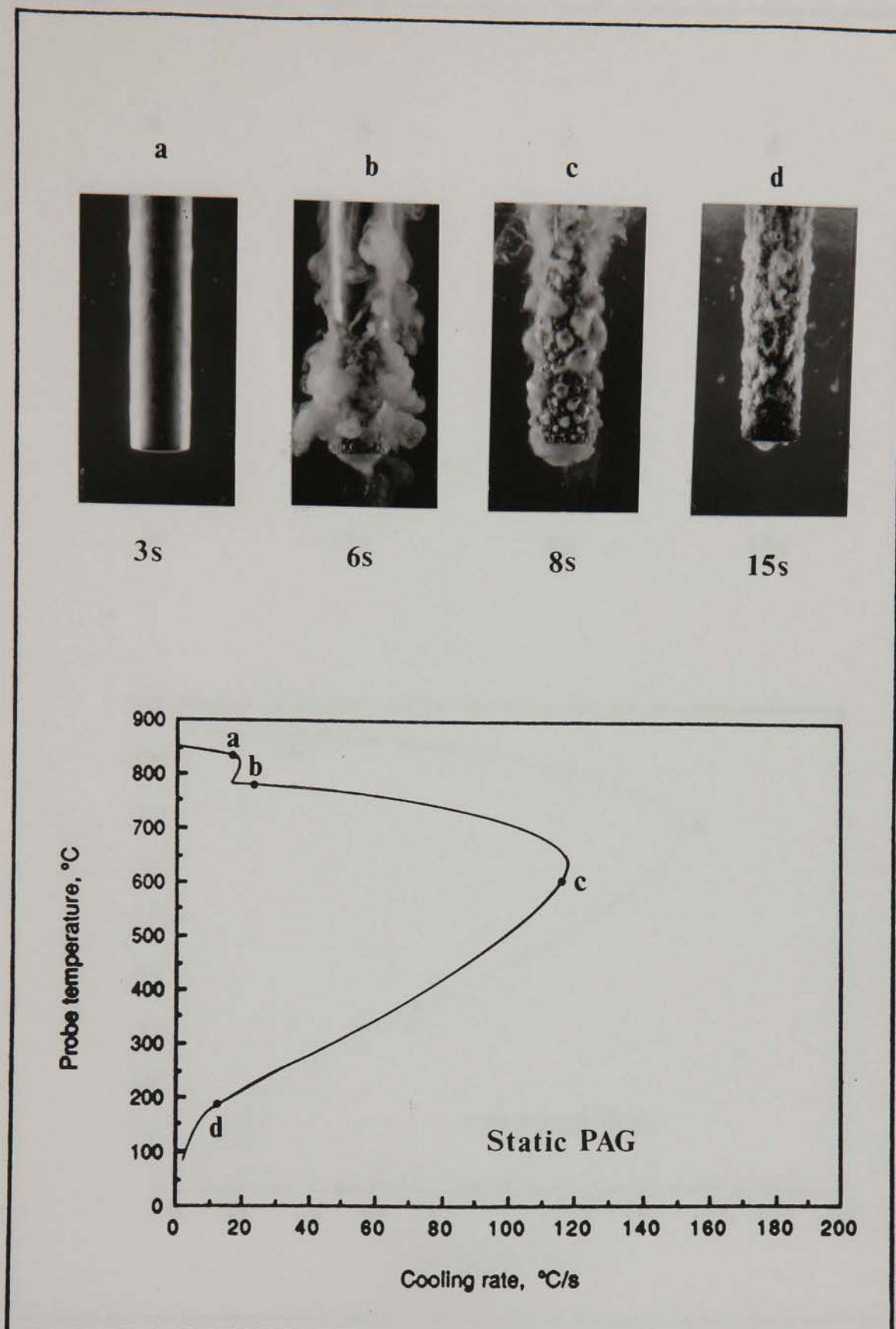


Figure 107. Stages during quenching for a non-agitated 15 volume per cent PAG (Quendila PA) solution at 30 °C. Photographs a to d correspond synchronously with those points marked on the recorded cooling rate-temperature curve. See text.

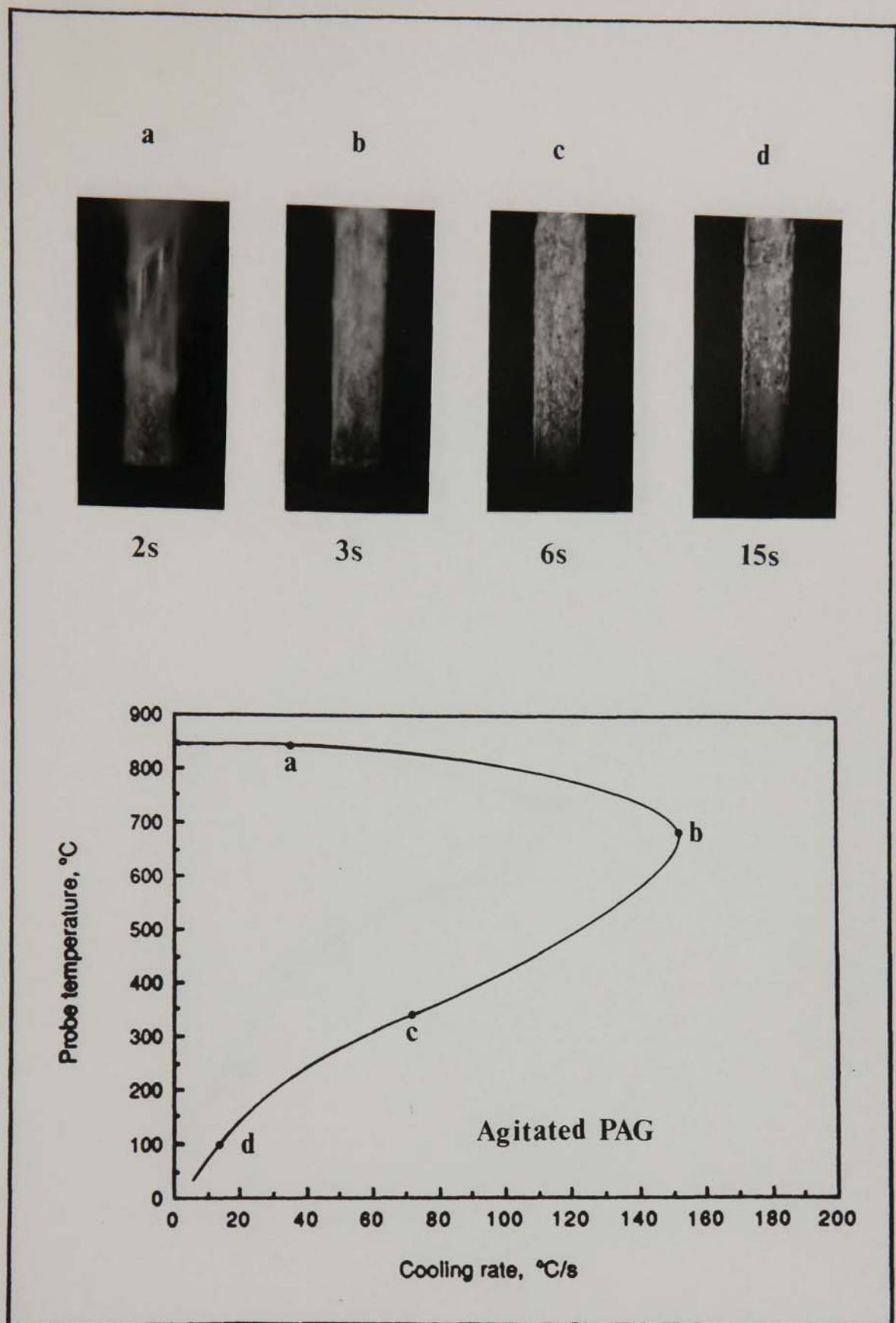


Figure 108. Stages during quenching for a 15 volume per cent PAG (Quendila PA) solution at 30 °C and 0.5m/s agitation. Photographs a to d correspond synchronously with those points marked on the recorded cooling rate-temperature curve See text.

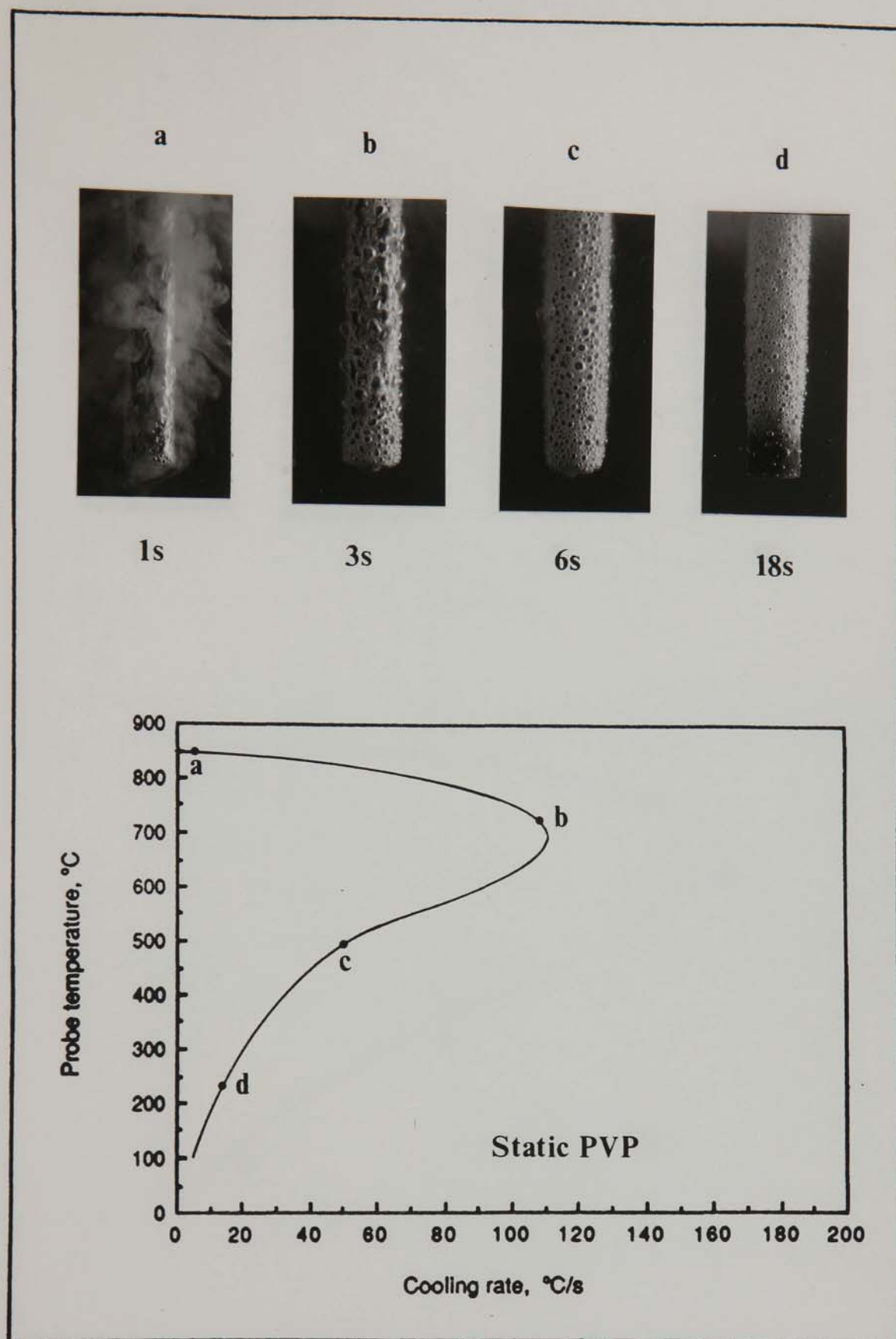


Figure 109. Stages during quenching for a non-agitated 15 volume per cent PVP (Parquench 90) solution at 30 °C. Photographs a to d correspond synchronously with those points marked on the cooling rate-temperature curve. See text.

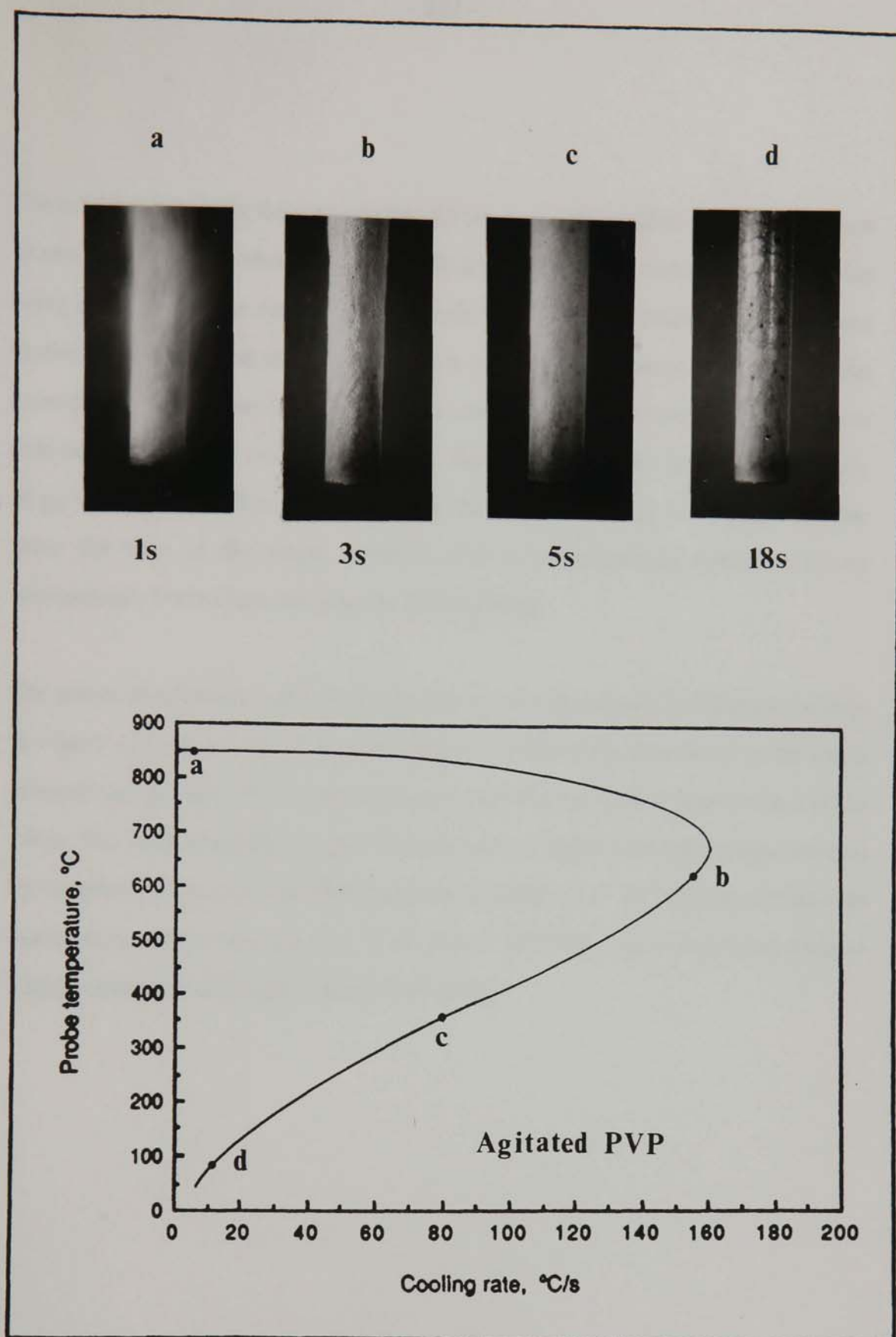


Figure 110. Stages during quenching for a 15 volume per cent PVP (Parquench 90) solution at 30 °C and agitated at 0.5m/s. Photographs a to d correspond synchronously with those points marked on the cooling rate-temperature curve. See text.

The cooling stages for the non-agitated 15 per cent polyacrylate solution at 30° are shown in *Figure 111* where: (a) film boiling is in operation, with the vapour blanket being stabilized by the surrounding polymer. (b) Transition boiling stage, with both partial-film-boiling and nucleate boiling occurring simultaneously. The polymer film surrounding the vapour blanket has been jettisoned. (c) Nucleate boiling has now commenced along the entire probe length. Some of the bubbles have grown to a size of up to 5mm before being detached. (d) The nucleate boiling has begun to decline from the base of the probe upwards, with a corresponding reduction in the characteristic bubble size and polymer film thickness.

The effect of agitation on the characteristics of this polyacrylate solution can be seen in *Figure 112* where: (a) nucleate boiling has started at the base of the probe and is proceeding upwards. (b) A continuous polymer film has formed near the base of the probe. The boiling regime changes from nucleate to partial-film-boiling upon moving up the probe, with a corresponding increase in bubble size. (c) The polymer film has started to redissolve near the base of the probe. (d) Only a trace of polymer remains visible around the midlength region of the probe.

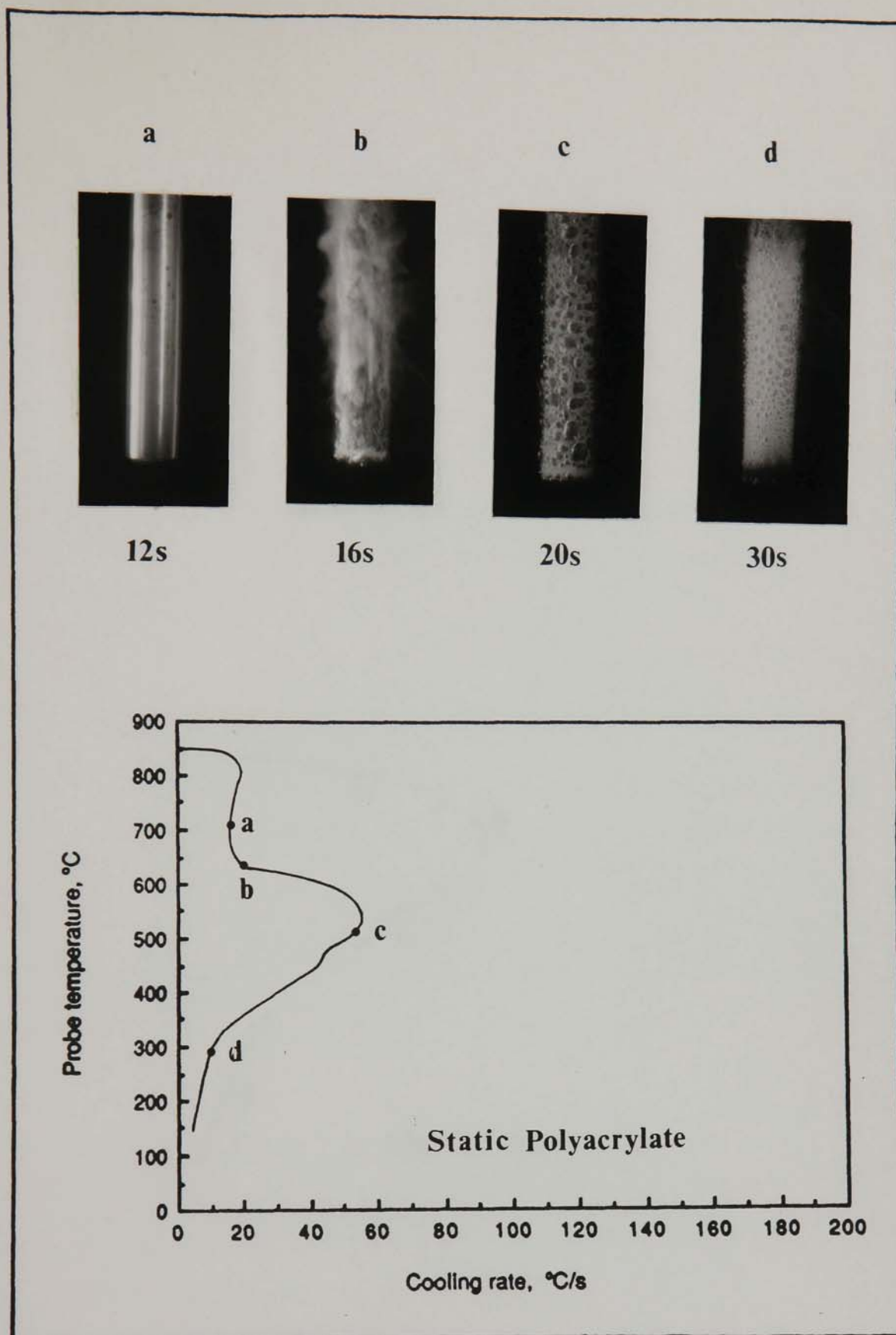


Figure 111. Stages during quenching for a non-agitated 15 volume per cent Polyacrylate (Aquaquench ACR) solution at 30 °C. Photographs a to d correspond synchronously with those points marked on the recorded cooling rate-temperature curve. See text.

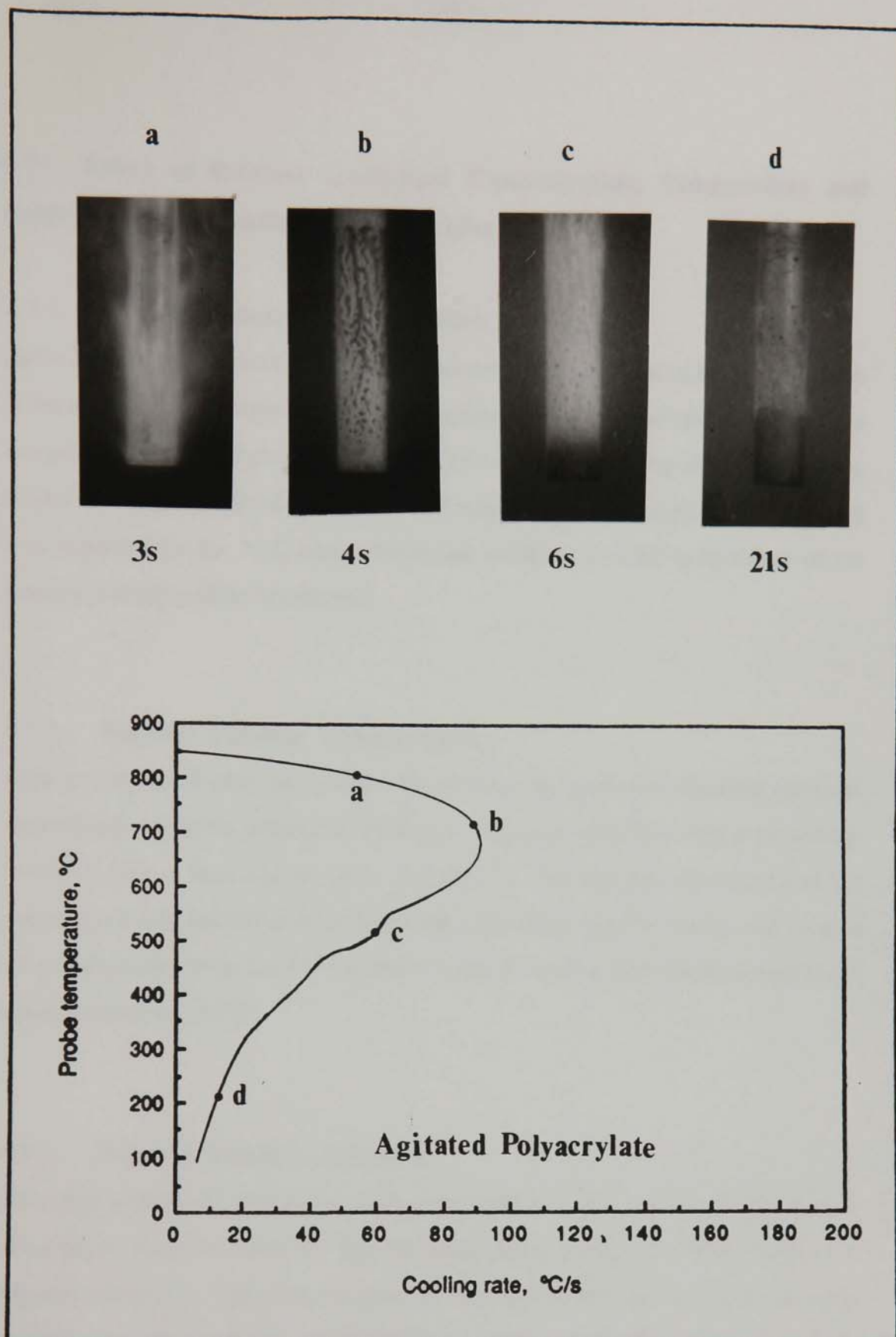


Figure 112. Stages during quenching for a 15 volume per cent Polyacrylate (Aquaquench ACR) solution at 30 °C and 0.5m/s agitation. Photographs a to d correspond synchronously with those points marked on the recorded cooling rate - temperature curve. See text.

4.7 Effect of Polymer Quenchant Concentration, Temperature and Agitation on the Cooling Characteristics.

4.7.1 Polymer Solution Concentration.

Table 21 shows the effect on the cooling characteristics of changing the concentration of each of the representative polymer quenchant types. Selective curves which show the general trends are given in *Figures 113 to 115*. Increasing the concentration tended to reduce the rate of cooling for each polymer quenchant type. Stage A cooling was extended for the PAG and polyacrylate solutions and the temperature of the maximum rate tended to be reduced.

4.7.2 Polymer Solution Temperature.

Figures 116 to 118 show the trends in the cooling characteristics observed when the representative polymer solution temperatures were increased. The cooling parameters for this series of tests can be found in *Table 22*. Raising the temperature of the polymer solution significantly increased the duration of stage A cooling and reduced the cooling rates. Even the PVP exhibited stage A cooling for solution temperatures equal to and above 50°C.

4.7.3 Polymer Solution Agitation.

The effect of fluid velocity on the cooling characteristics of the representative polymer solutions is shown in *Table 23*. Typical curves for each polymer type are given in *Figures 119 to 121*. The effect of agitation was as described in Section 4.4.2. Stage A cooling was progressively reduced for both the PAG and polyacrylate samples, and the cooling rates increased for each polymer type.

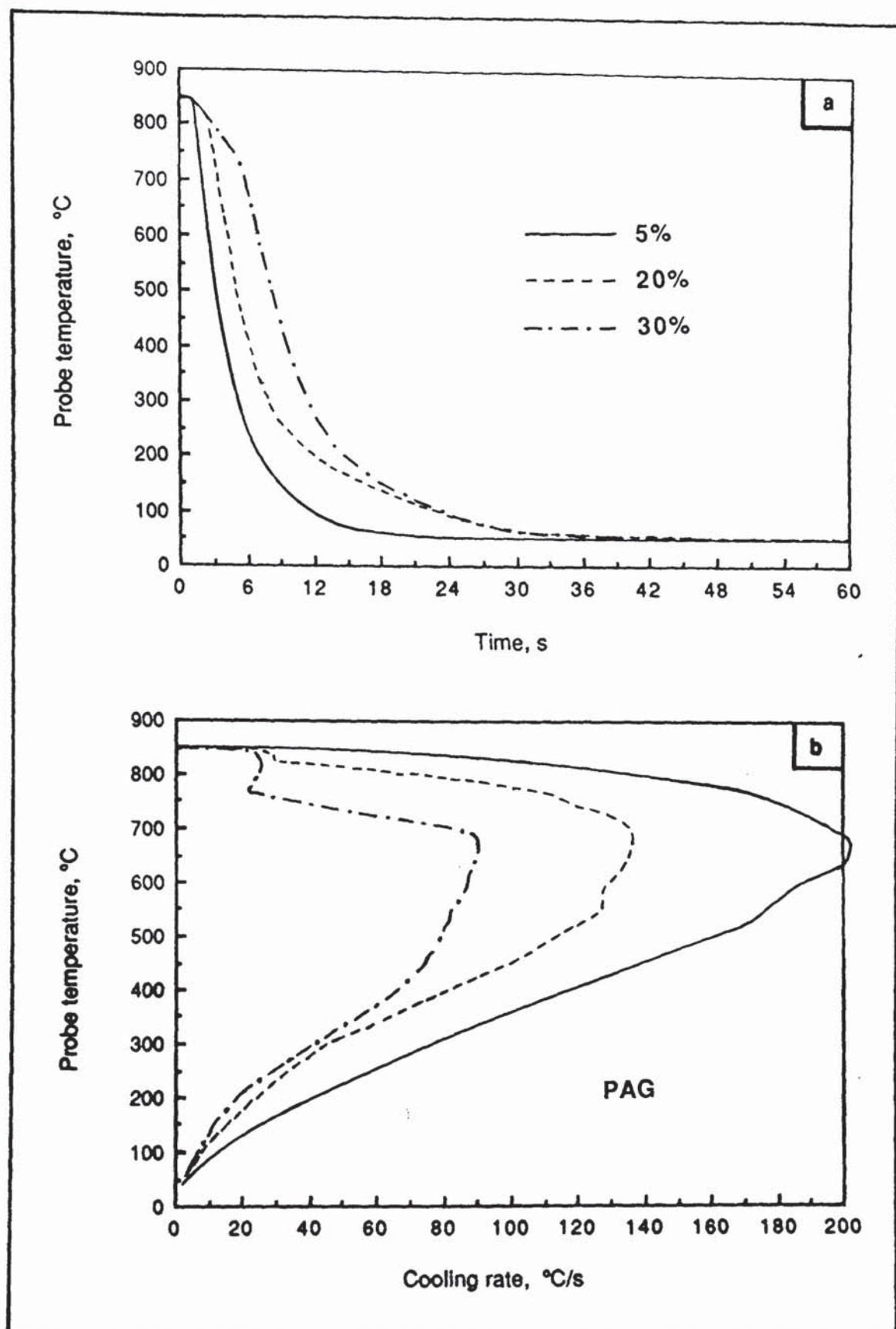


Figure 113. Typical cooling data for various concentration PAG (Quendila PA) solutions tested at 30 °C and 0.5 m/s agitation.

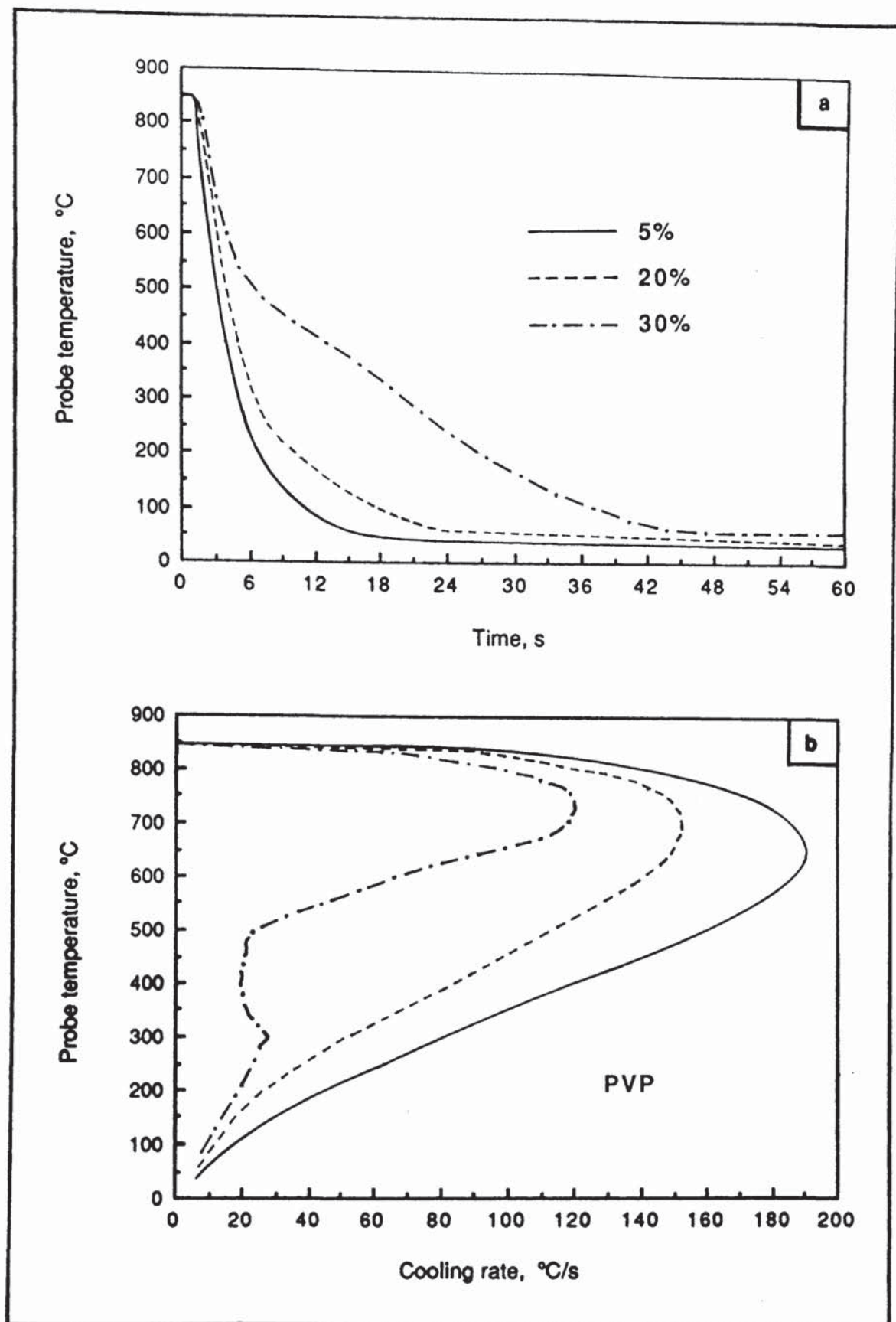


Figure 114. Typical cooling data for various concentration PVP (Parquench 90) solutions tested at 30 °C and 0.5 m/s agitation.

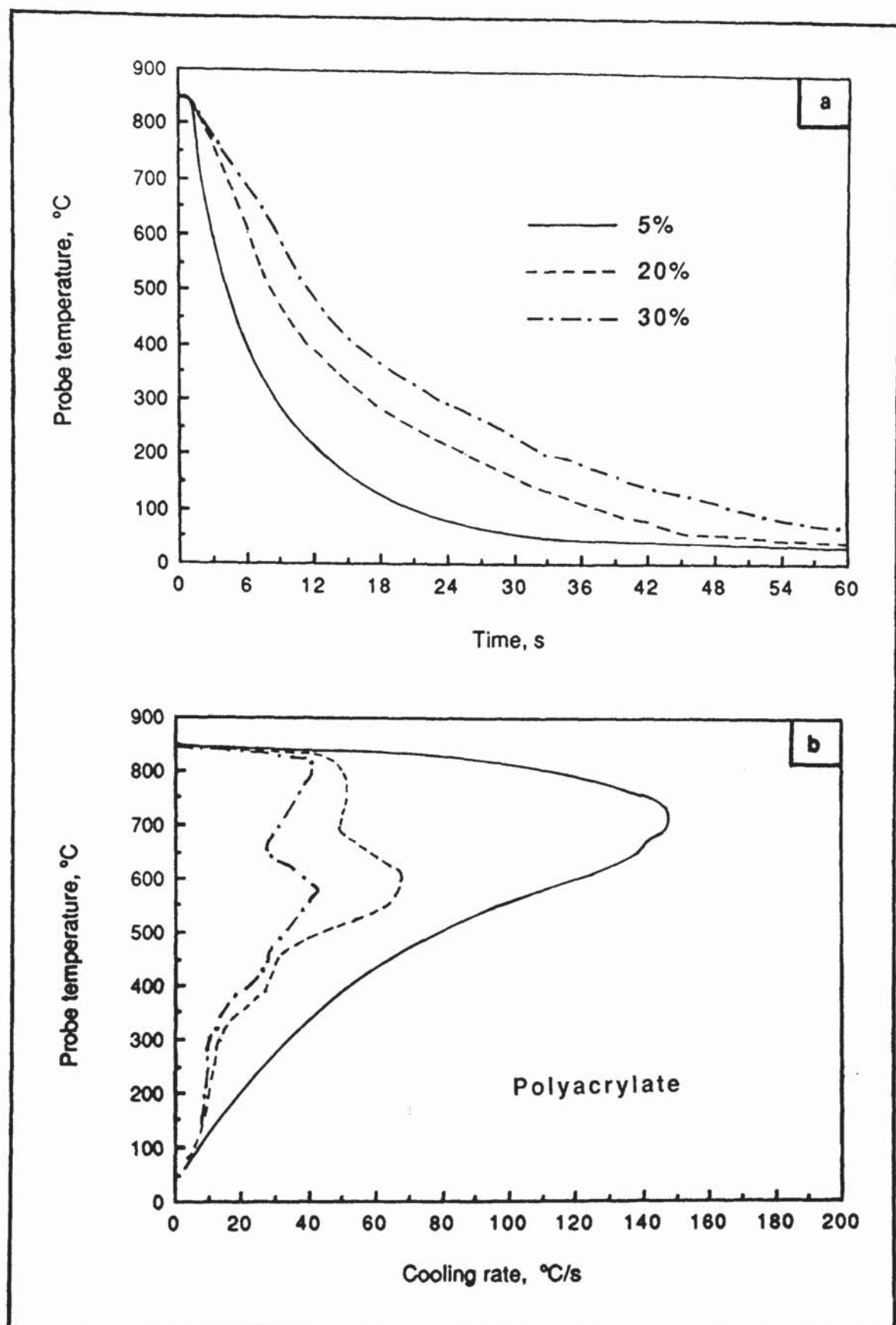


Figure 115. Typical cooling data for various concentration polyacrylate (Aquaquench ACR) solutions tested at 30 °C and 0.5 m/s agitation.

Table 22. Cooling characteristics for 15 volume per cent solutions of the representative polymer quenchants tested at various temperatures and 0.5m/s agitation.

| Polymer solution temp. (°C) | Time (s) to | | Maximum cooling rate (°C/s) | Temp. of max ^m rate (°C) | Cooling rate at 300°C (°C/s) | Stage A/B transition | |
|-----------------------------|-------------|----------|-----------------------------|-------------------------------------|------------------------------|----------------------|-------------|
| | 600°C | 400°C | 200°C | | | Temp. (°C) | Rate (°C/s) |
| PAG | | | | | | | |
| 10 | 2.7±0.1 | 4.4±0.1 | 8.8±0.1 | 703 ± 7 | 52 ± 1 | - | - |
| 20 | 2.8±0.1 | 4.5±0.1 | 9.2±0.2 | 662 ± 28 | 50 ± 1 | - | - |
| 30 | 3.4±0.2 | 5.0±0.1 | 9.4±0.2 | 676 ± 16 | 50 ± 1 | 831 ± 5 | 32 ± 1 |
| 40 | 4.5±0.1 | 6.2±0.1 | 11.7±0.2 | 648 ± 26 | 46 ± 1 | 820 ± 1 | 28 ± 1 |
| 50 | 5.6±0.1 | 7.6±0.1 | 13.4±0.2 | 645 ± 18 | 43 ± 1 | 800 ± 5 | 23 ± 1 |
| 60 | 9.1±0.1 | 11.4±0.1 | 17.4±0.3 | 535 ± 18 | 41 ± 1 | 730 ± 6 | 20 ± 1 |
| 70 | 17.1±1.1 | 21.4±1.7 | 28.2±1.7 | 435 ± 21 | 38 ± 1 | 631 ± 2 | 15 ± 1 |
| PVP | | | | | | | |
| 10 | 2.5±0.1 | 4.1±0.1 | 7.6±0.1 | 690 ± 13 | 62 ± 1 | - | - |
| 20 | 2.7±0.1 | 4.3±0.1 | 7.8±0.1 | 673 ± 9 | 61 ± 1 | - | - |
| 30 | 2.8±0.1 | 4.4±0.1 | 8.1±0.2 | 676 ± 23 | 60 ± 1 | - | - |
| 40 | 2.9±0.1 | 4.7±0.1 | 8.4±0.1 | 715 ± 22 | 60 ± 1 | - | - |
| 45 | 3.3±0.1 | 6.5±0.2 | 10.7±0.1 | 735 ± 20 | 51 ± 1 | - | - |
| 50 | 4.1±0.1 | 8.2±0.6 | 18.9±1.1 | 720 ± 20 | 21 ± 1 | 837 ± 7 | 21 ± 1 |
| 60 | 6.1±0.5 | 11.2±0.8 | 24.2±1.7 | 681 ± 2 | 18 ± 1 | 810 ± 3 | 21 ± 1 |
| 70 | 10.1±0.6 | 14.6±0.1 | 28.0±1.3 | 615 ± 3 | 16 ± 1 | 770 ± 5 | 20 ± 1 |
| Polyacrylate | | | | | | | |
| 10 | 4.0±0.1 | 7.8±0.1 | 13.5±1.7 | 720 ± 13 | 45 ± 11 | - | - |
| 20 | 4.3±0.3 | 8.4±0.1 | 19.2±0.2 | 674 ± 21 | 19 ± 2 | 811 ± 10 | 76 ± 1 |
| 30 | 5.0±0.2 | 9.0±0.2 | 21.2±0.3 | 670 ± 2 | 17 ± 1 | 796 ± 9 | 61 ± 1 |
| 40 | 6.1±0.4 | 10.2±0.2 | 24.7±0.2 | 612 ± 25 | 12 ± 1 | 681 ± 7 | 56 ± 1 |
| 50 | 7.9±0.2 | 12.2±0.4 | 30.0±0.7 | 608 ± 30 | 10 ± 1 | 688 ± 8 | 40 ± 3 |
| 60 | 11.6±0.1 | 16.4±0.4 | 36.7±0.6 | 582 ± 18 | 8 ± 1 | 677 ± 9 | 29 ± 1 |
| 70 | 14.7±0.5 | 19.3±0.6 | 40.7±0.7 | 547 ± 17 | 8 ± 2 | 655 ± 9 | 18 ± 1 |

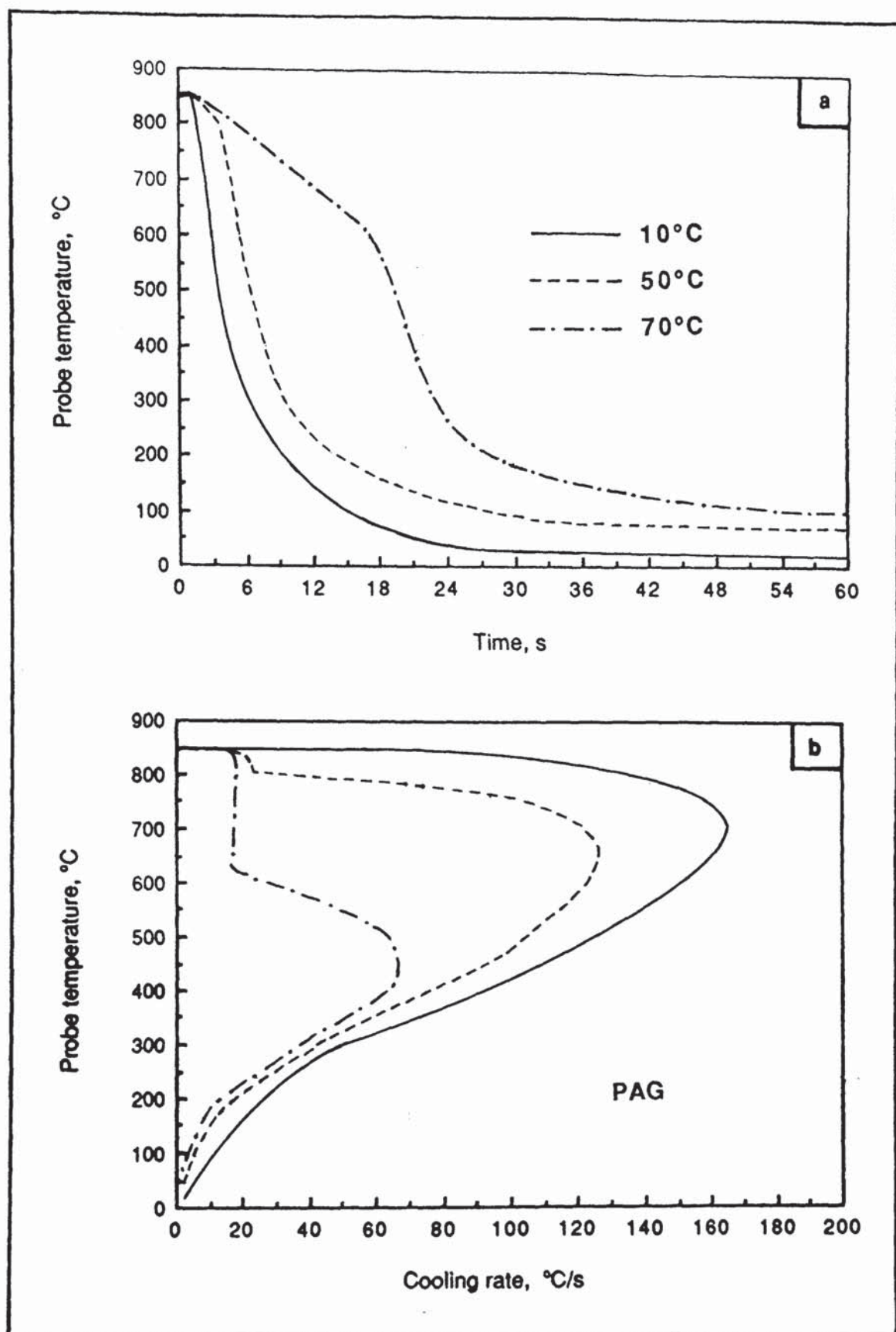


Figure 116. Typical cooling data for a 15 volume per cent PAG (Quendila PA) solution tested at various temperatures and 0.5m/s agitation.

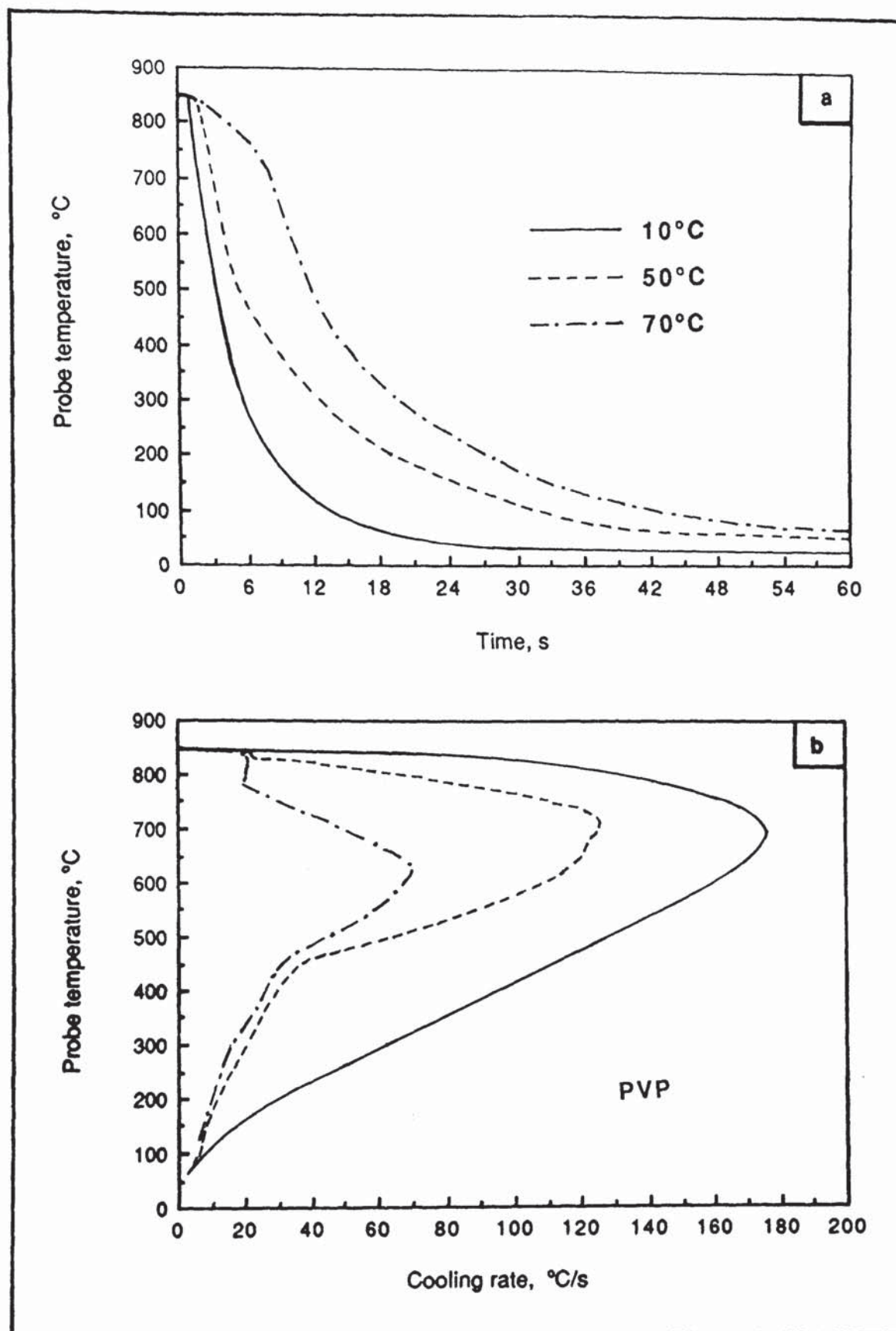


Figure 117. Typical cooling data for a 15 volume per cent PVP (Parquench 90) solution tested at various temperatures and 0.5m/s agitation.

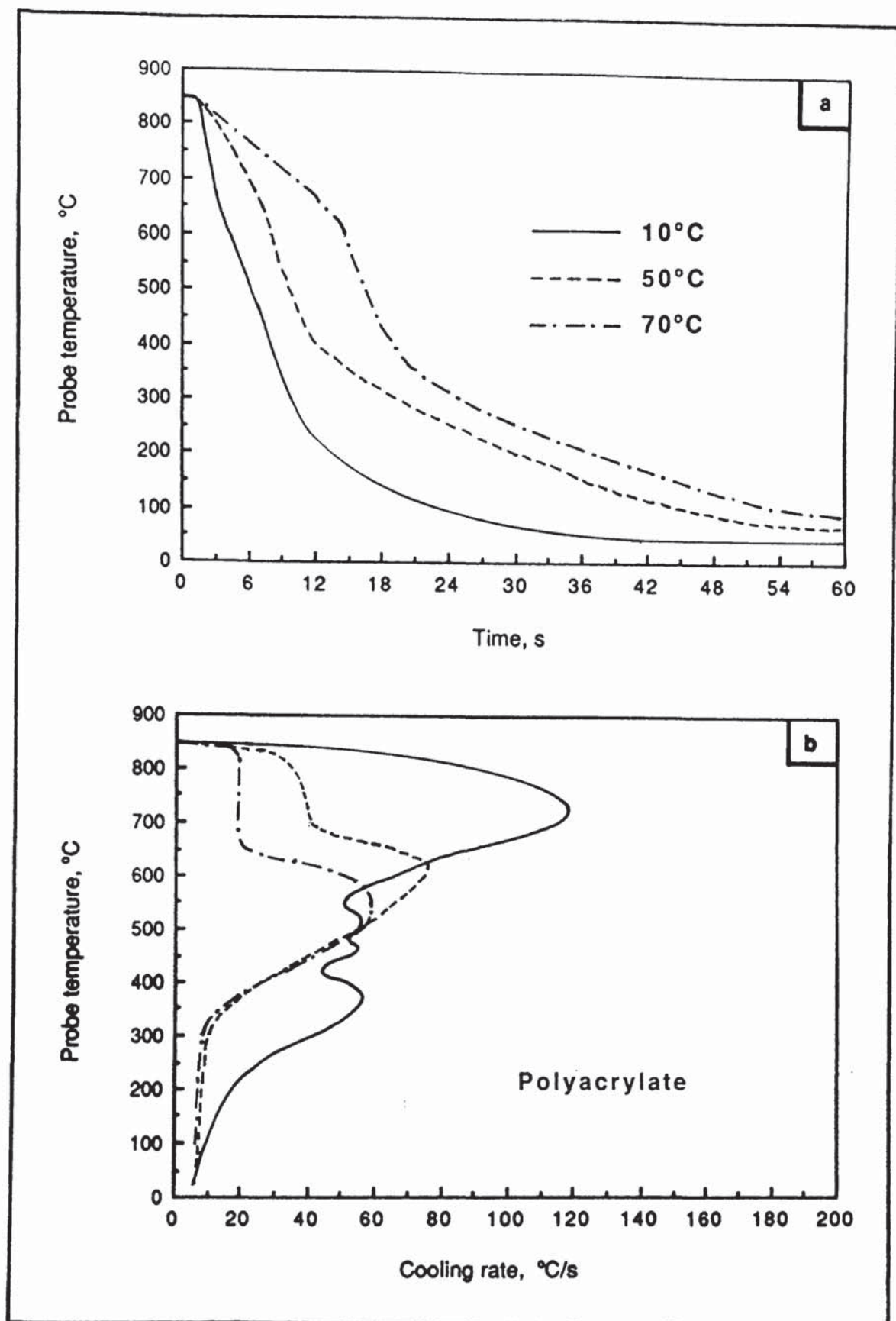


Figure 118. Typical cooling data for a 15 volume per cent polyacrylate (Aquaquench ACR) solution tested at various temperatures and 0.5ml/s agitation.

Table 23. Cooling characteristics for 15 volume per cent solutions of the representative polymer quenchants tested at 30°C and agitated at various fluid velocities.

| Fluid velocity (m/s) | Time (s) to | | Maximum cooling rate (°C/s) | Temp. of max ^m rate (°C) | Cooling rate at 300°C (°C/s) | Stage A/B transition | | |
|----------------------|-------------|----------|-----------------------------|-------------------------------------|------------------------------|----------------------|------------|-------------|
| | 600°C | 400°C | | | | 200°C | Temp. (°C) | Rate (°C/s) |
| PAG | | | | | | | | |
| static | 7.6±0.4 | 9.5±0.3 | 14.0±0.7 | 119 ± 3 | 634 ± 27 | 48 ± 3 | 776 ± 8 | 18 ± 2 |
| 0.1 | 5.7±1.5 | 7.4±1.5 | 12.3±1.5 | 135 ± 6 | 655 ± 35 | 49 ± 1 | 810 ± 3 | 22 ± 2 |
| 0.2 | 4.5±0.1 | 6.2±0.1 | 11.1±0.1 | 144 ± 1 | 668 ± 17 | 49 ± 1 | 831 ± 1 | 25 ± 1 |
| 0.3 | 4.0±0.1 | 5.7±0.1 | 10.7±0.1 | 149 ± 3 | 662 ± 28 | 49 ± 1 | 832 ± 10 | 28 ± 6 |
| 0.4 | 3.4±0.1 | 5.1±0.3 | 10.0±0.1 | 152 ± 1 | 665 ± 24 | 50 ± 1 | - | - |
| 0.5 | 3.4±0.2 | 5.0±0.2 | 9.4±0.2 | 154 ± 1 | 676 ± 16 | 50 ± 1 | 835 ± 1 | 32 ± 1 |
| 0.6 | 3.3±0.1 | 5.0±0.1 | 9.3±0.1 | 156 ± 2 | 666 ± 36 | 50 ± 1 | 835 ± 1 | 33 ± 4 |
| PVP | | | | | | | | |
| static | 3.9±0.4 | 8.2±0.3 | 19.7±1.9 | 112 ± 3 | 690 ± 3 | 21 ± 4 | - | - |
| 0.1 | 4.8±0.3 | 8.6±2.7 | 14.1±5.5 | 131 ± 7 | 664 ± 71 | 47 ± 18 | - | - |
| 0.2 | 3.1±0.1 | 4.8±0.1 | 8.5±0.1 | 142 ± 1 | 683 ± 25 | 60 ± 1 | - | - |
| 0.3 | 3.0±0.1 | 4.6±0.1 | 8.3±0.1 | 151 ± 4 | 642 ± 6 | 60 ± 1 | - | - |
| 0.4 | 2.9±0.1 | 4.5±0.1 | 8.2±0.1 | 157 ± 1 | 665 ± 1 | 60 ± 1 | - | - |
| 0.5 | 2.8±0.1 | 4.4±0.1 | 8.1±0.2 | 162 ± 3 | 676 ± 23 | 60 ± 1 | - | - |
| 0.6 | 2.7±0.1 | 4.4±0.1 | 8.0±0.1 | 166 ± 2 | 666 ± 1 | 62 ± 1 | - | - |
| 0.7 | 2.6±0.1 | 4.3±0.1 | 8.0±0.1 | 168 ± 1 | 711 ± 64 | 63 ± 1 | - | - |
| Polyacrylate | | | | | | | | |
| static | 17.2±1.1 | 22.2±2.0 | 48.2±3.2 | 56 ± 2 | 528 ± 56 | 8 ± 1 | 640 ± 25 | 14 ± 1 |
| 0.2 | 8.2±0.7 | 12.8±0.6 | 29.1±0.1 | 59 ± 4 | 634 ± 10 | 9 ± 1 | 744 ± 13 | 33 ± 1 |
| 0.3 | 8.7±0.7 | 12.9±0.4 | 29.0±0.3 | 64 ± 1 | 598 ± 1 | 11 ± 1 | 726 ± 11 | 40 ± 1 |
| 0.4 | 6.2±0.5 | 10.3±0.4 | 24.7±0.7 | 76 ± 4 | 632 ± 56 | 13 ± 2 | 797 ± 6 | 50 ± 5 |
| 0.5 | 5.0±0.2 | 9.0±0.2 | 21.2±0.3 | 90 ± 3 | 670 ± 2 | 17 ± 1 | 782 ± 10 | 60 ± 2 |
| 0.6 | 4.0±0.1 | 7.7±0.1 | 19.5±0.6 | 115 ± 3 | 687 ± 20 | 18 ± 1 | - | - |

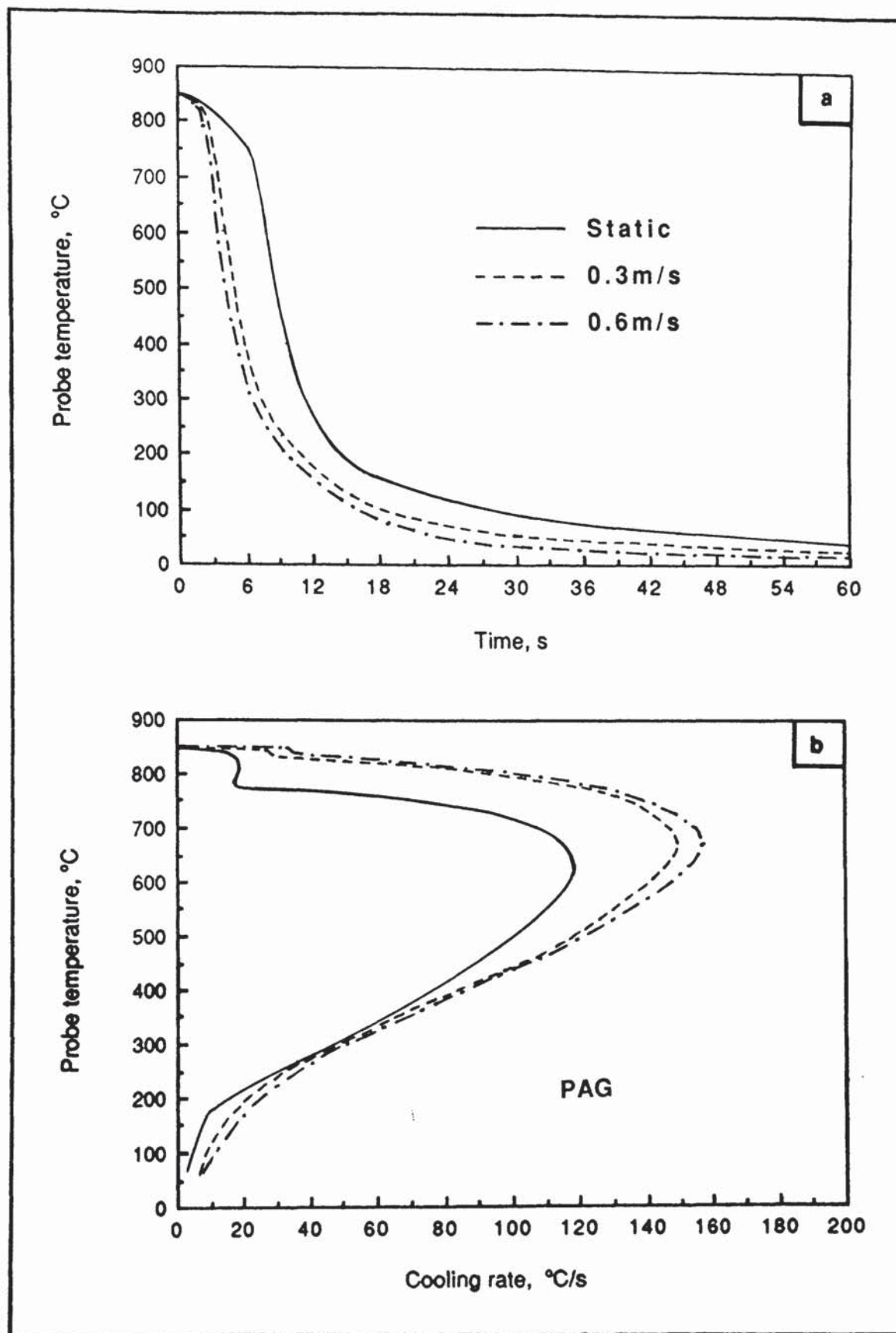


Figure 119. Typical cooling data for a 15 volume per cent PAG (Quendila PA) solution at 30 °C and agitated at various fluid velocities.

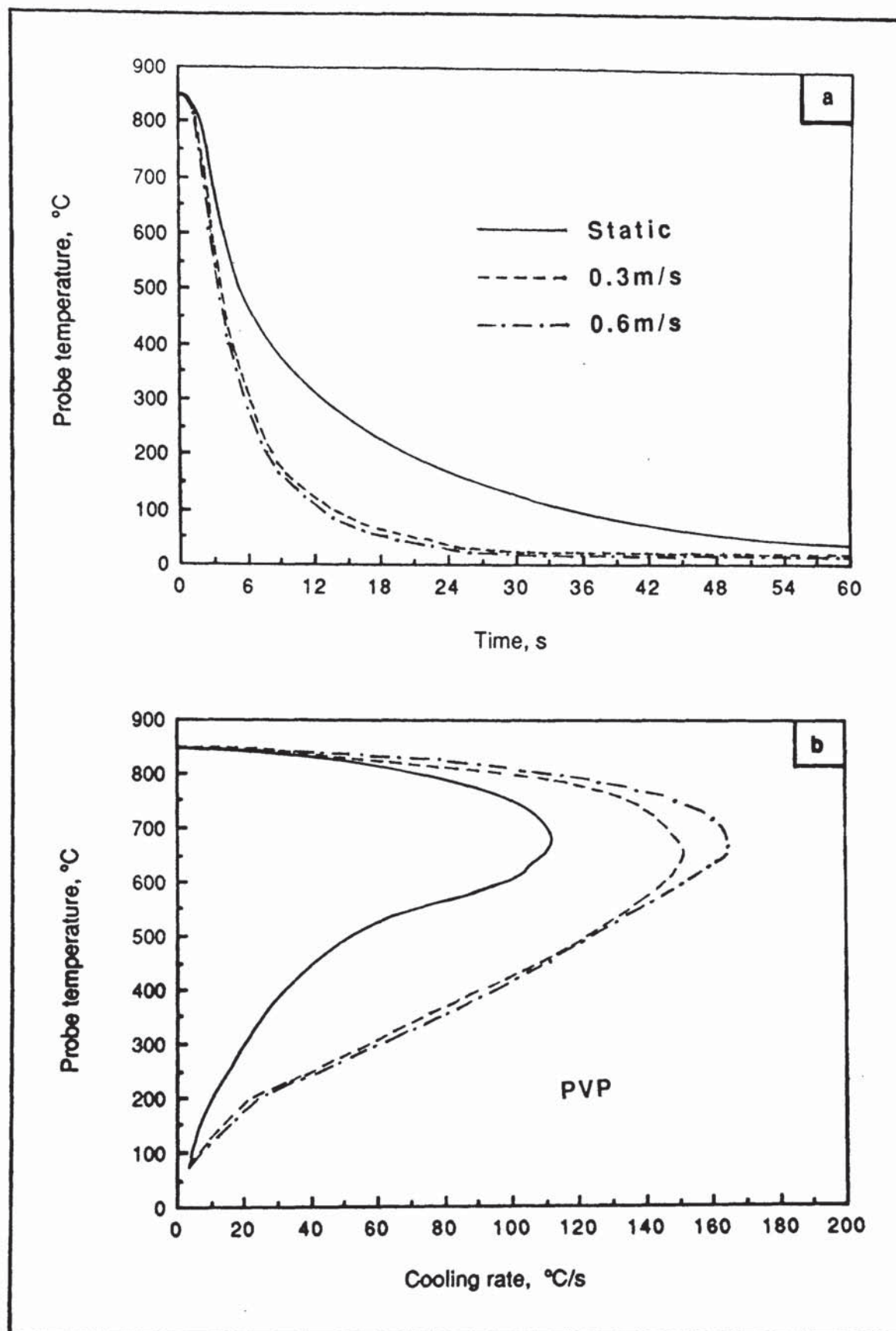


Figure 120. Typical cooling data for a 15 volume per cent PVP (Parquench 90) solution at 30 °C and agitated at various fluid velocities.

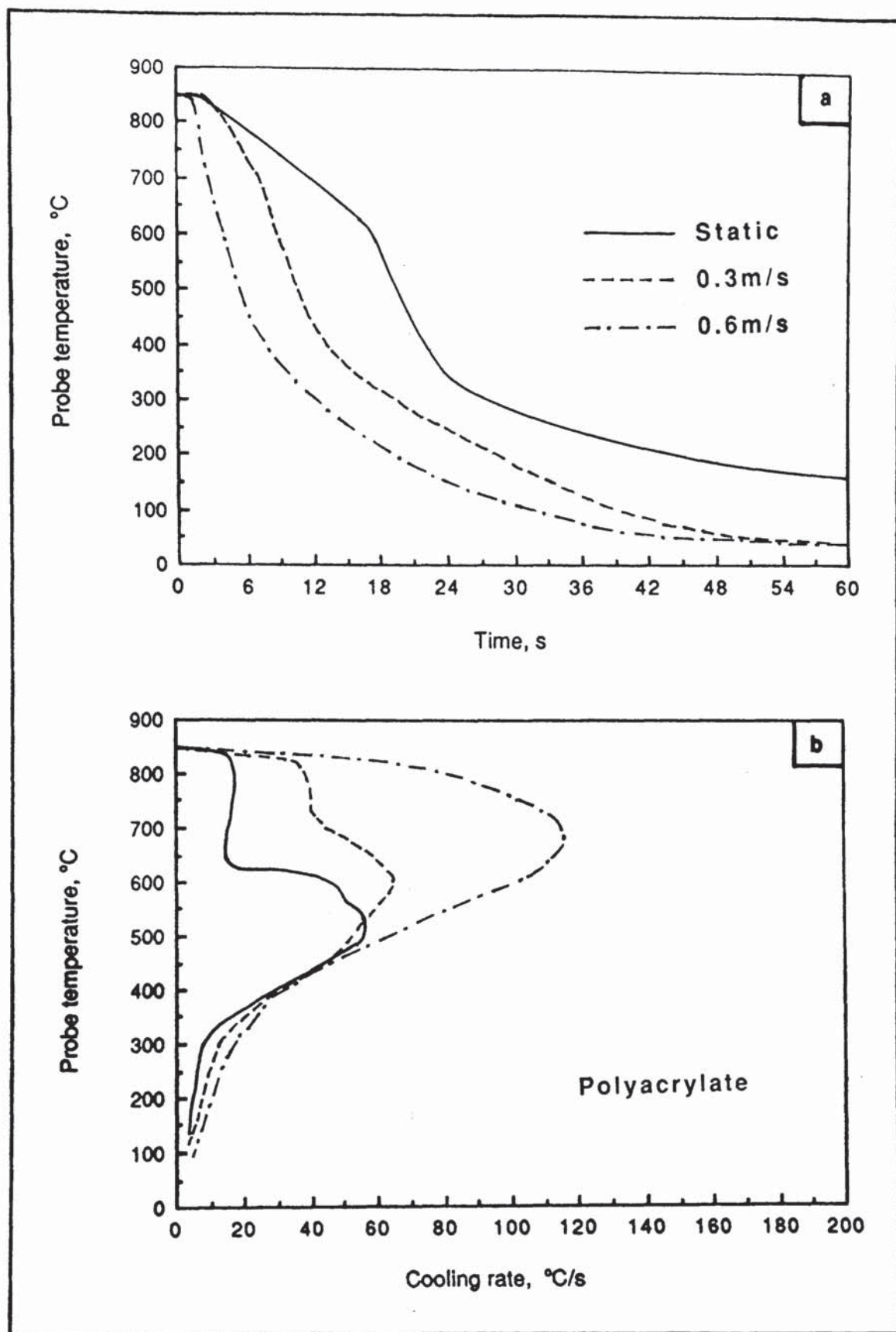


Figure 121. Typical cooling data for a 15 volume per cent polyacrylate (Aquaquench ACR) solution at 30 °C and agitated at various fluid velocities.

Table 24. Cooling characteristics for the nominal 15 volume per cent PAG (Quendila PA) solution at 30°C and 0.5m/s agitation following various throughput in the simulated ageing test.

| Cumulative quench load (kg/litre) | Time (s) to | | | Maximum cooling rate (°C/s) | Temp. of max ^m rate (°C) | Cooling rate at 300°C (°C/s) | Stage A/B | | Kinematic viscosity at 40°C (mm ² /s) |
|---|-------------|---------|---------|--------------------------------------|--|---------------------------------------|---------------|------------------------------|---|
| | 600°C | 400°C | 200°C | | | | Temp. (°C) | transition Rate (°C/s) | |
| 0 | 3.4±0.1 | 5.0±0.2 | 9.4±0.1 | 154 ± 1 | 676 ± 16 | 50 ± 1 | 831 ± 5 | 32 ± 1 | 3.69 |
| 10 | 3.7±0.2 | 5.5±0.2 | 9.1±0.6 | 153 ± 3 | 672 ± 5 | 58 ± 1 | 837 ± 3 | 32 ± 1 | 3.61 |
| 20 | 3.0±0.1 | 4.5±0.1 | 8.3±0.1 | 162 ± 1 | 655 ± 24 | 63 ± 1 | - | - | 3.56 |
| 30 | 2.8±0.1 | 4.4±0.1 | 8.1±0.1 | 167 ± 1 | 675 ± 1 | 62 ± 1 | - | - | 3.53 |
| 40 | 3.0±0.1 | 4.6±0.1 | 8.3±0.1 | 161 ± 2 | 699 ± 5 | 63 ± 1 | - | - | 3.46 |
| 50 | 2.8±0.1 | 4.5±0.1 | 8.3±0.2 | 162 ± 1 | 698 ± 3 | 62 ± 1 | - | - | 3.49 |
| 60 | 3.0±0.1 | 4.6±0.1 | 8.6±0.1 | 161 ± 2 | 686 ± 16 | 61 ± 1 | - | - | 3.42 |
| 70 | 3.0±0.5 | 4.6±0.3 | 8.1±0.3 | 166 ± 2 | 658 ± 54 | 64 ± 1 | - | - | 3.33 |
| 80 | 2.7±0.1 | 4.3±0.1 | 7.9±0.1 | 170 ± 2 | 675 ± 4 | 65 ± 1 | - | - | 3.18 |
| 90 | 2.7±0.1 | 4.2±0.1 | 7.8±0.1 | 168 ± 1 | 677 ± 11 | 66 ± 1 | - | - | 3.20 |
| 100 | 2.9±0.1 | 4.4±0.2 | 7.8±0.1 | 170 ± 2 | 669 ± 27 | 67 ± 1 | - | - | 3.17 |

Table 25. Cooling characteristics for the nominal 15 volume per cent PVP (Parquench 90) solution at 30°C and 0.5m/s agitation following various throughput in the simulated ageing test.

| Cumulative quench load (kg/litre) | Time (s) to | | | Maximum cooling rate (°C/s) | Temp. of max ^m rate (°C) | Cooling rate at 300°C (°C/s) | Stage A/B | | Kinematic viscosity at 40°C (mm ² /s) |
|---|-------------|---------|---------|--------------------------------------|--|---------------------------------------|---------------|----------------|---|
| | 600°C | 400°C | 200°C | | | | Temp. (°C) | Rate (°C/s) | |
| 0 | 2.8±0.1 | 4.4±0.1 | 8.1±0.2 | 162 ± 3 | 676 ± 23 | 60 ± 1 | - | - | 2.67 |
| 2.5 | 3.0±0.1 | 4.6±0.1 | 8.1±0.1 | 160 ± 3 | 649 ± 5 | 64 ± 1 | - | - | - |
| 5 | 2.8±0.1 | 4.3±0.1 | 7.3±0.1 | 168 ± 2 | 671 ± 36 | 69 ± 1 | - | - | - |
| 10 | 2.5±0.1 | 3.9±0.1 | 7.0±0.1 | 178 ± 2 | 655 ± 30 | 76 ± 2 | - | - | 1.97 |
| 20 | 3.0±0.1 | 5.2±0.2 | 8.2±0.2 | 144 ± 1 | 748 ± 17 | 75 ± 2 | - | - | 1.56 |
| 30 | 3.2±0.1 | 5.4±0.3 | 8.9±0.7 | 133 ± 2 | 767 ± 12 | 71 ± 4 | - | - | 1.66 |
| 40 | 3.2±0.1 | 5.4±0.1 | 8.5±0.1 | 133 ± 2 | 761 ± 6 | 72 ± 1 | - | - | 1.68 |
| 50 | 3.4±0.1 | 5.3±0.1 | 8.6±0.3 | 137 ± 1 | 768 ± 18 | 69 ± 6 | - | - | 1.76 |
| 60 | 3.3±0.1 | 5.2±0.2 | 8.3±0.1 | 123 ± 1 | 763 ± 6 | 74 ± 1 | - | - | 1.80 |
| 70 | 3.1±0.1 | 4.7±0.1 | 7.6±0.1 | 139 ± 2 | 528 ± 3 | 77 ± 1 | - | - | 1.46 |
| 80 | 3.0±0.1 | 4.5±0.2 | 7.3±0.1 | 146 ± 9 | 567 ± 50 | 82 ± 1 | - | - | 1.33 |
| 90 | 2.7±0.1 | 4.1±0.1 | 6.9±0.3 | 169 ± 1 | 641 ± 19 | 84 ± 1 | - | - | 1.46 |
| 100 | 2.6±0.1 | 4.0±0.1 | 6.7±0.1 | 173 ± 6 | 625 ± 2 | 85 ± 1 | - | - | 1.40 |

Table 26. Cooling characteristics for the nominal 15 volume per cent polyacrylate (Aquaquench ACR) solution at 30°C and 0.5m/s agitation following various throughput in the simulated ageing test.

| Cumulative quench load (kg/litre) | Time (s) to | | | Maximum cooling rate (°C/s) | Temp.of max ^m rate (°C) | Cooling rate at 300°C (°C/s) | Stage A/B transition | | Kinematic viscosity at 40°C (mm ² /s) |
|---|-------------|---------|----------|--------------------------------------|---|---------------------------------------|-------------------------|----------------|---|
| | 600°C | 400°C | 200°C | | | | Temp. (°C) | Rate (°C/s) | |
| 0 | 5.0±0.2 | 9.0±0.2 | 21.2±0.3 | 90 ± 3 | 670 ± 2 | 17 ± 1 | 782 ± 10 | 60 ± 2 | 12.49 |
| 2.5 | 5.0±0.5 | 8.5±0.8 | 19.4±0.3 | 107 ± 3 | 638 ± 21 | 19 ± 1 | - | - | - |
| 5 | 5.3±0.2 | 8.9±0.5 | 20.2±3.2 | 108 ± 2 | 624 ± 3 | 19 ± 3 | - | - | - |
| 10 | 3.7±0.1 | 7.9±0.3 | 19.5±0.6 | 128 ± 3 | 707 ± 11 | 20 ± 1 | - | - | 7.64 |
| 20 | 3.5±0.2 | 7.3±0.4 | 15.6±0.8 | 126 ± 8 | 685 ± 17 | 26 ± 1 | - | - | 5.74 |
| 30 | 3.7±0.1 | 7.5±0.4 | 18.1±0.9 | 130 ± 8 | 707 ± 13 | 23 ± 4 | - | - | 5.57 |
| 40 | 4.3±0.2 | 7.6±0.3 | 14.1±0.5 | 127 ± 3 | 685 ± 39 | 32 ± 2 | - | - | 5.19 |
| 50 | 3.4±0.1 | 7.1±0.2 | 16.2±2.2 | 136 ± 3 | 724 ± 15 | 29 ± 1 | - | - | 4.98 |
| 60 | 3.9±0.1 | 7.4±0.1 | 13.9±0.1 | 132 ± 4 | 684 ± 10 | 35 ± 2 | - | - | 5.07 |
| 70 | 3.7±0.1 | 6.8±0.2 | 12.1±0.4 | 137 ± 3 | 702 ± 9 | 42 ± 2 | - | - | 4.56 |
| 80 | 3.4±0.3 | 6.2±0.5 | 11.4±0.3 | 143 ± 6 | 706 ± 8 | 43 ± 2 | - | - | 4.33 |
| 90 | 3.1±0.1 | 6.3±0.2 | 11.7±0.2 | 144 ± 5 | 720 ± 12 | 43 ± 2 | - | - | 4.33 |
| 100 | 3.3±0.2 | 6.2±0.2 | 11.4±0.5 | 145 ± 1 | 700 ± 13 | 44 ± 3 | - | - | 4.16 |

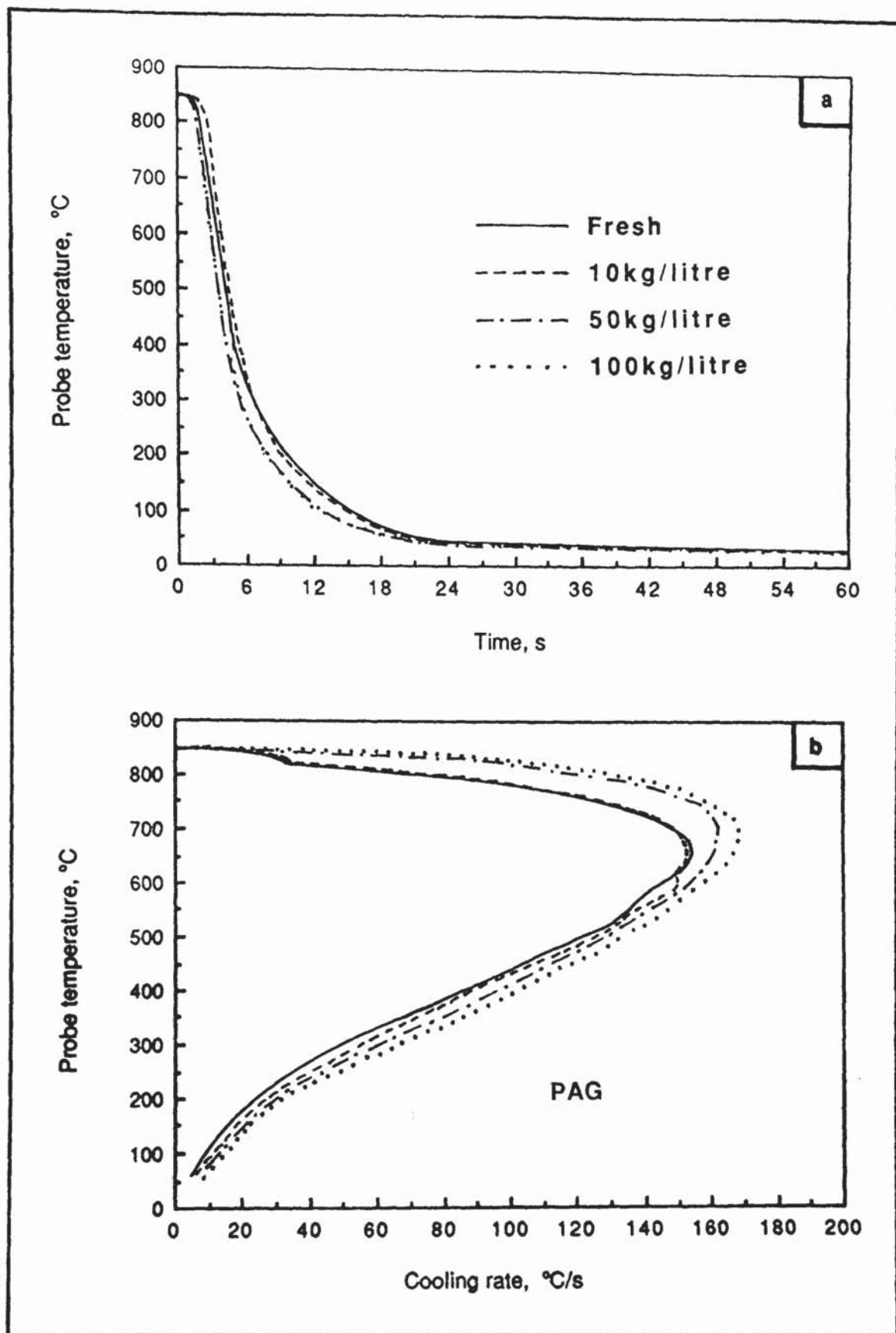


Figure 122. Typical cooling data for a 15 volume per cent PAG (Quendila PA) solution at 30°C and agitated at 0.5m/s following various cumulative quench loads in the simulated ageing test.

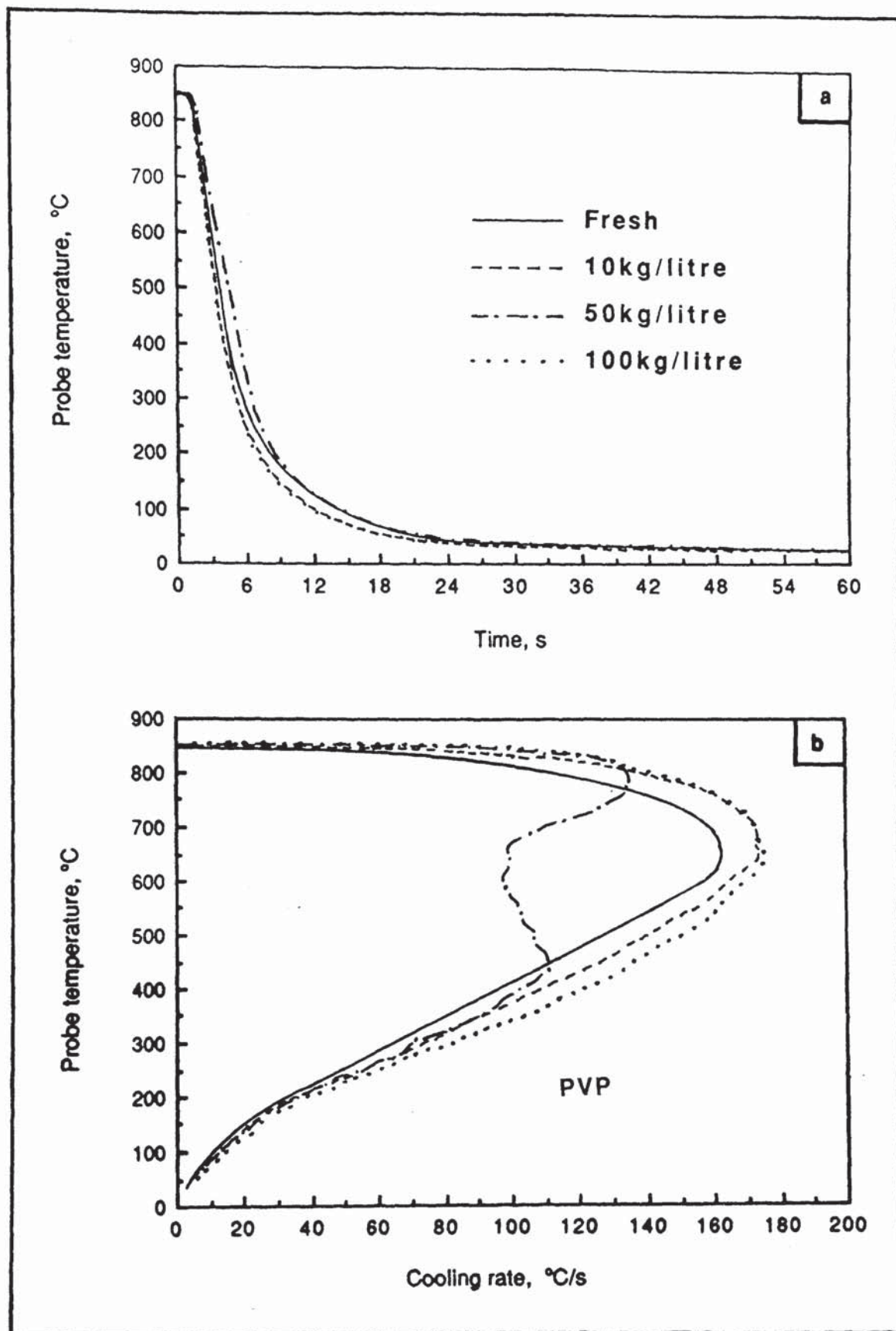


Figure 123. Typical cooling data for a 15 volume per cent PVP (Parquench 90) solution at 30 °C and agitated at 0.5m/s following various cumulative quench loads in the simulated ageing test.

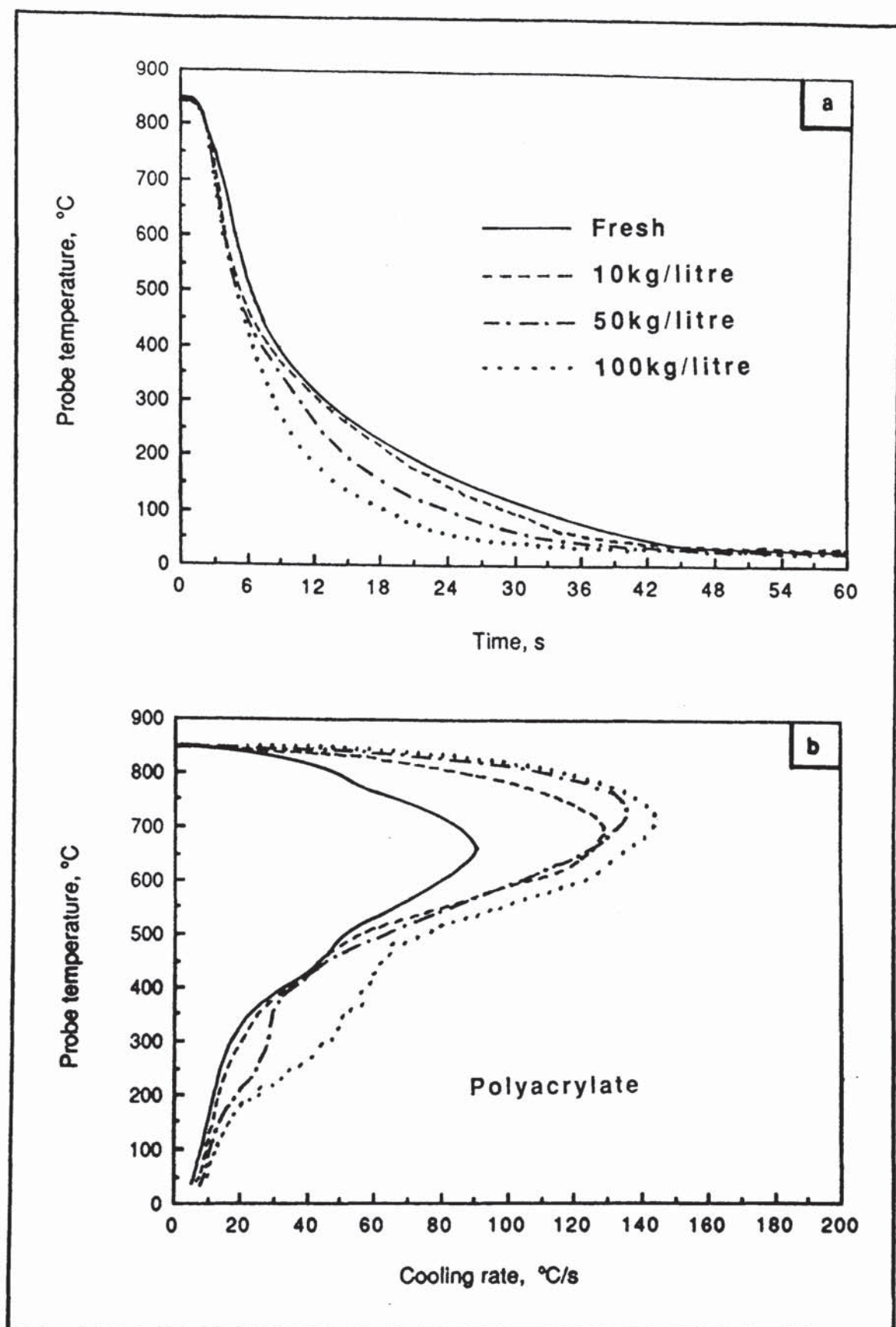


Figure 124. Typical cooling data for a 15 volume per cent polyacrylate (Aquaquench ACR) solution at 30 °C and agitated at 0.5m/s following various cumulative quench loads in the simulated ageing test.

4.8 Ageing Data for the Representative Polymer Quenchants.

Tables 24 to 26 indicate the changes in the cooling characteristics of the representative polymer products after being subjected to increased throughput during the accelerated ageing programme. The cooling characteristics were assessed at the standardized conditions. The effect of increasing quench load on the kinematic viscosities of the solutions at 40°C is also shown in the tables. The changes with use in the shape of the cooling curves are shown in *Figures 122 to 124*. Increasing the throughput tended to reduce any stage A cooling and to increase the severity of the quench. The kinematic viscosity of each of the polymer solutions dropped with usage; the drop was particularly severe for the polyacrylate in the first 20kg/litre.

The changes in the molecular weight distributions for the PAG and PVP samples after 100kg/litre were given in *Figures 76 and 82 (Table 13)*. Viscosity-average molecular weight data for the aged PVP and polyacrylate were given in Section 4.2.2. The PAG solution became slightly more acidic with usage, its pH dropped from 7.79 when fresh to 6.90 after 100kg/litre. There was no measured change in the pH of the PVP which remained at 8.33. The pH of the polyacrylate solution dropped slightly from the freshly prepared value of 8.25 to 8.04 upon completion of the accelerated ageing programme.

Table 27. Fresh polymer concentrate and distilled water additions required to maintain a 2 litre sample of constant refractive index (equivalent to an initial 15 volume per cent solution) following a cumulative quench load of 100kg/litre in the simulated ageing test.

| Polymer | PAG | PVP | Polyacrylate |
|-----------------------------------|------|------|--------------|
| Polymer concentrate addition (ml) | 262 | 194 | 416 |
| Distilled water addition (ml) | 2184 | 1247 | 3592 |

Table 27 lists the amount of water and fresh polymer concentrate which were required to be added in order to maintain a 2 litre sample of constant refractometer reading. More distilled water than polymer was needed in order to compensate for evaporation. The colour of the polymer quenchants changed with usage as shown in *Plates 6 to 8*. A progressively-increasing flocculent phase was developed in the polyacrylate sample. Upon standing, this phase settled to produce a sedimentary layer as seen in *Plate 8*.

Figure 125 shows the change in the shape of the cooling curves with increased usage for the polyacrylate samples supplied by T.I. Desford Tubes Ltd. The corresponding parametric data for these curves is given in *Table 28*. The kinematic viscosity of this nominally 18 volume per cent solution dropped from 14.9mm²/s at 40°C in the fresh condition, to 8.8mm²/s after 3200 tonnes. These used polyacrylate solutions were also black and "oil-like" in appearance and contained traces of particulate floc.

Plate 9 shows the appearance of the representative polymer solutions 14 days after the addition of 1.0 weight per cent of oxidized mild steel filings. There was no apparent interaction between the filings and the PAG and PVP solutions. However, a dark flocculent phase can clearly be seen above the filings in the polyacrylate sample. There was no change in the refractometer readings for the PAG and the PVP samples after the 14 day period, whereas the reading for the polyacrylate decreased from 4.5 to 4.0 Brix.



Plate 6. Change in appearance of a nominally 15 volume per cent solution of the representative PAG (Quendila PA) with increased throughput in the accelerated ageing test. (a) Fresh, (b) 10kg/litre, (c) 50kg/litre and (d) 100kg/litre.



Plate 7. Change in appearance of a nominally 15 volume per cent solution of the representative PVP (Parquench 90) with increased throughput in the accelerated ageing test. (a) Fresh, (b) 10kg/litre, (c) 50kg/litre and (d) 100kg/litre.



Plate 8. Change in appearance of a nominally 15 volume per cent solution of the representative Polyacrylate (Aquaquench ACR) with increased throughput in the accelerated ageing test. (a) Fresh, (b) 10kg/litre, (c) 50kg/litre and (d) 100kg/litre.

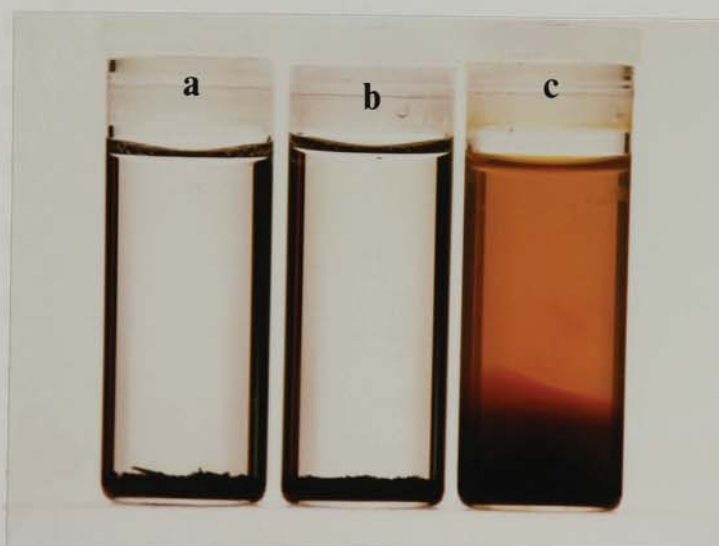


Plate 9. Change in appearance of 15 volume per cent solutions of each representative polymer quenchant 14 days after the addition of 1 weight per cent of oxidized mild steel filings. (a) PAG (Quendila PA), (b) PVP (Parquench 90) and (c) Polyacrylate (Aquaquench ACR).

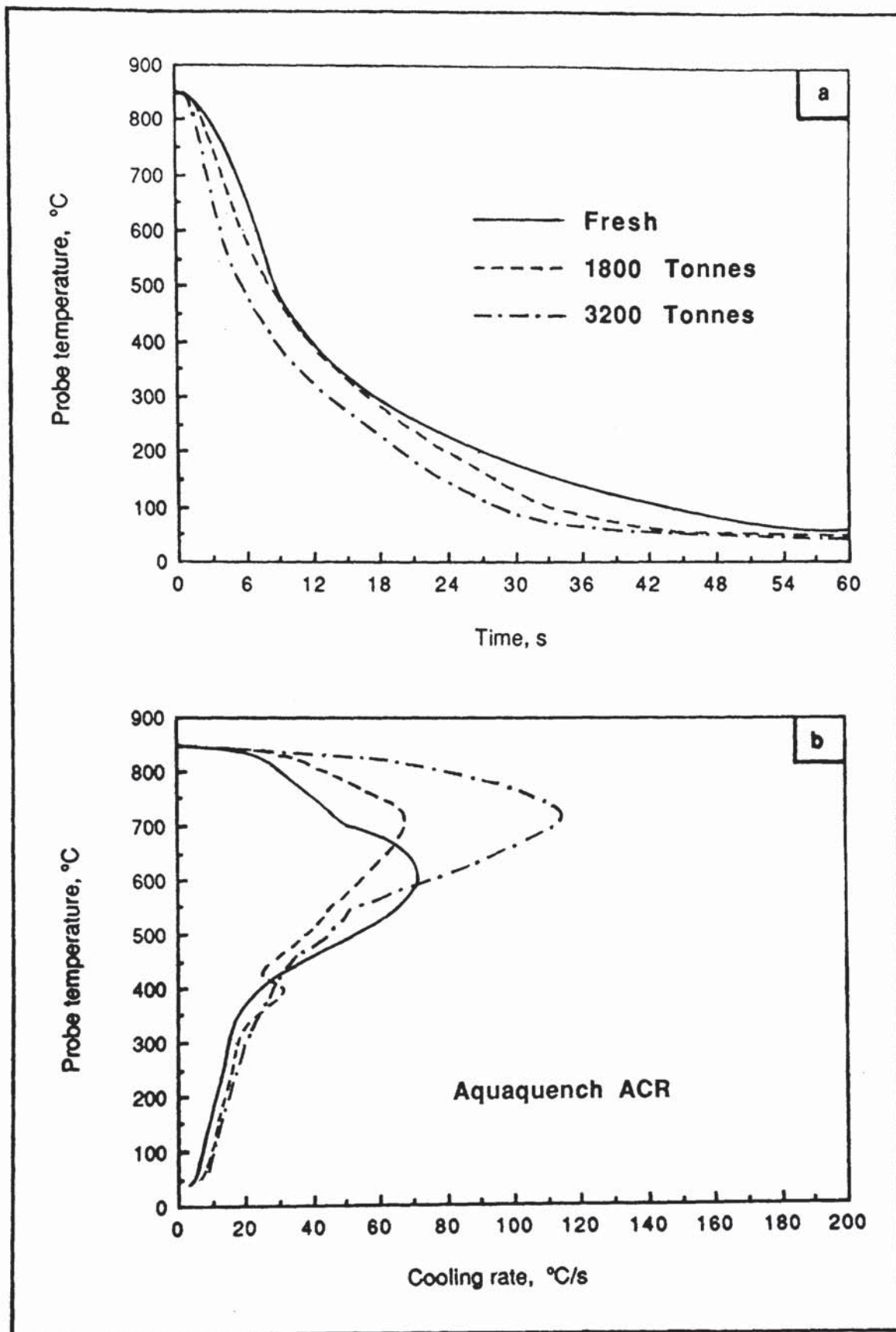


Figure 125. Typical cooling data for nominally 18 volume per cent polyacrylate (Aquaquench ACR) solutions supplied by T.I. Desford Tubes Ltd. following various periods of use. Test conditions 30 °C and 0.5m/s agitation.

Table 28. Cooling characteristics for nominally 18 volume per cent polyacrylate (Aquaquench ACR) solutions supplied by T.I. Desford Tubes Ltd, following various periods of use.
Test conditions 30°C and 0.5m/s agitation

| Cumulative quench load (Tonnes) | Time (s) to | | 200°C | Maximum cooling rate (°C/s) | Temp.of max ^m rate (°C) | Cooling rate at 300°C (°C/s) | Stage A/B | | Kinematic viscosity at 40°C (mm ² /s) |
|---------------------------------------|-------------|----------|----------|--------------------------------------|---|---------------------------------------|-----------|------------------------------|---|
| | 600°C | 400°C | | | | | Temp. | transition Rate (°C/s) | |
| Fresh | 7.0±0.5 | 11.6±0.6 | 26.6±1.2 | 71 ± 5 | 619 ± 25 | 13 ± 1 | 700 ± 14 | 50 ± 1 | 14.9 |
| 1800 | 6.1±0.2 | 11.8±0.3 | 24.3±0.6 | 65 ± 1 | 718 ± 42 | 16 ± 1 | - | - | 11.6 |
| 3200 | 4.1±0.1 | 8.5±0.6 | 19.8±0.1 | 114 ± 1 | 695 ± 47 | 18 ± 2 | - | - | 8.8 |

4.8.1 Polymer Quenchant Shear Stability Data.

Figure 126 gives an indication of the shear stability for a 15 volume per cent solution of each representative polymer tested using the Kurt Orbahn diesel injector method. After 90 cycles, the kinematic viscosity for the PAG (Quendila PA) had increased by 6 per cent, whilst there was a drop of 33 per cent for the PVP (Parquench 90) and of 22 per cent for the polyacrylate (Aquaquench ACR).

4.9 Polymer Quenchant Solution Rheology Data.

The shear stress-shear rate characteristics for 15 volume per cent solutions of each representative polymer quenchant at 15°C are shown in *Figure 127*. Ideal liquids, such as water, show what is known as Newtonian behaviour: i.e. the viscosity is independent of shear. The upward curvature plots shown in *Figure 127* demonstrate that the polymer solutions exhibit shear thinning or pseudoplastic behaviour, since the viscosity decreases as the shear rate increases. *Table 29* gives apparent viscosity results for the three samples at shear rates of 2000s⁻¹ and 4000s⁻¹. These latter results were calculated using equation (25), from shear stress values extrapolated from the curves. It can be seen that the viscosity of the polyacrylate solution was more sensitive to shear rate than either the PAG or the PVP.

Table 29. Apparent viscosity values for 15 per cent solutions of each representative polymer quenchant type measured at 15°C.

| Polymer type | Apparent viscosity (mPas) | |
|----------------------------------|-----------------------------------|-----------------------------------|
| | Shear rate 2000s ⁻¹ | Shear rate 4000s ⁻¹ |
| PAG (Quendila PA) | 3.60 | 3.10 |
| PVP (Parquench 90) | 2.43 | 2.10 |
| Polyacrylate (Aquaquench ACR) | 15.90 | 12.40 |

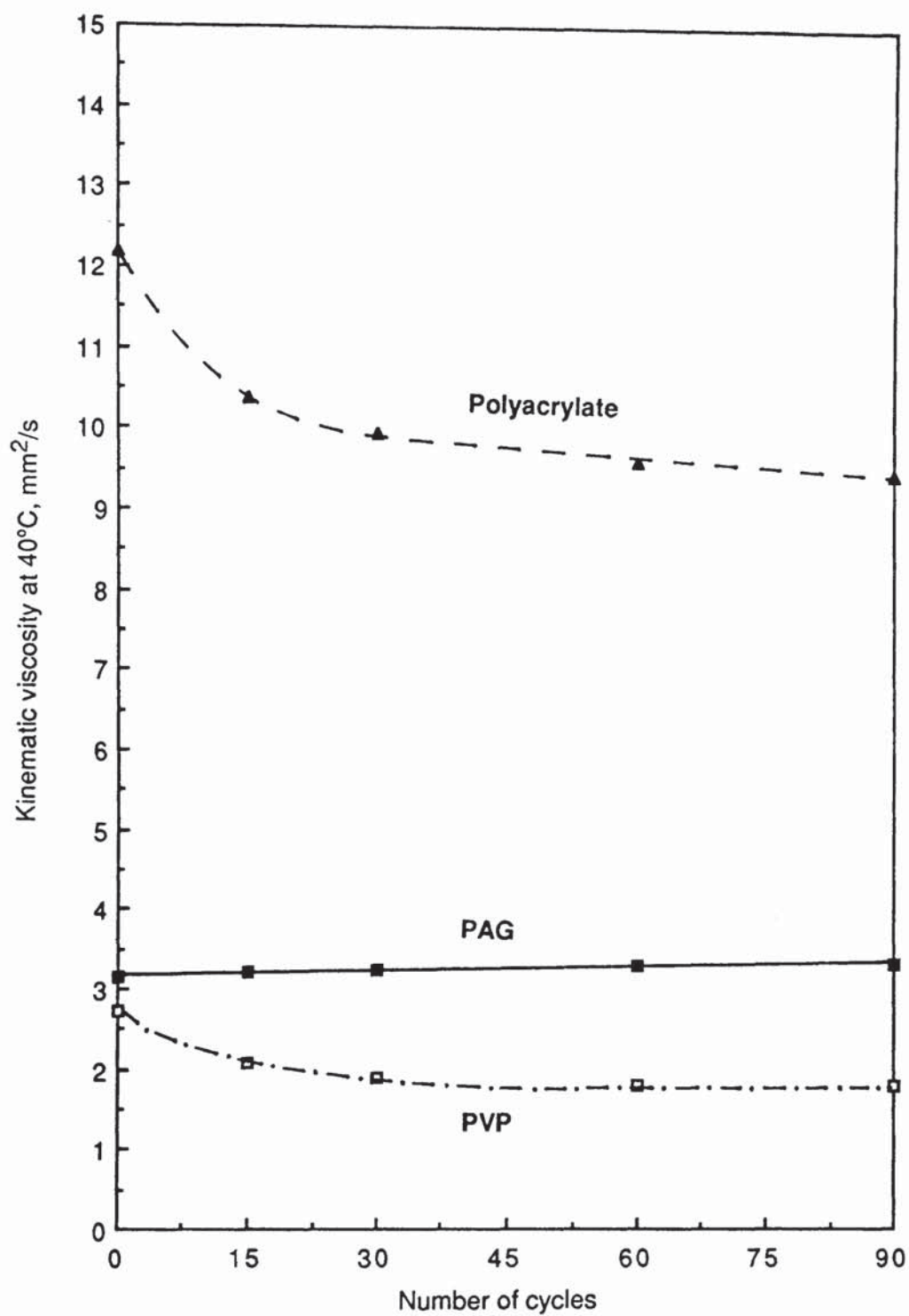


Figure 126. Kurt Orbahn shear stability results for 15 volume per cent solutions of the representative polymer quenchants.

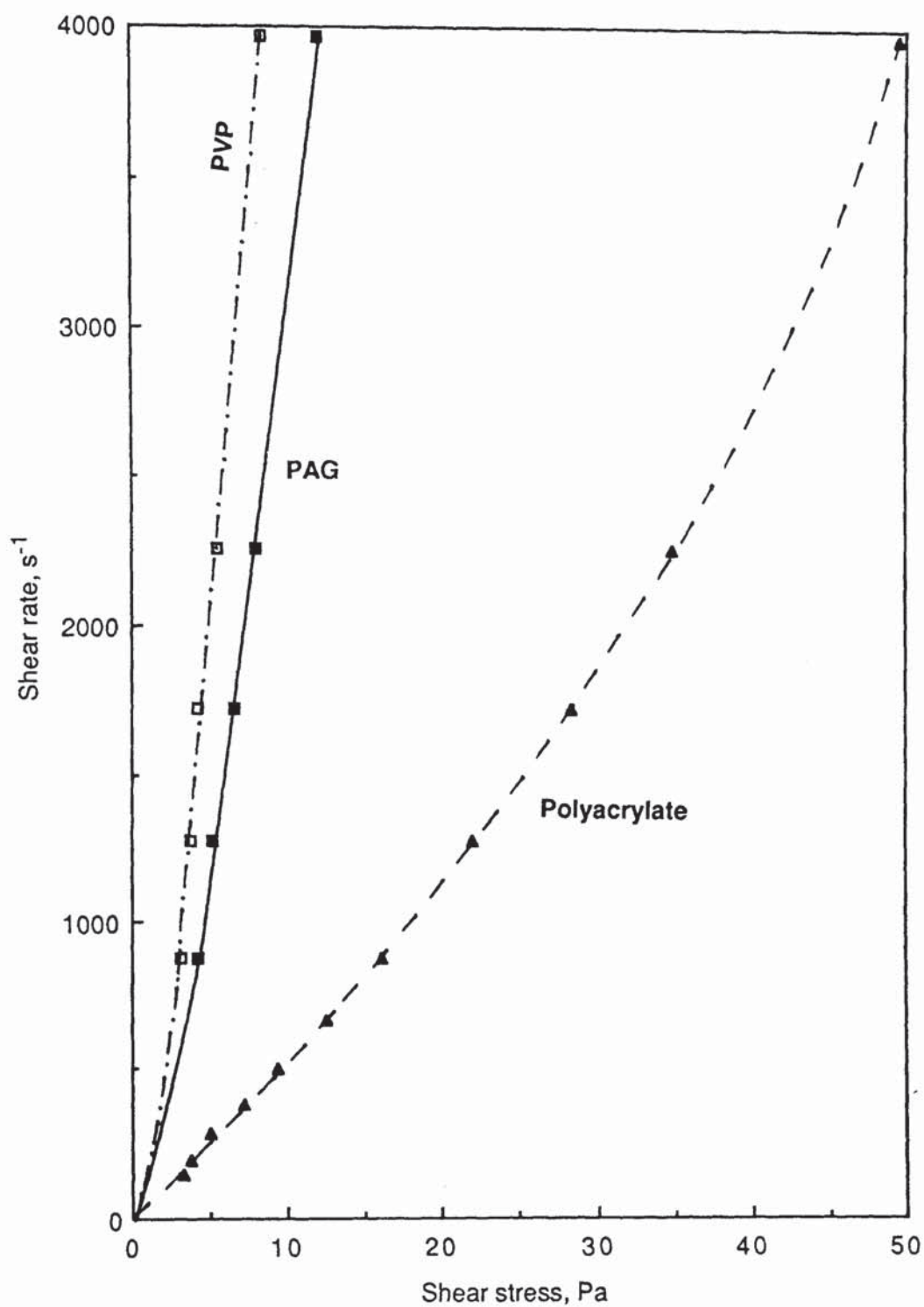


Figure 127. Epprecht Rheomat cone-and-plate viscometer results for 15 volume per cent solutions of the representative polymer quenchants at 15 °C.

4.10 Polymer Quenchant Contamination Data.

4.10.1 **Contamination with Oil.** The effect of quench oil contamination on the shape of the cooling curves, for each of the representative polymer solutions tested at the standardized conditions, can be seen in *Figures 128 to 131*. The corresponding cooling parameter data, plus the effect of the oil contaminant on the refractometer readings, is given in *Table 30*. Increasing the level of oil tended to prolong stage A cooling and reduce the maximum rate. There was a slight increase in the cooling rate at 300°C for the PAG and polyacrylate samples, but a significant drop for the PVP above 1 weight per cent. For a given level of contamination the water washable oil tended to reduce the maximum rate of the PAG to a greater extent than the equivalent non water soluble product. The refractometer readings for each polymer solution increased slightly as the level of oil contamination was raised.

4.10.2 **Contamination with Ammonia.** *Figures 132 to 134* illustrate the effect of ammonia contamination on the cooling characteristics of the representative polymer solutions. *Table 31* lists the parametric and refractometer reading data. There was a linear increase in the refractometer readings with ammonia contamination level for each product. Ammonia contamination resulted in extended stage A cooling and reduced maximum rates and temperatures of maximum rate. There was little effect on the cooling rate at 300°C with increased ammonia content for the PAG, a slight drop for the polyacrylate, and a considerable decrease for the PVP. The fresh PVP experienced no stage A cooling and a rate at 300°C of $61 \pm 1^\circ\text{C/s}$. The addition of 5 weight per cent ammonia to the PVP resulted in the formation of a stage A cooling regime down to a temperature of $707 \pm 9^\circ\text{C}$, plus a drop in the rate at 300°C to $23 \pm 1^\circ\text{C/s}$.

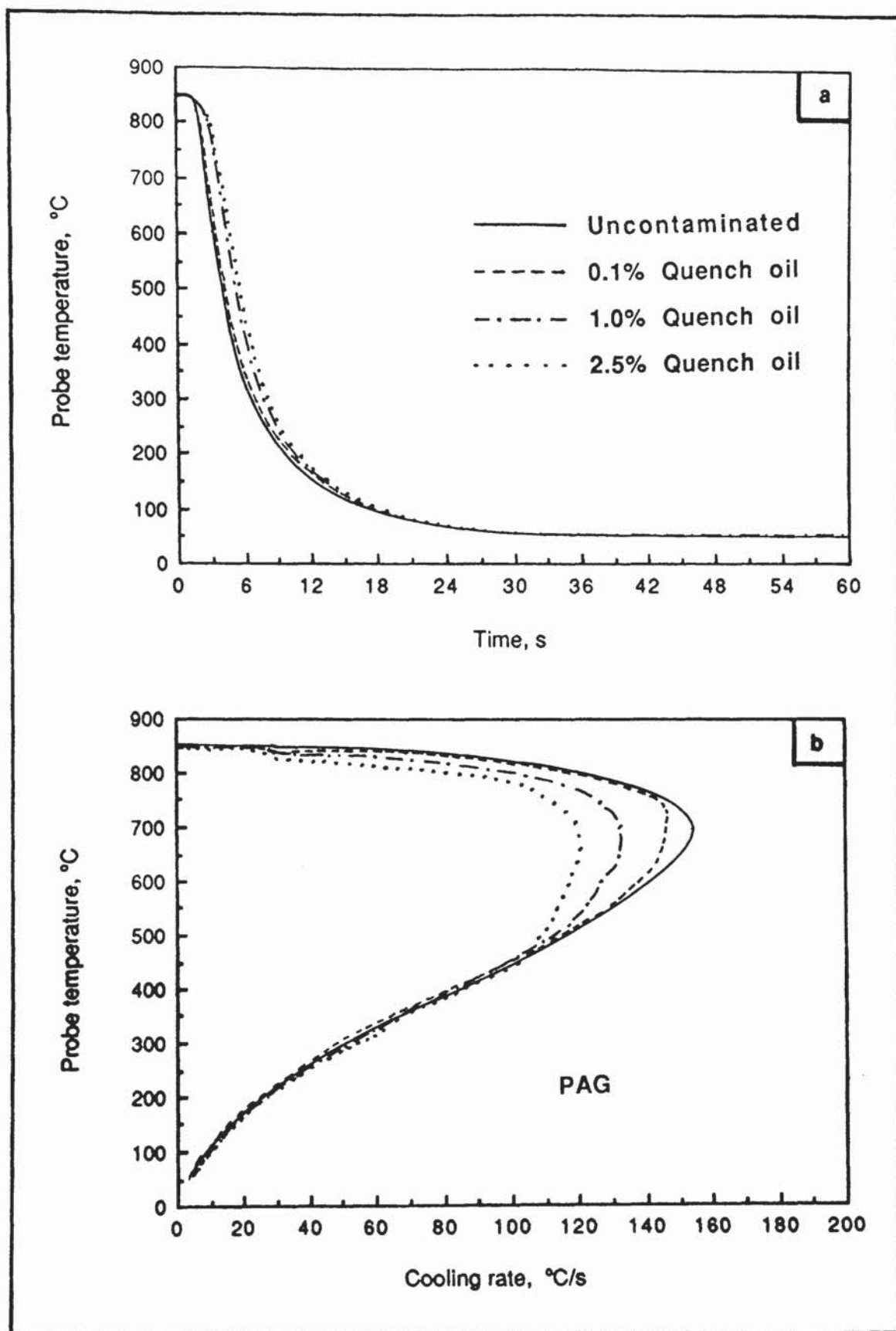


Figure 128. Typical cooling data for a 15 volume per cent PAG (Quendila PA) solution at 30 °C and agitated at 0.5m/s with various weight per cent levels of quench oil contamination (Houghtoquench 3s).

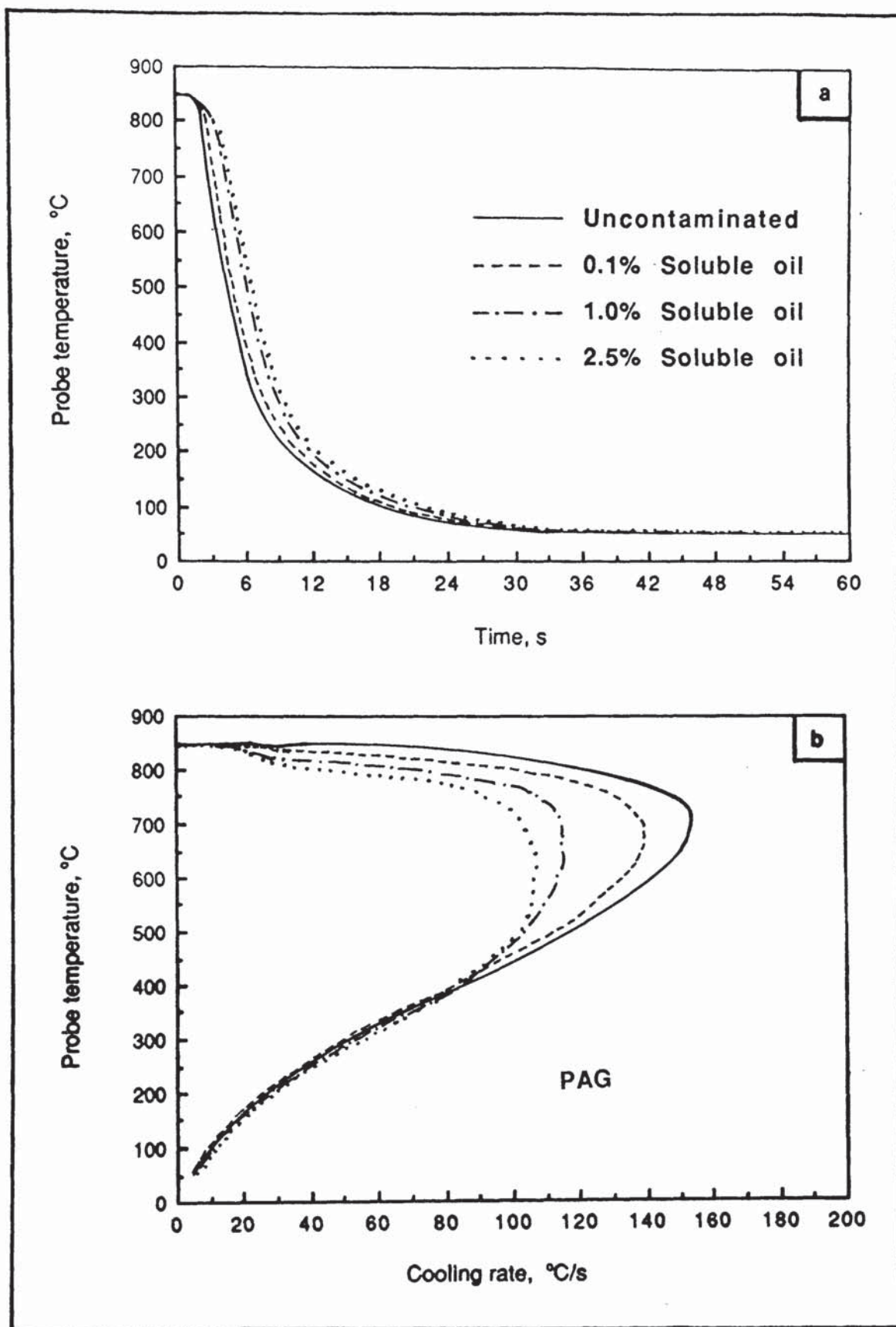


Figure 129. Typical cooling data for a 15 volume per cent PAG (Quendila PA) solution at 30 °C and agitated at 0.5 m/s with varying weight per cent levels of soluble quench oil contamination (Klenquench 3).

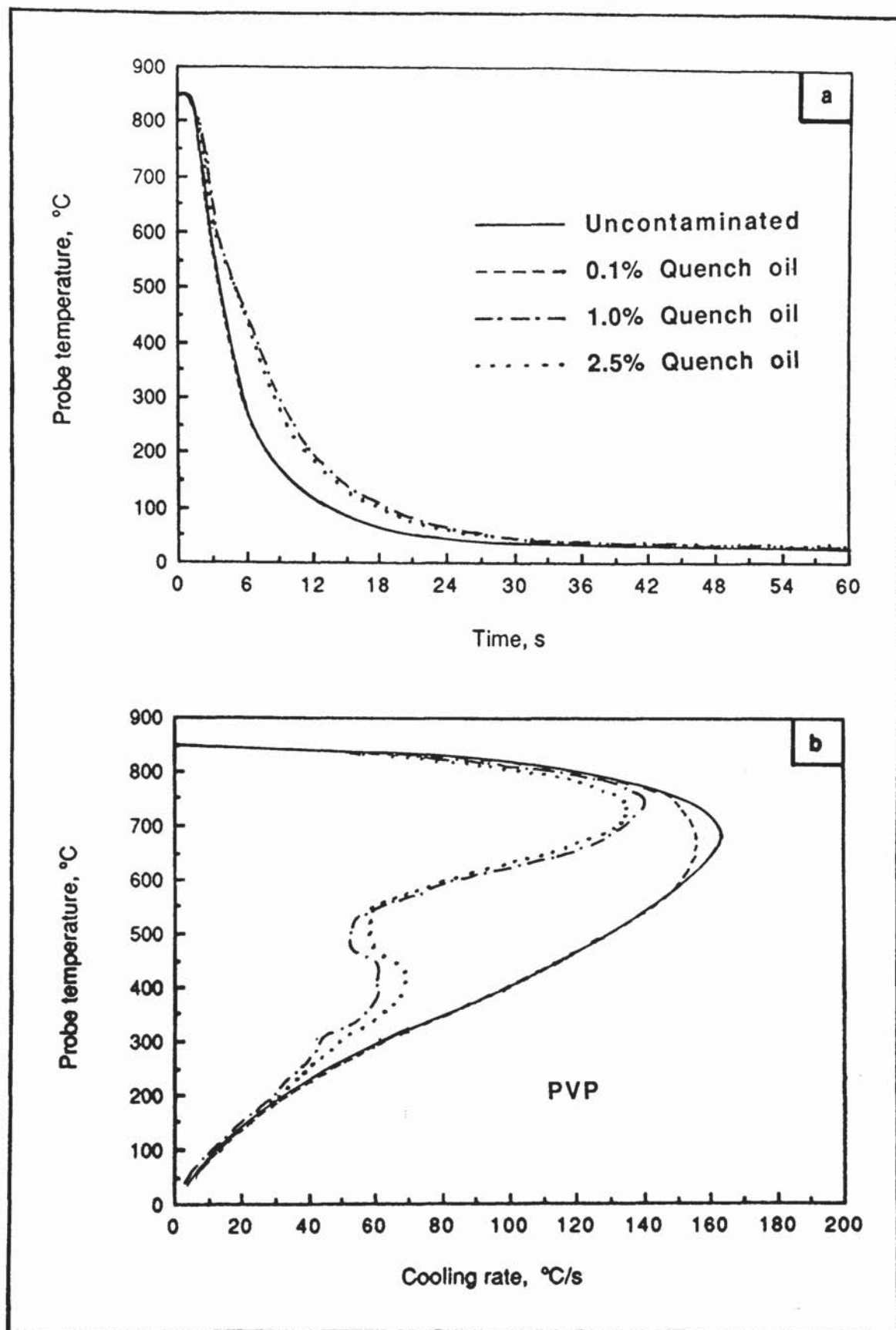


Figure 130. Typical cooling data for a 15 volume per cent PVP (Parquench 90) solution at 30 °C and agitated at 0.5m/s with varying weight per cent levels of quench oil contamination (Houghtoquench 3s).

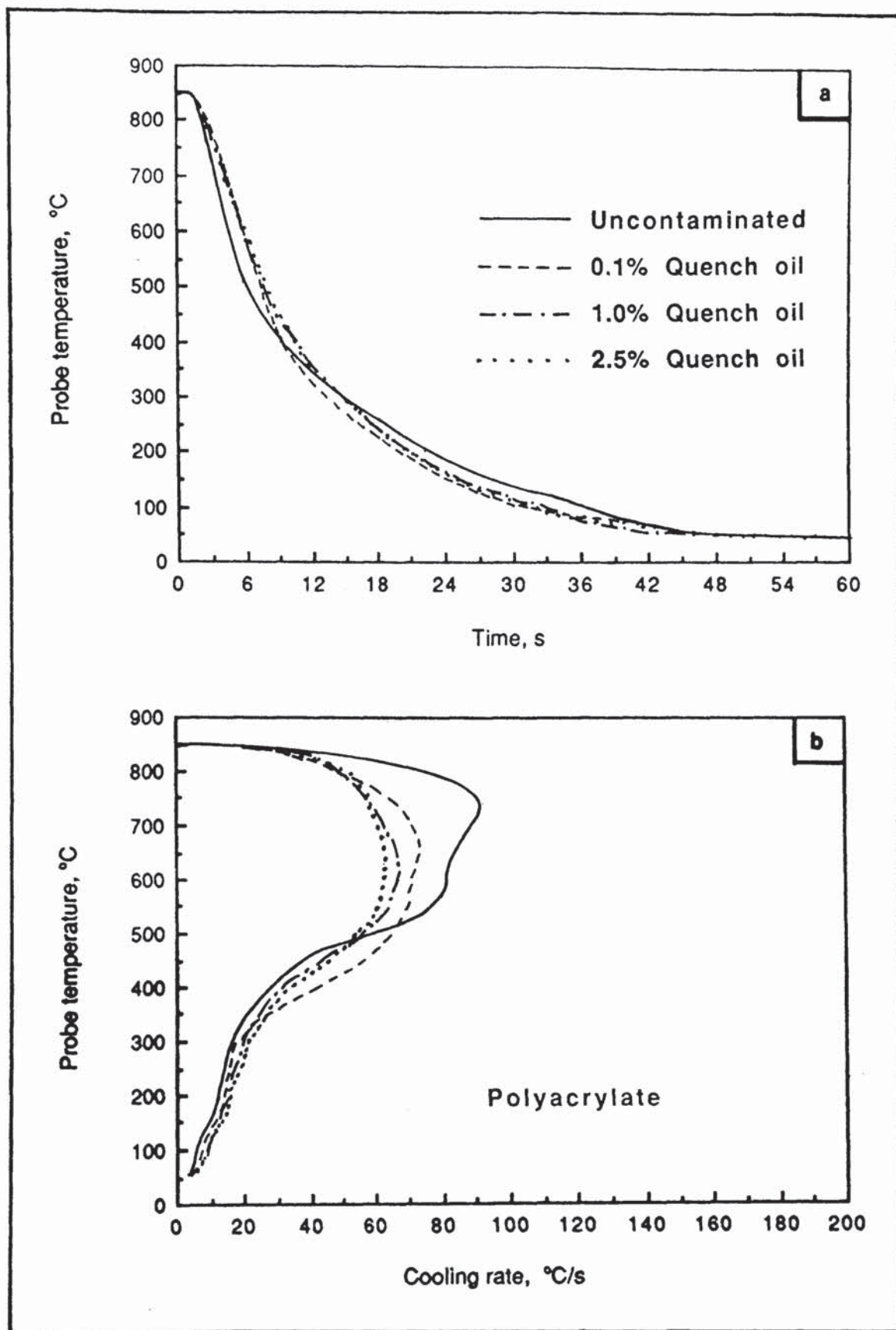


Figure 131. Typical cooling data for a 15 volume per cent polyacrylate (Aquaquench ACR) solution at 30 °C and agitated at 0.5m/s with varying weight per cent levels of quench oil contamination (Houghtoquench 3s).

Table 30. Cooling characteristics for 15 volume per cent representative polymer quenchant solutions contaminated with quench oil and tested at 30°C and 0.5m/s agitation

| Test | Time (s) to | | | Maximum cooling rate (°C/s) | Temp. of max ^m rate (°C) | Cooling rate at 300°C (°C/s) | Stage A/B transition | | Refractometer reading (Brix no.) |
|--------------|-------------|----------|----------|-----------------------------|-------------------------------------|------------------------------|----------------------|-------------|----------------------------------|
| | 600°C | 400°C | 200°C | | | | Temp. (°C) | Rate (°C/s) | |
| PAG | | | | | | | | | |
| Uncontam. | 3.1±0.1 | 4.8±0.1 | 9.2±0.1 | 153 ± 3 | 693 ± 11 | 51 ± 1 | 833 ± 3 | 32 ± 1 | 7.9 |
| 0.1 wt % | 3.1±0.3 | 4.9±0.2 | 9.7±0.1 | 147 ± 3 | 683 ± 37 | 51 ± 1 | 830 ± 6 | 30 ± 1 | 8.1 |
| 1.0 wt % | 4.2±0.1 | 6.1±0.1 | 10.2±0.1 | 135 ± 2 | 670 ± 23 | 52 ± 1 | 829 ± 2 | 28 ± 1 | 8.3 |
| 2.5 wt % | 4.6±0.1 | 6.6±0.1 | 10.7±0.1 | 122 ± 1 | 613 ± 23 | 57 ± 1 | 826 ± 1 | 26 ± 1 | 8.4 |
| Soluble oil | | | | | | | | | |
| Uncontam. | 3.5±0.3 | 5.1±0.1 | 9.5±0.3 | 153 ± 1 | 650 ± 22 | 51 ± 1 | 833 ± 5 | 32 ± 1 | 7.9 |
| 0.1 wt % | 3.7±0.2 | 5.5±0.2 | 10.2±0.2 | 141 ± 1 | 679 ± 12 | 50 ± 1 | 837 ± 1 | 31 ± 1 | 8.2 |
| 1.0 wt % | 4.9±0.2 | 6.9±0.2 | 11.4±0.2 | 115 ± 1 | 663 ± 44 | 52 ± 1 | 824 ± 2 | 26 ± 1 | 8.3 |
| 2.5 wt % | 5.3±0.1 | 7.3±0.1 | 12.2±0.1 | 110 ± 1 | 594 ± 48 | 53 ± 1 | 811 ± 10 | 25 ± 1 | 8.5 |
| PVP | | | | | | | | | |
| Uncontam. | 2.9±0.2 | 4.5±0.3 | 7.9±0.3 | 161 ± 4 | 655 ± 32 | 60 ± 3 | - | - | 1.8 |
| 0.1 wt % | 2.9±0.1 | 4.4±0.1 | 7.7±0.1 | 156 ± 1 | 667 ± 37 | 62 ± 1 | - | - | 1.8 |
| 1.0 wt % | 3.1±0.3 | 6.2±0.6 | 11.6±0.6 | 141 ± 2 | 738 ± 24 | 41 ± 2 | - | - | 1.9 |
| 2.5 wt % | 3.4±0.1 | 6.4±0.2 | 11.3±0.1 | 135 ± 1 | 737 ± 20 | 45 ± 3 | - | - | 2.0 |
| Polyacrylate | | | | | | | | | |
| Uncontam. | 4.7±0.3 | 8.7±0.1 | 21.8±0.7 | 91 ± 6 | 742 ± 6 | 17 ± 1 | - | - | 4.5 |
| 0.1 wt % | 5.5±0.1 | 8.9±0.3 | 19.9±0.4 | 76 ± 5 | 650 ± 35 | 18 ± 2 | - | - | 4.5 |
| 1.0 wt % | 5.5±0.2 | 9.8±0.1 | 20.5±0.1 | 67 ± 2 | 612 ± 7 | 19 ± 2 | - | - | 4.6 |
| 2.5 wt % | 6.0±0.2 | 10.6±0.6 | 20.8±0.6 | 62 ± 2 | 609 ± 95 | 20 ± 2 | - | - | 4.7 |

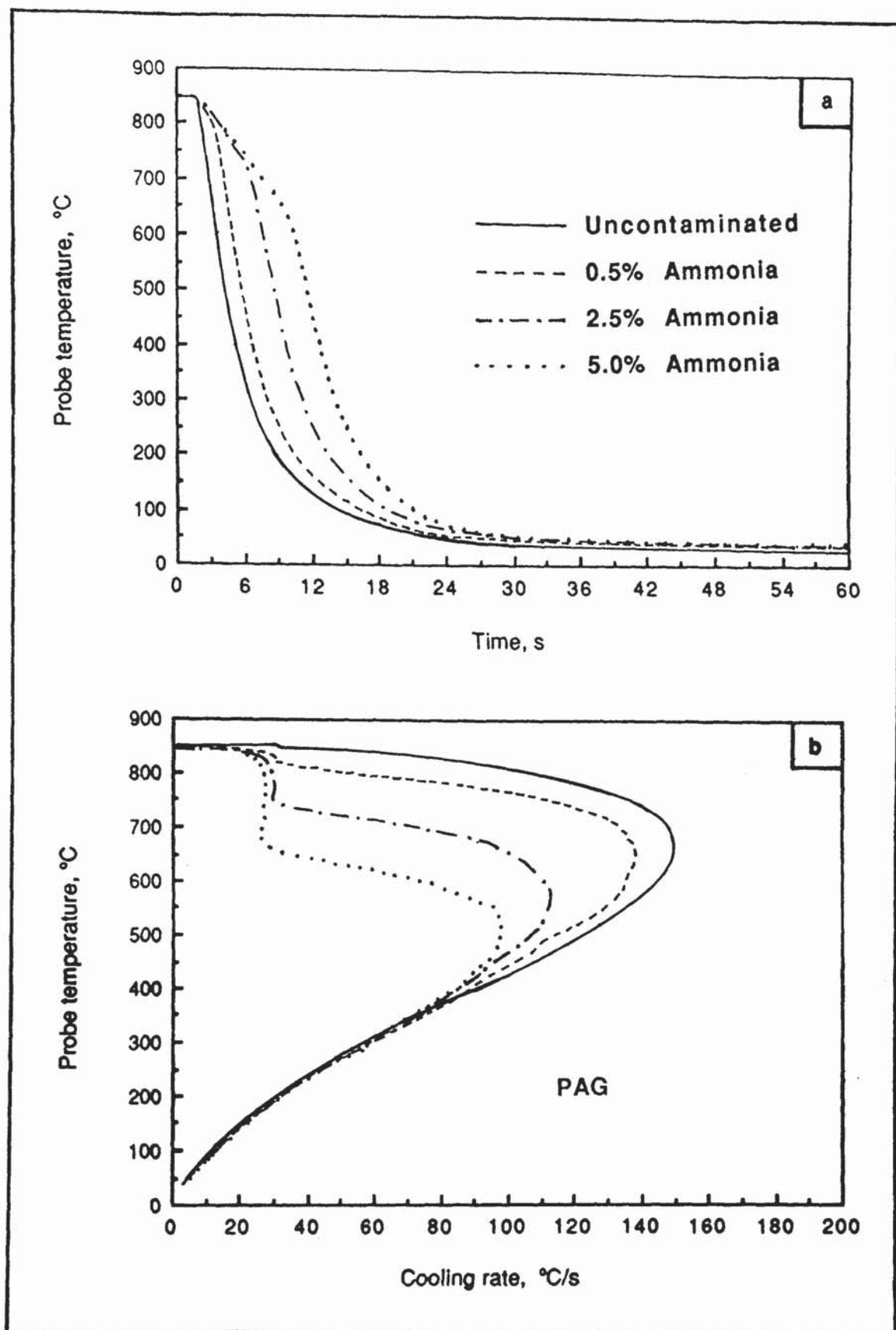


Figure 132. Typical cooling data for a 15 volume per cent PAG (Quendila PA) solution contaminated with various weight per cent additions of ammonia. Test conditions 30 °C, 0.5m/s agitation.

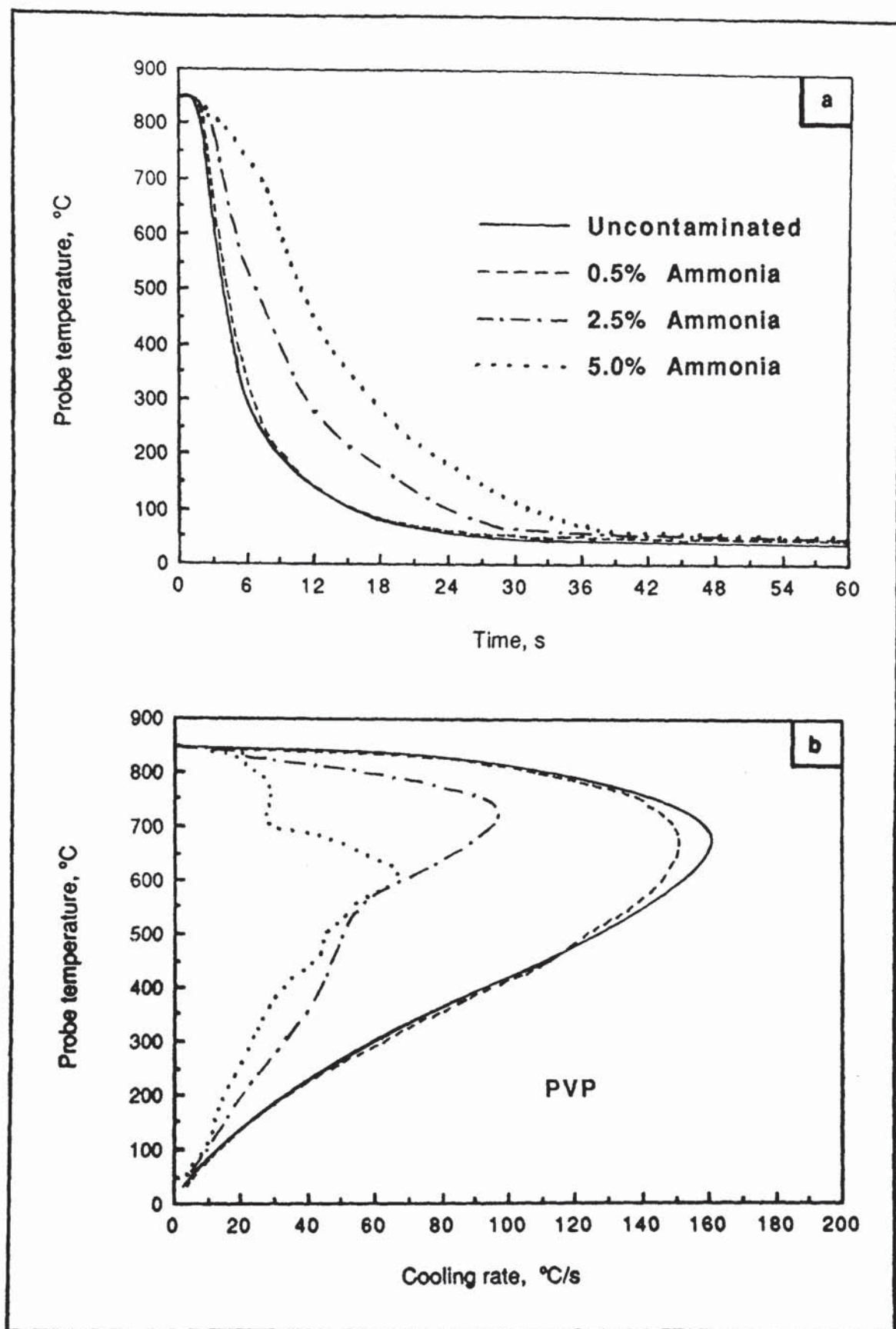


Figure 133. Typical cooling data for a 15 volume per cent PVP (Parquench 90) solution contaminated with various weight per cent additions of ammonia. Test conditions 30 °C, 0.5m/s agitation.

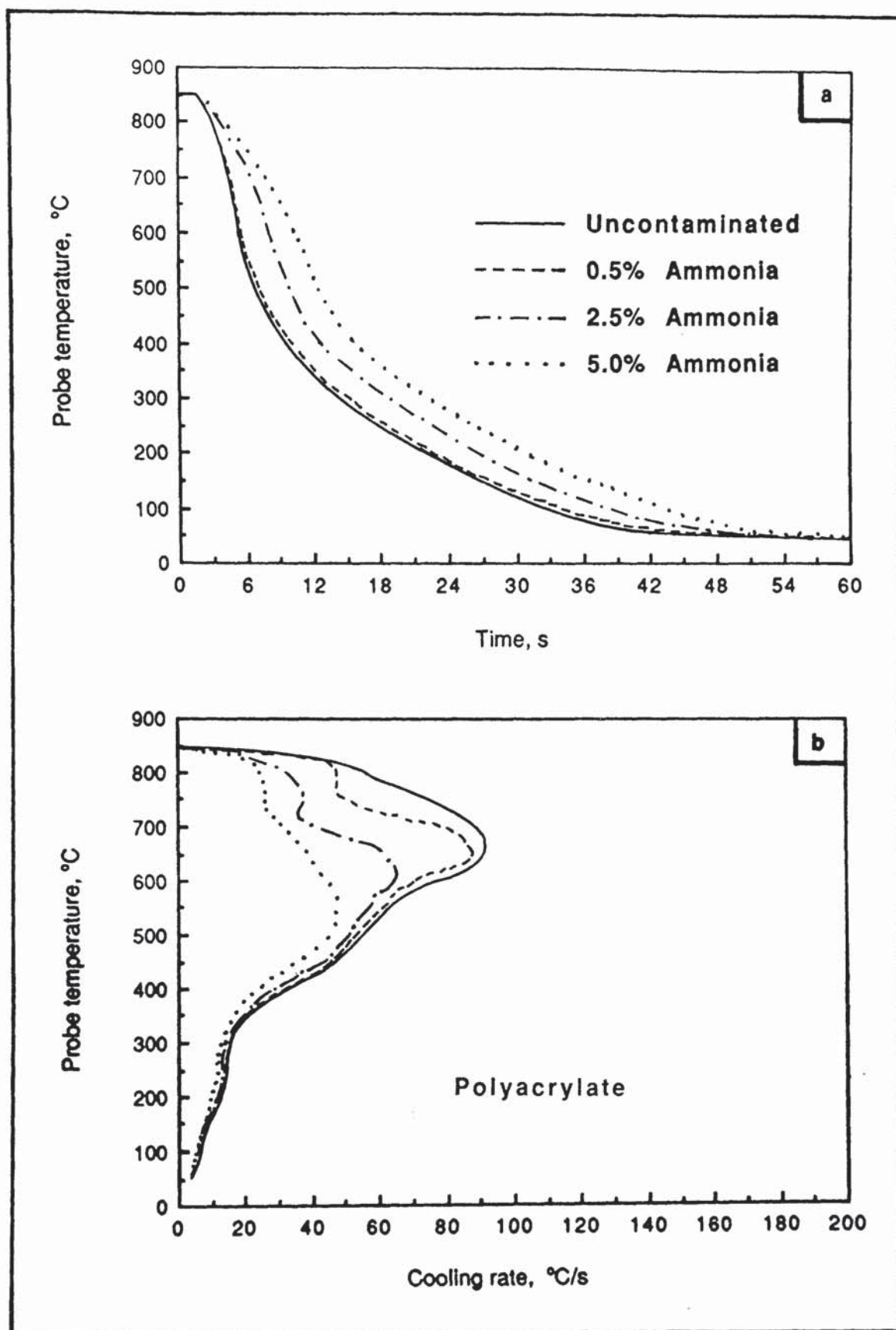


Figure 134. Typical cooling data for a 15 volume per cent polyacrylate (Aquaquench ACR) solution contaminated with various weight per cent additions of ammonia. Test conditions 30 °C, 0.5m/s agitation.

Table 31. Cooling characteristics for 15 volume per cent representative polymer quenchant solutions contaminated with ammonia and tested at 30°C and 0.5m/s agitation

| Test | Time (s) to | | | Maximum cooling rate (°C/s) | Temp.of max ^m rate (°C) | Cooling rate at 300°C (°C/s) | Stage A/B transition | | Refractometer reading (Brix no.) |
|---------------------|-------------|----------|----------|-----------------------------|------------------------------------|------------------------------|----------------------|-------------|----------------------------------|
| | 600°C | 400°C | 200°C | | | | Temp. (°C) | Rate (°C/s) | |
| PAG | | | | | | | | | |
| Uncontam. | 3.6±0.5 | 5.2±0.6 | 8.9±0.7 | 150 ± 3 | 668 ± 18 | 59 ± 2 | 833 ± 2 | 32 ± 1 | 7.85 |
| 0.5 wt % | 4.5±0.1 | 6.3±0.1 | 10.0±0.1 | 140 ± 2 | 646 ± 5 | 60 ± 1 | 818 ± 5 | 31 ± 1 | 10.98 |
| 2.5 wt % | 7.5±0.1 | 9.4±0.1 | 13.2±0.1 | 113 ± 1 | 567 ± 2 | 60 ± 1 | 744 ± 4 | 29 ± 1 | 8.10 |
| 5.0 wt % | 9.9±0.2 | 12.1±0.3 | 15.9±0.3 | 96 ± 1 | 517 ± 32 | 59 ± 2 | 670 ± 7 | 28 ± 1 | 8.35 |
| PVP | | | | | | | | | |
| Uncontam. | 3.0±0.2 | 4.5±0.1 | 8.2±0.1 | 160 ± 3 | 679 ± 4 | 61 ± 1 | - | - | 1.70 |
| 0.5 wt % | 3.1±0.1 | 4.7±0.1 | 8.4±0.2 | 155 ± 4 | 675 ± 22 | 62 ± 2 | - | - | 1.85 |
| 2.5 wt % | 5.2±0.1 | 9.1±0.1 | 16.6±1.9 | 96 ± 5 | 726 ± 5 | 32 ± 8 | 837 ± 3 | 20 ± 3 | 2.25 |
| 5.0 wt % | 8.7±0.5 | 13.2±0.6 | 22.7±0.6 | 68 ± 1 | 637 ± 10 | 23 ± 1 | 707 ± 4 | 29 ± 1 | 2.75 |
| Polyacrylate | | | | | | | | | |
| Uncontam. | 5.1±0.3 | 9.3±0.9 | 22.1±1.2 | 92 ± 5 | 686 ± 24 | 16 ± 1 | 798 ± 6 | 59 ± 1 | 4.7 |
| 0.5 wt % | 5.3±0.1 | 9.3±0.3 | 22.2±0.1 | 86 ± 5 | 649 ± 5 | 16 ± 1 | 763 ± 4 | 47 ± 1 | 4.8 |
| 2.5 wt % | 7.9±0.2 | 12.1±0.1 | 26.1±0.4 | 68 ± 3 | 610 ± 13 | 15 ± 1 | 725 ± 6 | 35 ± 1 | 5.0 |
| 5.0 wt % | 10.2±0.2 | 15.4±0.1 | 31.0±0.5 | 50 ± 1 | 518 ± 9 | 13 ± 1 | 689 ± 11 | 26 ± 1 | 5.4 |

4.10.3 Salt Contamination. *Tables 32 to 35* give data describing the effect of additions of AVS 250 (sodium nitrite-nitrate salt) on the cooling characteristics of distilled water, on 15 and 30 per cent PAG solutions, and on 15 per cent PVP and polyacrylate solutions. These additions were made in order to simulate the contamination of quenchants used when precipitation-hardening aluminium alloys are heated in salt baths. For this same reason the Wolfson probe preheat temperature had been set at 500°C. Typical cooling curves for the 15 volume per cent PAG (Quendila PA) solution are shown in *Figure 135*. The effect of the salt additions on the refractometer readings and kinematic viscosities for the solutions is shown in *Figures 136 and 137*.

Table 32. Cooling characteristics for distilled water at 30°C contaminated with various sodium nitrite/nitrate salt additions (AVS 250). Test conditions 30°C and 0.5m/s agitation, probe preheat temperature 500°C.

| AVS 250 addition (wt %) | 400°C | Time (s) to 200°C | 100°C | Maximum cooling rate (°C/s) | Temp. of max ^m rate (°C) | Cooling rate at 300°C (°C/s) |
|-------------------------------|---------|----------------------|----------|-----------------------------------|---|------------------------------------|
| Uncont. | 2.1±0.1 | 5.0±0.1 | 9.0±0.1 | 106 ± 3 | 420 ± 10 | 73 ± 1 |
| 0.5 | 2.1±0.1 | 4.9±0.1 | 8.6±0.1 | 104 ± 1 | 396 ± 14 | 77 ± 1 |
| 1.0 | 2.1±0.1 | 5.0±0.1 | 8.7±0.2 | 104 ± 1 | 404 ± 4 | 73 ± 5 |
| 2.5 | 2.1±0.1 | 5.1±0.1 | 8.9±0.1 | 103 ± 1 | 418 ± 32 | 72 ± 1 |
| 5.0 | 2.1±0.1 | 5.1±0.1 | 9.3±0.2 | 102 ± 4 | 428 ± 5 | 70 ± 1 |
| 10.0 | 2.1±0.1 | 5.2±0.1 | 9.8±0.2 | 104 ± 3 | 431 ± 5 | 68 ± 1 |
| 15.0 | 2.1±0.1 | 5.4±0.1 | 10.1±0.1 | 102 ± 3 | 424 ± 16 | 64 ± 2 |
| 20.0 | 2.1±0.1 | 5.5±0.1 | 10.4±0.2 | 100 ± 1 | 426 ± 17 | 63 ± 1 |
| 25.0 | 2.1±0.1 | 5.6±0.1 | 10.4±0.3 | 99 ± 2 | 425 ± 7 | 62 ± 2 |

With each of the polymer solutions there was a critical salt level above which the cooling characteristics were equivalent to those for water with the same salt addition. With the PAG solutions the salt additions raised the severity of the quenches until these critical levels were reached. The critical levels were 2.5 and 5 weight per cent salt for the 15 and 30 per cent PAG solutions respectively.

Increasing the level of salt contamination reduced the inversion temperature for the PAG solutions as shown in *Figure 138*.

Table 33. Cooling characteristics for 15 and 30 volume per cent PAG (Quendila PA) solutions contaminated with various sodium nitrite/nitrate salt additions (AVS 250). Test conditions 30°C and 0.5m/s agitation, probe preheat temperature 500°C.

| AVS 250 addition (wt %) | Time (s) to | | | Maximum cooling rate (°C/s) | Temp. of max ^m rate (°C) | Cooling rate at 300°C (°C/s) |
|-------------------------------|-------------|---------|----------|-----------------------------------|---|------------------------------------|
| | 400°C | 200°C | 100°C | | | |
| 15 Vol% PAG | | | | | | |
| 0 | 2.4±0.1 | 6.7±0.2 | 12.5±0.9 | 79 ± 2 | 418 ± 16 | 53 ± 1 |
| 0.5 | 2.5±0.1 | 7.2±0.1 | 13.9±0.4 | 78 ± 1 | 415 ± 1 | 50 ± 1 |
| 1.0 | 2.4±0.1 | 6.8±0.1 | 13.4±0.4 | 79 ± 1 | 416 ± 8 | 52 ± 2 |
| 2.5 | 2.2±0.1 | 5.3±0.1 | 10.2±0.1 | 105 ± 1 | 405 ± 6 | 71 ± 1 |
| 5.0 | 2.1±0.1 | 5.2±0.1 | 10.4±0.4 | 106 ± 1 | 417 ± 8 | 70 ± 1 |
| 10.0 | 2.1±0.1 | 5.5±0.1 | 10.8±0.2 | 102 ± 2 | 427 ± 9 | 67 ± 1 |
| 12.5 | 2.1±0.1 | 5.6±0.1 | 10.9±0.6 | 101 ± 2 | 451 ± 3 | 66 ± 1 |
| 15.0 | 2.2±0.1 | 5.7±0.1 | 11.4±0.3 | 101 ± 3 | 434 ± 21 | 64 ± 2 |
| 20.0 | 2.2±0.1 | 5.6±0.1 | 11.1±0.1 | 101 ± 3 | 432 ± 11 | 64 ± 2 |
| 25.0 | 2.2±0.1 | 5.8±0.1 | 11.6±0.6 | 100 ± 1 | 426 ± 13 | 62 ± 3 |
| 30 Vol% PAG | | | | | | |
| 0 | 2.7±0.1 | 9.3±0.3 | 21.0±0.5 | 71 ± 1 | 431 ± 2 | 40 ± 1 |
| 0.5 | 2.8±0.1 | 8.0±0.2 | 18.6±0.1 | 71± 1 | 425 ± 2 | 47 ± 1 |
| 1.0 | 2.7±0.1 | 6.7±0.2 | 15.1±1.3 | 81 ± 3 | 389 ± 6 | 60 ± 1 |
| 1.5 | 2.6±0.1 | 6.3±0.1 | 13.5±0.5 | 89 ± 1 | 406 ± 2 | 64 ± 2 |
| 2.0 | 2.6±0.1 | 6.1±0.1 | 13.2±0.1 | 96 ± 3 | 402 ± 8 | 67 ± 1 |
| 2.5 | 2.6±0.1 | 5.8±0.1 | 11.5±0.2 | 98 ± 1 | 416 ± 12 | 68 ± 1 |
| 3.75 | 2.5±0.1 | 6.1±0.1 | 13.9±1.4 | 102±3 | 408 ± 35 | 70 ± 1 |
| 5.0 | 2.3±0.1 | 5.6±0.1 | 12.1±0.1 | 102±2 | 412 ± 26 | 68 ± 1 |
| 10.0 | 2.2±0.1 | 5.9±0.3 | 13.3±0.6 | 103±1 | 421 ± 19 | 66 ± 2 |
| 15.0 | 2.1±0.1 | 6.2±0.1 | 14.0±0.2 | 102±2 | 445 ± 16 | 66 ± 2 |

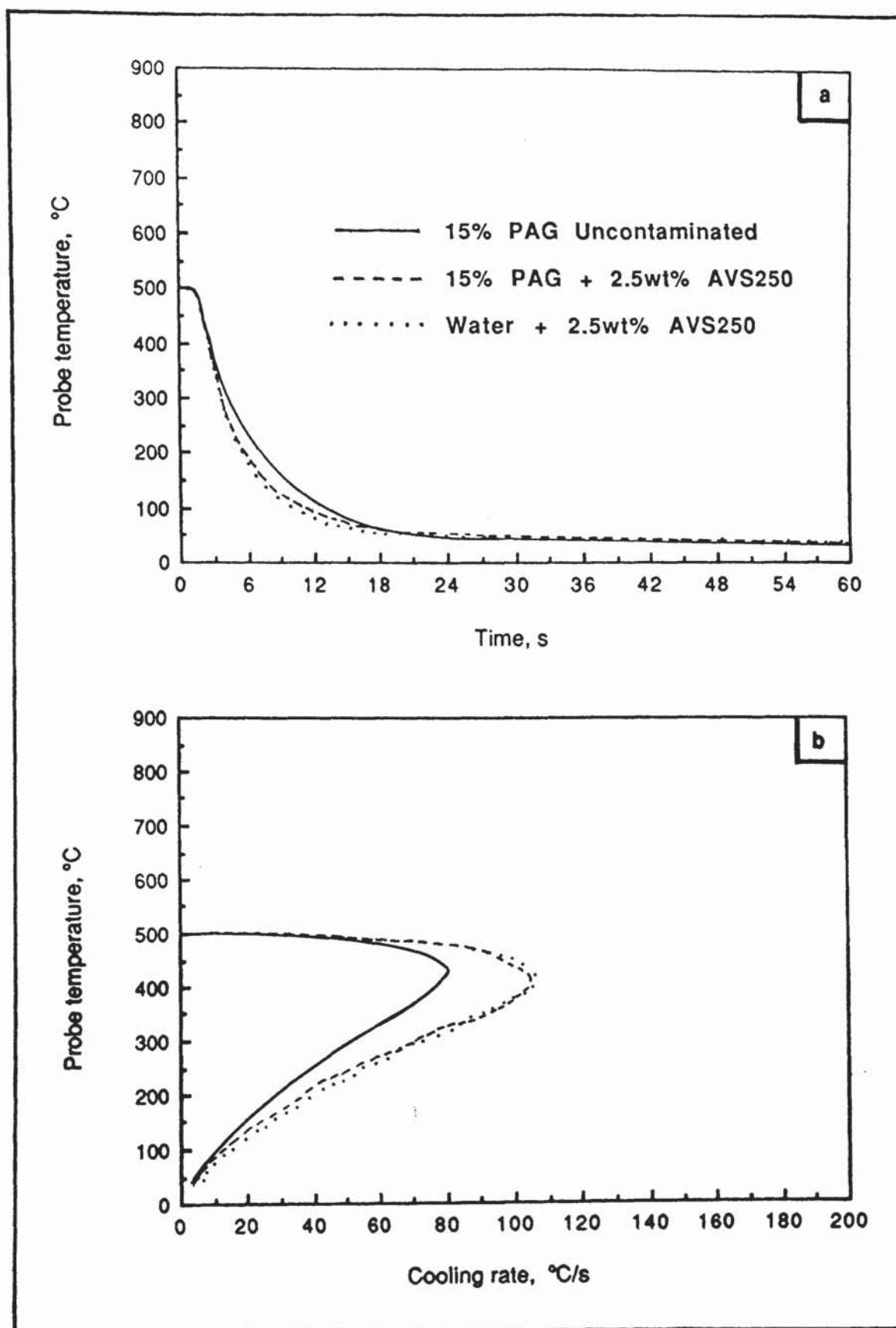


Figure 135. Typical cooling curves for a 15 volume per cent PAG (Quendila PA) solution, and for water contaminated with AVS 250 sodium nitrite/nitrate salt. Test conditions 30 °C, 0.5m/s agitation, probe preheat temperature 500 °C.

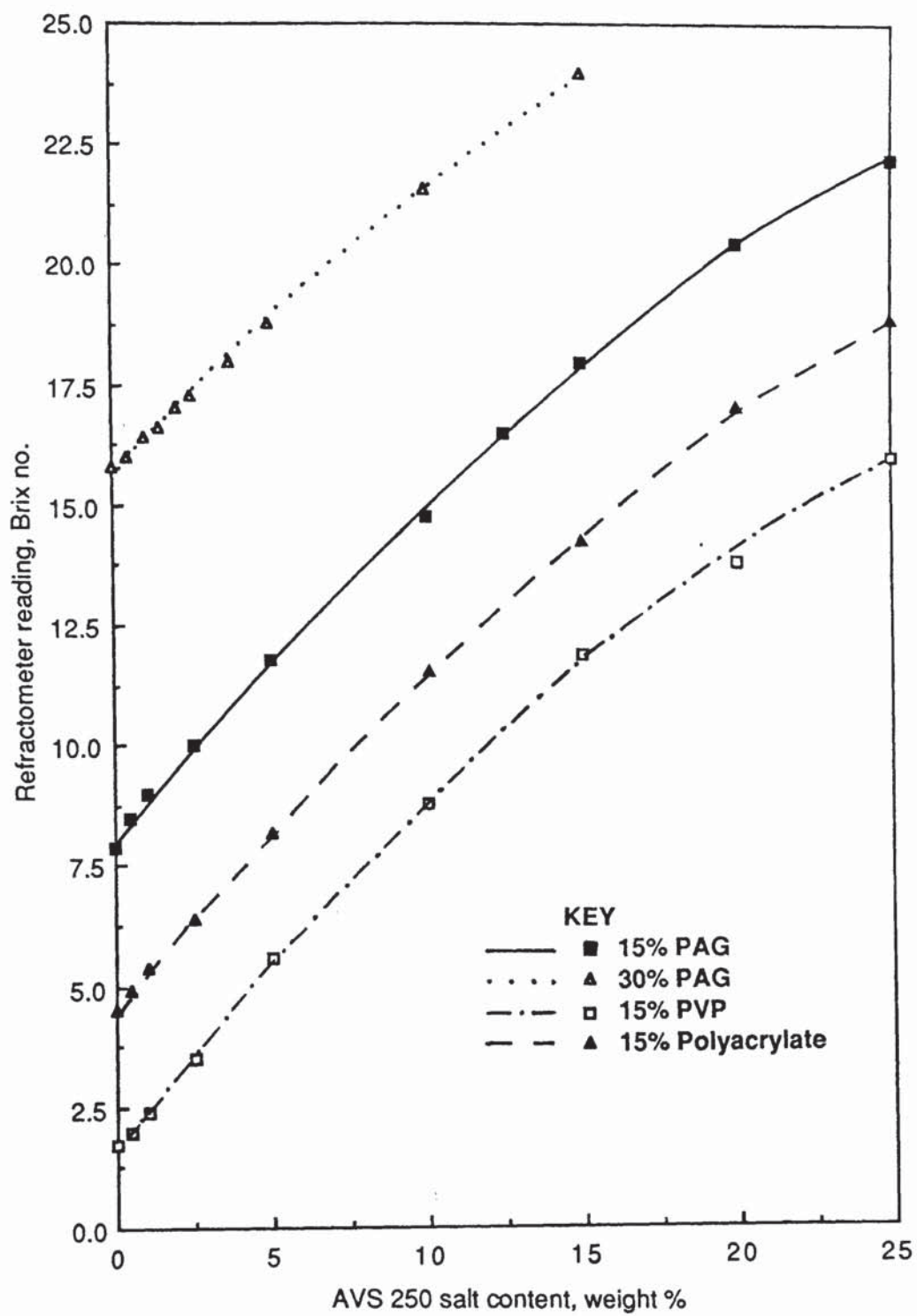


Figure 136. The effect of sodium nitrite/nitrate salt additions on the refractometer readings for the representative polymer quenchant solutions.

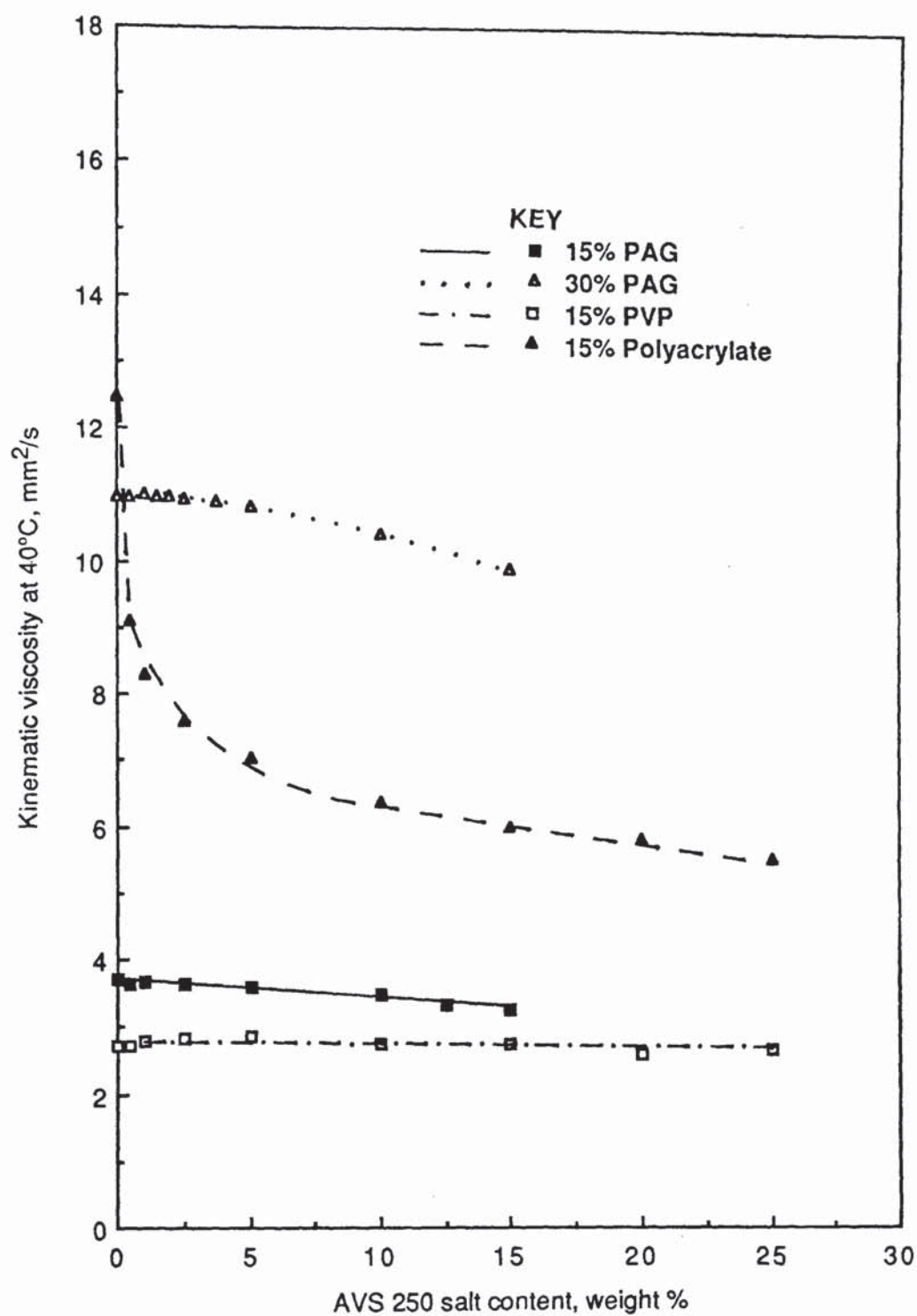


Figure 137. The effect of sodium nitrite/nitrate salt additions on the kinematic viscosities of the representative polymer solutions.

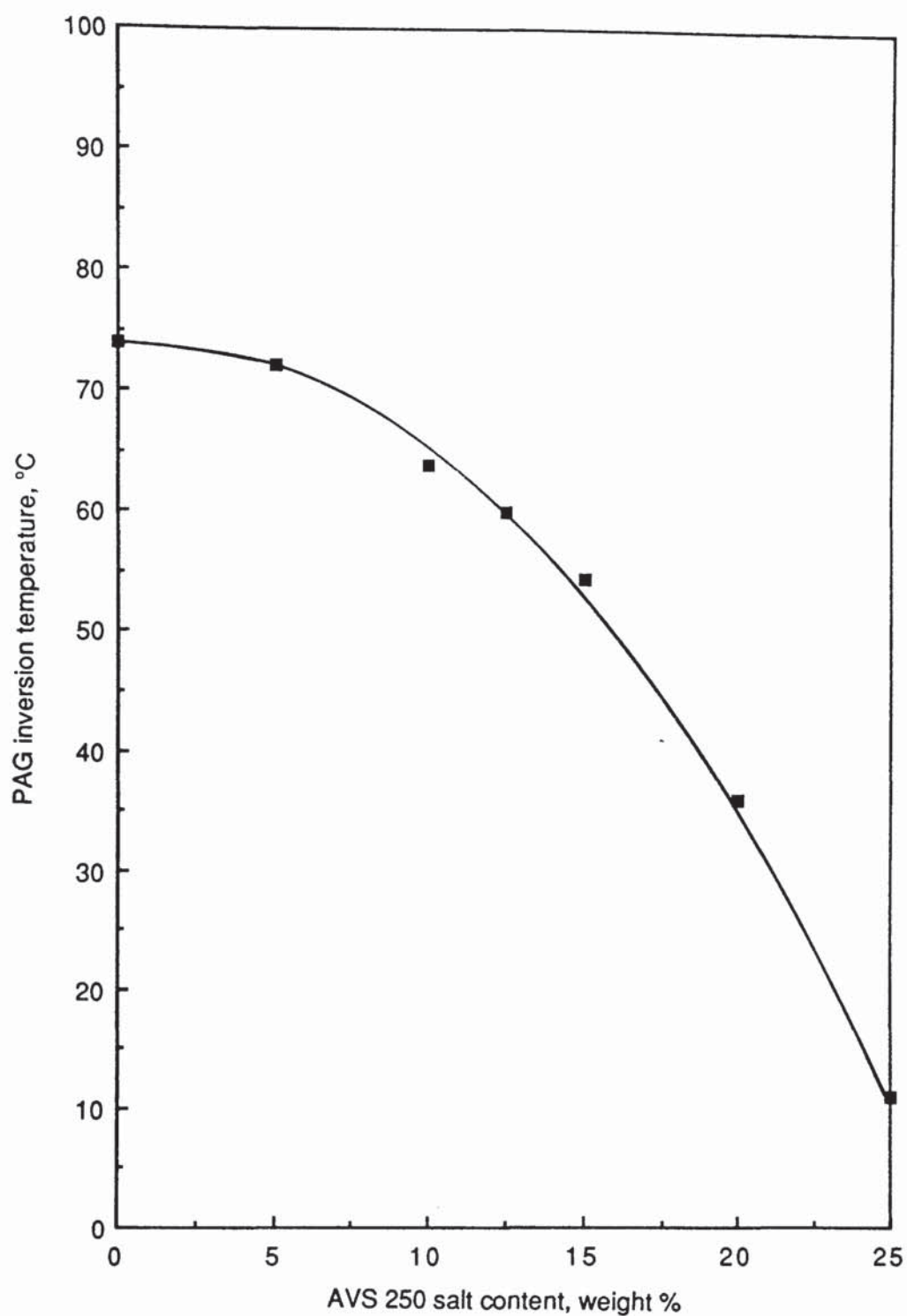


Figure 138. The effect of sodium nitrite/nitrate salt additions on the inversion temperature for 15 and 30 volume per cent PAG (Quendila PA) solutions.

Table 34. Cooling characteristics for 15 volume per cent PVP (Parquench 90) solutions contaminated with various sodium nitrite/nitrate salt additions (AVS 250). Test conditions 30°C and 0.5m/s agitation, probe preheat temperature 500°C.

| AVS 250 addition (wt %) | Time (s) to | | | Maximum cooling rate (°C/s) | Temp. of max ^m rate (°C) | Cooling rate at 300°C (°C/s) |
|-------------------------------|-------------|----------|----------|-----------------------------------|---|------------------------------------|
| | 400°C | 200°C | 100°C | | | |
| Uncontam. | 2.2±0.1 | 5.2±0.1 | 10.9±0.1 | 98 ± 1 | 408 ± 11 | 74 ± 1 |
| 0.5 | 2.8±0.1 | 12.8±0.1 | 21.4±0.2 | 59 ± 2 | 451 ± 10 | 20 ± 1 |
| 1.0 | 3.0±0.2 | 10.3±0.7 | 18.8±0.6 | 54 ± 1 | 456 ± 19 | 31 ± 5 |
| 2.5 | 2.6±0.1 | 7.7±0.1 | 14.0±0.2 | 70 ± 1 | 423 ± 21 | 42 ± 3 |
| 5.0 | 2.5±0.1 | 7.2±0.2 | 12.8±0.3 | 76 ± 1 | 424 ± 5 | 46 ± 2 |
| 10.0 | 2.2±0.1 | 5.6±0.1 | 11.0±0.2 | 103 ± 1 | 421 ± 22 | 67 ± 2 |
| 15.0 | 2.2±0.2 | 5.6±0.2 | 11.8±0.3 | 104 ± 1 | 425 ± 9 | 66 ± 3 |
| 20.0 | 2.2±0.1 | 5.6±0.1 | 11.4±0.3 | 102 ± 2 | 442 ± 11 | 63 ± 3 |
| 25.0 | 2.2±0.1 | 5.6±0.1 | 11.0±0.2 | 102 ± 1 | 430 ± 28 | 65 ± 3 |

The quench severity for the PVP solution decreased with the addition of up to 1 weight per cent salt. However, with further additions it increased until the critical level of around 10 weight per cent.

The polyacrylate solution exhibited an initial rapid decrease in quench severity with the addition of 0.5 weight per cent salt, followed by a less rapid progressive rise until the critical level was achieved (25 weight per cent).

Table 35. Cooling characteristics for 15 per cent polyacrylate (Aquaquench ACR) solutions contaminated with various sodium nitrite/nitrate salt additions (AVS 250). Test conditions 30°C and 0.5m/s agitation, probe preheat temperature 500°C.

| AVS 250 addition (wt %) | Time (s) to 400°C | Time (s) to 200°C | Time (s) to 100°C | Maximum cooling rate (°C/s) | Temp. of max ^m rate (°C) | Cooling rate at 300°C (°C/s) |
|-------------------------------|----------------------|----------------------|----------------------|-----------------------------------|---|------------------------------------|
| Uncontam. | 3.4±0.2 | 17.2±0.2 | 28.1±0.3 | 50 ± 1 | 456 ± 6 | 15 ± 1 |
| 0.5 | 2.5±0.1 | 7.7±0.2 | 17.5±0.8 | 84 ± 1 | 410 ± 1 | 56 ± 1 |
| 1.0 | 2.5±0.1 | 6.9±0.1 | 15.9±0.1 | 85 ± 4 | 409 ± 8 | 59 ± 1 |
| 2.5 | 2.4±0.1 | 6.7±0.1 | 15.7±0.2 | 88 ± 3 | 425 ± 10 | 60 ± 1 |
| 5.0 | 2.3±0.1 | 6.7±0.1 | 15.5±0.2 | 89 ± 1 | 395 ± 2 | 60 ± 2 |
| 10.0 | 2.2±0.1 | 6.9±0.3 | 15.1±0.8 | 91 ± 1 | 423 ± 8 | 48 ± 1 |
| 15.0 | 2.4±0.1 | 6.7±0.1 | 14.5±0.2 | 93 ± 2 | 421 ± 8 | 54 ± 1 |
| 20.0 | 2.4±0.1 | 6.3±0.1 | 13.3±0.6 | 93 ± 1 | 410 ± 9 | 56 ± 2 |
| 25.0 | 2.2±0.1 | 6.0±0.1 | 13.2±0.5 | 98 ± 3 | 419 ± 17 | 64 ± 2 |

4.11 Drag-Out

The post quench weight gain of the arbitrary test piece (previously shown in *Figure 73*) was used to compare the amount of drag-out for each representative polymer. *Figure 139* shows the amount of drag-out for 5, 15 and 25 per cent solutions of each polymer, tested at 30°C in both the static and agitated condition. Each result is the mean figure from five tests. *Table 36* lists the standard deviations for this data. To put these results into perspective, static water at 30°C resulted in a drag-out of 40 ± 2mg, whereas a static normal speed quench oil (Fenso 40) at 40°C produced a figure of 137 ± 20mg. The histogram (*Figure 139*) indicates that the level of drag-out increased as the concentration of the solutions was raised and that agitation reduced the drag-out, particularly for high concentrations. The polyacrylate solutions had

higher levels of drag-out when compared with the PAG, which in turn had higher levels than the PVP.

Table 36. Drag-out for various quenchants.

| Sample | Drag-out (mg) |
|------------------------------|---------------|
| 5% PAG 30°C static | 48.0 ± 3.2 |
| 0.5m/s | 44.1 ± 1.1 |
| 15% PAG 30°C static | 90.5 ± 6.9 |
| 0.5m/s | 67.5 ± 4.4 |
| 25% PAG 30°C static | 156.0 ± 16.0 |
| 0.5m/s | 114.4 ± 2.1 |
| <hr/> | |
| 5% PVP 30°C static | 42.2 ± 2.9 |
| 0.5m/s | 41.6 ± 4.4 |
| 15% PVP 30°C static | 80.7 ± 5.6 |
| 0.5m/s | 57.2 ± 0.9 |
| 25% PVP 30°C static | 128.6 ± 10.4 |
| 0.5m/s | 105.8 ± 2.8 |
| <hr/> | |
| 5% Polyacrylate 30°C static | 237.1 ± 29.0 |
| 0.5m/s | 185.7 ± 16.6 |
| 15% Polyacrylate 30°C static | 371.4 ± 18.0 |
| 0.5m/s | 214.8 ± 11.3 |
| 25% Polyacrylate 30°C static | 585.1 ± 42.5 |
| 0.5m/s | 281.3 ± 20.3 |
| <hr/> | |
| Distilled water 30°C static | 40.0 ± 2.0 |
| <hr/> | |
| Quench oil 40°C static | 137.3 ± 19.6 |

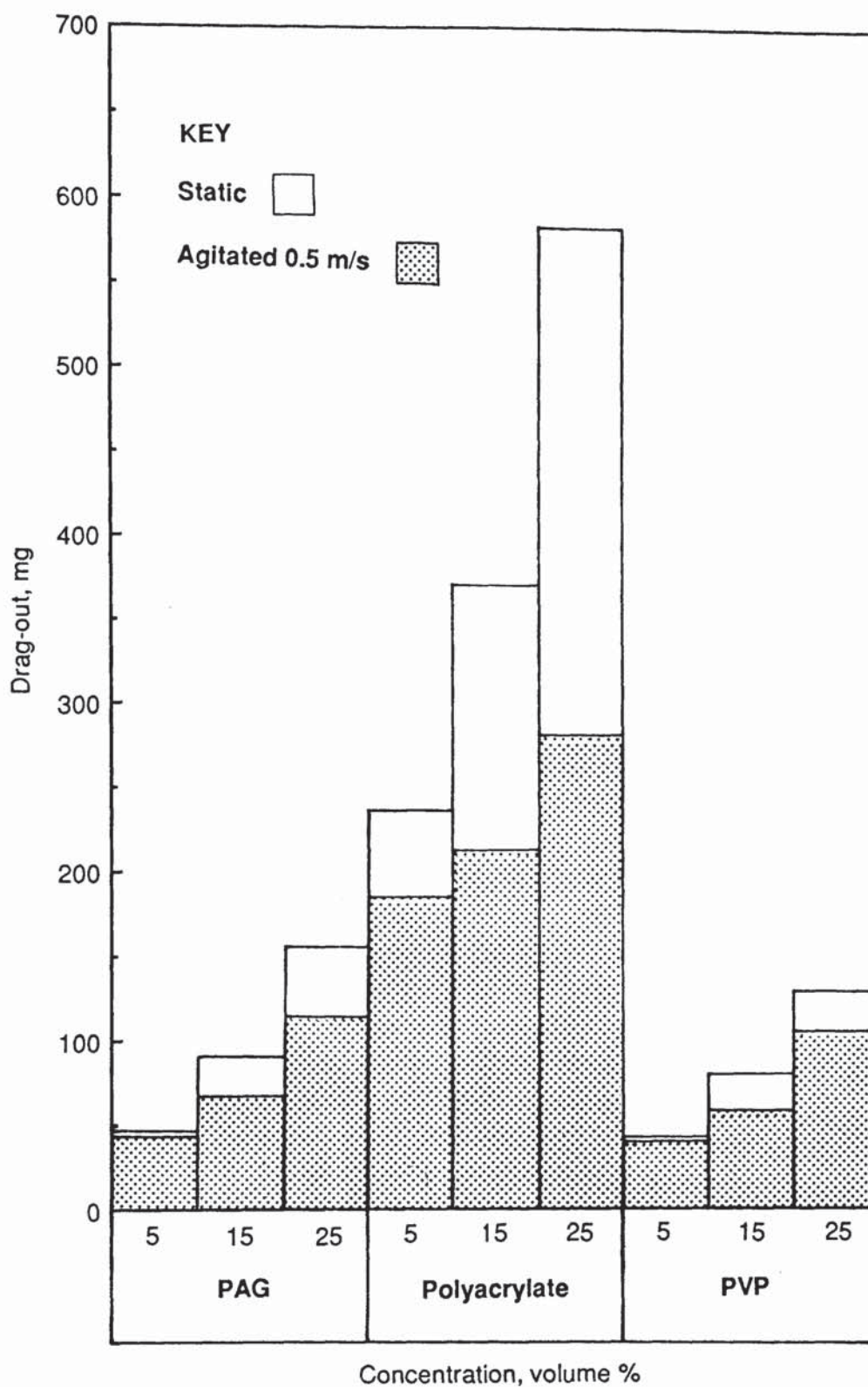


Figure 139. Results of drag-out experiment for representative polymer quenchant solutions of various concentrations at 30 °C in both the static and the agitated conditions.

4.12 Quenchant Hardness and Residual Stress Data.

Typical examples of the (211) martensite/ferrite X-ray diffraction profiles, obtained for the heat treated 080H41 steel specimens (*Figure 74*), are given in *Figures 140 to 143*. The intensity of the diffraction peaks was always greater at $\psi = 45^\circ$. This is as would be expected since the parafocus technique was employed and the focal length of the diffracted beam decreases as ψ increases (*Figure 75*). The diffraction line profile for the annealed specimen exhibited a clearly resolved K_α doublet as seen in *Figure 40*. In this case the surface residual hoop macrostress was found to be 78 ± 2 MPa when using the K_{α_1} peak for the calculation. This specimen had a core hardness of 176HV₃₀.

The breadth of the diffraction profiles for the specimens which had been quenched into each of the representative polymer quenchants at the standardized conditions (*Figures 141 to 143*) reflected the severity of the quenches. The peak breadth is related to non-uniform microstrain which is proportional to the hardness. For example, the peaks for the specimen quenched into the agitated PVP solution (*Figure 142*) were much broader than those for the polyacrylate (*Figure 143*). The corresponding core hardness values were 579 and 422HV₃₀ respectively.

Table 37 lists the calculated surface residual hoop macrostresses together with the measured core and near surface hardness values for each quenched specimen. The stress results are the average values from at least duplicate tests, the hardness values the mean from five impressions. Tensile residual macrostresses were developed in the surface of each specimen. These stress results can only be considered as comparative, since published values for the steel's elastic constants were used in the calculations, and no corrections made to take into account the curvature of the specimens. Also included in *Table 37* are the quenchant maximum cooling rates and cooling times to 360°C (which corresponds with the M_s temperature for this steel) measured using the Wolfson Engineering Group test. It is clear from this data that as the quench severity increased, so in turn did the resulting hardness and stress. The highest stress, $265 \pm$

19MPa was generated at the surface of the 40°C static water quenched bar, this specimen also had the highest core hardness (657HV₃₀). The specimen quenched into the distilled water at 30°C suffered longitudinal cracking. Since the section size for these specimens was approaching the maximum for through hardening, this cracking is not surprising. Thelning⁽⁷⁴⁾ outlined that specimens within this critical size range are susceptible to longitudinal cracks which emanate from the surface. This is because tensile stresses exceeding the tensile strength of the steel build up in these outer layers. High cooling rates and surface stress raisers increase the likelihood of such cracking. However, the magnitude of the measured stresses was lower than that anticipated for exceeding the tensile strength of untempered martensite.

Table 37. Surface residual hoop stress and hardness data for 12.5mm diameter 080H41 cylinders quenched under various conditions, including selected Wolfson quench test data.

| Sample | Surface residual hoop stress (MPa) | Hardness (HV ₃₀) near core surface | | Maximum cooling rate (°C/s) | Cooling time (s) to 360°C |
|--------------------------------|------------------------------------|--|-----|-----------------------------|---------------------------|
| 15% PAG 30°C | | | | | |
| static | 219 ± 6 | 564 | 554 | 119 ± 3 | 9.9 ± 0.7 |
| 0.5m/s | 241 ± 3 | 606 | 586 | 154 ± 1 | 7.1 ± 0.3 |
| 15% PVP30°C | | | | | |
| static | 207 ± 10 | 537 | 517 | 112 ± 3 | 10.5 ± 0.5 |
| 0.5m/s | 242 ± 11 | 594 | 579 | 162 ± 3 | 5.2 ± 0.3 |
| 15% polyacrylate | | | | | |
| 30°C static | 101 ± 4 | 290 | 283 | 56 ± 2 | 24.4 ± 2.1 |
| 0.5m/s | 191 ± 4 | 452 | 422 | 90 ± 3 | 10.8 ± 0.5 |
| Distilled water 40°C static | 265 ± 14 | 671 | 657 | 192 ± 4 | 4.7 ± 0.5 |
| Quench oil 40°C static | 147 ± 3 | 427 | 413 | 70 ± 1 | 19.3 ± 0.8 |

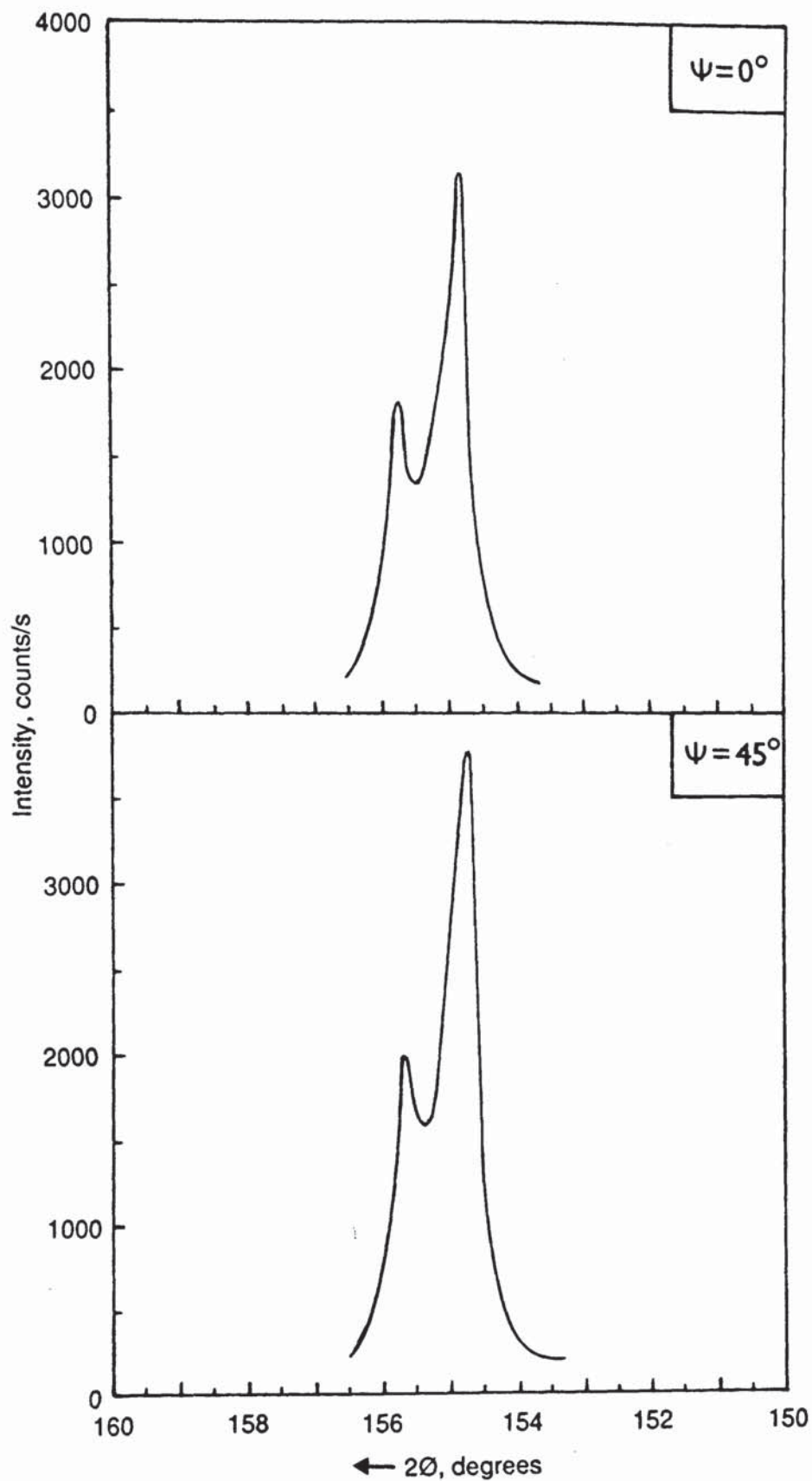


Figure 140. Chromium K_{α} diffraction profiles from the body-centred cubic 211 crystallographic planes for the fully annealed 12.5mm diameter 080H41 specimen at orientations $\psi = 0$ and 45° .

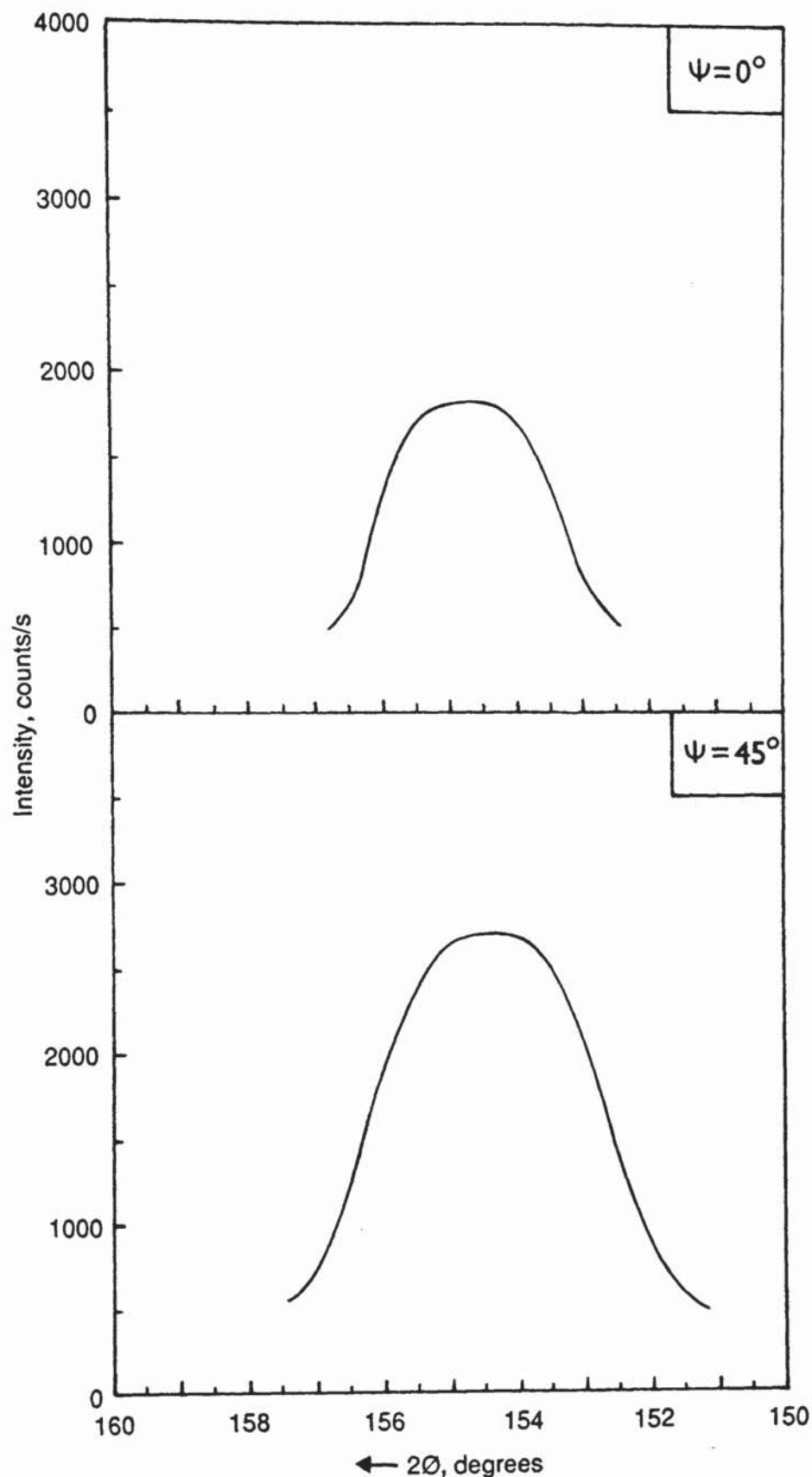


Figure 141. Chromium K_{α} diffraction profiles (at orientations $\psi = 0$ and 45°) from the body-centred cubic 211 crystallographic planes for the 12.5mm diameter 080H41 specimen quenched into a 15 volume per cent PAG (Quendila PA) solution at 30°C and 0.5m/s agitation

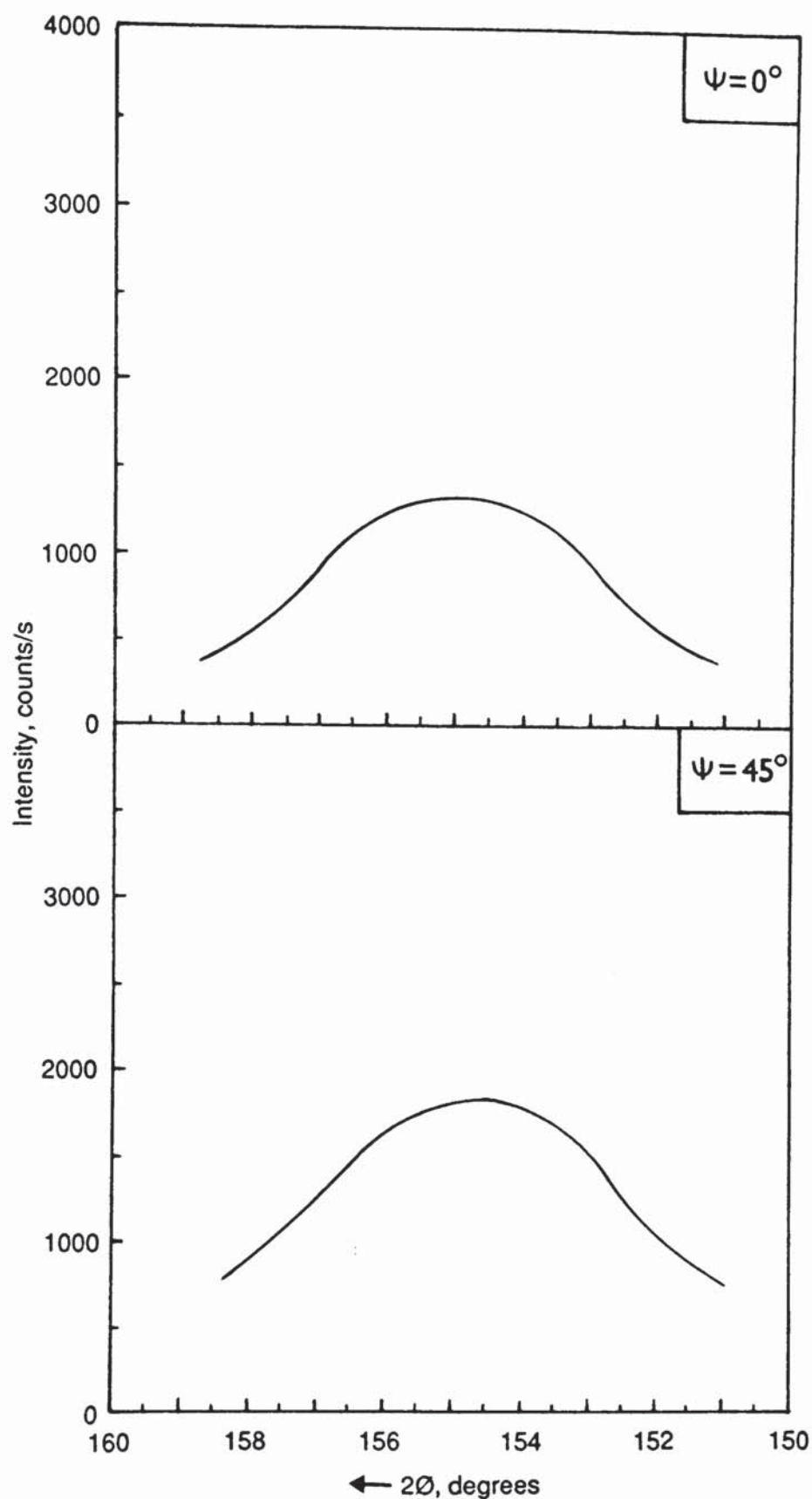


Figure 142. Chromium $K\alpha$ diffraction profiles (at orientations $\psi = 0$ and 45°) from the body-centred cubic 211 crystallographic planes for the 12.5mm diameter 080H41 specimen quenched into a 15 volume per cent PVP (Parquench 90) solution at 30 °C and 0.5m/s agitation.

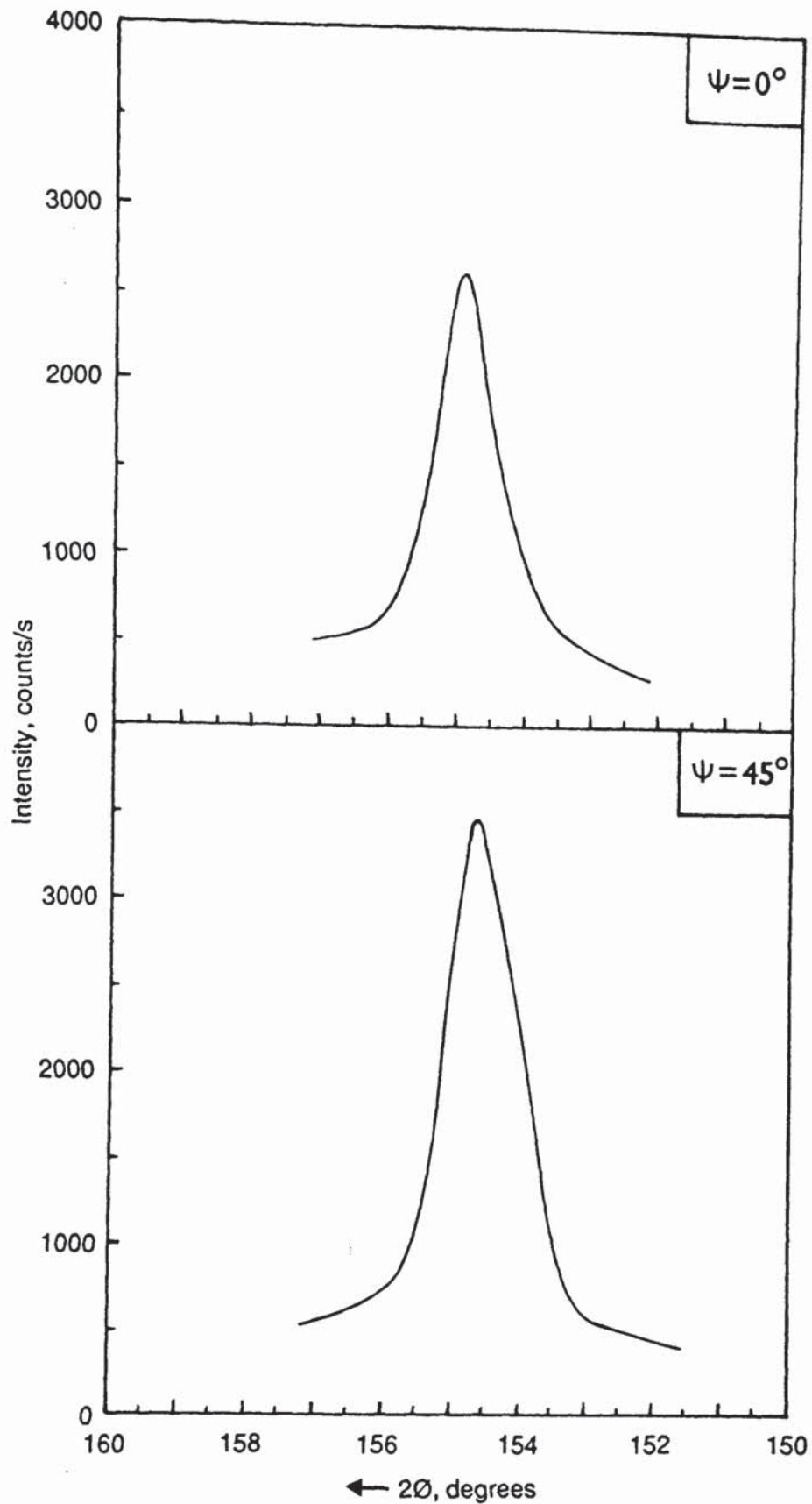


Figure 143. Chromium K_α diffraction profiles (at orientations $\psi = 0$ and 45°) from the body-centred cubic 211 crystallographic planes for the 12.5mm diameter 080H41 specimen quenched into a 15 volume per cent polyacrylate (Aquaquench ACR) solution at 30°C and 0.5m/s agitation.

4.13 Cooling Data for New Polymer Quenchant Systems.

Figures 144 to 146 show both the time-temperature and the cooling rate-temperature curves for the prototype quenchants incorporating poly(ethyloxazoline) with a weight-average molecular weight of 500,000. The parametric cooling data for these tests is given in *Table 38*.

Figure 144 represents a 2.25 weight per cent PEO_x solution tested at 30°C in both the static condition and agitated at 0.5m/s. This solution had a kinematic viscosity of 3.25mm²/s at 40°C and a refractometer reading of 2.6 Brix. Like the PAG's the PEO_x solutions exhibit inverse solubility in water. This particular solution had a cloud point of 59 ± 1 °C.

Figure 145 shows the static and agitated curves for the solution containing 1.5 weight per cent of a PVP:PEO_x mixture in the ratio 3:1. Parquench 90 was the PVP used in this formulation. The solution had a 40°C kinematic viscosity of 2.26mm²/s and a refractometer reading of 1.8 Brix.

Finally, the curves for the solution containing a 10 weight per cent mixture of PAG:PEO_x in the ratio 9:1 are given in *Figure 146*. The PAG product used in this mixture was Quendila PA. The kinematic viscosity for this solution was 5.17mm²/s at 40°C and it had a refractometer reading of 8.8 Brix. The inversion temperature for this solution was 45 ± 1 °C.

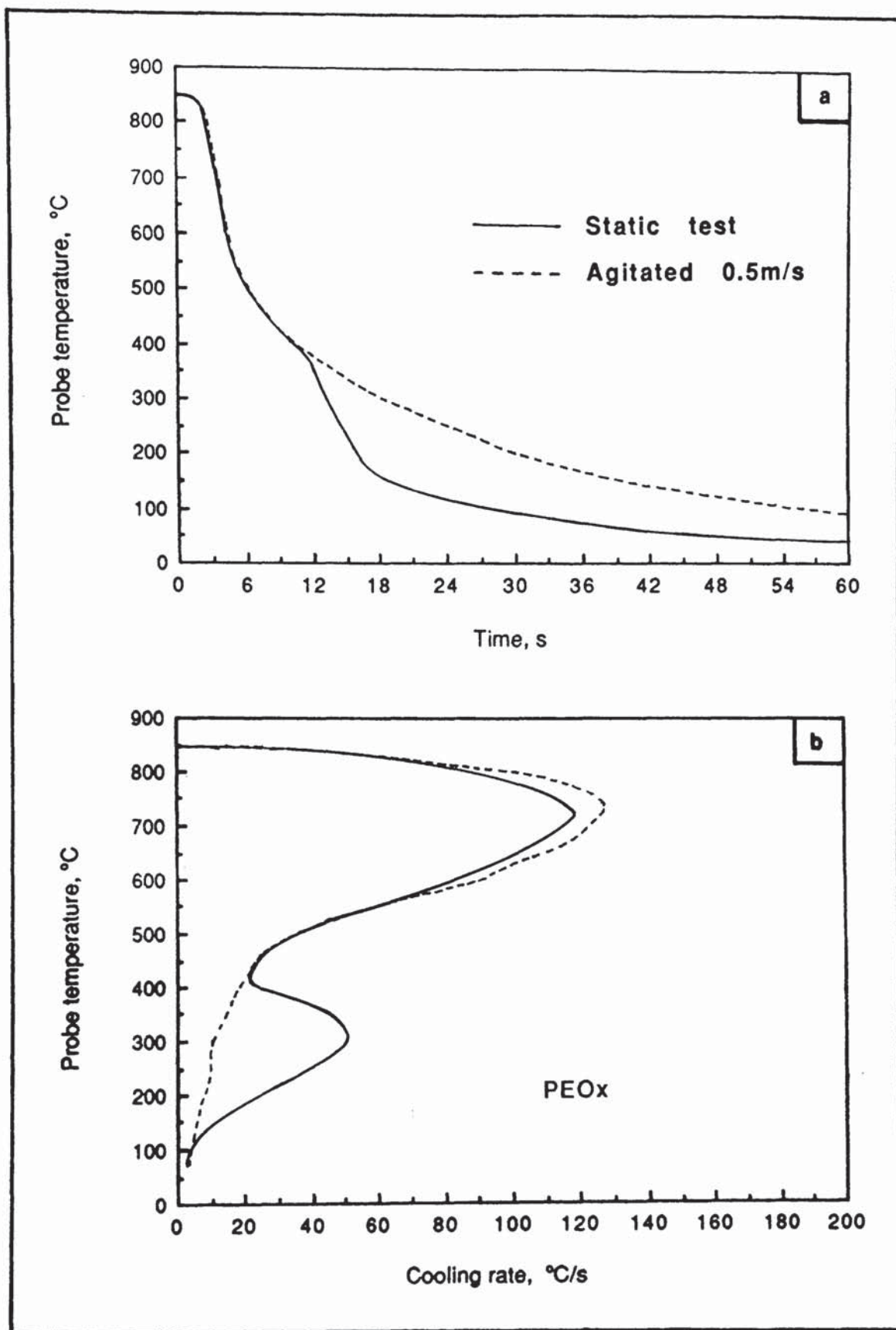


Figure 144. Cooling data for a 2.25 weight per cent solution of poly(ethyloxazoline) tested at 30 °C in both the static condition and 0.5m/s agitation.

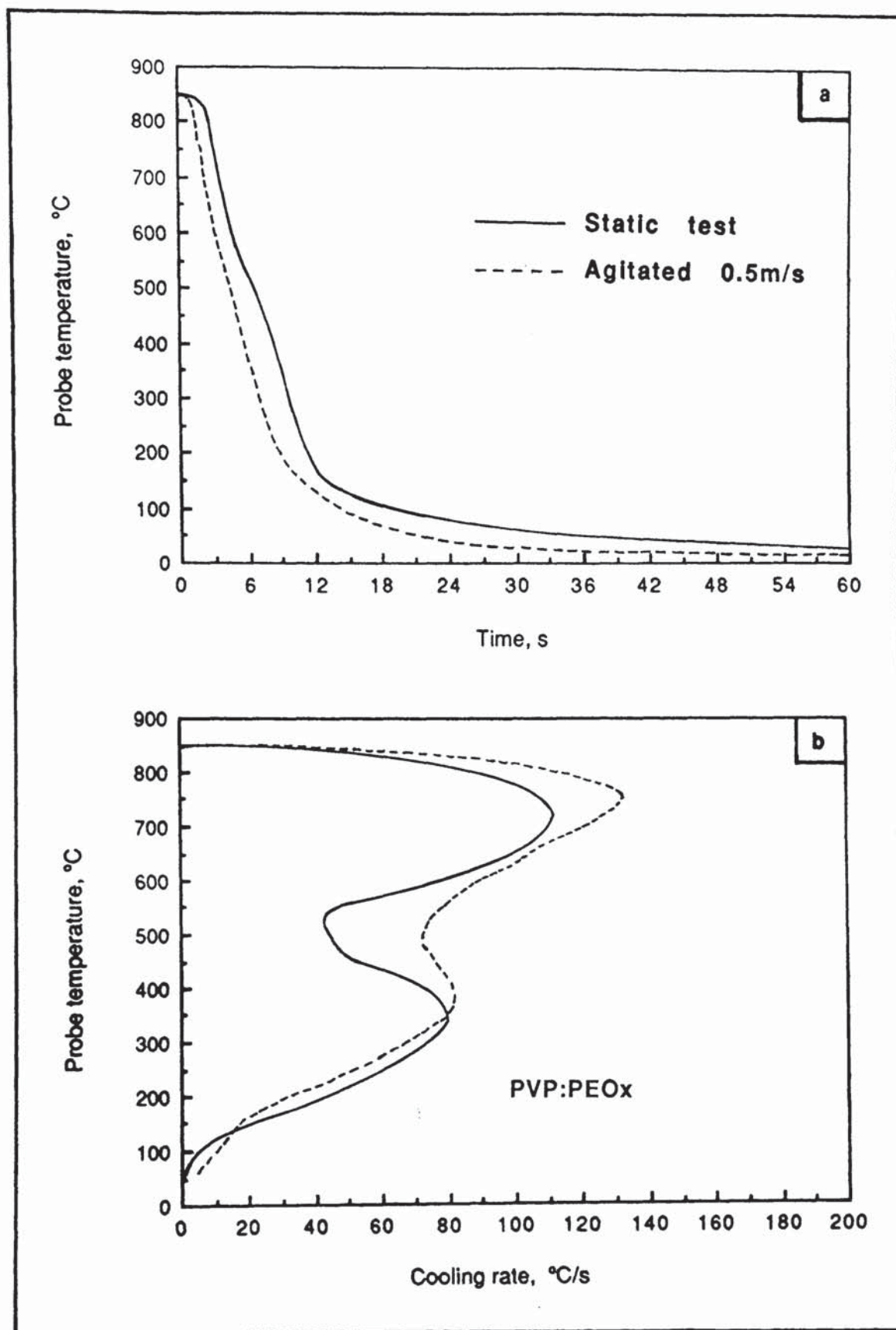


Figure 145. Cooling data for a solution containing 1.5 weight per cent Parquench 90: poly(ethyloxazoline) mixed in the ratio 3:1, and tested at 30 °C in both the static condition and 0.5m/s agitation.

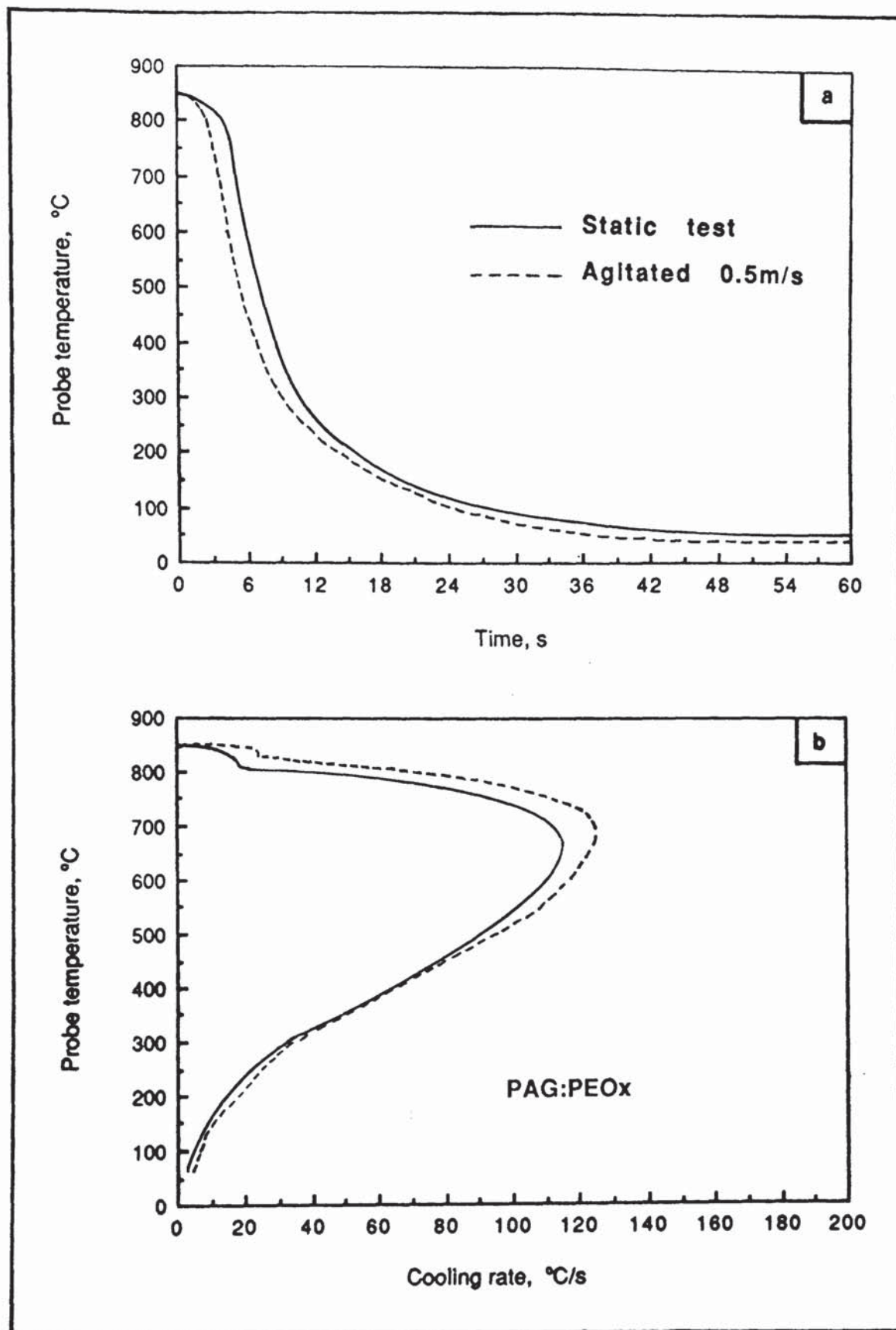


Figure 146. Cooling data for a solution containing 10 weight per cent of Quendila PA: poly(ethyloxazoline) mixed in the ratio of 9:1, and tested at 30 °C in both the static condition and 0.5m/s agitation.

Table 38. Cooling characteristics for the prototype quenchant solutions containing poly(ethyloxazoline)
($\bar{M}_w = 500,000$) tested at 30°C.

| Test | Time (s) to | | | Maximum cooling rate (°C/s) | Temp. of max ^m rate (°C) | Cooling rate at 300°C (°C/s) | Stage A/B | |
|--------------------------------------|-------------|----------|----------|--------------------------------------|--|---------------------------------------|---------------|----------------|
| | 600°C | 400°C | 200°C | | | | Temp. (°C) | Rate (°C/s) |
| 2.25wt% PEO _x | | | | | | | | |
| static | 4.0±0.1 | 10.0±0.8 | 15.2±1.3 | 119 ± 4 | 719 ± 8 | 50 ± 4 | - | - |
| 0.5 m/s | 4.3±0.1 | 10.7±0.1 | 32.2±0.8 | 126 ± 1 | 738 ± 17 | 10 ± 1 | - | - |
| 1.5wt% PVP:PEO _x (3:1) | | | | | | | | |
| static | 4.5±0.2 | 8.1±0.3 | 11.2±0.5 | 112 ± 2 | 711 ± 5 | 73 ± 1 | - | - |
| 0.5 m/s | 3.3±0.1 | 5.8±0.1 | 9.2±0.1 | 131 ± 3 | 751 ± 15 | 67 ± 1 | - | - |
| 10wt% PAG:PEO _x (9:1) | | | | | | | | |
| static | 6.0±0.6 | 8.3±0.6 | 15.9±0.8 | 115 ± 4 | 655 ± 17 | 30 ± 1 | 805 ± 21 | 18 ± 1 |
| 0.5 m/s | 4.7±0.2 | 7.0±0.1 | 14.6±0.1 | 124 ± 1 | 681 ± 7 | 29 ± 1 | 827 ± 8 | 24 ± 1 |

CHAPTER 5

5.0 DISCUSSION OF EXPERIMENTAL RESULTS

5.1 Development of an Agitated Quench Test System.

The principal characteristic of any quenchant is its ability to cool components consistently at the required rate in order to produce desired microstructures. Thus, when examining the behaviour of polymer quenchants, the most valuable test is that for assessing the cooling characteristics of the solutions. As described in Section 2.6.1.2, the most satisfactory technique for the routine evaluation of quench oils is the one developed by the Wolfson Heat Treatment Centre Engineering Group. However, since agitation is known to be necessary for the realistic evaluation of polymer quenchants, the first objective of this work was to develop a reliable means for providing a controllable forced convection current over the hot test probe surface.

Initial trials with impeller/baffle systems proved unsatisfactory (*Table 17*). Impeller speeds up to 1300rpm had little effect on the overall characteristics, whilst higher speeds of rotation resulted in air entrapment and foaming problems. Flat-bladed-impellers drive the fluid radially and are therefore fairly inefficient at providing effective circulation. Similar inconsistent trends were shown by Close,⁽²⁶⁾ who used an identical arrangement (*Figure 40*). The reduction in the maximum cooling rates at the higher stirrer speeds is believed to be due to cavitation and the consequent adsorption of insulating air bubbles on the hot metal surface. The purpose of the baffle is to inhibit tangential flow, to break the primary vortex and to reinforce the axial pumping effect. Pitched-bladed (marine) propellers are designed to pump fluid upwards near the shaft and downwards at their periphery. This explains why the 40mm diameter model boat propeller (preferred by Lakin⁽¹¹⁾) was more effective at increasing the maximum cooling rate. However, for both systems examined, the H-shaped baffle arrangement was ineffective. The circulation could be improved by using a close tolerance draft tube around the propeller, plus a number of supplementary directional baffles.

In essence, there are two types of fluid motion: laminar and turbulent flow. In laminar flow, the fluid advances in separate layers, "gliding" one over the other. Turbulent flow, on the other hand, is disorderly with small portions of fluid, known as eddies, moving about in a chaotic manner for a short period of time before losing their identity. A dimensionless parameter, known as the Reynolds Number, represents the ratio of inertial to viscous forces, and determines the stability of flow. The Reynolds number for fluid flow adjacent to a flat-bladed impeller is calculated using the following equation:⁽⁴⁴⁾

$$Re = \frac{N D^2}{\mu} \quad (32)$$

where N is the speed of rotation, D the impeller diameter and μ the kinematic viscosity of the fluid. For values of $Re > 10,000$ the flow is considered fully turbulent. Since the kinematic viscosity of the 20 per cent Quendila PA solution at 30°C was 6.26mm²/s, fully turbulent conditions were obtained adjacent to the 75mm diameter impeller at speeds above 668rpm. However, because of the inefficiency of the H-shaped baffle used, the turbulence eddies would have been dissipated rapidly, and the actual flow in the vicinity of the probe would have been much more stable.

The results shown in *Figure 93* illustrate that directional high-velocity fluid flow from a pump has a much more significant effect on the cooling characteristics, than agitation created using impeller/baffle systems. Fluid velocity is a much more objective means of quantifying agitation than quoting impeller speeds, the effects of which are highly dependent on the shape and size of the impeller and baffle and on the geometry of the quench tank used. Consequently, a pump/orifice system would appear to be a more suitable method for assessing the effects of agitation on polymer quenchants in a laboratory scale test.

In addition to the fluid velocity, the flow pattern is also very important. Horizontal flow with respect to the axis of the probe was found to be more effective in destabilizing stage A cooling than vertical flow. There are two explanations for this: firstly, the fluid flow impinges in a greater surface area of the probe and, secondly,

because of the non-ideal flow characteristics of viscous liquids, a turbulent wake would be formed along the surface of the probe furthest from the orifice. A critical fluid velocity to eliminate stage A heat transfer could be used as a parameter to characterize the effect of agitation on the cooling characteristics as was shown in *Figure 94*. However, certain polymers do not normally produce stage A cooling, and large flow rates would be required for other high-concentration polymer solutions, which would render the test unrepresentative of industrial conditions.

Table 18 listed the cooling data from the tests performed using the large scale pump system at West Bromwich College of Commerce and Technology (*Figure 41*). With this system, the probe was inserted into a tube through which the quenchant was pumped. The probe, therefore, formed an annulus with the outlet. The maximum cooling rate for the test solution was higher when using the larger diameter outlet tube for an equivalent 0.5m/s fluid velocity past the probe. This can be explained by examining the stability of the flow through the annuli. The Reynolds number for flow through an annulus is given by:⁽⁴⁴⁾

$$Re = \frac{D_c V}{\mu} \quad (33)$$

where D_c is the hydraulic diameter (which in this case equalled the internal diameter of the pump outlet minus the probe diameter), V the fluid velocity and μ the kinematic viscosity. Equation (33) was used to calculate the value of Re for each of the tests listed in *Table 18*. *Figure 147* shows the maximum cooling rates plotted as a function of Re . At a fluid velocity of 0.5m/s the value of Re for the 42mm diameter annulus was 2356; this compares with a figure of 998 for the 25mm annulus. Therefore, the fluid flow through the larger diameter annulus was less stable, thus explaining the increased maximum cooling rate. Increasing levels of turbulence occurred for values of Re greater than 2200. As the fluid velocity increased, so in turn did the maximum cooling rate. Surprisingly, the maximum rate increased more rapidly in the laminar flow region, the rate of increase slowing down with increasing turbulence.

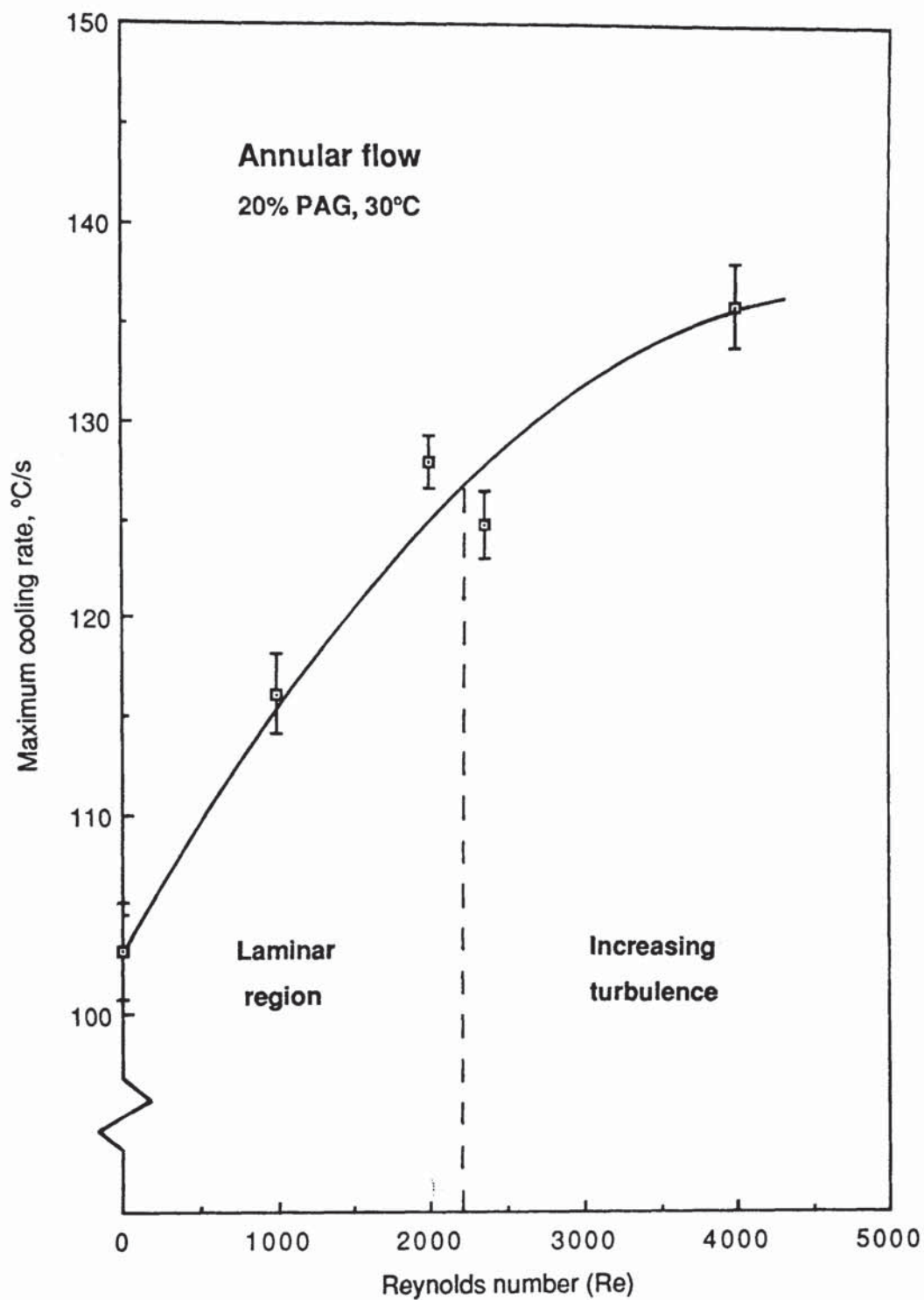


Figure 147. Maximum cooling rates for a 20 volume per cent PAG (Quendila PA) solution as a function of calculated Reynolds numbers for annular flow produced using the West Bromwich College of Commerce and Technology agitation system.

The calculated values of Re are all likely to be considerably lower than their true values because of the design of the quenching unit (*Figure 69*). The fluid flow through the outlet tube is unlikely to be laminar, even at low velocities. This is because the length of the outlet tube is less than twenty times its diameter, resulting in undeveloped flow. Considerable turbulence is also likely to result from the way in which the fluid flow from each of the pumps is forced to converge and its direction reversed, at the base of the unit.

This system offers the advantage that the actual velocity of the fluid flowing over the surface of the probe can be specified. However, it also has many shortcomings. The principal problem is the large volume of test sample required: over 25 litres. This obviously precludes its usage for routine laboratory scale testing. In addition, the close proximity of the outlet tube to the probe's surface is likely to produce unrealistic cooling characteristics, and prevents visual examination of the cooling mechanism.

Upon increasing the fluid velocity the maximum cooling rate was increased, the temperature of maximum rate decreased and stage A cooling was eliminated between 0.5 and 1.0m/s. There was little change in the cooling rate at 300°C. These trends are in agreement with the findings of Mason and Capewell⁽³⁴⁾ (*Figure 42*), who used this same system, and with the results from the earlier series of pump circulation tests which were conducted using the system shown in *Figure 68*. This prototype system was inconvenient to operate because the Charles Austen centrifugal pump was not self-priming. This problem was alleviated in the pump system finally chosen (*Figure 70*), by positioning the quench tank directly above the pump. The dimensions of the tank were those specified by the Wolfson Engineering Group for static oil testing.^(24,25) The system was portable and had a total capacity of 2 litres, which made it suitable for routine tests.

Vertical flow was preferred, since it produced a more symmetrical flow pattern around the probe. A fluid velocity of 0.5m/s was chosen as the optimum, since greater consistency in the cooling characteristics had been achieved at this speed, and it is within the range estimated for most industrial units. Obviously, in practice, the

flow conditions vary considerably from unit to unit and with position within the tank. The 25mm diameter outlet orifice size enabled a fluid velocity of 0.5m/s to be obtained for fluids with kinematic viscosities of up to 30mm²/s at 40°C. This enabled all the popular polymer quenchants to be tested over their normal range of concentration. The preferred probe height above the outlet was 25mm, which resulted in the thermocouple hot junction coinciding with the centre of the quenchant sample volume.

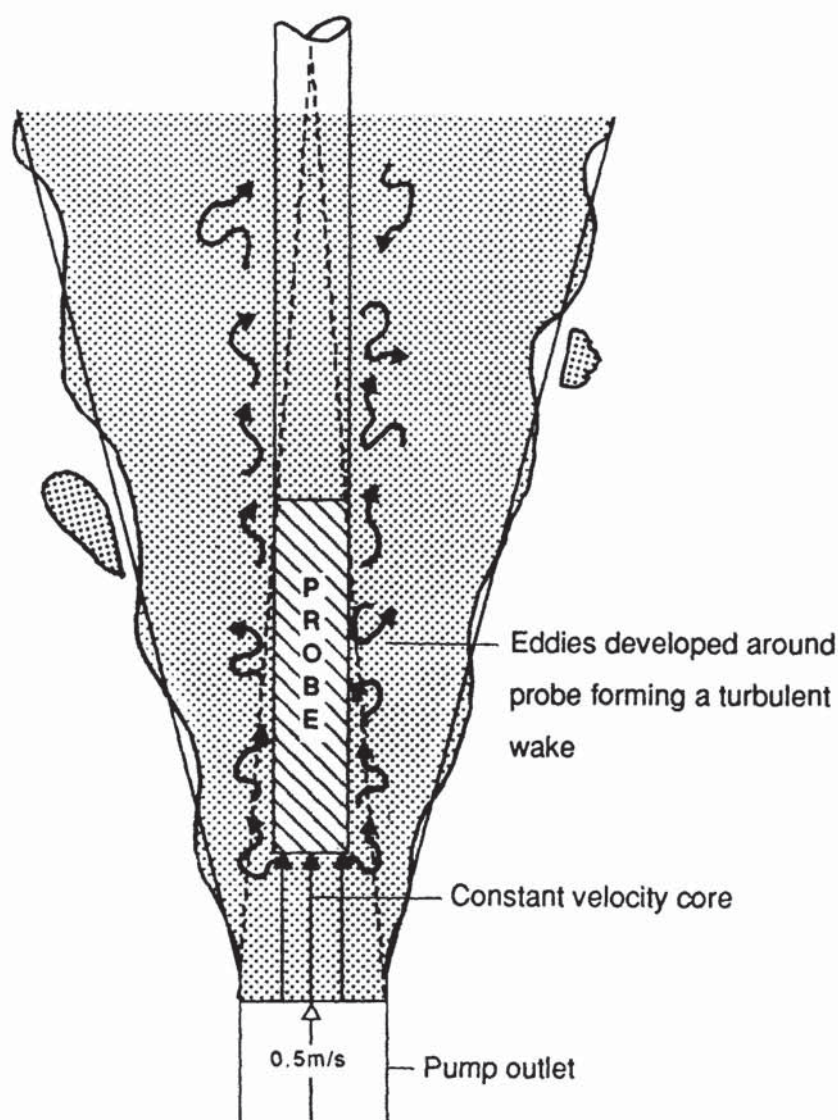


Figure 148. Schematic representation of the flow pattern seen in Plate 5 for a 15% PAG solution at 0.5m/s, illustrating turbulent flow establishment.

Figure 95 revealed a linear reduction in the cooling rate upon increasing the height of the probe, H , above the orifice. Lateral displacements from the geometric centre of the orifice, X , of up to 10mm resulted in only a slight reduction in the cooling rates (*Figure 96*). The decrease became much more pronounced for values of X greater than 10mm. These effects can be explained by examining the ink-injection flow visualization photograph, *Plate 5*, obtained using the representative PAG solutions at the standard conditions. This flow pattern is typical of a jet emerging from a submerged nozzle into a large volume of fluid. A schematic representation of the flow pattern is given in *Figure 148*. Shortly after emerging from the circular orifice, the jet entrains some of the miscible stationary liquid and expands at an angle of approximately 15° . It therefore can be seen that the jet of fluid no longer circumvents the base of the probe for values of X greater than 10mm. Consequently, it can be seen that precise positioning of the probe above the pump outlet is critical. This was achieved by the pneumatic probe transfer system.

The nature of the fluid flow around the hot probe obviously has a significant effect on the rate of heat transfer. The velocity of a fluid flowing past a solid object drops to zero at its surface, producing what is known as a "boundary layer"⁽⁴⁴⁾. The boundary layer is very important since it controls the major temperature and concentration changes. The optimum means of characterizing the level of agitation around the probe would be to quote a Reynolds number. However, the effectiveness of the agitation is going to vary from one position to the next on the probe's surface; a complete solution to this complex problem poses considerable mathematical difficulties. Nevertheless, it is possible to estimate a value of Re for the fluid flowing through the pump outlet tube using equation (3). The kinematic viscosities of the three representative 15 per cent PAG, PVP and polyacrylate solutions at 30°C were $5.40\text{mm}^2/\text{s}$, $3.85\text{mm}^2/\text{s}$ and $17.20\text{mm}^2/\text{s}$ respectively. Consequently, at the standard test fluid velocity of 0.5m/s , the Reynolds number for the PAG was 2300, for the PVP 3300 and for the polyacrylate 730. These results are all likely to be lower than the true values, firstly because the polymer solutions exhibit pseudoplastic flow characteristics and, secondly, because the flow in the pump outlet tube is not fully developed (since the tube length is less than twenty times its diameter in order to

reduce the scale of the system.). These results highlight the fact that although the fluid velocities are identical, the stability of the flows are different, due to variations in the fluid viscosities. Therefore, in order to truly compare the cooling characteristics of polymer quenchants, the flow conditions around the probe should be the same for each solution. Consequently, when standardizing a pump agitation system precise details must be given regarding the specification of not only the pump, but also the geometry of the quench tank and its associated pipework.

The value of Re for the PAG solution flowing through the outlet tube was 2300. The transition from laminar to turbulent flow occurs for values of Re greater than 2200, with full turbulence occurring when Re exceeds 10,000. This result is in agreement with *Figure 148 (Plate 5)*, since an essentially laminar (parallel) jet of fluid can be seen progressing from the outlet for a distance of approximately 5mm. However, this flow arrangement satisfies the three main criteria for inducing turbulence:⁽⁴⁴⁾

- (a) Fluid flowing rapidly past a solid surface.
- (b) Fluid flowing rapidly into a slow moving or stationary fluid.
- (c) A solid object and fluid in relative motion, producing form drag and eddy shedding.

A region of turbulent flow establishment around the probe can be seen clearly in *Figure 148 (Plate 5)*. The profile of the flow around the probe is typical of a submerged free turbulent jet; but this jet cannot be considered to be totally "free" since its cross-sectional area is greater than 20 per cent of that of the tanks, by the time it is parallel with the probe's midlength position. At the point at which the jet impinges on the base of the probe it may still be considered to be free. Consequently, the fluid velocity of the jet at the point of impingement will still equal 0.5m/s, since there is a constant velocity core which extends to about 6.4 orifice diameters,⁽⁴⁴⁾ as shown in *Figure 148*.

The design of this preferred agitation system ensures a region of turbulent flow establishment around the probe for normal-concentration polymer quenchant solutions tested at 0.5m/s. This is believed to be a realistic test, although the actual stability of

the fluid around the probe will depend upon its viscosity. Truly equivalent levels of agitation would require the testing of polymer solutions of identical apparent viscosity at a particular fluid velocity, or the development of fully turbulent conditions. The latter could only be achieved by using very large pumps capable of generating sufficiently high flow-rates. Obviously this is totally impractical for the routine analysis of quenchant samples.

5.2 Commercial Polymer Quenchants Examined.

The characteristics of polymer quenchant products of the same basic polymer type, as supplied by different manufacturers, will vary. This was clearly demonstrated in *Table 12* and *Figures 98 to 106*. These differences in cooling performance can be explained by variations in the molecular architecture of the polymer itself, and by the different levels and types of additives used. The molecular weight distribution of the polymer obviously has a profound effect on its characteristics, as does its configuration and its conformation in solution. Commercial polymers are polydisperse and therefore no two batches of polymer quenchant will have identical characteristics. Nevertheless, by carefully controlling the polymerization reaction, the manufacturers of the base polymers can usually control the viscosity of the product to within a few percent.

Due to the high inherent viscosity of the neat polymers, water is always included in the commercial concentrate to aid subsequent further handling and dilution. The polymer concentrates also contain some form of corrosion inhibitor. Other additives which may be used in the concentrate formulation include anti-oxidants, defoamers, buffers and bactericides. The level of water in the as-supplied concentrate depended on the type of polymer and varied between proprietary products. If, for example, the solids-content levels in *Table 12* are examined, it is clear that the PVP concentrates contained less polymer than the polyacrylates, which in turn contained less than the PAG's. This was reflected by the slopes of the refractometer calibration plots for each of the representative polymer quenchants examined (*Figure 91*).

Higher-molecular-weight polymers are required at lower concentrations to produce equivalent solution viscosities. This can be understood by considering a schematic representation of the polymer molecules as flexible randomly-coiled chains in solution. The viscosity of the polymer solution is related to the number of chain entanglements between separate molecules. In dilute solutions the chains will be relatively far apart, but as the polymer concentration is raised there will be a corresponding increase in the solution viscosity due to an increased number of chain entanglements. Obviously, as the molecular weight is increased the chains become longer and there is a greater statistical chance of effective entanglement. The effect of molecular weight on the solution viscosity for linear chains was given in equation (18).

The GPC analysis for the PAG's revealed that they had polystyrene-equivalent weight average molecular weights ranging from about 12,000 to 20,000. The Quendila products had nearly equivalent \overline{M}_w values around 12,500, whilst the result was nearer 14,000 for Aquaquench 1250 (*Table 13*). The chromatogram for this last product (*Figure 79*) exhibited a lower molecular weight hump corresponding to the addition of a second polymer with a \overline{M}_w value around 7000. This product had the broadest molecular weight distribution of all the PAG's tested, with a polydispersity ratio of 3.67. Aquaquench 1250 is therefore believed to be a mixed (Type II) polymer system. The lower molecular weight addition is unlikely to have a significant effect on this product's cooling characteristics.

Although not absolute, this molecular weight data for the PAG's is in agreement with Blackwood and Cheesman's patent,⁽⁹¹⁾ which stated preferred average molecular weights between 12,000 and 14,000. The more recently introduced PAG quenchants such as Breox NF-18 and Ucon E had higher polystyrene-equivalent \overline{M}_w values of nearly 18,000 and 20,000 respectively. The former had the narrowest molecular weight distribution with a polydispersity ratio of 1.95, whilst the latter exhibited a distinct lower molecular weight tail (*Figure 80*). The latest patent filed by Union Carbide Corporation regarding PAG quenchants, disclosed preferred \overline{M}_n values from about 10,000 to 15,000.⁽¹⁶²⁾ The measured polystyrene-equivalent \overline{M}_n for Ucon E

was 9580. The Ucon E concentrate had the lowest solids-content figure (40 weight per cent) of all the PAG products examined, and yet exhibited the slowest cooling characteristics in the comparative quench tests (*Figure 102*). This is believed to be due to its higher molecular weight, combined with a modification to its structure to incorporate hydrophobic capping groups as described in European patent 206,347.⁽¹⁶²⁾

Breox NF-18 had the highest maximum cooling rate of the PAG's examined in the comparative tests, but its rate of cooling at 300°C was almost equivalent to that of Quendila PA and slower than either Quendila PHT or Aquaquench 1250. The different trends shown by Breox NF-18, when compared with the earlier Quendila products, can be attributed to the former's higher molecular weight, its lower solids-content and its different corrosion inhibition mechanism. Sodium nitrite is still the most common corrosion inhibitor. However, on the grounds of health and safety, the more recent products such as Breox NF-18 contain nitrite-free systems such as those based on amines. Sodium nitrite is a cathodic inhibitor and operates by mopping up the oxygen and suppressing the cathodic corrosion cell reaction. Organic amine inhibitors, on the other hand, are strongly adsorbed onto the metal at the anodic sites. Furthermore, all polymer quenchants are maintained slightly alkaline in order to reduce corrosion problems.

The PVP products had much higher molecular weights than the PAG's and lower solids-contents. The K-value of the PVP used in the Parquench concentrates is incorporated in the product tradename. This was confirmed using Fikentsher's equation (29). The Parquench 60 product was found to have a K-value of 60.4, whilst that for Parquench 90 was 88.7. The limiting viscosity numbers measured for these PVP's were in fairly close agreement with published data. The values of $[\eta]$ for Parquench 60 and 90 were found to be 0.74dl/g and 1.59dl/g respectively; these figures compare with published values of 0.76dl/g for K-60 and 1.61dl/g for K-90 grade PVP's.⁽¹⁶³⁾ The measured values of $[\eta]$ are both slightly lower than the published figures. This is most probably due to the other additives present in the quenchant concentrate formulation. These additives could be present at levels of up to

several per cent of the total solids-content of the concentrate, and were not accounted for when preparing the solutions for the viscosity number determinations.

There is considerable confusion in the literature regarding the values of the Mark-Houwink-Sakurada parameters for PVP's in aqueous solution. The two main suppliers of PVP, GAF and BASF have until recently reported different values of \bar{M}_v for products of equivalent K-value. GAF originally employed values of κ and a in equation (18) of 1.6×10^{-5} and $a = 0.7$. Both manufacturers have recently elected to adopt the latter constants.⁽¹⁶³⁾ Table 39 gives \bar{M}_v values using both sets of constants for the products examined during this work.

Table 39. Viscosity-average molecular weight data for the PVP's examined during this work.

| PVP sample | $[\eta]$ (dl/g) | Old GAF \bar{M}_v | New GAF \bar{M}_v |
|------------------------------------|-----------------|------------------------|------------------------|
| Parquench 60 | 0.74 | 152,566 | 208,314 |
| Parquench 90 | 1.59 | 356,886 | 621,214 |
| Aged Parquench 90 (100kg/litre) | 0.68 | 138,885 | 184,611 |

Haaf et al⁽¹⁶⁴⁾ have claimed K-90 grade PVP has a \bar{M}_w of 1.1 million, and a \bar{M}_n of 150,000. The GPC analysis for Parquench 90 revealed a polystyrene-equivalent \bar{M}_w of 74,560 and a corresponding \bar{M}_n of 25,040. These relative values are obviously considerably lower than the absolute figures claimed by Haaf et al for an equivalent K-90 grade PVP. The discrepancy between these results is not surprising in light of the fact that the molecular weights obtained during this work were measured using GPC columns which had been calibrated for polystyrene in THF. Furthermore, the PVP samples were eluted using chloroform as the solvent. The results do nevertheless reflect the relative distributions for these PVP products. For example, the limiting viscosity number data revealed that Parquench 60 had a value of \bar{M}_v around

66 per cent lower than Parquench 90. The GPC analysis was fairly close since it showed that Parquench 60 had a 63 per cent lower \bar{M}_w , and a 59 per cent lower \bar{M}_n compared with Parquench 90. The Parquench 90 molecular weight distribution was slightly broader than that for Parquench 60, as indicated by its polydispersity ratio which was 0.27 higher (*Table 13*). This would be anticipated because higher molecular weight PVP chains are known to exhibit more branching due to grafting during polymerization.⁽¹⁶⁴⁾ The solids-content value for each of the PVP products was about 10 weight per cent. Therefore, the results from the comparative quench tests *Figures 103* and *104* are for virtually equivalent concentration solutions. The maximum cooling rates for the higher molecular weight Parquench 90 solution were approximately 7.5 per cent lower than those for Parquench 60, the rates at 300°C about 20 per cent lower.

The industrially approved manner of quoting polymer quenchant concentrations as a volume percentage of the as-supplied concentrate is misleading. This is because the actual solids-content values for the concentrates vary considerably, as seen in *Table 12*. When the kinematic viscosity of true 1.5 weight per cent solutions of each representative product were measured at 40°C, it was discovered that the polyacrylate had the highest value (6.65mm²/s), whilst the PVP had a value (2.67mm²/s) nearly three times higher than the PAG (0.94mm²/s). Generally higher molecular weight polymers produce more viscous solutions with correspondingly reduced cooling rates. Thus when comparing the true polymer concentrations for the representative solutions with the measured cooling characteristics, it would appear that the polyacrylate is likely to have the highest molecular weight. However, the situation is more complex, since sodium polyacrylates are extremely effective aqueous thickening agents.⁽¹⁶⁵⁾

Unlike PAG's and PVP's which are nonionic, sodium polyacrylates (*Figure 49*) are anionic or negatively charged in solution. This type of polymer quenchant therefore acts as a polyelectrolyte, which means that its viscosity in solution varies in a complex fashion with pH. When aqueous solutions of polyacrylic acid are neutralized by the addition of sodium hydroxide, the molecules expand with an enormous increase in

solution viscosity. This is because ionization occurs producing a combination of polymeric ions and sodium counterions. As the number of ionized carboxyl groups increases, the polymer chain uncoils due to mutual repulsion of the charges and the solution viscosity increases. The viscosity reaches a maximum near the neutral point. The increase in viscosity with neutralization is greater the higher the molecular weight, and with polyacrylic acid, the greater the isotacticity⁽¹⁶⁶⁾. On adding excess sodium hydroxide a build-up of sodium counterions occurs, with a gradual repression of the effective ionization of the polymer chain resulting in a slow decrease in the viscosity.

When measuring the molecular weight of polyelectrolyte, the result will be affected by the ambient ionic atmosphere in which the determinations are made. The \bar{M}_v value for Aquaquench ACR was found to be 245,884 when using the Mark-Houwink-Sakurada constants given in *Table 5*, for sodium polyacrylate dissolved in 1.25M aqueous sodium thiocyanate and tested at 30°C. These conditions result in the polymer assuming its so called "theta-state", where it behaves like an ideal statistical coil.⁽¹⁵¹⁾ The exponent, a , in equation (18) is equal to 0.5 for a polymer in the theta-state, and the value of κ remains virtually constant over the whole molecular weight range. Thus it can be seen that the representative polyacrylate quenchant examined (Aquaquench ACR) had a molecular weight higher than any of the PAG's tested, marginally higher than the PVP product Parquench 60, yet lower than Parquench 90. However, for a given concentration it produced a solution with a much higher viscosity because of its polyelectrolyte character.

5.3 Cooling Mechanism For Polymer Quenchants.

The traditional theory of quenching involves 3 distinct stages of heat transfer, as described in Section 2.4. However, this is an oversimplification when the quenching liquid is not pure, as is clearly the case with polymer quenchants. Additives to the liquid affect the stability, and hence the duration, of each stage of cooling. When salt, for example, is added to water it reduces the duration of stage A cooling because

recrystallization occurs on the surface of the hot metal, providing enhanced nucleation sites for boiling. Conversely, water-soluble polymer additions stabilize stage A by encapsulating the steam blanket within a polymer-rich film. The way in which the polymer-rich film is formed depends on the structure of the polymer. For polymers such as PVP and polyacrylate, which exhibit normal solubility in water, localized evaporation occurs adjacent to the hot metal surface, producing a polymer concentration gradient which increases towards the liquid-gas interface. As the concentration increases, so too does the level of chain entanglement until eventually a stage is reached where a temporary three-dimensional entanglement network is created. At this point, a "gel-like" polymer-rich film is formed: this extends to the vapour blanket interface.

With PAG quenchants, the polymer-rich film is actually precipitated from solution at a critical temperature below the boiling point of water. This inverse solubility phenomenon is not well understood, and will now be considered in more detail.

5.3.1 PAG Inverse Solubility Phenomenon. Inverse solubility occurs quite generally with polymer solutions at temperatures above the boiling point of the solvent, and at pressures of several hundred kPa. Polymer-solvent systems that invert at lower temperatures are much more rare. The most commonly reported form of inverse solubility phenomenon is the cloud point exhibited by certain nonionic surfactant solutions. These relatively low molecular weight surfactants generally have structures similar to the PAG quenchant polymers, consisting of a water-insoluble moiety combined with a larger proportion of ethylene oxide units. At the inversion temperature (cloud point) these surfactant solutions become turbid, only clearing again upon cooling. Like the PAG quenchants, these surfactants also separate into two distinct layers when maintained at a temperature above the inversion point for several minutes.

Inverse solubility can be explained using either a mechanistic or a thermodynamic approach. The mechanistic approach is based on the amphipathic nature of the polymer molecules, which means they contain both hydrophilic and hydrophobic

portions.⁽¹⁶⁷⁾ As seen from *Figure 37*, the PAG chains consist of hydrophilic polyoxyethylene segments, and polyoxypropylene segments which are totally insoluble in water when in excess of 900 units.⁽¹⁶⁸⁾ By varying the proportion of the oxyethylene and oxypropylene units, the molecular weight of the final product, the initiator substrate, catalyst and other polymerization conditions PAG's may be produced with a wide range of viscosities and inversion temperatures. Commercial PAG quenchant products are generally random copolymers, since block products tend to exhibit more detergent-like properties which result in excessive foaming. The PAG chains can be linear or branched, depending on the functionality of the initiator used in the polymerization reaction. Linear chains would be produced if initiators such as water, monohydric alcohols (such as methanol or butanol), or dihydric alcohols (such as ethylene glycol) were used. Branched chains would result from using polyfunctional compounds such as trimethylpropane. The traditional PAG quenchants such as Quendila PA are most likely to be linear chains since they act as the most efficient thickeners for a given molecular weight. However, in recent years, much higher molecular weight PAG's have been produced on an industrial scale: therefore it is likely that the new generation PAG products have branched structures.

At low temperatures, the PAG molecules are taken into solution by hydration of their hydrophilic oxyethylene units, but at the inversion temperature this loosely-bound hydration sheaf is sufficiently broken down to render the polymer insoluble because of the remaining hydrocarbon segments. At inversion, the polymer will first exhibit a cloud point before stratifying to form two distinct layers. These layers do not comprise pure polymer and pure water. Instead, the polymer layer will be rich in polymer but will still contain a few per cent of chemically bound water. Likewise, the aqueous layer will still retain minor amounts of polymer. Since the polymer-rich layer is the most dense it will stratify at the bottom.

Upon raising the temperature of the PAG solution, the polymer will undergo a conformational change as the thermally labile H-bonds between the water and the ether-oxygen atoms become less numerous. The precise nature of this conformational change is unclear, as can be seen from the considerable confusion in the

literature.^(169,170,171,172) Block copolymer PAG derivatives are sold commercially as nonionic surfactants under the name Pluronic⁶, and are known to form "micelles" in solution.^(171,172) These micelles are molecular aggregates which are formed to minimize their interaction with the aqueous phase. A conformational change in the copolymer gives rise to a close packed molecule with the hydrophobic units orientated towards its interior, shielded by the oxyethylene units. These block copolymer PAG solutions exhibit a striking increase in their bulk viscosity near the cloud point, which is ascribed to the formation of large polymolecular micelles.⁽¹⁷²⁾ No increase in the kinematic viscosities of the Quendila PA random copolymer PAG solutions were observed near the inversion temperatures as seen in *Figures 86* and *87*. Thus it is unlikely that polymolecular micelles are formed. This is not surprising because of the PAG quenchant's much higher molecular weight, and its random distribution of hydrophobic groups. It is far more likely that these polymer chains undergo a gradual folding as the temperature is raised, the extent of the folding depending on the degree of hydration. The limiting viscosity number data obtained for Quendila PA at 25°C, 40°C and 60°C supports this hypothesis (*Figure 85*). From equation (20), it was seen that $[\eta]$ is related to the root mean square end-to-end distance for the polymer chain. Thus it is clear that, since $[\eta]$ decreased from 0.28 dl/g at 25°C to 0.02dl/g at 60°C, the PAG chains contracted as the temperature was raised.

The inversion temperatures for the PAG quenchants remain constant over their normal range of concentration. For example, the inversion point for Quendila PA was normally 74°C as was shown in *Figure 87*. However, at very low concentrations, where polymer-polymer interactions are minimal, the inversion temperature is higher. This was demonstrated in *Figure 86* where a 1 weight per cent solution of the dehydrated Quendila PA concentrate exhibited inversion at 78°C. The inversion temperature for PAG quenchants can be tailored to suit specific requirements by controlling the molecular weight of the polymer and its ratio of hydrophilic

⁶Pluronic is a tradename of BASF Wyandotte
Chemicals Corporation

oxyethylene units to hydrophobic oxypropylene units (i.e. the hydrophile-lipophile balance, HLB). This effect was confirmed by the NMR analysis of both Quendila PA and PHT. Quendila PA has an inversion temperature of 74°C and an oxyethylene:oxypropylene ratio of about 75:25, whereas inversion occurred at 88°C for Quendila PHT which had a respective ratio of around 85:15. The GPC analysis revealed that both these products had polystyrene-equivalent \bar{M}_w values around 12,500. Thus it can be seen that the inversion temperature for the polymer was raised by enlarging the proportion of oxyethylene units, and thus increasing the effective HLB. Quendila PHT's higher inversion temperature is beneficial in situations where bulk inversion problems arise, such as in sealed quench furnaces.⁽¹¹⁸⁾ The increased number of hydrophilic oxyethylene units in Quendila PHT resulted in it having a more extended conformation in solution, and hence a higher viscosity. The kinematic viscosity of the Quendila PA concentrate at 40°C was 430mm²/s, compared with 558mm²/s for Quendila PHT. Both these concentrates had solids-content values around 60 weight per cent.

From a thermodynamic standpoint, inverse solubility can be explained in terms of an exothermic heat of mixing and a negative entropy of dilution : this is because of the large dissimilarity in the free volumes of the polymer and the solvent. Upon mixing the dense polymer with the expanded solvent, there is actually an ordering of the system and a corresponding contraction. In the literature regarding the thermodynamics of polymer solutions the inversion point is confusingly called a lower critical solution temperature (LCST): this is because it lies at the bottom of a two-phase region and in spite of the fact that it occurs at a higher temperature than the usual upper critical solution temperature.

The traditional Flory-Huggins theory of polymer solution thermodynamics is inadequate for describing real solutions which exhibit this inverse solubility phenomenon. More elaborate corresponding-state theories such as those developed by Prigogine⁽¹⁷³⁾ are required. The basic concept will now be briefly described, more precise information can be found in a review by Patterson.⁽¹⁷⁴⁾ Upon heating the PAG solution, the water expands much faster than the polymer which is restrained by

the covalent bonding between its segments. If mixing is to occur at the higher temperatures, the spaces between the water molecules have to be reduced. The negative enthalpy, associated with the LCST, arises from the effective condensation of the water in the polymer. Since $\Delta G^m = \Delta H^m - T\Delta S^m$, this contributes to a negative Gibbs free energy of mixing and greater solubility with increased temperature. However, as the temperature increases, the overall solubility is dominated by the negative entropy. Two effects contribute to ΔS^m ; (i) combinatorial mixing and (ii) molecular ordering arising from the contraction of the expanded solvent to fit the polymer. This non-combinatorial term is negative and unfavourable, since it results in a positive contribution to ΔG^m . Upon raising the solution temperature, it becomes increasingly difficult for the water to contract sufficiently to fit the polymer, and the non-combinatorial term predominates. When this occurs, ΔG^m becomes positive and phase separation takes place.

Returning now to the cooling mechanism for polymer quenchants: it is believed that they all operate by the same fundamental principle. This mechanism is associated, firstly, with the increased viscosity of their solutions compared with water and, secondly, with their ability to produce a viscous insulating polymer-rich film around the hot metal. The action of this polymer-rich film is the same, irrespective of how it is formed.

Stage A cooling tends to be prolonged by the formation of this polymer-rich film since it encapsulates the superheated vapour blanket and stabilizes it. This theory is contrary to that proposed in the original PAG quenchant patent.⁽⁹¹⁾ Blackwood and Cheesman believed that the PAG formed a covering layer over the entire metal surface to the exclusion of the water component of the solution, with the result that no vapour formed at the interface. This is clearly not the case as was demonstrated in *Figure 107*. High molecular weight polymers and high concentration solutions tend to increase the stability and hence duration of stage A because they produce thicker films. The stability also depends on the solution temperature and the level of agitation; under realistic quenching conditions, it is not uncommon for stage A to be eliminated,

with nucleate/partial film boiling occurring instantaneously upon immersion. The vapour film component comprises essentially of steam, although there may also be a minor contribution from volatile polymer degradation products such as CO₂, produced when the quenchant initially wetted the hot metal surface. The vapour film pressure (P_{vf}) is in dynamic equilibrium with the atmospheric pressure (P_{at}), the pressure created by the column of liquid (P_{cl}), and the pressure created by the surface tension (P_{st}):

$$P_{vf} = P_{at} + P_{cl} + P_{st} \quad (34)$$

The total film pressure equals the sum of the partial pressures of its constituents, as described by Dalton's Law. However, since the heat flow through the insulating vapour blanket / polymer film is insignificant, superheating occurs with an increase in the vapour film pressure. Eventually the polymer-rich sheaf becomes incapable of constraining the vapour, and an explosive reaction occurs as the superheated vapour punctures the polymer sheaf at its weakest point. The hot metal is then rewetted and nucleate boiling spreads out from the point of initiation. Generally, the nucleate boiling commenced at the free end of the quenched probe, as shown in *Figure 107(b)*, since this is the region which cools fastest and is therefore where the polymer film is thinnest. This is in agreement with the findings of Tensi et al^(56,175) who examined the rewetting kinetics using conductivity measurements between a quenched cylindrical test piece and the electrode surrounding it. Thus it is clear that more than one of the traditional stages of cooling can co-exist along the length of the probe.

During stage B cooling, two processes are in competition: polymer-encapsulated steam bubbles are trying to escape from the surface of the hot metal, whilst the surrounding polymer-rich film is attempting to restrain the release and thus reproduce a more stable film equivalent to stage A cooling. Alternate periods of nucleate boiling and stable film cooling could occur with high molecular weight polymers, or high concentration solutions, where the driving force for film reformation is high. The bubbles will be preferentially nucleated over imperfections (cavities) at the hot metal

surface where vapour has been entrapped (*Figure 149*). Any non-volatile polymer thermal degradation products, formed during the wetting of the hot metal, could also act as potential bubble nucleation sites. Once the bubbles have attained a size greater than that for unstable equilibrium, they will grow spontaneously. Their growth will tend to be limited by the inertia of the surrounding viscous polymer-rich film. This will be further enhanced by elastic stresses in the bulk liquid, since polymer solutions exhibit slight viscoelastic properties. For vaporization and bubble growth to continue, water must be diffused from the bulk solution through the polymer-rich film. The bubble growth rate will thus be reduced since mass diffusivity is an order of magnitude smaller than thermal diffusivity.⁽¹⁷⁶⁾

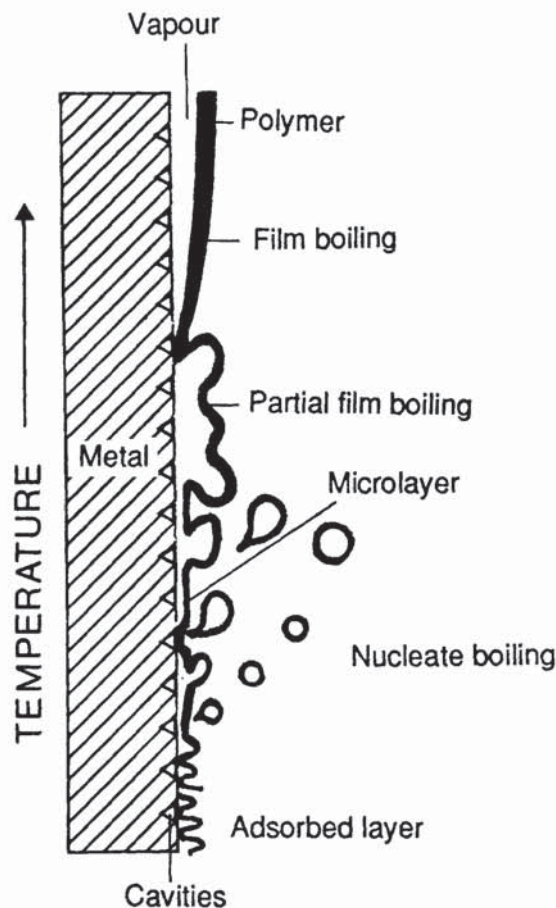


Figure 149. Schematic representation of the cooling mechanism for polymer quenchants

This retardation of the bubble growth rate by the viscous polymer-rich film formed at the vapour interface, combined with its insulating properties, explains the reduced stage B cooling rates experienced by polymer quenchants when compared with water.

When the surface temperature of the metal is high, bubble coalescence can occur, sometimes resulting in partial film boiling (e.g. *Figure 109(a)*). Bubble coalescence occurs extensively when pure water is boiled, resulting in high rates of heat extraction.⁽¹⁷⁷⁾ The bubbles eventually reach a size at which their buoyancy is greater than the restraining surface tension and polymer forces; they then escape, pumping away the liquid superheat. The polymer will actually reduce the surface tension and thus tend to increase the rate of heat transfer but, as the polymer concentration increases, viscosity enhancement and film formation effects predominate, reducing the heat transfer.

The more recent theories concerning nucleate boiling involve the formation of a thin "microlayer" of vapour which is maintained between the heating surface and the bubbles.⁽¹⁷⁸⁾ With polymer quenchants, the microlayer will also contain an outer polymer-rich component. The vapour layer will thus effectively isolate the polymer from the hot metal surface (i.e. similar to stage A). During stage B cooling, the polymer is only likely to rewet the hot metal surface for a fraction of a second upon bubble departure. Therefore, thermal degradation of the polymer will be minimized, since it will mostly be adjacent to the vapour which, although superheated, will be cooler than the hot metal surface which additionally acts as a potential catalyst.

The industrial acceptance of polymer quenchants has been limited by their higher cooling rates compared with oils at the lower temperatures, with the increased likelihood of cracking and distortion problems. Most quench oils have an initial boiling point within the range 300 to 450°C. Polymer quenchants, being aqueous solutions, have boiling points only slightly above 100°C. This means that stage C convective cooling in polymer quenchants occurs when the surface temperature of the component has fallen much lower than with oils. Consequently, polymer quenchants generally exhibit higher cooling rates than oils at 300°C in the Wolfson Engineering Group test.

It is not possible to significantly increase the boiling point of water by the addition of moderate amounts of polymer. Thus, other than by raising the pressure above the liquid surface, the only effective means of reducing the rate of cooling at 300°C for polymer quenchants is to maintain a stable insulating polymer-rich film. This can only be achieved using high molecular weight polymers, polymers with limited solubility or high concentration solutions. Less hydrophilic macromolecules will produce more tenacious polymer-rich films. For example, Quendila PA had a lower cooling rate at 300°C, compared with Quendila PHT which had a smaller proportion of oxypropylene units. Ucon E was the PAG with the lowest cooling rate at 300°C: this product had the highest molecular weight of its class, and is also suspected to have been modified by hydrophobic capping.

The dilemma faced by the polymer quenchant formulator is that of trying to balance a low cooling rate at 300°C with an acceptable level of drag-out. When the surface temperature of the metal has fallen below the boiling point of the solution, a certain amount of residual polymer-rich film will come into direct contact with the metal and thus reduce the cooling rate during stage C. The speed with which this residual polymer redissolves depends upon its structure and the bath conditions. It is known that adsorbed layers of polymer are permanently formed on metal surfaces which are immersed in polymer solutions.⁽¹⁷⁹⁾ The amount of polymer adsorbed increases with the polymer's molecular weight and reaches a limiting value with increased concentration. It has been shown that this limiting concentration is usually well in excess of that which would be expected for a monomolecular layer of polymer adsorbed flat on the metal surface. This suggests that the adsorbed polymer is anchored to the surface only at a few points, with the remainder of the polymer in the forms of loops and tails moving more or less freely in the liquid phase. Since the level of adsorption is reduced as the temperature increases, this phenomenon is only likely to influence stage C cooling. The level of adsorption is likely to be higher for the polyacrylate quenchants because of their charged character.

5.4 Effect of Polymer Quenchant Concentration, Temperature and Agitation on the Cooling Characteristics.

5.4.1 Polymer Solution Concentration The effect of polymer concentration on the maximum cooling rate for the representative solutions, tested at 30°C and agitated at 0.5m/s, is shown in *Figure 150*. For each polymer quenchant, the maximum rate was reduced linearly over its normal range of concentration. This agrees with the findings of Mason and Lake⁽⁹⁹⁾ who also demonstrated a linear reduction in maximum rate with increasing concentration (*Figure 39*), for non-agitated PAG solutions tested with an austenitic stainless steel probe. However, *Figure 150* shows deviations from linearity for all polymer concentrations below 5 per cent and for polyacrylate concentrations above about 20 per cent. In fact, the PAG exhibited higher cooling rates than water for concentration levels below 2.5 per cent. This class of polymer will be the most effective at reducing the surface tension of water because of its amphipathic character. Consequently, at concentrations below the level at which viscosity enhancement and film formation effects dominate, increased wetting will result in higher rates of cooling. For each concentration, the polyacrylate had a lower maximum rate than either the PAG or the PVP. For concentrations up to 10 per cent, the PVP had a lower maximum rate than the PAG, but above this level the situation was reversed. *Figure 151* shows the effect of concentration on the cooling rates at 300°C for each representative polymer quenchant. The rate at 300°C is an important parameter, since that temperature is within or near the martensite transformation range for a number of common engineering steels. Therefore a low rate of cooling at 300°C is desirable in order to minimize the risks of distortion and cracking.

As would be expected, the data for the rate at 300°C exhibit similar trends to those for the maximum rate. They differ in that the 5 per cent PVP solution had a higher rate at 300°C than pure water; above this concentration, the rate continued to drop linearly. On the other hand, the rates for the polyacrylate and the PAG tended to level off above concentrations of about 10 and 15 per cent respectively. The rate at 300°C was actually lower for the PVP, compared with the PAG, for solution concentrations above about 25 per cent.

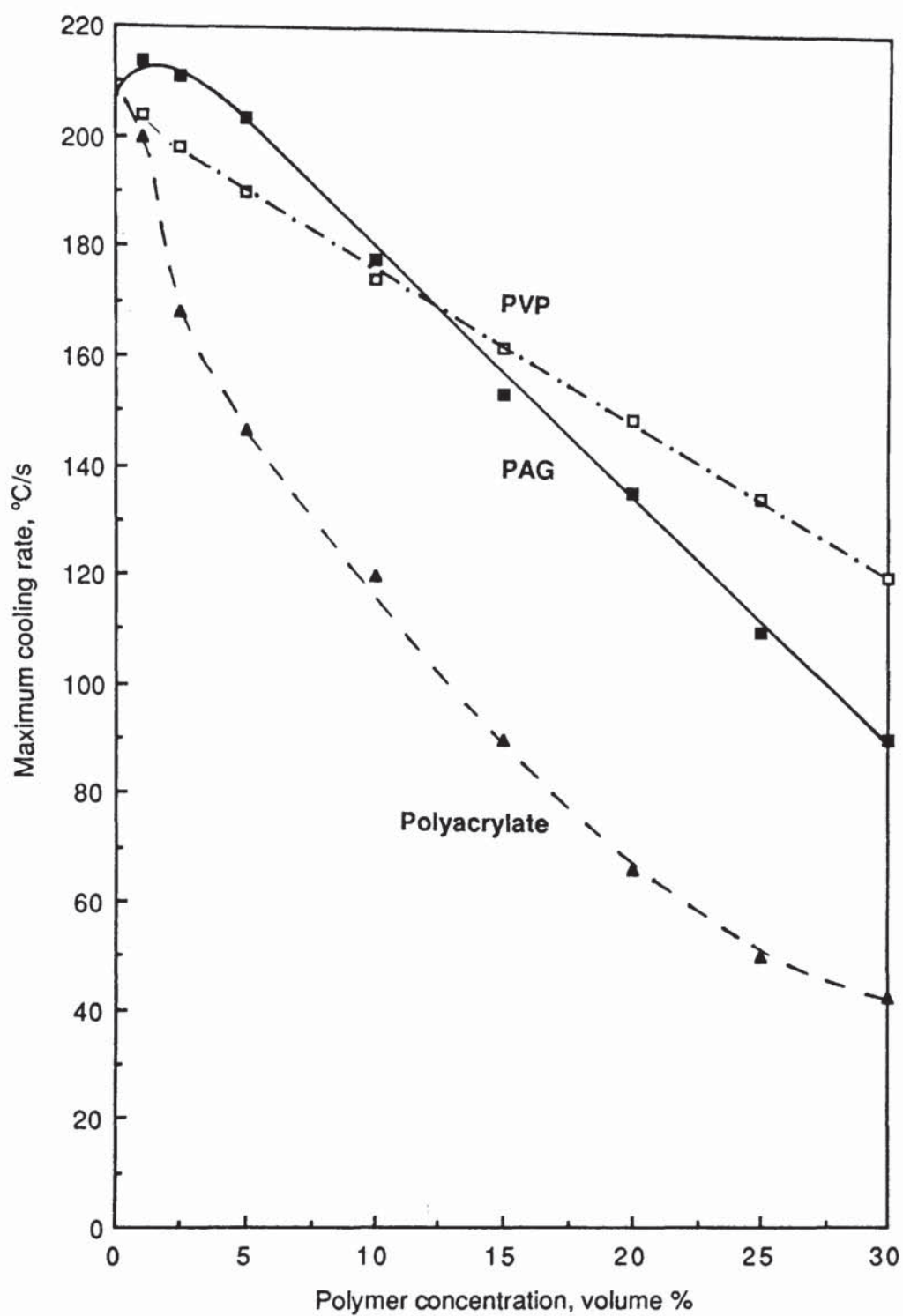


Figure 150. The effect of solution concentration on the maximum cooling rate for each of the representative polymers tested at 30 °C, 0.5m/s fluid velocity.

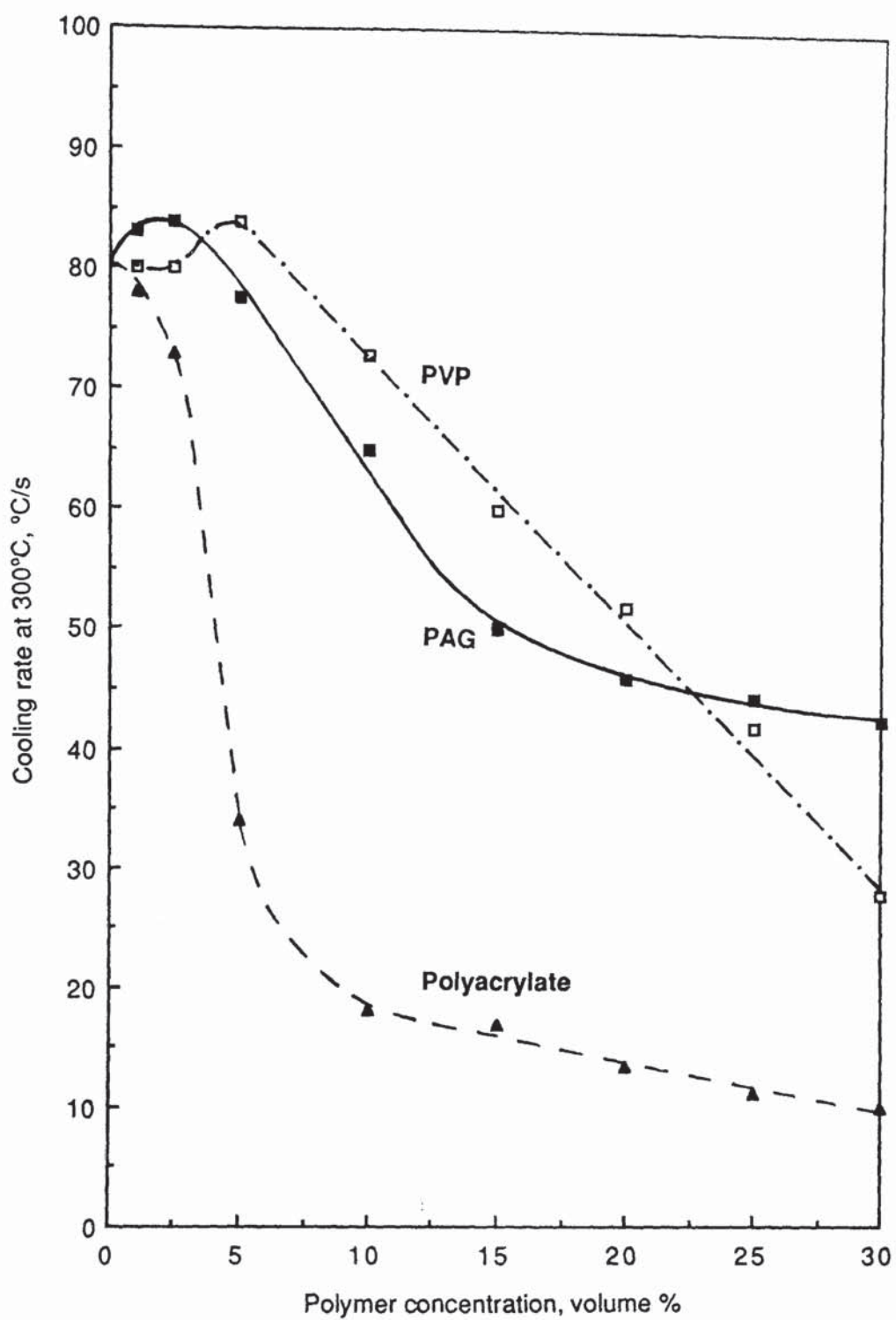


Figure 151. The effect of solution concentration on the cooling rate at 300 °C for each of the representative polymers tested at 30 °C, 0.5m/s fluid velocity.

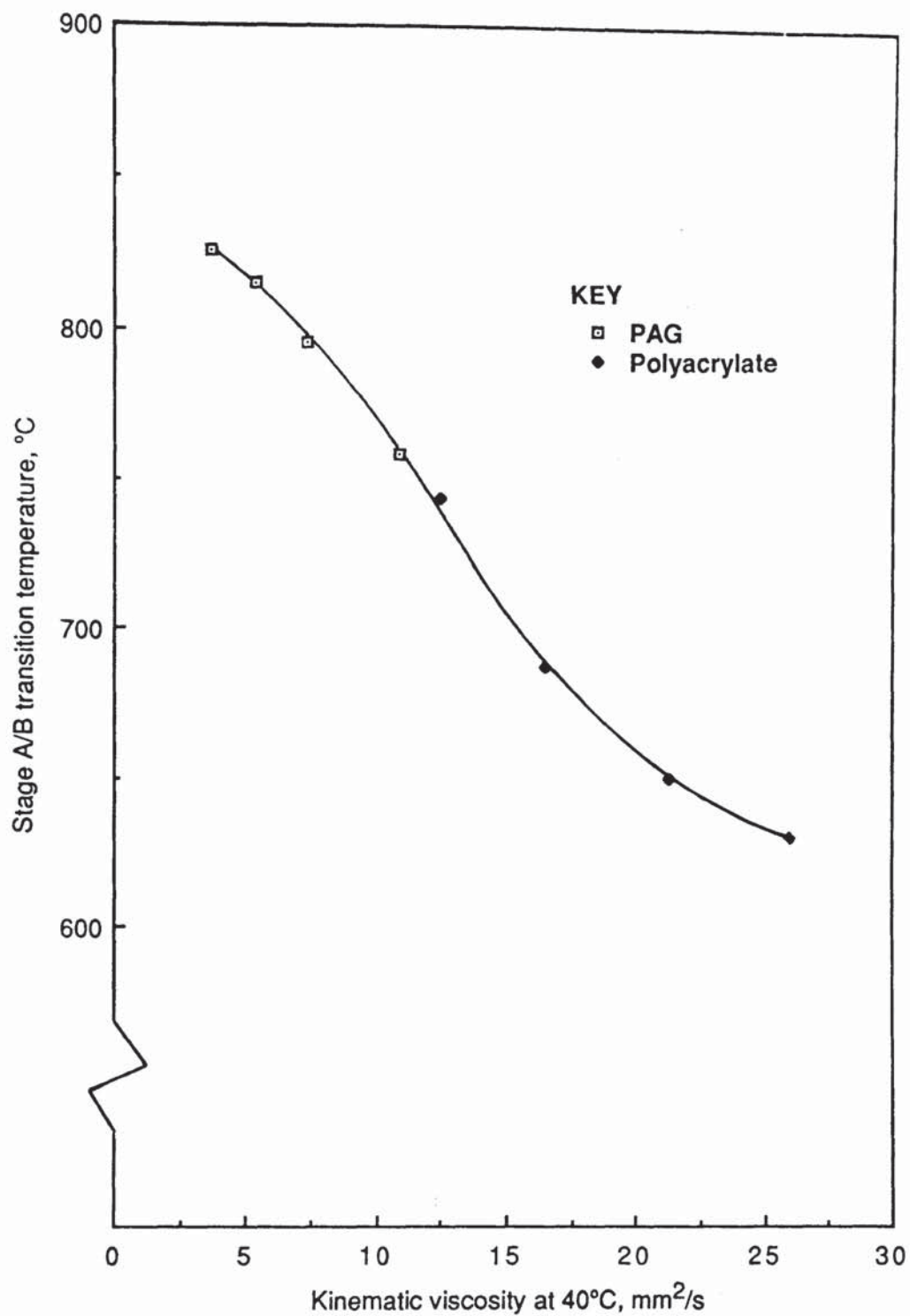


Figure 152. Effect of solution kinematic viscosity measured at 40 °C on the stage A/B transition temperature for the various concentration PAG (Quendila PA) and polyacrylate (Aquaquench ACR) solutions tested at 30 °C, and 0.5m/s agitation.

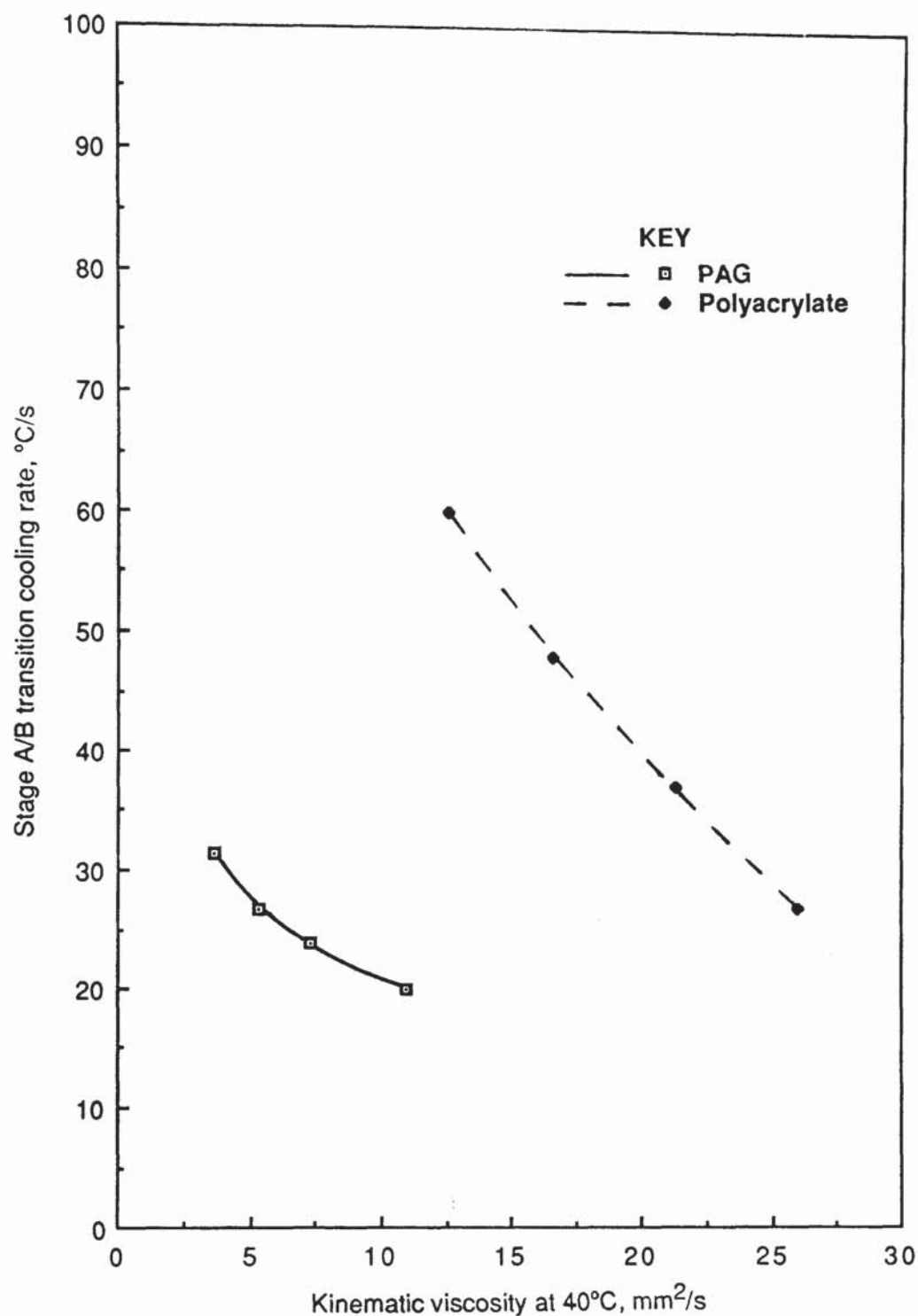


Figure 153. Effect of solution kinematic viscosity measured at 40 °C on the stage A/B transition cooling rates for the various concentration PAG (Quendila PA) and polyacrylate (Aquaquench ACR) solutions, tested at 30 °C, and 0.5m/s agitation.

In general, there was a reduction in the rate of cooling as the polymer concentration was increased. Stage A was extended for the PAG and polyacrylate solutions and the temperature of the maximum rate tended to be reduced. Increased concentration results in a thicker and more stable insulating polymer-rich film being formed around the hot metal. In addition, as the concentration increases, so too does the viscosity of the solutions. There are some interesting correlations which can be made between the measured cooling characteristics for the agitated polymer solutions and their kinematic viscosities which were measured at 40°C. For example, as the solution viscosity increased, there was a curvilinear reduction in the stage A/B transition temperature, shown in *Figure 152*, which is associated with a thicker encapsulating polymer-rich sheaf around the probe, and reduced levels of turbulence. The PVP (Parquench 90) did not support stage A cooling even at a solution concentration of 30 per cent of the as-supplied concentrate. This is believed to be due to its much lower true solution concentration, since the as-supplied concentrate had a solids-content of only 10 weight per cent. Parquench 90 solutions with concentration levels above 20 volume per cent had kinematic viscosities in excess of 3.5mm²/s at 40°C. From *Figure 152*, it would have been predicted that these solutions would have exhibited a period of stage A cooling. However, no such cooling regime was observed.

Figure 153 compares the stage A/B transition rate data with the polymer solution kinematic viscosities. Curvilinear relationships exist for both the PAG and the polyacrylate, with the stage A/B transition rate decreasing with increasing kinematic viscosity. The transition rates were lower for the PAG than the polyacrylate. Since the PAG exhibits inverse solubility, a stable polymer-rich film is formed more rapidly. However, this continuous film is more rapidly broken down because of the PAG's lower molecular weight.

By combining *Figure 92* and *Figure 150*, it can be seen that there is an exponential reduction in the maximum cooling rate with increased kinematic viscosity, irrespective of the polymer type (*Figure 154*). This supports the relationship proposed by Rohsenow,⁽¹⁸⁰⁾ which indicates that the viscosity η is the most influential liquid property in determining nucleate boiling performance:

$$c = A \frac{(\Delta T)^2}{S_p^{2.1} \eta^{4.1} (\Delta H)^2} \sqrt{\left(\frac{K g (\rho_l - \rho_v)}{\sigma} \right)} \quad (35)$$

where c = heat transfer coefficient in nucleate boiling, A is a constant, ΔT is the thermal driving force, S_p is the heat capacity of the liquid, η is the liquid viscosity, ΔH is the heat of vaporization, K is the thermal conductivity of the liquid, ρ_l and ρ_v are the density of the liquid and the vapour respectively, and σ the surface tension. The more viscous the fluid surrounding the hot metal, the greater the inertia which retards the rate of bubble growth. Furthermore, the viscosity of the solution also reflects the molecular weight and the concentration of the added polymer and hence the stability of the film formed.

Figure 154 suggests that little advantage is to be gained in terms of reducing the maximum rate, by increasing the kinematic viscosity of the solution above approximately 20mm²/s at 40°C. A similar effect was observed by Bozhko et al,⁽¹⁴⁰⁾ who proposed that there is a critical viscosity for polymer solutions, above which there is little effect on the cooling rate. This Soviet work was based on solutions containing various molecular weight derivatives of a nonionic polymer, described only as "PPS". These workers obtained a value for the "critical" kinematic viscosity of about 4.5mm²/s, but they did not state the temperature at which these measurements were made. Furthermore, the kinematic viscosity in this instance was correlated with the average cooling rate measured at the centre of a steel specimen of unspecified dimensions, which was quenched into unagitated solutions of the polymer.

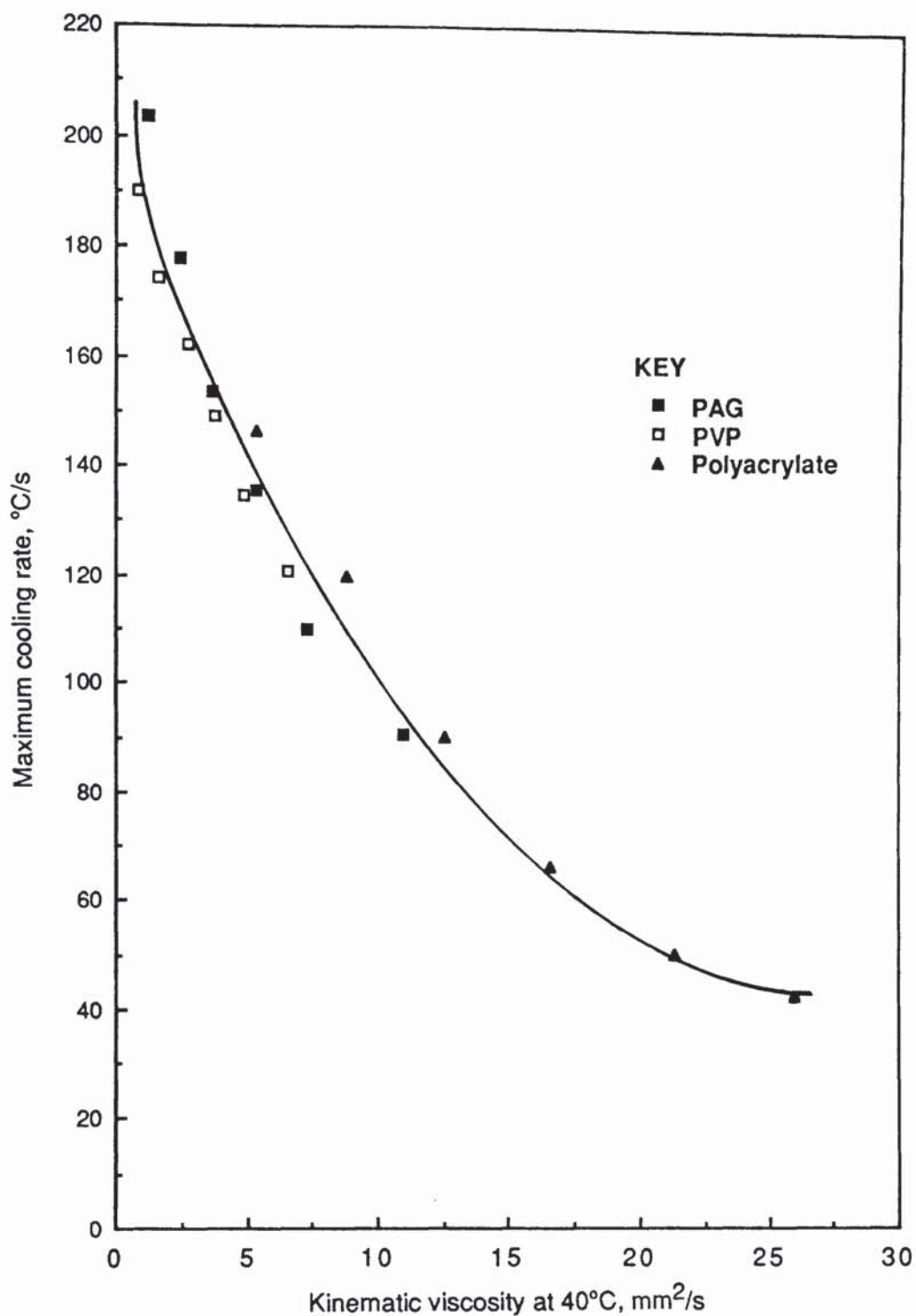


Figure 154. The maximum cooling rate for the various concentration representative polymer solutions measured at 30 °C and 0.5m/s agitation, as a function of kinematic viscosity.

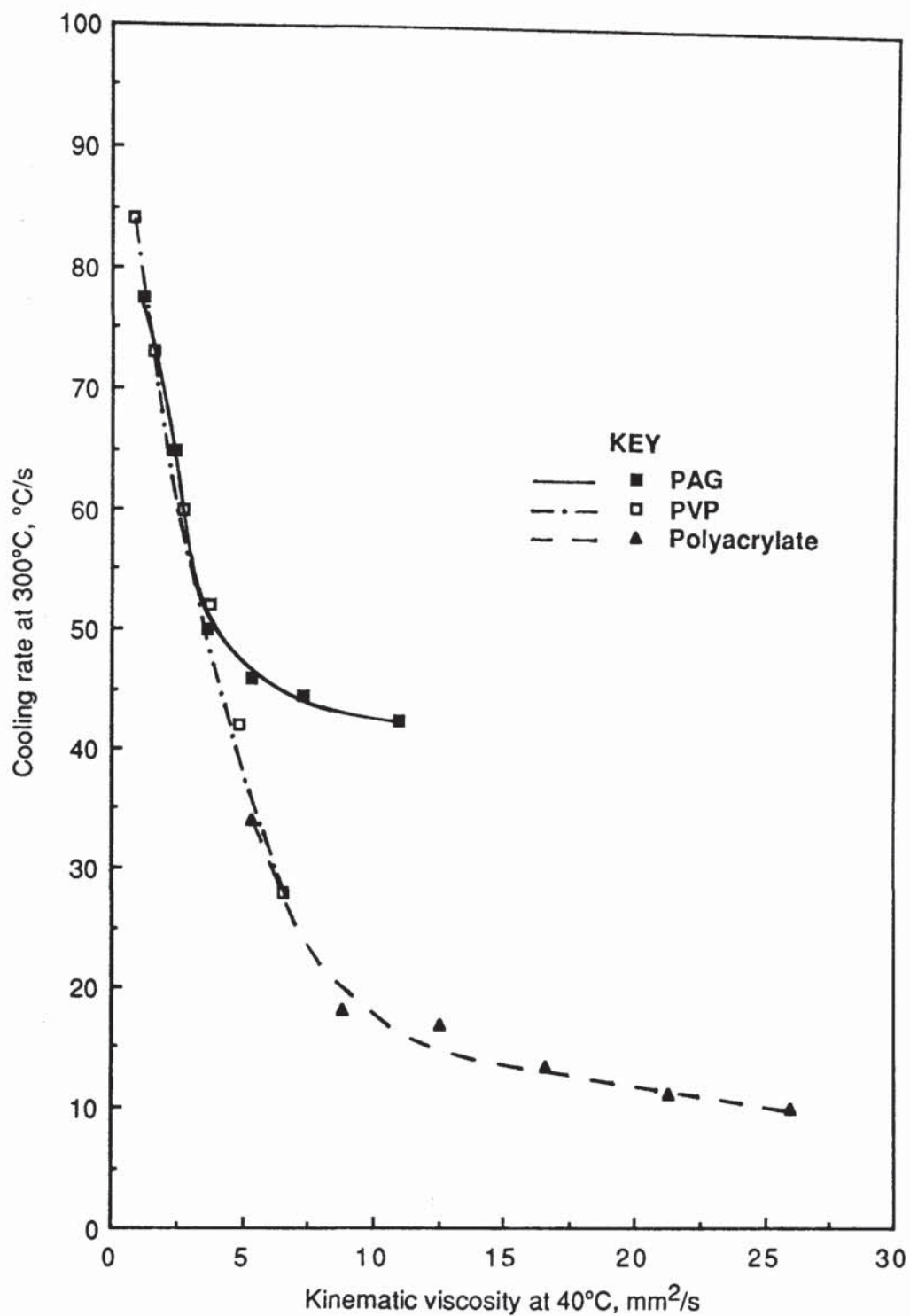


Figure 155. The cooling rate at 300 °C for the various concentration representative polymer solutions measured at 30 °C and 0.5m/s agitation, as a function of kinematic viscosity.

When this same treatment is applied to the cooling rate data at 300°C, obtained for the various concentration representative polymer quenchant solutions agitated at 0.5m/s (*Figure 155*), it can be seen that the situation is more complex. The reduction in the rate at 300°C begins to level off at a 40°C kinematic viscosity of about 5mm²/s for the PAG, and at around 8mm²/s for the polyacrylate. The rate at 300°C continued to drop rapidly for the PVP, up to the highest concentration solution examined, that was 30 per cent, with a kinematic viscosity of 6.52mm²/s. The viscosity at which the retardation in the 300°C cooling rate begins to level off is believed to be associated with the formation of a stable insulating polymer-rich film. The cooling rate at which this occurs depends upon the effectiveness of the insulating film produced. The PAG, which exhibits inverse solubility, produced a limiting thickness film at a lower viscosity than the polyacrylate; the latter produced a thicker and more insulating film with a correspondingly lower rate of cooling, because of its higher molecular weight. Upon further increasing the concentration of the Parquench 90 solution it would be anticipated that it would produce a limiting polymer film of greater thickness than that for Aquaquench ACR, with a lower 300°C cooling rate, because of the PVP's higher molecular weight.

5.4.2 Polymer Solution Temperature. As the temperature of the solution was raised, the maximum cooling rate for each representative polymer was reduced as shown in *Figure 156*. This is the opposite effect to most normal speed quench oils, where raising the oil temperature within this range generally reduces the viscosity sufficiently to increase the maximum rate. Raising the temperature of aqueous solutions also reduces their viscosity (as demonstrated in *Figures 86 and 87*); but this effect is outweighed by an increased contribution to the latent heat of vaporization, since the temperature of the solution is now nearer to its boiling point. Consequently, raising the solution temperature tended to stabilize and considerably prolong stage A cooling with a corresponding reduction in the temperature of the maximum rate. Stage A cooling was observed for PVP solution temperatures above 50°C. There was very little difference between the maximum rates for all three polymers at a solution temperature of 70°C; note that this temperature is perilously close to the bulk inversion temperature (74°C) for this particular PAG (Quendila PA).

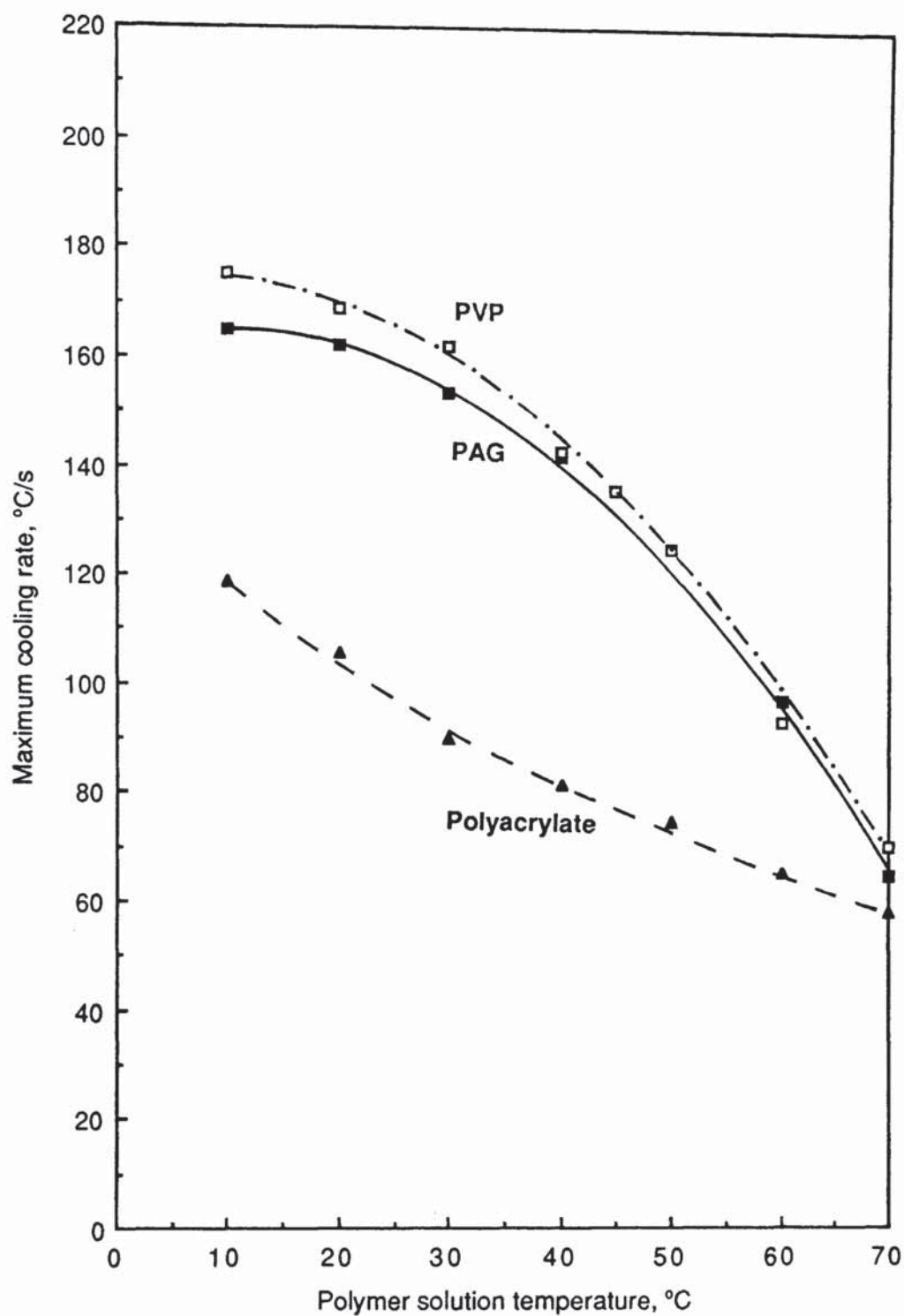


Figure 156. The effect of solution temperature on the maximum cooling rate for each of the representative polymers tested at 15 volume per cent concentration and 0.5m/s agitation.

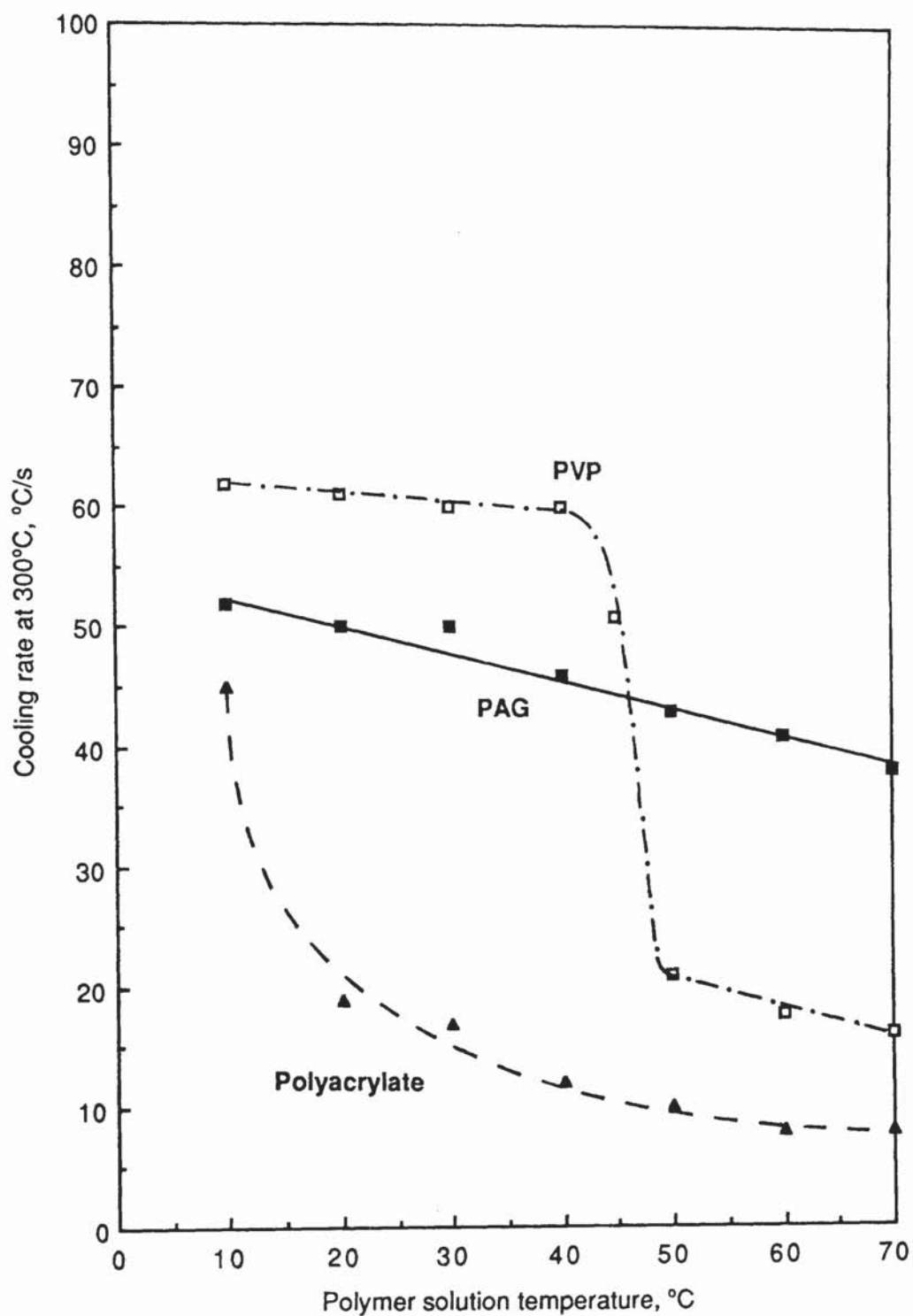


Figure 157. The effect of solution temperature on the cooling rate at 300 °C for each of the representative polymers tested at 15 volume per cent concentration and 0.5m/s agitation.

Raising the solution temperature also reduced the cooling rate at 300°C, as shown in *Figure 157*. There was a slight linear decrease for the PAG between 10°C and 70°C. The polyacrylate exhibited a fairly significant drop in rate at 300°C between 10°C and 20°C, but a further increase in the solution temperature resulted in a much less pronounced reduction, similar to that observed for the PAG. The results for the PVP are the most interesting: for solution temperatures up to 40°C, there was little effect on the cooling rate at 300°C, but between 40°C and 50°C the rate fell dramatically, a 65 per cent decrease in fact, before slowing down in a similar manner to the other two polymer types. This sudden drop is believed to be due to the formation of a more stable polymer-rich film, which takes place as nucleate boiling, and its associated high rates of cooling, begin to subside.

5.4.3 Polymer Solution Agitation. Agitation, or externally-produced fluid movement, has been established as critical for the successful use of polymer quenchants in order to prevent thermal stratification and inconsistent performance under production conditions. *Figure 158* shows the effect of agitation, measured in terms of fluid velocity, on the maximum cooling rate for each polymer type. As can be seen, the maximum cooling rate increased as the level of agitation was raised in all cases. Increasing the level of agitation had the effect of reducing the stability and hence the duration of stage A cooling, until a point was reached where instantaneous nucleate boiling occurred. This was true for both the PAG and the polyacrylate solutions with critical fluid velocities in excess of 0.6m/s and around 0.5m/s respectively. The critical velocity for the PAG could be predicted as 0.8m/s from examination of *Figure 94*. However, this data was obtained using the prototype tank (shown in *Figure 68*) which, because of its different pipework, will have produced submerged jets of unequal stability for a given fluid velocity compared with the preferred system. This helps to explain the discrepancies between the measured maximum cooling rates of the 15 per cent PAG (Quendila PA) and those predicted from *Figure 93*. The overall effect of the agitation was the same for both systems. The maximum cooling rate increased more rapidly at the lower fluid velocities, and then began to level off as the level of agitation was raised further. This is believed to be associated with increasing turbulence, and it is suspected that a limiting value

would be reached when fully turbulent conditions around the entire probe are established.

Increasing fluid velocity had the same effect on the maximum cooling rate of the PVP, as for the PAG. The rate of increase in the maximum rate of the PVP was slightly greater than for the PAG, presumably because of its lower true solution concentration. The polyacrylate exhibited a different response, with an exponential increase in maximum rate as the fluid velocity was raised. This is most probably due to its higher solution viscosity, which results in increased flow stability (i.e. lower Reynolds number: equations (3) and (7)). It is likely that upon increasing the fluid velocity of the polyacrylate above 1m/s, the maximum cooling rate will begin to rise less quickly, in a similar fashion to the PAG and PVP, before reaching a plateau at the velocity at which full turbulence is induced.

Another factor which could contribute to the polyacrylates different response to agitation, is its more pronounced pseudoplastic behaviour, as was shown in *Figure 127*. Polymer solutions commonly exhibit this behaviour which is characterized by a reversible reduction in viscosity with increased shear rate. It occurs because of the tendency of the applied force to disturb the long polymer chains from their favoured equilibrium conformation, causing elongation in the direction of shear. From *Table 29*, it was seen that between shear rates of 2000s^{-1} and 4000s^{-1} , the apparent viscosities for the PAG and PVP solutions dropped by about 14 per cent, whilst the drop for the polyacrylate was nearer 22 per cent. Since the polyacrylate is a polyelectrolyte, its chains will be more extended (i.e. rod-like) in solution and thus more susceptible to shear alignment.

Figure 159 shows the corresponding cooling rate data at 300°C . As the fluid velocity was increased, there was a very small linear increase for the PAG, whilst the polyacrylate showed a slightly greater curvilinear increase, and the PVP exhibited a rapid initial increase up to 0.2m/s. The large difference between the static and agitated PVP results can also be explained in terms of a more stable polymer-rich film.

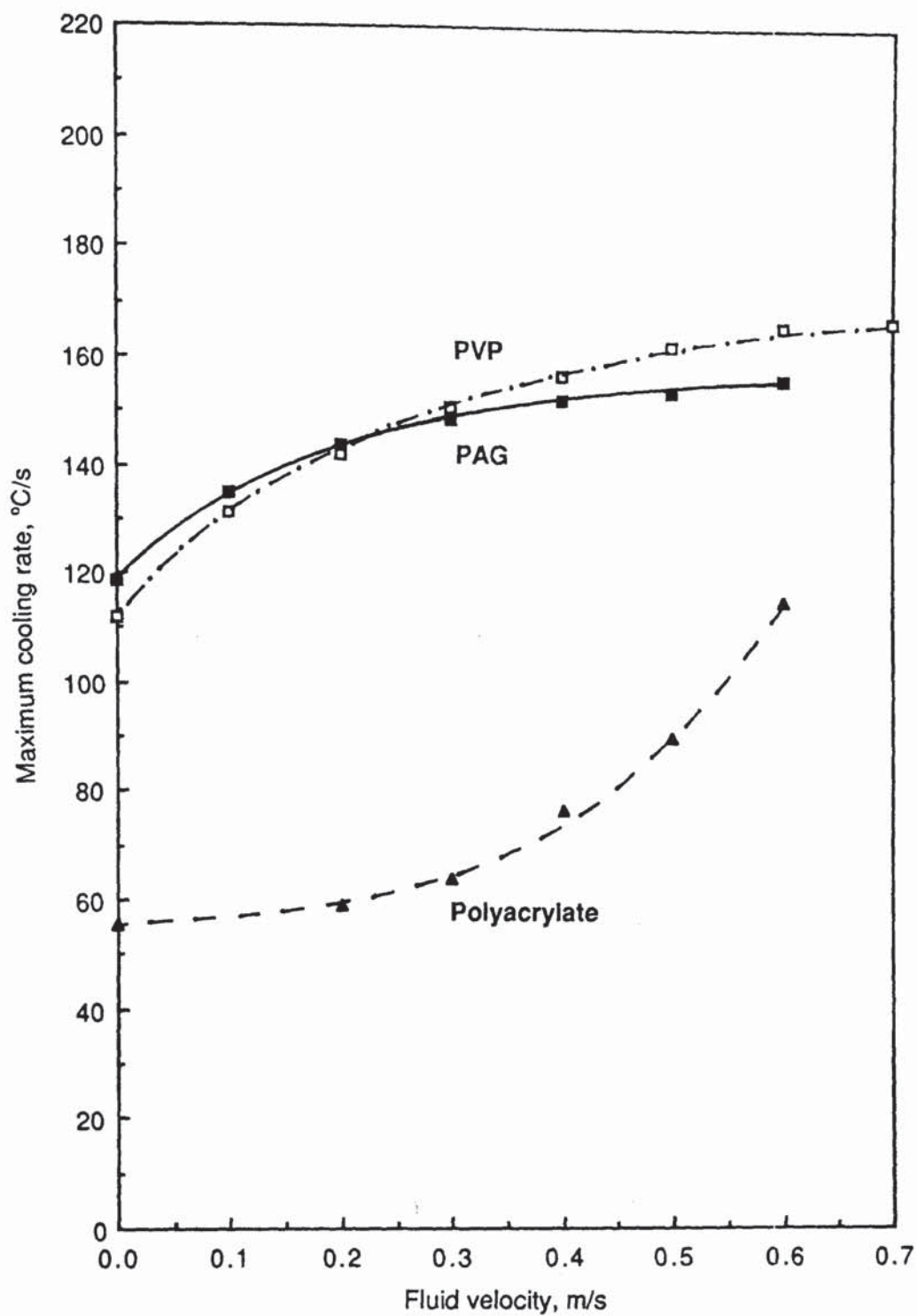


Figure 158. The effect of agitation on the maximum cooling rate for 15 volume per cent solutions of the representative polymers at 30 °C.

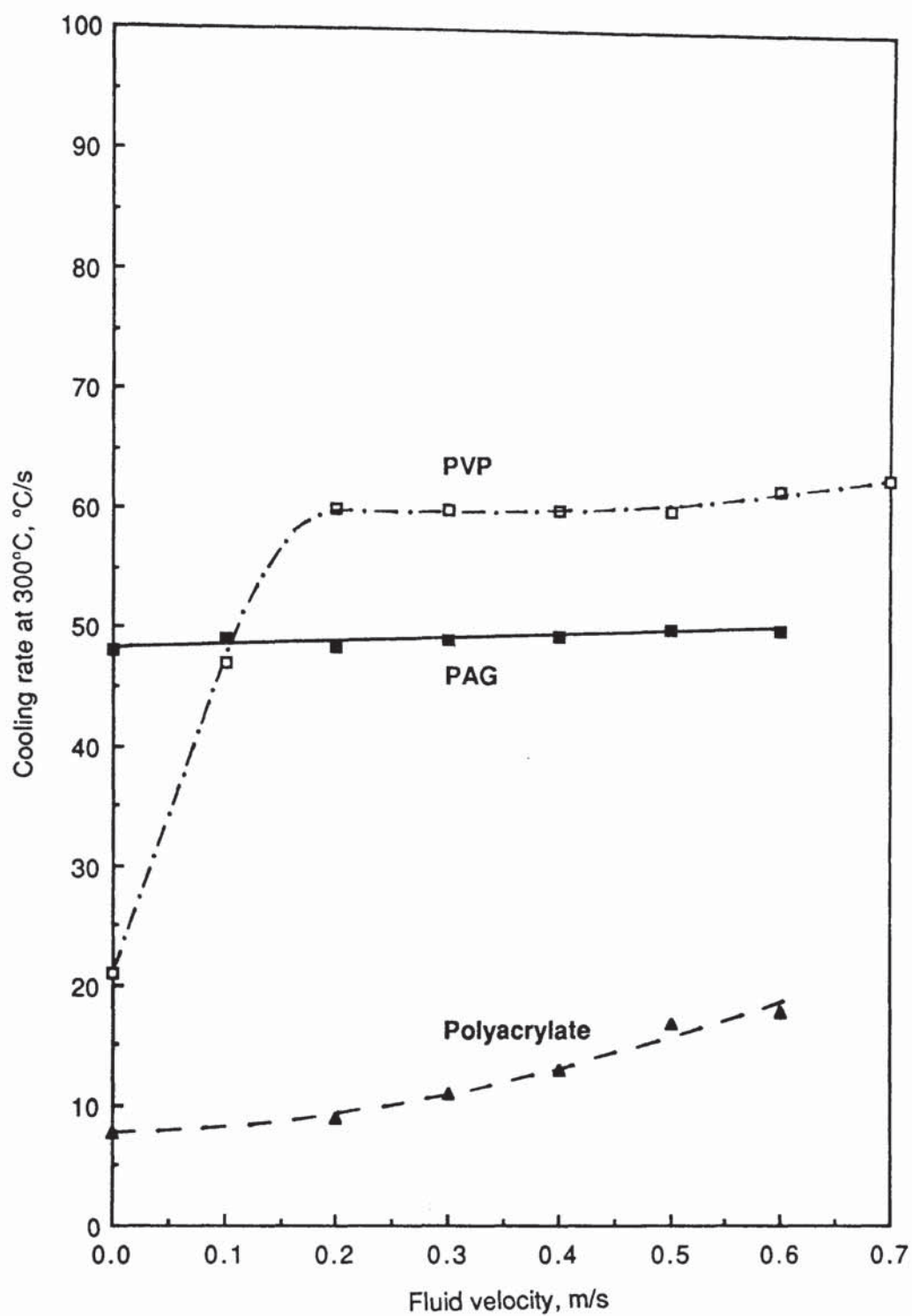


Figure 159. The effect of agitation on the cooling rate at 300 °C for 15 volume per cent solutions of the representative polymers at 30 °C.

Agitation produces thinner, more uniform, polymer-rich films around the hot metal. It also disperses the polymer-encapsulated steam bubbles and directs cooler fluid against the hot metal. Consequently, the cooling rates are increased as the level of turbulence rises. From equation (3), it can be seen that a reduction in the polymer concentration for a given fluid velocity reduces the solution viscosity and hence increases the level of turbulence and heat transfer. However, increased turbulence also results in enhanced mass transfer, diffusion and mixing. Therefore insulating polymer-rich film, jettisoned from the hot metal surface during nucleate boiling, is more rapidly replaced. These points help explain why agitation of the polymer quenchant solutions results in faster, more uniform cooling.

5.4.4 Summary of the Effect of Polymer Quenchant Concentration, Temperature and Agitation on Cooling Characteristics. The following effects generally occur if the polymer quenchant concentration is increased, its solution temperature raised, or the level of agitation in the quench tank reduced:

- (1) Stage A cooling will be prolonged with a corresponding reduction in the stage A/B transition temperature and rate.
- (2) There will be a reduction in the maximum cooling rate and temperature of maximum rate.
- (3) The cooling rate at 300°C will be reduced.

Linear multiple regression analysis of the combined data for each polymer quenchant has enabled derivation of equations which predict either the maximum cooling rate or the rate at 300°C from knowledge of the concentration, temperature and fluid velocity. The multiple correlation coefficients r , for these equations, are all within the 99 per cent confidence level.⁽¹⁸¹⁾ Armed with the relevant equation, and with a certain amount of practical experience, it should be possible to suggest the optimum conditions for particular industrial applications.

For the representative polymer quenchants tested during this work, the following equations apply, where:

MR = Maximum cooling rate ($^{\circ}\text{C/s}$)

R_{300} = Cooling rate at 300°C ($^{\circ}\text{C/s}$)

C = Polymer concentration (volume %)

T = Solution temperature ($^{\circ}\text{C}$)

V = Fluid velocity (m/s)

ν = Multiple correlation coefficient

PAG (Quendila PA)

$$\text{MR} = 244.7 - 4.3\text{C} - 1.7\text{T} + 47.2\text{V} \quad \nu = 0.98 \quad (36)$$

$$R_{300} = 83 - 1.68\text{C} - 0.36\text{T} + 14.1\text{V} \quad \nu = 0.92 \quad (37)$$

PVP (Parquench 90)

$$\text{MR} = 223.7 - 2.94\text{C} - 1.9\text{T} + 71.9\text{V} \quad \nu = 0.98 \quad (38)$$

$$R_{300} = 96.3 - 1.8\text{C} - 1.02\text{T} + 37.68\text{V} \quad \nu = 0.91 \quad (39)$$

Polyacrylate (Aquaquench ACR)

$$\text{MR} = 160.59 - 5.63\text{C} - 1.10\text{T} + 114.8\text{V} \quad \nu = 0.97 \quad (40)$$

$$R_{300} = 58.6 - 2.5\text{C} - 0.57\text{T} + 43.4\text{V} \quad \nu = 0.87 \quad (41)$$

5.5 Simulated Ageing of Polymer Quenchants.

Figure 160 shows that there was a slight linear increase in the maximum cooling rate for the PAG as the quench load was increased. The polyacrylate exhibited a fairly rapid initial increase for quench loads up to between 10 and 20kg/litre after which the maximum rate rose less quickly, in a linear manner similar to the results for the PAG. The results for the PVP appear quite erratic in comparison. For quench loads up to 10kg/litre, the maximum cooling rate increased but then, surprisingly, dropped to a value below the original starting level. The situation was reversed with quench load values above about 50kg/litre. At 100kg/litre, the maximum rate again exceeded the starting value. After 100kg/litre, the maximum cooling rate for the PAG had increased approximately 11 per cent, the PVP 6 per cent and the polyacrylate 60 per cent.

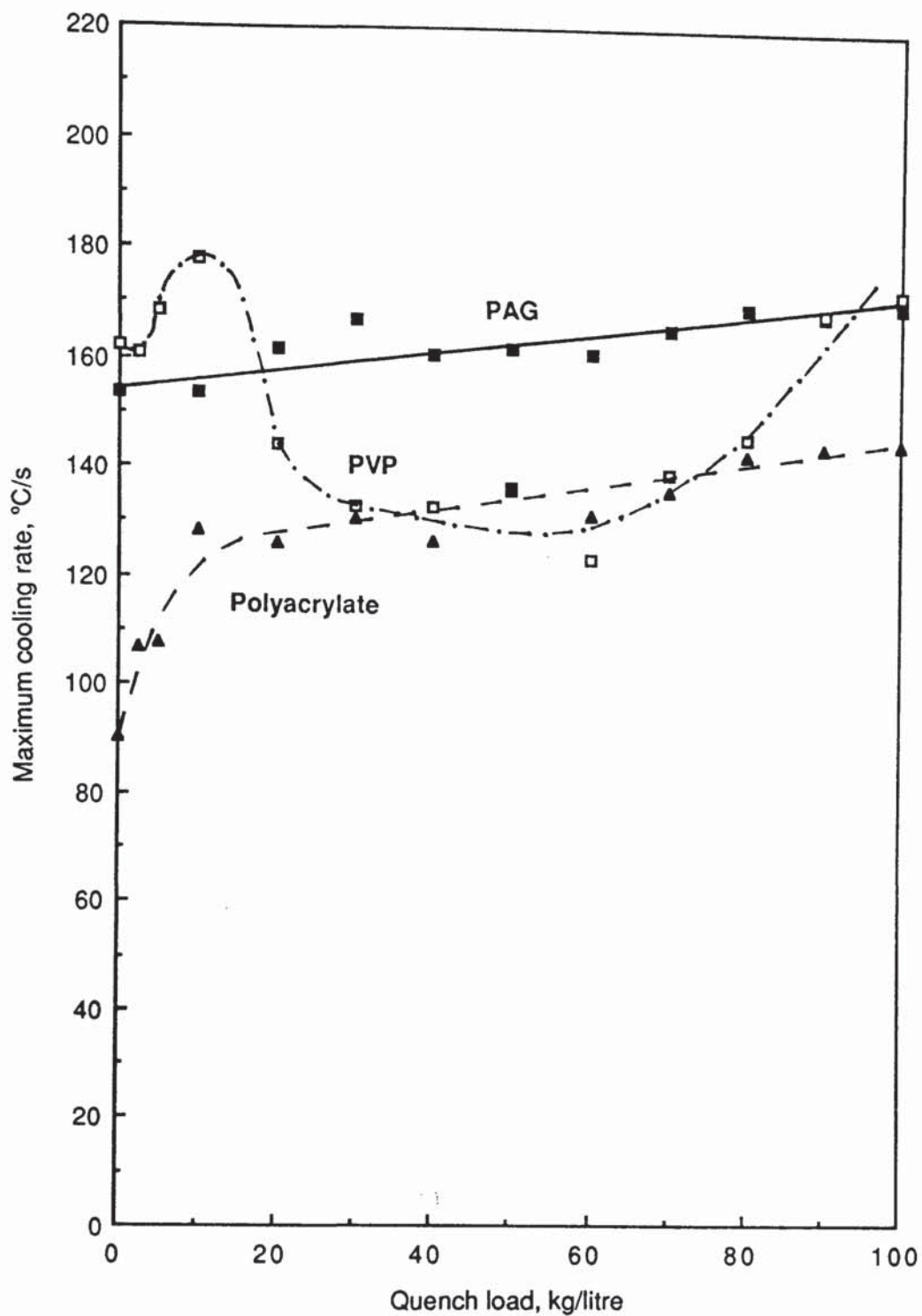


Figure 160. The effect of usage on the maximum cooling rate for a nominal 15 volume per cent solution of each representative polymer quenchant, tested at 30 °C and 0.5m/s agitation.

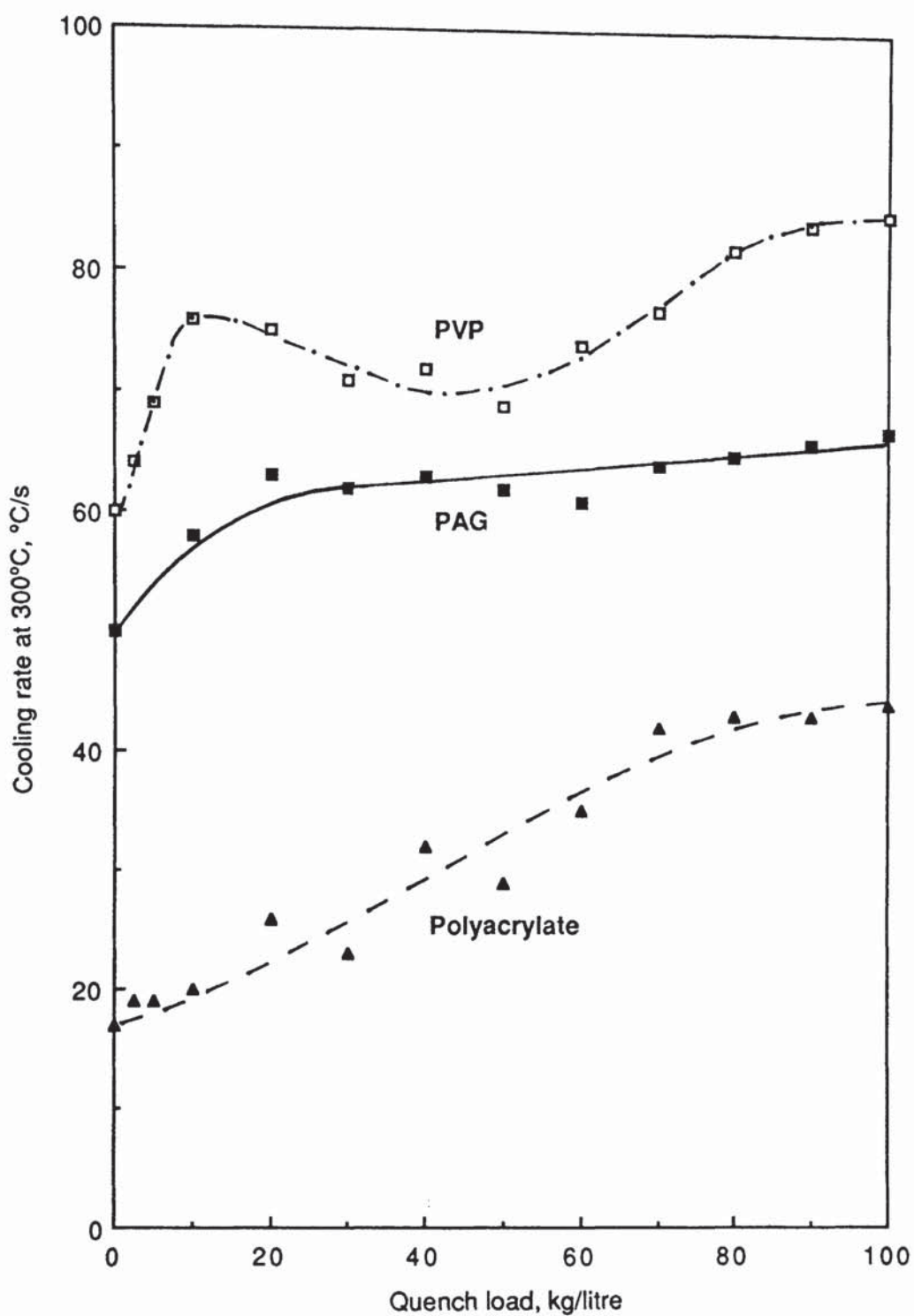


Figure 161. The effect of usage on the cooling rate at 300 °C for a nominal 15 volume per cent solution of each representative polymer quenchant, tested at 30 °C and 0.5m/s agitation.

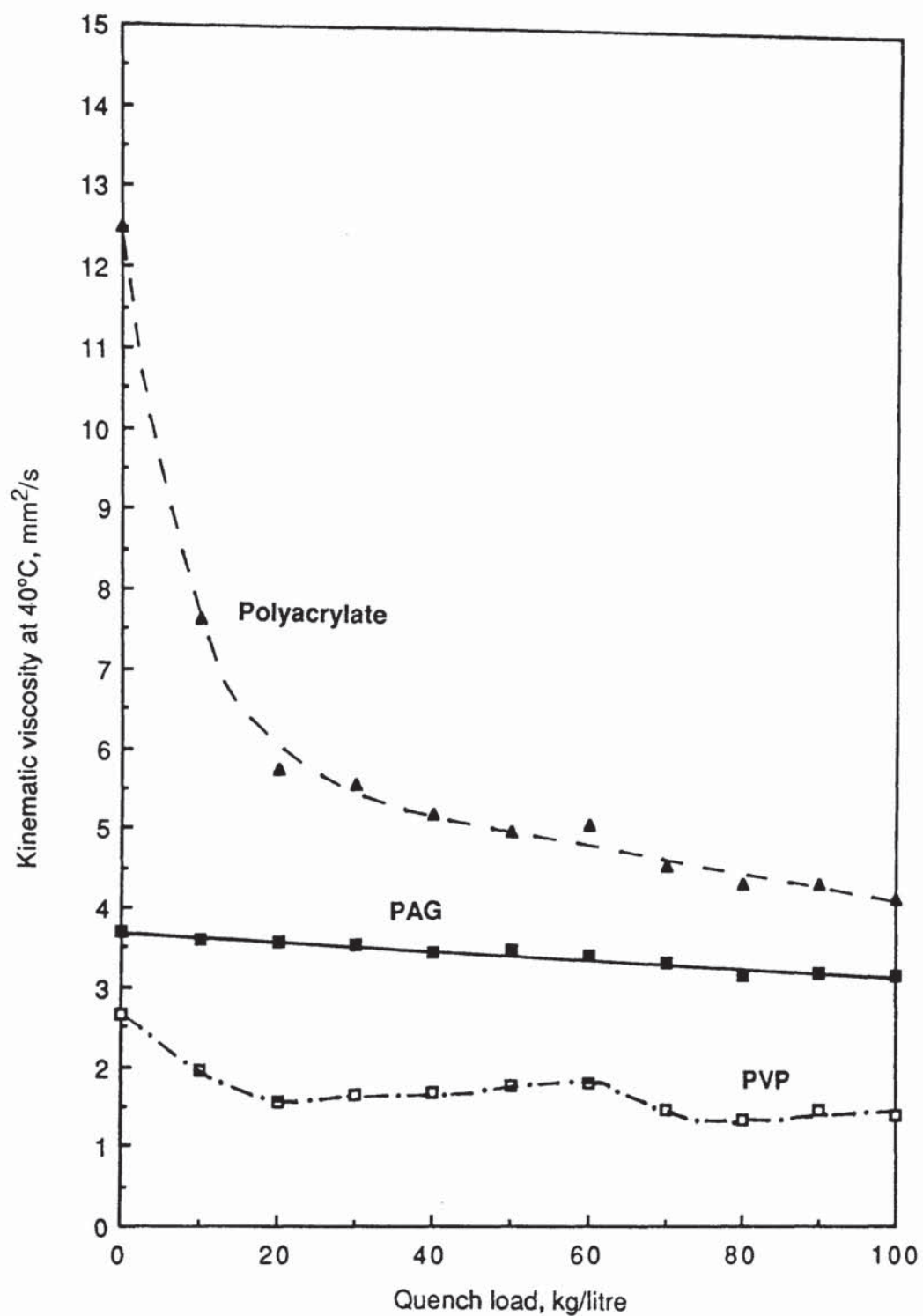


Figure 162. The effect of usage on the kinematic viscosity of nominal 15 volume per cent solutions of each representative polymer quenchant at 40 °C.

As described earlier, a slow rate of cooling at 300°C is desirable in view of that temperature's correspondence with the martensite transformation range for many engineering steels. *Figure 161* shows that as the quench load was increased, the cooling rate at 300°C likewise increased for each polymer type. After 100kg/litre, the rate at 300°C had increased 34 per cent for the PAG, 43 per cent for the PVP and 160 per cent for the polyacrylate. Nevertheless, even after 100kg/litre, the polyacrylate still retained slower cooling characteristics than the other two polymer types.

Very little information has been published concerning the cooling characteristics of used polymer quenchants. The only notable exception is a paper by Kopietz,⁽⁹⁴⁾ who compared a number of PAG quenchants from industrial units after prolonged use. His findings showed that used PAG solutions exhibited extended stage A cooling, increased maximum cooling rates, and increased rates during the convection stage. The results for the PAG (Quendila PA) solution tested during this work show the same basic trends in cooling rate, although stage A cooling was reduced rather than extended. The solutions tested by Kopietz were taken from industrial units, so contamination almost certainly also had an effect. On the other hand, the polymer solutions tested during the present work were aged under carefully controlled conditions to prevent contamination.

Figure 162 shows the effect of quench load on the kinematic viscosity of the polymer solutions measured at 40°C. There was a corresponding drop in kinematic viscosity as the quench load increased for each polymer type. The PAG showed a slight linear decrease; initially, the PVP showed a fairly rapid decrease for loads up to 20kg/litre before rising and falling in an erratic fashion; while the kinematic viscosity for the polyacrylate, after a considerable initial reduction, began to level off. In fact, the kinematic viscosity for the polyacrylate dropped by nearly 50 per cent after only 20kg/litre.

Mueller⁽¹²¹⁾ introduced the concept of a "delta" value, which quantifies the extent of contamination of polymer quenchants. The difference in concentration measured by

refractometer and the effective concentration measured by kinematic viscosity, delta values are a useful means of indicating the relative amounts of degradation for the samples aged during this work. After 100kg/litre the respective delta values were 2.1 for the PAG, 5.6 for the PVP and 11.7 for the polyacrylate.

The changes in both the viscosity and the cooling characteristics of the polymer quenchant solutions with usage can be explained, at least partly, in terms of degradation of the macromolecules, with a corresponding reduction in their molecular weight. The PVP (Parquench 90), which had the highest molecular weight when fresh ($\bar{M}_v = 621,214$), also experienced the greatest reduction in molecular weight after 100kg/litre in the accelerated ageing test ($\bar{M}_v = 184,611$, 70 per cent reduction). The polyacrylate (Aquaquench ACR) had an initial \bar{M}_v equal to 245,884 which dropped 51 per cent to 120,483 upon completion of the test. The PAG, which had the lowest initial molecular weight also experienced the smallest reduction in molecular weight with usage. Its polystyrene-equivalent \bar{M}_w fell 10 per cent from 12,480 to 11,280 after 100kg/litre. It would therefore appear from these results that the higher the molecular weight of the polymer the more susceptible it is to degradation during quenching, irrespective of polymer type.

Degradation of all organic quenchants in use is unavoidable due to the very severe nature of the quenching operation, i.e., thermal shock combined with the catalytic effect of the metal. For example, Bashford and Mills,⁽⁷⁶⁾ using a service simulation test, have shown the dramatic deterioration in the properties of certain quench oils with usage (*Figure 32*).

Degradation of polymer quenchants results in chain scission and a corresponding skewing of the normal molecular weight distribution towards lower molecular weights. This depolymerization was demonstrated in *Figures 76* and *82* which compared the GPC chromatograms for the fresh representative PAG and PVP polymers with those after a quench load of 100kg/litre in the accelerated ageing test. The chromatogram for the used PAG clearly exhibited a lower molecular weight tail, and there was a 10 per cent drop in the polystyrene-equivalent \bar{M}_w , and an 18 per cent

drop in the \bar{M}_n (Table 13). The molecular weight distribution for this polymer quenchant became slightly broader with use as indicated by the 0.33 increase in its polydispersity ratio. These distribution results for the PAG are typical of those for a polymer that has undergone chain scission. This was reflected in the 14 per cent drop in the PAG solutions kinematic viscosity after 100kg/litre.

The degradation of polymer quenchant molecules is highly complex, involving the synergistic influence of thermal, oxidative, biological and mechanical processes. Techniques such as dynamic thermogravimetric analysis (TGA) and differential thermal analysis (DTA), combined with analytical methods such as infrared-adsorption spectroscopy or gas-liquid chromatography would be required to study thermal degradation mechanisms. Consequently, it is beyond the scope of this work to propose detailed degradation mechanisms for the polymer quenchants examined. Nevertheless, tentative suggestions can be made regarding what are considered to be the most influential processes affecting the performance of each class of quenchant with use. For example, since the PAG's contain oxygen atoms in the main chain, they are more susceptible to autoxidation than either the PVP's or the polyacrylates which have a backbone of only carbon atoms. The most likely degradation products from such a reaction would be hydroperoxides which could decompose further resulting in scission of the main chain to form aldehydes, ketones or carboxylic acids. Polyvalent metal ions and acidic conditions will accelerate this process, whilst alkylated phenols will act as antioxidants when added in quantities of 100 to 5000 parts per million of product by weight.⁽¹⁸²⁾ The PAG solution actually became slightly more acidic with use, its pH dropped from 7.79 when fresh to 6.90 after 100 kg/litre.

The GPC chromatogram for the PVP sample after 100kg/litre exhibited a broadening of the distribution with shifts towards both higher and lower molecular weights (Figure 82). The distribution was bimodal with a secondary peak corresponding to a polystyrene-equivalent molecular weight of around 20,000. The chromatogram for the used PVP, like the PAG, exhibited a pronounced lower molecular weight tail. The polystyrene-equivalent \bar{M}_n for this used sample dropped by about 70 per cent. This was in agreement with the \bar{M}_v figure which also fell 70 per cent. However, the

polystyrene-equivalent \bar{M}_w decreased by only around 12 per cent. This is because the \bar{M}_w is more sensitive to high molecular weight chains, and there was also a higher molecular weight contribution towards the increased breadth of the used distribution. Following a quench load of 100kg/litre, the polydispersity ratio for the PVP almost trebled.

At least two processes are believed to be affecting the molecular weight and hence the characteristics of the PVP with usage. Firstly, chain scission is occurring with a corresponding reduction in the molecular weight, and secondly, certain chains are concurrently being cross-linked to produce polymers with a higher molecular weight than the original fresh product. These factors help to explain the erratic nature of both the kinematic viscosity and cooling characteristic data for this polymer with use. Furthermore, concentration control is more difficult with PVP solution since they tend to have much lower refractive indexes than the other two polymer types as shown in *Figure 91*. For example, one Brix number is equivalent to over eight volume per cent of concentrate for Parquench 90.

The results for the Kurt Orbahn shear stability test (*Figure 126*) revealed that the PVP was more susceptible to mechanical degradation than the other polymer quenchants examined. This test method obviously subjects the polymer solutions to much higher levels of shear than they would normally encounter in industrial practice. However, in vigorously agitated quench tanks, shear almost certainly contributes to the breakdown of very high molecular weight polymers. After 90 cycles, the kinematic viscosity for the PAG actually increased by 6 per cent: this was most probably due to evaporation during the test. There was a drop of 33 per cent for the PVP and 22 per cent for the polyacrylate. These non-reversible reductions in the viscosity are associated with mechanical scission of the polymer chains. It has been shown that polymers under mechanical shear initially degrade relatively rapidly before levelling off to a limiting, though still quite high, molecular weight.⁽¹⁸³⁾ This could possibly explain the lower molecular weight peak which appeared on the chromatogram for the aged PVP. The much higher molecular weight of the PVP,

combined with its large pendant groups, make it far more susceptible to shear damage than the PAG. Generally, linear polymer chains of high molecular weight are more susceptible to mechanical degradation than branched chains, which are less extended and can therefore move more freely. However, from the point of view of oxidation and thermal stability, linear chains would be preferred.⁽¹⁸³⁾

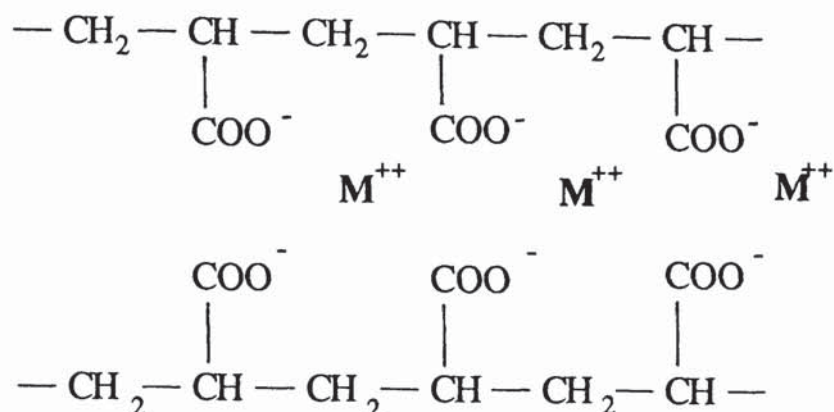
Schildknecht⁽¹⁸⁴⁾ has shown that aqueous PVP can be made permanently insoluble by heating with alkali. This is associated with free radical opening of the pyrrolidone ring and the subsequent reactions which occur across the different chains. Since the PVP quenchants are maintained alkaline to minimize corrosion problems (the pH of the representative PVP solution remained around 8.3 with use), it is quite conceivable that permanent cross-linking could occur between the polymer chains in closest proximity to the hot metal. Oxidation of the PVP could also result in cross-linking, if peroxides are formed.⁽¹⁶⁴⁾ As the degree of cross-linking increases the polymer becomes less soluble, eventually forming a permanent soft gel. The glazed appearance of components which have been quenched into PVP solutions could also be explained by this effect. This same phenomenon limited the usefulness of polyvinyl alcohol (PVA) solutions as quenchants. PVA is much more susceptible to cross-linking than PVP, because of its secondary hydroxyl groups (*Figure 35*). The control problem with PVA quenchants was exacerbated by their much lower working concentration range (0.05-0.3 weight per cent).⁽⁸⁸⁾

The drop in the kinematic viscosities of the polymer solutions with increased usage was reflected in the increased cooling rates. This effect is clearly exemplified by examining the polyacrylate results. The significant drop in the kinematic viscosity for quench loads up to 20kg/litre resulted in a corresponding rise in the maximum cooling rate. This is as would have been predicted from *Figure 154*. After 100kg/litre the \bar{M}_v for the polyacrylate had dropped 51 per cent, this was reflected in a 67 per cent reduction in the kinematic viscosity of the actual solution. A reduction in the molecular weight results in shorter polymer chains and therefore less stable insulating polymer-rich films. Reduced stage A cooling is likely to increase the rate of

degradation, since the polymer would come into intimate contact with the hot metal more rapidly. However, as described previously, it is believed that a boundary microlayer of vapour effectively isolates the polymer-rich film from the searing hot metal surface. Thus, even during stage B cooling, the polymer only momentarily contacts the metal as a consequence of bubble departure. Prolonged contact therefore only begins during stage C, when the surface temperature of the metal has fallen to around 100°C, and at which most polymers remain fairly stable. This explains the lower rate of degradation of polymer quenchants than would be anticipated from consideration of the very severe nature of the quenching process, combined with the intrinsic thermal instability associated with macromolecules.

The colour of the polymer quenchant solutions changed with usage as was shown in *Plates 6 to 8*. When fresh, all three representative polymer solutions were transparent pale straw-coloured fluids. With prolonged use, the PAG and PVP solutions developed a slightly darker hue and became more translucent. The polyacrylate (Aquaquench ACR), on the other hand, became black and "oil-like" in appearance after about only 10kg/litre. A progressively-increasing flocculent phase was also observed with this polymer, as seen by the levels of sediment in *Plate 8*. Both the colour change and the floc are believed to be associated with the formation of an insoluble polyvalent metal ion complex. Since sodium polyacrylate is an anionic polyelectrolyte in solution, multivalent cations such as Fe^{3+} , Ca^{2+} and Mg^{2+} will tend to replace water molecules orientated around individual carboxyl groups causing partial dehydration. This effect is not observed for Na^+ ions since the extent of the water displacement is dependent on the degree of ion binding which is related to the ionic potential of the cation (counterion). The polyanionic chain exerts an electrostatic attraction on the small counterions which are thus constrained to remain in the vicinity of the polyanion. This ion binding eventually gives rise to gelation and precipitation of the polyelectrolyte.

A diagrammatic representation of the structure of a polyacrylic acid salt formed with a bivalent metal cation is given below:⁽¹⁸⁵⁾



This phenomenon explains the flocculent polyacrylate gel which was formed adjacent to the oxidized mild steel filings in *Plate 9*. The refractometer reading for this solution decreased as the polymer was precipitated from solution. The PAG and the PVP samples showed no such effect. Hard water, caused by the presence of Ca^{2+} and Mg^{2+} ions, could thus similarly affect polyacrylate quenchants, thus causing control problems as predicted by Mueller.⁽⁸³⁾ The representative polyacrylate solution became slightly more acidic with use, its pH falling from 8.25 when fresh, to 8.04 after 100kg/litre. This change in pH could affect the viscosity of the solution because of the polyacrylate's polyelectrolyte character.

The polyacrylate solutions supplied by T.I. Desford Tubes Ltd. showed the same trends in appearance and cooling characteristics as the representative sample examined during the simulated ageing programme. The similarity in the cooling characteristics with increased quench load can be seen by comparing *Figures 124* and *125*. The concentration of the Aquaquench ACR solution used by T.I. was 3 volume per cent higher than the representative polyacrylate sample examined during the accelerated test. Since the quench tank at Desford had a capacity of about 55,000 litres, a quench load of 3200 tonnes was equivalent to 7.8kg/litre in the accelerated test which was considered to be approximately 7.5 times more severe. This assumption appears to be

reasonable since the kinematic viscosity of the industrial solution at 40°C dropped from 14.9mm²/s when fresh, to 8.8mm²/s after 3200 tonnes, with a corresponding increase in the maximum cooling rate from 71 ± 5°C/s to 114 ± 1°C/s. This is essentially what would have been predicted from examining *Figures 162 and 154*.

5.6 Contamination of Polymer Quenchants.

Several authors have shown that the cooling characteristics of PAG quenchants are sensitive to certain contaminants.^(28,121) The results from this work extend these findings to include the other two popular polymer quenchant types.

5.6.1 Contamination with Oil or Ammonia *Figures 163 and 164* show the effect of additions of quench oil and ammonia on the maximum cooling rate for each representative polymer tested using the standard conditions. The results for the PAG are in agreement with the findings of Burgdorf and Kopietz,⁽²⁸⁾ i.e., volatile contaminants such as ammonia (a constituent of carbonitriding atmospheres) and oils tend to extend stage A cooling and reduce the maximum cooling rate and temperature of maximum rate. This is because the dissolved ammonia tends to come out of solution at the hot metal surface, whilst the hydrophobic oils are attracted towards it. Fresh liquid containing the contaminant is continually brought to the heating surface by forced convection.

As the level of contaminations increased, the cooling rate at 300°C remained virtually unchanged for both the PAG and polyacrylate solutions. The PVP solutions actually exhibited a drop in the cooling rate at 300°C as the volatile contaminant additions increased. The fresh PVP solution had a cooling rate at 300°C of 60°C/s. With the addition of 2.5 weight per cent quench oil it dropped to 45°C/s, and with a 5 weight per cent addition it fell to 23°C/s. These reductions at 300°C are once again believed to be due to reformation of a more stable composite film. The oil contaminant will be emulsified by each of the polymers, particularly the PAG, because of their surface active characteristics. These contaminants could result in uneven distributions of vapour, thus increasing the risk of soft spotting problems. Furthermore, as the level of contamination increased, the refractometer reading for each solution was raised (*Tables 30 and 31*), thus rendering the calibration plots shown in *Figure 91* meaningless.

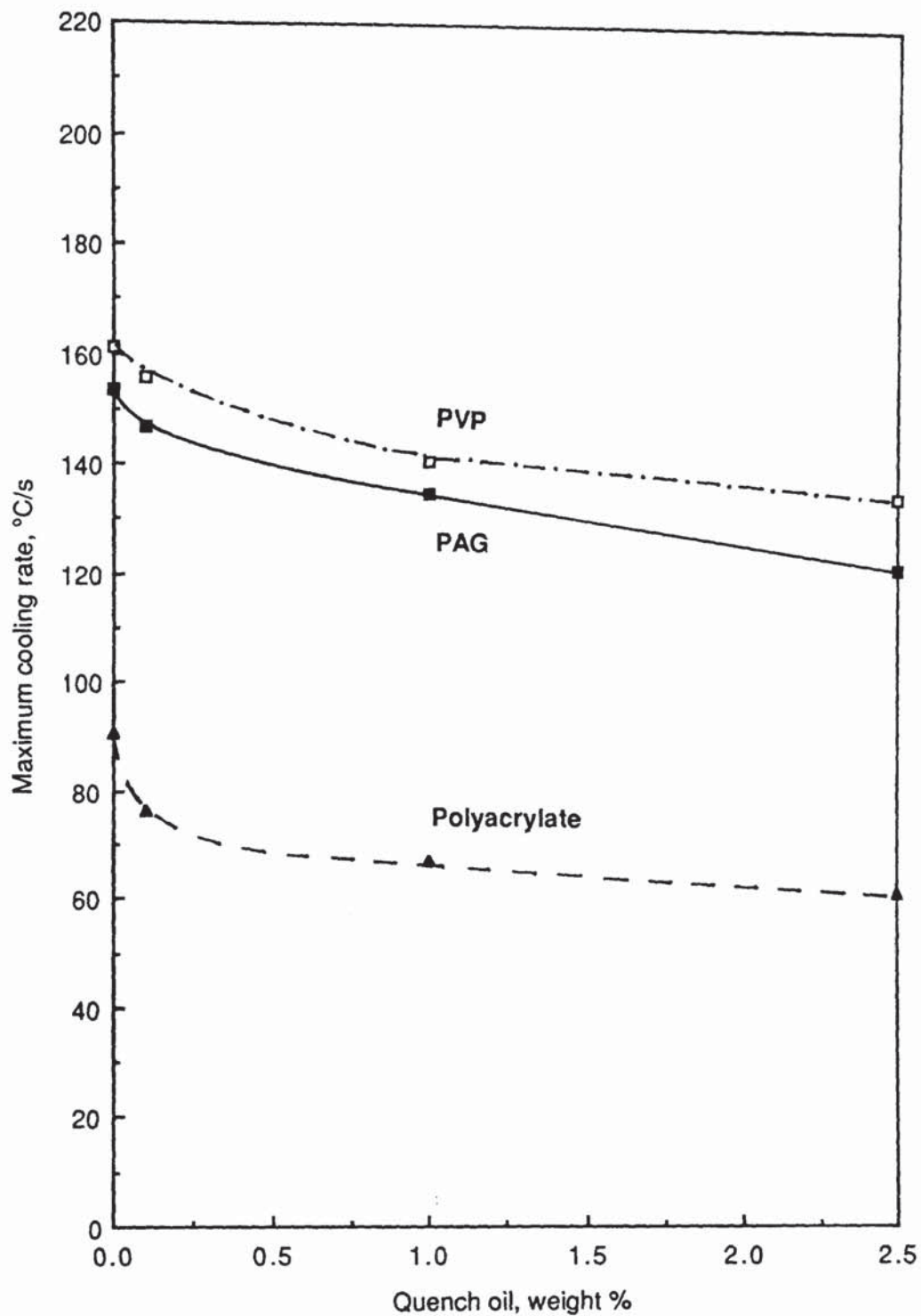


Figure 163. The effect of oil contamination (Houghtoquench 3S) on the maximum cooling rate of 15 volume per cent solutions of each representative polymer quenchant, tested at 30 °C, 0.5m/s fluid velocity.

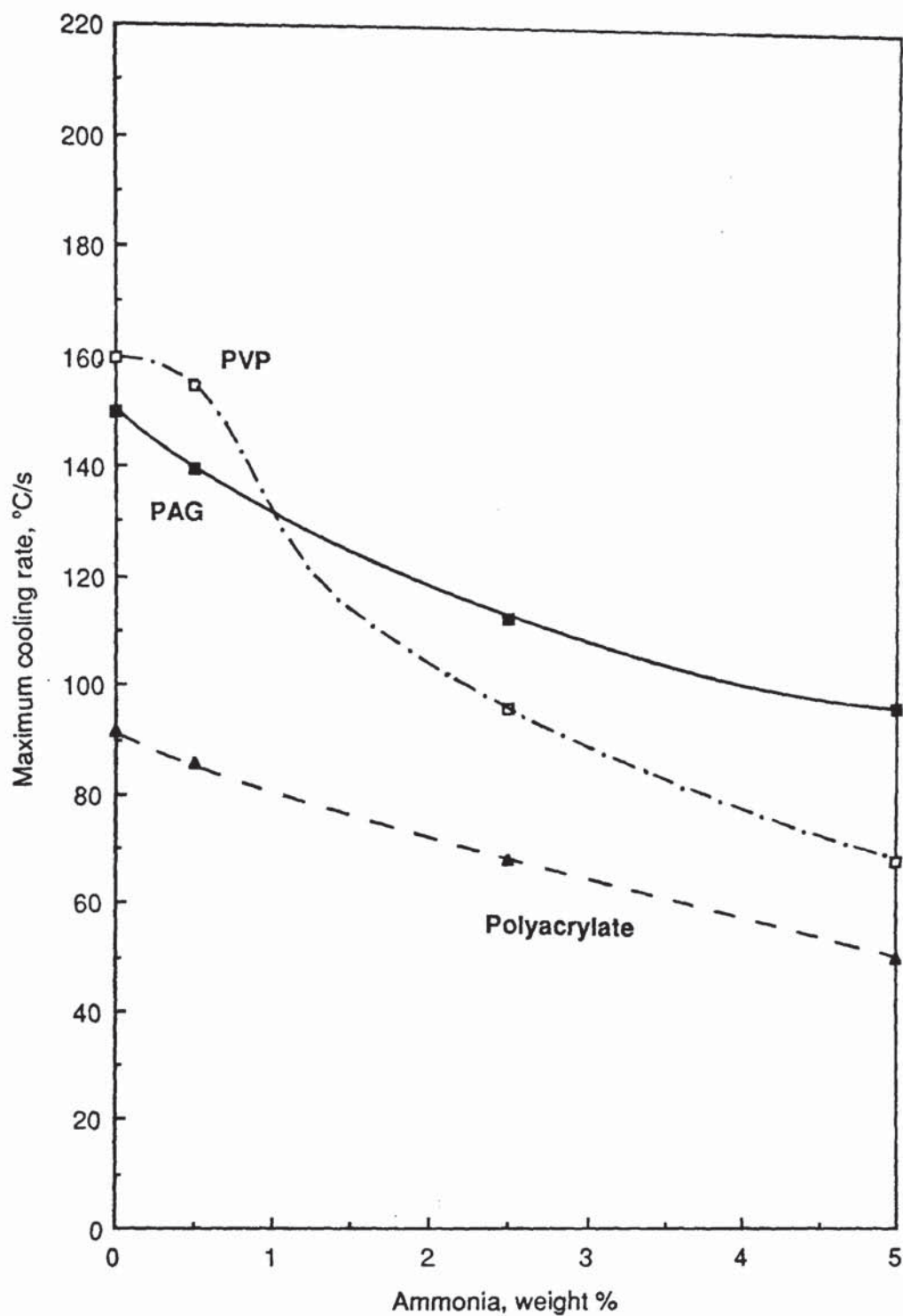


Figure 164. The effect of ammonia contamination on the maximum cooling rate of 15 volume per cent solutions of each representative polymer quenchant, tested at 30 °C, 0.5m/s fluid velocity.

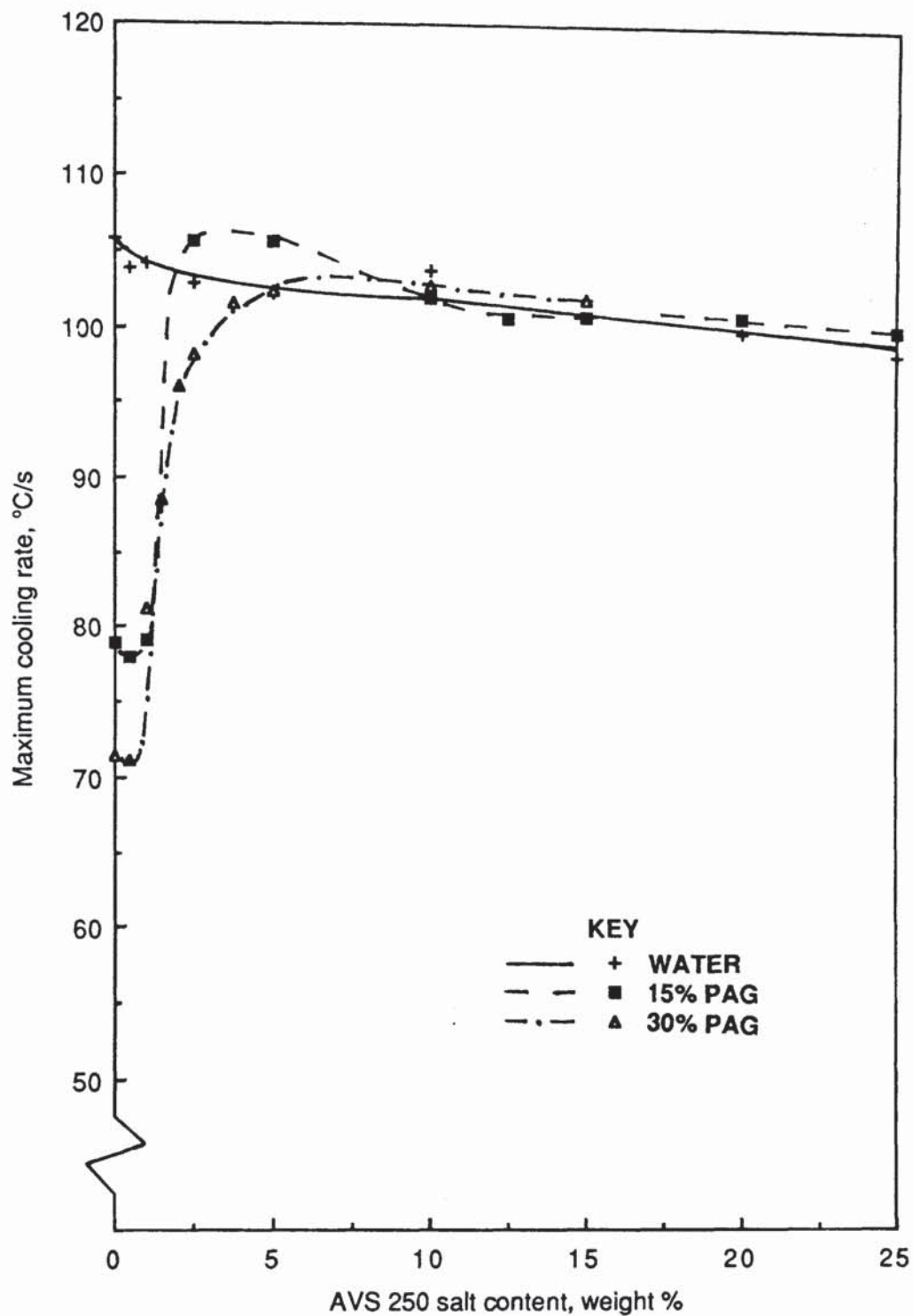


Figure 165. The effect of additions of AVS 250 nitrite/nitrate salt on the maximum cooling rate of water and both 15 and 30 volume per cent PAG (Quendila PA) solutions. Tested at 30 °C, 0.5m/s with probe preheated to 500 °C.

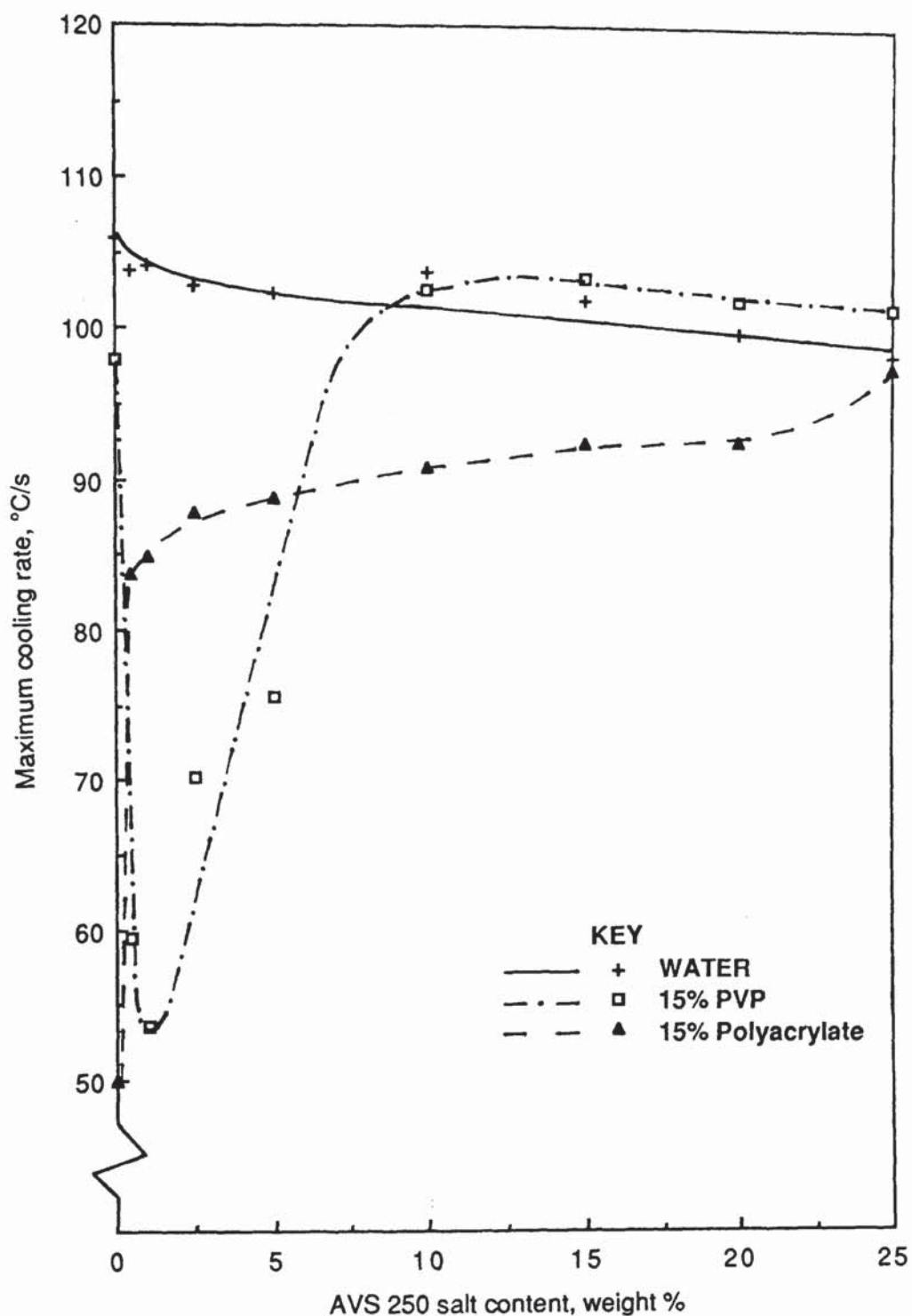


Figure 166. The effect of additions of AVS 250 nitrite/nitrate salt on the maximum cooling rate of water and 15 volume per cent solutions of a typical PVP (Parquench 90) and a polyacrylate (Aquaquench ACR) quenchant, tested at 30 °C, 0.5m/s with probe preheated to 500 °C.

5.6.2 Salt Contamination. Contamination of aqueous quenchants with relatively low levels of salt will tend to increase the rate of cooling by destabilizing stage A, as has already been described. The effect of salt contamination will therefore be less pronounced for those quench conditions which do not normally support stage A cooling. High salt concentrations may actually result in reduced cooling due to the precipitation of an insulating layer of salt around the hot metal.

In the aerospace industry, precipitation-hardenable aluminium alloys are quenched from nitrite/nitrate salt baths at around 500°C to produce a supersaturated solid solution. A high cooling rate is required in order to avoid undesirable pre-precipitation effects which diminish the material's response to subsequent ageing in terms of mechanical properties and corrosion resistance. Contamination of the quenchant is unavoidable and fairly rapid, because of the molten salt retained on the surface of the components. To reduce distortion hot water quenches were used originally, but in recent years PAG solutions have become increasingly popular. PAG's are currently the only class of polymer quenchant permitted by US military specifications for this application.⁽¹¹¹⁾ However, these specifications are currently being revised in order to include other classes of polymer. *Figure 165* shows the effect of AVS 250 sodium nitrite/nitrate salt content on the maximum cooling rate for water and both 15 and 30 per cent PAG (Quendila PA) solutions. It is clear from this figure that there is little difference between the maximum cooling rate for water and the 15 per cent PAG solution with salt levels above 2.5 weight per cent. Similarly, the critical level for the 30 per cent PAG solution was 5 weight per cent salt. Thus, from the point of view of minimizing distortion by reducing the cooling rate, there are no apparent advantages over water in using this particular PAG contaminated with salt above these critical levels. This is in agreement with the experience of Anderson et al.⁽¹²⁴⁾ Nevertheless, the contaminated solutions could still help reduce distortion since they enhance the wetting of the hot aluminium, thus producing more uniform cooling.

The polymer quenchant suppliers actually recommend thermal separation of the PAG from the salt-rich aqueous phase for salt contamination levels between 12 and 14 weight per cent.^(95,123) The salt-rich phase can then be discarded and the polymer

rediluted with fresh water. This 12 to 14 weight per cent range was probably chosen because of the influence of the salt in the inversion temperature for the PAG, which was shown in *Figure 138*. Between 12 and 14 weight per cent salt, the inversion temperature fell to a value between 50 and 60°C. This is close to the operating temperature for some quench tanks and bulk inversion problems could arise. In addition, as the level of salt increases, so too does the specific gravity of the aqueous phase. Therefore, above approximately 12 weight per cent salt, thermal inversion causes the polymer-rich phase to stratify on top. This facilitates the removal of the salt-rich aqueous phase which is drained from the bottom of the tank.

The PAG is "salted-out" because of the solutions changing electrolytic character. The PAG is nonionic, whereas the salt acts as an electrolyte. Since water is a better solvent for the salt ions than it is for the nonionic polymer, increasing the amount of salt raises the activity of the polymer and it is "salted-out". Debye and McAulay⁽¹⁸⁶⁾ showed that the upper temperature limit for neutral molecules in water should be lowered in a manner proportional to the size, amount and valences of the ionic species added. Upon increasing the salt content, the kinematic viscosities of the PAG solutions were reduced (*Figure 137*). This is associated with the increased number of hydration shells around the ions, leading to a reduction in the number of water molecules available for the solution of the polymer, and a decrease in its hydrodynamic volume.

Figure 166 shows the effect of the sodium nitrite/nitrate salt additions on the maximum cooling rate for water and 15 volume per cent solutions of the representative PVP and polyacrylate quenchants. The PVP (Parquench 90) exhibited a 45 per cent decrease in maximum cooling rate upon increasing the salt content to 1 weight per cent. This pronounced decrease in cooling rate is difficult to explain since there was little change in the kinematic viscosity of the solution as seen in *Figure 137*. PVP's are known to exhibit exceptional complexing ability, being able to bind a wide variety of small molecules and ions.⁽¹⁴⁸⁾ This initial decrease in cooling rate could thus possibly be the result of complex formation. In a similar fashion to the

PAG, the solubility of the PVP will tend to decrease upon increasing the salt content, because of its nonionic character.

The polyacrylate had the lowest maximum cooling rate ($50 \pm 5^\circ\text{C/s}$) in the uncontaminated condition. However, the addition of just 0.5 weight per cent salt increased this rate to $83.7 \pm 0.8^\circ\text{C/s}$. The increase in cooling rate was reflected in a rapid decrease in kinematic viscosity (*Figure 137*). This decrease in viscosity is most probably associated with the increased number of sodium counterions. Polyelectrolytes exhibit chain coiling and reduced solubility in the presence of excess counterions. The critical level of AVS250 for this polyacrylate solution was 25 weight per cent. Thus, in terms of reducing the level of distortion in quenched aluminium components by reducing the cooling rate, the polyacrylate would appear to be the best choice since it had the highest tolerance to salt contamination. The PVP, although having a much higher maximum rate than the PAG solutions when fresh, was superior to even the 30 per cent PAG solution at salt contamination levels above 0.5 weight per cent.

5.7 Drag-Out.

The amount of drag-out for 5, 15 and 25 per cent solutions of each representative polymer, tested at 30°C in both the static and agitated condition, was shown in the form of a histogram (*Figure 139*). The level of drag-out increased as the concentration of the solutions was raised. Agitation reduced the drag-out level especially for high concentration solutions. *Figure 167* shows that there was a roughly linear relationship between the levels of drag-out for the static tests and the kinematic viscosities of the solutions measured at 40°C . Consequently, the polyacrylate solutions tended to suffer higher drag-out levels compared with the PAG, which in turn had higher levels than the PVP. However, upon closer inspection of *Figure 167*, it can be seen that each class of polymer exhibited its own particular trend.

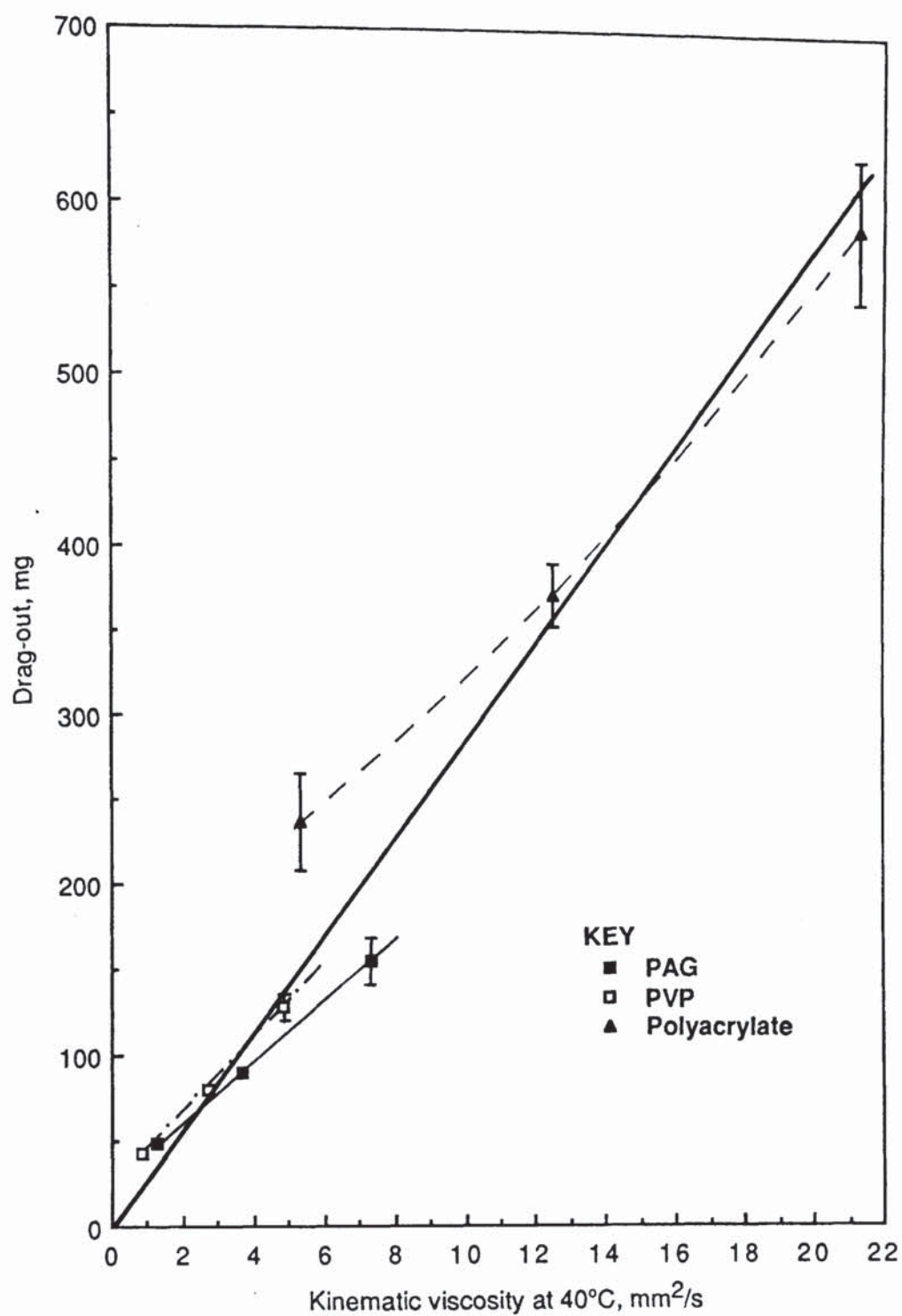


Figure 167. The effect of the representative polymer solution viscosity on the level of drag-out in the static tests.

The amount of water and fresh polymer required to maintain a 2 litre sample of each representative polymer quenchant during the accelerated ageing test was given in *Table 27*. This data also reflects the amount of drag-out for these nominally 15 volume per cent solutions since a lid was employed to minimize evaporative losses. Nevertheless, in order to maintain a constant refractometer reading for each of these solutions more distilled water than polymer concentrate had to be added. More polyacrylate concentrate than PAG was required, and less PVP concentrate than PAG. This is as would be expected from *Figure 167*. However, it would have been predicted from this figure that the concentrate additions would have been in the ratio 1 : 0.89 : 4.10 (PAG : PVP : Polyacrylate), whereas the actual additions were in the respective ratio 1 : 0.74 : 1.58. Thus, much less polyacrylate concentrate was added than would have been predicted from the drag-out test. One of the reasons for this is almost certainly the large decrease in the kinematic viscosity of the polyacrylate solution with usage as was shown in *Figure 162*. If the mean kinematic viscosity of the solutions during the accelerated ageing test is considered, the ratio now becomes 1 : 0.50 : 1.74 (compared with 1 : 0.72 : 3.38 when fresh). The fit is therefore much closer for the polyacrylate when its change in viscosity is taken into account. On this basis the drag-out for the PVP is now higher than would be anticipated. Furthermore, from *Table 27* it can be seen that the proportion of polymer concentrate to water added during the accelerated test was higher for the PVP than the other two classes of polymer. The PAG concentrate constituted 10.7 per cent of the total addition, the PVP 13.5 per cent and the polyacrylate 10.4 per cent. The total accelerated test solution volume (2 litres) was replaced 1.2 times for the PAG, 0.7 times for the PVP and twice for the polyacrylate. Consequently, the influence of polymer degradation is likely to be more pronounced for the PVP.

As described previously, polymer quenchants produce an insulating polymer-rich film around the workpiece. This film is a consequence of either localized evaporation producing a "gel-like" temporary three-dimensional chain-entanglement network, or a precipitation reaction depending on the polymer structure. Regardless of how the film is formed, it does not redissolve instantaneously once the surface of the quenched

metal has fallen below the boiling point of the solution or the inversion temperature for phase separation. High polymer concentrations or molecular weights produce thicker films which are more difficult to dissolve. From *Figure 167*, it can be seen that at a kinematic viscosity of $5\text{mm}^2/\text{s}$ at 40°C the PAG would exhibit lower drag-out than the PVP. This is believed to be associated with the PVP's much higher molecular weight and its possible susceptibility to cross-linking adjacent to the hot metal. Higher molecular weight chains are more likely to be dragged out, thus shifting the molecular weight distribution to lower weights and contributing to the change in the cooling characteristics with usage. Those degradation mechanisms which induce chemical cross-linking make the polymer films insoluble and hence increase the level of drag-out. This could explain the PVP's higher drag-out in the accelerated ageing test than was predicted from the solution's mean kinematic viscosity. The polyacrylate exhibited significantly higher drag-out than the other two classes of polymer for a solution of given kinematic viscosity as seen in *Figure 167*. This was despite the fact that the polyacrylate examined had a lower molecular weight than the PVP. The charged character of the polyacrylate means that it is likely to be permanently adsorbed onto the quenched metal surface to a greater extent than the other two nonionic polymers. This effect is likely to be more pronounced at lower solution viscosities as suggested by the curved nature of the plot for the polyacrylate in *Figure 167*.

Agitation of the solutions tended to displace the residual polymer-rich films which were formed at high temperatures and increased the speed at which they redissolved. This is because increased turbulence results in enhanced mass transfer. Forced convection is thus an effective means of reducing the level of drag-out.

Segerberg⁽¹²⁰⁾ conducted a similar drag-out experiment using flat hexagonal test pieces (*Figure 52(a)*) quenched into static quenchants. He showed that polyacrylates tended to produce lower drag-out losses when compared with PAG's of equivalent quenching intensity, and that polymer solutions generally resulted in less drag-out than quench oils (*Figure 52(b)*). The drag-out data from the current work shows that both the PVP and the PAG solutions, over their normal concentration range, exhibited

lower drag-out than a normal speed quench oil at 40°C (*Table 36*). However, the polyacrylate solutions (even at 5 per cent concentration) tended to have higher levels of drag-out than either the oil or the PAG solution. Differences in the shapes of the test pieces could explain the discrepancy between the results. The test piece used during the present work (*Figure 73*) contained a hole and a sharp angle incision which tended to entrap polymer-rich film, especially for the polyacrylate, and thus increase the amount of drag-out. Nevertheless, the findings of this work are in general agreement with Segerberg's overall conclusion that the amount of drag-out is dependent on six variables: the type of polymer; its concentration and temperature; the surface temperature of the component when taken out of the bath; and its shape and surface condition.

5.8 Polymer Quenchant Control.

Segerberg⁽¹²⁰⁾ questioned the validity of refractometer readings for polymer quenchant control, by comparing the cooling data for polluted quenchants with those for a freshly prepared solution with the same refractive index (*Figure 43*). The present findings confirm Segerberg's doubts, even for uncontaminated aged quenchants. The refractometer reading is a measure of the total dissolved solids content. *Figure 136* clearly demonstrated how salt contamination significantly increased the refractometer reading for each class of polymer quenchant. With uncontaminated solutions, the refractive index reflects the amount of polymer in solution, but takes no account of changes in the molecular weight distribution of that polymer which influences the cooling characteristics. Kinematic viscosity measurements, although more time consuming to perform, are sensitive to changes in molecular weight and are therefore more effective as a means of monitoring the condition of the quenchant. However, the polymer solution viscosity may also be affected by contaminants as was demonstrated in *Figure 137*.

An ideal quenchant would consistently maintain the optimum cooling characteristics for a particular application. Unfortunately the cooling characteristics of all quenchants change with usage. Due to the larger number of variable parameters affecting the

cooling characteristics of polymer solutions, control is more critical than with quench oils. As has been demonstrated during this work, the polymer solution temperature, concentration and level of agitation all have a significant influence on the cooling characteristics. Furthermore, the intensity of the quench is also significantly affected by contamination and degradation, whilst the concentration is influenced by drag-out and evaporation. The Wolfson Engineering Group quench test has been found to be sensitive to variations in each of these parameters. It is therefore ideally suited for routine process control, and could be readily incorporated within a heat treatment shops statistical process control (SPC) programme. Subtle changes in the cooling characteristics would be instantly detected, enabling prompt remedial action, thus avoiding the risk of costly cracked or distorted components. The test is also eminently suitable for the judicious selection of quenchant and for the development of new products.

5.9 Quenched Hardness and Residual Stress.

Due to the highly complex unsteady-state nature of the quenching process, accurate predictions of the hardening response of even simple geometry steel components poses considerable difficulties. The hardness developed at each position within the component depends on the composition of the steel and its thermal history. Traditional predictive methods, such as those based on Grossmann's quench severity factor or on the tables of Atkins and Andrews, are insensitive to the characteristics of the quenchant and can only give a rough guide (Section 2.9). A universally acceptable hardness equivalence criterion will need to be flexible enough to take into account the characteristics of the quenchant plus the transformation kinetics for the particular material being cooled. Accurate predictions will certainly require a powerful computer technique such as that proposed by Hildenwall.⁽⁶¹⁾ Provided reliable physical data for the material being quenched is available, finite difference or finite element heat transfer programmes could be employed to calculate the time-temperature profiles for regular spatial positions within the quenched component. Huge amounts of physical data would need to be collated due to the variation with temperature. However, the fundamental problem faced is that of trying to relate the cooling characteristics of a

quenchant monitored with a test probe to those of a quenched component, since the interfacial heat transfer coefficient c varies with the size, shape and surface finish of the quenched piece.⁽⁵⁴⁾

These factors must be borne in mind when interpreting the hardness and residual stress results for the 080H41 steel specimens which had been quenched into a number of quenchants. The steel cylinders were of equivalent geometry to the Wolfson test probe and had been quenched using the same conditions that were used when evaluating the cooling characteristics of the quenchants. *Figure 168* shows the relationship between the maximum cooling rate measured for the various quenchants and the surface residual hoop stresses generated in the quenched specimens. It is clear that as the maximum rate increased, so in turn did the resulting level of stress. The highest stress ($265 \pm 19\text{MPa}$), was generated at the surface of the water quenched bar. Tensile residual macrostresses were developed in the surface of each specimen.

When quench hardening steels, the residual stress pattern produced is a consequence of differential expansions and contractions within the part associated with the thermal gradient and phase transformations. When austenite transforms to produce either martensitic, bainitic or pearlitic structures there is a corresponding expansion. Compressive residual macrostresses are induced by the thermal gradient, and when the phase transformation begins at the interior of the quenched part. Tensile residual macrostresses, on the other hand, are produced when the transformation starts in the surface. This is commonly associated with the formation of martensite. When the part is through hardened, for example, the martensitic expansion (about 4 per cent) begins at the surface because it reaches the M_s temperature first, whilst the interior is at a higher temperature. The hot ductile austenite in the interior follows the outside expansion plastically. When the inside of the part subsequently transforms and expands, the cold outside surface shell is stretched elastically. Generally, the larger the dimensions of the part, the greater the stresses developed (Section 2.14).

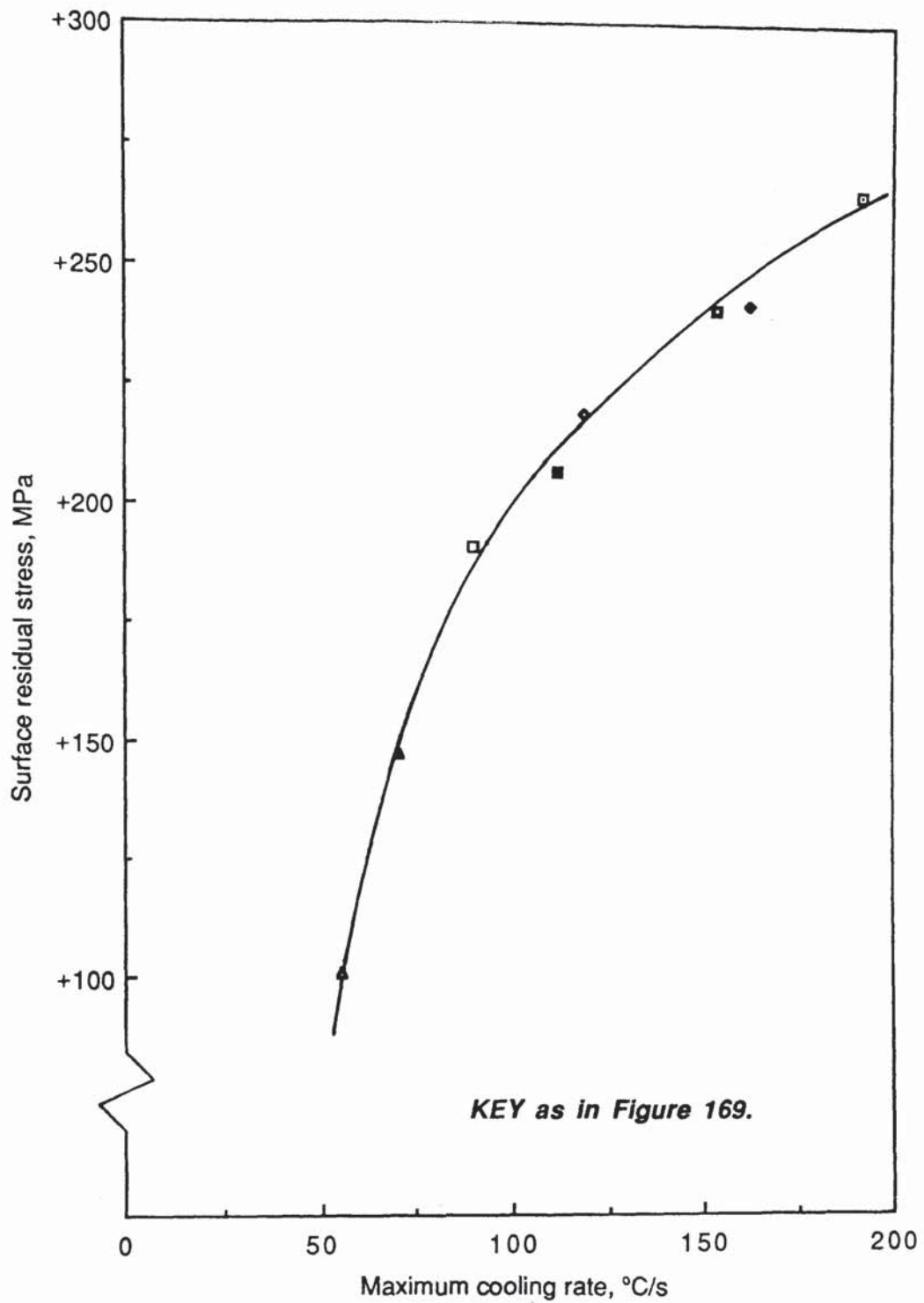


Figure 168. The relationship between the residual hoop stress in quenched 12.5mm diameter 0.45%C steel bars and the maximum cooling rates for the various quenchants measured using the Wolfson Engineering Group test.

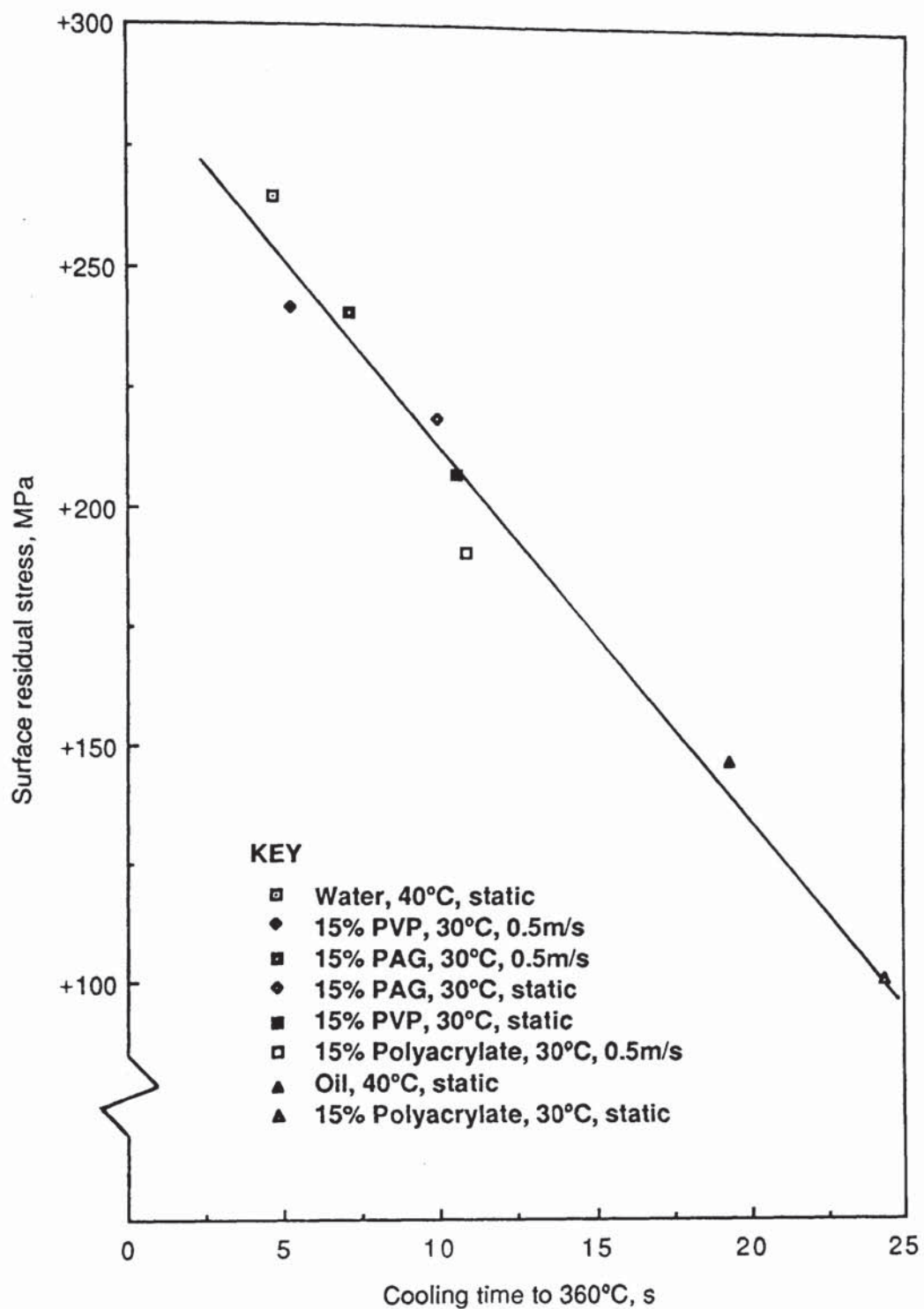


Figure 169. The relationship between the residual hoop stress in quenched 12.5mm diameter 0.45%C steel bars and the cooling times to 360 °C for the various quenchants measured using the Wolfson Engineering Group test.

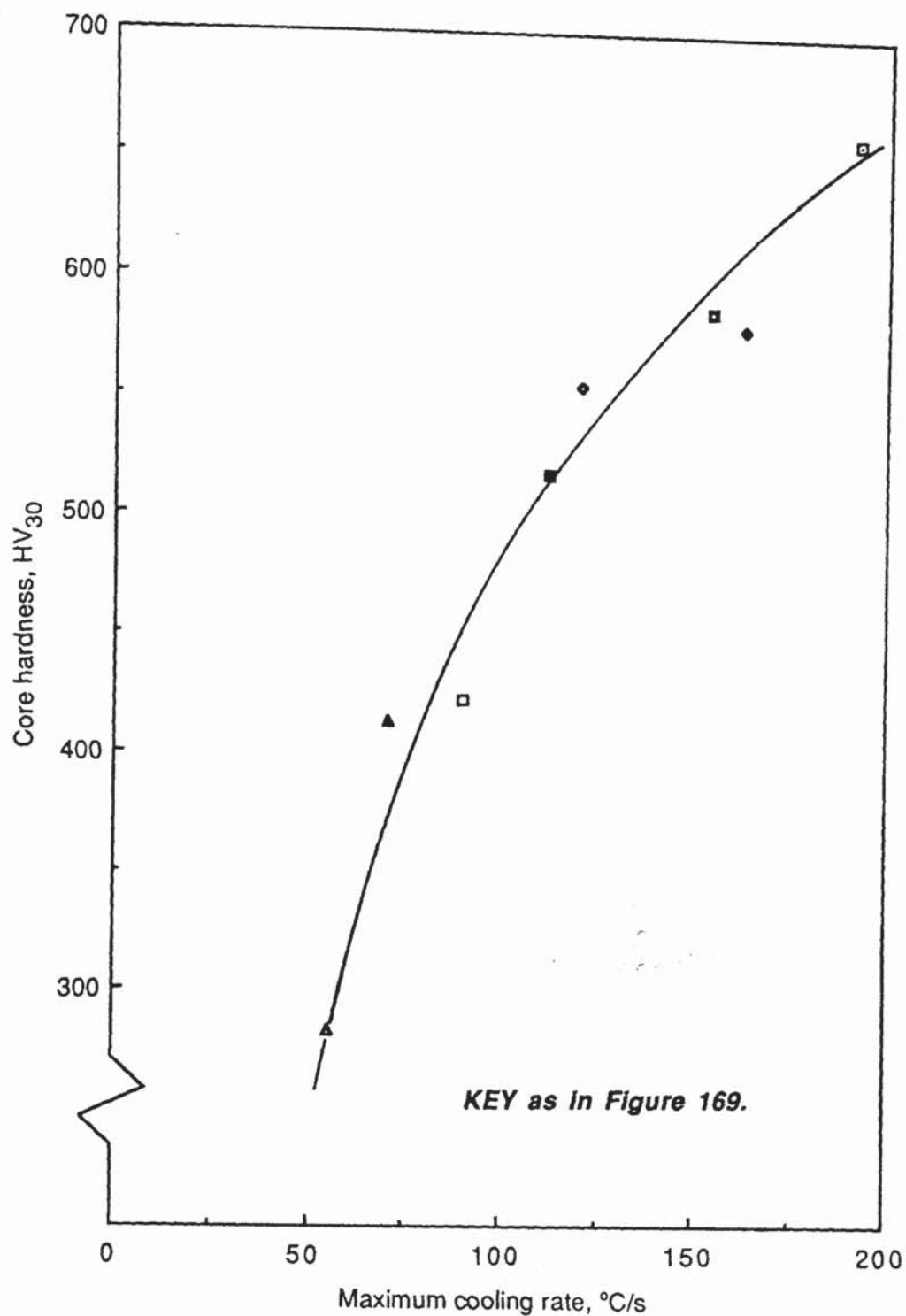


Figure 170. The relationship between the core hardness in quenched 12.5mm diameter 0.45%C steel bars and the maximum cooling rates for the various quenchants measured using the Wolfson Engineering Group test.

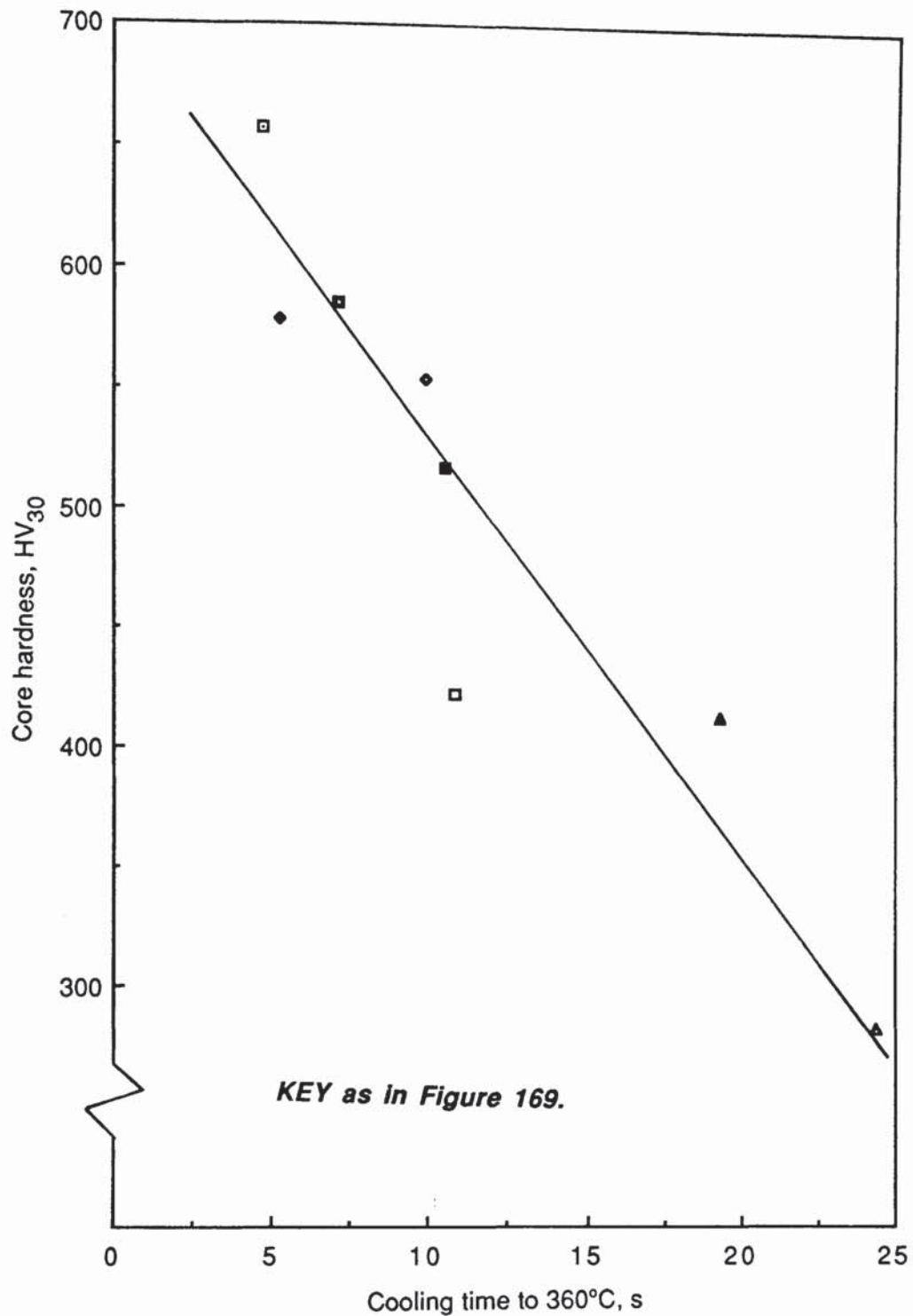


Figure 171. The relationship between the core hardness in quenched 12.5mm diameter 0.45%C steel bars and the cooling times to 360 °C for the various quenchants measured using the Wolfson Engineering Group test.

Figure 169 reveals an approximately linear relationship between the cooling time to 360°C (M_s temperature for the steel) measured using the Wolfson Engineering Group test and the surface residual macrostress for the quenched steel cylinders. However, it must be noted that the thermal history of the quenched specimens will have been different to that of the Wolfson test probe quenched under the same conditions, even though they are both of the same geometry. This can be attributed not only to differences in the thermal diffusivities of Inconel and the steel, but also to the influence of the heats of transformation associated with the steel.

Figures 170 and 171 illustrate that the core hardness values exhibited similar relationships to maximum cooling rate and cooling time to 360°C as those of residual stress. There was a linear relationship between the surface hardness and the surface residual macrostress as indicated by the following regression equation with a correlation coefficient of 0.99:

$$\text{Surface stress} = 0.440 (\text{surface hardness}) - 26 \quad (42)$$

where the stress is given in MPa and the hardness in HV₃₀. The specimen quenched in static water at 40°C produced a core hardness of 657HV₃₀, compared with 413HV₃₀ for the static normal speed quench oil at the same temperature. The polymer-quenched specimens generally exhibited hardnesses and residual stresses intermediate between those obtained with the water quench and the oil.

Agitation of the polymer quenchants tended to increase both the hardness values and the residual macrostresses. Agitation of the PAG solution raised the residual macrostress by approximately 10 per cent and the hardness value by around 7 per cent. The influence of agitation on the PVP was to increase the stress by 17 per cent and the hardness by about 12 per cent. The static polyacrylate solution at 30°C produced residual stress and hardness values lower than those developed in the static oil quench at 40°C; however, when agitated, the measured stress increased by 89 per cent and the hardness values by about 50 per cent. Nevertheless, both the hardness

and residual stress values for the specimen quenched in the agitated polyacrylate solution were lower than those obtained with the other polymer quenchant types, even in the static condition.

The correlation for these particular specimens proposed by Nicklin⁽⁷⁰⁾ (equation (14)), for predicting core hardness values from the cooling times to 600°C measured from static Wolfson Engineering Group tests, was found to be unsatisfactory when dealing with aqueous quenchants. For example, the specimen quenched into the static 15 per cent PVP solution at 30°C had a core hardness of 517HV₃₀. The value predicted using equation (14) is 910HV₃₀: this is higher than the maximum attainable hardness for this grade of steel. However, the fit was better for the static oil sample where the predicted hardness was 469HV₃₀ and the measured value 413HV₃₀. This is not surprising since Nicklin derived equation (14) using data from oil tests alone. Consequently, the cooling times to 600°C ranged from only 9.2s to 12.2s, the range for the quenchants examined during this work was 2.8s to 17.2s. A modified form of Nicklin's regression equation is given below for the samples examined during this work:

$$HV = 644.4 + 126.8V - 18.7t_{600} \quad (43)$$

where HV = core hardness for quenched 12.5mm diameter 080H41 bars (HV₃₀).

V = fluid velocity (m/s)

t = cooling time to 600°C in a static Wolfson Engineering Group quench test (s).

The correlation coefficient for this equation is 0.92. However, equations such as this are facile and serve little or no scientific purpose, because they are only valid for the particular geometry and composition of specimen examined. Furthermore, they take no real account of the transformation behaviour of the material (although in this case the cooling time to 600°C corresponds approximately with the ferrite nose on the CCT diagram for this material (*Figure 13(b)*). Such analysis may, however, be useful for companies providing large quantities of one component and experiencing variation in HV when using a variety of furnaces and quench facilities.

5.10 New Polymer Quenchants.

The quench test results for the prototype quenchant formulations incorporating the 500,000 \overline{M}_w (poly(ethyloxazoline)) were very interesting (*Figures 144 to 146*). However, these prototype formulations would not be suitable as commercial quenchants without the addition of certain other additives, such as corrosion inhibitors. The straight 2.25 weight per cent PEOx solution exhibited no stage A cooling, and twin boiling peaks when tested in the static condition (*Figure 144*). When agitated the cooling rate profile for this sample looked much more attractive. The forced convection increased the maximum cooling rate, eliminated the second boiling peak and hence considerably reduced the rate of cooling at 300°C from $50 \pm 4^\circ\text{C/s}$ to $10 \pm 1^\circ\text{C/s}$. The cooling rate profiles were reminiscent of those for the PVP's, which is not surprising since they are both high molecular weight polymers used at relatively low true solution concentrations. Consequently, control of this class of nonionic polymer may prove to be a problem. Furthermore, the industrial usefulness of this particular polymer is limited by its low cloud point ($59 \pm 1^\circ\text{C}$). This problem could be reduced by the use of a lower molecular weight product.

The cooling rate profiles for the 1.5 weight per cent PVP : PEOx (3:1) mixed polymer solution proved disappointing (*Figure 145*). Twin boiling peaks were evident in both the static and agitated tests, resulting in much higher rates of cooling at 300°C than a straight 1.5 weight per cent Parquench 90 solution.

Figure 146 showed the cooling curves for the 10 weight per cent PAG : PEOx (9:1) mixed polymer solution. The results for both the static and agitated tests looked promising, since lower cooling rates at 300°C were produced than for higher concentration single polymer PAG solutions. For example, the rate of cooling at 300°C for a 30 per cent Quendila PA solution (true PAG concentration approximately 18 weight per cent) tested at 30°C and 0.5m/s was $43 \pm 1^\circ\text{C/s}$ (*Figure 113*). This compares with a value of $29 \pm 1^\circ\text{C/s}$ for the 10 weight per cent PAG : PEOx (9:1) mixture which was tested at the same conditions. However, the inversion temperature for this mixture was only $45 \pm 1^\circ\text{C}$.

CHAPTER 6

6.0 CONCLUSIONS

1. The Wolfson Heat Treatment Centre Engineering Group test is a highly sensitive means of monitoring the cooling characteristics of quenchants. When assessing polymer quenchants, agitation of the sample is required in order to produce a realistic test and to improve the reproducibility of the results. Following the examination of a number of forced convection systems, the preferred method comprises positioning the preheated test probe 25mm above the geometric centre of a 25mm diameter outlet tube through which the quenchant sample is being pumped at a fluid velocity of 0.5m/s. By inserting the probe into this submerged jet of fluid, turbulent flow conditions are established around it. However, the actual stability of the flow depends on the viscosity of the fluid. A small variable speed centrifugal pump is employed and the quench tank is of the same dimensions as that outlined in the internationally approved Wolfson standard method for evaluating quench oils. The total capacity of the system is only 2 litres which, unlike previously reported pump agitation systems, makes it suitable for routine laboratory scale tests.

2. Three commercial polymer quenchant types have been studied (PAG, PVP and polyacrylate). Each was capable of providing a wide range of cooling rates depending on the molecular architecture of the polymer, the product formulation, the solution concentration, the solution temperature and the level of agitation. Generally, the cooling performance of these polymer quenchants is intermediate between that of quench oils and of water.

3. All polymer quenchants are believed to operate by the same fundamental mechanism. This mechanism is associated firstly with the increased viscosity of their solutions compared with water and, secondly, with their ability to produce an insulating polymer-rich film around the hot metal. The way in which this film forms depends on the structure of the polymer. For polymers which exhibit normal solubility in water, such as PVP and polyacrylate, localized evaporation occurs

adjacent to the hot metal surface producing a polymer concentration gradient increasing towards the liquid-gas interface. This results in the formation of a temporary three-dimensional polymer chain entanglement network or gel. With amphipathic polymers which exhibit inverse solubility (i.e. a lower critical solution temperature), such as PAG's, the polymer is actually precipitated below the boiling point of the solution. This is because the thermally labile H-bonds between the water and the polymer become less numerous as the temperature increases, causing a reduction in the hydrodynamic volume of the polymer.

During stage A cooling the polymer-rich film encapsulates the vapour blanket, thus stabilizing it. This view is contrary to previously proposed mechanisms. Bubble growth rate and hence heat transfer are retarded during stage B by the inertia of the viscous polymer film. However, for each class of polymer quenchant examined, there was little advantage to be gained in terms of reducing the maximum cooling rate, by increasing the kinematic viscosity of the solution above about $20\text{mm}^2/\text{s}$ at 40°C . A microlayer of vapour beneath the polymer-rich film during nucleate boiling minimizes thermal degradation of the macromolecules. The rate of cooling during stage C is reduced by raising the viscosity of the solution which in addition enhances adsorption of residual polymer on the surface of the metal. One or more of these traditional stages of cooling may occur simultaneously at different positions upon the quenched metal surface. These points were demonstrated using photographs of a Wolfson test probe quenched into representative solutions of each class of polymer.

4. Higher molecular weight polymers are required at lower solution concentrations to produce equivalent solution viscosities and heat transfer rates. Increasing the concentration or temperature of the solution tends to decrease the rate of cooling by producing more stable polymer-rich films, whilst increasing the level of agitation decreases film stability and therefore increases the rate of cooling. The rate of heat transfer will increase upon raising the level of agitation until fully turbulent conditions are developed around the quenched piece. Nevertheless, turbulent flow around the hot metal is essential when using polymer quenchants in order to produce more uniform polymer-rich films which, although thinner, result in more consistent

cooling and less likelihood of cracking and distortion.

5. Close control of polymer quenchants is essential, since their characteristics change with usage. Contamination, for example, can have a significant effect: volatile contaminants generally tend to increase stage A and reduce the maximum cooling rate, while salts have the opposite effect. Salts also reduce the solubility of the polymers, especially the PAG's.

During long-term use, degradation of the polymers (due to the combined influence of thermal, oxidative, mechanical and biological processes) also affect their characteristics. A reduction in the polymer's average molecular weight results in a corresponding reduction in the solution viscosity, and an increase in the maximum cooling rate and rate at 300°C. This would increase the possibility of cracking and distortion problems. High molecular weight polymers, such as PVP's, are more susceptible to chain scission. In addition, PVP's are capable of being chemically cross-linked adjacent to the hot metal surface. Consequently, this class of polymer exhibits erratic quenching performance with usage. The polyacrylates, being anionic polyelectrolytes, are very effective aqueous thickening agents, producing the most "oil-like" cooling characteristics. However, they are precipitated from solution by polyvalent metal cations, and their solution viscosity drops very rapidly with initial use with a corresponding increase in cooling rate. The lower molecular weight PAG which was used at higher true solution concentrations had greater stability, and provided more consistent cooling with usage.

Evaporation of water tends to increase the concentration of polymer quenchants with usage. Drag-out of residual polymer on the surface of the cool metal, on the other hand, reduces the effective solution concentration. The level of drag-out is associated with the viscosity of the solution: the higher the molecular weight of the polymer and hence the viscosity for a given concentration, the greater the drag-out. The charged character of the polyacrylate results in enhanced adsorption and higher drag-out. However, the level of drag-out is reduced for each class of polymer quenchant by

agitating the solution; this is particularly true for high concentration solutions.

6. Refractometer readings are an unreliable means of monitoring the concentration of polymer quenchants. Contaminants tend to raise the readings, and in long term usage the shift in the polymer's molecular weight distribution to lower molecular weights is not accounted for. Kinematic viscosity measurements are more reliable but lack the superior sensitivity of the Wolfson Engineering Group test, in instantly detecting subtle changes in the cooling characteristics.

7. Good correlation has been obtained between the Wolfson cooling data and the hardness and surface residual macrostress measured for 0.45 per cent plain carbon steel specimens of the same geometry as the Wolfson probe and quenched under exactly the same conditions. The higher the cooling rate, the higher the levels of hardness and residual stress developed. However, no satisfactory method is currently available to compare the cooling characteristics of a test probe with the hardening response of industrial components using a variety of steels.

8. Improved polymer quenchant products (such as those incorporating poly(ethyloxazoline), combined with more effective process control, will undoubtedly result in the more widespread use of polymer quenchants in the near future, with considerable technical and environmental benefits.

CHAPTER 7

7.0 SUGGESTIONS FOR FURTHER WORK

1. To perform trials using the preferred agitation system described during this work but with the incorporation of some method of inducing fully turbulent flow within the pump outlet tube.
2. To conduct chemical analyses on the degradation products of the representative polymer quenchants examined.
3. To develop a solution to the inverse problem of conduction for a standard Wolfson Heat Treatment Centre Engineering Group quench test probe, thus enabling surface heat transfer coefficients to be estimated.
4. To examine the efficacy of poly(ethyloxazoline) solutions, and those based on polyalkylene glycols with branched structures and molecular weights greater than 20,000, during prolonged usage.
5. To investigate various automated polymer concentration control systems. For example, the flowrate through a pump agitation system could be used to indirectly measure the solution viscosity. A microprocessor controller could then be used to add either fresh polymer concentrate from a holding vessel, or water from the mains to the quench tank via a series of electrically operated valves.
6. Since polyacrylate polymer quenchants are anionic polyelectrolytes it may be possible to control the rate of heat transfer using an electric field. It is already known that stage A cooling is suppressed, with an increase in steel hardening response, when a moderate electric field strength of about 10kV/cm is employed.⁽¹⁸⁷⁾ By making the quenched component anodic, negatively charged polyacrylate will be transferred by electrophoresis, therefore aiding the formation of an insulating polymer-rich film, even below the boiling point of the solution. Once cool the polarity could be reversed in order to rapidly dissipate the polymer, thus minimizing drag-out.

APPENDICES

APPENDIX A

Computer Program for the Analysis of the Gel Permeation Chromatograms written in BASIC for the Apple II plus

```
1      REM *** GPC CALCULATION ***
5      HOME :D$ = CHR$(4)
10     PRINT D$:"OPEN";"CALIB GPC"
15     PRINT D$;"READ";"CALIB GPC"
18     INPUT N
19     DIM D(N),B(N),L(N)
20     FOR I = 0 TO N - 1
22     INPUT D(I)
23     INPUT B(I)
24     INPUT L(I)
25     NEXT
27     INPUT G
29     INPUT C
30     INPUT R
35     REM "D(I)=MOL.WT.AT B(I)(ELUTION VOL)"
40     PRINT D$;"CLOSE";"CALIB GPC" VTAB 12
50     PRINT "PROGRAM FOR CALCULATED N OF MN AND MW OF"
51     PRINT "POLYMER FROM GPC TRACE"
52     PRINT
53     PRINT
55     INPUT "WHAT IS THE CODE NAME FOR THIS SAMPLE?";NAME$
56     IF NAME$ = "" THEN GOTO 55
57     INPUT "DATE OF ANALYSIS";TIME$
60     PRINT "HOW MANY SETS OF DATA HAVE YOU?"
70     INPUT K
72     K=K-1
76     PRINT
77     PRINT
85     PRINT
86     PRINT "PRESS ANY KEY TO CONTINUE"
90     GET A$
100    HOME
105    SPEED= 105
110    PR# 2
113    PRINT "GPC ANALYSIS FOR SAMPLE";NAME$;" ";TIME$:PRINT: PRINT
114    PR# 0
120    DIM V(K),H(K),W(K),N(K),X(K),Y(K)
130    PRINT "YOU MAY EITHER TYPE IN EACH ELUTION VOL OR IF THE Y ARE AT
        REGULAR INTERVALS YOU"
131    PRINT "MAY TYPE IN THE FIRST AND LAST VALUES TOGETHER WITH THE
        INTERVAL"
132    PRINT "1-INDIVIDUAL VALUES"
133    PRINT "2-FIRST LAST AND INTERVAL"
134    PRINT "PRESS THE APPROPRIATE KEY"
135    GET AN$
136    IF AN$ = "1" GOTO 150
137    IF AN$ = "2" GOTO 140
```

```
138 GOTO 135
140 GOSUB 8000
145 GOTO 175
150 HOME: PRINT "TYPE IN YOUR DATA IN PAIRS AS ELUTION VOLUME(RETURN) AND
      HEIGHT(RETURN)"
152 PRINT TAB( 2)"ELUTION VOL(ML)"; TAB( 25)"HEIGHT(MM)"
153 I = 0
155 INPUT "VE(ML)= ";V(I): INPUT"H(MM)=";H(I)
160 I =I + 1
170 IF I <=K GOTO 155
175 GOSUB 400
176 GOSUB 6000
180 S1 = 0
190 S2 =0
200 S3 = 0
210 FOR I=0 TO K
215 REM "FIND VALUE OF M(I)"
220 GOSUB 2000
230 S1 = S1 + (H(I) * M(I))
240 S2 =S2 +H(I)
250 S3 = S3 + (H(I) * M(I))
254 W(I) = H(I)
256 N(I) = H(I) / M(I)
260 NEXT I
270 MW = S1 /S2
280 MW =S2 /S3
290 D = MW /MN
300 MW = INT (MW / 10) * 10
310 MN = INT (MN / 10)*10
320 D = INT (D* 100) / 100
330 PR£2
340 PRINT "WEIGHT AVERAGE M WT =";MW
342 PRINT
343 PRINT
350 PRINT "NO.AVERAGE M WT = ";MN
352 PRINT
354 PRINT
356 PRINT "POLYDISPERSITY=";D
360 PR£ 0
400 PRINT "DO YOU WANT INFORMATION ON THE DISTRIBUTION? Y?N"
410 INPUT A$
420 HOME
430 IF A$ = "N" GOTO 740
435 PR£2
437 POKE 36,2: PRINT "ELUTION VOL";: POKE 36,15: PRINT "HEIGHT";: POKE 36,32:
      PRINT "M W T";: POKE 36,47: PRINT "WT,FRACT";: POKE 36,60: PRINT
      "NO.FRACT"
455 PRINT
460 FOR I = 0 TO K
462 W(I) =INT (N(I)*1000 /S2) / 1000
464 N(I) = INT (N(I) *1000 /S3)/ 1000
470 POKE 36,3: PRINT V(I);: POKE 36,33: PRINT INT (M(I));: POKE 36, 48: PRINT
      W(I);:POKE 36, 61: PRINT N(I)
475 PRINT
480 NEXT I
490 PR£ 0
```



```
495 GOSUB 5000
500 PRINT "DO YOU WISH TO SEE A WT.FRACT.CURVE? Y/N"
510 INPUT A$
515 HOME
520 IF A$ = "N" GOTO 620
525 HOME
530 PRINT "WHAT IS THE MAX. VALUE OF W(I)?"
540 INPUT WL
545 HOME
550 GOSUB 3000
555 VTAB 22
556 PRINT "RANGE OF W(I) FROM 0 TO"; WL
560 FOR I = 0 TO K
570  $X(I) = (200 * M(I) / M(0)) + 20$ 
580  $Y(I) = 150 - (140 * W(I) / WL)$ 
590 HPLOT X(I),Y(I)
600 NEXT I
602 PRINT "DO YOU WANT TO CHANGE UPPER LIMIT? Y/N"
604 INPUT A$
605 TEXT
606 IF A$ = "Y" GOTO 525
620 PRINT "DO YOU WANT TO CHANGE UPPER LIMIT? Y/N"
630 INPUT A$
640 HOME
650 IF A$ = "N" GOTO 740
652 HOME
655 PRINT "WHAT IS THE UPPER LIMIT OF N(I)?"
660 INPUT NU
670 GOSUB 3000
672 VTAB 22
675 PRINT "RANGE OF N(I) FROM 0 to "; NU
680 FOR I = 0 TO K
690  $X(I) = (200 * M(I) / M(0)) + 20$ 
700  $Y(I) = 150 - (140 * N(I) / NU)$ 
710 HPLOT X(I), Y(I)
720 NEXT I
725 PRINT "DO YOU WISH TO CHANGE THE UPPER LIMIT? Y/N"
728 INPUT A$
730 TEXT
732 IF A$ = "Y" GOTO 652
733 PRINT "DO YOU WISH TO KEEP A DISC FILE OF THESE RESULTS? Y/N"
734 GET ANS$
735 IF ANS$ = "Y" THEN GOSUB 7000
740 PRINT "DO YOU WISH TO ANALYSE ANOTHER CURVE? Y/N"
745 SPEED= 255
750 INPUT A$
755 HOME
760 IF A$ = "Y" GOTO 60
770 END
2000  $M(I) = 10 + (C+(G * V(I)))$ 
2010 RETURN
3000 REM SET HGR
3010 HGR
3020 REM DRAW GRID
3030 FOR A = 20 to 220 step 50
3040 HPLOT A, 10 TO A,152
3050 NEXT A
```

```
3060 FOR B = 10 TO 150 STEP 70
3070 HPLOT 20, B TO 220,B
3080 NEXT B
3085 VTAB 21
3087 T = INT (M(O) / 1000)* 1000
3090 PRINT TAB ( 3 )0; TAB ( 15) T /2; TAB (3) T
3100 RETURN
4000 PRINT:PRINT "THE COLUMNS ARE CALIBRATED FOR ": PRINT "POLYSTYRENE. DO
YOU WISH TO CHANGE THE": PRINT "CALIBRATION CURVE?"
4010 PRINT "TO DO SO YOU NEED TO INPUT THE MARK-": PRINT "HOUWINK
PARAMETERS FOR POLYMER IN THE "
4020 PRINT "SOLVENT USED. PRESS THE APPROPRIATE KEY": PRINT "Y- TO
RECALIBRATE": PRINT "N- TO CONTINUE UNCHANGED"
4030 PRINT : GET ANS$
4040 IF ANS$ = "Y" THEN GOTO 4060
4050 RETURN
4060 HOME : PRINT : PRINT "MARK-HOUWINK PARAMETERS FOR YOUR POLYMER"
4070 INPUT "K=";P2,"A=";A2
4080 PRINT "THE COLUMNS HAVE BEEN CALIBRATED USING": PRINT "THF AS THE
SOLVENT THE MARK HOUWINK": PRINT "PARAMETERS ARE K=7,2*10+5 AND A=
.76"
4090 PRINT "IF THE VALUES FOR POLYSTYRENE IN YOUR ": PRINT"SOLVENT DIFFER
SIGNIFICANTLY FROM THESE ": PRINT "YOU ARE ADVISED TO CHANGE THE
PARAMETERS"
4100 PRINT "DO YOU NEED TO CHANGE THE PARAMETERS" Y/N"
4110 PRINT : GET ANS$
4120 IF ANS$ = "Y" THEN GOTO 4150
4130 INPUT "K=";P1,"A=";A1: GOTO 4150
4140 P1 =7. * 10 + 5:A1 = .76
4150 G = G *(1+A1) / (1 + A2): C=C* (1+A1) / (1 + A2) + (( LOG (P1 / P2) / LOG
(10)) / (1 + A2))
4160 RETURN
5000 PR# 2
5010 PRINT:PRINT: PRINT "INFORMATION CONCERNING THE CALIBRATION CURVE"
5015 PRINT
5020 PRINT "THE CALIBRATION CURVE FOR YOUR POLYMER OBEYS THE EQUATION-"
5030 PRINT "LOG M(l) = ";G; ""V(l)+";C
5040 PRINT:PRINT: PRINT "THE HIGHEST MOLECULAR WEIGHT CALIBRANT WAS
";D(0);" AND THE LOWEST"
5050 PRINT "WAS ";D(N-1)
5060 PRINT "THEIR RESPECTIVE ELUTION VOLUMES WERE";B(0);" AND ";B(N-1)
5065 PR# 0
5070 RETURN
6000 PRINT TAB( 2)"SAMPLE"; TAB(14)"ELUTION VOL"; TAB(30)"HEIGHT"
6010 FOR I = 0 TO K
6020 PRINT TAB(3) I + 1; TAB(15)V(I); TAB( 31) H(I)
6030 NEXT
6040 PRINT: PRINT "ARE THESE VALUES CORRECT? Y/N"
6050 GET ANS$
6060 IF ANS$ = "N" THEN GOTO 6080
6070 RETURN
6080 INPUT "SAMPLE NO. TO BE CHANGED?";I:I =I-1
6090 PRINT "THE ELUTION VOLUME F OR ";I= 1;" IS ";V(I); AND HEIGHT"; H(I)
6100 INPUT "ELUTION VOLUME"; V(I)
6120 INPUT "HEIGHT";H(I)
6130 HOME : GOTO 6000
7000 SPEED= 255 : PRINT :PRINT D$;OPEN";NAME$
```

```
7010 PRINT D$;"WRITE";NAME$
7020 PRINT K + 1
7030 FOR I = 0 TO K
7040 PRINT M(I)
7050 PRINT V(I)
7060 PRINT H(I)
7070 PRINT W(1)
7080 PRINT N(1)
7090 NEXT
7100 PRINT G
7120 PRINT R
7130 PRINT D(0)
7140 PRINT D(N - 1)
7150 PRINT B(0)
7160 PRINT D$;"CLOSE";NAME$
7180 REM FILE K,M(1),V(1),H(1),W9i),N9i) AND CALIBRATION DATA
7190 REM LAST 4 ENTRIES ARE MWT OF STANDARDS AND ELUTION VOLS.
7200 RETURN
8000 HOME:INPUT "LOWEST VALUE OF ELUTION VOLUME";V(0)
8010 INPUT "FINAL VALUE OF THE ELUTION VOLUME";V(K)
8020 INPUT "ELUTION VOLUME INTERVAL";U
8030 FOR I = 0 TO K
8040  $V(I) = V(0) + (I * U)$ 
8050 PRINT "HEIGHT FOR ELUTION VOLUME ";V(I)
8060 INPUT H(I)
8070 NEXT
8080 RETURN
```


APPENDIX B

Computer Programs for Wolfson Engineering Group Quench Test
written in BASIC for the BBC B (155).

```
10  REM  ***QUENCH***
20  MODE 0
21  CAL=OPENIN("CALIB.DAT")
22  IF CAL=0 THEN PRINT TAB(20,15);"CALIBRATION FILE MISSING": END
23  INPUT £CAL, ZERO,BITCAL,RECALERROR,ABCALERROR
24  CLOSE £CAL
25  DTA=OPENIN ("PARAM.DAT.")
26  IF DTA=0 THEN PRINT TAB (20,15);"PARAMETER FILE MISSING": END
27  INPUT £DTA, TTIME,RATE,NOAV,SIZE$
28  CLOSE 3DTA
30  *Fx16,1
40  LF4=CHR$(10)
50  *Fx18
60  FLAG=0
70  PRINT TAB(1,29);" f0  f1  f2  f3  f4  f5  f6  f7  f8  f9"
80  PRINT TAB(0,30);"CHECK LIST RE  COLLECT  LIST  EDIT  ANALYSE
90  PRINT TAB(0,31);"CALIB CALIB CAL DATA  PARAMS  PARAMS  DATA"
100 VDU28,0,27,79,0
110 VDU24,0;95;1279;1023;
120 *KEY 0 0:M
130 *KEY 1 1:M
140 *KEY 2 2:M
150 *KEY 3 3:M
160 *KEY 4 4:M
179 *KEY 5 5:M
180 *KEY 6 6:M
190 *KEY 7 7:M
200 *KEY 8 8:M
210 *KEY 9 9:M
220 *KEY 10 "OLD :M RUN :M"
230 *Fx229,1
240 CLS
250 VDU 19,0,4,0;
260 VDU 19,1,3,0;
270 INPUT TAB(27,15) "Enter selection" IN
280 *Fx21,0
290 CLS
300 IF IN<0 OR IN>9 THEN 270 ELSE IN=IN+1
310 ON IN GOSUB 410,728,880,5000,388,1080,1230,380,380,1440
320 IF FLAG=1 THEN FLAG=0:GOTO 240
325 CLS
330 PRINT TAB(930,15);"EXIT (Y/N)";
340 IN$=GET$
350 IF IN$="N" THEN 240
360 IF IN$="Y" THEN CLS: PRINT TAB(30,15); "ARE YOU SURE(Y/N)";:X$=GET$: IF
X$="Y" THEN CLS: END ELSE CLS: GOTO 330
370 GOTO 330
380 REM *****DUMMY SUBROUTINE*****
390 FLAG=1
400 RETURN
```

```
410 REM*****CHECK CALIBRATION ROUTINE*****
420 CLS
470 PRINT TAB(20,5);"PLACE THERMOCOUPLE AT KNOWN TEMPERATURE"
480 INPUT TAB(20,5) "TEMPERATURE OF BATH:      "BATHTEMP
490 PRINT TAB(20,10); "WAIT FOR TEMPERATURE TO STABILIZE ANND PRESS KEY"
500 X$=GET$
510 VOLT=0
520 FOR X%=1 TO 100
530 *FX 17,1
540 IF ADVAL(0) DIV 256=0 THEN 540
550 VOLT=VOLT+ADVAL91)
560 NEXT X%
570 MEASTEMP=ZERO+VOLT/(100*BITCAL)
580 CLS
590 DIFF=ABS(BATHTEMP-MEASTEMP)
600 PERC=INT(100*DIFF/BATHTEMP)
610 PRINT TAB(20,5);"REAL TEMPERATURE=";INT(BATHTEMP);"DEGREES"
620 PRINT TAB(16,10);"TEMPERATURE DIFFERENCE=";INT(MEASTEMP);"DEGREES"
630 PRINT TAB(14,15);"TEMPERATURE
    DIFFERENCE=";INT(DIFF);"DEGREES(";INT(PERC);"%)"
640 IF DIFF>ABCALERROR OR PERC>RECALERROR THEN VDU 19,1,11,0; PRINT
    TAB(31,20);"OUT OF CALIBRATION" ELSE PRINT TAB(33,20);"IN CALIBRATION"
650 NOW=TIME
660 REPEAT UNTIL TIME=NOW+500
670 PRINT TAB(27,25); "PRESS ANY KEY TO CONTINUE";
680 X$=GET$
690 CLS
700 VDU 19,1,3,0;
710 RETURN
720 REM ****LIST CALIBRATION ROUTINE****
730 CLS
780 PRINT TAB(34,2);"CALIBRATIONS"
790 PRINT TAB(34,3);"-----"
800 PRINT TAB(40,5);"ZERO ERROR=";ZERO
810 PRINT TAB(28,9);"BITS/DEGREE CENTIGRADE=";BITCAL
820 PRINT TAB(27,13);"MAX % CALIBRATION ERROR=";RECALERROR
830 PRINT TAB(29,17);"MAX CALIBRATION ERROR=";ABCALERROR
840 PRINT TAB(27,25);"PRESS ANY KEY TO CONTINUE";
850 X$=GET$
860 CLS
870 RETURN
880 REM ***RE-CALIBRATION ROUTINE***
890 CLS
900 PRINT TAB(0,5);"TO CALIBRATE YOU NEED TO HAVE THE THERMOCOUPLE AT A
    MINIMUM OF TWO TEMPERATURES"
910 PRINT TAB(26,7);"AS WIDELY SPACED AS POSSIBLE"
920 PRINT TAB(3,90);"Allow temperature to stabilize at each temperature before
    pressing RETURN"
930 INPUT TAB(20,15) "NUMBER OF POINTS (2-5): "NUM%
940 IF NUM%<2 OR NUM%>5 THEN 930
950 DIM X(NUM%-1,1)
955 FOR X%=0 :SX2=0: SY=0: SY2=0: SXY=0
960 FOR X%=0 TO NUM%-1
965 VOLT=0
970 PRINT TAB(20,19+2*X%);"TEMPERATURE NUMBER";X%+1;";";
980 INPUT " " X(X%,0)
990 FOR Y%=1 TO 100
```



```
1000 *FX 17,1
1010 IF ADVAL(0) DIV 256=0 THEN 1010
1020 VOLT=VOLT+ADVAL(1)
1030 NEXT Y%
1040 X(X%,1)=VOLT/100
1042 SX=SX+X(X%,1)
1044 SX2=SX2+X(X%,1)^2
1046 SY=SY+X(X%,0)
1048 SY2=SY2+X(X%,0)^2
1049 SXY=SXY+X(X%,1)*(X%,0)
1050 NEXT X%
1051 B=(NUM%*SXY-SX*SY)/(NUM%*SX2-SX^2)
1052 A=(SY-B*SX)/NUM%
1053 R=(NUM%*SXY-SX*SY)/SQR(NUM%*SX2-SX^2)*(NUM%8SY2-SY^2) )
1054 CLS
1060 CAL=OPENOUT("CALIB.DAT")
1061 PRINT £CAL,A
1062 PRINT £CAL,1/B
1063 PRINT £CAL,RECALERROR
1064 PRINT £CAL,ABCALERROR
1065 CLOSE £CAL
1066 PRINT TAB(20,15);"CALIBRATION FINISHED"
1067 PRINT TAB(10,20);"CORRELATION COEFFICIENT = ";R
1068 PRINT TAB(18,250);"PRESS ANY KEY TO CONTINUE";
1069 X$=GET$
1070 CLS
1071 RETURN
1080 REM ***LIST PARAMETERS ROUTINE***
1090 CLS
1140 PRINT TAB(33,2);"PARAMETERS"
1150 PRINT TAB(33,3);"-----"
1160 PRINT TAB(20,5);"QUENCH TIME="; TTIME;"SECONDS"
1170 PRINT TAB(18,10);"SAMPLING RATE=";RATE;"PER SECOND"
1180 PRINT TAB(20,15);"AVERAGED OVER";NOAV;"SAMPLES"
1190 PRINT TAB(22,20);"PLOT SIZE=";SIZE$
1200 PRINT TAB(27,25);"PRESS AY KEY TO CONTINUE";
1210 X$=GET$
1220 RETURN
1230 REM ***EDIT PARAMETERS ROUTINE***
1240 GOSUB 1080
1250 IF DTA=0 THEN RETURN
1260 PRINT TAB(27,25);" ";
1270 INPUT TAB(16,5) "NEW QUENCH TIME =" TTIME
1280 IF TTIME>200 THEN 1270
1290 INPUT TAB(14,10) "NEW SAMPLING RATE=" RATE
1300 IF RATE>1000 THEN 1290
1310 INPUT TAB(16,15) "NEW AVERAGED OVER" NOAV
1320 IF NOAV>30/RATE THEN 1310
1330 INPUT TAB(18,20) "NEW PLOT SIZE="SIZE$
1340 IF SIZE$<>"A3" ANDSIZE$<>"A4" THEN 1330
1350 PRINT TAB(27,25); "ACCEPT DATA (Y/N)";
1360 X$=GET$
1370 IF X$="N" THEN 1260
1380 IF X$<>"Y" THEN 1350
1390 DTA=OPENOUT ("PARAM.DAT")
1400 PRINT £DTA, TTIME,RATE,NOAVSIZE$
1410 CLOSE £DTA
```



```
1420 CLS
1430 RETURN
1440 REM ***ANALYSE DATA***
1450 CLS
1460 CHAIN "ANALYSE"
1470 RETURN
500 REM ****COLLECT DATA ROUTINE****
5010 CHAIN "COLLECT"
5020 RETURN
```

```
10 REM ***COLLECT DATA ROUTINE (FOR QUENCH)***
20 CLS
30 CAL=OPENIN("CALIB.DAT")
40 IF CAL=0 THEN TAB(20,15); "CALIBRATION FILE MISSING": CLOSE £0: END
50 INPUT £CAL, ZERO, BITCAL, RECALERROR, ABCALERROR
60 CLOSE £CAL
70 DTA=OPENIN ("PARAM. DAT")
80 IF DTA=0 THEN PRINT TAB(20,150;"PARAMETER FILE MISSING": CLOSE £0 : END
90 INPUT £DTA, TTIME, RATE, NOAV, SIZE$
100 CLOSE £DTA
110 NOPTS=TTIME+RATE :DIM TEMP%(NOPTS-1)
120 *FX16,1
130 INPUT TAB(20,5) "OIL TEMPERATURE : "OILTEMP
140 INPUT TAB(16,10) "FURNACE TEMPERATURE : "FURTEMP
150 INPUT TAB(19,15) "DATE (DD-MMM-YY) : "DATES$
160 INPUT TAB(30,20) "TITLE: "TITLE$
170 INPUT TAB (27,25) "OIL TYPE : "OIL$
180 PRINT TAB(27,27) "ACCEPT DATA (Y/N)
190 X$=GET$
200 IF X$="N" THEN 130
210 IF X$<>"Y" THEN 180
220 CLS
230 PRINT TAB(20,15); "WAITING FOR PROBE TO BE INSERTED"
240 VOLT=0
250 FOR X%=1 TO 100
260 X=ADVAL(0) AND 3
270 IF X <>1 THEN 340
280 *FX 17,1
290 IF ADVAL(0) DIV 256=0 THEN 290
300 VOLT=VOLT+ADVAL(1)
310 NEXT X%
320 PRINT TAB(35,20);INT9ZERO+VOLT/(BITCAL+100))
330 GOTO 240
340 CLS
350 PRINT TAB(27,15); "DATA BEING COLLECTED";
360 FOR Y%=0 TO NOPTS-1
370 VOLT=0
380 REPEAT UNTIL TIME MOD (100/RATE)=0
390 FOR X%=1 TO NOAV
400 *FX 17,1
410 IF ADVAL (0) DIV 256=0 THEN 410
```

```
420 VOLT=VOLT+ADVAL(1)
430 NEXT X%
440 TEMP%(Y%)=INT(10*(ZERO+VOLT/(BITCAL*NOAV)))
450 NEXT Y%
460 CLS
470 INPUT TAB(30,15) "FILENAME: "FILENAME$
480 IF LEN(FILENAME$)>8 THEN 468 ELSE FILENAME$="B:"+FILENAME$+".TMP"
490 FILENUM=OPENOUT(FILENAME$)
500 PRINT£FILENUM,TTIME,RATE,NOAV,SIZE$,ZERO,BITCAL,OILTEMP,FURTEMP,DATE
    $,TITLE$,OIL$
510 FOR X%=0 TO NOPTS-1
520 PRINT £FILENUM, TEMP%(X%)
530 NEXT X%
540 CLOSE £FILENUM
550 CHAIN "QUENCH"
560 FOR X%=1 TO 10000
570 X=ADVAL(0) AND 3
580 PRINT X
590 NEXT X%
```

```
10 REM *****ANALYSE*****
20 CLOSE £0:FLAG1=0:FLAG2=0:NOPL0T=0:NOPL0T2=0:P$="1";MODE0:DFLAG=0
140 PRINTTAB(0,29);"f0 f1 f2 f3 f4 f5 f6
    TAB(0,30);" READ PRINT SCNPL0T SCNPL0T PENPL0T PENPL0T NEWPPER
160 PRINTTAB(0,31);DATA DATA TEMP QCHRATE TEMP QCHRATE PLOTTER
    f7 f8 f9";
    SET EXIT"
    PLOTTER UP"
170 VDU 28,0,27,79,0,19,0,4;0;19,1,3;0;
210 CLS:PROCBOX:DRAW 0,0;DRAW 1279,0; DRAW 1279,128
220 PRINTTAB (28,150;"ENTER SELECTION";
230 X$=GET$:CLS:"FX15,1
260 IFX4<"0" DRX$> "9" THEN220 ELSE IN=VAL(X$)+1
270 ONIN GOSUB320,640,860,970,1160,1410,1660,2070,2210,2240
280 IFFLAG=1 THENCHAIN"QUENCH"
290 IFFLAG2=1 THENCLS:END
300 GOTO210
320 CLS
340 INPUTTAB(30,15)*FILENAME;"FILENAME$:D1FLAG=0:IFFILENAME$="?"
    THEND1FLAG =1:CLS:"DIR B:".TMP
350 INPUT£FILENUM,TTIME,RATE,NOAV,SIZE$,ZERO,BITCAL,OILTEMP,DATE$,TITLE$,
    OIL$:NOPTS=TTIME*RATE:IFDFLAG=0 THENDIMTEMP%(NOPTS-1):DFLAG=1
360 FORX5=0 TONOPTS-1
370 INPUT3FILENUM,TEMP%(X%):NEXT
380 CLOSE£FILENUM:RETURN
640 CLS:PRINTTAB(27,15);"PRESS P FOR PRINTER";X$=GET$:IFX$="P" THEN
    VDU2:"FX5,1
690 PRINTTAB(43-LEN(OIL$))/2;"DATA FOR";OIL$;" PRODUCED ON";DATE$:PRINT
710 PRINTTAB(11);"OIL TEMPERATURE:";OILTEMP;TAB(43);"FURNACE
    TEMPERATURE:";FURTEMP:PRINT
730 PRINTTB(80-LEN(TITLE$))/2;TITLE$:PRINT:PRINT
750 PRINTTAB(21);"TIME TEMPERATURE QUENCH RATE"
760 PRINTTAB(20);"seconds degrees C/s":PRINT
```



```
780 FORX%=0 TONOPTS-1
790 PRINTTAB(23);X%/RATE;TAB937);TEMP%(X%)/10;TAB(44)
800 IF X%<>0 AND X%<NOPTS-1 THENPRINT(TEMP%(X%+1)-TEMP%(X%-
1))/(20*(1/RATE))
810 NEXT
820 IFNDAV>1 THENPRINT:PRINT:PRINTTAB(26);"EACH SAMPLE THE AVERAGE
OF";NOAV:VDU3:RETURN
860 PROCBOX:AVND=INT(1280/NOPTS):YSCALE=895/99800
890 FORX%=0 TO (NOPTS-1)*AVNO
STEPAVNO;PLOT5,X5,128+INT(TEMP%(X%/AVNO)*YSCALE0:NEXT
920 PRINTTAB927,27);:X$=GET$:CLS:RETURN
970 PROCBOX:QMAX=0
1030 QMAX=2000:MOVE0,128+FURTEMP*895/900
1040 FORX%=1 TONOPTS2:QRATE=ABS(RATE*(TEMP%(X%+1))/2:XVAL=QRATE*120
0/QMAX:YVAL=128+TEMP%(X%)*895/9000:PLOT5,XVAL:NEXT
1110 PRINTTAB(27,27);:X$=GET$:CLS:RETURN
1160 *FX5,2
1165 *FX3,7
1170 VDU2:PRINT"J";VAL(P$):XSCALE=3300/NOPTS:YSCALE=24/90
1210 PRINT "L";INT(NOPLOT):PRINT"M200,2600":PRINT"YO";
1250 FORX%=0 TONOPTS1:PRINT",";200+INT(XSCALE*(X%+1));",";200+INT(YSCALE
*TEMP%(X%));:NEXT
1290 PRINT:PRINT"S5":PRINT"M1000.":2500-50*NOPL0T;"PRINT"R25,-21":
PRINT "P";OIL$;"AT ";PILTEMP;"C";TITLE$;"DATE$
1340 NOPL0T=NOPL0T+1:PRINT"J0":*FX3,0
1350 VDU3:CLS:RETURN
1410 *FX5,2
1415 *FX3,7
1420 VDU2:PRINT"J";VAL(P4):XSCALE=16.5:YSCALE=24/90:PRINT"L";INT(NOPLOT2)
:PRINT "M200,2600":PRINT "Y0";
1500 FORX5=1 TONOPTS-2:PRINT",";200+XSCALE*AB(RATE*(TEMP%(X%+1)-
TEMP%(X%-1))/20);",";200=INT(YSCALE*TEMP5(X%));:NEXT
1540 PRINT:PRINT"S5":PRINT"M1000.":25000-50*NOPL0T2:PRINT"1100,0":PRINT
"R25,-21":PRINT"P";OIL$;"AT";OILTEMP;"C";TITLE$;" ";DATE
1600 PRINT "J0":*FX3,0
1610 VDU3:CLS:RETURN
1660 CLS:PRINTTAB(10,15);"TEMP-TEMP OR TEMP-QUENCH RATE (T/Q): ";X$=GET$
1690 IFX$<>"T" ANDX$<>"Q" THEN1660
1700 *FX5,2
1705 *FX3,7
1710 VDU2: PRINT":PRINT"M0,0":PRINT "D3600,0,3600,2700,0,2700,0,0:"
PRINT "M2000,200":PRINT"XS,3300,20":PRINT"I0,2400,-3300,0":PRINT
" X2-2400,18":PRINT "S10:PRINT "M520,2685"
1793 PRINT"D590,2685,590,2615,520,2615,520,2685,530,2682,540,2673,550,
2660,560,2640,570,2627,580,2618,590,2615"
1794 PRINT "M710,2610":PRINT "PWOLFSON HEAT TREATMENT CENTRE":PRINT
"S5":PRINT "M188,140":PRINT "P0"
1830 IFX$="Q" THEN 1890
1835 NOPL0T=0
1840 FORX%=1 TO 10
1842 IFX%*TTIME/10<19 THENPRINT"M":188+X%*330;"",140*ELSEIF
X%*TTIME/10<100 THENPRINT"M";167+X%*330",140 ELSEPRINT"M";146
+X%*330
1844 PRINT"P";INT(TTIME*X%/10):NEXT
1860 PRINT"M1398,80":PRINT"PTIME s ": GOTO1930
1890 NOPL0T2=0
1892 FORX%=1 TO10
```



```
1894 IFX%*20<100 THENPRINT "M";167+X%*330;"",140"
      ELSEPRINT"M";146+X%*330;140"
1896 PRINT "P";20*X%
1898 NEXT
1910 PRINT"M1188,80":PRINT"PQUENCH RATE C/s"
1930 PRINT "Q1":PRINT"M60,1106":PRINT"PTEMPERATURE C":PRINT"W25,1617,
      7,7,0,3600":PRINT"M158,179":PRINT"Q0":PRINT"P0"
2000 FORX%=1 TO9:PRINT"M74,";INT(179+X%*2400/9):PRINT"P";100*X%:NEXT
2020 *FX3,0
2030 VDU3:CLS:RETURN
2070 CLS:PRINTTAB(25,15);"ENTER NUMBER OF PEN DESIRED";:P$=GET$
2100 FIP$<"0" ORP$>"6" THEN 2070
2110 X=VAL(P$):*FX5,2
2115 *FX3,7
2120 VDU2:PRINT"J";X:VDU3:*FX3,4
2130 CLS:RETURN
2210 FLAG1=1:RETURN
2240 FLAG2=1:RETURN
2270 DEFPROCBOX
2280 CLS:MOVE0,128:DRAW1279,128:DRAW1279,1023:DRAW0,1023:DRAW0,128
2340 ENDPROC
```

```
10 REM ***PARSETUP***
20 X=OPENOUT("PARAM.DAT")
30 PRINT £X,100
40 PRINT £X,20
50 PRINT £X,10
60 PRINT £X,"A4"
70 CLOSE £X
80 END
```

```
10 REM ***CALSETUP***
20 X=OPENOUT ("CALIB.DAT")
30 PRINT £X,1
40 PRINT£X,72.8
50 PRINT £X,2
60 PRINT £X,5
70 CLOSE £X
80 END
```

APPENDIX C

Computer Program for the Calculation of Residual Stress, from X-ray Diffraction Data, written in BASIC for the Apple IIe.

```
50 REM *** RESIDUAL STRESS ***
100 D$ = CHR$ (4)
110 DIM TIME (100): DIM PAR (5)
120 HOME :: VTAB (5): HTAB (5)
130 PRINT "FOLLOWING OPTIONS ARE AVAILABLE"
140 PRINT :: PRINT
150 PRINT "1. ENTER DATA TO SAVE ON DISC": PRINT
160 PRINT "2. SAVE DATA IN A FILE": PRINT
170 PRINT "3. DISPLAY AND MODIFY DATA": PRINT
180 PRINT "4. COMPUTE RESULTS": PRINT
190 PRINT "WHICH?": GET KEY$
200 FLAG = VAL (KEY$): IF FLAG > 4 THEN 180
210 ON FLAG GOTO 400, 550, 7=0,840
400 HOME: REM** ENTER DATA**
410 GOSUB 1500
420 GOSUB 120
550 HOME: REM ** SAVE DATA**
560 PRINT "CAUTION:THIS SECTION WILL NOT WORK UNLESS DATA HAS BEEN
ENTERED"
570 INPUT "DO YOU WISH TO GO BACK TO THE MAIN MENU?": Z3$
580 IF Z3$ = "Y" THEN 620
590 IF Z3$ = "N" THEN 600
595 GOTO 570
600 INPUT "ENTER FILE NAME" ; F$
610 GOSUB 2000
620 GOSUB 120
700 HOME: REM ** DISPLAY AND MODIFY**
710 INPUT "IS DATA ON DISC?": Z4$
720 IF Z4$ = "Y" THEN 740
730 IF Z4$ = "N" THEN 780
735 GOTO 710
740 INPUT "ENTER FILE NAME": F$
750 GOSUB 3000
760 GOSUB 4000
770 GOTO 830
780 PRINT "CAUTION: THIS SECTION WILL NOT WORK UNLESS DATA HAS BEEN
ENTERED"
790 INPUT "DO YOU WISH TO GO BACK TO MAIN MENU?": Z5$
800 IF Z5$ = "N" THEN 820
810 IF Z5$ = "Y" THEN 830
815 GOTO 790
820 GOSUB 4000
830 GOTO 120
840 HOME: REM ** COMPUTATION **
850 INPUT "ENTER SAMPLE NO. ":C$
860 PR# 1: PRINT CHR$ (14); "SAMPLE NO. ":C$ PR# 0
865 INPUT "IS THE DATA ON DISC?": Z6$
870 IF Z6$ = "N" THEN 890
880 IF Z6$ = "Y" THEN 1030
```

```
885 GOTO 865
890 GOSUB 1500
900 GOSUB 5000
910 PR# 1
920 PRINT "PEAK POSITION FOR PSI ";P; " IS ";PK
930 PRINT "PEAK POSIOTION FOR PSI"; P;" is "; PK
940 IF P<> 0 THEN 980
950 T1 = PK: V2 =PK
960 GOTO 890
970 REM
980 T2 =PK: V2 = VK
990 PRINT "DELTA 20 = ";(T1 -T2)
1000 PRINT "STD(20) = "; SQR (V1 = V2)
1010 GOSUB 6000
1020 PR# 0: GOTO 1190
1030 INPUT "ENTER FILE NAME FOR PSI=0";F$
1040 GOSUB 3000
1050 GOSUB 5000
1060 PR# 1
1070 PRINT "PEAK POSITION FOR PSI = "; P; " is "; PK
1080 PRINT "SQR (VK)= "; SQR (VK)
1090 T1 = PK: V1 = VK: PR# 0
1100 INPUT "ENTER FILE NAME FOR PSI=45";F$
1110 GOSUB 3000
1120 GOSUB 5000
1130 PR# 1
1140 PRINT "PEAK POSITION FOR PSI = "; P;" IS "; PK
1150 PRINT "SQR (VK) = "; SQR (VK)
1160 T2 = PK: V2 = VK
1170 GOSUB 6000
1180 PR# 0
1190 GOTO 120
1200 END
1500 REM SUBROUTINE FOR DATA INPUT
1510 INPUT "PAR1. STARTING ANGLE 201 "; PAR(1)
1520 INPUT "PAR2. ANGLE PSI "; PAR(2)
1530 INPUT "PAR3. NUMBER OF POINTS "; PAR (3)
1540 INPUT " PAR4. STEP 2DO "; PAR (4)
1550 INPUT "PAR5. NUMBER OF COUNTS "; PAR(5)
1560 FOR I = 1 TO 100: TIME (I) = 0: NEXT I
1570 DUMMY = PAR (1) - PAR (4)
1580 FOR J = 1 TO PAR (3)
1590 DUMMY = DUMMY +PAR(4)
1600 PRINT DUMMY
1610 INPUT TIME (J)
1620 NEXT J
1630 RETURN
2000 REM WRITE TO FILE
2010 PRINT D$;"WRITE"; F$;"L7"
2020 FOR I = 1 TO 5
2030 PRINT D$; "WRITE ";F$;"R";I
2040 PRINT PAR (1)
2050 NEXT I
2060 FOR J = 1 TO PAR (3)
2070 PRINT D$; "WRITE ";F$;"R";J + 5
2080 PRINT TIME (J)
2090 NEXT J
```



```
2100 RETURN
3000 REM : READ FROM FILE
3010 PRINT D$;"OPEN ";F$;"L7
3020 FOR I = 1 TO 5
3030 PRINT D$; "READ "; F$;"R";I
3040 INPUT PAR (1)
3050 NEXT I
3060 FOR I = 1 TO 100: TIME (1) = 0: NEXT I
3070 FOR J =1 TO PAR (3)
3080 PRINT D$; "READ " ; F$;"R";J +5
3090 INPUT TIME (J)
3100 NEXT J
3110 PRINT D$; "CLOSE ";F$
3120 RETURN
4000 REM DISPLAY AND MODIFY VALUES
4020 PRINT "PAR1. STARTING ANGLE 201 "; PAR(1)
4030 PRINT "PAR2. ANGLE PSI "; PAR(2)
4040 PRINT "PAR3. NUMBER OF POINTS ";PAR (3)
4050 PRINT "PAR4. STEP 2DO"; PAR(4)
4060 PRINT "PAR5. NUMBER OF COUNTS ";PAR(5)
4070 DUMMY = PAR (1) - PAR(4)
4080 FOR J = 1 TO PAR (3)
4090 DUMMY = DUMMY + PAR(4)
4100 PRINT J;" "; DUMMY;" "; TIME(J)
4110 NEXT J
4120 PRINT
4130 INPUT "ANY CORRECTIONS?"; Z1$
4140 IF Z1$ = "Y" THEN 4160
4150 IF Z1$ = "N" THEN 4310
4155 GOTO 4130
4160 INPUT "WHICH DATA ITEM DO YOU WISH TO CHANGE
(PARAMETERS/TIME)?" ;Z2$
4170 IF Z2$ = "PARAMETER" THEN 4190
4180 IF Z2$ = "TIME" THEN 4250
4185 GOTO 4160
4190 INPUT "WHICH PARAMETER?";I
4200 INPUT "ENTER NEW VALUE"; PAR (1)
4210 INPUT "ANY MORE?";Z3$
4220 IF Z3$ = "N" THEN 4120
4230 IF Z3$ = "Y" THEN 4190
4240 GOTO 4210
4250 INPUT "WHICH DATA ITEM?";J
4260 INPUT "ENTER NEW VALUE "; TIME (J)
4270 INPUT "ANY MORE?";Z4$
4280 IF Z4$ = "N" THEN 4120
4290 IF Z4$ = "Y" THEN 4250
4300 GOTO 4270
4310 RETURN
5000 REM ** COMPUTE RESULTS **
5010 CM = 0: YB = 0: S2 = 0: C =0
5020 N = (PAR(3) - 1) /2
5030 CM=(N*(N+1) * (2*N+1)*(2*N+3)*(2*N-1)*(2*N+3)*(2*N-1)) / 2700
5040 P=PAR(2)*3.1416 180:D = PAR(4):CT=PAR(5)
5050 S1= PAR910 - PAR (4)
5060 FX= - (2*N+3)*(2*N-1) / 30
5070 M=N*(N+1) / 3
5080 M1 = 0:M2 = 0
```

```
5090  FOR X = -N TO N
5100  S1 = S1 + PAR(4)
5110  J = X + N + 1
5120  Y = TIME (J)
5140  S = S1 * 3.1416 / 180
5150  F = 2 * (SIN (S / 2) ^ 2) / ((1 + COS (S)^2) * (1-TAN (P)/ TAN (S/2)))
5160  Y = Y/F
5170  C = C + Y
5180  M1 = M1 + X * Y
5190  M2 = M2 + (X * X - M) * Y
5200  NEXT X
5210  YB = C/(2*N+1): S2 =(YB*YB)/(CT)
5220  K = FX * M1/M2
5230  VK = ((D*D*S2*CM) / (M2 * M2)) * (1+60*K*K/((2*N=30*(2*N-1)))
5240  PK = (S1-N*D)+K*D
5250  P = P * 180 / 3.1416
5260  RETURN
6000  REM ** CALC RESIDUAL STRESS **
6010  PI = 3.1416
6020  T1 = T1 * PI / 360
6030  T2 = T2 * PI / 360
6040  P = P * PI / 360
6050  NUM = ( SIN (T1) / SIN (T2) - 1)
6060  DEN = 1. 29 * (SIN (P) * SIN (P))
6070  Z = 206850 * NUM /DEN
6080  PRINT "RESIDUAL STRESS IS =";Z
6090  RETURN
```

REFERENCES

- 1) Glossary of Metallurgical Terms and Engineering Tables. *American Society for Metals. Metals Park, Ohio. 1979.*
- 2) **Cook W.T.** Quenching Media. *British Steel Corporation, Special Steels Division. Report No. PROD/SA/7471/-/75/B. July 1975.*
- 3) Quenching and Martempering. *ASM Committees on Quenching and Martempering. American Society for Metals. Metals Park, Ohio, 1964.*
- 4) **Masseria V. and Kirkpatrick C.W.** (Editors). Quenching of Steel. "Heat Treating" *Metals Handbook, 9th Edition, Vol.4. American Society for Metals. Metals Park, Ohio. 1981, 31-69.*
- 5) **Segerberg S. and Bodin J.** Polymer quenchants show benefits in metal heat treatment. *Metallurgia. Sept.1986, Vol.53, No.9, 425-426.*
- 6) **Pilling N.B. and Lynch T.D.** Cooling properties of technical quenching liquids. *Transactions, American Institute of Mining and Metallurgical Engineers. 1920, Vol.62, 665.*
- 7) **Scott H.** The problem of quenching media for the hardening of steel. *Transactions, American Society for Metals. 1934, Vol.22, 577-604.*
- 8) **Beck G., Dumont F., Moreaux F. and Simon A.** Guiding principles in choosing and selecting hardening oil. *Harterei-Technische Mitteilungen. 1975, Vol.30, No.6, 346-358. (In German).*
- 9) **Segerberg S.** Correlation between the quenching characteristics of quenching media and hardness distribution in steel. *Heat Treatment '84. Book No. 312, 19.1-19.7. The Metals Society, London. 1984.*
- 10) **Price R.F. and Fletcher A.J.** Determination of surface heat-transfer coefficients during quenching of steel plates. *Metals Technology. May 1980, Vol.7, No.5, 203-211.*
- 11) **Lakin J.J.** Adaption of the Wolfson test technique to polymer quenchants. *Paper presented at the Wolfson Heat Treatment Centre conference "Advances in Quenching Technology", Aston University, Birmingham, 23 Nov. 1983 (See Heat Treatment of Metals. 1983.3, Vol.10, 69-71).*
- 12) **Close D.** Wolfson Engineering Group quench test adopted for international standard. *Heat Treatment of Metals. 1985.3, Vol.12, 62.*
- 13) **Blanchard P.M.** Properties of Quenchants. *Metallurgia and Metal Forming. June 1973, Vol.40, No.6, 177-180.*
- 14) **Lakin J.J.** Testing of quenching media. *Heat Treatment of Metals. 1979.3, Vol.6, 59-62.*
- 15) **French H.J.** The Quenching of Steels. *American Society for Metals, Cleveland, Ohio. 1930, 12-20.*
- 16) **Heins R.W. and Mueller E.R.** Characterisation of polymer quenchants by cooling curves. *Metal Progress. Sept.1982, Vol.122, No.4, 33-39.*

- 17) **Tennent R.M.** (Editor) Science Data Book, *The Open University. Oliver and Boyd, Edinburgh.* 1979, 60.
- 18) **Rogen G. and Sidan H.** Testing the quenching capacity of liquid quenching media, particularly oils. *Berg-und (Huttenmannische Monatshefte.* 1972, Vol.117, No.7, 250-258 (In German).
- 19) **Rohsenow W.M., Hartnett J.P. and Ganic E.N.** (Editors). Handbook of Heat Transfer Fundamentals. 2nd Edition. *McGraw-Hill Book Company, New York.* 1985.
- 20) **Sayettat C. and Bournicon C.** Characterization of the properties of quench fluids. *Traitement Thermique.* Jun-July 1981, No.156, 41-46. (In French).
- 21) **Murakami Y.** Application of JIS test on polymer quenchants. *Journal of the Japan Society for Heat Treatment.* 1985, Vol.25, No.1, 31-33. (In Japanese).
- 22) **Tamura I., Shimizu N. and Okada T.** Engineering method to judge the quench hardening of steel from cooling curves of quenchants. *Paper presented at the 7th ASM Heat Treating Conference / Workshop, Chicago, 10-12 May.* 1983.
- 23) **Thelning K.E.** New aspects on the appraisal of the cooling process during hardening of steel. *Scandinavian Journal of Metallurgy.* 1983, Vol.12, 189-194.
- 24) **Laboratory Test for Assessing the Cooling Characteristics of Industrial Quenching Media.** *Wolfson Heat Treatment Centre Engineering Group Specification.* *Wolfson Heat Treatment Centre. Aston University, Birmingham.* 1982.
- 25) **Hick A.** (Editor) Quench test specification published. *Heat Treatment of Metals.* 1982.2, Vol.9, 36.
- 26) **Close D.** The Wolfson Engineering Group quench test-scope and interpretation of results. *Heat Treatment of Metals.* 1984.1, Vol.11, 1-6 (Based on the paper presented at the Wolfson Heat Treatment Centre conference "Advances in Quenching Technology", Aston University, Birmingham, 23 Nov. 1983).
- 27) **Mansion J.** Properties and choice of quenching oils. *Traitement Thermique.* April 1976, No.104, 59-66. (In French).
- 28) **Burgdorf E.H. and Kopietz K.H.** Effect of contamination on polymer quenchants. *Industrial Heating.* Oct.1981, Vol.48, No.10, 18-25.
- 29) **Von Bergen R.T.** New developments in the technology and application of polymer quenchants. *Paper presented at the Wolfson Heat Treatment conference "Advances in Quenching Technology", Aston University Birmingham, 23 Nov.1983. (see Heat Treatment of Metals.* 1984.1, Vol.11, 7-8).
- 30) **Luty W.** Investigation of repeatability of cooling characteristics for water based polymer quenchants and quenching oils. *Metalozn. Orbrobka Ciepi.* May - June 1984, Vol.69, 12-16 (In Polish).

- 31) **Tensi H.M., Steffen E. and Kunzel T.H.** Laboratory test for assessing the cooling characteristics of polymer quenchants. *Submission on behalf of the Technical University of Munich, as part of Task 2 of the International Federation for the Heat Treatment of Materials (IFHT) Technical Committee on "Scientific and Technological Aspects of Quenching" working plan 1980-1985, to develop a "laboratory method for the testing of the quenching power of polymer quenchants". Minutes of the meeting at the 5th IFHT International Congress on Heat Treatment of Materials, Budapest, Oct.20, 1986. (In German)*
- 32) **Liscic B.** Assembling the absolute quenching capacity during hardening from the surface temperature gradient. *Harterei-Technische Mitteilungen. 1978, Vol.33, No.4, 179-191. (In German).*
- 33) **Monroe R.W. and Bates C.E.** Evaluating quenchants and facilities for hardening steel. *Paper presented at the 7th ASM Heat Treating Conference/Workshop. Chicago, 10-12 May, 1983. (see Journal of Heat Treating. Dec. 1983, Vol.3, No.2, 83-99).*
- 34) **Mason K.J. and Capewell I.** The effect of agitation on the quenching characteristics of oil and polymer quenchants. *Heat Treatment of Metals, 1986.4, Vol.13, 99-102.*
- 35) **Hilder N.A.** A pump agitation system for assessing the cooling characteristics of quenchants. *Heat Treatment of Metals. 1985.3, Vol.12, 63-68 (Based on submission, on behalf of the Wolfson Heat Treatment Centre Engineering Group working party on "Testing of Quenching Media", to the International Federation for the Heat Treatment of Materials (IFHT) Technical Committee on "Scientific and Technological Aspects of Quenching". 4th IFHT International Congress on Heat Treatment of Materials, Berlin, June 1985.*
- 36) **Hilder N.A.** The behaviour of polymer quenchants. *Heat Treatment of Metals. 1987.2, Vol.14, 31-46. (Based on the paper presented at the Wolfson Heat Treatment Centre conference "Advances in Heat Treatment Practice", Metropole Hotel, National Exhibition Centre, Birmingham, 4th Sept. 1986).*
- 37) **Mason K.J.** Assessment of quenching media characteristics. *Heat Treating. Nov. 1979, Vol.11, No.11, 20-22.*
- 38) **Wyatt O.H. and Dew-Hughes D.** *Metals, Ceramics and Polymers. Cambridge University Press. London. 1974.*
- 39) **Siebert C.A., Doane D.V. and Breen D.H.** The Hardenability of Steels. *American Society for Metals, Metals Park, Ohio. 1977.*
- 40) **Cook W.T.** The role of hardenability in the choice of a quenching system. *Heat Treatment of Metals. 1980. 4, Vol.7, 83-87*
- 41) **Wever F. and Rose A.** Atlas zur Warmbehandlung der Stähle (*Atlas for the heat treatment of steels*) Vol.1, Verlag Stahleisen M.B.H., Dusseldorf. 1958. (In German).

- 42) **Sachs K.** Presentation of transformation data. *Heat Treatment of Metals*. 1974.2, Vol.1, 43-57.
- 43) **Terrier A.** Quenching tank technology. *Traitement Thermique*. April 1976, No.104, 89-100. (In French).
- 44) **Davies J.T.** Turbulence Phenomena. *Academic Press Incorporated Limited*. London. 1972
- 45) **Russell T.F.** Some Mathematical Considerations on the Heating and Cooling of Steel. *First Report of the Alloyed Steel Research Committee, Iron and Steel Institute, Special Report No.14*, 1936, 149-187.
- 46) **Grossmann M.A., Assimow M. and Urban S.F.** Hardenability of Alloy Steels. *American Society for Metals*. Cleveland, Ohio. 1939.
- 47) **Asimow M., Craig W.F. and Grossmann M.A.** Correlation between Jominy test and quenched rounds. *Transactions, Society of Automotive Engineers*. 1941, Vol.49, No.1, 283-292.
- 48) **Carney D.J. and Janulionis A.D.** An examination of the quenching constant H. *Transactions, American Society for Metals*. 1951, Vol.43, 480-496.
- 49) **Hopkins A.D. and Riley D.** Hardenability re-examined. *Iron and Steel*. Oct.1969, Vol.42, 287-296.
- 50) **Heindlhofer K.** Quenching: a mathematical study of various hypotheses in rapid cooling. *Physical Review*. 1922, Vol.20, 221-242.
- 51) **Atkins M.** The Cooling of Round Steel Bars Determination of Heat Transfer Coefficient. *United Steel Companies Limited*. Report No. PTM.54621-166. April 1966.
- 52) **Carney D.J.** Another look at quenchants, cooling rates and hardenability. *Transactions, American Society for Metals*. 1954, Vol.46, 1500-1526.
- 53) **Austin J.B.** Quenching Flow of Heat in Metals. *American Society for Metals*. Cleveland, Ohio. 1942, 50.
- 54) **Chevrier J.C. and Beck G.** Quest for a general definition of the cooling power of a quenching liquid. *Memores Scientifiques de la Revue de Metallurgie*. 1972 Vol.69, No.9, 623-632. (In French).
- 55) **Bamburger M. and Prinz B.** Determination of heat transfer coefficients during water cooling of metals. *Materials Science and Technology*. April 1986, Vol.2, No.4, 410-415.
- 56) **Tensi H.M., Welzel G., Kunzel T. and Steffen E.** Controlled heat treatment using quenching characteristics of fluids. *International Federation for the Heat Treatment of Materials (IFHT)*. 5th IFHT International Congress on Heat Treatment of Materials, Budapest, 20-24 Oct. 1986, Proceedings Vol.3, 784-1791.
- 57) **Stolz G.** Numerical solution to an inverse problem of heat conduction for simple shapes. *Transactions, American Society of Mechanical Engineers, Series C. Journal of Heat Transfer*. 1960, Vol.82, 20-26.

- 58) **Beck J.V.** Nonlinear estimation applied to the nonlinear inverse heat conduction problem. *International Journal of Heat and Mass Transfer*. 1970, Vol.13, 703-716.
- 59) **Qun H. and Xijing L.** Application of heat transfer method to measuring cooling power of quenchants with silver cylindrical probe. *International Federation for the Heat Treatment of Materials (IFHT). 5th IFHT International Congress on Heat Treatment of Materials, Budapest, 20-24 Oct. 1986, Proceedings Vol.3, 1822-1829.*
- 60) **Xijing L.** Private communication. *Department of Mechanical Engineering, Jiangxi Institute of Technology, Nanchang, China. Sep.1986.*
- 61) **Hildenwall B.** Predictions of the Residual Stresses Created During Quenching (Especially the Quench Response in Carburized Steel). *Linköping Studies in Science and Technology. Dissertation No.39. Division of Engineering Materials, Department of Mechanical Engineering, Linköping University, Sweden, 1979.*
- 62) **Grossmann M.A. and Bain E.C.** Principles of Heat Treatment. *American Society for Metals. Cleveland, Ohio. 1944.*
- 63) **Rose A.** The cooling power of quenching agents for steel. *Archiv fur das Eisenhüttenwesen. Feb.1940, Vol.13, 345. (In German).*
- 64) **Krainer V.H. and Swoboda K.** The role of the quenchant in the hardening of alloy steel. *Archiv fur das Eisenhüttenwesen. 1944, Vol.17, 163. (In German).*
- 65) **Lamont J.L.** How to estimate hardening depth in bars. *The Iron Age. Oct 14th 1943, Vol.152, 64-70.*
- 66) **Russell T.F.** Some Theoretical Considerations of the Jominy Hardenability Test. *Iron and Steel Institute, Special Report No.36, 1946, 25-33.*
- 67) **Jaczak C.F.** Determining hardenability from composition. *Metal Progress. Sept.1971, Vol.100, 60-65.*
- 68) **Bateman C.** Private communication. *Garringtons, Bromsgrove, March 1984.*
- 69) **Hampshire J.M.** Private communication. *RHP (Ransome Hoffman Pollard Ltd.) Bearing Research Centre, Newark, March 1984.*
- 70) **Nicklin S.E.** An Investigation into the Relationship Between Quench Severity Assessed from Industrial Furnaces and from a Laboratory Oil Test. *MSc Thesis, Aston University, Birmingham. 1982.*
- 71) **Jones F.W. and Pumphrey W.I.** Some experiments on quenching media. *Journal of the Iron and Steel Institute. May 1947, Vol.156, Part 1, 37-54.*
- 72) **Jominy W.E.** Hardenability of Alloy Steels. *American Society for Metals. Cleveland, Ohio. 1939, 66-84.*
- 73) **Thelning K.E.** Correlation of the measured quenching intensity with the hardness distribution in quenched parts. *IFHT Task 4. International Federation for the Heat Treatment of Materials (IFHT). 5th IFHT International*

- Congress on Heat Treatment of Materials, Budapest, 20-24 Oct. 1986, Proceedings Vol.3, 1737-1759.*
- 74) **Thelning K.E.** Steel and its Heat Treatment. (*Bofors Handbook*). 2nd Edition. Butterworth, London. 1984, 260-283.
 - 75) **Dicken T.W.** Modern quenching oils: an overview. *Heat Treatment of Metals*. 1986.1, Vol.13, 6-8. (Based on the paper presented at the Wolfson Heat Treatment Centre conference "Progress in Quenching Technology", Aston University, Birmingham, 13 Nov. 1985).
 - 76) **Bashford A. and Mills A.J.** The development of improved additives for quenching oils using laboratory simulations. *Heat Treatment of Metals*. 1984.1, Vol.11, 9-14. (Based on the paper presented at the Wolfson Heat Treatment Centre conference "Advances in Quenching Technology", Aston University, Birmingham, 23 Nov. 1983).
 - 77) **Hewitt W.** Monitoring of quench media in the production heat treatment shop. *Heat Treatment of Metals*. 1986.1, Vol.13, 9-14. (Based on the paper prepared for the Wolfson Heat Treatment Centre conference "Progress in Quenching Technology", Aston University, Birmingham, 13 Nov. 1985).
 - 78) **Skidmore C.** Salt-bath quenching - a review. *Heat Treatment of Metals*. 1986.2, Vol.13, 34-38.
 - 79) **Bless F. and Bouwman J.W.** Application of high-pressure gas quenching in vacuum heat treatment furnaces. *Heat Treatment of Metals*. 1986.4, Vol.13, 95-98 (Based on the paper presented at the Wolfson Heat Treatment Centre conference "Progress in Quenching Technology", Aston University, Birmingham, 13 Nov. 1985).
 - 80) **Sommer P.** Quenching in fluidised beds. *Heat Treatment of Metals*. 1986.2, Vol.13, 39-44. (Based on the paper presented at the Wolfson Heat Treatment Centre conference "Progress in Quenching Technology", Aston University, Birmingham, 13 Nov. 1985).
 - 81) **Von Bergen R.T.** Practical experience with acrylate polymer quenchants. Paper presented at the Wolfson Heat Treatment Centre conference "Progress in Quenching Technology", Aston University, Birmingham, 13 Nov. 1985 (See *Heat Treatment of Metals*. 1986.1, Vol. 13, 4).
 - 82) **Foreman R.W. and Meszaros A.** Polymer quenching update. *Industrial Heating*. Jan. 1984, Vol. 51, No. 1, 22-24 & 29.
 - 83) **Mueller E.R.** A look at the polymers - past, present and future. *Heat Treating*. Oct. 1980, Vol. 12, No.10, 30-33.
 - 84) **Quenching Principles and Practice.** Trade Brochure. Edgar Vaughan and Co. Ltd., Birmingham. 1985.
 - 85) **Hilder N.A.** Polymer quenchants - a review. *Heat Treatment of Metals*. 1986.1, Vol. 13, 15-26.
 - 86) **Corneil E.R.** Process for quench-hardening steel. U.S. patent 2,600,290. 10 June 1952.

- 87) **Davidson R.L. and Sittig M. (Editors).** Water-Soluble Resins. 2nd Edition. *Reinhold Book Corporation, New York. 1968.*
- 88) **Cary P.E., Magnus E.O. and Herring W.E.** A new quenchant for steel. *Metal Progress. March 1958, Vol. 73, No. 3, 79-81.*
- 89) **Curme G.O. and Johnston F. (Editors).** Glycols. *Reinhold Publishing Corporation, New York, 1953, 280-281.*
- 90) **Roberts F.H. and Fife H.R.** Mixtures of polyoxyalkylene mono-hydroxy compounds and methods of making such mixtures. *U.S. patent 2,425,755. Aug.1947.*
- 91) **Blackwood R.R. and Cheesman W.D.** Metal quenching medium. *U.S. patent 3,220,893. Nov. 1965.*
- 92) **Parker R.J.L.** Chemical quenching media for metal heat treatment. *Paper presented at the 3rd International Process Heating Conference, "Heatex '67", London. 1967.*
- 93) **Blackwood R.R. and Mueller E.R.** Installation and control of polyglycol quenchants. *Heat Treating. Oct. 1981, Vol. 13, No.10, 26-36.*
- 94) **Kopietz K.H.** How ageing affects quenching with PAG polymer solutions. *Heat Treating. Sep. 1984, Vol. 16, No. 9, 20-26.*
- 95) **Von Bergen R.T.** Private communication. *Edgar Vaughan and Co. Ltd., Birmingham. Jan. 1984.*
- 96) **Lakin J.J.** Private communication. *Hythe Chemicals Ltd., (British Petroleum Company p.l.c.), Fawley, April 1985.*
- 97) **Mueller E.R.** Polymer quenchants : what about corrosion? *Heat Treating. Sep. 1986, Vol. 18, No. 9, 24-26.*
- 98) **Lewis M. and Welsh P.J.** Method of quenching. *U.S. patent 3,475,232. Oct. 1969.*
- 99) **Mason K.J. and Lake R.N.** The hardening response of En 43 steel to polymer quenchants. *The Metallurgist and Materials Technologist. March 1981, Vol.13, No. 3, 157-158.*
- 100) **Lauderdale R.H.** A new quenchant for thin-gauge aluminium. *Metal Progress. Dec. 1967, Vol. 92, No. 6, 79-81.*
- 101) **Singleton O.R.** An analysis of new quenchants for aluminium. *Journal of Metals. Nov. 1968, Vol. 20, No.11, 60-67.*
- 102) **Croucher T.R. and Schuler M.D.** Distortion control of aluminium products using synthetic quenchants. *Metals Engineering Quarterly, Aug. 1970, Vol. 10, No. 3.*
- 103) **Croucher T.R.** Applying synthetic quenchants to high strength alloy heat treatment. *Metals Engineering Quarterly. May 1971, Vol. 11, No. 2, 6-11.*
- 104) **Turley R.V. and Gassner R.H.** Large aluminium alloy forgings fly high in the DC-10. *Metal Progress. March 1972, Vol. 101, No. 3, 48-50.*
- 105) **Croucher T.R.** Synthetic quenchants eliminate distortion. *Metal Progress. Nov. 1973, Vol. 104, No. 6, 52-55.*

- 106) **Collins J.F. and Maduell C.E.** Polyalkylene glycol quenching of aluminium alloys. *Materials Performance*. July 1977, Vol. 16, No. 7, 20-23.
- 107) **Suttie N.R.** The use of polymer quenchants for aluminium alloy heat treatment. *Heat Treatment of Metals*. 1979.1, Vol. 6, 19-21.
- 108) **Croucher T.R. and Butler D.** Quenching: major stress source in treated aluminium alloys. *Heat Treating*. Oct. 1980, Vol. 12, No. 10, 34-37.
- 109) **Croucher T.R. and Butler D.** Polymer quenching of top quality, high strength aluminium castings. *Heat Treating*. Oct. 1982, Vol. 14, No. 10, 28-31.
- 110) **Bates C.E., Landig T. and Seitanakis G.** Quench factor analysis : a powerful tool comes of age. *Heat Treating*. Dec. 1985, Vol. 17, No. 12, 13-17. (Presented at 9th American Society for Metals Heat Treating Conference and Exposition, O'Hare Convection Centre, 29 April - 1 May 1986, Chicago).
- 111) **Polyalkylene Glycol Heat Treat Quenchant.** *Aerospace Material Specification AMS 3025*. Society of Automotive Engineers, Warrendale, Pennsylvania, April 1980.
- 112) **Lasday S.B.** Metal quenching with oils and synthetic media. *Industrial Heating*. Oct. 1976, Vol. 43, No. 10, 8-19.
- 113) **Chandler E. (Editor)** Experience with synthetic quenchants for steel. *Metal Progress*. Nov. 1976, Vol. 110, No.6, 46-50.
- 114) **Beck A.J.** Some factors to consider in quench tank design using polymer quenchants. *Heat Treating*. May 1977, Vol. 9, No. 5, 55-60.
- 115) **Boulter W.** Using nitrogen-based atmospheres and polymer quenchants for the continuous heat treatment of fasteners. *Heat Treatment of Metals*. 1979.4, Vol. 6, 93-96.
- 116) **Robertshaw J. and von Bergen R.T.** Practical experience with polymer quenchant in sealed quench furnaces used for carburising. *Heat Treatment of Metals*. 1981.1, Vol. 8, 13-16.
- 117) **Robertshaw J. and von Bergen R.T.** In service tests on polymer based quenchants in a cementation furnace incorporating a quench tank. *Traitement Thermique*. Aug-Sept. 1981, No. 157, 65-69. (In French).
- 118) **Lakin J.J.** The use of polymer quenchants in surface heat treatments. *Heat Treatment of Metals*. 1982.3, Vol.9, 73-76.
- 119) **Creal R.** Working with polymers: a survey of commercial shops. *Heat Treating*. Oct. 1982, Vol. 14, No. 10, 24-26.
- 120) **Seegerberg S.** Polymer quenchants: an evaluation of technical and environmental properties. *Paper presented at the 4th International Congress on Heat Treatment of Materials*. International Federation for the Heat Treatment of Materials. 3-7 June 1985, Berlin. *Proceedings* Vol.2, 1252-1265; and at the Wolfson Heat Treatment Centre conference "Progress in Quenching Technology", Aston University, Birmingham, 13 Nov. 1985. (See *Heat*

- Treatment of Metals. 1986.1, Vol. 13, 1-3).*
- 121) **Mueller E.R.** Polyglycol quenchant cleanliness: are there benefits? *Heat Treating. Oct. 1983, Vol. 15, No. 10, 24-27.*
 - 122) **Blackwood R.R., Lorbach M.M. and Mueller E.R.** Is something bugging your polymer quenchant? *Heat Treating. July 1985, Vol. 17, No. 7, 40-42.*
 - 123) **Simmonds P.J.** Salt contamination of polymer quenchants. *Heat Treatment of Metals. 1985.3, Vol. 12, 85.*
 - 124) **Anderson K., Croucher T.R. and Butler D.** Room temperature separation of glycol quenchants. *Metal Progress. May 1983, Vol. 123, No. 6, 37-40.*
 - 125) **Croucher T.R.** Glycol separators show potential for varied heat treat operations. *Heat Treating. Sept. 1984, Vol. 16, No. 9, 27-30.*
 - 126) **Goettsh H.B.G., Lien L.A. and Butler D.R.** Glycol quenchant control with a membrane system. *Paper presented at the 9th American Society for Metals Heat Treating Conference and Exposition, O'Hare Convention Centre, 29 April- 1 May 1986, Chicago. (See Heat Treatment of Metals 1986.3, Vol. 13, 69).*
 - 127) **Meszaros A.G.** Water-based quenching composition comprising polyvinylpyrrolidone and method quenching. *US patent 3,902,929. Sept. 1975.*
 - 128) **Hart B.J.** PVP polymer products claim quench operation advantages. *Heat Treating. Oct. 1982, Vol. 14, No. 10, 24-26.*
 - 129) **Foreman R.W. and Meszaros A.G.** Method for restoring molecular weight distribution of polymeric quenchant. *US patent 4,251,292.*
 - 130) **Kopietz K.H.** Quenching in polymer solutions to obtain non-martensitic structures. *Paper presented at the American Society for Metals (ASM) Heat Treating Conference/Workshop '77, Cobo Hall, 25 May 1977, Detroit.*
 - 131) **Kopietz K.H. and Munjat F.S.** Process for the controlled cooling of ferrous metal. *US patent 4,087,290, May 1978.*
 - 132) **Kopietz K.H.** Controlled quenching of ferrous metals in sodium polyacrylate aqueous solutions. *Industrial Heating. June 1979, Vol. 46, No. 6, 30-38.*
 - 133) **Mason K.J. and Griffin T.** The use of polymer quenchants for the patenting of high-carbon steel wire and rod. *Heat Treatment of Metals. 1982.3, Vol. 9, 77-83.*
 - 134) **von Bergen R.T.** New developments in polymer quenching technology. *Heat Treatment '84. Book no. 312, 17.1-17.4. The Metals Society. London, 1984.*
 - 135) **Hausen D.F.** Success with polymer synthetic quenchant to eliminate oil at a commercial heat treating plant. *Industrial Heating. Aug. 1980, Vol. 47, No.8, 22-24.*

- 136) **Khina M.L., Vasil'kov V.F. and Kobzev N.S.** Quenchants based on water-soluble polymers. *Metal Science and Heat Treatment*. 1978, Vol. 20, No. 1-2, 680-681.
- 137) **Tolstousov A.V. and Bannykh O.A.** New quenching method based on water-soluble polymers. *Metal Science and Heat Treatment*. 1981, Vol. 23, No. 1-2, 104-106.
- 138) **Zakamaldin A.A., Kochurkina Y.I. and Tikhonov G.I.** New quenchants. *Metal Science and Heat Treatment*. 1983, Vol. 25, No. 1-2, 13-18.
- 139) **Bedarev A.S., Konyukhov G.P., Il'yushko E.G. and Beloboradov G.I.** Use of water-soluble polymers for quenching aluminium alloys. *Metal Science and Heat Treatment*. 1978, Vol. 20, No. 1-2, 48-52.
- 140) **Bozhko G.T., Bannykh O.A., Tropkina M.N., Manikhin P.I. and Popov A.V.** Effect of aqueous polymer solution viscosity on cooling capacity. *Metal Science and Heat Treatment*. 1983, Vol. 25, No. 11-12, 810-813.
- 141) **Warchol J.F.** New polymers for use in aqueous quenching. *Paper presented at the 8th American Society for Metals Heat Treating Conference/Workshop, 18-20 Sept. 1984, Detroit.*
- 142) **Warchol J.F.** Polyoxazolines in aqueous quenchants. *US patent 4,486,286. Dec. 1984*
- 143) **Warchol J.F.** Aqueous quenchants containing polyoxazolines and N-vinyl heterocyclic polymers and their use in quenching steel. *US patent 4,528,044. July 1985.*
- 144) **Hasson J.A.** Glycol quenching takes the heat off steel. *Metal Progress*. Sept. 1985, Vol. 128, No. 4, 67-72.
- 145) **Masseria V. and Kirkpatrick C.W. (Editors).** Induction Hardening and Tempering. "Heat Treating" *Metals Handbook, 9th Edition, Vol. 4, American Society for Metals, Metals Park, Ohio. 1981, 451-483.*
- 146) **Billmeyer F.W.** Textbook of Polymer Science. 3rd Edition. *John Wiley and Sons Incorporated, New York. 1984.*
- 147) **Simpson C.F. (Editor).** Practical High Performance Liquid Chromatography. *Heyden, London. 1976.*
- 148) **Morawetz H.** Macromolecules in Solution. 2nd Edition. *John Wiley and Sons Incorporated, New York. 1975.*
- 149) **Rose A.** Internal stresses resulting from heat treatment and transformation processes. *Harterei-Technische Mitteilungen*. 1966, Vol. 21, No. 1, 1-6. (In German).
- 150) **Child H.C.** Residual stress in heat-treated components. *Heat Treatment of Metals*. 1981.4, Vol. 8, 89-94.
- 151) **Brandrup J. and Immergut E.H. (Editors).** Polymer Handbook. *John Wiley and Sons, New York. 1966.*

- 152) Methods for determination of the viscosity of liquids. *BS 188:1977. British Standards Institution. 1977.*
- 153) Cloud point of nonionic surfactants. *ASTM standard test designation : D2024-65. American Society for Testing and Materials. 1965.*
- 154) **Greff R.A. and Flanagan P.W.** The characterization of nonionic surfactants by NMR. *The Journal of the American Oil Chemists Society. March 1963, Vol.40, No. 3, 118-120.*
- 155) **Taylor J.** Private communication, *GKN (Guest Keen and Nettlefolds plc), Group Technological Centre, Wolverhampton, July 1984.*
- 156) Shear stability of polymer-containing fluids using a diesel injector nozzle *ASTM standard test, designation : D3945-80. American Society for Testing and Materials. 1980.*
- 157) **Kirk D.** Theoretical aspects of residual stress measurements by X-ray diffractometry. *Strain. Feb. 1970, Vol. 6, No. 2, 75-80.*
- 158) **Kirk D.** X-ray measurement of residual stresses. *Paper presented at the Institute of Non-Destructive Testing seminar "Non-Destructive Measurement of Residual and Other Stresses in Components", Institute of Non-Destructive Testing, Northampton, 9 Feb. 1984.*
- 159) **Hilley M.E., Larson J.A., Jatzak C.F. and Riclefs R.E.(Editors).** Residual Stress Measurement by X-Ray Diffraction. *SAE Handbook J784a. Society of Automotive Engineers, Warrendale, Pennsylvania. 1971.*
- 160) **Cullity B.D.** Elements of X-Ray Diffraction. 2nd Edition, *Addison Wesley Publishing Company Incorporated, Reading, Massachusetts. 1978.*
- 161) **Kirk D.** Experimental features of residual stress measurement by X-ray diffractometry. *Strain. Jan. 1971, Vol. 7, No. 1, 1-8.*
- 162) **Harding R.H. and Matlock P.L.** Method of quenching. *European patent 0206,347. June 1986.*
- 163) **Grayson M. (Editor).** Kirk-Othmer Encyclopedia of Chemical Technology, 3rd Edition, Vol. 23. *John Wiley and Sons, New York. 1983, 967-968.*
- 164) **Haaf F., Sanner A. and Straub F.** Polymers of N-vinylpyrrolidone : synthesis, characterization and uses. *Polymer Journal. Jan. 1985, Vol. 17, No. 1, 143-152.*
- 165) **Horn M.B.** Acrylic Resins. *Reinhold Publishing Corporation, New York. 1960.*
- 166) **Conrad J. (Editor)** Encyclopedia of Polymer Science and Technology, Vol. 1. *John Wiley and Sons, New York. 1964.*
- 167) **Doolittle A.K.** The Technology of Solvents and Plasticizers. *Chapman and Hall Ltd, London. 1954.*
- 168) **Coreza R.J. (Editor)** Block and Graft Copolymerization, Vol. 2. *John Wiley and Sons, London. 1976.*

- 169) **Jayasuriya D.S., Dwivedi A.M. and Gage M.C.** A DSC study of hydration of poly(ethylene oxide). *Polymer Preprints*. Sept. 1986, Vol. 27, No. 2, 284-285.
- 170) **Matsura H. and Fukuhara K.** Hydration of the oxyethylene chain. *Bulletin Chemical Society of Japan*. March 1986, Vol. 59, No. 3, 763-768.
- 171) **Kucharaski G. and Chlebicki J.** The effect of polyoxypropylene chain length on the critical micelle concentration of propylene oxide - ethylene oxide block copolymers. *Journal of Colloid and Interface Science*. March 1974, Vol. 46, No. 3, 518-521.
- 172) **Prasad K.N., Luong T.T., Florence A.T., Paris J., Kaution C., Seiller M. and Puisieux F.** Surface activity and association of ABA polyoxyethylene - polyoxypropylene block copolymers in aqueous solution. *Journal of Colloid and Interface Science*. April 1979, Vol. 69, No. 2, 225-232.
- 173) **Prigogine I.** The Molecular Theory of Solutions. *North Holland Publishing Co, Amsterdam*. 1957.
- 174) **Patterson D.** Free volume and polymer solubility. *Macromolecules*. Nov-Dec. 1969, Vol. 2, No. 6, 672-277.
- 175) **Kunzel T., Tensi H.M. and Welzel G.** Rewetting rate - the decisive characteristic of a quenchant. *International Federation for Heat Treatment of Materials (IFHT)*. 5th IFHT International Congress on Heat Treatment of Materials, Budapest, 20-24 Oct. 1986, *Proceedings* Vol. 3, 1806-1813.
- 176) **Collier J.G.** Convective Boiling and Condensation. 2nd Edition. *McGraw-Hill International Book Company, London*. 1981.
- 177) **Kotchaphakdee P. and Williams M.C.** Enhancement of nucleate pool boiling with polymeric additives. *International Journal of Heat and Mass Transfer*, 1970, Vol. 13, 835-846.
- 178) **Winter E.R.F., Merte H.M. and Hertz H.M.** Recent Developments in Boiling and Condensation. *Weinheim, New York*. 1977.
- 179) **Oscik J.** Adsorption. *John Wiley and Sons, Chichester*. 1982.
- 180) **Rohsenow W.M.** Correlation of nucleate boiling heat transfer data. *Paper presented at the conference "Boiling and Two Phase Flow for Heat Transfer Engineers"*, University of California, Berkeley and Los Angeles, May 27-28. 1965.
- 181) **Lipson C. and Sheth N.J.** Statistical Design and Analysis of Engineering Experiments. *McGraw-Hill Kogakusha Ltd., Tokyo*. 1973. 496.
- 182) **Leis D.G. and Stout E.C.** Stabilization of polyoxyalkylene compounds *US patent 2,942,033*. June 1960.
- 183) **Reich L. and Stivala S.S.** Elements of Polymer Degradation. *McGraw-Hill International Book Company, London*. 1971.
- 184) **Schildknecht C.E.** Vinyl and Related Polymers. *John Wiley and Sons, New York*. 1952.

- 185) **Holliday L.** Ionic Polymers. *Applied Science Publishers, London. 1975.*
- 186) **Debye V.P. and McAulay J.M.** Das elektrische feld der ionen und die neutralsalzwirkung. *Physikalische Zeitschrift, 1925, Vol.26, 22-29. (In German).*
- 187) **Cheng K.J., Pearsall G.W. and Chaddock J.B.** Enhancement of the steel quenching process by an electric field. *Journal of Materials Science, 1987, Vol.22, 103-108*